INHERITED METABOLIC DISEASES IN PEDIATRICS: CLINICAL AND MOLECULAR FEATURES

EDITED BY: Yuan-Zong Song, Hui Xiong and Huiwen Zhang

PUBLISHED IN: Frontiers in Genetics and Frontiers in Pediatrics

frontiers Research Topics

frontiers

ISSN 1664-8714
ISBN 978-2-83250-847-3
DOI 10.3389/978-2-83250-847-3

About Frontiers

Frontiers is more than just an open-access publisher of scholarly articles: it is a pioneering approach to the world of academia, radically improving the way scholarly research is managed. The grand vision of Frontiers is a world where all people have an equal opportunity to seek, share and generate knowledge. Frontiers provides immediate and permanent online open access to all its publications, but this alone is not enough to realize our grand goals.

Frontiers Journal Series

The Frontiers Journal Series is a multi-tier and interdisciplinary set of open-access, online journals, promising a paradigm shift from the current review, selection and dissemination processes in academic publishing. All Frontiers journals are driven by researchers for researchers; therefore, they constitute a service to the scholarly community. At the same time, the Frontiers Journal Series operates on a revolutionary invention, the tiered publishing system, initially addressing specific communities of scholars, and gradually climbing up to broader public understanding, thus serving the interests of the lay society, too.

Dedication to Quality

Each Frontiers article is a landmark of the highest quality, thanks to genuinely collaborative interactions between authors and review editors, who include some of the world's best academicians. Research must be certified by peers before entering a stream of knowledge that may eventually reach the public - and shape society; therefore, Frontiers only applies the most rigorous and unbiased reviews.
Frontiers revolutionizes research publishing by freely delivering the most outstanding research, evaluated with no bias from both the academic and social point of view. By applying the most advanced information technologies, Frontiers is catapulting scholarly publishing into a new generation.

What are Frontiers Research Topics?

Frontiers Research Topics are very popular trademarks of the Frontiers Journals Series: they are collections of at least ten articles, all centered on a particular subject. With their unique mix of varied contributions from Original Research to Review Articles, Frontiers Research Topics unify the most influential researchers, the latest key findings and historical advances in a hot research area! Find out more on how to host your own Frontiers Research Topic or contribute to one as an author by contacting the Frontiers Editorial Office: frontiersin.org/about/contact

INHERITED METABOLIC DISEASES IN PEDIATRICS: CLINICAL AND MOLECULAR FEATURES

Topic Editors:
Yuan-Zong Song, First Affiliated Hospital of Jinan University, China
Hui Xiong, Peking University, China
Huiwen Zhang, Xinhua Hospital Shanghai, China

Citation: Song, Y.-Z., Xiong, H., Zhang, H., eds. (2022). Inherited Metabolic Diseases in Pediatrics: Clinical and Molecular Features.
Lausanne: Frontiers Media SA. doi: 10.3389/978-2-83250-847-3

Table of Contents

frontiers in Pediatrics

CASE REPORT
published: 27 August 2021
doi: 10.3389/fped.2021.725930

Novel *GLDC* Compound Heterozygous Variant Leading to Nonketotic Hyperglycinemia: Case Report and Literature Review

Yanyan Cao[1†], *Lingzhi Meng*[2†], *Yudong Zhang*[2], *Jiancheng Jiao*[2], *Weicong Pu*[2] *and Li Ma*[2*]

[1] *Institute of Pediatric Research, Children's Hospital of Hebei Province, Shijiazhuang, China,* [2] *Department of Neonatology, Children's Hospital of Hebei Province, Shijiazhuang, China*

Nonketotic hyperglycinemia (NKH) is a lethal autosomal recessive disease resulting from alterations in glycine metabolism, commonly caused by mutations in glycine decarboxylase (*GLDC*). The symptoms of NKH usually manifest in the neonatal period, and can be categorized into severe NKH and attenuated NKH based on the clinical outcome. To date, only a few NKH cases have been reported in China. We here report a case of a neonate with severe NKH carrying a novel compound heterozygous variant in *GLDC.* The patient was a 68-h-old girl who had progressive lethargy, no crying, and poor sucking ability from birth, and was therefore transferred to our department. On admission, the patient was supported by intubation and ventilation and presented with profound coma. Metabolic investigation indicated a markedly increased glycine concentration both in the plasma and cerebrospinal fluid (CSF). Symptomatic treatments were administered, but the patient's condition did not improve substantially. Whole-exome sequencing identified compound heterozygous mutations (c.1261G>C, p.G421R and c.450 C>G, p.N150K) in *GLDC*, which were inherited from the mother and the father, respectively. The patient was hospitalized for 8 days in our department and died 2 days after discharge. We further summarize the clinical features, genetic characteristics, administered treatment, and prognosis of previously reported Chinese NKH patients for context. Our results highlight that due to the non-specific clinical phenotypes of NKH and difficulty in obtaining CSF samples, genetic testing is a crucial tool, not only for a diagnosis but also for predicting the clinical outcome and can potentially help to determine the optimal therapeutic strategy.

Keywords: nonketotic hyperglycinemia, *GLDC* variation, compound heterozygous variant, glycine cleavage enzyme system, inherited metabolic disease

OPEN ACCESS

Edited by:
Huiwen Zhang,
Xinhua Hospital, China

Reviewed by:
Enrique Lin Shiao,
University of California, Berkeley, United States
Sinem Firtina,
University of Istinye, Turkey

***Correspondence:**
Li Ma
mary801@sina.com

[†]These authors have contributed equally to this work

Specialty section:
This article was submitted to Genetics of Common and Rare Diseases, a section of the journal Frontiers in Pediatrics

Received: *16 June 2021*
Accepted: *06 August 2021*
Published: *27 August 2021*

Citation:
Cao Y, Meng L, Zhang Y, Jiao J, Pu W and Ma L (2021) Novel GLDC Compound Heterozygous Variant Leading to Nonketotic Hyperglycinemia: Case Report and Literature Review. Front. Pediatr. 9:725930. doi: 10.3389/fped.2021.725930

INTRODUCTION

Nonketotic hyperglycinemia (NKH) is an autosomal recessive inherited metabolic disease characterized by deficient activity of the glycine cleavage enzyme system (GCS), leading to the accumulation of glycine in almost all body tissues. The GCS consists of four components: glycine decarboxylase (also known as P protein), aminomethyl transferase (T protein), hydrogen carrier

protein (H protein), and dihydrolipoamide dehydrogenase (L protein), encoded by *GLDC*, *AMT*, *GCSH*, and *DLD*, respectively. *GLDC* mutations account for ∼80% of NKH cases, whereas *AMT* variants account for ∼20% of cases (1). In the majority of NKH cases, symptoms first appear in the neonatal period or during early infancy. According to the clinical outcomes, NKH is classified into severe NKH and attenuated NKH. Approximately 85% of cases with neonate onset are classified as severe NKH (2), mainly presenting with progressive lethargy and marked hypotonia, as well as severe apnea that requires ventilation.

We here report the case of a neonate with NKH carrying a novel compound heterozygous variant in *GLDC*, and summarize the clinical and genetic features of children with NKH reported in China to date.

CASE DESCRIPTION

A 68-h-old girl presenting with lethargy and a poor nutritional state among other symptoms was transferred from a local hospital to our department. She was born at 37 + 3 weeks of gestation by cesarean section due to cephalopelvic disproportion from a gravida 1, parity 1 (G1P1) mother. She had a birth weight of 2,600 g, an Apgar score of 10, and did not present asphyxia. Her parents were healthy and non-consanguine. After birth, the child manifested with progressive lethargy, no crying, and poor sucking ability. She was admitted to a neonatal department in the local hospital at 40 h of life, where she showed low spirit, decreased spontaneous breathing, poor terminal circulation, and blood pressure of 39/22 mmHg. She was intubated and ventilated, and administered 0.9% sodium chloride and dopamine (12 $\mu g \cdot kg^{-1} \cdot min^{-1}$) intravenously, as well as cefoperazone. However, the patient's condition did not substantially improve, and she was therefore transferred to our department.

On admission, physical examination showed profound coma with intubation and ventilation, yellowish skin, no autonomic activity, no autonomic breathing, no response to orbital pressure stimulation, slow pupil response to light, soft limbs, and poor peripheral blood circulation. Blood gas analysis showed respiratory acidosis (pH = 7.197, P_{CO2} = 65.7 mmHg, P_{O2} = 93.4 mmHg, $[HCO_3]$ = 24.9 mM, [Be] = 4.1 mM, and O_2 saturation of 97.4%). Electrolytes and lactic acid levels were normal, and blood glucose was slightly high (7.8 mM).

DIAGNOSTIC ASSESSMENT

After admission, the patient continued to be supported by intubation and ventilation, indwelling catheterization, and administration of cefoperazone and sulbactam sodium to combat any potential infection. Because a diagnosis of congenital metabolic diseases could not be excluded, a regimen including

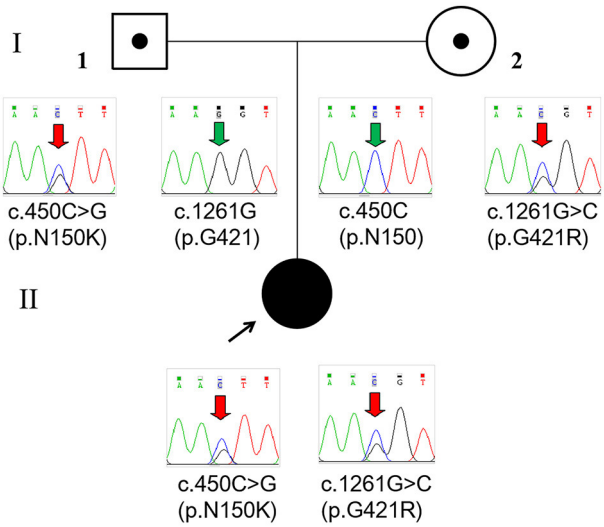

FIGURE 2 | Pedigree and *GLDC* variations confirmed by Sanger sequencing of the family. The patient (II) had a compound heterozygous variation c.450C>G (p.N150K) and c.1261G>C (p.G421R), which were inherited from her father (I-1) and mother (I-2), respectively.

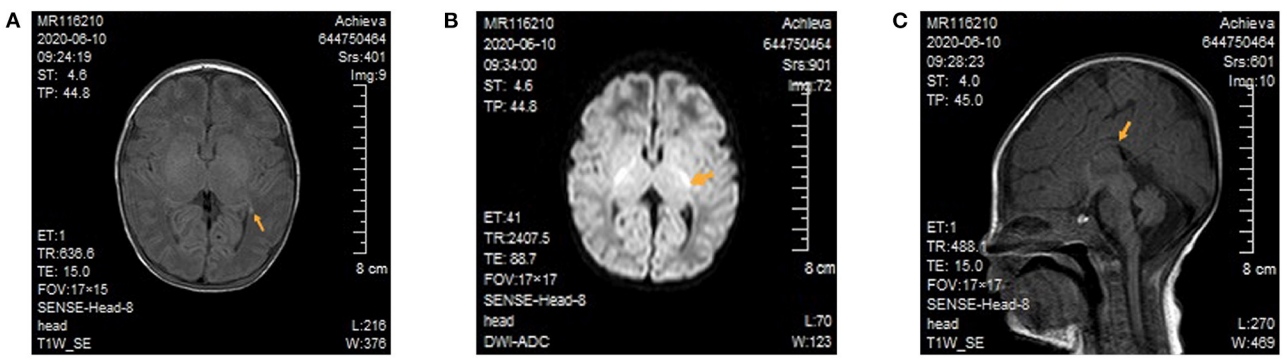

FIGURE 1 | Cranial magnetic resonance imaging of the patient. **(A)** Focal cerebral hemorrhage of the left paraventricular brain. There was no high T1 signal in the posterior limb of bilateral internal capsule. **(B)** In the diffusion-weighted image, high signals can be seen for the posterior limb of the internal capsule. **(C)** The thin and short of corpus callosum.

TABLE 1 | Clinical characteristics and *GLDC* variants in Chinese NKH children.

Case	Sex	Age of onset	Clinical presentation	Exons	Mutation	Inherited	Plasma glycine (normal range) (μmol/L)	CSF glycine (normal range) (μmol/L)	CSF/plasma ratio (normal ratio)	Treatment	Outcome	References
1	Male	1 d	poor feeding and decreased activity, lethargy, hypotonia, absent deep tendon reflexes, developmental delay, myoclonic seizures	21/20	c.2516A>G (p.Y839C)/c.2457 + 2T>A	Mother/father	947.8 (115–600)	226.4 (3–20)	0.24 (< 0.02)	Sodium benzoate, pyridoxine, dextromethorphan, dietary restriction of natural protein intake	Alive at 1 year 7 months: improved deep tendon reflexes and muscular hypotonia; but still poor feeding and intellectual disability	Liu S, et al. (5)
2	Male	11 h	early metabolic encephalopathy and Ohtahara syndrome	15/4–15	c.1786 C>T (p.R596X)/Exon 4–15 deletion	Mother/father	Normal	NA	NA	Adreno-cortico-tropic-hormone, topiramate and dextromethorphan	Died at 4 m	Gao Z, et al. (6)
3	Male	after birth	progressively poor reaction and weak crying	21/21	c.2198 C>T (p.A733V)	Mother/father[a]	1304.32 (130–650)	NA	NA	Antibiotics, mechanical ventilation and nutritional support	Died after 4 d	Dai H, et al. (7)
4	Male	5 d	poor reaction, feeding difficulty and limb tremor	13/9p24.3p22.3	c.1607G>A(p.R536Q)/ 9p24.3p22.3 deletion	Mother/NA[b]	1409.16 (125–750)	NA	NA	Cardiopulmonary resuscitation and trachea intubation and mechanical ventilation	Died at 6 d	Cheng L, et al. (8)
5	Male	9 m	intractable seizure	25/9	c.3006C>G (p.C1002W)/c.1256C>G (p.S419X)	Mother/father	75 (0∼276)	45.3 (1.6∼19.5)	0.06 (≤0.02)	NA	Alive at 6 year 8 months: intractable seizure, severe bilateral spastic paralysis and intellectual disability	Jiang T, et al. (9)
6	Female	2 year	ataxia, chorea and behavioral abnormality	25/9	c.3006C>G (p.C1002W)/c.1256C>G (p.S419X)	Mother/father	Normal	36.7 (1.6–19.5)	0.13 (≤0.02)	NA	Alive at 3 year 5 months: language retardation, ataxia, chorea and behavioral problem	
7	Male	2 d	Lethargy, hypotonia, seizures, apnea	23/3	c.2680A>G(p.T894A)/ Exon 3 deletion	Mother/father	NA	NA	NA	NA	Died at 11 d	Lin Y, et al. (10)
8	Male	2 d	Lethargy, hypotonia, seizures, apnea, hiccup	23/3	c.2680A>G(p.T894A)/ Exon 3 deletion	Mother/father	1587.87 (232-740)	260.2 (2.2-14.2)	0.164 (<0.08)	NA	Died at 13 d	

(Continued)

TABLE 1 | Continued

Case	Sex	Age of onset	Clinical presentation	Exons	Mutation	Inherited	Plasma glycine (normal range) (μmol/L)	CSF glycine (normal range) (μmol/L)	CSF/plasma ratio (normal ratio)	Treatment	Outcome	References
9	Female	3d	Lethargy, hypotonia, seizures, hiccup	23/3	c.2680A>G(p.T894A)/ Exon 3 deletion	Mother/father	1038.25 (232-740)	157.2 (2.2-14.2)	0.151 (<0.08)	Sodium benzoate, dextromethorphan	Alive at 7 m: severe intellectual disability, frequent seizures	
10	Female	after birth	Lethargy, no crying, poor feeding and hypotonia	9/3	c.1261 G>C (p.G421R)/c.450 C>G (p.N150K)	Mother/father	942 (100–500)	Markedly elevated	0.12 (<0.08)	Antibiotics, mechanical ventilation, vitamin B12, B6 and C, folic acid, coenzyme Q10 and levocarnitine	Died at 13 d	This study

[a] *The patient's sample was not obtained, and his parents carried a heterozygous mutation in GLDC.*

[b] *Copy number variation was not analyzed in the parents.*

NA, Not available.

vitamin B12, vitamin B6, vitamin C, folic acid, coenzyme Q10, and levocarnitine was administered. Several subsequent blood ammonia checks were in the normal range, and there was no obvious metabolic/respiratory acidosis in the repeated blood gas analysis. Amplitude-integrated electroencephalogram both on 3 and 5 days of life all indicated a burst suppression pattern (the amplitude ranged from 1μV to nearly 100 μV), absence of sleep-wake cycle and no convulsive activity. Cranial magnetic resonance imaging (MRI) demonstrated focal cerebral hemorrhage of the right frontal lobe and left paraventricular brain (**Figure 1A**), focal long T2 signal of the bilateral frontal parietal lobes, and high signals of diffusion-weighted imaging of several brain areas, including the bilateral radial crown, posterior limb of the internal capsule (**Figure 1B**), and pontine arm, and the thin corpus callosum (**Figure 1C**). On day five of admission, the blood amino acid and acylcarnitine spectrum analyses to check for inherited metabolic diseases showed that the glycine concentration was increased at 942 μM (normal range 100–500 μM). The metabolic spectrum of the cerebrospinal fluid (CSF) also showed a markedly elevated glycine level, reaching a value of 3,460 times the control. The ratio of CSF to plasma glycine was 0.12 (normal < 0.08). A comprehensive panel of urine organic acids was normal.

Whole-exome sequencing (Beijing Fulgent Technologies Inc., Beijing, China) indicated that the patient had compound heterozygous variants in *GLDC* (reference genome hg 19, NM_000170.2): c.1261G>C (p.G421R) in exon 9 and c.450 C>G (p.N150K) in exon 3, which have not been previously reported. Sanger sequencing also confirmed that the two mutations were inherited from her mother and father, respectively (**Figure 2**). According to American College of Medical Genetics and Genomics guidelines, these two missense mutations are classified as likely pathogenic. The two mutations were inherited from the mother and father, respectively. Mutations were absent from controls in the GnomAD, 1000 Genomes Project, Exome Aggregation Consortium, and dbSNP databases. Bioinformatic prediction analyses using Mutation_Taster, PolyPhen2, and SIFT indicated that they were deleterious. Two other two missense mutations, p.G421V and p.N150T, at the same amino acid position had been identified as pathogenic. A diagnosis of NKH was finally made based on the clinical symptoms, elevated glycine concentration in the plasma and CSF, and increased glycine CSF/plasma ratio.

After 8 days of comprehensive anti-infection treatment, mechanical ventilation, and other symptomatic care, the patient's conscious reaction, limb movement, and peripheral circulation improved, although she still had no obvious spontaneous breathing. Considering the poor prognosis, the parents ceased treatment, and the patient died 2 days after discharge.

DISCUSSION

Approximately 80% of the NKH-causing *GLDC* mutations are sequence variations, whereas the remainder are exonic copy number variations (CNVs) (3). Among the sequence variations, missense mutations are the most frequent, followed by nonsense mutations, splice-site mutations, and small insertions/deletions.

In addition, some recurrent mutations have been identified in the United Kingdom and Finland, because of a founder effect, almost all of them unique (3, 4).

To date, 13 *GLDC* variants, including seven missense mutations (53.8%), three CNVs (23.1%), two nonsense mutations (15.4%), and one splice-site mutation (7.7%), have been identified in 10 Chinese children with NKH from 7 different families (**Table 1**) (5–10). Among 11 alleles identified with single-nucleotide variants, three (27.3%) were in exon 21 and two (18.2%) were in exon 9. No mutations in *AMT* have been identified in Chinese children suffering from NKH to date. In this study, we detected two heterozygous missense mutations in a neonate with severe NKH, c.1261G>C (p.G421R) and c.450 C>G (p.N150K), which were inherited from the mother and the father, respectively.

Different types of genetic variants can lead to a complete absence or different degrees of residual GCS enzyme activity, thus leading to distinct clinical phenotypes. For example, loss-of-function mutations such as a copy number (11), frameshift, nonsense, or splice site variation (12) causing complete depletion of GCS activity can lead to a severe phenotype (3, 13–15). However, it is difficult to assess the residual GSC activity in the case of missense mutations (4, 16). In addition to the present report of a severe case of NKH, there have been seven severe cases of NKH and two cases of attenuated NKH reported in China. Among the 12 alleles associated with severe NKH (eight cases from six unique families), seven (58.3%) were missense mutations, whereas in the two alleles associated with the attenuated cases (two cases from one family), only one was a missense mutation. Although the effect of the novel mutations identified in this study, p.G421R and p.N150K, on GCS activity is not clear, this patient was diagnosed with severe NKH according to the age of onset and clinical characteristics, suggesting that both of them were null mutations. Furthermore, the same amino acid positions of *GLDC*, p.G421V and p.N150T have been previously reported in three different patients with NKH. A patient carrying the p.N150T and p.R790W mutations presented with hypotonia apnea, coma intraventricular hemorrhage since the 3 days of life; her electroencephalogram showed a suppression burst pattern and brain MRI was normal; the concentration of glycine in CSF and in serum, and the CSF/serum ratio were 270 umol/L, 880umol/L and 0.31, respectively. At 16 days of age, sodium benzoate and dextromethorphan were administered. Imipramine was initiated at 7 years of age. *In vitro* expression analyses showed that the mutant glycine decarboxylases with p.N150T had 1% normal enzyme activity. However, the patient had far better psychomotor development because the other mutation, p.R790W, retained 14% of the enzyme activity (16). Kure et al. reported another Asian patient with p.N150T and c.1926 + 1G>A mutations (14). Her glycine level in CSF and the CSF/serum ratio were 148 mM and 0.12, respectively. No other phenotype was described. For residue 421 of glycine decarboxylase, variations of p.G421V and p.A729Efs*3 have already been described as associated with NKH (3). No other clinical data are available.

Currently, there are no formal management guidelines for NKH. The current treatment strategy focuses on reducing the plasma glycine concentration, blocking N-methyl-D-aspartate receptors, and symptomatic care (17, 18). Treatment information is available for six patients with severe NKH previously described in the literature (**Table 1**). Among three cases treated with dextromethorphan and/or sodium benzoate, one died at 4 months (case 2 in **Table 1**) and two were alive with severe intellectual disability when followed up at 1 year 7 months (case 1 in **Table 1**) and 7 months (case 9 in **Table 1**), respectively. The remaining three cases treated only with symptomatic care died from 4 to 13 days of life. Although information about the treatment provided was not available for the two siblings with attenuated NKH (case 5 and case 6 in **Table 1**), valproate administration leading to aggravation of the condition in the early stage of the disease was reported for case 5. Based on this, valproate is contraindicated for controlling epileptic seizures in NKH patients (19). In addition, based on previous case reports, vigabatrin should be avoided to treat West syndrome in NKH (20).

Since the genetic basis of NKH is well-defined and increased residual GCS activity has been associated with an improved clinical outcome, therapeutic strategies that can enhance the residual activity associated with a mutation should be pursued. For example, a translational read-through inducer has been used to promote translation through a premature stop codon (21), chemical chaperones have been used for unstable missense mutations to restore protein folding (22), and antisense oligonucleotides have been used to correct a splicing variation (23). Considering that CSF samples of neonatal children are not easily obtained, genetic testing is a powerful tool for diagnosing NKH, especially for patients with a normal plasma glycine level (case 2 in **Table 1**). Early use of genetic testing to diagnose NKH can avoid unnecessary drug-induced damage, as well as provide guidance to the family for future pregnancies.

CONCLUSION

We reported a patient with severe NKH who carried a novel compound heterozygous mutation and summarized the genetic and phenotypic characteristics, as well as the treatment strategy followed and prognosis of other NKH cases reported in China to date. This case report highlights the importance of genetic testing not only as a tool for NKH diagnosis but also for clinical outcome prediction, and the potential development of novel therapeutic strategies in the future.

DATA AVAILABILITY STATEMENT

The original contributions presented in the study are included in the article/supplementary materials, further inquiries can be directed to the corresponding author/s.

ETHICS STATEMENT

The studies involving human participants were reviewed and Hebei Province. Written informed consent to participate in this study was provided by the participants' legal guardian/next of kin.

Written informed consent was provided by the participants' legal guardian/next of kin for the publication of this case report.

AUTHOR CONTRIBUTIONS

YC wrote the manuscript. LM, YZ, JJ, and WP followed-up the patient and conducted data collection. LM conceived the study and supervised this research. All authors performed critical reading and approved the final version of manuscript.

FUNDING

This study was supported by Medical Science Research Program of Hebei province (20210056).

ACKNOWLEDGMENTS

We thank the patient and her parents for their participation in this study, and Editage (www.editage.cn) for English language editing.

REFERENCES

1. Toone JR, Applegarth DA, Coulter-Mackie MB, James ER. Recurrent mutations in P- and T-proteins of the glycine cleavage complex and a novel T-protein mutation (N145I): a strategy for the molecular investigation of patients with nonketotic hyperglycinemia (NKH). *Mol Genet Metab.* (2001) 72:322–5. doi: 10.1006/mgme.2001.3158
2. Van Hove JLK, Coughlin CII, Swanson M, Hennermann JB. Nonketotic hyperglycinemia. 2002 Nov 14 [Updated 2019 May 23]. In: Adam MP, Ardinger HH, Pagon RA, Wallace SE, Bean LJH, Mirzaa G, et al., editors. GeneReviews® [Internet]. Seattle (WA): University of Washington, Seattle. 1993–2021.
3. Coughlin CR. 2nd, Swanson MA, Kronquist K, Acquaviva C, Hutchin T, Rodríguez-Pombo P, et al. The genetic basis of classic nonketotic hyperglycinemia due to mutations in GLDC and AMT. *Genet Med.* (2017) 19:104–11. doi: 10.1038/gim.2016.74
4. Kure S, Takayanagi M, Narisawa K, Tada K, Leisti J. Identification of a common mutation in Finnish patients with nonketotic hyperglycinemia. *J Clin* Invest. (1992) 90:160–4. doi: 10.1172/JCI115831
5. Liu S, Wang Z, Liang J, Chen N, Ou Yang H, Zeng W, et al. Two novel mutations in the glycine decarboxylase gene in a boy with classic nonketotic hyperglycinemia: case report. *Arch Argent Pediatr*. (2017) 115:e225–e9. doi: 10.5546/aap.2017.eng.e225
6. Gao Z, Jiang Q, Chen Q, Xu K. Clinical and molecular genetic study of nonketotic hyperglycinemia in a Chinese family. *Zhongguo Dang Dai Er Ke Za Zhi (Chinese)*. (2017) 19:268–71. doi: 10.7499/j.issn.1008-8830.2017.03.003
7. Dai H, Cai L, Wu Z. A neonate with nonketotic hyperglycinemia. *Neural Injury And Functional Reconstruction (Chinese)*. (2017) 12:18. doi: 10.16780/j.cnki.sjssgncj.2017.02.033
8. Cheng L, Song T, Li Y, Xu H, Xu Y, Wan S, et al. Identification and analysis of a novel mutation of glycine decarboxylase gene in a neonata with nonketotic hyperglycinemia. *Chinese Journal of Perinatal Medicine (Chinese)*. (2017) 20:527–9. doi: 10.3760/cma.j.issn.1007-9408.2017.07.010
9. Jiang T, Jiang J, Xu J, Zhen J, Jiang P, Gao F. Clinical and genetic analyses of a family with atypical nonketotic hyperglycinemia caused by compound heterozygous mutations in the GLDC gene. *Zhongguo Dang Dai Er Ke Za Zhi (Chinese)*. (2017) 19:1087–91. doi: 10.7499/j.issn.1008-8830.2017.10.011
10. Lin Y, Zheng Z, Sun W, Fu Q. A novel compound heterozygous variant identified in GLDC gene in a Chinese family with non-ketotic hyperglycinemia. *BMC Med Genet.* (2018) 19:5. doi: 10.1186/s12881-017-0517-1
11. Kanno J, Hutchin T, Kamada F, Narisawa A, Aoki Y, Matsubara Y, et al. Genomic deletion within GLDC is a major cause of non-ketotic hyperglycinaemia. *J Med Genet*. (2007) 44:e69. doi: 10.1136/jmg.2006.043448
12. Xiong HY, Alipanahi B, Lee LJ, Bretschneider H, Merico D, Yuen RKC, et al. RNA splicing. The human splicing code reveals new insights into the genetic determinants of disease. *Science*. (2015) 347:1254806. doi: 10.1126/science.1254806
13. Swanson MA, Coughlin CR Jr, Scharer GH, Szerlong HJ, Bjoraker KJ, Spector EB, et al. Biochemical and molecular predictors for prognosis in nonketotic hyperglycinemia. *Ann Neurol.* (2015) 78:606–18. doi: 10.1002/ana.24485
14. Kure S, Kato K, Dinopoulos A, Gail C, DeGrauw TJ, Christodoulou J, et al. Comprehensive mutation analysis of GLDC, AMT, and GCSH in nonketotic hyperglycinemia. *Hum Mutat.* (2006) 27:343–52. doi: 10.1002/humu.20293
15. Conter C, Rolland MO, Cheillan D, Bonnet V, Maire I, Froissart R. Genetic heterogeneity of the GLDC gene in 28 unrelated patients with glycine encephalopathy. *J Inherit Metab Dis.* (2006) 29:135–42. doi: 10.1007/s10545-006-0202-6
16. Kure S, Ichinohe A, Kojima K, Sato K, Kizaki Z, Inoue F, et al. Mild variant of nonketotic hyperglycinemia with typical neonatal presentations: mutational and in vitro expression analyses in two patients. *J Pediatr.* (2004) 144:827–9. doi: 10.1016/j.jpeds.2004.02.044
17. Hamosh A, McDonald JW, Valle D, Francomano CA, Niedermeyer E, Johnston MV. Dextromethorphan and high-dose benzoate therapy for nonketotic hyperglycinemia in an infant. *J Pediatr.* (1992) 121:131–5. doi: 10.1016/S0022-3476(05)82559-4
18. Bjoraker KJ, Swanson MA, Coughlin CR. 2nd, Christodoulou J, Tan ES, Fergeson M, et al. Neurodevelopmental outcome and treatment efficacy of benzoate and dextromethorphan in siblings with attenuated nonketotic hyperglycinemia. *J Pediatr*. (2016) 170:234–9. doi: 10.1016/j.jpeds.2015.12.027
19. Hall DA, Ringel SP. Adult nonketotic hyperglycinemia (NKH) crisis presenting as severe chorea and encephalopathy. *Mov Disord.* (2004) 19:485–6. doi: 10.1002/mds.106815
20. Tekgul H, Serdarolu G, Karapinar B, Plat M, Yurtsever S, Tosun A, et al. Vigabatrin caused rapidly progressive deterioration in two cases with early myoclonic encephalopathy associated with nonketotic hyperglycinemia. *J Child* Neurol. (2006) 21:82–4. doi: 10.1177/08830738060210011801
21. Sánchez-Alcudia R, Pérez B, Ugarte M, Desviat LR. Feasibility of nonsense mutation readthrough as a novel therapeutical approach in propionic acidemia. *Hum Mutat.* (2012) 33:973–80. doi: 10.1002/humu.22047
22. Majtan T, Liu L, Carpenter JF, Kraus JP. Rescue of cystathionine beta-synthase (CBS) mutants with chemical chaperones: purification and characterization of eight CBS mutant enzymes. *J Biol Chem.* (2010) 285:15866–73. doi: 10.1074/jbc.M110.107722
23. Hua Y, Sahashi K, Hung G, Rigo F, Passini MA, Bennett CF, et al. Antisense correction of SMN2 splicing in the CNS rescues necrosis in a type III SMA mouse model. *Genes Dev.* (2010) 24:1634–44. doi: 10.1101/gad.1941310

Conflict of Interest: The authors declare that the research was conducted in the absence of any commercial or financial relationships that could be construed as a potential conflict of interest.

Publisher's Note: All claims expressed in this article are solely those of the authors and do not necessarily represent those of their affiliated organizations, or those of the publisher, the editors and the reviewers. Any product that may be evaluated in this article, or claim that may be made by its manufacturer, is not guaranteed or endorsed by the publisher.

frontiers in Genetics

ORIGINAL RESEARCH
published: 20 October 2021
doi: 10.3389/fgene.2021.729777

Correlation Between Genotype and Age of Onset in Leukoencephalopathy With Vanishing White Matter

*Jiong Deng, Ling Zhou, Jie Zhang, Xuting Chang, Yuwu Jiang, Jingmin Wang and Ye Wu**

Department of Pediatrics, Peking University First Hospital, Beijing, China

Purpose: Leukoencephalopathy with vanishing white matter (VWM) is an autosomal recessive leukoencephalopathy caused by mutations in any of the five genes encoding the subunits of eukaryotic translation initiation factor 2B (eIF2B). The severity of the disease varies considerably, and its genotypic-phenotypic correlation is still unclear. Age of onset is the only independent clinical predictor for VWM severity. In this study, the correlation between genotype and age at onset of patients was investigated.

Methods: Data were collected from patients with VWM in the available literature reports and from those diagnosed in Peking University First Hospital. The age of onset was divided into early-onset (≤4 years) and late-onset type (>4 years) for the analysis of the correlation between genotype and age of onset in patients with VWM.

Results: A total of 341 patients were included, 281 were reported in 87 available articles and 60 were diagnosed in our center. A total of 180 different mutations were found, among which 86.1% were missense. The gene (*EIF2B1-5*) in which the mutation located, and the number of null alleles were not associated with age of onset in these patients. Certain mutations such as eIF2Bε[Arg195His] and eIF2Bε[Arg269Gln] that were predicted to have a serious influence on eIF2B structure were related to earlier age of onset. EIF2Bγ [Ala87Val] which was predicted to have a minimal influence on eIF2B structure, was related to later age of onset. Whereas eIF2Bβ[Glu213Gly], eIF2Bβ[Gly200Val] and eIF2Bε [Thr91Ala], also predicted having a small effect on the structure of eIF2B, did not show correlation with the age of onset. The onset age of patients with one or biallelic missense mutations located in the catalytic domain or other homologous domains in catalytic subunits (eIF2Bγ, ε) was earlier than that of patients with biallelic mutations located in the NT domain.

Conclusion: The onset age of patients with different genotypes varied greatly. The degree of influence in protein structure of some missense mutations was correlated with phenotypic severity, but the results were not completely consistent. The combined effect of biallelic mutations, the role of regulatory genes, environmental stress and other potential factors on phenotypes need to be further explored.

Keywords: leukoencephalopathy with vanishing white matter, EIF2B1-5, genotype, age of onset, correlation

OPEN ACCESS

Edited by:
Yuan-Zong Song,
First Affiliated Hospital of Jinan University, China

Reviewed by:
Alessio Di Fonzo,
IRCCS Ca 'Granda Foundation Maggiore Policlinico Hospital, Italy
Li Jiang,
Children's Hospital of Chongqing Medical University, China

****Correspondence:***
Ye Wu
dryewu@263.net

Specialty section:
This article was submitted to Genetics of Common and Rare Diseases, a section of the journal Frontiers in Genetics

Received: *23 June 2021*
Accepted: *08 October 2021*
Published: *20 October 2021*

Citation:
Deng J, Zhou L, Zhang J, Chang X, Jiang Y, Wang J and Wu Y (2021) Correlation Between Genotype and Age of Onset in Leukoencephalopathy With Vanishing White Matter. Front. Genet. 12:729777. doi: 10.3389/fgene.2021.729777

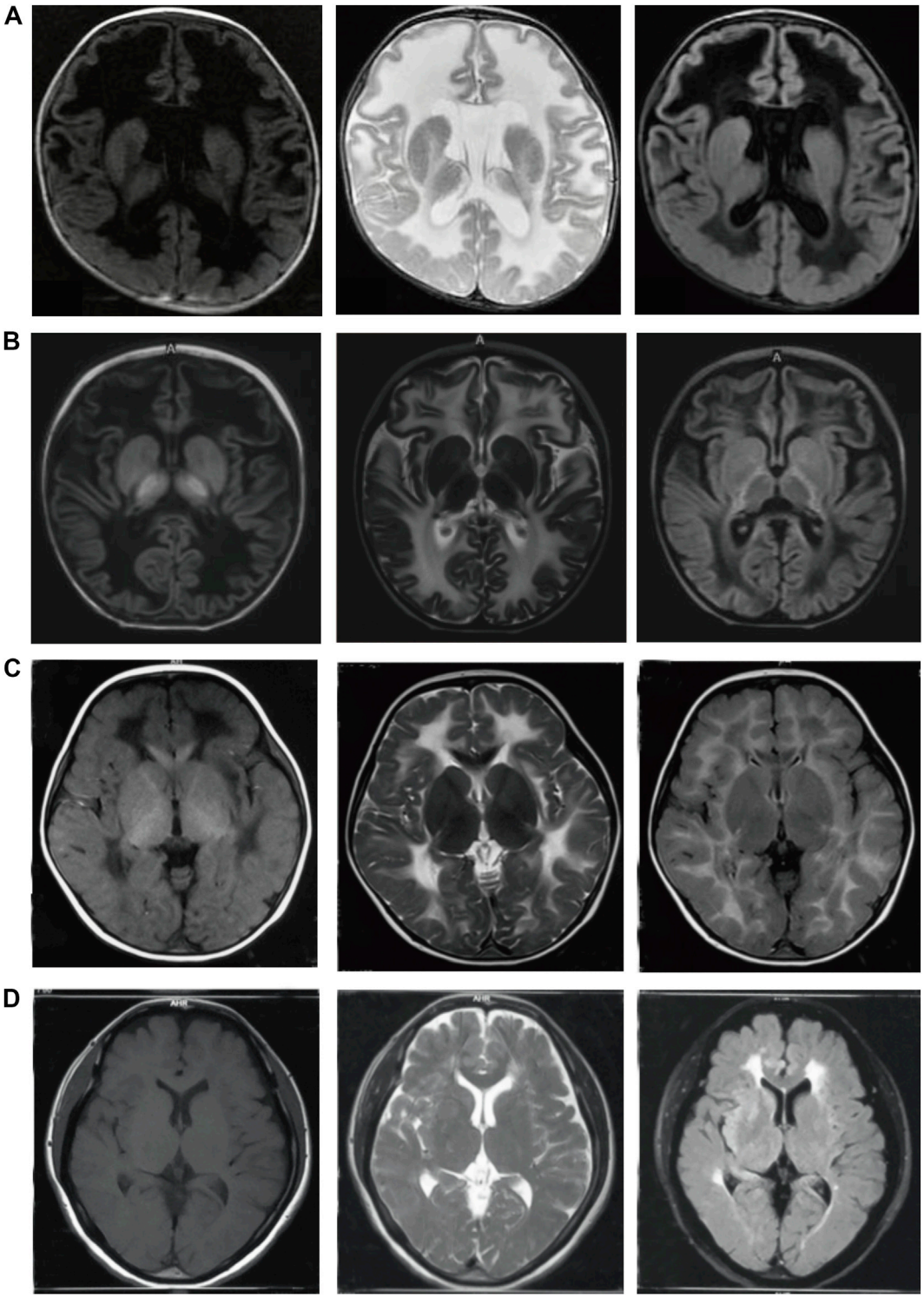

FIGURE 1 | Brain MRI of four patients with VWM at different onset ages. **(A)**: case 1 with onset in neonatal period, the age at MRI was 3 months; **(B)**: case 2 with onset in infancy, the age at onset was 11 months, the age at MRI was 18 months; **(C)**: case 3 with onset in childhood, the age of onset was 3 years old, the age at MRI was 3 years old; **(D)**: case 4 with onset in adulthood, the age of onset was 43 years old, the age at MRI was 43 years old. The left column:T1 weighted sequences (T1WI); The middle column:T2 weighted sequences (T2WI); The right column: T2 FLAIR sequences. The white matter showed low signal on T1WI, high signal on T2WI and low signal liquefaction on T2 FLAIR. The earlier the age of onset, the wider the range of white matter liquefaction, while the liquefaction sign was not evident in adult patients. Furthermore, the subcortical white matter was involved in the early stage.

INTRODUCTION

Leukoencephalopathy with vanishing white matter (VWM) is an autosomal recessive leukoencephalopathy. In 1997, van der Van Der Knaap et al. (1997) reported the first clinically diagnosed case of VWM. From 2001 to 2002, it was revealed to be caused by mutations in any one of the five following subunits of the eukaryotic translation initiation factor 2B(eIF2B): *EIF2B*1(12q24), *EIF2B*2(14q24), *EIF2B*3(1p34), *EIF2B*4(2p23) and *EIF2B*5(3q27) (Leegwater et al., 2001; Van Der Knaap et al., 2002). The typical phenotype in children is progressive regression in motor function exacerbated by fever or head trauma. Brain MRI shows that the white matter liquefies progressively (**Figure 1**). Age of onset and disease severity vary substantially from neonatal period to adulthood. Early onset of this disease is usually correlated to fast progression and poor prognosis (Hamilton et al., 2018). Although the pathogenesis of VWM is increasingly recognized, the reasons for the wide phenotype are still unknown. A clear genotype-phenotype correlation has not been established. The relationship between genotype and phenotype is important in elucidating the pathogenesis of VWM, predicting the prognosis of VWM, and promoting genetic consultation. Previous studies have confirmed that age of onset is the only independent clinical predictor of disease severity (Fogli et al., 2004a; Hamilton et al., 2018). A thorough search on patients from published literatures and those diagnosed in our center (Pediatric Department, Peking University First Hospital) were conducted to analyze the correlation between the genotype and the age of onset.

PATIENTS AND METHODS

Inclusion of Patients

Literature Searching Strategy

Case series studies or case reports on VWM containing information on the clinical and genotypic spectra of patients were searched from the following databases: PubMed, Embase, Cochrane Library, Web of Science, China National Knowledge Infrastructure, and WAN FANG DATA (the latter two are Chinese public searching databases). The following search terms were used: leukoencephalopathy with vanishing white matter, vanishing white matter disease, childhood ataxia with central nervous system hypomyelination or Cree leukoencephalopathy (CLE). The publications were in either English or Chinese. The searching deadline was January 2021.

Inclusion Criteria of Patients From Our Center

The inclusion criteria were as follows: brain MRI showing symmetric abnormal signals on T1WI, T2WI and T2 FLAIR images in the white matter that was partially rarefied, and biallelic pathogenic or likely pathogenic variants in *EIF2B1-5* according to the American College of Medical Genetics Guidelines confirmed by sequencing (Richards et al., 2015). The study was approved by the Medical Ethics Committee of Peking University First Hospital. Informed consents were obtained from the parents of the children.

Correlation Analysis of Genotype and Age of Onset

Age of onset was divided into early-onset type (≤4 years) and late-onset type (>4 years). It was used as a typical phenotypic index to analyze the genotype-phenotype correlation. All data were analyzed using SPSS 20.0 software. $p < 0.05$ was considered statistically significant.

Correlation Between the Mutant Gene (*EIF2B1-5*) and Age of Onset

Enumeration data were expressed as frequency and percentage, and measurement data were expressed as median (range). Chi-square test was performed to compare the difference in mutant genes between the early- and late-onset patients. If the data were normally distributed, one-way ANOVA was used; otherwise, Kruskal-Wallis test was applied.

Correlation Between Numbers of Null Allele and Age of Onset

Null allele was defined as loss-of-function allele, which included nonsense, frameshift, +1 or +2 splicing mutations, −1 and −2 intronic mutations, and single or multiple exon deletion. They were divided into 1 and 0 null allele in accordance with the number of null alleles carried by the patients. If the data were normally distributed, T test was used to analyze the age of onset between the two groups; otherwise, non-parametric test was applied.

Correlation Between Missense Mutations With Reported Structural Effects and Age of Onset

Some missense mutations were reported to have multiple effects on eIF2B structure, but the variant was not completely related to the phenotype, thus suggesting the influence of another allele or other modifiers on the phenotype. In this study, patients with biallelic missense variants were included for the analysis. The differences in age of onset among patients with 0, 1 or 2 missense mutations reported to show structural effects were analyzed.

Correlation Between Missense Mutations Located Indifferent Structural Domain and Age of Onset

The eIF2B decamer consists of regulatory (α, β, δ) and catalytic (γ, ε) subunits. Catalytic subcomplexes elF2Bγ and elF2Bε have four different domains (**Figure 2**): 1) NT domain; 2) I-patch domain: the NT domain and I-patch domain alone do not interact with other subunits, but certain mutations or disruptions within them affected the formation of eIF2B holo-complexes; 3) Catalytic domain: responsible for the interaction of eIF2B with elF2 (the substrate); 4) other domains: except for the above three domains, the sequences are all highly homologous regions, but functional significance is still unclear. Given the wide range of effects of null allele on eIF2B and the unclear effects of intron mutations, the

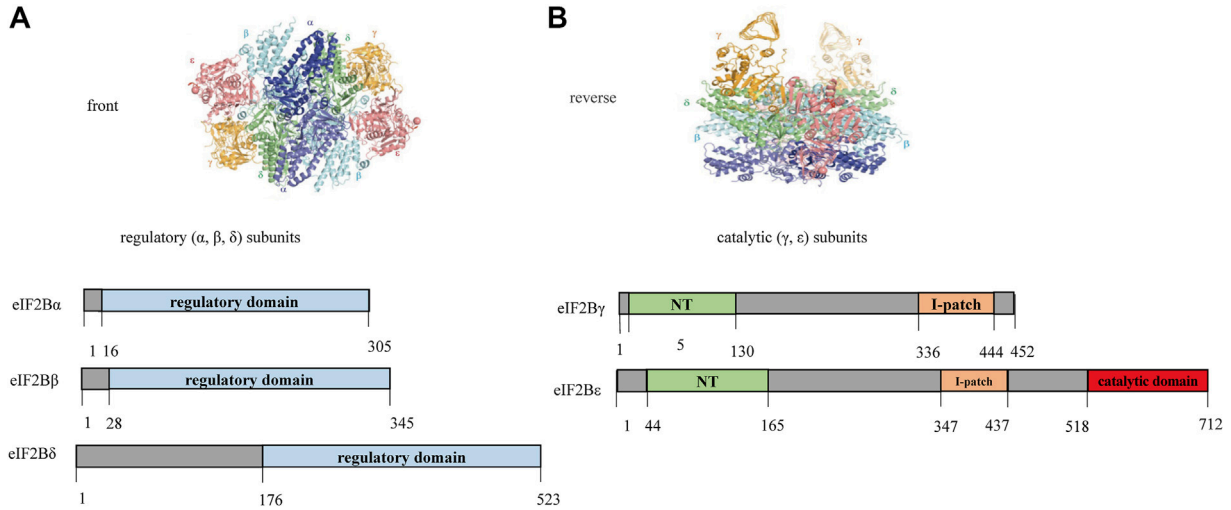

FIGURE 2 | Schematic diagram of the homologous structure of human *eIF2B* (Kashiwagi et al., 2016). The eIF2B decamer is a heterodimer structure composed of regulatory (α, β, δ) and catalytic (γ, ε) subunits. The γ and ε subunits have two homology domains, the first is NT domain which sequence similarities with nucleotidyl transferases (shown in green in 5–130 amino acids of eIF2Bγ and 44–165 amino acids of eIF2Bε); the second is I-patch domain which has sequence similarities with acyl transferases (shown in yellow in 336–444 amino acids of eIF2Bγ and 347–437 amino acids of eIF2Bε), which have approximate hexad spacing of the hydrophobic branched-chain amino acids isoleucine (Ile), valine (Val), and leucine (Leu). The catalytic domain is located at the C-terminus of eIF2Bε(shown in red in 518–712 amino acids of eIF2Bε).

correlation between the affected structural domain and age of onset was compared among patients with biallelic missense variants. If the data were normally distributed, ANOVA was used to analyze the age of onset between groups affected by different structural domains; otherwise, Kruskal-Wallis test was applied.

RESULTS

General Information of the Mutations

A total of 341 patients were included, among which, 281 were reported in 87 available articles and 60 were diagnosed in our center (**Supplementary Table S1**). In addition, 196 patients belonged to the early-onset type and 145 patients were categorized as late-onset type. The proportions of patients with mutations in *EIF2B1, EIF2B2, EIF2B3, EIF2B4,* and *EIF2B5* were 1.5% (5/341), 15.2% (52/341), 11.1% (38/341), 10.3% (35/341) and 61.9% (211/341), respectively. A total of 180 mutations were identified, including 154 missense (86.1%), 11 frameshift (6.1%), eight nonsense (4.4%), three in-frame small deletion (1.7%), 2 splice-site, and 2 intronic mutations (not splice-site).

Correlation Between the Mutant Gene and Age of Onset

Five patients carried mutations in *EIF2B1*, of which two were early-onset and three were late-onset, and the median age of onset was 10.0 (0.7–29.0) years. Fifty-two patients carried mutation in *EIF2B2*, of which 31 were early-onset and 21 were late-onset, and the median age of onset was 3.8 (0.2–43.0) years. Thirty-eight patients carried mutation in *EIF2B3*, of which 24 were early-onset and 14 were late-onset, and the median age of onset was 3.6 (0–61.0) years. Thirty-five patients carried mutation in *EIF2B4*, of which 21 were early-onset and 14 were late-onset, and the median age of onset was 3.5 (0–41.0) years. A total of 211 cases carried mutation in *EIF2B5*, of which 119 were early-onset and 92 were late-onset, and the median age of onset was 3.5 (0–62.0) years. No statistical difference was observed between the proportions of patients with early-onset and late-onset types among different mutant genes ($\chi 2 = 1.51$, $p > 0.05$). No statistical difference also was observed in the age of onset among the five mutant genes ($H = 3.39$, $p > 0.05$) (**Figure 3A**).

Correlation Between Numbers of Null Allele and Age of Onset

Among the study population, 36 patients carried one null allele with the median age at onset of 2.5 (0–24.0) years, and 303 patients carried zero null allele with the median age at onset of 3.6 (0–62.0) years (two patients carried intronic variants in non-splicing sites were excluded). No statistical difference in the age of onset was observed between patients with one or zero null allele ($Z = 1.57$, $p > 0.05$) (**Figure 3B**).

Correlation Between Missense Mutations With Reported Structural Effects and Age of Onset

Some missense mutations were predicted to show variable structural effects on the protein, including eIF2Bβ[Thr91Bla], eIF2Bβ[Ser171Phe], eIF2Bβ[Gly200Val], eIF2Bγ [Arg91His], eIF2Bδ [Arg264Trp], eIF2Bδ[Arg357Trp], eIF2Bδ[Arg483Trp],

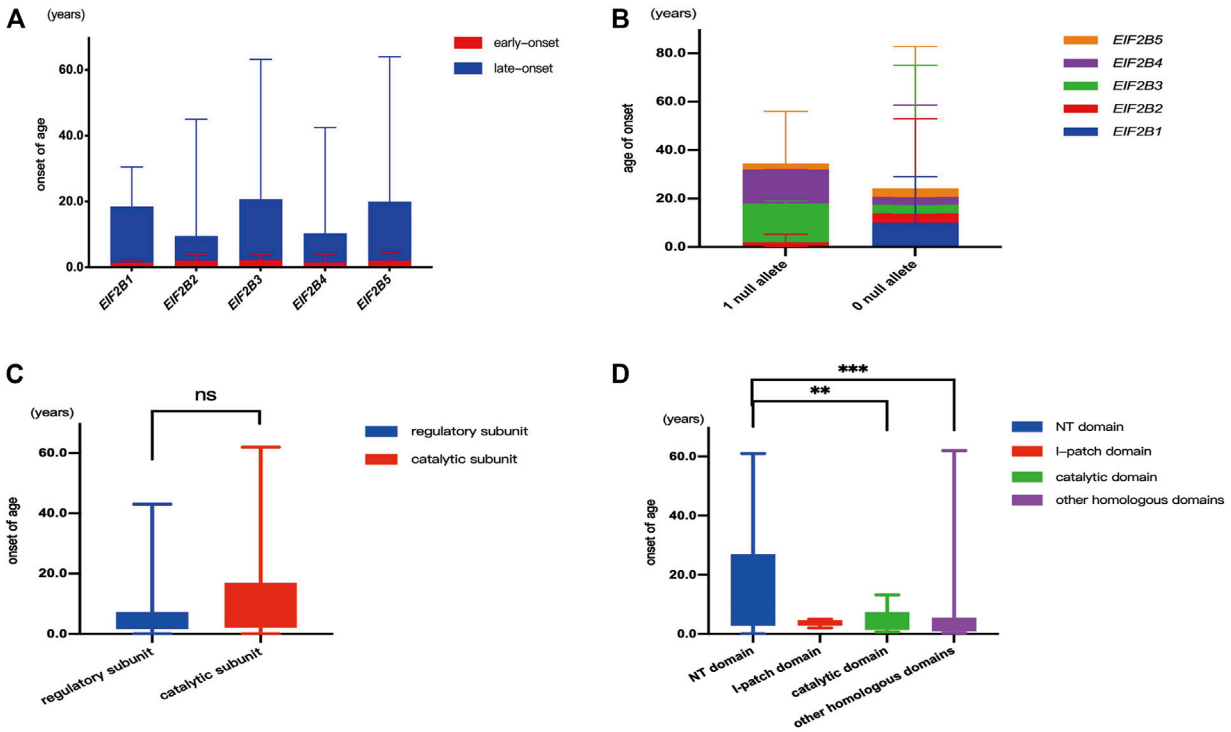

FIGURE 3 | Genotype-age of onset correlation. **(A)**: Correlation between the mutant gene (*EIF2B*1-5) and age of onset. **(B)**: Correlation between number of null alleles and age of onset. **(C)**: Correlation between missense mutations located in different subunit and age at onset. **(D)**: Correlation between missense mutations located in different structural domain and age of onset. "**"denotes $p < 0.01$, "***" denotes $p < 0.001$, "ns" indicates no statistical difference.

TABLE 1 | Correlation between age of onset among patients with 0, 1 or 2 above missense mutations and structural effect.

Predicted structural effects	Mutations	Numbers of mutations	N[a]	Age of onset(years)	Variable	P
substantial effect	eIF2Bε[Arg195His]	1–2	13	0.8(0.3–34)	13.08	<0.001
		2	6	0.7(0.3–0.9)	H_a = 3.63	<0.001
					H_b = 0.09	>0.05
		1	7	4.5(0.3–34.0)	H_c = 0.41	>0.05
		0	290	3.6(0–62.0)		
substantial effect	eIF2Bε[Arg269Gln]	1–2	9	1.2(0.7–4.5)	2.77	<0.01
		2	2	(1.2–1.6)		
		1	7	1.1(0.7–4.5)	H_d = 2.34	<0.05
		0	294	3.7(0–62.0)		
small effect	eIF2Bβ[Glu213Gly]	1–2	22	5.5(1.5–17.0)	1.84	>0.05
		2	17	5.0(1.5–17.0)		
		1	5	7.0(1.7–17.0)		
		0	281	3.5(0–62.0)		
small effect	eIF2Bβ[Gly200Val]	1	7	1.7(0.3–22.0)	0.94	>0.05
		0	296	3.6(0–62.0)		
small effect	eIF2Bε[Thr91Ala]	1–2	5	2.0(1.5–3.0)	0.11	>0.05
		0	298	3.6(0–62.0)		
small effect	eIF2Bγ[Ala87Val]	1–2	10	29.0(2.1–61.0)	2.68	<0.01
		2	6	26.5(2.1–61.0)		
		1	4	38.5(2.3–57.0)		
		0	293	3.5(0–62.0)		

[a]N: *number of patients with 0, 1 or 2 missense mutations;* H_a: *people carried two eIF2Bε[Arg195His] compared with those without eIF2Bε[Arg195His] mutation;* H_b: *people carried two eIF2Bε[Arg195His] compared with those carried one eIF2Bε[Arg195His] mutation;* H_c: *people carried one eIF2Bε[Arg195His] compared with those without eIF2Bε[Arg195His] mutation.* H_d: *people carried one eIF2Bε[Arg269Gln] compared with those without eIF2Bε[Arg269Gln] mutation.*

eIF2Bε [Thr79Ile], eIF2Bε[Glu81Leu], eIF2Bε[Arg136His], eIF2Bε[Arg195His], eIF2Bε[His269Pro], eIF2Bε[Arg316Gln], eIF2Bε[Thr91Ala], eIF2Bε[Glu213Gly], eIF2Bε[Arg133His], eIF2Bε[Gly386Val], [Ala403Val] and [Thr432Ile](Slynko et al., 2021).

In this study, due to the small number of the above mutations in these patients, we only analyzed eIF2Bε[Arg195His], eIF2Bε [Arg269Gln], eIF2Bβ[Gly200Val], eIF2Bβ[Glu213Gly], eIF2Bγ [Ala87Val] and eIF2Bε[Thr91Ala]. Among them, eIF2Bε [Arg195His] and eIF2Bε[Arg269Gln] were considered to have a serious effect on the structure of eIF2B and associated with a more serious phenotype, whereas eIF2Bβ[Gly200Val], eIF2Bβ [Glu213Gly], eIF2Bγ[Ala87Val] and eIF2B[Thr91Ala] were predicted to have a small effect on the structure of eIF2B and associated with a mild phenotype. Only patients with biallelic missense mutations were included for the analysis.

Differences in the age of onset among patients with 0, 1 or 2 above missense mutations were analyzed (**Table 1**). The age of onset in patients with eIF2Bε[Arg195His] or eIF2Bε[Arg269Gln] mutation was significantly earlier than that in patients without the mutations ($Z = 2.14$, $p < 0.05$; $Z = 2.77$, $p < 0.01$), thus supporting the previous results that patients with these two mutations have a more serious clinical phenotype. In addition, the patients with two eIF2Bε[Arg195His] variants had an earlier age of onset than those with one or no eIF2Bε[Arg195His], and patients with one eIF2Bε[Arg195His] showed no statistically significant difference in the age of onset with those without the mutation. Similarly, the patients with one eIF2Bε [Arg269Gln] had an earlier age of onset than those without the mutation. The age at onset in patients with eIF2Bγ [Ala87Val] or eIF2Bγ[Arg269Gln] mutation was significantly later than that in patients without the mutation ($Z = 2.68$, $p < 0.01$), indicating that the slight structural effect predicted mild disease severity. However, no significant difference in the age of onset was observed among patients with eIF2Bβ[Gly200Val], eIF2Bβ[Glu213Gly] or eIF2Bε [Thr91Ala] compared with other patients ($Z = 1.34$, $p > 0.05$; $Z = 0.94$, $p > 0.05$; $Z = 0.11$, $p > 0.05$, respectively), suggesting that eIF2Bβ[Glu213Gly], eIF2Bβ[Gly200Val] and eIF2Bε[Thr91Ala] have a slight correlation with age of onset in these patients.

Correlation Between Missense Mutations Located in Different Structural Domain and Age of Onset

Among the 154 missense mutations, four were *EIF2B*1 mutations, 17 were *EIF2B*2 mutations, 23 were *EIF2B*3 mutations, 28 were *EIF2B*4 mutations, and 82 were *EIF2B*5 mutations (**Supplementary Table S2**).

Correlation Between Missense Mutations Located in Different Subunit and Age at Onset

Among the 303 patients carrying biallelic missense mutations, 81 patients carried mutations affecting the regulatory subunit, and the median age of onset was 4.0 (0–43.0) years, while 222 patients carried mutations affecting the catalytic subunit, and the median age of onset was 3.5 (0–62.0) years. No statistically significant difference in the age of onset was observed among patients carrying mutations affecting the regulatory or catalytic submit ($Z = 1.26$, $p > 0.05$) (**Figure 3C**).

Correlation Between Missense Mutations Located in Different Structural Domain and Age of Onset

A total of 222 patients carrying missense mutations in the catalytic subunit were classified into the following four groups: 1) 106 patients carried biallelic mutations in the NT domain, with the median age of onset 9.0 (0–61.0) years; 2) five patients carried biallelic mutations in the I-patch domain, with the median age of onset 4.0 (2.0–5.0) years; 3) eight patients carried one mutation affected the catalytic domain, with the median age of onset 2.5 (0.7–13.2) years; and 4) 49 patients carried biallelic mutations affecting the other domains, with the median age of onset 2.5 (0.3–62.0) years. Significant difference in the age of onset was observed among these four groups ($H = 19.19$, $p < 0.001$). The age of onset in patients carrying one mutation in the catalytic domain was significantly earlier than that of patients with two mutations in the NT domain ($Z = 2.28$, $p < 0.05$). The age of onset in patients carrying biallelic mutations affecting other domains was earlier than that in patients with biallelic mutations in the NT domain ($Z = 3.99$, $p < 0.001$) (**Figure 3D**).

DISCUSSION

A genotype-phenotype correlation was reported in patients with VWM, but certain differences were found, in part because of differences in the phenotypic measures used in the studies (Fogli et al., 2004a; Van Der Lei et al., 2010; Matsukawa et al., 2011). Age of onset is the only independent clinical predictor of disease severity (Hamilton et al., 2018), which is easily accessible from the literature, and therefore served as a relatively reliable index of phenotype in our study. Data from 341 patients with VWM were collected, including 180 different mutations in *EIF2B1-5*, of which 86.1% were missense mutations. In this study, the proportions of patients with mutations in *EIF2B1, EIF2B2, EIF2B3, EIF2B4,* and *EIF2B5* were 1.5, 15.2, 11.1, 10.3 and 61.9%, respectively. Similar to the results of previous reports (Bugiani et al., 2010), the most common mutant gene was *EIF2B5*, followed by *EIF2B2*. The correlation between the age of onset and the different mutant genes was not identified.

EIF2B1-5 are house-keeping genes that play an important role in eukaryotic cells. They encode eIF2B, which is a critical factor in the initiation of protein translation. Null allele may result in the inability to synthesize eIF2B protein and loss of translation initiation function. Therefore, individuals carrying two null alleles could not survive to be born. No patients carrying two null alleles have been reported yet. In this study, we analyzed the correlation between numbers of null allele and age of onset. We did not find significant difference between the age of onset in patients with one or zero null allele. This finding may be due to the relatively small proportion of patients with null allele (10.5%).

Previous studies have reported a certain correlation between the degree of influence of missense mutations on protein structure and phenotypes, but the results are not consistent.

Results from protein prediction software or model analysis of the mutation site function prediction revealed that some mutations with multiple or substantial effects on the eIF2B structure were associated with severe phenotypes, such as eIF2Bε[Thr79Ile], eIF2Bε[Glu81Leu], eIF2Bε[Arg136His], eIF2Bε[Arg195His], eIF2Bε[His269Pro], eIF2Bε[Arg269Gln], eIF2Bε[Arg316Gln]; eIF2Bδ[Arg264Trp], eIF2Bδ[Arg357Trp], eIF2Bδ[Arg483Trp], and eIF2Bγ[Arg91His] (Slynko et al., 2021). Mutations such as eIF2Bβ[Thr91Bla], eIF2Bε[Thr91Ala], eIF2Bε[Ala87Val] and eIF2Bε[Glu213Gly], with predicted minimal influence on the eIF2B structure, were associated with mild disease severity. However, the functional prediction of missense variants could not completely explain the phenotype. For example, mutations such as eIF2Bε[Arg133His] and eIF2Bβ[Ser171Phe] were predicted to have a huge effect on protein structure, but they were related to mild phenotype. Mutations such as eIF2Bβ [Gly200Val], eIF2Bε[Gly386Val] [Ala403Val] and [Thr432Ile], with small predict effects, were linked to serious phenotype (Fogli et al., 2004b; Campbell and Ashe, 2006; Slynko et al., 2021). In this study, 303 patients with biallelic missense mutations were analyzed. Those with eIF2Bε[Arg195His] and eIF2Bε [Arg269Gln] had a significantly earlier age of onset than those without the mutations. This finding is consistent with the genotype-phenotype correlation from previous reports. The phenotype of children carrying eIF2Bε[Arg195His] mutation usually manifested as Cree leukoencephalopathy, a rapidly fatal phenotypic variant of infantile VWM with disease onset in prenatal or infancy; almost all of the affected patients died before 2 years of age (Van Der Knaap et al., 2003; Harder et al., 2010). In the present study, patients carrying eIF2Bγ[Ala87Val] had a significantly later age of onset than those without the mutation. Contrary to the results of previous studies, eIF2Bβ [Glu213Gly], [Gly200Val], and eIF2Bε[Thr91Ala] showed a minimal correlation with the age of onset. Fogli et al. (2004a) reported that eIF2Bβ[Glu213Gly] mutation was associated with a mild phenotype, relatively late age of onset, and slow progression. van der Van Der Lei et al. (2010) found that the disease severity of patients with homozygous eIF2Bε[Arg113His] was milder than that of patients with heterogeneous eIF2Bε[Arg113His] and homozygous eIF2Bε [Thr91Ala]. Meanwhile, the phenotype of patients with eIF2Bε [Arg113His/Arg339any] was milder than that of patients with eIF2Bε[Thr91Ala/Arg339any]. In our study, the age of onset among patients with two, one or without eIF2Bε[Arg195His] variants were compared. The patients with biallelic eIF2Bε [Arg195His] showed earlier onset than those with one or no variant, and the patients with one eIF2Bε[Arg195His] showed no statistically significant difference in terms of age of onset compared with those without the variant. Similarly, the patients with one eIF2Bε [Arg269Gln] mutation had an earlier age of onset than those without the mutation. These findings suggested that the correlation between genotype and phenotype required consideration of the combined effects of biallelic variants.

Whether the location of the missense mutations in different types of subunits or functional domains was associated with the age of onset was further analyzed. The results showed that the age of onset was not correlated with the location of the mutations in the regulatory (α, β, δ) or catalytic (γ, ε) subunits. Catalytic subcomplexes eIF2Bγ and eIF2Bε have four different domains: NT domain, I-patch domain, catalytic domain and other domains. eIF2Bε has the most important catalytic domain (amino acids 518–712 at the C-terminus) with GEF activity (GDP/GTP conversion). Knockout of the catalytic domain fragment in the mouse model could substantially reduce GEF activity and eIF2Bε binding to other subunits, suggesting that this region is important for the stability and activity of the eIF2B complex (Wortham et al., 2016; Moon and Parker, 2018a). Therefore, we further analyzed whether the location of missense mutations in different domains of the catalytic subunits influenced the age of onset. The results showed that patients carrying mutations located in the catalytic domain and other homologous domains had an earlier age of onset.

In VWM, stress is the triggering or aggravating factor, including head trauma, acute startle, and febrile infection (Labauge et al., 2009). Different cellular stresses lead to eIF2α phosphorylation, which then acts as a competitive inhibitor of eIF2B, inhibiting mRNA translation. A central mechanism in a cellular stress response is the inhibition of protein synthesis, known as unfolded protein response (Wong et al., 2019). This process aims to reduce the accumulation of denatured and misfolded proteins and escape translation inhibition through the transcription of mRNA with a special open reading frame (ORF), thus preserving cellular energy to enhance cell survival under stress. However, if the cellular stress state remains uncorrected for a long time and the unfolded protein response is overactivated and could not be recovered over a long period of time, it may lead to the logical deterioration and possible multi-organ dysfunction, which may be the possible cause of exacerbation of VWM (Moon and Parker, 2018b). Therefore, the observed considerable phenotypic variability indicated that genotype is not the only factor that determines phenotype; the environment may be an essential influential entity that affects disease severity. Exposure to factors causing episodic exacerbations could worsen the disease. Measures to prevent trauma and infection can improve the prognosis, and other factors, such as the regulation of upstream and downstream gene variation and epigenetics, have possible implications.

This study has some limitations. Most mutations have not been functionally studied, and their effects on protein functions need to be confirmed. The variants of only one allele were analyzed, and the other allele also contributed to the phenotype. The combined effect of the two alleles requires a larger sample data. Other regulatory genes and environmental factors also influence phenotypes, and they were not considered in this study. Age of onset is an independent risk factor for phenotypic severity. It was used as a phenotypic factor in this study to simplify and facilitate the extraction from the literature. However, it was likely to be inaccurate, and including indicators, such as the speed of motor function progression, is preferable.

CONCLUSION

A detailed genotypic-phenotypic association analysis was performed in 341 patients with VWM. The gene (*EIF2B1-5*) in which the mutation located, and the number of null alleles were not associated with age of onset in these patients. Certain mutations, such as eIF2Bε[Arg195His] and eIF2Bε

[Arg269Gln], which were predicted to have a serious influence on eIF2B structure, were related to earlier age of onset. And eIF2Bγ [Ala87Val], which was predicted to have a minimal influence on eIF2B structure, was related to later onset. eIF2Bβ[Glu213Gly], eIF2Bβ[Gly200Val] and eIF2Bε[Thr91Ala] showed a slight correlation with age of onset. The age of onset in patients with one or biallelic missense mutations located in the catalytic domain or other homologous domains in the catalytic subunits was earlier than that of patients with biallelic variants located in the NT domain. The combined effect of biallelic mutations, the role of regulatory genes, environmental stress and other potential factors on phenotypes need to be further explored.

DATA AVAILABILITY STATEMENT

The original contributions presented in the study are included in the article and **Supplementary Material**, further inquiries can be directed to the corresponding author.

ETHICS STATEMENT

The studies involving human participants were reviewed and approved by Medical Ethics Committee of Peking University First Hospital. Written informed consent to participate in this study was provided by the participants' legal guardian/next of kin.

AUTHOR CONTRIBUTIONS

Conceptualization: JD, LZ, and YW; Data curation: JD, LZ, JZ, and XC; Formal analysis: JD; Writing original draft: JD; Review and editing: JW, YJ, and YW.

FUNDING

This study was supported by the Beijing Natural Science Foundation (L202034) and National Science and Technology Major Project of the Ministry of Science and Technology of China (Grant Nos. 2017ZX09304029-006).

ACKNOWLEDGMENTS

We thank all the families of these children for their participation and cooperation.

SUPPLEMENTARY MATERIAL

The Supplementary Material for this article can be found online at: https://www.frontiersin.org/articles/10.3389/fgene.2021.729777/full#supplementary-material

REFERENCES

Bugiani, M., Boor, I., Powers, J. M., Scheper, G. C., and Van Der Knaap, M. S. (2010). Leukoencephalopathy with Vanishing white Matter: a Review. *J. Neuropathol. Exp. Neurol.* 69, 987–996. doi:10.1097/nen.0b013e3181f2eafa

Campbell, S. G., and Ashe, M. P. (2006). Localization of the Translational Guanine Nucleotide Exchange Factor eIF2B: a Common Theme for GEFs?. *Cell Cycle* 5, 678–680. doi:10.4161/cc.5.7.2607

Fogli, A., Schiffmann, R., Bertini, E., Ughetto, S., Combes, P., Eymard-Pierre, E., et al. (2004a). The Effect of Genotype on the Natural History of eIF2B-Related Leukodystrophies. *Neurology* 62, 1509–1517. doi:10.1212/01.wnl.0000123259.67815.db

Fogli, A., Schiffmann, R., Hugendubler, L., Combes, P., Bertini, E., Rodriguez, D., et al. (2004b). Decreased Guanine Nucleotide Exchange Factor Activity in eIF2B-Mutated Patients. *Eur. J. Hum. Genet.* 12, 561–566. doi:10.1038/sj.ejhg.5201189

Hamilton, E. M. C., Van Der Lei, H. D. W., Vermeulen, G., Gerver, J. A. M., Lourenço, C. M., Naidu, S., et al. (2018). Natural History of Vanishing White Matter. *Ann. Neurol.* 84, 274–288. doi:10.1002/ana.25287

Harder, S., Gourgaris, A., Frangou, E., Hopp, K., Huntsman, R., Lowry, N., et al. (2010). Clinical and Neuroimaging Findings of Cree Leukodystrophy: a Retrospective Case Series. *AJNR Am. J. Neuroradiol* 31, 1418–1423. doi:10.3174/ajnr.a2108

Kashiwagi, K., Takahashi, M., Nishimoto, M., Hiyama, T. B., Higo, T., Umehara, T., et al. (2016). Crystal Structure of Eukaryotic Translation Initiation Factor 2B. *Nature* 531, 122–125. doi:10.1038/nature16991

Labauge, P., Horzinski, L., Ayrignac, X., Blanc, P., Vukusic, S., Rodriguez, D., et al. (2009). Natural History of Adult-Onset eIF2B-Related Disorders: a Multi-Centric Survey of 16 Cases. *Brain* 132, 2161–2169. doi:10.1093/brain/awp171

Leegwater, P. A. J., Vermeulen, G., Könst, A. A. M., Naidu, S., Mulders, J., Visser, A., et al. (2001). Subunits of the Translation Initiation Factor eIF2B Are Mutant in Leukoencephalopathy with Vanishing white Matter. *Nat. Genet.* 29, 383–388. doi:10.1038/ng764

Matsukawa, T., Wang, X., Liu, R., Wortham, N. C., Onuki, Y., Kubota, A., et al. (2011). Adult-onset Leukoencephalopathies with Vanishing white Matter with Novel Missense Mutations in EIF2B2, EIF2B3, and EIF2B5. *Neurogenetics* 12, 259–261. doi:10.1007/s10048-011-0284-7

Moon, S. L., and Parker, R. (2018a). Analysis of eIF2B Bodies and Their Relationships with Stress Granules and P-Bodies. *Sci. Rep.* 8, 12264. doi:10.1038/s41598-018-30805-y

Moon, S. L., and Parker, R. (2018b). EIF2B2 Mutations in Vanishing white Matter Disease Hypersuppress Translation and Delay Recovery during the Integrated Stress Response. *Rna* 24, 841–852. doi:10.1261/rna.066563.118

Richards, S., Aziz, N., Aziz, N., Bale, S., Bick, D., Das, S., et al. (2015). Standards and Guidelines for the Interpretation of Sequence Variants: a Joint Consensus Recommendation of the American College of Medical Genetics and Genomics and the Association for Molecular Pathology. *Genet. Med.* 17, 405–423. doi:10.1038/gim.2015.30

Slynko, I., Nguyen, S., Hamilton, E. M. C., Wisse, L. E., De Esch, I. J. P., De Graaf, C., et al. (2021). Vanishing white Matter: Eukaryotic Initiation Factor 2B Model and the Impact of Missense Mutations. *Mol. Genet. Genomic Med.* 9, e1593. doi:10.1002/mgg3.1593

Van Der Knaap, M. S., Barth, P. G., Gabreëls, F. J. M., Franzoni, E., Begeer, J. H., Stroink, H., et al. (1997). A New Leukoencephalopathy with Vanishing white Matter. *Neurology* 48, 845–854. doi:10.1212/wnl.48.4.845

Van Der Knaap, M. S., Leegwater, P. A. J., Könst, A. A. M., Visser, A., Naidu, S., Oudejans, C. B. M., et al. (2002). Mutations in Each of the Five Subunits of Translation Initiation Factor eIF2B Can Cause Leukoencephalopathy with Vanishing white Matter. *Ann. Neurol.* 51, 264–270. doi:10.1002/ana.10112

Van Der Knaap, M. S., Van Berkel, C. G. M., Herms, J., Van Coster, R., Baethmann, M., Naidu, S., et al. (2003). eIF2B-related Disorders: Antenatal Onset and Involvement of Multiple Organs. *Am. J. Hum. Genet.* 73, 1199–1207. doi:10.1086/379524

Van Der Lei, H. D. W., Van Berkel, C. G. M., Van Wieringen, W. N., Brenner, C., Feigenbaum, A., Mercimek-Mahmutoglu, S., et al. (2010). Genotype-phenotype

Correlation in Vanishing white Matter Disease. *Neurology* 75, 1555–1559. doi:10.1212/wnl.0b013e3181f962ae

Wong, Y. L., Lebon, L., Basso, A. M., Kohlhaas, K. L., Nikkel, A. L., Robb, H. M., et al. (2019). eIF2B Activator Prevents Neurological Defects Caused by a Chronic Integrated Stress Response. *Elife* 8, e42940. doi:10.7554/eLife.42940

Wortham, N. C., Stewart, J. D., Harris, S., Coldwell, M. J., and Proud, C. G. (2016). Stoichiometry of the eIF2B Complex Is Maintained by Mutual Stabilization of Subunits. *Biochem. J.* 473, 571–580. doi:10.1042/bj20150828

Conflict of Interest: The authors declare that the research was conducted in the absence of any commercial or financial relationships that could be construed as a potential conflict of interest.

Publisher's Note: All claims expressed in this article are solely those of the authors and do not necessarily represent those of their affiliated organizations, or those of the publisher, the editors and the reviewers. Any product that may be evaluated in this article, or claim that may be made by its manufacturer, is not guaranteed or endorsed by the publisher.

frontiers in Pediatrics

ORIGINAL RESEARCH
published: 12 November 2021
doi: 10.3389/fped.2021.771922

Three Novel and One Potential Hotspot *CPT1A* Variants in Chinese Patients With Carnitine Palmitoyltransferase 1A Deficiency

Weifeng Zhang[1], *Yanru Chen*[2], *Chunmei Lin*[2], *Weilin Peng*[2], *Qingliu Fu*[2] *and Yiming Lin*[2]*

[1] Department of Neonatology, Quanzhou Maternity and Children's Hospital, Quanzhou, China, [2] Center of Neonatal Disease Screening, Quanzhou Maternity and Children's Hospital, Quanzhou, China

Carnitine palmitoyltransferase 1A (CPT1A) deficiency is an inherited disorder of mitochondrial fatty acid β-oxidation that impairs fasting ketogenesis and gluconeogenesis in the liver. Few studies implementing newborn screening (NBS) for CPT1A deficiency in the Chinese population have been reported. This study aimed to determine the biochemical, clinical, and genetic characteristics of patients with CPT1A deficiency in China. A total of 204,777 newborns were screened using tandem mass spectrometry at Quanzhou Maternity and Children's Hospital between January 2017 and December 2018. Newborns with elevated C0 levels were recruited, and suspected patients were subjected to further genetic analysis. Additionally, all Chinese patients genetically diagnosed with CPT1A deficiency were reviewed and included in the study. Among the 204,777 screened newborns, two patients were diagnosed with CPT1A deficiency; thus, the estimated incidence in the selected population was 1:102,388. In addition to the two patients newly diagnosed with CPT1A deficiency, we included in our cohort 10 Chinese patients who were previously diagnosed. Five of these 12 patients were diagnosed *via* NBS. All patients exhibited elevated C0 and/or C0/(C16+C18) ratios. No clinical symptoms were observed in the five patients diagnosed *via* NBS, while all seven patients presented with clinical symptoms, including fever, cough, vomiting, diarrhea, and seizures. Eighteen distinct *CPT1A* variants were identified, 15 of which have been previously reported. The three novel variants were c.272T>C (p.L91P), c.734G>A (p.R245Q), and c.1336G>A (p.G446S). *in silico* analysis suggested that all three novel variants were potentially pathogenic. The most common variant was c.2201T>C (p.F734S), with an allelic frequency of 16.67% (4/24). Our findings demonstrated that NBS for CPT1A deficiency is beneficial. The three novel variants expand the mutational spectrum of *CPT1A* in the Chinese population, and c.2201T>C (p.F734S) may be a potential hotspot *CPT1A* mutation.

Keywords: newborn screening, carnitine palmitoyltransferase 1A deficiency, *in silico* prediction, *CPT1A* gene, tandem mass spectrometry

OPEN ACCESS

Edited by:
Huiwen Zhang,
Xinhua Hospital, China

Reviewed by:
Yi-Jun Chen,
First Affiliated Hospital of Fujian Medical University, China
Xinwen Huang,
Children's Hospital of Zhejiang University, China

***Correspondence:**
Yiming Lin
linyiming0819@sina.com

Specialty section:
This article was submitted to Genetics of Common and Rare Diseases, a section of the journal Frontiers in Pediatrics

Received: *07 September 2021*
Accepted: *07 October 2021*
Published: *12 November 2021*

Citation:
Zhang W, Chen Y, Lin C, Peng W, Fu Q and Lin Y (2021) Three Novel and One Potential Hotspot CPT1A Variants in Chinese Patients With Carnitine Palmitoyltransferase 1A Deficiency. Front. Pediatr. 9:771922. doi: 10.3389/fped.2021.771922

INTRODUCTION

Carnitine palmitoyltransferase 1A (CPT1A) (OMIM 255120; EC 2.3.1.21) deficiency is an inherited autosomal recessive disorder of mitochondrial fatty acid β-oxidation that impairs fasting ketogenesis and gluconeogenesis in the liver. The causative gene, *CPT1A* (OMIM 600528), is located on chromosome 11q13.1-q13.2. Patients may present with a variety of symptoms, including seizures, lethargy, hypoglycemia, vomiting, diarrhea, fever, and hepatomegaly triggered by fasting. Sudden infant death and hypoketotic hypoglycemia have been reported in patients with severe deficiency (1).

Tandem mass spectrometry (MS/MS) has been widely used in newborn screening (NBS) for inherited metabolic diseases. CPT1A deficiency can be detected by MS/MS, with free carnitine (C0) and C0 to free long-chain acylcarnitine [C0/(C16+C18)] as the primary screening markers (2, 3). As early identification and timely treatment can prevent clinical symptoms, NBS is an important tool for diagnosing CPT1A deficiency.

Several patients have been reported worldwide since the first description of this disorder in 1981 (4). In particular, a high prevalence of CPT1A deficiency was observed in the Inuit, First Nations, and Alaska Native populations (5–8). However, few studies have used NBS to diagnose CPT1A deficiency in the Chinese population (9–13). In this study, we used NBS to diagnose CPT1A deficiency in a southern Chinese population. Furthermore, we systematically reviewed Chinese patients previously diagnosed with CPT1A deficiency to improve our understanding of this rare disorder.

MATERIALS AND METHODS

Study Population

A total of 204,777 newborns were screened by MS/MS at Quanzhou Maternity and Children's Hospital between January 2017 and December 2018, and newborns with elevated C0 levels (C0 > 60 μmol/L, cut-off value: 10–60 μmol/L) were recruited for the study. Additionally, all Chinese patients previously genetically diagnosed with CPT1A deficiency were reviewed and included in the study. Data from these patients were retrieved from PubMed (http://www.ncbi.nlm.nih.gov/pubmed) by searching the keywords "carnitine palmitoyltransferase 1A deficiency" or "CPT1A deficiency," "Chinese" or "China," and "*CPT1A*." Written informed consent was obtained from the parents of all patients. This study was approved by the Ethical Committee of Quanzhou Maternity and Children's Hospital. Written informed consent was obtained from the parents of all patients for the collection of samples and the publication of medical data.

Abbreviations: CPT1A, carnitine palmitoyltransferase 1A; MS/MS, tandem mass spectrometry; NBS, newborn screening; C0, free carnitine; C0/(C16+C18), C0 to free long-chain acylcarnitine; NGS, next-generation sequencing; PCR, polymerase chain reaction; 3D, three-dimensional; ACMG/AMP, American College of Medical Genetics and Genomics and the Association for Molecular Pathology.

NBS for CPT1A Deficiency

Sample collection, delivery, and pre-processing were performed as described in our previous article (14). Amino acids and acylcarnitines were quantitated using an ACQUITY TQD mass spectrometer (Waters, Milford, MA, USA). Newborns with elevated C0 levels (cut-off value: 10–60 μmol/L) and/or C0/(C16+C18) ratios (cut-off value: 0–40) were recalled. Those who tested positive were subjected to genetic testing.

Genetic Analysis

Targeted next-generation sequencing (NGS) was performed as previously described (15). A multigene panel covering 94 genes associated with inherited metabolic disorders (including *CPT1A*) was applied. All candidate variants identified by NGS were validated using Sanger sequencing. *CPT1A* exons and flanking intron sequences were amplified by polymerase chain reaction (PCR) under standard conditions. Primer sequences are available upon request. PCR products were sequenced directly using an ABI Prism 3500 Genetic Analyzer (Applied Biosystems, Foster City, CA, USA). The sequencing results were analyzed using Chromas 2.6.5 (Technelysium Pty Ltd, Australia), and the sequences were aligned using the *CPT1A* transcript (NM_001876). DNAMAN 8 (Lynnon Biosoft, San Ramon, CA, USA) was used to identify nucleotide variants.

All candidate variants were searched in several frequently used databases, as previously described (15). The pathogenicity of the novel missense variants was predicted using several *in silico* tools, including SIFT, PolyPhen-2, PROVEAN, and MutationTaster. Evolutionary conservation was analyzed using ClustalX (http://www.clustal.org/clustal2), and homology modeling was performed using the Swiss Model Workspace to analyze changes in the three-dimensional (3D) structure. Finally, all novel variants were evaluated based on the standard recommendations and guidelines for sequence variant interpretation, as published by the American College of Medical Genetics and Genomics and the Association for Molecular Pathology (ACMG/AMP) (16).

RESULTS

NBS for CPT1A Deficiency

Of the 204,777 screened newborns, 199 exhibited elevated C0 levels during initial NBS, of which 3 had extremely high C0 levels and 18 were accompanied by elevated C0/(C16+C18) ratios. During the recall stage, 12 newborns had elevated C0 levels, and 6 had elevated C0/(C16+C18) ratios. Two patients were finally diagnosed with CPT1A deficiency; thus, the incidence in the selected population was estimated to be 1:102,388.

Biochemical and Clinical Characteristics

In addition to the two patients newly diagnosed with CPT1A deficiency, we included in our cohort 10 Chinese patients who were previously diagnosed. Five of these 12 patients were diagnosed *via* NBS. All 12 patients exhibited elevated C0 levels; 11 patients (91.7%) also exhibited elevated C0/(C16+C18) ratios. The median C0 concentration and C0/(C16+C18) ratio were 136.00 ± 39.13 μmol/L (range: 79.65–193.61 μmol/L, cut-off

TABLE 1 | Biochemical, clinical, and molecular features of 11 Chinese patients with CPT1A deficiency.

Patient	Sex	Type	Acylcarnitine analysis		Genotype		Onset	Clinical manifestions	References
			C0	C0/(C16+C18)	Allele 1	Allele 2			
1	F	NBS	113.46	34.49	**c.734G>A (p.R245Q)**	**c.1336G>A (p.G446S)**	None	None	This study
2	M	NBS	79.65	379.29	c.1131G>C (p.E377D)	**c.272T>C (p.L91P)**	None	None	This study
3	M	NBS	128.1	512.4	c.1318G>A (p.A440T)	c.2201T>C (p.F734S)	None	None	(11)
4	F	SMS	179.68	499.5	c.1846G>A (p.V616M)	c.2201T>C (p.F734S)	1 y, 10 m	Seizure	(13)
5	M	SMS	191.5	1,473	c.693+1G>A	c.967+81C>T	1 y, 2 m	Fever, vomiting, diarrhea, seizure	(12)
6	M	SMS	144.9	920	c.968-8C>T	c.946C>T (p.R316W)	1 y, 2 m	Fever, vomiting, diarrhea, seizure	(12)
7	M	SMS	160.9	1,641	c.1787T>C (p.L596P)	c.2201T>C (p.F734S)	8 m	Fever, seizure, hypoglycemia	(12)
8	F	SMS	111.6	558	c.1131G>C (p.E377D)	c.124_126delAAG (p.K42del)	6 m	Fever, seizure, hypoglycemia	(12)
9	M	NBS	107.4	571	c.281+1G>A	c.956C>T (p.G319V)	None	None	(12)
10	M	NBS	84.3	843	c.740C>T (p.P247L)	c.577delC (p.M194*)	None	None	(12)
11	F	SMS	193.61	1,595.54	c.281+1G>A	Deletion of exon 15-18	1 y, 6 m	Fever, diarrhea, seizure	(10)
12	M	SMS	136.88	1,059.37	c.1787T>C (p.L596P)	c.2201T>C (p.F734S)	8 m	Fever, cough, diarrhea, seizure	(9)

M, male; F, female; NBS, newborn screening; SMS, selective metabolic screening; y, years; m, months; cut-off value, C0: 10–60 μmol/L, C0/(C16+C18): 0–40; the novel CPT1A variants are in boldface type.

value: 10–60 μmol/L) and 840.55 ± 513.80 (range: 34.49–1,595.54 μmol/L, cut-off value: 0–40), respectively.

No clinical symptoms were observed in the five patients diagnosed *via* NBS. The follow-up period of patients (no. 1–3) were between 2 and 3 years, while follow-up data of patients (no. 9 and 10) were not available. In contrast, all seven patients presented with clinical symptoms, including fever, cough, vomiting, diarrhea, and seizures. The age of onset ranged from 6 months to 1 year and 10 months. Detailed information on the biochemical and clinical manifestations of these patients is presented in **Table 1**.

Genetic Findings

All patients harbored compound heterozygous *CPT1A* variants. Eighteen distinct variants were identified, among which 61.11% (11/18) were missense variants, 22.22% (4/18) affected splicing, 11.11% (2/18) were frameshift variants, and 5.56% (1/18) were large deletions. Fifteen of these *CPT1A* variants were previously reported, and the other three were novel. The novel variants were c.272T>C (p.L91P), c.734G>A (p.R245Q), and c.1336G>A (p.G446S). The most common variant was c.2201T>C (p.F734S), with an allelic frequency of 16.67% (4/24). Relatively common variants were c.281+1G>A, c.1131G>C (p.E377D), and c.1787T>C (p.L596P), which were each identified twice. Each of the remaining 14 variants was identified only once (**Figure 1**).

None of these novel variants were recorded in disease databases such as ClinVar and HGMD. The novel variants were absent or had extremely low allelic frequencies in the dbSNP, ExAC, 1000 Genome, and GnomeAD databases. *In silico* analysis suggested that all three novel variants were potentially pathogenic (**Supplementary Table 1**). Alignment of the CPT1A sequences revealed that the amino acid residues at positions 91, 245, and 446 were strictly conserved (**Figure 2**). Protein modeling showed that Leu-91 was located in the extracellular segment between two transmembrane domains; the p.L91P variant may affect the quaternary structure of CPT1A by causing the loss of the side chain hydrogen bond with Thr-90, which may result in abnormal folding. p.R245Q was located in the C-terminal catalytic domain, which may affect the quaternary structure of CPT1A by eliminating the side chain hydrogen bonds with Gly-244, Gly-319, and Asp-323, possibly resulting in abnormal folding. Likewise, p.G446S was located in the C-terminal catalytic domain, and the beta turn in the secondary structure of CPT1A became a random coil, resulting in protein instability (**Figure 3**). All variants were classified as variants of unknown significance (PM2+PP3) according to the ACMG/AMP guidelines for interpretation of sequence variation.

Although the pathogenicity of these novel variants could not be confirmed, we provided the following evidence supporting an association between these variants and CPT1A deficiency: (i) the variants were inherited from the parents, who were carriers; (ii) the variants were not present or had extremely low allelic frequencies in population databases, altered the strictly conserved amino acid residues of CPT1A, and were predicted to be deleterious by different computational tools; and (iii) protein modeling analysis indicated that the variants could lead to structural damage or CPT1A dysfunction.

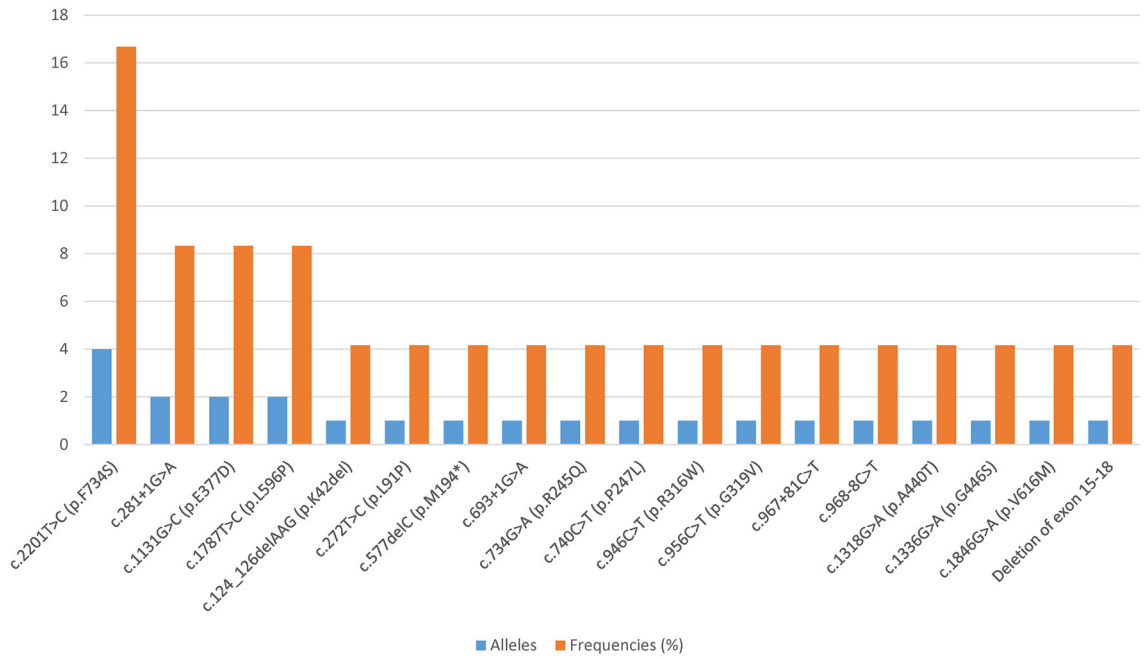

FIGURE 1 | Overview of all *CPT1A* variants found in the Chinese population.

	p.L91P	p.R245Q	p.G446S
Homo sapiens (human)	IAKINRTLETANCMSS...WWEEYIYLRGRGPLMVNSNYYA...DSYAKSLLHGRCYDRWFDKSFTF		
Pan troglodytes (chimpanzee)	IAKINRTLETANCMSS...WWEEYIYLRGRGPLMVNSNYYA...DSYAKSLLHGRCYDRWFDKSFTF		
Macaca nemestrina (macaque)	IAKINRTLETTDCMSS...WWEEYIYLRGRGPLMVNSNYYA...DSYAKSLLHGQCYDRWFDKSFTF		
Canis lupus dingo (dog)	IAKINRTLDTTGYMSS...WWEEYIYLRGRGPLMVNSNYYA...DSYAKSLLHGRCFDRWFDKSFTF		
Vulpes vulpes (fox)	IAKINRTLDTTGYMSS...WWEEYIYLRGRGPLMVNSNYYA...DSYAKSLLHGRCFDRWFDKSFTF		
Felis catus (cat)	IAKINRTLDTSGYMSS...WWEEYIYLRGRGPLMVNSNYYA...DSYAKSLLHGRCYDRWFDKSFTF		
Equus caballus (horse)	IAKINRTLDTTGYMSS...WWEEYIYLRGRGPLMVNSNYYA...DSYAKSLLHGRCSDRWFDKSFTF		
Myotis lucifugus (bat)	IAKINRTLDTTGSMSS...WWEEYIYLRGRGPLMVNSNYYA...DNYAKSLLHGRCFDRWFDKSFTF		
Bos taurus (bovine)	IAKINRTLDTTGCMSS...WWEEYIYLRGRGPLMVNSNYFA...DSYAKSLLHGRCFDRWFDKSFTF		
Loxodonta africana (elephant)	IAKINRTLDTTGYMSD...WWEEYIYLRGRGPLMVNSNYYA...DSYAKSLLHGKCFDRWFDKSFTF		
Mus musculus (mouse)	IAKINRTLDTTGRMSS....WWEEYIYLRGRGPIMVNSNYYA...DSYAKSLLHGRCFDRWFDKSITF		
Rattus norvegicus (rat)	IAKISRTLDTTGRMSS.....WWEEYIYLRGRGPLMVNSNYYA..DSYAKSLLHGRCFDRWFDKSITF		

FIGURE 2 | Multiple sequence alignment using ClustalX. Alignment of the CPT1A sequences revealed that the amino acid residues at positions 91, 245, and 446 (highlighted in box) were strictly conserved.

DISCUSSION

Except for in a few specific ethnic groups, CPT1A deficiency seems to be very rare in the general population. This study presented the biochemical, clinical, and genetic characteristics of Chinese patients with CPT1A deficiency, highlighting the value of NBS, and contributing to the body of knowledge needed for early diagnosis and timely intervention of this rare disorder.

The incidence of CPT1A deficiency varies significantly among different ethnic groups. NBS data from Germany, Australia, and the USA showed that the incidence of CPT1A deficiency was as low as 1:750,000 to 1:2,000,000 in 2010 (17). The actual incidence of CPT1A deficiency in China remains unclear. The largest nationwide cross-sectional study using a standardized questionnaire showed that the overall incidence of CPT1A deficiency in mainland China is 1:546,128 (18). We identified two Chinese patients with CPT1A deficiency through our NBS program, which indicated an estimated prevalence of 1:102,388 in the southern Chinese newborn population. This incidence is higher than that reported in previous studies, and this variation may be due to differences in ethnic backgrounds, cut-off value settings, recall criteria, diagnostic methods, and awareness of the disease. It is noteworthy that the availability of NBS is relatively limited, and there

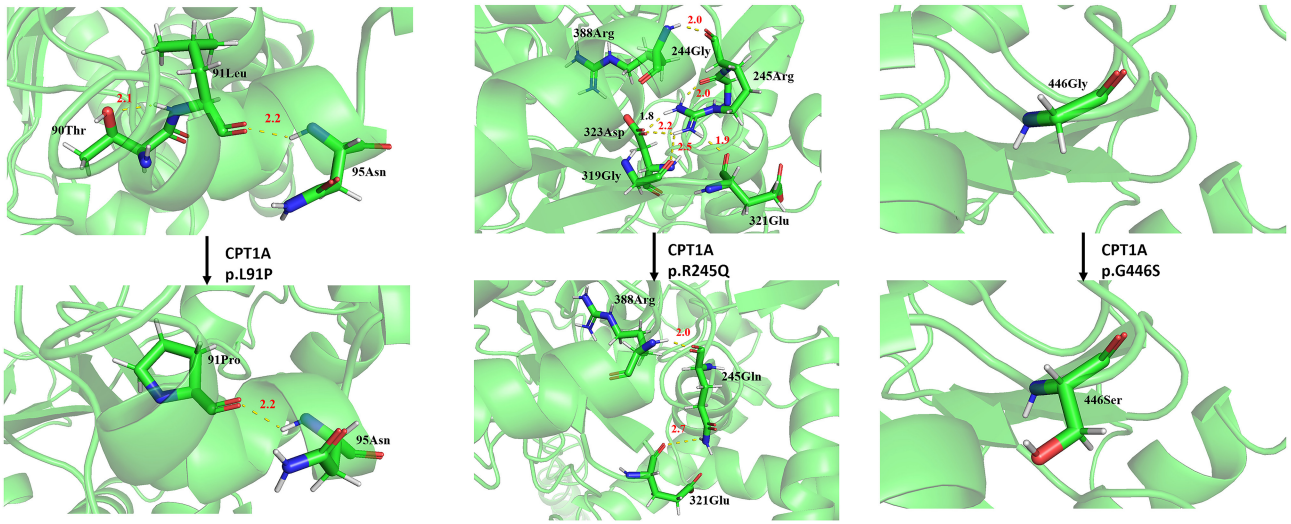

FIGURE 3 | Three-dimensional structural modeling of wild-type and mutant CPT1A proteins. The yellow dashed lines represent hydrogen bonds, and the red numbers represent the hydrogen bond distances. Leu-91 is located in the extracellular segment between two transmembrane domains. The p.L91P variant may affect the quaternary structure of CPT1A by causing the loss of the side chain hydrogen bond with Thr-90, which may result in abnormal folding of CPT1A. p.R245Q is located in the C-terminal catalytic domain, which may affect the quaternary structure of CPT1A by eliminating the side chain hydrogen bonds with Gly-244, Gly-319, and Asp-323, possibly resulting in abnormal folding. p.G446S is located in the C-terminal catalytic domain; the beta turn in the CPT1A secondary structure was changed to a random coil, resulting in an unstable protein.

may be some patients that cannot be identified by MS/MS-based NBS.

All patients showed elevated C0 levels and/or C0/(C16+C18) ratios, and one patient had a normal C0/(C16+C18) ratio. Therefore, these two screening markers do not necessarily increase at the same time, and any significant increase in one marker should be interpreted as a positive NBS result. Although patients with CPT1A deficiency can be identified by NBS, previous studies have shown that milder forms of CPT1A deficiency can be difficult to diagnose because screening markers may be normalized or only slightly increased during follow-up (19, 20). These patients may be missed or not diagnosed until the patient presents with acute metabolic decompensations. To avoid delayed diagnosis, it has been proposed that all patients with abnormal NBS results suspected of CPT1A deficiency should undergo mandatory *CPT1A* sequencing and/or enzyme analysis (20).

None of the five patients diagnosed *via* NBS had any clinical symptoms, while all of the clinically diagnosed patients presented with a variety of clinical symptoms, indicating that NBS for CPT1A deficiency is beneficial. However, we should note that patients diagnosed using NBS may also develop clinical manifestations when energy demands increase, such as during fasting or febrile illness. Therefore, dietary management and avoidance of prolonged fasting are recommended, and careful follow-up is required to ensure that the patient has a good prognosis.

CPT1A is located on chromosome 11q13.3 and contains 19 exons spanning more than 60 kb of genomic DNA. To date, at least 30 *CPT1A* pathogenic variants have been reported. Most pathogenic variants appear to be unique or identified only in a few pedigrees, except c.1436C>T (p.P479L) and c.2129G>A (p.G710E). c.1436C>T (p.P479L) was found to be highly prevalent in northern Canada, Greenland, Siberia, and the Alaska Native population (5, 7, 21). c.2129G>A (p.G710E) was recognized as a founder mutation in the Hutterite population (22, 23). Reports on Chinese patients with CPT1A deficiency are limited, and no hotspot *CPT1A* mutations have been reported to date. The cohort of Chinese patients in our study was characterized by wide allelic heterogeneity, with 18 different variants identified. c.2201T>C (p.F734S) was the most frequent variant, suggesting that c.2201T>C (p.F734S) may be a potential hotspot *CPT1A* mutation in the Chinese population. This variant has not yet been found in other populations; therefore, it could be unique to the Chinese population. The remaining variants were detected only once or twice. Three novel variants were identified, further expanding the mutational spectrum of *CPT1A*. Although computational prediction is helpful for assessing potential pathogenicity, further functional investigations are warranted to confirm the pathogenicity of these novel variants.

In conclusion, the incidence of CPT1A deficiency in Quanzhou, China, was estimated to be 1:102,388. Furthermore, the biochemical, clinical, and genetic characteristics of Chinese patients with CPT1A deficiency documented in this study may facilitate early diagnosis and intervention. Moreover, our findings demonstrated that NBS for CPT1A deficiency is beneficial. This cohort of Chinese patients was characterized by wide allelic heterogeneity. The three novel variants identified in this study expand the mutational spectrum of *CPT1A* in the Chinese population. c.2201T>C (p.F734S), the most frequent variant, may be a potential hotspot *CPT1A* mutation in this population.

DATA AVAILABILITY STATEMENT

The data presented in the study are deposited in FigShare, accession number 10.6084/m9.figshare.16920841.

ETHICS STATEMENT

The studies involving human participants were reviewed and approved by the Ethical Committee of Quanzhou Maternity and Children's Hospital. Written informed consent to participate in this study was provided by the participants' legal guardian/next of kin. Written informed consent was obtained from the individual(s), and minor(s)' legal guardian/next of kin, for the publication of any potentially identifiable images or data included in this article.

AUTHOR CONTRIBUTIONS

WZ performed the data analysis and drafted, and revised the manuscript. YC revised the manuscript. CL, WP, and QF assisted with data collection. YL designed and supervised the research study. All authors contributed to the data analysis and revised and approved the final manuscript for publication.

FUNDING

This work was funded by the Natural Science Foundation of Fujian Province (Grant Nos. 2020J01130 and 2021J01538) and the Youth Research Project in the Health System of Fujian Province (Grant No. 2020QNA083).

ACKNOWLEDGMENTS

We thank all the patients and their families for their participation. We would like to thank Editage (www.editage.cn) for English language editing.

SUPPLEMENTARY MATERIAL

The Supplementary Material for this article can be found online at: https://www.frontiersin.org/articles/10.3389/fped.2021.771922/full#supplementary-material

REFERENCES

1. Sinclair GB, Collins S, Popescu O, McFadden D, Arbour L, Vallance HD. Carnitine palmitoyltransferase I and sudden unexpected infant death in British Columbia First Nations. *Pediatrics.* (2012) 130:e1162–1169. doi: 10.1542/peds.2011-2924
2. Tsuburaya R, Sakamoto O, Arai N, Kobayashi H, Hasegawa Y, Yamaguchi S, et al. Molecular analysis of a presymptomatic case of carnitine palmitoyl transferase I (CPT I) deficiency detected by tandem mass spectrometry newborn screening in Japan. *Brain Dev.* (2010) 32:409–11. doi: 10.1016/j.braindev.2009.03.004
3. Roomets E, Polinati PP, Euro L, Eskelin PM, Paganus A, Tyni T. Carrier frequency of a common mutation of carnitine palmitoyltransferase 1A deficiency and long-term follow-up in Finland. *J Pediatr.* (2012) 160:473–9 e471. doi: 10.1016/j.jpeds.2011.08.032
4. Bougneres PF, Saudubray JM, Marsac C, Bernard O, Odievre M, Girard J. Fasting hypoglycemia resulting from hepatic carnitine palmitoyl transferase deficiency. *J Pediatr.* (1981) 98:742–6. doi: 10.1016/S0022-3476(81)80834-7
5. Collins SA, Sinclair G, McIntosh S, Bamforth F, Thompson R, Sobol I, et al. Carnitine palmitoyltransferase 1A (CPT1A) P479L prevalence in live newborns in Yukon, Northwest Territories, and Nunavut. *Mol Genet Metab.* (2010) 101:200–4. doi: 10.1016/j.ymgme.2010.07.013
6. Gessner BD, Gillingham MB, Birch S, Wood T, Koeller DM. Evidence for an association between infant mortality and a carnitine palmitoyltransferase 1A genetic variant. *Pediatrics.* (2010) 126:945–51. doi: 10.1542/peds.2010-0687
7. Gessner BD, Gillingham MB, Johnson MA, Richards CS, Lambert WE, Sesser D, et al. Prevalence and distribution of the c.1436C–>T sequence variant of carnitine palmitoyltransferase 1A among Alaska Native infants. *J Pediatr.* (2011) 158:124–9. doi: 10.1016/j.jpeds.2010.07.031
8. Clemente FJ, Cardona A, Inchley CE, Peter BM, Jacobs G, Pagani L, et al. A selective sweep on a deleterious mutation in CPT1A in arctic populations. *Am J Hum Genet.* (2014) 95:584–9. doi: 10.1016/j.ajhg.2014.09.016
9. Cui D, Hu Y, Shen D, Tang G, Zhang M, Duan J, et al. Clinical features and genetic analysis of a case with carnitine palmitoyltransferase 1A deficiency. *Chin J Med Genet.* (2017) 34:228–31. doi: 10.3760/cma.j.issn.1003-9406.2017.02.017
10. Zhang H, Yuan Y, Tang L, Tan Y, Li S. Clinical characteristics of one case of carnitine palmitoyltransferase 1A deficiency and analysis of CPT1A gene mutation. *J Pediatr Pharm.* (2019) 25:23–7. doi: 10.13407/j.cnki.jpp.1672-108X.2019.11.007
11. Gan Y, Yu F, Fang H. Novel mutation in carnitine palmitoyltransferase 1A detected through newborn screening for a presymptomatic case in China: a case report. *Ital J Pediatr.* (2021) 47:154. doi: 10.1186/s13052-021-01136-y
12. Yu Y, Shen LH, Qiu WJ, Zhang HW, Ye J, Liang LL, et al. Clinical features and gene mutations of 6 patients with carnitine palmitoyltransferase 1A deficiency. *Chin J Med Genet.* (2021) 101:1041–4. doi: 10.3760/cma.j.cn112137-20200724-02206
13. Zhou Z, Yang L, Liao H, Ning Z, Chen B, Jiang Z, et al. Analysis of a child with carnitine palmitoyl transferase 1A deficiency due to variant of CPT1A gene. *Chin J Med Genet.* (2021) 38:184–7. doi: 10.3760/cma.j.cn511374-20200309-00146
14. Lin Y, Zhang W, Chen Z, Lin C, Lin W, Fu Q, et al. Newborn screening and molecular features of patients with multiple acyl-CoA dehydrogenase deficiency in Quanzhou, China. *J Pediatr Endocrinol Metab.* (2021) 34:649–52. doi: 10.1515/jpem-2020-0694
15. Lin Y, Gao H, Lin C, Chen Y, Zhou S, Lin W, et al. Biochemical, clinical, and genetic characteristics of short/branched chain Acyl-CoA dehydrogenase deficiency in Chinese patients by newborn screening. *Front Genet.* (2019) 10:802. doi: 10.3389/fgene.2019.00802
16. Richards S, Aziz N, Bale S, Bick D, Das S, Gastier-Foster J, et al. Standards and guidelines for the interpretation of sequence variants: a joint consensus recommendation of the American College of Medical Genetics and Genomics and the Association for Molecular Pathology. *Genet Med.* (2015) 17:405–24. doi: 10.1038/gim.2015.30
17. Lindner M, Hoffmann GF, Matern D. Newborn screening for disorders of fatty-acid oxidation: experience and recommendations from an expert meeting. *J Inherit Metab Dis.* (2010) 33:521–6. doi: 10.1007/s10545-010-9076-8
18. Deng K, Zhu J, Yu E, Xiang L, Yuan X, Yao Y, et al. Incidence of inborn errors of metabolism detected by tandem mass spectrometry in China: a census of over seven million newborns between 2016 and 2017. *J Med Screen.* (2020) 2020:969141320973690. doi: 10.1177/0969141320973690
19. Borch L, Lund AM, Wibrand F, Christensen E, Sondergaard C, Gahrn B, et al. Normal levels of plasma free carnitine and acylcarnitines in follow-up samples from a presymptomatic case of carnitine palmitoyl transferase 1 (CPT1) deficiency detected through newborn screening in Denmark. *JIMD Rep.* (2012) 3:11–5. doi: 10.1007/8904_2011_35

20. Dowsett L, Lulis L, Ficicioglu C, Cuddapah S. Utility of genetic testing for confirmation of abnormal newborn screening in disorders of long-chain fatty acids: a missed case of carnitine palmitoyltransferase 1A (CPT1A) deficiency. *Int J Neonatal Screen.* (2017) 3:20010. doi: 10.3390/ijns3020010
21. Fohner AE, Garrison NA, Austin MA, Burke W. Carnitine palmitoyltransferase 1A P479L and infant death: policy implications of emerging data. *Genet Med.* (2017) 19:851–7. doi: 10.1038/gim.2016.202
22. Prasad C, Johnson JP, Bonnefont JP, Dilling LA, Innes AM, Haworth JC, et al. Hepatic carnitine palmitoyl transferase 1 (CPT1 A) deficiency in North American Hutterites (Canadian and American): evidence for a founder effect and results of a pilot study on a DNA-based newborn screening program. *Mol Genet Metab.* (2001) 73:55–63. doi: 10.1006/mgme.2001.3149
23. Prip-Buus C, Thuillier L, Abadi N, Prasad C, Dilling L, Klasing J, et al. Molecular and enzymatic characterization of a unique carnitine palmitoyltransferase 1A mutation in the Hutterite community. *Mol Genet Metab.* (2001) 73:46–54. doi: 10.1006/mgme.2001.3176

Conflict of Interest: The authors declare that the research was conducted in the absence of any commercial or financial relationships that could be construed as a potential conflict of interest.

Publisher's Note: All claims expressed in this article are solely those of the authors and do not necessarily represent those of their affiliated organizations, or those of the publisher, the editors and the reviewers. Any product that may be evaluated in this article, or claim that may be made by its manufacturer, is not guaranteed or endorsed by the publisher.

frontiers in Genetics

CASE REPORT
published: 22 November 2021
doi: 10.3389/fgene.2021.734481

Clinical and Genetic Characteristics of Chinese Children With GLUT1 Deficiency Syndrome: Case Report and Literature Review

Qingqing Hu[1,2], *Yuechi Shen*[1], *Tangfeng Su*[1], *Yan Liu*[1] *and Sanqing Xu*[1]*

[1]*Department of Pediatrics, Tongji Hospital, Tongji Medical College, Huazhong University of Science and Technology, Wuhan, China,* [2]*Department of Pediatrics, The First Affiliated Hospital of Nanchang University, Nanchang, China*

Objective: GLUT1 deficiency syndrome (GLUT1-DS) is a rare, treatable neurometabolic disorder. However, its diagnosis may be challenging due to the various and evolving phenotypes. Here we report the first Chinese familial cases with genetically confirmed GLUT1-DS and analyze the characteristics of Chinese children with GLUT1-DS from clinical, laboratory, and genetic aspects.

Methods: We reported a Chinese family with three members affected with GLUT1-DS and searched for relevant articles up to September 2020 from PubMed, WOS, CNKI, and WanFang databases. A total of 30 Chinese patients diagnosed with GLUT1-DS (three newly identified patients in one family and 27 previously reported ones) were included and analyzed in this study.

Results: The median age of onset of the 30 patients (male: 18, female: 12) was 8.5 months (range, 33 days to 10 years). Epileptic seizures were found in 25 patients, most with generalized tonic–clonic and focal ones. Movement disorders were found in 20 patients—frequently with ataxia and dystonia, developmental delay in 25 patients, and microcephaly only in six patients. The cerebrospinal fluid (CSF) analysis showed decreased CSF glucose (median: 1.63 mmol/L, range: 1.1–2.6 mmol/L) and glucose ratio of CSF to blood (median: 0.340; range: 0.215–0.484). The genetic testing performed in 28 patients revealed 27 cases with pathogenic variations of the SLC2A1 gene, including 10 missense, nine frameshift, three nonsense, three large fragment deletions, and two splice-site mutations. Most patients had a good response to the treatment of ketogenic diet or regular diet with increased frequency. Although three patients in this Chinese family carried the same pathogenic mutation c.73C > T (p.Q25X) in the SLC2A1 gene, their symptoms and responses to treatment were not exactly the same.

Conclusion: The clinical manifestations of GLUT1-DS are heterogeneous, even among family members sharing the same mutation. For children with unexplained epileptic seizures, developmental delay, and complex movement disorders, detection of low CSF glucose or SLC2A1 gene mutations is helpful for the diagnosis of GLUT1-DS. Early initiation of ketogenic diet treatment significantly improves the symptoms and prognosis of GLUT1-DS.

Keywords: GLUT1 deficiency syndrome, epilepsy, developmental delay, movement disorders, SLC2A1 gene

OPEN ACCESS

Edited by:
Huiwen Zhang,
Xinhua Hospital, China

Reviewed by:
Emanuele Micaglio,
IRCCS Policlinico San Donato, Italy
Yuwu Jiang,
Peking University First Hospital, China

***Correspondence:**
Sanqing Xu
sanqingx@163.com

Specialty section:
This article was submitted to Genetics of Common and Rare Diseases, a section of the journal Frontiers in Genetics

Received: *01 July 2021*
Accepted: *18 October 2021*
Published: *22 November 2021*

Citation:
Hu Q, Shen Y, Su T, Liu Y and Xu S (2021) Clinical and Genetic Characteristics of Chinese Children With GLUT1 Deficiency Syndrome: Case Report and Literature Review. Front. Genet. 12:734481. doi: 10.3389/fgene.2021.734481

INTRODUCTION

Glucose transporter type 1 deficiency syndrome (GLUT1-DS) is caused by impaired glucose transport through the blood–brain barrier and inherited in an autosomal dominant trait, which results from mutations of SLC2A1 gene encoding GLUT1 (Brockmann et al., 2001; Klepper et al., 2001). Autosomal recessive transmission has also been described in rare cases, whereas homozygosity showed embryonic lethality in a mouse model (Wang et al., 2006; Klepper et al., 2009; Rotstein et al., 2010). The classic phenotype is characterized by refractory infantile epilepsy, developmental delay, acquired microcephaly, and complex movement disorders, such as ataxia, dystonia, and spasticity, which was first described by De Vivo *et al.* in 1991 (De Vivo et al., 1991). Over the past few decades, its clinical spectrum has broadened to include non-classic phenotypes, such as paroxysmal exercise-induced dyskinesia and epilepsy, paroxysmal choreoathetosis with spasticity, atypical childhood absence epilepsy, and myoclonic astatic epilepsy (Wang et al., 2018). Additionally, paroxysmal non-epileptic events, including intermittent ataxia, paroxysmal eyeball movements, dysarthria, migraine, alternating hemiplegia, spastic paraparesis, and periodic confusion (De Giorgis and Veggiotti, 2013; Pearson et al., 2013; Nicita et al., 2019), and some extraneurologic features, like hemolytic anemia and cataracts, have also been described (Weber et al., 2008; Flatt et al., 2011; Bawazir et al., 2012). Despite its complex and variable clinical manifestations, GLUT1-DS can be diagnosed based on the presence of hypoglycorrhachia and pathogenic variants of SLC2A1 gene. Ketogenic diet (KD) is recognized as the most effective treatment, which can provide ketone bodies to serve as an alternative fuel for the brain, and the earlier it is used, the better the prognosis will be (Kass et al., 2016).

In 2008, Bao *et al*. diagnosed a Chinese GLUT1-DS patient for the first time in mainland China and then reported three Chinese GLUT1-DS ones in 2012 (Liu et al., 2012). However, most (90%) detected SCL2A1 gene mutations are sporadic and *de novo*, whereas familial cases are rare (Pearson et al., 2013). Here we reported a Chinese family with three members affected with genetically confirmed GLUT1-DS and evaluated the efficacy of KD. Meanwhile, we analyzed and summarized the clinical and genetic characteristics of GLUT1-DS in the newly identified and previously reported Chinese GLUT1-DS cases.

PATIENTS AND METHODS

Case Presentation

The clinical data and blood and cerebrospinal fluid (CSF) samples of three GLUT1-DS patients from one Chinese family were collected at the pediatric neurology clinics of Tongji Hospital. The study was approved by the Medical Ethics Committee of Tongji Hospital, Tongji Medical College, Huazhong University of Science and Technology. Informed consent was obtained from the patients and their parents.

Patient 1

The proband was a 6-year-old girl born to non-consanguineous parents. The pregnancy and the delivery were normal. She began to speak and walk independently at the age of 19 months and had a normal head circumference. The seizures occurred at the age of 8 months and 1 year, respectively, presenting with eyes rolling involuntarily and lips cyanosis, but there were no seizures in the next 2 years. Until the age of 4 years, her symptoms evolved into dystonia, majorly with the head backward, stiffness of the right lower limbs, and hallux dorsal flexion. Occasionally, her right arm was rotated inward and could not be flexed, accompanied by crying and shaking of the whole body. At the early stage, these symptoms were mild, with a frequency of three to eight times per month, each lasting about 1 to 2 min. The electroencephalogram (EEG) showed sharp waves and sharp slow waves in the right central temporal and left central region with a normal background during wake and sleep. Oral oxcarbazepine was then administered, but the attacks were not controlled completely. Since the age of 5 years, the frequency and duration of the attacks increased, ranging from once every 2 to 3 days to twice to thrice a day and lasting up to half an hour each time. Additionally, she experienced frequent paroxysmal hypokinesia with low muscle tone, which were relieved after resting. Nervous system physical examination was performed during the interictal period, and there was no abnormal muscle tension or strength and no positive ataxia signs, while the Assessment of the Child Development Scale indicated that her development was lagging behind mildly. The metabolic screening and other blood examinations were normal. KD was introduced along with oral oxcarbazepine when she was 5 years old, and it was tolerated well during the follow-up. Up to now, she has been free of these symptoms for nearly a year. The EEG returned to normal after initiating KD for 2 months.

Patient 2

The older brother of the proband was a 9-year-old boy without microcephaly. He started speaking after more than 12 months and still walked unsteadily at the age of 2 years and easily fell down. He also had paroxysmal hypokinesia which occurred about once to twice a month and lasted 1–5 min each time. At 3 years old, he had binocular gaze in a daze with clear consciousness, similar to an atypical absence seizure. His physical examination was unremarkable, and the developmental assessment showed that his development was lagging behind mildly as well. His brain magnetic resonance imaging (MRI), video EEGs, serum biochemistry values, and metabolic screening results were all normal. Considering the possible diagnosis of paroxysmal events related to epilepsy, sodium valproate (VPA) was added. He displayed some responses to VPA, with the symptoms alleviated only partly. Then, he received CSF analysis and gene panel sequencing, which indicated hypoglycorrhachia (CSF glucose: 2.6 mmol/L; CSF/blood glucose ratio: 0.481) and a pathogenic mutation in the SLC2A1 gene c.73C > T (p.Q25X). All these results clarified the final diagnosis of "GLUT1-DS," but his family did not pay attention to it further. His symptoms worsened at the age of 6 years when VPA was discontinued by his

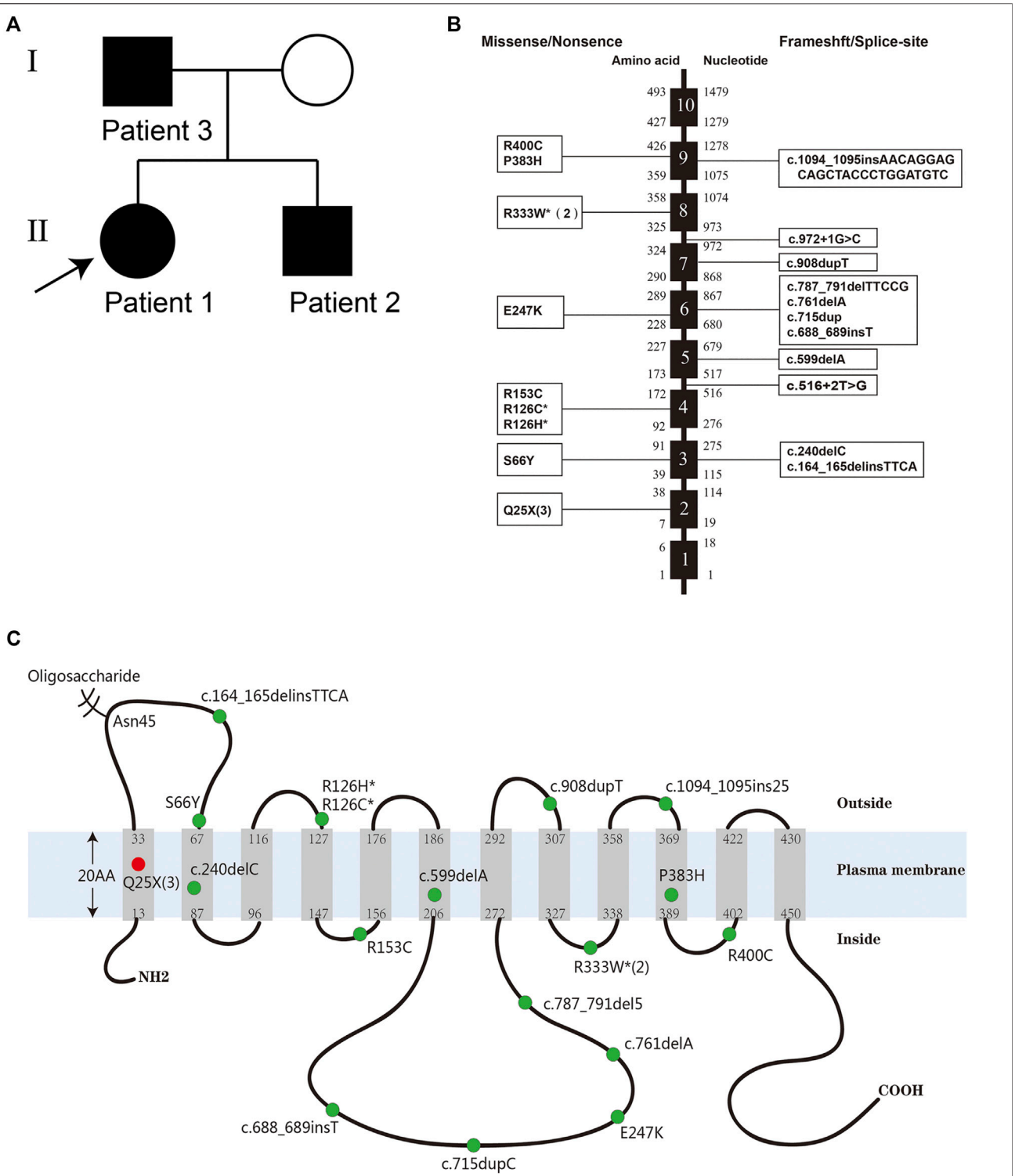

FIGURE 1 | (A) The pedigree of the reported family with GLUT1-DS caused by a nonsense mutation c.73C > T (p.Q25X) in SLC2A1 gene. **(B)** Distribution of the reported mutations of SLC2A1 gene. The black boxes represent exons. The numbers to the left and the right of the intron–exon boundaries represent amino acid residues and nucleotides, respectively. The three large fragment deletion mutations and one missense mutation with limited information are not listed. **(C)** The conformational model of GLUT1 and the location of the reported mutations of the SLC2A1 gene. The three large fragment deletions and two splice-site mutations are not listed. The red dot represents a novel mutation c.73C > T (p.Gln25*) found in the familial cases. Some numbers between brackets represent the total number of patients identified with the mutation. Mutation hotspots are represented with an asterisk.

parents, accompanied with an inability to speak or speaking vaguely—also called dysarthria and attacks of hallux-dorsiflexion, which lasted for a few minutes each time and were relieved spontaneously. Therefore, KD was introduced, and his symptoms remitted within 1 month. Up to now, he could go to school normally.

Patient 3

The father of patients 1 and 2, now at 31 years old, began to experience paroxysmal hypokinesia and could not move or walk for up to 10 min every time since he was 10 years old, without typical epileptic seizures. Surprisingly, although without any therapy, his symptom disappeared about 2 years ago. All these data were obtained from his description but no adult nervous physical examinations have been conducted.

Family History

The pedigree is shown in **Figure 1A**. The uncle of patient 3 had similar attacks of movement disorder, but his information was incomplete and unavailable.

Genetic Analyses and *In Silico* Analyses

Whole-exome sequencing was performed in the proband (patient 1), and it revealed the pathogenic mutation c.73C > T (p.Q25X) in the SLC2A1 gene, which was identical to that of patient 2. The mutation was confirmed by Sanger sequencing in their parents and verified to be inherited from their father (patient 3). The nonsense variant was predicted by PVS1 as pathogenic based on the guidelines of the American College of Medical Genetics and Genomics.

The heterozygous substitution c.73C > T (p.Q25X) is a novel nonsense mutation in exon 2 that has not been previously reported, which is predicted to cause a premature termination at position 25 and the deletion of 467 amino acids (**Figures 1B,C**). The truncated protein contains only less than one of the wild type 12 transmembrane domains and easily degrades in the cell. A previous study has shown that, when the last 37 carboxyl-terminal amino acids of GLUT1 were lost, the truncated proteins would abolish transport activity completely (Oka et al., 1990).

Systematic Review

We searched literatures about Chinese case reports of GLUT1-DS in PubMed, WOS, CNKI, and WanFang databases (until September 2020). Patients who were described more than once in the literatures were included only one time. Based on the systematic review, 15 articles describing 27 Chinese patients with GLUT1-DS were found (Fung et al., 2011; Liu et al., 2012; Ye et al., 2012; Liu et al., 2013; Li et al., 2014; Yu and Long, 2015; Duan et al., 2016; Zhang et al., 2017; Ji et al., 2018; Liang et al., 2019; Wang et al., 2019; Wei et al., 2019; Zha et al., 2019; Pei et al., 2020; Wang et al., 2020). Thus, together with the three newly identified familial cases, a total of 30 Chinese patients diagnosed with GLUT1-DS were included in this study.

RESULTS

Among the 30 patients, there were 18 males and 12 females. The median age of onset was 8.5 months (range, 33 days to 10 years). Epileptic seizures were reported in 25 patients (83.3%), presenting as the first symptom in 23 patients (76.7%) during infancy. The seizures were of mixed types, including 11 cases of generalized tonic–clonic (GTC) (36.7%), nine cases of focal (30%), four cases of tonic (13.3%), three cases of absence (10%), two cases of atonic (6.7%), one case of spasm (3.3%), one case of myoclonic–atonic (3.3%), and one case of febrile seizures (3.3%). Most seizures were resistant to antiseizure medications (ASMs), such as phenobarbital, valproic acid, lamotrigine, levetiracetam, and oxcarbazepine. Movement disorders were reported in 20 patients (66.7%), including ataxia in 15 cases (50.0%), dystonia in 14 cases (46.7%), gait disturbance in eight cases (26.7%), dysarthria in seven cases (23.3%), paroxysmal hypokinesia in three cases (10.0%), tremor in two cases (6.7%), paroxysmal limb paralysis in two cases (6.7%), and paroxysmal eye movement disorder in two cases (6.7%). Developmental delay was observed in 25 patients (83.3%), and microcephaly was found only in six patients (20%). The clinical characteristics of 30 Chinese patients with GLUT1-DS are summarized in **Table 1**.

A fasting lumber puncture was performed in 24 patients, but only 17 patients reported definite values of CSF analysis, with low CSF glucose at 1.1–2.6 mmol/L (median, 1.63 mmol/L) and low CSF/blood glucose ratio of 0.215–0.484 (median, 0.340).

EEG was performed in 28 of 30 patients, showing generalized or focal epileptiform discharges or background slowing in 19 cases. No abnormalities were found in the remaining nine cases. Brain MRI was performed in 25 patients. Only nine cases exhibited abnormalities, such as mild brain atrophy, bilateral ventricle enlargement, hypomyelination, abnormal signals in the bilateral frontal cortex, widening of the bilateral frontotemporal sulci, and cerebral dysplasia.

Genetic testing was performed in 28 patients. Except for one patient who was negative for SLC2A1 gene mutation, 27 patients carried pathogenic mutations in the SLC2A1 gene, including 10 with missense, nine with frameshift, three with nonsense, three with large fragment deletion, and two with splice-site mutations (**Table 2**).

Twenty-three patients were treated with KD, 21 of whom became free from seizures and movement disorders. Two cases gave up KD treatment for intolerance, and their symptoms were not improved. Besides this, four patients were given a regular diet with increased frequency or advised to eat candy, three of whom had a significant improvement in their outcomes. The other three patients refused any treatment for their mild symptoms or were still counseled for KD treatment.

TABLE 1 | Clinical characteristics of 30 Chinese patients with GLUT1-DS identified from 2008 to 2020.

Pt	Sex/ age at onset	Seizure type	MD	DD	MC	CSF glucose (mmol/L)	CSF/ blood glucose ratio	EEG	Brain MRI/CT	Genetic testing	Treatment (response)	Ref
1	M/ 18m	Spasm#	Ataxia, dystonia	+	+	1.80	0.382	-	-	+	KD (+)	Fung et al. (2011)
2	F/8m	Absence#	Ataxia	+	-	1.90	0.387	-	-	+	Counseling for MAD	Fung et al. (2011)
3	M/2m	GTCS#	-	+	-	1.10	0.215	δ activity	-	N/A	KD (+)	Ye et al. (2012)
4	M/ 41d	Focal#, tonic	-	+	-	low	Low	Epileptiform discharge	Mild brain atrophy	+	KD (+)	Liu et al. (2013)
5	M/ 60d	Focal#	-	+	-	low	Low	-	-	+	KD (+)	Liu et al. (2013)
6	M/ 33d	Focal#, tonic	Gait disturbance, ataxia	+	-	low	Low	-	Bilateral ventricle plump	+	Increased frequency of regular diet (+)	Liu et al. (2013)
7	F/1y	-	Ataxia#, dysarthria, gait disturbance, dystonia	+	-	1.63	0.402	-	Mild hypomyelination	+	KD (intolerance)	Liu et al. (2012)
8	M/ 5y9m	-	Gait disturbance #, ataxia#, dystonia	-	-	2.40	0.484	Epileptiform discharge	-	+	Increased frequency of regular diet (+)	Liu et al. (2012)
9	F/2y	Focal	Gait disturbance #, ataxia#, dystonia	+	+	1.74	0.375	-	-	+	Increased frequency of regular diet (+)	Liu et al. (2012)
10	F/6m	GTCS#	Dystonia	+	+	1.60	0.240	Background slowing	N/A	-	KD (intolerance)	Li et al. (2014)
11	F/73d	Focal#	-	+	-	2.10	0.340	Epileptiform discharge, background slowing	N/A	+	Increased frequency of regular diet (+-); KD is planned	Li et al. (2014)
12	M/2m	GTCS#	Ataxia	+	-	1.50	0.319	Background slowing	-	+	KD (+)	Yu and Long, (2015)
13	M/9m	GTCS#	Ataxia	-	+	1.87	0.368	Epileptiform discharge	-	+	N/A	Duan et al. (2016)
14	F/ 1y6m	-	Dystonia#, ataxia#, gait disturbance	+	+	N/A	N/A	N/A	White matter dysplasia	+	KD (+)	Zhang et al. (2017)
15	F/ 11m	Tonic#, Atonic	Ataxia, dystonia, dysarthria, tremor, paroxysmal limb paralysis	+	-	low	Low	Epileptiform discharge	-	+	KD (+)	Ji et al. (2018)
16	M/ 15m	GTCS#, Atonic, Focal	Ataxia, dystonia, dysarthria, paroxysmal limb paralysis and eye movement disorders	+	-	low	Low	Epileptiform discharge	Abnormal signals in bilateral frontal cortex	+	KD (+)	Ji et al. (2018)
17	M/2m	GTCS#	Ataxia, dystonia, dysarthria, tremor, paroxysmal eye movement disorders	+	-	low	Low	Epileptiform discharge	Widened bilateral frontotemporal sulci	+	KD (+)	Ji et al. (2018)
18	F/6m	GTCS#	Ataxia, dystonia, dysarthria	+	-	low	Low	Few atypical sharp waves	-	+	KD (+)	Ji et al. (2018)
19	M/2m	Focal#, GTCS	-	+	+,-	1.22	0.312	Epileptiform discharge	-	+	KD (+)	Wang et al. (2019)
20	F/ 2y7m	FS#, Absence	-	-	-	1.62	0.337	Epileptiform discharge	-	+	KD (+)	Liang et al. (2019)

(Continued on following page)

TABLE 1 | (*Continued*) Clinical characteristics of 30 Chinese patients with GLUT1-DS identified from 2008 to 2020.

Pt	Sex/ age at onset	Seizure type	MD	DD	MC	CSF glucose (mmol/L)	CSF/ blood glucose ratio	EEG	Brain MRI/CT	Genetic testing	Treatment (response)	Ref
21	M/ 3y7m	-	Ataxia, dystonia, gait disturbance dysarthria	+#	-	N/A	N/A	-	-	+	KD (+)	Liang et al. (2019)
22	F/ 1y3m	GTCS#	-	+	-	N/A	N/A	Epileptiform discharge	Cerebral dysplasia	+	KD (+)	Liang et al. (2019)
23	M/1y	MAE#	Gait disturbance	+	-	N/A	N/A	Epileptiform discharge	N/A	+	KD (+)	Wei et al. (2019)
24	M/ 45d	GTCS#	-	+	-	1.33	0.246	-	-	+	KD (+)	Zha et al. (2019)
25	F/65d	GTCS#	Ataxia, dystonia	+	-	1.43	0.332	Background slowing	Hypomyelination	N/A	KD (+)	Zha et al. (2019)
26	M/ 6y8m	Focal#	-	-	-	1.83	0.373	Borderline	Arachnoid cyst, hippocampal sclerosis	+	KD (+)	Pei et al. (2020)
27	M/2m	Tonic #	-	+	-	1.38	0.238	Epileptiform discharge	-	+	KD (+)	Wang et al. (2020)
28	F/8m	Focal#	Dystonia, paroxysmal hypokinesia	+	-	N/A	N/A	Epileptiform discharge	N/A	+	KD (+)	This study
29	M/2y	Absence	Gait disturbance #, paroxysmal hypokinesia #, dystonia, dysarthria	+	-	2.60	0.481	-	-	+	KD (+)	This study
30	M/10y	-	Paroxysmal hypokinesia #	-	-	N/A	N/A	N/A	N/A	+	N/A	This study

Pt, patient; F, female; M, male; m, months; y, years; d, days; MD, movement disorder; DD, developmental delay; MC, microcephaly; GTCS, generalized tonic–clonic seizure; FS, febrile seizures; MAE, myoclonic–atonic epilepsy; CSF, cerebrospinal fluid; KD, ketogenic diet; MAD, modified Atkins diet; N/A, not available; +, positive; -, negative; #, initial symptoms.

DISCUSSION

Glucose, the most essential energy source for brain metabolism, enters into the brain facilitated by GLUT1. The cerebral metabolic rate for glucose was low at birth and then increased rapidly to reach adult level by 2 years old. At about 3 to 4 years old, it reaches a peak that exceeds adult level by over two folds, keeps up until 9 years of age, and then gradually decreases to adult rate again by the age of 20 years (Chugani et al., 1987; Chugani, 1998). Consequently, the seizures generally occur at 1–6 months after birth as the most common initial symptom of GLUT1-DS and gradually reduce in adolescence, whereas these rarely appear during the neonatal period, but cyanotic or apnea episodes and paroxysmal eyeball movements—named aberrant gaze saccades—may occur before seizures in infancy (Pearson et al., 2017), which are easily ignored or misdiagnosed as focal seizures. Among the 30 patients in our study, the earliest onset age was 33 days, and the median age was 8.5 months. About 76.7% of the patients presented epileptic seizures as the first symptom.

Approximately 90% of GLUT1-DS patients have seizures of various types, including GTC, absence, focal, myoclonic, atonic, tonic, and spasm seizures, in which GTC and absence seizures are the most common (Pong et al., 2012). Although seizures are often resistant to ASMs, some of which even inhibit the GLUT1 function *in vitro*, such as phenobarbital, valproate, chloral hydrate, and diazepam (Klepper et al., 1999; Klepper et al., 2003; Wong et al., 2005), there are still about 8% of patients who respond positively to them (Pong et al., 2012). In this study, 83.3% of the 30 patients had epileptic seizures, and the seizure types in some patients evolved with age, with GTC (36.7%) and focal (30%) seizures mostly observed. Some patients achieved partial relief of seizures and motor disorders by taking ASMs, such as oxcarbazepine and levetiracetam. However, the epileptic seizures in such GLUT1-DS patients are not closely related to the epileptiform discharges on EEG. Our study showed that one patient without seizures was found to be with epileptiform discharges, while seven cases with seizures had normal EEG findings.

TABLE 2 | Twenty-four different mutations of the SLC2A1 gene in 27 Chinese patients with GLUT1-DS.

Mutation	Pt.	Exon	Nucleotide	Location	Mutation origin
Missense					
R333W	2, 22	8	c. 997C > T	Cytoplasmic loop 8–9	*De novo*
E247K	5	6	c.741G > A	Cytoplasmic loop 6–7	*De novo*
P383H	8	9	c.1148C > A	TMD10	*De novo*
R400C	9	9	c.1198C > T	Cytoplasmic loop 10–11	*De novo*
N/A	14#	8	N/A	N/A	*De novo*
R126C	16	4	376G > A	Extracellular loop 3–4	*De novo*
R126H	17	4	377G > A	Extracellular loop 3–4	*De novo*
S66Y	19	3	197C > A	Extracellular loop 1–2	*De novo*
R153C	20	4	457C > T	Cytoplasmic loop 4–5	*De novo*
Nonsense					
Q25X	28–30	2	73C > T	TMD1	Paternal
Frameshift					
c.240delC	1	2	240delC	TMD2	N/A
c.599delA	6	5	599delA	TMD6	*De novo*
c.761delA	7	6	761delA	Cytoplasmic loop 6–7	N/A
c.787_791del5	15	6	787_791del TTCCG	Cytoplasmic loop 6–7	*De novo*
c.688_689insT	18	6	688_689insT	Cytoplasmic loop 6–7	*De novo*
c.715dupC	21	6	715dupC	Cytoplasmic loop 6–7	*De novo*
c.1094_1095ins25	23	9	1094_1095insAACAGGAGC AGCTACCCTGGATGTC	Extracellular loop 9–10	*De novo*
c.908dupT	26	7	908dupT	Extracellular loop 7–8	N/A
c.164_165delinsTTCA	27	3	164_165delinsTTCA	Extracellular loop 1–2	*De novo*
Large fragment deletion					
Large fragment deletion	4	2	exon 2 large fragment deletion	-	*De novo*
c.350_385del	13	4	350_385del	-	*De novo*
Large fragment deletion	24#	N/A	chr1:43392702–43409002	-	*De novo*
Splice site		Intron			
c.972+1G > C	11	7	972+1G > C	-	N/A
c.516+2T > G	12	4	516+2T > G	-	*De novo*

Two patients (Pt. 14 and Pt. 24) only showed limited information of mutations. One patient (Pt. 10) negative for SLC2A1 gene mutation and two (Pt. 3 and Pt. 25) without available mutation data were not presented here.

Compared with epileptic seizures, movement disorders are more common in older children and tend to replace seizures over the years (Leen et al., 2014). In this study, 66.7% of the 30 patients had movement disorders, with ataxia (50.0%), dystonia (46.7%), gait disturbance (26.7%), and dysarthria (23.3%) being more commonly observed.

Since infancy, the developing brain of GLUT1-DS patients is unable to obtain enough energy for its growth, leading to cerebral dysfunction and limited head growth. The majority of patients with GLUT1-DS have experienced some degree of cognitive impairment, ranging from mild learning disability to severe intellectual impairment. In this study, developmental delay was observed in 83.3% of the 30 patients, while microcephaly was not a key sign, only observed in 20% of patients. Furthermore, one patient with microcephaly had no developmental delay, indicating that microcephaly was not always accompanied by developmental delay.

The laboratory hallmark for GLUT1-DS is low glucose of the CSF (hypoglycorrhachia) when normoglycemic. Generally, fasting CSF glucose values are less than 3.3 mmol/L (60 mg/dl). In the majority (>90%) of cases, the values are less than 2.2 mmol/L (40 mg/dl). Another less reliable biomarker is the glucose ratio of CSF to blood below 0.45 (De Vivo and Wang, 2008; Yang et al., 2011; Klepper, 2012; Leen et al., 2013), but normal CSF glucose has also been reported in some patients with milder phenotypes. In addition, the CSF lactate level from normal to low (<1.4 mmol/L) can help differentiate GLUT1-DS from other causes of hypoglycorrhachia, such as meningitis, encephalitis, subarachnoidal haemorrhage, and some metabolic disorders, in which the CSF lactate level is elevated (>2.0 mmol/L) (Chow, 2005). Leen et al. (2013) suggested that it was unlikely to diagnose GLUT1-DS if the CSF lactate was increased. The CSF glucose and CSF/blood glucose ratio were low in this study, ranging 1.1–2.6 mmol/L (median 1.63 mmol/L) and 0.215–0.484 (median 0.340), respectively, which was consistent with that described above.

To date, SLC2A1 is recognized as the only gene associated with GLUT1-DS mapped to the short arm of chromosome 1 (1p34.2), with a length of about 35 kb and containing 10 exons (Shows et al., 1987; Fukumoto et al., 1988). Its coded protein GLUT1 is a transmembrane glycoprotein and composed of 492 amino acids. It has 12 transmembrane domains that span the plasma membrane in an α-helical structure, forming a pore for the transport of glucose and other substrates, and is mainly distributed on brain endothelial cells, astrocytes, and erythrocytes (Mueckler et al., 1985). Since the first elucidation of its genetic–pathogenic roles (Seidner et al., 1998), more than 200 SLC2A1 gene mutations have been described, including missense, nonsense, frameshift, splice-site, and large fragment deletion mutations. Several mutation hotspots within the SLC2A1 gene have been identified, such as Asn34, Gly91, Ser113, Arg126, Arg153, Arg264, Thr295, and Arg333 (Leen et al., 2010).

However, about 5–10% of GLUT1-DS cases were reported with absence of mutations in the SLC2A1 gene (Yang et al., 2011; Klepper, 2013). In our study, there was one case with a negative SLC2A1 gene mutation as well. Therefore, some studies have suggested that GLUT1-DS may have undetectable variants in the non-coding regions or downstream of the DNA that could affect posttranscriptional modifications, such as mRNA splicing, protein assembly, folding, transportation, intracellular storage, and activation (Klepper and Leiendecker, 2007).

Furthermore, the phenotypes and symptom severity of GLUT1 patients with the same mutations were heterogeneous even among affected family members sharing the same mutation, indicating that secondary genes (such as PURA gene) and other modifying proteins might be involved in glucose transport or that DNA variant regulatory elements of the wild-type allele may modulate the expression level of GLUT1 (Leen et al., 2010; Mayorga et al., 2018). Mayorga et al. (2018) reported a patient with a PURA gene mutation that had marked hypoglycorrhachia, overlapping the clinical findings with GLUT1-DS, though no variants were found on the SLC2A1 gene. By western blot assays, they confirmed a significantly reduced expression of GLUT1 in the peripheral blood cells of the patient compared to controls. Based on the known functions of PURA as a transcriptional and translational regulator, they proposed GLUT1 as a new PURA target, and mutations in PURA can decrease GLUT1 expression.

Though familial cases were usually correlated with milder manifestations compared to sporadic *de novo* cases (De Giorgis et al., 2015), attention should be paid to prenatal genetic counseling in familial cases because of phenotypic heterogeneity—even if a patient has very few and mild symptoms, and it is possible that offspring with the same mutation will be severely affected. Herein the familial cases in this study, who carried a nonsense mutation c.73C > T (p.Gln25*) and inherited in an autosomal dominant manner, presented mild to moderate clinical phenotypes with overlapping but variable symptoms. The clinical manifestations of the father of the proband were mild, with only episodic hypokinesia but no intelligence or language disorder, which might be related to the late onset of the disease, while the phenotypes of the proband and her brother were moderate, including three main symptoms, and even evolved with age.

KD is the gold standard treatment for GLUT1-DS, which should be started as early as possible and maintained at least until adolescence to meet the increased energy demand of the developing brain (Klepper, 2012; Kass et al., 2016). In our study, most patients were free of seizures and movement disorders after initiation of KD, and intelligence development and the head circumference of some patients recovered to normal levels. The other three patients treated with a regular diet of increased frequency also showed an improvement that might be classified as "carbohydrate-responsive" phenotype.

In conclusion, the diagnosis of GLUT1-DS is challenging due to its clinical heterogeneity. When children presented with unexplained epileptic seizures, developmental delay, and complicated movement disorder, GLUT1-DS should be suspected and a fasting lumbar puncture or genetic testing is recommended. Once the diagnosis of GLUT1-DS is confirmed, KD should be administered earlier and timely in order to gain a better prognosis.

DATA AVAILABILITY STATEMENT

The datasets for this article are not publicly available due to concerns regarding participant/patient anonymity. Requests to access the datasets should be directed to the corresponding author.

ETHICS STATEMENT

The studies involving human participants were reviewed and approved by the Medical Ethics Committee of Tongji Hospital, Tongji Medical College, Huazhong University of Science and Technology. Written informed consent to participate in this study was provided by the legal guardian/next-of-kin of the participant. Written informed consent was obtained from the individual(s) and minor(s) legal guardian/next-of-kin for the publication of any potentially identifiable images or data included in this article.

AUTHOR CONTRIBUTIONS

QH drafted the manuscript and analyzed the data. YS checked the data. TS and YL revised the manuscript. SX performed critical revision of the whole work and edited the final manuscript. All authors have read and approved the final manuscript.

ACKNOWLEDGMENTS

We would like to thank the patients and their families for their support of our research.

REFERENCES

Bawazir, W. M., Gevers, E. F., Flatt, J. F., Ang, A. L., Jacobs, B., Oren, C., et al. (2012). An Infant with Pseudohyperkalemia, Hemolysis, and Seizures: Cation-Leaky GLUT1-Deficiency Syndrome Due to aSLC2A1Mutation. *J. Clin. Endocrinol. Metab.* 97, E987–E993. doi:10.1210/jc.2012-1399

Brockmann, K., Wang, D., Korenke, C. G., Von Moers, A., Ho, Y.-Y., Pascual, J. M., et al. (2001). Autosomal Dominant Glut-1 Deficiency Syndrome and Familial Epilepsy. *Ann. Neurol.* 50, 476–485. doi:10.1002/ana.1222

Chow, S. L. (2005). The Significance of Elevated Csf Lactate. *Arch. Dis. Child.* 90, 1188–1189. doi:10.1136/adc.2005.075317

Chugani, H. T. (1998). A Critical Period of Brain Development: Studies of Cerebral Glucose Utilization with Pet. *Prev. Med.* 27, 184–188. doi:10.1006/pmed.1998.0274

Chugani, H. T., Phelps, M. E., and Mazziotta, J. C. (1987). Positron Emission Tomography Study of Human Brain Functional Development. *Ann. Neurol.* 22, 487–497. doi:10.1002/ana.410220408

De Giorgis, V., Teutonico, F., Cereda, C., Balottin, U., Bianchi, M., Giordano, L., et al. (2015). Sporadic and Familial Glut1ds Italian Patients: a Wide Clinical Variability. *Seizure* 24, 28–32. doi:10.1016/j.seizure.2014.11.009

De Giorgis, V., and Veggiotti, P. (2013). Glut1 Deficiency Syndrome 2013: Current State of the Art. *Seizure* 22, 803–811. doi:10.1016/j.seizure.2013.07.003

De Vivo, D. C., Trifiletti, R. R., Jacobson, R. I., Ronen, G. M., Behmand, R. A., and Harik, S. I. (1991). Defective Glucose Transport across the Blood-Brain Barrier as a Cause of Persistent Hypoglycorrhachia, Seizures, and Developmental Delay. *N. Engl. J. Med.* 325, 703–709. doi:10.1056/NEJM199109053251006

De Vivo, D. C., and Wang, D. (2008). Glut1 Deficiency: Csf Glucose. How Low Is Too Low. *Revue Neurologique* 164, 877–880. doi:10.1016/j.neurol.2008.10.001

Duan, L., Wang, H., Sun, Y., Yang, Y., and Zhou, L. (2016). The Clinical Feature of Glucose Transporter 1 Deficiency Syndrome and Literature Review(in Chinese). *Chin. Pediatr. Emerg. Med.* 23, 337–341.

Flatt, J. F., Guizouarn, H., Burton, N. M., Borgese, F., Tomlinson, R. J., Forsyth, R. J., et al. (2011). Stomatin-deficient Cryohydrocytosis Results from Mutations in Slc2a1: a Novel Form of Glut1 Deficiency Syndrome. *Blood* 118, 5267–5277. doi:10.1182/blood-2010-12-326645

Fukumoto, H., Seino, S., Imura, H., Seino, Y., and Bell, G. I. (1988). Characterization and Expression of Human Hepg2/erythrocyte Glucose-Transporter Gene. *Diabetes* 37, 657–661. doi:10.2337/diab.37.5.657

Fung, E. L.-w., Ho, Y. Y., Hui, J., Wong, J. H., Ng, T.-B., Fong, N.-Y. F., et al. (2011). First Report of Glut1 Deficiency Syndrome in Chinese Patients with Novel and Hot Spot Mutations in Slc2a1 Gene. *Brain Develop.* 33, 170–173. doi:10.1016/j.braindev.2010.03.009

Ji, X. N., Xu, C. J., Gao, Z. J., Chen, S. H., Xu, K. M., and Chen, Q. (2018). Glucose Transporter 1 Deficiency Syndrome: Features of Movement Disorders, Diagnosis and Treatment. *Zhongguo Dang Dai Er Ke Za Zhi* 20, 209–213.

Kass, H. R., Winesett, S. P., Bessone, S. K., Turner, Z., and Kossoff, E. H. (2016). Use of Dietary Therapies Amongst Patients with Glut1 Deficiency Syndrome. *Seizure* 35, 83–87. doi:10.1016/j.seizure.2016.01.011

Klepper, J. (2013). Absence of Slc2a1 Mutations Does Not Exclude Glut1 Deficiency Syndrome. *Neuropediatrics* 44, 235–236. doi:10.1055/s-0033-1336015

Klepper, J., Fischbarg, J., Vera, J. C., Wang, D., and De Vivo, D. C. (1999). Glut1-deficiency: Barbiturates Potentiate Haploinsufficiency *In Vitro*. *Pediatr. Res.* 46, 677. doi:10.1203/00006450-199912000-00006

Klepper, J., Flörcken, A., Fischbarg, J., and Voit, T. (2003). Effects of Anticonvulsants on Glut1-Mediated Glucose Transport in Glut1 Deficiency Syndrome *In Vitro*. *Eur. J. Pediatr.* 162, 84–89. doi:10.1007/s00431-002-1112-8

Klepper, J. (2012). Glut1 Deficiency Syndrome in Clinical Practice. *Epilepsy Res.* 100, 272–277. doi:10.1016/j.eplepsyres.2011.02.007

Klepper, J., and Leiendecker, B. (2007). GLUT1 Deficiency Syndrome - 2007 Update. *Dev. Med. Child. Neurol.* 49, 707–716. doi:10.1111/j.1469-8749.2007.00707.x

Klepper, J., Scheffer, H., Elsaid, M. F., Kamsteeg, E.-J., Leferink, M., and Ben-Omran, T. (2009). Autosomal Recessive Inheritance of Glut1 Deficiency Syndrome. *Neuropediatrics* 40, 207–210. doi:10.1055/s-0030-1248264

Klepper, J., Willemsen, M., Verrips, A., Guertsen, E., Herrmann, R., Kutzick, C., et al. (2001). Autosomal Dominant Transmission of Glut1 Deficiency. *Hum. Mol. Genet.* 10, 63–68. doi:10.1093/hmg/10.1.63

Leen, W. G., Klepper, J., Verbeek, M. M., Leferink, M., Hofste, T., van Engelen, B. G., et al. (2010). Glucose Transporter-1 Deficiency Syndrome: the Expanding Clinical and Genetic Spectrum of a Treatable Disorder. *Brain* 133, 655–670. doi:10.1093/brain/awp336

Leen, W. G., Taher, M., Verbeek, M. M., Kamsteeg, E. J., van de Warrenburg, B. P., and Willemsen, M. A. (2014). Glut1 Deficiency Syndrome into Adulthood: a Follow-Up Study. *J. Neurol.* 261, 589–599. doi:10.1007/s00415-014-7240-z

Leen, W. G., Wevers, R. A., Kamsteeg, E.-J., Scheffer, H., Verbeek, M. M., and Willemsen, M. A. (2013). Cerebrospinal Fluid Analysis in the Workup of GLUT1 Deficiency Syndrome. *Jama Neurol.* 70, 1440–1444. doi:10.1001/jamaneurol.2013.3090

Li, X., Chaolumen, Q., Wang, J., Fu, J., Zhang, X., Duo, H., et al. (2014). Two Cases of Glucose Transporter Type 1 Deficiency Syndrome (in Chinese). *Chin. J. Appl. Clin. Pediatr.* 29, 1593–1594.

Liang, C., Wang, L., and Guo, H. (2019). Three Cases Report of Glucose Transporter 1 Deficiency Syndrome and Literature Review (in Chinese). *J. Southeast University(Medical Sci. Edition)* 38, 865–868.

Liu, Y., Bao, X., Wang, D., Fu, N., Zhang, X., Cao, G., et al. (2012). Allelic Variations of Glut-1 Deficiency Syndrome: the Chinese Experience. *Pediatr. Neurol.* 47, 30–34. doi:10.1016/j.pediatrneurol.2012.04.010

Liu, Y. Y., Bao, X. H., Wang, S., Fu, N., Liu, X. Y., Song, F. Y., et al. (2013). Clinical and Genetic Characteristics of Glucose Transporter Type 1 Deficiency Syndrome. *Zhonghua Er Ke Za Zhi* 51, 443–447.

Mayorga, L., Gamboni, B., Mampel, A., and Roqué, M. (2018). A Frame-Shift Deletion in the Pura Gene Associates with a New Clinical Finding: Hypoglycorrhachia. Is Glut1 a New Pura Target. *Mol. Genet. Metab.* 123, 331–336. doi:10.1016/j.ymgme.2017.12.436

Mueckler, M., Caruso, C., Baldwin, S. A., Panico, M., Blench, I., Morris, H. R., et al. (1985). Sequence and Structure of a Human Glucose Transporter. *Science* 229, 941–945. doi:10.1126/science.3839598

Nicita, F., Schirinzi, T., Stregapede, F., Vasco, G., Bertini, E., and Travaglini, L. (2019). Slc2a1 Mutations Are a Rare Cause of Pediatric-Onset Hereditary Spastic Paraplegia. *Eur. J. Paediatric Neurol.* 23, 329–332. doi:10.1016/j.ejpn.2018.12.004

Oka, Y., Asano, T., Shibasaki, Y., Lin, J.-L., Tsukuda, K., Katagiri, H., et al. (1990). C-terminal Truncated Glucose Transporter Is Locked into an Inward-Facing Form without Transport Activity. *Nature* 345, 550–553. doi:10.1038/345550a0

Pearson, T. S., Akman, C., Hinton, V. J., Engelstad, K., and De Vivo, D. C. (2013). Phenotypic Spectrum of Glucose Transporter Type 1 Deficiency Syndrome (Glut1 Ds). *Curr. Neurol. Neurosci. Rep.* 13, 342. doi:10.1007/s11910-013-0342-7

Pearson, T. S., Pons, R., Engelstad, K., Kane, S. A., Goldberg, M. E., and De Vivo, D. C. (2017). Paroxysmal Eye-Head Movements in Glut1 Deficiency Syndrome. *Neurology* 88, 1666–1673. doi:10.1212/WNL.0000000000003867

Pei, P., Ai, R., Liu, W., Cheng, S., and Zhang, W. (2020). A Case Report of Glucose Transporter 1 Deficiency Syndrome in Children(in Chinese). *J. Epileptology Electroneurophysiology* 29, 113–115.

Pong, A. W., Geary, B. R., Engelstad, K. M., Natarajan, A., Yang, H., and De Vivo, D. C. (2012). Glucose Transporter Type I Deficiency Syndrome: Epilepsy Phenotypes and Outcomes. *Epilepsia* 53, 1503–1510. doi:10.1111/j.1528-1167.2012.03592.x

Rotstein, M., Engelstad, K., Yang, H., Wang, D., Levy, B., Chung, W. K., et al. (2010). Glut1 Deficiency: Inheritance Pattern Determined by Haploinsufficiency. *Ann. Neurol.* 68, 955–958. doi:10.1002/ana.22088

Seidner, G., Alvarez, M. G., Yeh, J.-I., O'Driscoll, K. R., Klepper, J., Stump, T. S., et al. (1998). Glut-1 Deficiency Syndrome Caused by Haploinsufficiency of the Blood-Brain Barrier Hexose Carrier. *Nat. Genet.* 18, 188–191. doi:10.1038/ng0298-188

Shows, T. B., Eddy, R. L., Byers, M. G., Fukushima, Y., Dehaven, C. R., Murray, J. C., et al. (1987). Polymorphic Human Glucose Transporter Gene (GLUT) Is on Chromosome 1p31.3->p35. *Diabetes* 36, 546–549. doi:10.2337/diab.36.4.546

Wang, D., Pascual, J. M., and De Vivo, D. (2018). Glucose Transporter Type 1 Deficiency Syndrome.

Wang, D., Pascual, J. M., Yang, H., Engelstad, K., Mao, X., Cheng, J., et al. (2006). A Mouse Model for Glut-1 Haploinsufficiency. *Hum. Mol. Genet.* 15, 1169–1179. doi:10.1093/hmg/ddl032

Wang, H., Zhang, J., and Luo, Q. (2019). A Case of Glucose Transporter 1 Deficiency Syndrome(in Chinese). *Chin. J. Child Health Care* 27, 1039–1040.

Wang, Y., Hua, Y., Jing, M., and Tang, H. (2020). A Case Report of Glucose Transporter 1 Deficiency Syndrome(in Chinese). *Tianjin Med. J.* 48, 777–779. doi:10.1177/0300060520911269

Weber, Y. G., Storch, A., Wuttke, T. V., Brockmann, K., Kempfle, J., Maljevic, S., et al. (2008). Glut1 Mutations Are a Cause of Paroxysmal Exertion-Induced Dyskinesias and Induce Hemolytic Anemia by a Cation Leak. *J. Clin. Invest.* 118, 2157–2168. doi:10.1172/JCI34438

Wei, Z., Wang, L., and Deng, Y. (2019). Treatment of Myoclonic-Atonic Epilepsy Caused by Slc2a1 De Novo Mutation with Ketogenic Diet. *Medicine* 98, e15428. doi:10.1097/MD.0000000000015428

Wong, H. Y., Chu, T. S., Lai, J. C., Fung, K. P., Fok, T. F., Fujii, T., et al. (2005). Sodium Valproate Inhibits Glucose Transport and Exacerbates Glut1-Deficiency *In Vitro*. *J. Cel. Biochem.* 96, 775–785. doi:10.1002/jcb.20555

Yang, H., Wang, D., Engelstad, K., Bagay, L., Wei, Y., Rotstein, M., et al. (2011). Glut1 Deficiency Syndrome and Erythrocyte Glucose Uptake Assay. *Ann. Neurol.* 70, 996–1005. doi:10.1002/ana.22640

Ye, X., Zhao, Z., and Yang, B. (2012). To Report One Case of Glucose Transporter Type 1 Deficiency Syndrome and Literature Review(in Chinese). *Chin. J. Birth Health Hered.* 20, 124–126.

Yu, B., and Long, Y. (2015). Analysis of Misdiagnosis of Glucose Transporter Type 1 Deficiency Syndrome (in Chinese). *Clin. Misdiagnosis Mistherapy* 28, 54–55.

Zha, J., Huang, Z., Xie, J., Yi, Z., Yu, X., Chen, Y., et al. (2019). Clinical Observation of 2 Cases of Glucose Transporter Type 1 Deficiency Syndrome in a Family (in Chinese). *Jiangxi Med. J.* 54, 1077–1079.

Zhang, D., Guo, H., and Liu, S. (2017). Glucose Transporter 1 Deficiency Syndrome Misdiagnosed as Cerebral Palsy: a Case Report and Literature Review (in Chinese). *Chin. Manipulation Rehabil. Med.* 8, 50–51.

Conflict of Interest: The authors declare that the research was conducted in the absence of any commercial or financial relationships that could be construed as a potential conflict of interest.

frontiers in Pediatrics

ORIGINAL RESEARCH
published: 25 November 2021
doi: 10.3389/fped.2021.751895

Combined Malonic and Methylmalonic Aciduria Due to *ACSF3* Variants Results in Benign Clinical Course in Three Chinese Patients

Ping Wang[1,2†], *Jianbo Shu*[1,2†], *Chunyu Gu*[1,2,3†], *Xiaoli Yu*[4], *Jie Zheng*[1,2], *Chunhua Zhang*[5] *and Chunquan Cai*[1,2,6*]

[1] Tianjin Pediatric Research Institute, Tianjin Children's Hospital (Tianjin University Children's Hospital), Tianjin, China, [2] Tianjin Key Laboratory of Birth Defects for Prevention and Treatment, Tianjin, China, [3] Graduate College of Tianjin Medical University, Tianjin, China, [4] Department of Neurology, Tianjin Children's Hospital (Tianjin University Children's Hospital), Tianjin, China, [5] Matsumoto Institute of Life Science (MILS) International, Yokohama, Japan, [6] Department of Neurosurgery, Tianjin Children's Hospital (Tianjin University Children's Hospital), Tianjin, China

OPEN ACCESS

Edited by:
Hui Xiong,
Peking University First Hospital, China

Reviewed by:
Chunhua Zeng,
Guangzhou Women and Children's Medical Center, China
Leonardo Caporali,
IRCCS Institute of Neurological Sciences of Bologna (ISNB), Italy

***Correspondence:**
Chunquan Cai
cqcns6@126.com

[†]*These authors have contributed equally to this work*

Specialty section:
This article was submitted to Genetics of Common and Rare Diseases, a section of the journal Frontiers in Pediatrics

Received: *02 August 2021*
Accepted: *19 October 2021*
Published: *25 November 2021*

Citation:
Wang P, Shu J, Gu C, Yu X, Zheng J, Zhang C and Cai C (2021) Combined Malonic and Methylmalonic Aciduria Due to ACSF3 Variants Results in Benign Clinical Course in Three Chinese Patients. Front. Pediatr. 9:751895. doi: 10.3389/fped.2021.751895

Introduction: Combined malonic and methylmalonic aciduria (CMAMMA) is a rare metabolic disease caused by biallelic variants in *ACSF3* gene. The clinical phenotype is highly heterogeneous in this disorder, ranging from asymptomatic to severe symptoms. No cases with CMAMMA were reported in China.

Materials and Methods: In this study, three Chinese pediatric patients were diagnosed with CMAMMA unexpectedly while being treated for other ailments. To better characterize CMAMMA in a Chinese population, we made a multidimensional analysis with detailed clinical phenotype, semi-quantitative detection of urine organic acid, and analysis of *ACSF3* gene variants.

Results: The clinical presentation of these patients is quite different; their main complaints were anemia, jaundice, or abnormal urine test, respectively. They showed no symptoms of the classic methylmalonic academia, but urine organic acid analysis showed elevated malonic acid and methylmalonic acid in all the patients repeatedly. Variants were found at four sites in *ACSF3* gene. Patient 1 carried the compound heterogeneous variant c.689G>A (p.Trp230*)/c.1456G>A (p.Ala486Thr). A compound heterozygous variant c.473C>T (p.Pro158Leu)/c.1456G>A (p.Ala486Thr) was identified in patient 2. Patient 3 harbored a novel homozygous variant c.1447A>G (p.Lys483Glu).

Conclusions: Three Chinese patients were diagnosed with CMAMMA caused by *ACSF3* variants. Their clinical course revealed that CMAMMA can be a benign condition that does not affect individual growth and development, but severe clinical phenotype may appear when other triggers exist. This study systematically elaborates CMAMMA in a Chinese population for the first time, broadens the spectrum of gene variant, and provides a strong basis for the etiological study of this disorder.

Keywords: combined malonic and methylmalonic aciduria, *ACSF3* gene, benign condition, Chinese population, novel variant

INTRODUCTION

Methylmalonic academia (MMAemia) is a common inborn error of metabolism characterized by abnormal accumulation of methylmalonic acid in body fluids, resulting in many serious clinical manifestations. MMAemia is mainly caused by the defect of methylmalonyl-CoA mutase (MUT) or its coenzyme cobalamin (Cbl) (1). Combined malonic and methylmalonic aciduria (CMAMMA) is a rare atypical form of MMAemia featured with increased concentrations of malonic acid (MA) and methylmalonic acid (MMA) in urine (2). CMAMMA is caused by biallelic variants in the AcylCoA synthetase family member 3 (*ACSF3*, OMIM:614265) gene. *ACSF3* encodes a mitochondrial acyl-CoA synthetase, which is essential for the synthesis of malonyl-CoA as well as methylmalonyl-CoA (3). Patients who carried *ACSF3* gene variants excrete more MMA than MA in reported cases, which make them distinct from the patients with classical MMAemia (4).

The gene of *ACSF3* is located on chromosome 16q24.3. It consists of 11 exons and encodes a 576-amino-acid protein with the first 83 residues representing the predicted mitochondrial transit peptide (4). To date, more than 50 patients worldwide have been reported to have CMAMMA caused by homozygous or compound heterozygous variants in *ACSF3*, including missense, nonsense, deletion, frameshift, and splice site variants. The clinical presentation of CMAMMA is quite controversial. Signs and symptoms reported so far are involved in neurological abnormalities in adults and infection induced encephalopathy in pediatric patients. Nevertheless, asymptomatic patients with normal outcomes strongly suggest that CMAMMA can be a benign state (2, 4–9). No case of the disease has been reported in China so far.

In this study, we summarized the clinical course, urine organic acid screening results, and analysis of *ACSF3* gene variants in three Chinese patients with CMAMMA diagnosed in our hospital. We identified four variants inherited from the parents separately, among which c.1447A>G (p.K483E) is a novel variant. Based on the present study and literature review, we speculate that the CMAMMA is a benign state when other triggers are absent in Chinese population.

MATERIALS AND METHODS

Participants

Three patients at the age of 11 days to 8 months were diagnosed as CMAMMA in Tianjin Children's Hospital in China. There was no family history in these patients. The informed consents from guardians and the approval of the Medical Ethics Committee of Tianjin Children's Hospital were obtained.

Routine Tests and Metabolic Assay

Routine tests were conducted in three patients, such as physical examination, routine blood, urine and stool test, blood gas analysis, biochemical test, imaging examination, and etiological examination for infected patients. Semi-quantitative analysis of organic acid in urine was performed using gas chromatography–mass spectrometry (GC/MS).

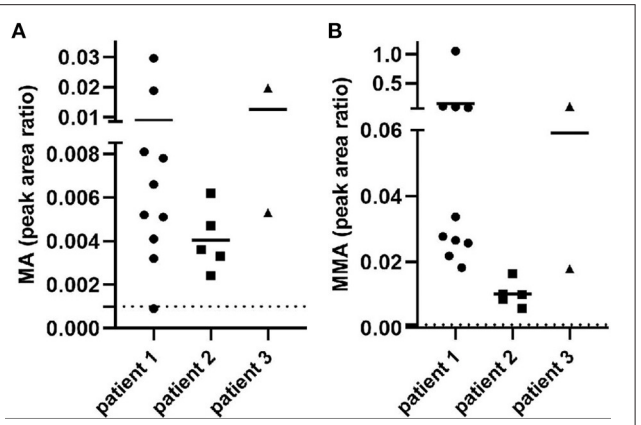

FIGURE 1 | MA and MMA excretion in urine from all the patients. The *x*-axis represents different patients, and the value of the *y*-axis means metabolite peak area ratio to creatinine (Cr). Dotted lines represent reference range. **(A)** Peak area ratio of MA/Cr indicated the MA excretion in patients. **(B)** Peak area ratio of MMA/Cr indicated the MMA excretion in patients.

Whole Exome Sequencing and Analysis

The peripheral blood samples were collected to extract the genomic DNA. Peripheral blood from the patients and their parents were collected. A Blood Genomic DNA Mini kit was used to extract the genomic DNA according to the manufacturer's protocol. WES was performed to detect the pathogenic gene variants. Paired-end sequencing was performed on more than 95% of the target regions, with a read length of 150 bp and an average coverage depth of 100-fold, covering all coding regions and exon–intron boundaries. The Burrows-Wheeler Aligner (BWA) software was used to align the raw data with the human reference genome hg19. Insertions, deletions, and single-nucleotide polymorphism sites (SNPs) were analyzed by the Genome Analysis Tool Kit (GATK) software. Annovar software was utilized to add the annotated information of databases such as HGMD, dbSNP, OMIM, and 1000 Genomes. Protein function was predicted by SIFT and Polyphen2 software. The filtering of the variants was performed based on the phenotype, gene frequency, variant type, inherited pattern, and bioinformatics analysis. Suspected variants were validated by Sanger sequencing.

RESULTS

Clinical Data

Patient 1 was a 3-month-old girl. She was admitted to the hospital due to pale face for 2 weeks, fever, and cough for 2 days. Detailed physical examination and laboratory tests revealed that the patient had anemia, splenomegaly, hepatomegaly, thrombocytopenia, and bronchitis. Widened interval outside the cerebrum was noted in computed tomography. These clinical features were mainly attributed to suspected Evans syndrome and viral infection. The patient is 5 years old now and shows no sign of physical or psychomotor retardation.

Patient 2 was an 11-day-old boy. He was born at term by normal delivery. He was referred to the hospital due to

TABLE 1 | Genetic and phenotypic finding of patients with CMAMMA.

Patient	Age and sex	Clinical feature	Variants			References
1	3mo, F	Anemia, splenomegaly, hepatomegaly, thrombocytopenia, and bronchitis	c.689G>A[a] (p.W230*)		c.1456G>A[b] (p.A486T)	Present study
2	11d, M	Jaundice, neonatal omphalitis, myocardial damage, testicular hydrocele, and liver function damage	c.473C>T[a] (p.P158L)		c.1456G>A[b] (p.A486T)	Present study
3	8mo, M	Urinary tract infection, pneumonia, and diarrhea	c.1447A>G[a] (p.K483E)		c.1447A>G[b] (p.K483E)	Present study
4	14y, M	Asymptomatic	c.1411C>T (p.R471W)		c.1411C>T (p.R471W)	(4)
5	4y, F	Asymptomatic	c.1075G>A (p.E359K)		c.1075G>A (p.E359K)	(4)
6	2y, M	Asymptomatic	c.1075G>A (p.E359K)		c.1075G>A (p.E359K)	(4)
7	43y, F	Ocular migraine, memoryproblems, T2 hyperintensities on brain MRI	c.1385A>C (p.K462T) c.del1394_1411 (p.Q465_G470)		c.1672C>T (p.R558W)	(2)
8	51y, M	Complex partial seizures, and memory problems	c.1567C>T (p.R523*)		c.1672C>T (p.R558W)	(2)
9	55y, F	Psychiatric symptoms, T2 hyperintensities on brain MRI	c.1075G>A (p.E359K)		c.1672C>T (p.R558W)	(2)
10	22mo, F	Seizure, encephalopathy, ketoacidosis	c.1672C>T (p.R558W)		c.1672C>T (p.R558W)	(2)
11	4y, F	Hypoglycemia, acidosis, poor weight gain, diarrhea episodes	c.1073C>T (p.T358I)		c.1412G>A (p.R471Q)	(2)
12	66y, F	Incontinence, mild memory problems	c.1411C>T (p.R471W)		c.1411C>T (p.R471W)	(2)
13	6mo, M	Failure to thrive, elevated transaminases	c.728C>T (p.P243L)		c.728C>T (p.P243L)	(2)
14	17mo, M	Psychomotor delay, microcephly, dystonia, axial hypotonia, and speech delay	c.593T>G (p.M198R)		c.593T>G (p.M198R)	(2)
15	26mo, M	Psychomotor delay, hypotonia, and loss of speech	–		–	(2)
16	6y, F	Asymptomatic until 6y, encephalopathic event upon an influenza infection	c.1075G>A (p.E359K)		c.311A>T (p.N104I)	(5)
17	5.5y, F	Asymptomatic until 5.5y, encephalopathic event upon an influenza infection	c.1075G>A (p.E359K)		c.311A>T (p.N104I)	(5)
18	2y, F	Mild developmental delay and seizure disorder	c.1672C>T (p.R558W)		c.1673G>A (p.R558Q)	(6)
19	73y,M	Late-onset neurologic syndrome, rare axonal degeneration of segmental myelin thinning.	c.634G>C (p.V212L)	c.781G>T (p.G261*)	c.854C>T (p.P285L)	(6)
20	10y, F	Significant developmental and speech delays	c.1470G>C (p.E490D)		c.1470G>C (p.E490D)	(6)
21	8mo, F	Persistent elevation of MMA	c.1239+2T>G		c.1672C>T (p.R558W)	(6)
22	3y, F	Recurrentvomiting, febrile seizures	Chr16:87441993: 89171912deletion (spanning *ACSF3*)		c.1672C>T (p.R558W)	(6)
23	n/a	Asymptomatic at 3y	c.1446_1447delCA (p.Y482*)		c.424C>T (p.Q142*)	(7)
24	n/a	Hearing loss, psychomotor delay	c.1075G>A (p.E359K)		c.1075G>A (p.E359K)	(7)

(Continued)

TABLE 1 | Continued

Patient	Age and sex	Clinical feature	variants		References
25	n/a	Seizures, dystonia	c.1075G>A (p.E359K)	c.1672C>T (p.R558W)	(7)
26	n/a	Asymptomatic at 7 m	c.820C>T (p.Q274*)	c.820C>T (p.Q274*)	(7)
27	2y, M	Hydronephrosis, several renal cysts	c.1718delT	c.1672C>T (p.R558W)	(8)
28	7y, F	None	n/a	n/a	(8)
29	6y, F	None	c.1446_1447delCA (p.Y482*)	c.1075G>A (p.E359K)	(8)
30	24y, F	None	c.1075G>A (p.E359K)	c.1470G>C (p.E490D)	(8)
31	5y, F	Growth at 3rd percentile, consistent with parental heights, allergic rhinitis, eczema	c.1239+2T>G	c.1672C>T (p.R558W)	(8)
32	2y, M	Growth at 3–15th percentile, consistent with parental heights	n/a	n/a	(8)
33	11y, M	Hypopigmented spots	n/a	n/a	(8)
34	27y, F	Recurrent urinarytract infection, hives, and endometriosis	c.1672C>T (p.R558W)	c.1672C>T (p.R558W)	(8)
35	24y, M	Hepatomegaly and bovine protein intolerance in infancy, bilateral vesicoureteral reflux	c.1075G>A (p.E359K)	c.1075G>A (p.E359K)	(8)
36	22y, F	Attention deficit hyperactivity disorder	n/a	n/a	(8)
37	20y, M	Nissen fundoplication for GERD in infancy	n/a	n/a	(8)
38	23y, F	Neonatal cutaneous lupus erythematosus	c.1553C>A (p.A518D)	c.1553C>A (p.A518D) c.473C>T (p.P158L)	(8)
39	20y, F	Slightly smaller right kidney, and migraines	n/a	n/a	(8)
40	7y, M	None	c.1075G>A (p.E359K)	c.1672C>T (p.R558W)	(8)
41	13y, M	None	c.1075G>A (p.E359K)	c.1672C>T (p.R558W)	(8)
42	6 mo, F	Severe bronchiolitis/pneumonia at 1 month, lactic acidosis, mild valvular pulmonary stenosis, height and weight 0.1–3rd percentile	c.1075G>A (p.E359K)	c.1075G>A (p.E359K)	(8)
43	7y, M	None	c.774_775del (p.W259Gfs*10)	c.1672C>T (p.R558W)	(8)
44	14y, M	Attention deficit hyperactivity disorder, dysorthography	c.1470G>C (p.E490D)	c.1081G>A (p.G361S)	(8)
45	16y, M	Eczema, scoliosis, glaucoma and cataract, mild language and fine motor delay in 1st years, corrected by school age, cyclic vomiting in adolescence with no metabolic derangement	c.1239+2T>G	c.1075G>A (p.E359K)	(8)
46	30y, F	Dehydration and metabolic acidosis in the context of severe bloody diarrhea at 4 weeks of age, otherwise healthy	c.1075G>A (p.E359K)	c.1075G>A (p.E359K)	(8)
47	19y, M	Attention deficit hyperactivity disorder	c.1411C>T (p.R471W)	c.1411C>T (p.R471W)	(8)
48	8y, F	Bilateral congenital dacryostenosisy	c.1075G>A (p.E359K)	c.1075G>A (p.E359K)	(8)

(Continued)

TABLE 1 | Continued

Patient	Age and sex	Clinical feature	variants		References
49	7y, M	None	c.1075G>A (p.E359K)	c.1075G>A (p.E359K)	(8)
50	6y, M	None	c.1075G>A (p.E359K)	c.1672C>T (p.R558W)	(8)
51	7y, M	Latent nystagmus	c.634G>A (p.V212 M)	c.1470G>C (p.E490D)	(8)
52	6y, M	Neonatal jitteriness, developmental delay, Autism, Joint hypermobility	c.1453A>C (p.S485R)	c.1453A>C (p.S485R)	(9)

mo, month; d, day; y, year; [a]variant was inherited from mother; [b]variant was inherited from father; –, no variant in coding exons or splice sites; n/a, not available.

jaundice for 7 days. Detailed physical examination showed neonatal omphalitis, myocardial damage, testicular hydrocele, and liver function damage. Laboratory tests showed that the direct bilirubin level was 17.1 μmol/L (normal: 0–5 μmol/L), and indirect bilirubin level was 184.4 μmol/L (normal: 3.4–10.3 μmol/L). These clinical manifestations were mainly caused by jaundice and infection. He is 3 years old now and attains a development milestone.

Patient 3 was an 8-month-old boy. He was born at term by cesarean section. He was admitted because of abnormal urine test for 3 months with red urine and urinary frequency. Urinary tract infection, pneumonia, and diarrhea were found in this patient. No obvious abnormality in his growth development was present. Infection factors were the main cause of his clinical presentations. He shows no sign of psychomotor retardation at the age of 5 in our recent follow-up.

Urine Analysis

GC/MS demonstrated elevated MA and MMA in all the patients repeatedly (**Figure 1**), which suggested the suspected diagnosis of MMAemia. However, the patients did not present with the clinical symptoms of classic MMAemia.

Gene Variation Analysis

All the patients were detected to carry variants in *ACSF3* gene (NM_174917.4) by WES. Patient 1 carried a compound heterozygous variant. The variant c.689G>A (p.Trp230*) was inherited from her mother and the other variant c.1456G>A (p.Ala486Thr) was inherited from her father. Besides, the compound heterozygous variant, c.473C>T (p.Pro158Leu)/c.1456G>A (p.Ala486Thr), was identified in the *ACSF3* gene in patient 2. The two heterozygous variants were inherited from the mother and father, respectively. Patient 3 harbored a homozygous variant of c.1447A>G (p.Lys483Glu) in *ACSF3* gene, which was inherited from his parents (**Table 1**). Sanger sequencing was used to confirm the variants (**Figures 2**–**4**). The homozygous variant c.1447A>G in *ACSF3* gene is a novel discovery.

DISCUSSION

CMAMMA is a rare inborn error of metabolism characterized by high excretion of MMA than MA in urine. The pathogenic gene *ACSF3* catalyzes the initial reaction in intramitochondrial fatty acid synthesis by activating MA and MMA into their respective CoA thioesters. To date, about 52 patients with 31 homozygous or compound heterozygous variants of *ACSF3* have been reported worldwide, including missense, nonsense, deletion, frameshift, and splice site variants. The locations of these variants in *ACSF3* are graphically displayed in **Figure 5**. Most of the variants are missense, mainly located at the carboxyl terminal of the protein (**Table 1**) (2, 4–9). The most common *ACSF3* variants reported so far are c.1075G>A (p.E359K) and c.1672C>T (p.R558W), which are also the most common variants in asymptomatic patients. It indicates that the two variants are more likely to have a mild effect on gene function. Patients who carried the heterozygous variant c.1470G>C (p.E490D) have mild clinical symptoms, while the homozygous variant can result in significant developmental and speech delays. In the present work, we identified four variants of the *ACSF3* gene (one nonsense and three missense mutations) in three Chinese patients from three unrelated families, among which the variant c.1447A>G (p.K483E) is novel. The heterozygous variant c.473C>T (p.P158L) has also been reported in another patient with benign clinical presentation (8).

Patients who carried *ACSF3* variants exhibit controversial clinical phenotypes. Based on the literature review we did, severe clinical manifestations are mainly reported in adults, with the most common symptoms of neurological problems and psychiatric features (2). Because of the long-term damage accumulation, older people are at high risk for neurological illness even without *ACSF3* variants. The phenotype of pediatric patients is relatively mild or even asymptomatic. Three pediatric patients diagnosed with CMAMMA due to *ACSF3* mutation were reported to be clinically asymptomatic, and they had age-appropriate development (4). A retrospective study described the course of 25 CMAMMA individuals and suggested that CMAMMA is probably a benign condition (8). Another study showed that infection factors could provoke metabolic dysregulation in pediatric patients with CMAMMA, and normal levels of development could be obtained at follow-up (5). Therefore, CMAMMA may be considered as a risk factor instead of a disease, which could lead to clinical symptoms when other influencing factors exist.

ACSF3 variants that were only reported in patients with benign manifestations include c.689G>A, c.1456G>A,

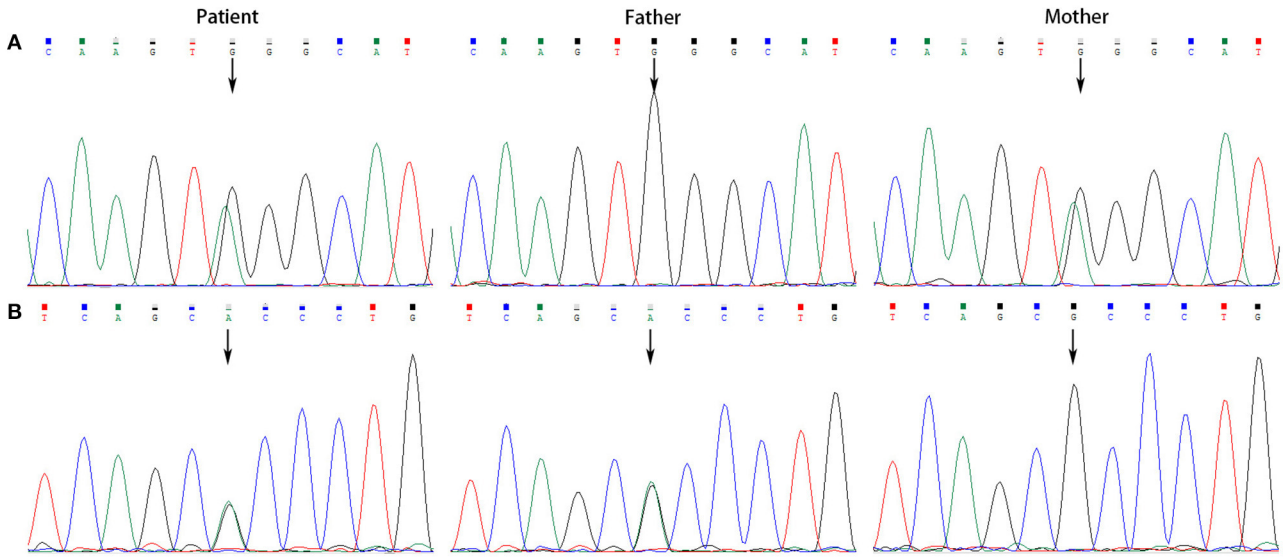

FIGURE 2 | Sanger sequencing of the genomic DNA from patient 1 and her parents. **(A)** Patient 1 carried with a heterozygous variant of c.689G>A, her father with a normal genotype, and mother with a heterozygous variant of c.689G>A. **(B)** Patient 1 carried with a heterozygous variant of c.1456G>A, her father with a heterozygous variant of c.1456G>A, and mother with a normal genotype.

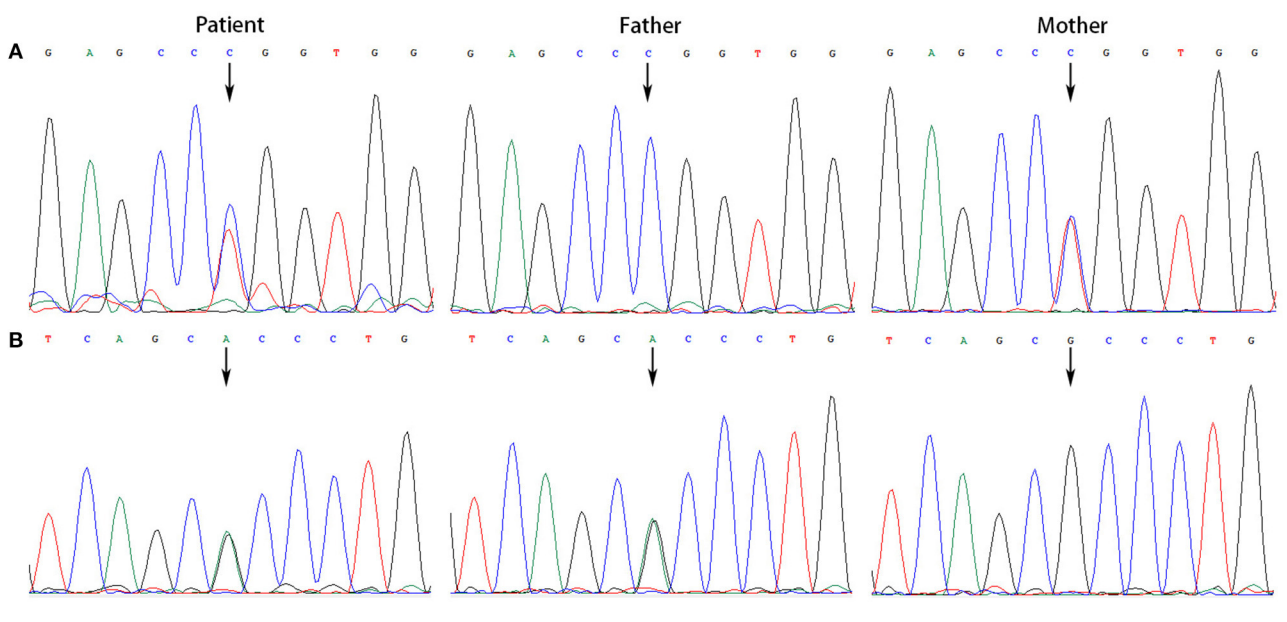

FIGURE 3 | Sanger sequencing of the genomic DNA from patient 2 and his parents. **(A)** Patient 2 with a heterozygous variant of c.473C>T, his father with a normal genotype, and mother with a heterozygous variant of c.473C>T. **(B)** Patient 2 with a heterozygous variant of c.1456G>A, his father with a heterozygous variant of c.1456G>A, and mother with a normal genotype.

c.473C>T, c.1447A>G, c.311A>T, c.1239+2T>G, c.1446_1447delCA, c.424C>T, c.820C>T, c.1553C>A, c.774_775del, and c.1081G>A. Patients carrying these variants were asymptomatic or had infection-induced symptoms that disappeared after treatment (2, 4–9). Besides, although the variant c.1456G>A has a high frequency in population, our present study showed that patients carrying this variant had repeatedly elevated biochemical phenotype without obvious clinical phenotype, which could also be observed in other inherited metabolic disease. The β-ureidopropionase deficiency patients carrying the homozygous or compound heterozygous c.977G>A variant (high prevalence in normal Japanese

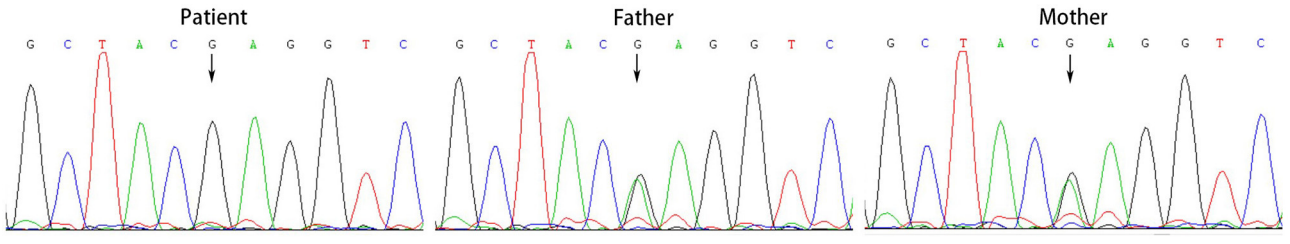

FIGURE 4 | Sanger sequencing of the genomic DNA from patient 3 and his parents. Patient 3 harbored a homozygous variant of c.1447A>G in *ACSF3* gene, both his father and mother carried this variant.

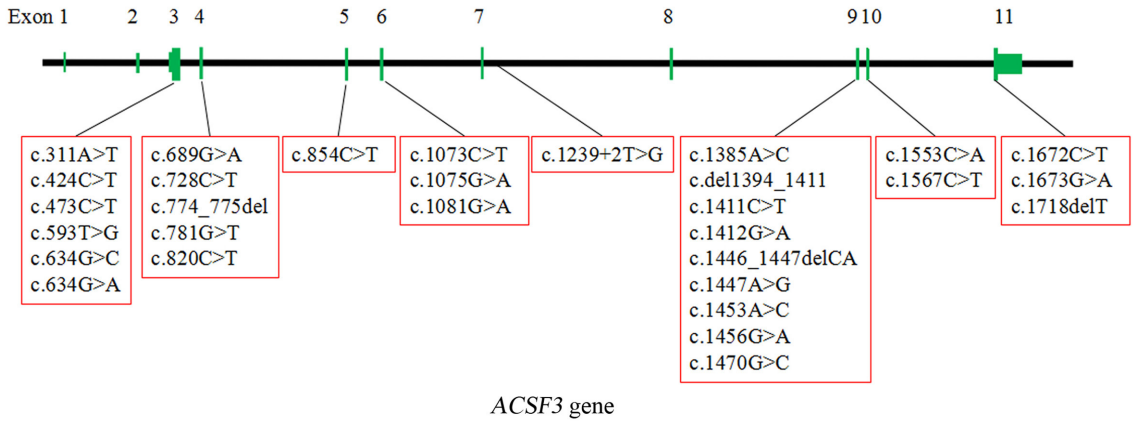

FIGURE 5 | The localization of 30 homozygous or compound heterozygous variants in *ACSF3* reported worldwide (except for a Chr16:87441993:89171912 deletion spanning *ACSF3*). The types of the variants include missense, nonsense, deletion, frameshift, and splice site variants. The most common type is missense.

population) in *UPB1* gene could be asymptomatic as well (10). We speculate that the c.1456G>A variant in *ACSF3* may act in a similar way. High frequency of c.1456G>A in population indicates that CMAMMA may not be as rare as generally considered, and this kind of variant may contribute to the benign condition in patients. Accumulations of free MA and MMA were neurotoxic *in vitro*, while the concentrations might be insufficient to produce disease in CMAMMA patients (8). Actually, we cannot completely exclude the possibility that the accumulation of metabolites is associated with the occurrence of neurological symptoms as the patients grow up, or that the people with the *ACSF3* gene variants are more genetic susceptible to neurological problems later in life. Increased dependency on β-oxidation for energy production were observed in fibroblasts from CMAMMA patients. As a result, the subsequent increased risk for hypoxia and oxidative stress may be crucial for the onset of neurological symptoms in the long run (11).

CONCLUSIONS

In conclusion, our study included three Chinese pediatric patients under the age of 4 years. Their clinical features were mainly caused by infection or other reasons. They showed no sign of physical or psychomotor retardation in our follow-up. Combined with reported cases, our study strongly suggested that the CMAMMA is a benign clinical course, especially for patients carrying certain variants. In addition, the present study had some limitations. Firstly, this study only involved the correlation analysis between genotype and phenotype. Functional verification of variants *in vitro* will help to elucidate the pathogenesis of CMAMMA, especially for the novel variant c.1447A>G (p.K483E), while functional studies were not available in this study due to the limitations of experimental condition. Secondly, a longer follow-up period is needed to better assess the growth and development of the patients.

DATA AVAILABILITY STATEMENT

The original contributions presented in the study are included in the article/supplementary material, further inquiries can be directed to the corresponding author/s.

ETHICS STATEMENT

The studies involving human participants were reviewed and approved by the Medical Ethics Committee of Tianjin Children's

Hospital. Written informed consent to participate in this study was provided by the participants' legal guardian/next of kin.

AUTHOR CONTRIBUTIONS

PW and JS conceived the concept and wrote the manuscript. CG contributed to literature review and revised the manuscript. XY provided clinical diagnosis. JZ contributed to interpretation of the results. CZ performed the analysis. CC participated in supervision of the project. All authors read and approved the final manuscript.

FUNDING

This research was supported by the National Natural Science Foundation of China (81771589), the Program of Tianjin Science and Technology Plan (18ZXDBSY00170), and the Public Health and Technology project of Tianjin (KJ20166, ZC20120).

REFERENCES

1. Baumgartner MR, Hörster F, Dionisi-Vici C, Haliloglu G, Karall D, Chapman KA, et al. Proposed guidelines for the diagnosis and management of methylmalonic and propionic acidemia. *Orphanet J Rare Dis.* (2014) 9:130. doi: 10.1186/s13023-014-0130-8
2. Sloan JL, Johnston JJ, Manoli I, Chandler RJ, Krause C, Carrillo-Carrasco N, et al. Exome sequencing identifies ACSF3 as a cause of combined malonic and methylmalonic aciduria. *Nat Genet.* (2011) 43:883–6. doi: 10.1038/ng.908
3. Bowman CE, Wolfgang MJ. Role of the malonyl-CoA synthetase ACSF3 in mitochondrial metabolism. *Adv Biol Regul.* (2019) 71:34–40. doi: 10.1016/j.jbior.2018.09.002
4. Alfares A, Nunez LD, Al-Thihli K, Mitchell J, Melançon S, Anastasio N, et al. Combined malonic and methylmalonic aciduria: exome sequencing reveals mutations in the ACSF3 gene in patients with a non-classic phenotype. *J Med Genet.* (2011) 48:602–5. doi: 10.1136/jmedgenet-2011-100230
5. de Sain-van der Velden MG, van der Ham M, Jans JJ, Visser G, Prinsen HC, Verhoeven-Duif NM, et al. A new approach for fast metabolic diagnostics in CMAMMA. *JIMD Rep.* (2016) 30:15–22. doi: 10.1007/8904_2016_531
6. Pupavac M, Tian X, Chu J, Wang G, Feng Y, Chen S, et al. Added value of next generation gene panel analysis for patients with elevated methylmalonic acid and no clinical diagnosis following functional studies of vitamin B12 metabolism. *Mol Genet Metab.* (2016) 117:363–8. doi: 10.1016/j.ymgme.2016.01.008
7. Brasil S, Leal F, Vega A, Navarrete R, Ecay MJ, Desviat LR, et al. Improving the diagnosis of cobalamin and related defects by genomic analysis, plus functional and structural assessment of novel variants. *Orphanet J Rare Dis.* (2018) 13:125. doi: 10.1186/s13023-018-0862-y
8. Levtova A, Waters PJ, Buhas D, Lévesque S, Auray-Blais C, Clarke JTR, et al. Combined malonic and methylmalonic aciduria due to ACSF3 mutations: Benign clinical course in an unselected cohort. *J Inherit Metab Dis.* (2019) 42:107–16. doi: 10.1002/jimd.12032
9. Reid ES, Papandreou A, Drury S, Boustred C, Yue WW, Wedatilake Y, et al. Advantages and pitfalls of an extended gene panel for investigating complex neurometabolic phenotypes. *Brain.* (2016) 139:2844–54. doi: 10.1093/brain/aww221
10. Nakajima Y, Meijer J, Dobritzsch D, Ito T, Meinsma R, Abeling NG, et al. Clinical, biochemical and molecular analysis of 13 Japanese patients with β-ureidopropionase deficiency demonstrates high prevalence of the c.977G > A (p.R326Q) mutation [corrected]. *J Inherit Metab Dis.* (2014) 37:801–12. doi: 10.1007/s10545-014-9682-y
11. Tucci S. Brain metabolism and neurological symptoms in combined malonic and methylmalonic aciduria. *Orphanet J Rare Dis.* (2020) 15:27. doi: 10.1186/s13023-020-1299-7

Conflict of Interest: The authors declare that the research was conducted in the absence of any commercial or financial relationships that could be construed as a potential conflict of interest.

Publisher's Note: All claims expressed in this article are solely those of the authors and do not necessarily represent those of their affiliated organizations, or those of the publisher, the editors and the reviewers. Any product that may be evaluated in this article, or claim that may be made by its manufacturer, is not guaranteed or endorsed by the publisher.

frontiers in Genetics

BRIEF RESEARCH REPORT
published: 17 December 2021
doi: 10.3389/fgene.2021.786294

Microhomology-Mediated Nonhomologous End Joining Caused Rearrangement of *EMD* and *FLNA* in Emery-Dreifuss Muscular Dystrophy

Danyu Song[1], *Xiaomei Li*[2], *Wei Wei*[3], *Xueqin Liu*[1], *Lin Wu*[4] *and Hui Xiong*[1]*

[1]Department of Pediatrics, Peking University First Hospital, Beijing, China, [2]Department of Pediatric Cardiology, The First Hospital of Tsinghua University (Beijing Huaxin Hospital), Beijing, China, [3]Beijing Kangso Medical Inspection Co., Ltd., Beijing, China, [4]Department of Cardiology, Peking University First Hospital, Beijing, China

Background: Emery–Dreifuss muscular dystrophy (EDMD) is a rare disease characterized by early joint contractures, slowly progressive muscular dystrophy, and cardiac involvement, which includes arrhythmia, dilated cardiomyopathy, hypertrophic cardiomyopathy, heart failure, and sudden death.

Methods: Clinical data of the proband and family members were collected. The next-generation sequencing technology was used to analyze the pathogenic variants and copy number variations. Polymerase chain reaction was used to sequence the breakpoints of gene locus rearrangements.

Results: Here, we report two siblings with EDMD in a family. The proband, a 17-year-old boy, manifested a dilated right heart, bradycardia, mild muscle weakness, and joint contractures. His younger brother only showed a mild bowing limitation with elevated creatine kinase. Next-generation sequencing revealed the complete deletion of *EMD* and a rearrangement in *FLNA* (exon29_48dup) in these two patients. The *EMD* deletion and partial *FLNA* duplication were accompanied by a 5 bp overlap (GTCCC) on the background of the *FLNA-EMD* inversion. These findings support the pathogenic mechanism of microhomology-mediated nonhomologous end joining.

Conclusion: We report two siblings with complete *EMD* deletion and *FLNA* duplication in a family. A microhomology-mediated nonhomologous end joining event involving *EMD* and *FLNA* acts as the underlying mechanism.

Keywords: Emery–Dreifuss muscular dystrophy, microhomology-mediated nonhomologous end joining, EMD, FLNA, right heart abnormalities

OPEN ACCESS

Edited by:
Desheng Liang,
Central South University, China

Reviewed by:
Shiwen Wu,
Chinese PLA General Hospital, China
Xiaoli Chen,
Capital Institute of Pediatrics, China

***Correspondence:**
Hui Xiong
xh_bjbj@163.com
xionghui03582@pkufh.com

Specialty section:
This article was submitted to Genetics of Common and Rare Diseases, a section of the journal Frontiers in Genetics

Received: *30 September 2021*
Accepted: *15 November 2021*
Published: *17 December 2021*

Citation:
Song D, Li X, Wei W, Liu X, Wu L and Xiong H (2021) Microhomology-Mediated Nonhomologous End Joining Caused Rearrangement of EMD and FLNA in Emery-Dreifuss Muscular Dystrophy. Front. Genet. 12:786294. doi: 10.3389/fgene.2021.786294

INTRODUCTION

Emery–Dreifuss muscular dystrophy (EDMD) is a rare inherited disease that is characterized by early joint contractures, slow-progressive muscular dystrophy, and cardiac involvement (Madej-Pilarczyk, 2018; Heller et al., 2020), including arrhythmias, cardiomyopathy, heart failure, and sudden death. In the Online Mendelian Inheritance in the Man (OMIM) database, EDMD is divided into seven phenotypes, namely, EDMD 1 to 7, based on their causative genes and inherited manner. These genes include *EMD*, *LMNA*, *SYNE1*, *SYNE2*, *FHL1*, and *TMEM43* (Heller et al., 2020). In addition, *SUN1*,

SUN2, and *TTN* can also cause EDMD (Heller et al., 2020). Among these causative genes, *EMD* and *LMNA* are the most common (Bonne and Quijano-Roy, 2013). EMD, located in Xq28, is assigned to the X-linked EDMD (also named EDMD 1). In patients with X-linked EDMD, joint contractures (elbows, Achilles tendons, and cervical spine) frequently emerge in the first decade of life, and muscle weakness (in a "humeroperoneal" pattern) usually occurs in the second decade of life. Cardiac involvement typically starts after joint contractures and muscle weakness. Here, we report two EDMD patients with an *EMD* deletion and partial *FLNA* (a neighboring gene of *EMD*) duplication in an unconsanguineous family, supporting the pathogenic mechanism of microhomology-mediated nonhomologous end joining.

MATERIALS AND METHODS

Clinical Data Collection

The research protocol (2015[916]) was reviewed and approved by the Ethics Committee of Peking University First Hospital. Written informed consent, which also included consent for the publication of medical data, was obtained from the patients and their parents.

Medical records of the patients were reviewed. Clinical and laboratory data, including age of onset, onset of recognizable symptoms, motor development, contractures, creatine kinase (CK) levels, electrocardiography (ECG), Holter, ultrasound cardiography (UCG), cardiac magnetic resonance imaging (MRI), limb muscle MRI, and muscle biopsy findings, were collected.

Variant Screening and Pathogenicity Verification

Genomic DNA of the proband, the younger brother, and their parents was extracted from leukocytes isolated from peripheral blood. A muscular disease gene panel and whole exome sequencing (WES) were successively used to detect genetic variations in the proband. Candidate variants in the probands were validated by Sanger sequencing in the family. Disease association databases and population databases, including the HGMD (HGMD: http://www.hgmd.cf.ac.uk/ac/index.php), LOVD (LOVD: http://www.dmd.nl/), ClinVar database (https://www.ncbi.nlm.nih.gov/clinvar/), 1000 Genomes (http://www.1000genomes.org/), ExAC (ExAC: http://exac.broadinstitute.org/), and gnomAD (gnomAD: http://gnomad.broadinstitute.org/) databases, were used to identify previously reported mutations and discover potential novel mutations. Predictions for the pathogenicity of missense mutations were obtained using PolyPhen-2, SIFT, and Mutation Taster. The predicted splicing mutations were tested through the Human Splicing Finder. The pathogenicity of candidate variants was classified according to the American College of Medical Genetics and Genomics and the Association for Molecular Pathology (ACMG-AMP) guidelines (Richards et al., 2015).

Next-Generation Sequencing Data Analysis for Copy Number Variation

Next-generation sequencing (NGS) data were also analyzed to detect copy number variations (CNVs) by comparing the number of sequence reads between the patient and control samples. First, the number of reads in each amplicon was counted for the patient and control samples. For the purposes of this comparison, sequencing data from at least three control samples (genomic sequencing had been performed for patients diagnosed with other diseases) were used as the reference. Subsequently, the patient/control ratios were calculated by dividing the number of patient reads in each amplicon with the average of the total reads regarding this amplicon from control samples. For the genes, including *EMD* and its neighboring gene *FLNA*, located on the X chromosome, patient/control ratios near 0.5 indicated the presence of heterozygous deletions in female patients (control samples were female). Ratios near 0 indicated deletions in male patients (control samples were male). In contrast, ratios near 1.5 indicated the presence of heterozygous duplications in female patients (control samples were female), and ratios higher than 1.75 indicated duplications in male patients (control samples were male). Polymerase chain reaction (PCR) was used to confirm the deletion of *EMD* in male patients. Statistical results were illustrated using GraphPad Prism 8 software (GraphPad Software, La Jolla, CA).

PCR for Deletion Validation and the Sequencing of Breakpoints of the CNVs

PCR and Sanger sequencing were performed to verify *EMD* deletion and to sequence the breakpoints of the CNVs. Primers were designed separately for exons 1–6 of *EMD* using Primer 5.0 (Premier Biosoft, Palo Alto, CA, United States). The two primers designed for exon 1 were Primer F 5′-ACCGCGAGA CCTTTTGCTC-3′ and Primer R 3′-GCGAGGCTCTCACCA GAGAA-5′. The two primers designed for exon 2 were Primer F 5′-CGCACGGGCCTGTAGTAGGT-3′ and Primer R 3′-GAC GAAGTCGGGTGAAGGTG-5′. The two primers designed for exon 3 were Primer F 5′-CGGCCAGGATCAACTCGTAG-3′ and Primer R 3′-TCCTAAGGCTGCTGGAGTGG-5′. The two primers designed for exon 4 were Primer F 5′-ACCTTCACC CGACTTCGTCA-3′ and Primer R 3′-TCCTGAATGGCTCTG GGTGT-5′. The two primers designed for exon 5 were Primer F 5′-GAGCCATTCAGGAGGGTGTG-3′ and Primer R 3′-GCT GAAACAGGGCGGTAGTG-5′. The two primers designed for exon 6 were Primer F 5′-TGTGGGTTCCTGGCCTCTAA-3′ and Primer R 3′- AAAAATGCGGACCCAACAAA-5′. For the breakpoints, two primers were designed for a location in exon 2 of *FLNA* (Primer F GRCh37/hg19, chrx:153599438-1535994, 5′-CACTTCAGGTGCTCGTT-3′) and exon 29 of *FLNA* (Primer R GRCh37/hg19, chrx:153585865-153585883, 3′-GGATCTCGT CACCACCGTA-5′). PCR amplifications were performed using GoldStar Taq DNA Polymerase in an Applied Biosystems Veriti Thermal Cycler (4375305, Thermo Fisher Scientific, Waltham, MA, United States). Each PCR amplification was repeated for 35 cycles (30 s at 95°C, 30 s at 60°C, and 45 s at 72°C). Before

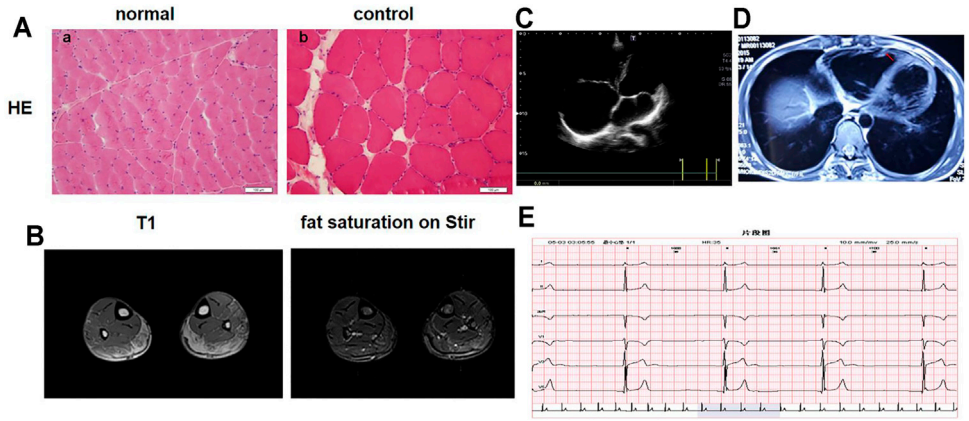

FIGURE 1 | Clinical Results. **(A)** Muscle biopsy. (a) Hematoxylin and eosin (H&E) staining of serial sections of the skeletal muscle from a normal control. (b) H&E staining of the skeletal muscle of the proband shows dystrophic changes: variability in the size of muscle fibers, fibrosis, and fat replacement. **(B)** Limb muscle MRI showed infiltration of fatty tissues in the soleus. **(C)** Echocardiography showed enlargement of the right heart. **(D)** Cardiac magnetic resonance imaging revealed an obviously enlarged right heart and evident thinning of the lateral wall of the right ventricle. The red arrows show fatty tissues in the local cardiac muscle. **(E)** Holter monitoring showed bradycardia and a junctional ectopic rhythm.

sequencing, the PCR products were analyzed by electrophoresis on a 2% agarose gel.

RESULTS

Clinical Findings of the Proband

The proband was referred to our hospital at the age of 17 due to suspected "skeletal muscle cardiomyopathy". He started to feel physical activity-related tiredness and chest distress at the age of 13. He was suspected of having "myocarditis" and was given nutritional therapy without regular follow up. At the age of 15, he visited the local hospital again due to poor exercise tolerance and chest discomfort. Subsequently, bradycardia and enlargement of the right heart were found by Holter monitoring and UCG. Due to the symptomatic right heart problem, he was suspected of having "right ventricular cardiomyopathy" and received indolapril as a treatment. At the age of 16, he presented with bilateral brachial muscle pain and aggravated chest distress. His motor and cognitive development was normal. None of his family members exhibited any clinical abnormalies. Physical examination at the age of 17 revealed a heart rate of 56 bpm, normal oxygen saturation, and no dyspnea at rest. Neurological examination showed obvious bilateral brachial and peroneal muscle atrophy, elbow contracture, a mild rigid spine, and a tight Achilles tendon with normal gait. The muscle strength grade of the upper proximal arms was IV^{+}, while that of the distal arms was V. The muscle strength grade of the proximal lower limbs was V^{-}, with a distal dorsal flexion power of IV and a plantar flexion power of V^{-}. Bilateral knee tendon reflex could not be induced. To confirm the diagnosis, laboratory tests were performed. The level of CK was 500–2,500 U/L (normal 0–200 IU/L). Skeletal muscle biopsy indicated muscular dystrophic changes (**Figure 1A**). Limb muscle MRI showed infiltration of fatty tissues, predominantly in the soleus (**Figure 1B**). UCG showed enlargement of the right heart with a left ventricular ejection fraction (LVEF) of 68% (**Figure 1C**), and the Holter monitoring showed a junctional ectopic rhythm of 36 bpm (**Figure 1E**). A cardiac MRI subsequently revealed a markedly enlarged right heart, evident thinning of the lateral wall of the right ventricle, and fatty tissues in the local cardiac muscle with LVEF of 57% (**Figure 1D**). Combining the predominant cardiac involvement, muscle weakness, and joint contractures, he was clinically diagnosed with EDMD. This was confirmed by genetic tests (listed below). Considering bradycardia and the risk of sudden cardiac death, he was referred to implant a cardiac pacemaker. In addition, he was suggested to undergo rehabilitation training with regular follow up.

Genetic Results

A muscular disease gene panel that was performed in a local hospital detected no pathogenic variation in the proband. We reanalyzed the NGS data. We did not find any pathogenic variation but found that the depth of coverage was low in the whole region of *EMD*. This suggests *EMD* deletion. The PCR results confirmed the entire deletion of *EMD* (exons 1–6) (**Figure 2A**) in the proband. Then, we needed to further detect the deleted region and breakpoints. Due to the lack of designed probes and the small size of *EMD*, we failed to analyze the deleted region by using multiplex ligation-dependent probe amplification (MLPA) and array CGH. Finally, we used the NGS data of WES combined with PCR to help verify the region of deletion. The depth of coverage was used to detect the CNV by comparing its copy number ratio between the patient and the control. The ratio was 0 in the region of *EMD*, suggesting the deletion of the entire *EMD* gene (**Figure 2B**). On the other hand, the ratios were almost all greater than 1.75 in one segment (exon 29_48) and approximately 1 in another segment (exon 2_28) of *FLNA*, a gene adjacent to *EMD*. These findings suggest partial duplication of *FLNA* corresponding to exons 29–48 (Hg19, NM_001110556, **Figure 2B**). However, due

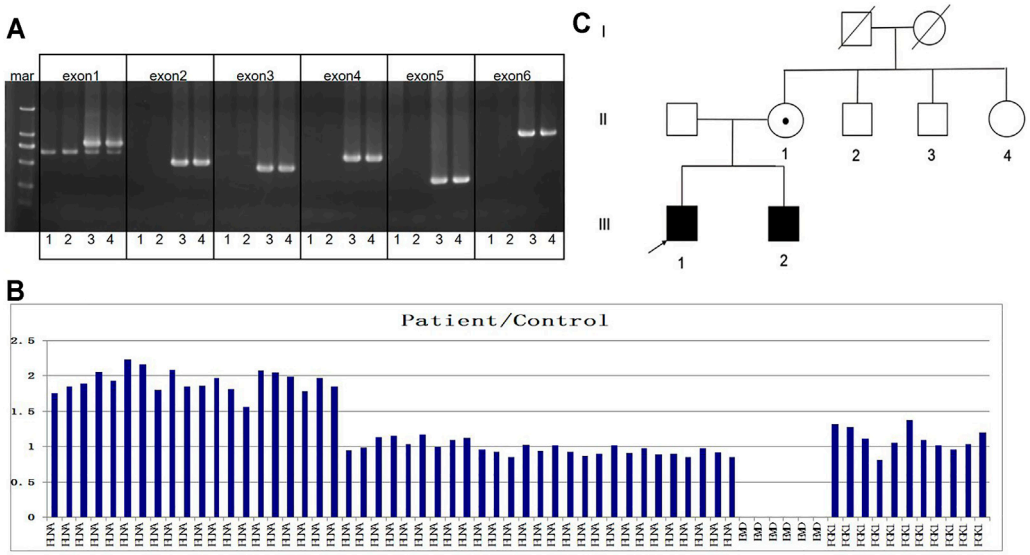

FIGURE 2 | Family pedigree and genetic results. **(A)** In the gel, numbers 1 to 4 represent the proband, his brother, his mother, and the control, respectively. The target bands of *EMD* exons 1–6 were deleted in the proband and his brother. **(B)** Column chart shows ratios between the patient and the control patients in terms of the number of reads, suggesting the deletion of exons 1–6 of *EMD* and the duplication of exons 29–48 of *FLNA* in the proband. **(C)** Family pedigree is shown.

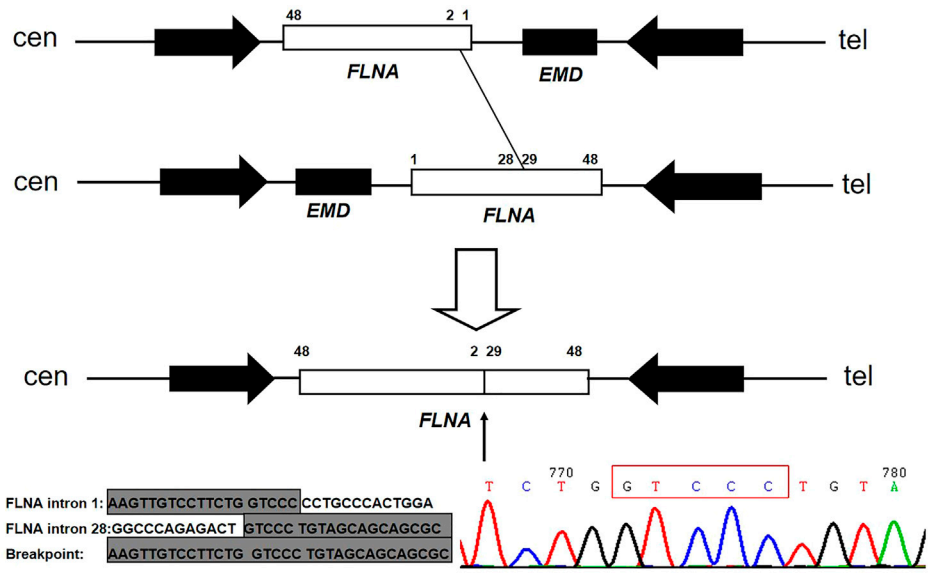

FIGURE 3 | Model of *FLNA* rearrangement and *EMD* deletion. The first allele shows the normal *FLNA-EMD* region. The second allele is a polymorphic inversion containing the entire *FLNA-EMD* region. The unshaded rectangle represents *FLNA*, whereas the shaded rectangle represents *EMD*. Two arrows point to the two large reverted repeats flanking the *FLNA-EMD* region. Between homologous X or sister chromatins, 5 bp (GTCCC) overlap between *FLNA* intron 28 and intron 1 on the background of *FLNA-EMD* inversion was confirmed.

to the lack of reads designed to cover exon 1 of *FLNA*, the WES data were lost in *FLNA* exon 1, which is a non-coding region (Patrosso et al., 1994). The whole *EMD* deletion involving partial *FLNA* duplication was similar to the genomic arrangement of the first reported EDMD case with *EMD* deletion (Small et al., 1997). Therefore, according to the case reported before (Small et al., 1997), we proposed that the genomic rearrangement in the proband may be caused by nonhomologous end joining on the background of *FLNA-EMD* inversion. Considering that the duplicated region of *FLNA* (exon 29_48) starts from exon 29, we proposed that one breakpoint in *FLNA* was located in intron 28 of *FLNA*. Besides, *FLNA* exon 2 was unaffected. Therefore, another

breakpoint in *FLNA* may occur in intron 1 of *FLNA* to the linkage region of *FLNA-EMD*. A model including the inversion of *FLNA-EMD* is shown (**Figure 3**) to explain the rearrangement of *FLNA*. To verify the breakpoints, PCR and Sanger sequencing were performed. Two primer sets were designed to be located in exon 2 of *FLNA* and exon 29 of *FLNA*. After sequencing, deletion boundaries and sequences were found. Between homologous X or sister chromatins, a microhomology-mediated nonhomologous end joining event was confirmed, accompanied by a 5 bp overlap (GTCCC) between *FLNA* intron 28 and *FLNA* intron 1 on the background of *FLNA-EMD* inversion.

Analysis of Other Family Members

The family pedigree is shown in **Figure 2C**. The family members were then evaluated. The 14-year-old younger brother complained of a mild bowing limitation. His CK level was 549 U/L. His echocardiograph and electrocardiograph revealed no problems. Their parents showed no symptoms, with normal CK and cardiac test results. After the same genetic test, the younger brother was identified as a patient with *EMD* deletion and partial *FLNA* duplication. He was followed up and given rehabilitation training regularly. The mother was confirmed as a carrier.

DISCUSSION

The proband had symptomatic right heart disease accompanied by mild muscle weakness. Due to his normal primary motor milestones, his mild elbow joint contracture and rigid spine may not have received enough attention. After a detailed physical examination, he was found to have mild muscle weakness, humeroperoneal muscle atrophy, mild elbow joint contracture, and a rigid spine. Based on his muscle weakness, high CK level, and pathological muscular dystrophic changes, the diagnosis of muscular dystrophy could be confirmed. Combining both cardiac and muscle involvement, skeletal muscle cardiomyopathy was confirmed. Given the severe cardiac involvement, humeroperoneal distributed muscle weakness, and special locations of the contractures, he was suspected to have EDMD. Finally, this diagnosis was confirmed by genetic analysis.

EMD, located in Xq28, encodes the nuclear protein emerin. The complete deletion of *EMD* in the proband caused an X-linked EDMD phenotype. The cardiac phenotype often emerges within the end of the second decade along the third decade of life in classical X-linked EDMD (Heller et al., 2020). The fact that the obvious right heart involvement started at 14 years of age is unusual. The involvement of the right side of the heart is also not a classical feature of the cardiological spectrum of X-linked EDMD. Significant right heart abnormalities and an early age of onset were features in the proband, with mild weakness and joint contractures. Regarding the mutation type, most mutations reported in *EMD* are nonsense mutations, missense mutations, frameshift mutations, or splicing mutations that cause a truncated protein. There have been five cases in which the complete deletion of *EMD* was reported (Small et al., 1997; Small and Warren, 1998; S et al., 1999), which was found in the proband.

Filamin-A is encoded by *FLNA*. It promotes orthogonal branching of actin filaments and links actin filaments to membrane glycoproteins with wide tissue expression. *FLNA* mutations can cause several severe syndromes, including periventricular nodular heterotopias, otopalatodigital syndromes, skeletal dysplasia, lung involvement, and cardiovascular abnormalities (Sankararaman et al., 2013; van der Werf et al., 2013; Deng et al., 2020; Meliota et al., 2021). In heterozygous females, the *FLNA*-related phenotype ranges from the absence of overall symptoms to severe manifestations. Male patients typically have a very severe phenotype and almost die prenatally or in the first years of life due to multisystem involvement (Sankararaman et al., 2013; van der Werf et al., 2013; Walsh et al., 2017; Cannaerts et al., 2018). This 17-year-old proband only manifested joint contractures and cardiac and muscle involvement without other systems involved. He had relatively minor symptoms compared with typical *FLNA*-related male patients. In addition, the duplication of exons 29–48 of *FLNA* did not influence the primary *FLNA* exons 2–48 (containing the entire open reading frame). Given this consideration, we predicted that *FLNA* is not a causative gene in this patient, despite the *FLNA* rearrangement.

For the molecular pathogenic mechanism, a microhomology-mediated nonhomologous end joining event involving *EMD* and *FLNA*, with a 5 bp overlap (GTCCC), acts as the underlying mechanism. Microhomology-mediated end joining is an error-prone repair mechanism for DNA double-strand breaks. It needs longer microhomology (more than 2 bp) and is independent of Ku70/Ku80, which is distinct from classic nonhomologous end joining (Kent et al., 2015; Sinha et al., 2016; Wang and Xu, 2017; Seol et al., 2018). The *FLNA-EMD* inversion in Xq28 is a common inversion mediated by inverted repeats (Small et al., 1997). The presence of an inversion of the *FLNA-EMD* region among X chromosomes was frequent (33% in females and 11% in males) (Small et al., 1997). The first reported case of EDMD with *EMD* deletion and a partial duplication of *FLNA* revealed an emerin-associated Alu with 2 bp of overlap between one pair of misaligned and inverted repeats (Small et al., 1997). Two other reported cases revealed 2 bp of overlap in *FLNA* (Small and Warren, 1998). They are all different from the proband reported here.

In conclusion, we reported two cases of EDMD with a complete *EMD* deletion and partial *FLNA* duplication. A microhomology-mediated nonhomologous end joining event involving *EMD* and *FLNA* acts as the underlying mechanism.

DATA AVAILABILITY STATEMENT

The datasets presented in this study can be found in online repositories. The names of the repository/repositories and accession number(s) can be found below: https://www.ncbi.nlm.nih.gov/genbank/, MH151792.

ETHICS STATEMENT

The research protocol was approved by the Ethics Committee of Peking University First Hospital.

AUTHOR CONTRIBUTIONS

HX: project lead and designing the project. DS, XL, WW, and LW: data collection. DS and HX: data analysis. DS: manuscript writing. XL and LW: manuscript editing. All authors contributed to the article and approved the submitted version.

REFERENCES

Bonne, G., and Quijano-Roy, S. (2013). Emery-dreifuss Muscular Dystrophy, Laminopathies, and Other Nuclear Envelopathies. *Handb Clin. Neurol.* 113, 1367–1376. doi:10.1016/B978-0-444-59565-2.00007-1

Cannaerts, E., Shukla, A., Hasanhodzic, M., Alaerts, M., Schepers, D., Van Laer, L., et al. (2018). FLNA Mutations in Surviving Males Presenting with Connective Tissue Findings: Two New Case Reports and Review of the Literature. *BMC Med. Genet.* 19 (1), 140. doi:10.1186/s12881-018-0655-0

Deng, X., Li, S., Qiu, Q., Jin, B., Yan, M., Hu, Y., et al. (2020). Where the Congenital Heart Disease Meets the Pulmonary Arterial Hypertension, FLNA Matters: a Case Report and Literature Review. *BMC Pediatr.* 20 (1), 504. doi:10.1186/s12887-020-02393-2

Fujimoto, S., Ishikawa, T., Saito, M., Wada, Y., Wada, I., Arahata, K., et al. (1999). Early Onset of X-Linked Emery-Dreifuss Muscular Dystrophy in a Boy with Emerin Gene Deletion. *Neuropediatrics* 30 (3), 161–163.

Heller, S. A., Shih, R., Kalra, R., and Kang, P. B. (2020). Emery-Dreifuss Muscular Dystrophy. *Muscle Nerve* 61 (4), 436–448. doi:10.1002/mus.26782

Kent, T., Chandramouly, G., Mcdevitt, S. M., Ozdemir, A. Y., and Pomerantz, R. T. (2015). Mechanism of Microhomology-Mediated End-Joining Promoted by Human DNA Polymerase θ. *Nat. Struct. Mol. Biol.* 22 (3), 230–237. doi:10.1038/nsmb.2961

Kurepa, D., Shen, Y., Kakkilaya, V., Ursin, S., Chen, H., and Sankararaman, S. (2013). Otopalatodigital Syndrome Type 2 in a Male Infant: A Case Report with a Novel Sequence Variation. *J. Pediatr. Genet.* 02 (1), 033–036. doi:10.3233/PGE-13045

Madej-Pilarczyk, A. (2018). Clinical Aspects of Emery-Dreifuss Muscular Dystrophy. *Nucleus* 9 (1), 314–320. doi:10.1080/19491034.2018.1462635

Meliota, G., Vairo, U., Ficarella, R., Milella, L., Faienza, M. F., and D'Amato, G. (2021). Cardiovascular, Brain, and Lung Involvement in a Newborn with a Novel FLNA Mutation. *Adv. Neonatal. Care* Publish Ahead of Print. doi:10.1097/ANC.0000000000000878

Patrosso, M. C., Repetto, M., Villa, A., Milanesi, L., Frattini, A., Faranda, S., et al. (1994). The Exon-Intron Organization of the Human X-Linked Gene (Fln1) Encoding Actin-Binding Protein 280. *Genomics* 21 (1), 71–76. doi:10.1006/geno.1994.1226

Richards, S., Aziz, N., Aziz, N., Bale, S., Bick, D., Das, S., et al. (2015). Standards and Guidelines for the Interpretation of Sequence Variants: a Joint Consensus Recommendation of the American College of Medical Genetics and Genomics and the Association for Molecular Pathology. *Genet. Med.* 17 (5), 405–423. doi:10.1038/gim.2015.30

Seol, J.-H., Shim, E. Y., and Lee, S. E. (2018). Microhomology-mediated End Joining: Good, Bad and Ugly. *Mutat. Research/Fundamental Mol. Mech. Mutagenesis* 809, 81–87. doi:10.1016/j.mrfmmm.2017.07.002

Sinha, S., Villarreal, D., Shim, E. Y., and Lee, S. E. (2016). Risky Business: Microhomology-Mediated End Joining. *Mutat. Research/Fundamental Mol. Mech. Mutagenesis* 788, 17–24. doi:10.1016/j.mrfmmm.2015.12.005

Small, K., Iber, J., and Warren, S. T. (1997). Emerin Deletion Reveals a Common X-Chromosome Inversion Mediated by Inverted Repeats. *Nat. Genet.* 16 (1), 96–99. doi:10.1038/ng0597-96

Small, K., and Warren, S. T. (1998). Emerin Deletions Occurring on Both Xq28 Inversion Backgrounds. *Hum. Mol. Genet.* 7 (1), 135–139. doi:10.1093/hmg/7.1.135

van der Werf, C. S., Sribudiani, Y., Verheij, J. B. G. M., Carroll, M., O'Loughlin, E., Chen, C.-H., et al. (2013). Congenital Short Bowel Syndrome as the Presenting Symptom in Male Patients with FLNA Mutations. *Genet. Med.* 15 (4), 310–313. doi:10.1038/gim.2012.123

Walsh, M., Hebbard, G., and Trainer, A. (2017). Update on a Previously Reported Male with a FLNA Missense Mutation. *Eur. J. Hum. Genet.* 25 (8), 905–906. doi:10.1038/ejhg.2016.156

Wang, H., and Xu, X. (2017). Microhomology-mediated End Joining: New Players Join the Team. *Cell Biosci* 7, 6. doi:10.1186/s13578-017-0136-8

FUNDING

This work was supported by grants from the National Natural Science Foundation of China (No. 82171393), the Natural Science Foundation of Beijing Municipality (No. 7212116), the National Key Research and Development Program of China (No. 2016YFC0901505), and the Beijing Key Laboratory of Molecular Diagnosis and Study on Pediatric Genetic Diseases (No. BZ0317).

ACKNOWLEDGMENTS

We are grateful to the patients and their families.

Conflict of Interest: WW was employed by the company Beijing Kangso Medical Inspection Co., Ltd.

The remaining authors declare that the research was conducted in the absence of any commercial or financial relationships that could be construed as a potential conflict of interest.

Publisher's Note: All claims expressed in this article are solely those of the authors and do not necessarily represent those of their affiliated organizations or those of the publisher, the editors, and the reviewers. Any product that may be evaluated in this article or claim that may be made by its manufacturer is not guaranteed or endorsed by the publisher.

frontiers in Genetics

CASE REPORT
published: 23 December 2021
doi: 10.3389/fgene.2021.763916

Case Report: A Novel Genetic Mutation Causes Idiopathic Infantile Arterial Calcification in Preterm Infants

*Liu Yunfeng, Han Tongyan, Wang Jing and Tong Xiaomei**

Department of Pediatrics, Peking University Third Hospital, Beijing, China

Idiopathic infantile arterial calcification (IIAC), also known as generalized arterial calcification of infancy (GACI), is a heritable ectopic mineralization disorder that results in diffuse arterial calcifications and or stenosis, which are attributed to mutations in the ENPP1 gene. In this case study, we report the development of IIAC in a 2-month-old male preterm infant. The patient presented with severe hypertension and seizures, which revealed diffused calcifications and c.130C > T and c.1112A > T mutations in the ENPP1 gene. With biphosphonate, antihypertensive, and control epilepsy therapy, his blood pressure was maintained at 110–120/50–60 mmHg. Intellectual motor development retardation was anticipated in this patient. To the best of our knowledge, this is the first case in which a novel c.130C > T mutation in the ENPP1 gene has been identified, and the administration of bisphosphonates to patients with IIAC has been assessed.

Keywords: genetic mutation, case, preterm, infant, hypertensive, artery, calcification, report

OPEN ACCESS

Edited by:
Yuan-Zong Song,
First Affiliated Hospital of Jinan University, China

Reviewed by:
Olivier Le Saux,
University of Hawaii, United States
Yuan Shi,
Children's Hospital of Chongqing Medical University, China

****Correspondence:***
Tong Xiaomei
tongxm2007@126.com

Specialty section:
This article was submitted to Genetics of Common and Rare Diseases, a section of the journal Frontiers in Genetics

Received: *24 August 2021*
Accepted: *07 December 2021*
Published: *23 December 2021*

Citation:
Yunfeng L, Tongyan H, Jing W and Xiaomei T (2021) Case Report: A Novel Genetic Mutation Causes Idiopathic Infantile Arterial Calcification in Preterm Infants. Front. Genet. 12:763916. doi: 10.3389/fgene.2021.763916

INTRODUCTION

Idiopathic infantile arterial calcification (IIAC), also known as generalized arterial calcification of infancy (GACI), is a rare autosomal recessive genetic disorder characterized by abnormalities in calcium and phosphorus metabolism. Approximately 69–80% of cases are caused by mutations in the ENPP1 gene on chromosome 6q23. A small fraction of cases results from mutations in the ABCC6 gene on chromosome 16p13.11. The first description of the clinical manifestation of GACI in the medical literature was published in 1901 (Bryant and White, 1901). IIAC is primarily diagnosed after observing hydroxyapatite deposits in the internal elastic layer of the large and medium arteries that causes vascular lesions, soft tissue calcification around joints, and various other life-threatening conditions due to the development of vascular lesions. Hypertension and heart failure are common clinical manifestations. Most infants develop arterial stenosis and heart failure within the first month of life. IIAC progresses rapidly; 80% of children with IIAC die within 6 months, and older children may die suddenly (Guimarães et al., 2010). This case report of neonatal GACI enriches the literature with data on a new familial mutation of the ENPP1 gene and provides details of the specific clinical course.

CASE DESCRIPTION

The boy was delivered at the 36th gestational period by cesarean section due to "suspected intrauterine distress" with a birth weight of 2,240 g. His Apgar scores were 7 at 1 min, 9 at

5 min, and 10 at 10 min. The amniotic fluid and umbilical cord were normal, and the placenta was calcified. The mother had two previous pregnancies and had complicated diabetes mellitus and hypothyroidism during pregnancy. At birth, he presented with respiratory distress, and blood gas analysis suggested severe respiratory failure. Echocardiography confirmed that the right ventricle was enlarged with moderate tricuspid regurgitation, and the pulmonary artery pressure was high, up to 70 mmHg. He developed severe hypertension 3 days after birth (systolic and diastolic blood pressure range, 100–120 and 40–70 mmHg, respectively). After Captopril treatment, the systolic blood pressure stabilized at 70–80/40–50 mmHg, and echocardiogram confirmed a thickened left ventricular wall, an enlarged left atrium, and a LVEF of 55%. Abdominal computed tomography (CT) detected diffuse calcifications of the abdominal aorta and its major branches and slight luminal stenosis (**Figure 1**).

Two months after birth, he presented with a hypertensive crisis with severe heart failure and persistent convulsions. The liver and renal functions of the patient were abnormal. The systolic blood pressure was high, at 170 mmHg; the diastolic blood pressure was high, at 120 mmHg; the blood calcium level was low, at 1.6 mmol/L (normal value 2.11–2.52 mmol/L); and the blood phosphorus level was high, at 2.27 mmol/L (normal value 0.85–1.51 mmol/L). Chest radiography showed a few exudative lesions in both lungs and an enlarged cardiac shadow. Echocardiography revealed significant thickening of the left ventricular wall, enlarged left atrium and left ventricle, patent ductus arteriosus (small left-to-right shunt), and LVEF of 50%. The EEG had persistent multichannel sharp waves. Arterial Doppler ultrasound was performed and showed extensive calcification of the walls of the bilateral common carotid, bilateral femoral, carotid, vertebral, and internal carotid arteries, extensive calcification of the walls of the abdominal aorta and the right renal artery, and local luminal stenosis (**Figures 2A–D**). Flow velocity in the calcified abdominal aorta increased, and blood flow velocity in both renal arteries increased. Cranial MRI revealed bilateral frontal, parietal, and temporal lobe atrophy with dilated ventricles (**Figure 3A**). The cranial MRA showed bilateral internal carotid artery patchy luminal stenosis, left vertebral artery fibrillation, and left anterior cerebral artery, left middle cerebral artery luminal stenosis, and bilateral posterior cerebral artery luminal stenosis (**Figure 3B**). Cranial ultrasound showed bilateral calcification of the lenticular artery on both sides. No joint or skeletal calcification was observed on radiography, and prenatal ultrasound images were also retrospectively reviewed, but no arterial calcifications were detected.

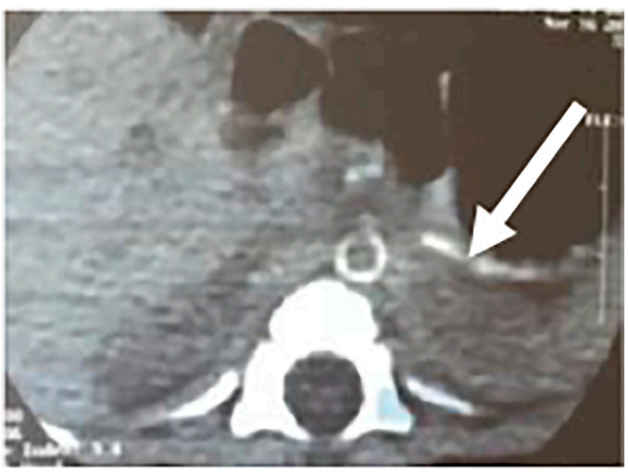

FIGURE 1 | Enhanced contrast CT scan of the abdomen shows calcification of the abdominal aorta and its branches.

These singularities were consistent with those of the IIAC. The genotype of the patient was analyzed. Genetic testing of the child and parents suggested two heterozygous mutations in the ENPP1 gene *1*) c.130C > T (mutation of nucleotide 130 in the coding region from cytosine to thymine), resulting in an amino acid change p.Q44X (nonsense mutation). The father had a suspected heterozygous variant at this locus. *2*) c.1112A > T (mutation of nucleotide 1112 in the coding region from adenine to thymine), resulting in an amino acid change p.Y371F (mutation of amino acid 371 from tyrosine to phenylalanine) which is a missense mutation. The father showed no mutation at this locus, and the mother had a heterozygous variant at this locus. The genetic results were consistent with those for idiopathic infantile arterial calcification. The c.130C > T mutation has not been described in the literature or mutation databases (**Figure 4**).

The main treatment consisted of three courses: *1*) Circulatory system: Severe heart failure treatment with cardiac and vasodilator therapy with Foxglove preparation and sodium nitroprusside (0.1 μg/kg min to 4 μg/kg min) and oral administration of Norvasc and Losartan. The blood pressure of the patient gradually reduced to approximately 120/60 mmHg (95–99th percentile). *2*) Nervous system: The child developed a persistent state of convulsions and was considered to have hypertensive encephalopathy. Luminal and midazolam were administered successively, and continuous multichannel sharp wave discharges were observed in the EEG. After propofol was administered for 2 days, the abnormal EEG discharge was reduced, and propofol and midazolam dosages were gradually reduced. *3*) Zoledronic acid was administered intravenously (0.02 mg/kg once every other week for three times). Blood pressure was maintained at 110–130/60–70 mmHg (approximately 95th percentile of normal blood pressure in children of the same age). Blood calcium level was 1.92 mmol/L and blood phosphorus level was 2.68 mmol/L. His blood pressure stabilized, heart failure was corrected, no further convulsions occurred, and he was discharged in good condition.

During the long-time follow-up, with Norvasc and Losartan antihypertensive treatment, his blood pressure leveled at around 110–120/50–60 mmHg. Currently, he orally takes Etidronic acid as well as Clonazepam and Topamax to control epilepsy. His Gesell testing at 2 years old suggested he has moderate intellectual-motor retardation. At 3 years old, ultrasound showed that extensive vascular calcification was still present

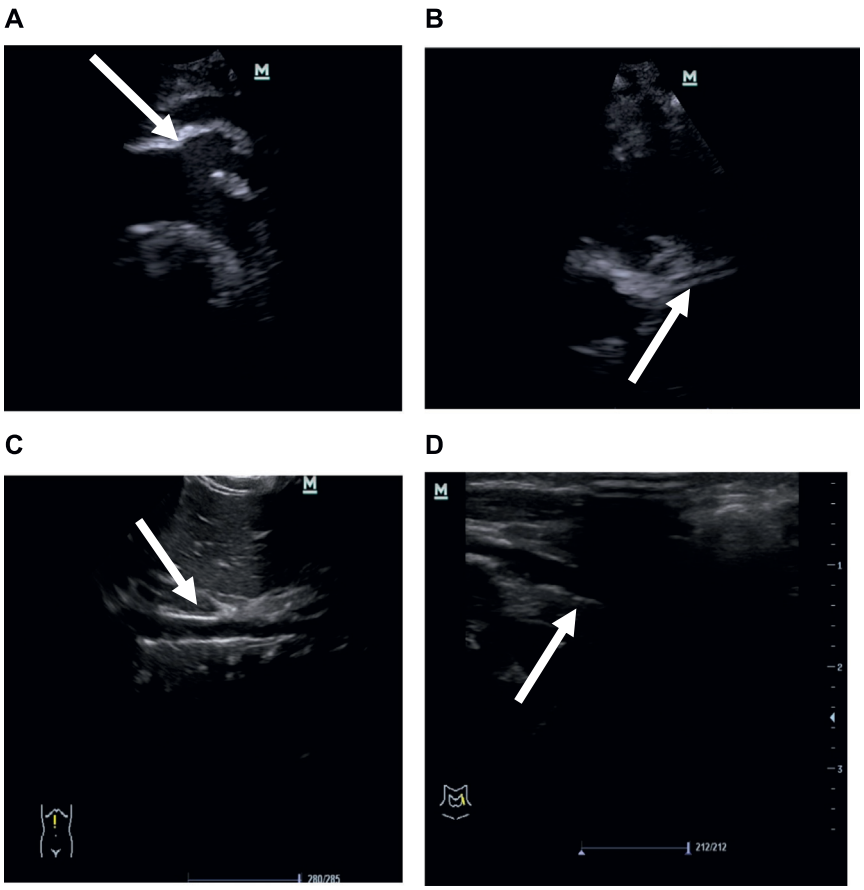

FIGURE 2 | Vascular ultrasound images. **(A)** Strong echo in the aortic arch and its branches is indicated by the arrows. **(B)** Strong echo in the left coronary artery wall is indicated by the arrows. **(C)** Strong echo in the abdominal aortic wall is indicated by the arrows. **(D)** Strong echo in the femoral artery wall is indicated by the arrows.

but was not progressing.The five-year-old child also suffers from cerebral palsy and receives rehabilitation training now.

His mother had another pregnancy 3 years ago, and prenatal genetic testing showed that the fetus carried the same mutations. A boy was born by full-term delivery, is now 3 years old, and is developing normally.

DISCUSSION

The first report of an association between IIAC and mutations in ENPP1 was reported by Rutsch et al. (2003). Animal experiments further confirmed that mutations in the ENPP1 gene can cause IIAC (Li et al., 2013, 2014). The gene is located on chromosomes 6q22 to q23, has a length of 83 kb, and contains 25 exons. ENPP1 is an external nucleotide pyrophosphatase/phosphodiesterase 1, an enzyme that causes vascular smooth muscle cells, chondrocytes, and osteoblasts to produce inorganic pyrophosphate (PPi). Mutations in the ENPP1 gene can lead to decreased levels of PPi and the production of hydroxyapatite crystals that are deposited in various layers of arteries, including the aorta, coronary arteries, heart valves, and renal arteries, causing vascular lesions, soft tissue calcification around joints, and various life-threatening conditions due to vascular lesions such as myocardial infarction, renal failure, cerebral infarction, and hypertensive encephalopathy (Numakura et al., 2006).

Less frequently, IIAC is linked to a mutation in the ATP-binding cassette subfamily C, member 6 (ABCC6) gene (GACI2, OMIM 614473) (Nitschke et al., 2012) which encodes ABCC6 (Nitschke and Rutsch, 2017). The ABCC6 gene on chromosome 16p13.11 is affected by the classic form of Pseudoxanthoma Elasticum (PXE). There is a genotypic overlap between IIAC and PXE, with some patients harboring mutations in ABCC6, and some patients with clinical manifestations consistent with PXE have mutations in ENPP1 (Nitschke et al., 2012). The main manifestations are calcification of the skin elastic fibers, systemic arterial vascular calcification, and cervical vertebral fusion (Ferreira et al., 2021a).

Genetic testing of our patient revealed two compound heterozygous mutations in the ENPP1 gene originating from his parents. Firstly, c.130C > T (mutation of nucleotide 130 in the coding region from cytosine to thymine) results in an amino acid change, p.Q44X, that causes a partial deletion of the protein from 44 amino acids onwards, a class I pathogenic form of mutation.

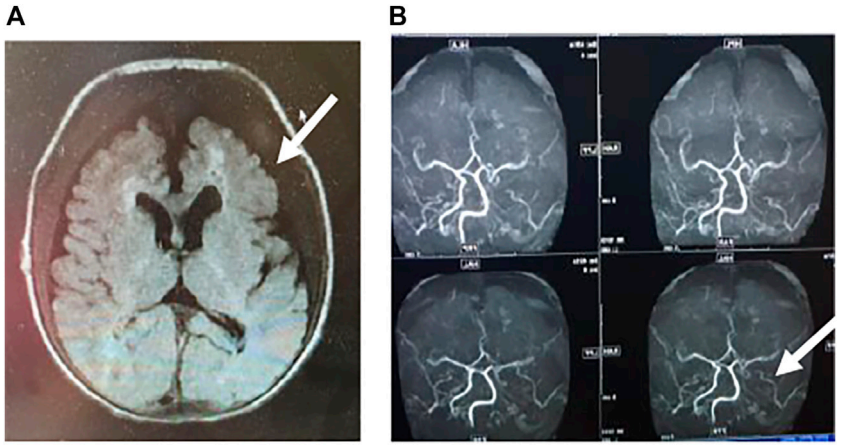

FIGURE 3 | A) Cranial MRI showing bilateral frontal and temporal lobe atrophy and abnormally high signal in the white matter around the anterior horn of the ventricle. The lesions are indicated by arrows. **(B)** Cerebrovascular artery MRI showing multiple luminal stenoses of the bilateral anterior, middle, and posterior cerebral arteries and vertebral arteries. The lesions are indicated by arrows.

This novel familial mutation in the ENPP1 gene has not yet been described in the literature or mutation databases. The other mutation is a missense mutation c.1112A > T (mutation of nucleotide 1112 in the coding region from adenine to thymine) that leads to an amino acid change, p.Y371F (mutation of amino acid 371 from tyrosine to phenylalanine), and is a pathogenic mutation that has been reported (Cheng et al., 2005) and is associated with IIAC.

The clinical manifestations of IIAC vary widely and can be broadly divided into two categories: early and late-onset (Sluis et al., 2006; Chong and Hutchins, 2008; Shaireen et al., 2013). Early onset (approximately 48%) refers to cases that occur in the fetal period or within 1 month of birth. The main manifestations are respiratory distress, fetal edema, severe heart failure, pulmonary hypertension, and hypertension. Late-onset (approximately 52%) refers to cases where the onset is 1 month after birth, and the main manifestations are respiratory failure, heart failure, cyanosis, hypertension, and nonspecific ischemic and hypoxic damage to other organs, such as abdominal pain and microvascular thrombosis (Rani et al., 2010; Zhang et al., 2011). Convulsive episodes and brain damage revealed old strokes and marked gliotic changes, but bilateral occipital necrosis is less commonly reported (Staretz-Chacham et al., 2019). If calcified plaques are deposited in the renal artery this can lead to renal artery stenosis and renal failure can occur. In our case, the child was born with heart failure, persistent hypertension, and progressive multisystem damage to liver function and kidney, consistent with the clinical features of the disease. The presence of the hypertensive crisis is suggestive of the aggressiveness of the disease. In contrast, the significant cerebrovascular calcification and neurological ischemic-hypoxic brain parenchymal damage presented in our case has not been reported previously.

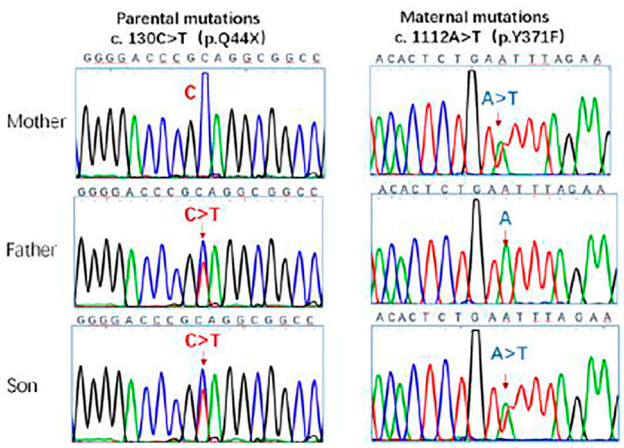

FIGURE 4 | Sanger sequencing of ENPP1 in the parents and the patient. The c.130C > T, c.1112A > T locus mutations were detected in the gene. The ENPP1 gene was inherited from both parents with heterozygous c. 130 C > T and c. 1112A > T compound heterozygous mutations. The mutation sites are indicated by the arrows.

Imaging examinations are of great value in the clinical diagnosis of IIAC. The main imaging manifestations are widespread calcification of the aorta and its branches, including the aortic arch, unnamed artery, abdominal aorta, femoral artery, and other large vessels. The inner wall of each vessel is not smooth; there are calcified plaques of different sizes attached, combined with stenosis of the diameter of the vessel, and the local blood flow velocity is significantly increased (Whitehall et al., 2003; Tran and Boechat, 2006; Bolster et al., 2015).

Based on the clinical features of large artery calcification combined with genetic testing, IIAC can be diagnosed (Borromini et al., 2016). Arterial biopsy indicates that hydroxyapatite deposits in the internal elastic membrane of large-and medium-sized arteries are the current gold standard bases for the diagnosis of IIAC (Dayapala et al., 2016).

The disease can be diagnosed during the fetal period. Fetal edema is the most common sign, and intrauterine distress and heart failure have been observed (Cansu et al., 2010; Esmer et al., 2015; Yi et al., 2017). Vascular ultrasound revealed intimal calcification and luminal stenosis of the aorta and abdominal aorta vessels, mostly in the second trimester. If an older sibling has a disease, the detection rate can be greatly improved by using multiple ultrasound examinations and genetic testing of amniotic fluid in the fetus of a subsequent pregnancy in early gestation (Mastrolia et al., 2015; Votava-Smith et al., 2017). In our case, no arterial calcifications were detected on prenatal ultrasound images.

As IIAC is a rare metabolic disorder, there are no guidelines for its treatment. Bisphosphonates are commonly used to treat IIAC, In 2008, (Rutsch et al., 2008). Rutsch used phosphonate analogs and performed a multicenter genetic study and retrospective observational analysis, suggesting that the survival of children was not significantly related to genetic mutations. Moreover, the survival rate was higher in children with well-controlled blood phosphate values and no hyperphosphaturia when treated with phosphonates. Therefore, phosphonate analogs are the first-line agents used in IIAC treatment (Ramjan et al., 2009). In recent years, different approaches for treating GACI have been intensively investigated, including early generation bisphosphonates, orally administered PPi, and soluble recombinant ENPP1-Fc protein (Albright et al., 2015; Dedinszki et al., 2017; Nitschke et al., 2018), and some cases have reported that sodium thiosulfate can improve ectopic calcification of IIAC (Omarjee et al., 2020), and animal experiments suggest that enzyme replacement therapy can have therapeutic effects on IIAC (Luo et al., 2020). The mechanism may be that this treatment reduces bone renewal, thus inhibiting further calcium deposition at sites of existing calcified injury, interferes with the formation of hydroxyapatite crystals, and/or provides analogs of inorganic pyrophosphates that can affect calcium deposition. Intravenous zoledronic acid therapy at doses of 0.25, 0.5, and 0.5 mg/kg for weeks 1, 2, and 3, respectively, and subsequent monthly doses of 0.5 mg/kg can be applied. It has recently been reported that switching administration to oral phosphonates at 20 mg/kg d after 3 weeks of intravenous therapy, with a gradual reduction to 50 mg/d for long-term oral maintenance, depending on vascular ultrasound treatment, can also provide relief (Edouard et al., 2011). In our case, treatment with symptomatic support and zoledronic acid every other week was switched to oral zoledronic acid after three courses, and blood pressure was largely maintained at the 95th–99th percentile of normal values in children of the same age, and the condition resolved. This also provides valuable insight for the treatment of other children with IIAC. The most common side effect of long-term administration of phosphonate preparations is severe skeletal lesions, similar to rickets manifestations (Otero et al., 2013; Ferreira et al., 2016) that must be monitored and treated.

The prognosis of patients with IIAC is poor. Combined coronary artery calcification is a major risk factor for a poor prognosis. Most deaths occur in infancy, and rapidly progressive malignant heart failure is often the main cause of death (Nael et al., 2014; Ferreira et al., 2021a). Individuals may die suddenly due to myocardial infarction. A small number of survivors may have intractable hypertension, recurrent cardiopulmonary failure (Nael et al., 2014) renal impairment, cervical spine fusion, and hearing loss (Ferreira et al., 2021b). Survivors require long-term oral antihypertensive drugs and medications to improve cardiac function. Patients with combined severe renal impairment require peritoneal dialysis (Stojanovic et al., 2013). Intractable heart failure eventually requires heart transplantation (Glatz et al., 2006; Giovannoni et al., 2014). Only two patients with IIAC who survived for 22 and 25 years have been reported. The patient in the present case successfully survived for 5 years, with hypertension and heart failure under effective control, but with severe brain damage and intellectual motor development retardation, and the long-term prognosis of the patient is not optimistic.

CONCLUSION

IIAC is a rare autosomal recessive disorder characterized by abnormal calcium metabolism due to genetic mutations. A novel c.130C > T mutation in ENPP1 was identified. Hypertension, heart failure, and central nervous system involvement due to vascular calcification are typical clinical manifestations. Treatment with oral phosphonates is expected to improve the long-term prognosis. Early recognition of the disease by obstetricians enables intrauterine diagnosis and prenatal genetic screening, which can effectively improve informed healthcare decision-making for parents. The limitation of this case was that vascular calcification was not treated. In the follow-up, his vascular calcification did not deteriorate further.

DATA AVAILABILITY STATEMENT

The original contributions presented in the study are included in the article/Supplementary Material, further inquiries can be directed to the corresponding authors.

ETHICS STATEMENT

Ethical approval was not provided for this study on human participants because this research was performed as part of a routine molecular diagnosis of patients. Written informed consent to participate in this study was provided by the participant's legal guardian/next of kin. Written informed consent was obtained from the individual(s) and minor(s) legal guardian/next of kin for the publication of any potentially identifiable images or data included in this article.

AUTHOR CONTRIBUTIONS

LY, HT, and WJ clinically followed the patient and were responsible for the initial manuscript writing as well as reviewing the literature. TX was responsible for the development of the final version of the manuscript. All authors contributed to the study and approved the manuscript for publication.

REFERENCES

Albright, R. A., Stabach, P., Cao, W., Kavanagh, D., Mullen, I., Braddock, A. A., et al. (2015). ENPP1-Fc Prevents Mortality and Vascular Calcifications in Rodent Model of Generalized Arterial Calcification of Infancy. *Nat. Commun.* 6, 10006. doi:10.1038/ncomms10006

Bolster, F., Ali, Z., Southall, P., and Fowler, D. (2015). Generalized Arterial Calcification of Infancy-Findings at Post-mortem Computed Tomography and Autopsy. *Forensic Sci. Int.* 254, e7–e12. doi:10.1016/j.forsciint.2015.06.017

Borromini, A., Rossi, G., Maggi, P., Speciale, D., Mirri, G., Cogliardi, A., et al. (2016). Molecular Biology as a Diagnostic Tool in the Newborn Emergency Department: A Rare Case of Idiopathic Infantile Arterial Calcification. *G Ital. Cardiol. (Rome)* 17 (3), 234–236. doi:10.1714/2190.23670

Bryant, J. H., and White, W. A. (1901). A Case of Calcification of the Arteries and Obliterative Endarteritis Associated with Hydronephrosis in a Child Aged 6 Months. *Guys Hosp. Rep.* 55, 17–28.

Cansu, A., Ahmetoglu, A., Mutlu, M., Guven, S., and Osmanagaoglu, M. A. (2010). Idiopathic Infantile Arterial Calcification: Prenatal Diagnosis and Postnatal Presentation. *Clin. Exp. Obstet. Gynecol.* 37 (1), 73–75.

Cheng, K.-S., Chen, M.-R., Ruf, N., Lin, S.-P., and Rutsch, F. (2005). Generalized Arterial Calcification of Infancy: Different Clinical Courses in Two Affected Siblings. *Am. J. Med. Genet.* 136A (2), 210–213. doi:10.1002/ajmg.a.30800

Chong, C. R., and Hutchins, G. M. (2008). Idiopathic Infantile Arterial Calcification: The Spectrum of Clinical Presentations. *Pediatr. Dev. Pathol.* 11 (5), 405–415. doi:10.2350/07-06-0297.1

Corbacioglu Esmer, A., Kalelioglu, I., Omeroglu, R. E., Kayserili, H., Gulluoglu, M., Has, R., et al. (2015). Prenatal Ultrasonographic Diagnosis of Generalized Arterial Calcification of Infancy. *J. Clin. Ultrasound* 43 (1), 50–54. doi:10.1002/jcu.22121

Dayapala, A., Rathnayake, I. L., and Pethiyagoda, P. (2016). A Case of Idiopathic Arterial Calcification of Infancy Diagnosed at Autopsy. *Ceylon Med. J.* 61 (3), 137–138. doi:10.4038/cmj.v61i3.8354

Dedinszki, D., Szeri, F., Kozák, E., Pomozi, V., Tőkési, N., Mezei, T. R., et al. (2017). Oral Administration of Pyrophosphate Inhibits Connective Tissue Calcification. *EMBO Mol. Med.* 9 (11), 1463–1470. doi:10.15252/emmm.201707532

Edouard, T., Chabot, G., Miro, J., Buhas, D. C., Nitschke, Y., Lapierre, C., et al. (2011). Efficacy and Safety of 2-year Etidronate Treatment in a Child with Generalized Arterial Calcification of Infancy. *Eur. J. Pediatr.* 170 (12), 1585–1590. doi:10.1007/s00431-011-1572-9

Ferreira, C. R., Hackbarth, M. E., Ziegler, S. G., Pan, K. S., Roberts, M. S., Rosing, D. R., et al. (2021b). Prospective Phenotyping of Long-Term Survivors of Generalized Arterial Calcification of Infancy (GACI). *Genet. Med.* 23 (2), 396–407. doi:10.1038/s41436-020-00983-0

Ferreira, C. R., Kintzinger, K., Hackbarth, M. E., Botschen, U., Nitschke, Y., Mughal, M. Z., et al. (2021a). Ectopic Calcification and Hypophosphatemic Rickets: Natural History of ENPP1 and ABCC6 Deficiencies. *J. Bone Miner Res.* 36, 2193–2202. doi:10.1002/jbmr.4418

Ferreira, C. R., Ziegler, S. G., Gupta, A., Groden, C., Hsu, K. S., and Gahl, W. A. (2016). Treatment of Hypophosphatemic Rickets in Generalized Arterial Calcification of Infancy (GACI) without Worsening of Vascular Calcification. *Am. J. Med. Genet.* 170 (5), 1308–1311. doi:10.1002/ajmg.a.37574

Giovannoni, I., Callea, F., Travaglini, L., Amodeo, A., Cogo, P., Secinaro, A., et al. (2014). Heart Transplant and 2-year Follow up in a Child with Generalized Arterial Calcification of Infancy. *Eur. J. Pediatr.* 173 (12), 1735–1740. doi:10.1007/s00431-014-2447-7

Glatz, A. C., Pawel, B. R., Hsu, D. T., Weinberg, P., and Chrisant, M. R. K. (2006). Idiopathic Infantile Arterial Calcification: Two Case Reports, a Review of the Literature and a Role for Cardiac Transplantation. *PediatrTransplant.Mar* 10 (2), 225–233. doi:10.1111/j.1399-3046.2005.00414.x

Guimarães, S., Lopes, J. M., Oliveira, J. B., and Santos, A. (2010). Idiopathic Infantile Arterial Calcification: A Rare Cause of Sudden Unexpected Death in Childhood. *Pathol. Res. Int.* 2010, 1–5. doi:10.4061/2010/185314

Li, Q., Brodsky, J. L., Conlin, L. K., Pawel, B., Glatz, A. C., Gafni, R. I., et al. (2014). Mutations in the ABCC6 Gene as a Cause of Generalized Arterial Calcification of Infancy: Genotypic Overlap with Pseudoxanthoma Elasticum. *J. Invest. Dermatol.* 134 (3), 658–665. doi:10.1038/jid.2013.370

Li, Q., Guo, H., Chou, D. W., Berndt, A., Sundberg, J. P., and Uitto, J. (2013). Mutant Enpp1asj Mice as a Model for Generalized Arterial Calcification of Infancy. *Dis. Model. Mech.* 6 (5), 1227–1235. doi:10.1242/dmm.012765

Luo, H., Li, Q., Cao, Y., and Uitto, J. (2020). Therapeutics Development for Pseudoxanthoma Elasticum and Related Ectopic Mineralization Disorders: Update 2020. *Jcm* 10 (1), 114. doi:10.3390/jcm10010114

Mastrolia, S. A., Weintraub, A. Y., Baron, J., Sciaky-Tamir, Y., Koifman, A., Loverro, G., et al. (2015). Antenatal Diagnosis of Idiopathic Arterial Calcification: A Systematic Review with a Report of Two Cases. *Arch. Gynecol. Obstet.* 291 (5), 977–986. doi:10.1007/s00404-014-3567-z

Nael, A., Siaghani, P. J., Chen, D., Romansky, S. G., and Shane, L. (201418985). Idiopathic Infantile Arterial Calcification: A Possible Cause of Refractory Cardiopulmonary Failure in Infancy. *Case Rep. Pathol.* 2014, 1–4. doi:10.1155/2014/189850

Nitschke, Y., Baujat, G., Botschen, U., Wittkampf, T., du Moulin, M., Stella, J., et al. (2012). Generalized Arterial Calcification of Infancy and Pseudoxanthoma Elasticum Can Be Caused by Mutations in Either ENPP1 or ABCC6. *Am. J. Hum. Genet.* 90 (1), 25–39. doi:10.1016/j.ajhg.2011.11.020

Nitschke, Y., and Rutsch, F. (2017). Inherited Arterial Calcification Syndromes: Etiologies and Treatment Concepts. *Curr. Osteoporos. Rep.* 15 (4), 255–270. doi:10.1007/s11914-017-0370-3

Nitschke, Y., Yan, Y., Buers, I., Kintziger, K., Askew, K., and Rutsch, F. (2018). ENPP1-Fc Prevents Neointima Formation in Generalized Arterial Calcification of Infancy Through the Generation of AMP. *Exp. Mol. Med.* 50 (10), 1–12. doi:10.1038/s12276-018-0163-5

Numakura, C., Yamada, M., Ariyasu, D., Maesaka, A., Kobayashi, H., Nishimura, G., et al. (2005). Genetic and Enzymatic Analysis for Two Japanese Patients with Idiopathic Infantile Arterial Calcification. *J. Bone Miner Metab.* 24 (1), 48–52. doi:10.1007/s00774-005-0645-0

Omarjee, L., Nitschke, Y., Verschuere, S., Bourrat, E., Vignon, M. D., Navasiolava, N., et al. (2020). Severe Early-onset Manifestations of Pseudoxanthoma Elasticum Resulting from the Cumulative Effects of Several Deleterious Mutations in ENPP1, ABCC6 and HBB: Transient Improvement in Ectopic Calcification with Sodium Thiosulfate. *Br. J. Dermatol.* 183 (2), 367–372. doi:10.1111/bjd.18632

Otero, J. E., Gottesman, G. S., McAlister, W. H., Mumm, S., Madson, K. L., Kiffer-Moreira, T., et al. (2013). Severe Skeletal Toxicity from Protracted Etidronate Therapy for Generalized Arterial Calcification of Infancy. *J. Bone Miner Res.* 28 (2), 419–430. doi:10.1002/jbmr.1752

Ramjan, K. A., Roscioli, T., Rutsch, F., Sillence, D., and Munns, C. F. (2009). Generalized Arterial Calcification of Infancy: Treatment with Bisphosphonates. *Nat. Rev. Endocrinol.* 5 (3), 167–172. doi:10.1038/ncpendmet1067

Rao, U., Rani, H., Rao, R., Dinesh, U., and Ramamurthy, B. (2010). Idiopathic Infantile Arterial Calcification with Thrombotic Microangiopathy -A Unique Case. *Fetal Pediatr. Pathol.* 29 (6), 413–418. doi:10.3109/15513815.2010.505625

Rutsch, F., Böyer, P., Nitschke, Y., Ruf, N., Lorenz-Depierieux, B., Wittkampf, T., et al.GACI Study Group (2008). Hypophosphatemia, Hyperphosphaturia, and Bisphosphonate Treatment Are Associated with Survival beyond Infancy in Generalized Arterial Calcification of Infancy. *Circ. Cardiovasc. Genet.* 1 (2), 133–140. doi:10.1161/CIRCGENETICS.108.797704

Rutsch, F., Ruf, N., Vaingankar, S., Toliat, M. R., Suk, A., Höhne, W., et al. (2003). Mutations in ENPP1 Are Associated with 'idiopathic' Infantile Arterial Calcification. *Nat. Genet.* 34 (4), 379–381. doi:10.1038/ng1221

Shaireen, H., Howlett, A., Amin, H., Yusuf, K., Kamaluddeen, M., and Lodha, A. (2013). The Mystery of Persistent Pulmonary Hypertension: An Idiopathic Infantile Arterial Calcification. *BMC Pediatr.* 13, 107. doi:10.1186/1471-2431-13-107

Staretz-Chacham, O., Shukrun, R., Barel, O., Pode-Shakked, B., Pleniceanu, O., Anikster, Y., et al. (2019). Novel Homozygous ENPP1 Mutation Causes Generalized Arterial Calcifications of Infancy, Thrombocytopenia, and Cardiovascular and central Nervous System Syndrome. *Am. J. Med. Genet.* 179 (10), 2112–2118. doi:10.1002/ajmg.a.61334

Stojanovic, V., Doronjski, A., Milak, G., and Barisic, N. (2013). Idiopathic Arterial Calcification of Infancy- Peritoneal Dialysis for Treatment of Hypertension. *Fetal Pediatr. Pathol.* 32 (6), 443–447. doi:10.3109/15513815.2013.802399

Tran, K. H., and Boechat, M. I. (2006). Idiopathic Infantile Arterial Calcification: Imaging Evaluation and the Usefulness of MR Angiography. *Pediatr. Radiol. Mar.* 36 (3), 247–253. doi:10.1007/s00247-0050044-7

van der Sluis, I. M., Boot, A. M., Vernooij, M., Meradji, M., and Kroon, A. A. (2006). Idiopathic Infantile Arterial Calcification: Clinical Presentation, Therapy and Long-Term Follow-Up. *Eur. J. Pediatr.* 165 (9), 590–593. doi:10.1007/s00431-006-0146-8

Votava-Smith, J. K., Pitukcheewanont, P., Randolph, L. M., and Chmait, R. H. (2017). Generalized Arterial Calcification in a Recipient Twin: Discordant Fetal Hemodynamics Result in Differing Phenotypes in Monozygotic Twins with an ABCC6 Mutation. *Fetal Diagn. Ther.* 41 (3), 234–236. doi:10.1159/000444852

Whitehall, J., Smith, M., and Altamirano, L. (2003). Idiopathic Infantile Arterial Calcification: Sonographic Findings. *J. Clin. Ultrasound* 31 (9), 497–501. doi:10.1002/jcu.10208

Yi, Y., Tong, T., Liu, T., Lin, Q., Xiong, Y., and Xu, J. (2017). Prenatal Diagnosis of Idiopathic Infantile Arterial Calcification Without Fetal Hydrops. *Echocardiography* 34 (2), 311–314. doi:10.1111/echo.13420

Zhang, E., Owen, R., Bruce, G., and Wiebe, S. (2011). Idiopathic Infantile Arterial Calcification in a 12-Year-Old Girl Presenting as Chronic Mesenteric Ischemia: Imaging Findings and Angioplasty Results. *Pediatr. Radiol.* 41 (11), 1476–1480. doi:10.1007/s00247-011-2030-6

Conflict of Interest: The authors declare that the research was conducted in the absence of any commercial or financial relationships that could be construed as a potential conflict of interest.

Publisher's Note: All claims expressed in this article are solely those of the authors and do not necessarily represent those of their affiliated organizations, or those of the publisher, the editors and the reviewers. Any product that may be evaluated in this article, or claim that may be made by its manufacturer, is not guaranteed or endorsed by the publisher.

frontiers in Genetics

ORIGINAL RESEARCH
published: 17 January 2022
doi: 10.3389/fgene.2021.811833

A Family Segregating Lethal Primary Coenzyme Q10 Deficiency Due to Two Novel *COQ6* Variants

Na Wang[1†], Youmin Zheng[2†], Lingzi Zhang[2], Xiong Tian[3], Yicheng Fang[4], Ming Qi[5,6,7], Juping Du[1], Shuaishuai Chen[1], Shiyong Chen[1], Jun Li[1], Bo Shen[1] and Lizhen Wang[2]**

[1]Department of Clinical Laboratory, Taizhou Hospital of Zhejiang Province Affiliated to Wenzhou Medical University, Linhai, China, [2]Department of Pediatrics, Taizhou Hospital of Zhejiang Province Affiliated to Wenzhou Medical University, Linhai, China, [3]Department of Public Research Platform, Taizhou Hospital of Zhejiang Province Affiliated to Wenzhou Medical University, Linhai, China, [4]Department of Radiology, Taizhou Hospital of Zhejiang Province Affiliated to Wenzhou Medical University, Linhai, China, [5]Sir Run Run Shaw Hospital Affiliated to Zhejiang University School of Medicine, Hangzhou, China, [6]DIAN Diagnostics, Hangzhou, China, [7]Department of Pathology and Laboratory Medicine, University of Rochester Medical Center, Rochester, NY, United States

OPEN ACCESS

Edited by:
Huiwen Zhang,
Xinhua Hospital, China

Reviewed by:
Eva Trevisson,
University of Padua, Italy
Nadia Akawi,
United Arab Emirates University, United Arab Emirates

***Correspondence:**
Bo Shen
shenb@enzemed.com
Lizhen Wang
wanglz@enzemed.com

[†]*These authors shared first authorship*

Specialty section:
This article was submitted to Genetics of Common and Rare Diseases, a section of the journal Frontiers in Genetics

Received: *09 November 2021*
Accepted: *06 December 2021*
Published: *17 January 2022*

Citation:
Wang N, Zheng Y, Zhang L, Tian X, Fang Y, Qi M, Du J, Chen S, Chen S, Li J, Shen B and Wang L (2022) A Family Segregating Lethal Primary Coenzyme Q10 Deficiency Due to Two Novel COQ6 Variants. Front. Genet. 12:811833. doi: 10.3389/fgene.2021.811833

Primary coenzyme Q10 deficiency-6 (COQ10D6), as a rare autosomal recessive disease caused by *COQ6* mutations, is characterized by progressive infantile-onset nephrotic syndrome resulting in end-stage renal failure and sensorineural hearing loss. Here, we report two Chinese siblings with COQ10D6 who primarily presented with severe metabolic acidosis, proteinuria, hypoalbuminemia, growth retardation, and muscle hypotonia and died in early infancy. Using whole-exome sequencing and Sanger sequencing, we identified two rare recessive nonsense mutations in the *COQ6* gene segregating with disease in affected family members: c.249C > G (p.Tyr83Ter) and c.1381C > T (p.Gln461Ter), resulting in two truncated protein products. Both mutations are located in a highly conserved area and are predicted to be pathogenic. Indeed, the death of our patients in early infancy indicates the pathogenicity of the p.Tyr83Ter and p.Gln461Ter variants and highlights the significance of the two variants for *COQ6* enzyme function, which is necessary for the biosynthesis of coenzyme Q10. In conclusion, we discovered a novel compound heterozygous pathogenic variant of the *COQ6* gene as a cause of severe COQ10D6 in the two siblings. Based on the clinical history and genetic characteristics of the patients, our cases expand the genotypic spectrum of COQ10D6 and highlight the heterogeneity and severity of clinical features associated with *COQ6* mutations. For patients with clinical manifestations suggestive of COQ10D6, early testing for *COQ6* mutations is beneficial for disease diagnosis and therapeutic interventions as well as disease prevention in future generations.

Keywords: *COQ6* mutation, nephrotic syndrome, primary coenzyme Q10 deficiency, genetics, infancy

INTRODUCTION

Nephrotic syndrome (NS) is a chronic kidney disease that involves massive proteinuria, hypoalbuminemia, hyperlipidemia, and edema. When occurring in the first year of life, NS is considered a life-threatening clinical condition with poor prognosis and high mortality if not treated in time (Noone et al., 2018). NS is generally classified as steroid-dependent nephrotic syndrome

(SDNS), steroid-resistant nephrotic syndrome (SRNS), or steroid-sensitive nephrotic syndrome (SSNS) based on its response to steroid therapy (Greenbaum et al., 2012; Trautmann et al., 2017). SRNS is a common cause of end-stage renal disease (ESRD) in children, affecting approximately 10–20% of all pediatric NS cases (Warejko et al., 2018; Park et al., 2020), and the renal biopsies of affected patients usually show focal segmental glomerulosclerosis (FSGS) (Lovric et al., 2016).

Recently, large cohort studies have shown that approximately 30% of childhood-onset SRNS cases are associated with genetic defects (Sadowski et al., 2015; Wang et al., 2017; Nagano et al., 2020). Different variants of the genes involved in coenzyme Q10 (CoQ10) biosynthesis may lead to a renal phenotype, either syndromic SRNS (*PDSS2*, *COQ2*, and *COQ6*) or isolated SRNS (*COQ8B*) (Cheong 2020). Primary CoQ10 deficiency-6 (COQ10D6, OMIM # 614650) is an autosomal recessive disorder that manifests as severe progressive infantile-onset NS resulting in end-stage renal failure and sensorineural hearing loss (SNHL) due to homozygous or compound heterozygous mutations in the *COQ6* gene located on chromosome 14q24.3, which encodes an evolutionarily conserved flavin-dependent monooxygenase required for CoQ10 biosynthesis. Heeringa et al. (Heeringa et al., 2011) first reported that 11 children from five families with COQ10D6 manifest as NS and SNHL, and some of these patients responded favorably to oral CoQ10 treatment. In addition, high-dose exogenous CoQ10 supplementation at early stages of the disease can ameliorate the neurological and renal symptoms (Heeringa et al., 2011; Quinzii et al., 2014; Stanczyk et al., 2018). Nevertheless, patients may not benefit from CoQ10 therapy when severe renal and neurological damage is established. Hence, an early and accurate diagnosis of COQ10D6 and simultaneous CoQ10 intervention are critical in improving prognosis.

In this study, we identified a novel compound heterozygous variant of the *COQ6* gene in a nonconsanguineous Chinese family with two siblings presenting severe metabolic acidosis, proteinuria, hypoalbuminemia, growth retardation, and muscle hypotonia; the female proband also developed seizures. Genetic findings showed that both mutations, located in the Ubi-OHase domain of *COQ6*, are present in a region that is highly evolutionarily conserved across species. The mutations are predicted to be pathogenic, as confirmed by the death of our patients in early infancy. Collectively, our findings widen the spectrum of known *COQ6* mutations and provide an expanded understanding of the clinical spectrum of the rare genetic disease COQ10D6.

RESULTS

Clinical Presentations of the Family

The two affected siblings were conceived by a healthy, nonconsanguineous couple who denied having hepatitis, tuberculosis, diabetes, allergic diseases, or a history of hereditary disease. The mother of the patients has a history of miscarriages. A summary of the molecular findings and clinical and biochemical characteristics of the two cases harboring *COQ6* mutations is shown in **Table 1**. The pedigree of the family and the confirmation of the *COQ6* mutations are presented in **Figure 1A**.

Patient 1

The proband (III-3) was a Chinese girl born at full term *via* spontaneous vaginal delivery who weighed 3.1 kg. According to her parents, the infant had not achieved the expected increases in height and body weight by the age of 3 months. At the age of 4 months and 28 days, she was sent to our hospital due to repeated convulsion for 5 days. Metabolic and hearing exams were normal. The blood gas analysis indicated compensatory metabolic acidosis with an elevated lactate level (5.4 mmol/L), a pH of 7.39, and a bicarbonate level of 13.4 mmol/L. Biochemical assays revealed significantly decreased albumin (23.7 g/L) and increased blood lipids (triglyceride (TG), 15.80 mmol/L; total cholesterol (TC), 9.54 mmol/L). A decline in immunity was also observed with IgG <0.75 g/L, IgA <0.01 g/L, and IgM <0.20 g/L. The urine organic acid (UOA) analysis showed increased levels of lactate, 3-hydroxybutyric acid-2, pyruvic acid-OX-2, 4-hydroxy-phenyllactate-2, palmitic acid-1, and malic acid-3. A widening of the bilateral frontotemporal subarachnoid space was detected by enhanced computed tomography (CT) (**Figure 2C**), though her electroencephalogram (EEG) was normal. During hospitalization, the patient developed a seizure during which her hands were clenched; the seizure abated after half a minute. The girl was then transferred to a higher-level hospital at the request of her parents. Magnetic resonance imaging (MRI) demonstrated a widening of the bilateral frontotemporal subarachnoid space (**Figures 2D,E**) and delayed myelination of white matter (**Figure 2F**), but long-term EEG showed no abnormality. Laboratory testing indicated a markedly elevated TC level of 9.79 mmol/L, an IgG level of 0.1 g/L, a $CD19^+$ B cell percentage of 14.7%, a $CD3^+$ T-cell percentage of 72.8%, and a $CD4^+$ T-cell percentage of 50.3%. The girl's parents declined further genetic testing, and she was discharged home the next day.

At the age of 5 months and 22 days, she was admitted again to the Department of Pediatrics of our hospital because of pneumonia and dyspnea. Physical examination indicated that she had growth retardation, with a height of 54 cm and body weight of 5.5 kg, which were both below −3 SD, and she was unable to raise her head steadily. Laboratory tests revealed hypoalbuminemia (16 g/L), massive proteinuria (3+, total urine protein of 2,570 mg/24 h), edema, and elevated blood lipids (TG, 27.51 mmol/L; TC, 13.77 mmol/L), accompanied by metabolic acidosis and electrolyte disturbances including decreased Na^+ (119 mmol/L) and elevated K^+ (6.48 mmol/L). After admission, the patient received anti-infection and symptomatic treatment including repeated albumin for protein supplementation and repeated acid correction. Given the proband's clinical symptoms and age of onset, NS was considered and a blood sample was then collected for genetic testing. Unfortunately, she had persistent metabolic acidosis, hyponatremia, and hypoalbuminemia. She continued to deteriorate and died of respiratory failure and heart failure at the age of 5 months and 26 days.

TABLE 1 | Clinical characteristics and molecular findings in subjects with COQ6 mutations.

	Proband (III-3)	Sibling of proband (III-2)
COQ6 mutation	c.249C > G/c.1381C > T	c.249C > G/c.1381C > T
Sex	Female	Male
Pregnancy duration	Full term	Full term
Type of delivery	Spontaneous vaginal delivery	Spontaneous vaginal delivery
Age at presentation	4 months + 23 days	3 months + 22 days
Birth Weight (kg)	3.1	2.95
Birth length (cm)	50	50
Feeding difficulties	–	–
Respiratory distress	+	+
Muscle hypotonia	+	+
Seizure	+	–
SNHL	–	–
Edema	+	+
Lactate (mmol/L)	5.4	7.8
Proteinuria (mg/24 h)	2,570	n/a
Serum albumin(g/L)	23.7	24.8
UOA	Lactic acid-2, pyruvic acid-OX-2, 3-hydroxybutyric acid-2, palmitic acid-1, 4-hydroxy-phenyllactate-2, malic acid-3	n/a
Brain MRI or head CT	Bifrontal widening frontotemporal of the subarachnoid space; delayed myelination of white matter	Bifrontal widening frontotemporal of the subarachnoid space
Age at death	5 months + 26 days	4 months + 13 days

Note: SNHL, sensorineural hearing loss; UOA, urine organic acid; MRI, magnetic resonance imaging; CT, computed tomography; n/a, not done or not available.

Patient 2

Patient III-2 was the brother of the proband. He was also born at full term *via* spontaneous vaginal delivery with a birth weight of 2.95 kg. At the age of 3 months and 22 days, he was admitted to our hospital because of repeated abdominal distension for 3 months, along with dyspnea and cyanosis for half an hour. Upon hospitalization, physical examination was unremarkable except for dyspnea and poor growth and development, with a body weight of 4.5 kg and a height of 57 cm, which were both below −2 SD. Laboratory examination showed cytomegalovirus infection, proteinuria (2+), and occult blood (2+). Blood gas analysis indicated compensatory respiratory alkalosis combined with metabolic acidosis with lactate at 7.8 mmol/L. Moreover, he exhibited significant decreases in albumin (24.8 g/L) and total protein (40.7 g/L), along with an IgA level of 0.02 g/L and increased lactic acid dehydrogenase (1123 U/L) and TG (6.02 mmol/L). Cardiac ultrasound revealed an atrial septal defect and pulmonary hypertension, and an electrocardiogram showed altered sinus rhythm T waves. The patient did not undergo a metabolic study, but his neonatal screening was normal. Regrettably, the boy remained in a critical condition after the application of symptomatic treatment.

The patient was then transferred to a higher-level hospital at the request of the parents. Chest and abdominal CT detected pulmonary inflammation and slightly enlarged liver, and abdominal ultrasound showed enlarged kidneys and poor liver texture. A widening of the bifrontal frontotemporal region of the subarachnoid space was indicated by the cranial CT exhibited (**Figures 2A,B**). Meanwhile, laboratory tests showed hypoalbuminemia, proteinuria (2+), and edema as well as a decreased level of IgG (2.2 g/L). However, hypoalbuminemia was not ameliorated by symptomatic treatment, and he subsequently developed exacerbated lung infection and degressive transcutaneous oxygen saturation. Unfortunately, despite all treatments, he died due to pulmonary hemorrhage and respiratory failure at the age of 4 months and 13 days.

Genetic Findings

The proband (III-3) underwent genetic testing by WES. DNA samples from her parents and brother were tested to verify the variants using Sanger sequencing. As illustrated in **Figure 1B**, novel compound heterozygous mutations in the *COQ6* gene (NM_182476.3:exon2:c.249C > G (p.Tyr83Ter) and exon12: c.1381C > T (p.Gln461Ter)) were found in the proband (III-3) and her brother (III-2), and Sanger sequencing validation identified their parents as heterozygous carriers for one of the mutations.

Figure 3A shows a schematic of the *COQ6* gene containing the two identified variants, and the COQ6 protein with its functional domains was created. The first variant c.249C > G (p.Tyr83Ter) in exon 2 of 12 causes a change of amino acid 83 from tyrosine to a stop codon that results in a truncated protein or degradation and thus probably greatly affects the structure and function of the *COQ6* enzyme. *COQ6* variant c.1381C > T (p.Gln461Ter) occurs at the last exon and leads to a deletion of seven amino acids from the Ubi-OHases domain of *COQ6*. Evolutionarily, a tyrosine at position 83 and a glutamine at position 461 of the *COQ6* enzyme are highly conserved among various species (**Figure 3B**). According to the gnomAD database, these variants are detected with no homozygosity at allele frequencies of 0.00003185 and 0.00003188, demonstrating that they are not common benign variants in the populations included in the database. Furthermore, both variants are absent from ClinVar, and no previous patient with either variant has been described in

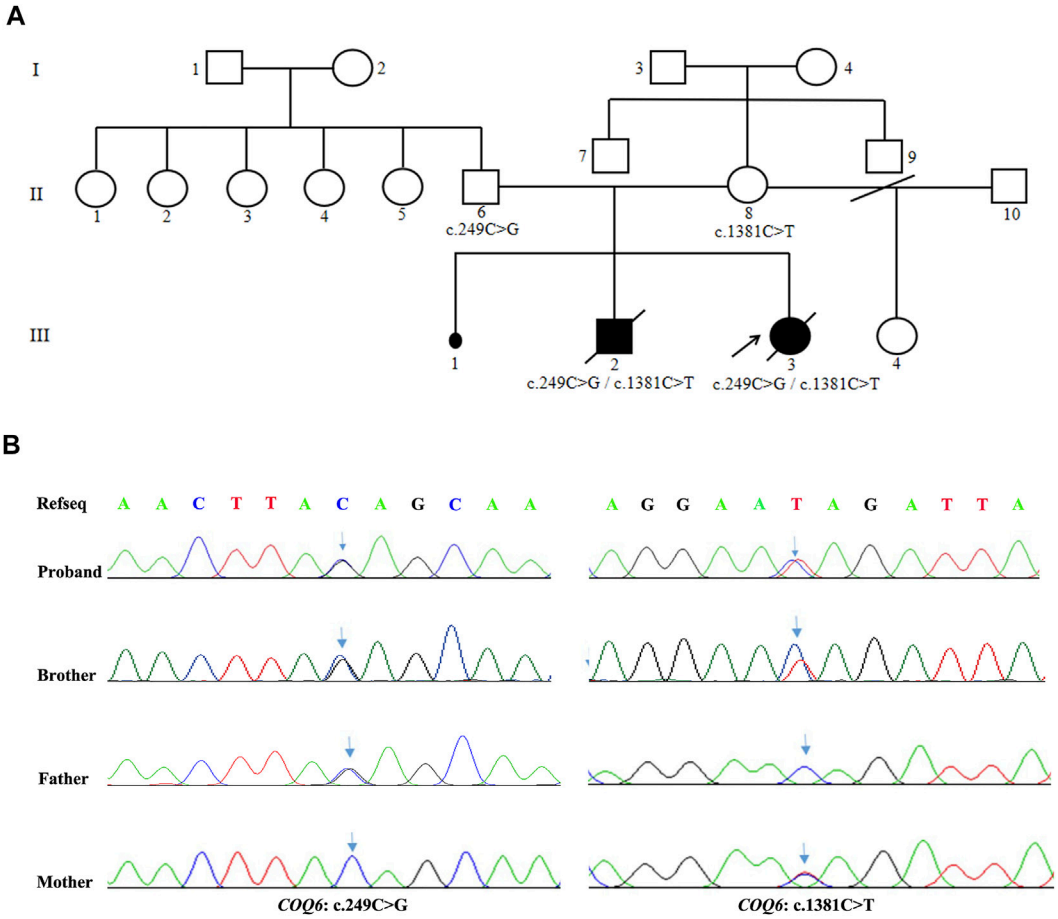

FIGURE 1 | Family pedigree and confirmation of the compound heterozygous variants of *COQ6*. **(A)** Pedigree shows the cosegregation of *COQ6* mutations in the family. The patient pointed by the arrow indicates the proband. Black symbols indicate clinically affected members, and open symbols represent unaffected individuals. **(B)** Validation of *COQ6* variants in the family by Sanger sequencing, and the arrows represent sites of mutation.

the literature to date. Using MutationTaster, p.Tyr83Ter and p.Gln461Ter are predicted to be disease-causing variants and p.Tyr83Ter may lead to nonsense-mediated decay (NMD).

DISCUSSION

In the present study, we report two novel pathogenic *COQ6* mutations: c.249C > G (p.Tyr83Ter) and c.1381C > T (p.Gln461Ter), which, in a compound heterozygous state, resulted in two siblings with clinical presentations of COQ10D6 characterized by renal involvements including hypoalbuminemia, proteinuria and edema, and extra-renal manifestations including growth retardation, muscle hypotonia, and/or seizures. Both mutations cosegregated with the disease, and the pathogenicity of the two *COQ6* variants was confirmed by the clinical symptoms of our patients, the analysis of human genome variation databases, and *in silico* predictions.

CoQ10, also known as ubiquinone, is an important component of the mitochondrial electron transport chain; this compound exerts many effects, such as countering oxidation, regulating calcium homeostasis, improving mitochondrial function, and preventing cellular apoptosis (Hargreaves et al., 2020). To date, pathogenic mutations in 10 genes (*PDSS1*, *PDSS2*, *COQ2*, *COQ4*, *COQ6*, *COQ7*, *COQ8A/ADCK3*, *COQ8B/ADCK4*, and *COQ9*) involved in the biosynthesis of CoQ10 have been reported to cause primary CoQ10 deficiency, which has variable clinical symptoms ranging from fatal neonatal multisystem disorder to adult-onset encephalopathy or nephropathy (Desbats et al., 2015; Acosta et al., 2016). Several pathogenic mutations in the *COQ6* gene are known to cause kidney dysfunction such as SRNS and extrarenal manifestations such as SHNL, seizures, growth retardation, and mild muscle weakness in the lower extremities (Heeringa et al., 2011; Cao et al., 2014; Park et al., 2017). The clinical manifestations in our cases and other reported patients are summarized in **Table 2**.

A mutation of the *COQ6* gene was first reported as a cause of primary CoQ10 deficiency in the study of Heeringa et al. (2011) The authors reported that all affected patients ($n = 11$) presenting with SRNS and SNHL showed proteinuria with a median onset age of 1.2 years (range, 0.2–6.4 years) and ESRD with a median onset age of 1.7 years (range, 0.4–9.3 years); five cases also

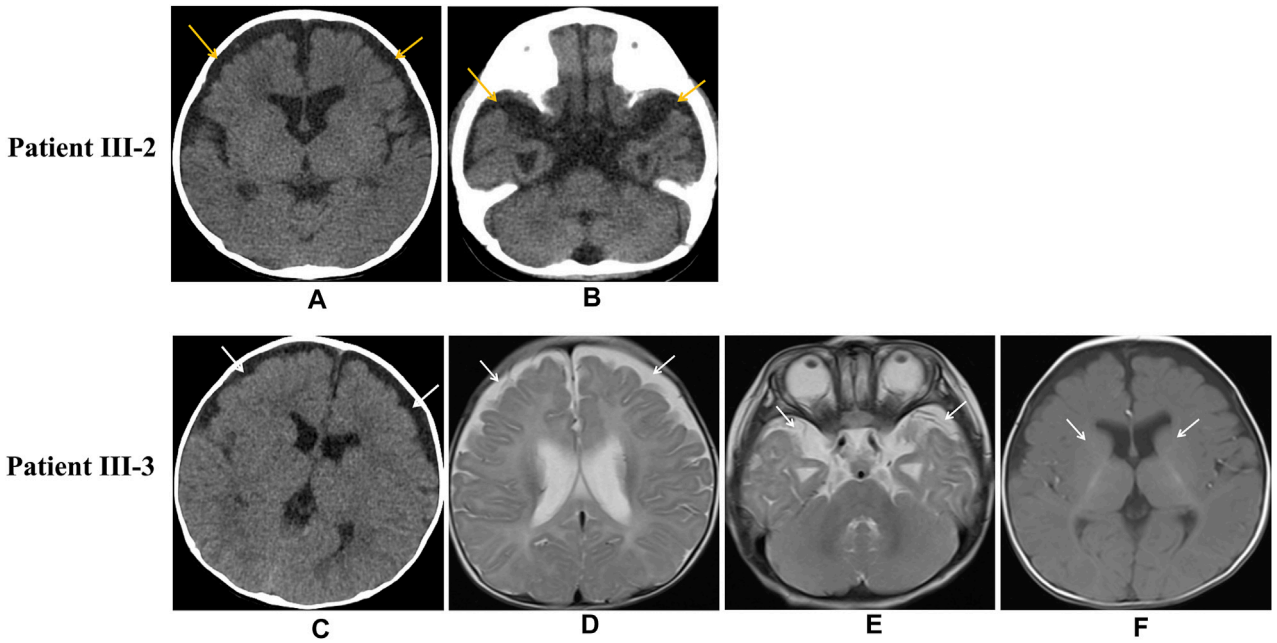

FIGURE 2 | Imaging of patient III-2 and patient III-3. Unenhanced head CT indicates widening of the bifrontal frontotemporal subarachnoid space in patient III-2 (**Figures 2A,B**) Unenhanced head CT of patient III-3 shows bifrontal widening frontotemporal of the subarachnoid space (**Figure 2C**), and axial MRI shows bifrontal widening frontotemporal of the subarachnoid space (**Figures 2D,E**) and delayed myelination of white matter (**Figure 2F**).

presented with extrarenal involvement such as white matter abnormalities, seizures, ataxia, and facial dysmorphism. Gigante et al. (2017) reported an 8-month-old Italian boy with SRNS that progressed to ESRD when he was 20 months old but with no extra-renal involvements; the pathogenicity of the *COQ6* p.Pro261Leu allele was then confirmed by rescue experiments in yeast. Park et al. (2017) reported six unrelated Korean children with SRNS and hearing loss, and mild muscle weakness of the lower extremities and ocular manifestations including bilateral optic nerve atrophy and exotropia were observed in four patients. The patients developed SRNS with onset at a median onset of 29 (range, 15–47) months and ERSD with onset at a median onset of 45 (range, 17–73) months; five of the patients underwent kidney transplantation without FSGS recurrence. Of note, these above patients with *COQ6* defects manifested SRNS during childhood, and all cases progressed to ERSD within 1–2 years of onset. Furthermore, some affected individuals received timely high-dosage oral CoQ10 administration after *COQ6* mutations were detected, and their renal function and psychomotor development have been improved (Cao et al., 2017; Stanczyk et al., 2018; Justine et al., 2020). Remarkably, patients may not benefit from CoQ10 therapy after severe renal and neurological damages occur. These observations suggest that once COQ10D6 is suspected clinically, immediate CoQ10 treatment and detection of *COQ6* mutations would be helpful for the improvement of patient prognosis.

Notably, clinical heterogeneity has been observed in patients carrying the same *COQ6* mutations (see **Table 2**). For example, a 7-year-old girl from Turkey showed only SRNS without other systemic symptoms due to a homozygous *COQ6* mutation c.1058C > A (p.Ala353Asp), while her elder brother harboring the same *COQ6* mutation exhibited normal renal functions without any neurological presentations and developed SNHL at 10 years old (Yuruk et al., 2020). Additionally, Heeringa et al. (Heeringa et al., 2011) reported six patients with the *COQ6* variant c.763G > A (p.Gln255Arg) who all had SRNS with or without other extrarenal presentations such as SNHL, seizures, white matter abnormalities, and facial dysmorphism. Similarly, our patients with the same *COQ6* mutations displayed variable clinical presentations, whereby the proband satisfying the diagnostic criteria of NS also showed growth retardation and muscle hypotonia in addition to seizures, which were not present in her older brother. Unlike most cases reported previously, our cases died in early infancy. Our findings highlight the clinical heterogeneity and the severity of the disorder caused by *COQ6* defects.

Moreover, we uncovered two novel and rare pathogenic mutations in *COQ6*, which are essential for CoQ10 biosynthesis, and these findings contribute to the known genotypic spectrum of COQ10D6. To date, seven mutations in *COQ6*, including missense mutations, indels, and frameshifts, have been reported in the Human Gene Mutation Database (HGMD). To confirm the deleterious effect of p.Gln461Ter on *COQ6* function, we evaluated the secondary structure of *COQ6* with p.Gln461Ter mutation using PredictProtein and found that it affected the secondary structure and solvent to some extent (**Figure 4A**). The Gln461Ter led to a deletion of seven amino acids of the *COQ6* C-terminus located on the surface of the active site (Doimo et al., 2014), which was confirmed to be functionally important by a recent study demonstrating that the deletion of 25 amino acids at the *COQ6* C-terminus leads to impaired CoQ10

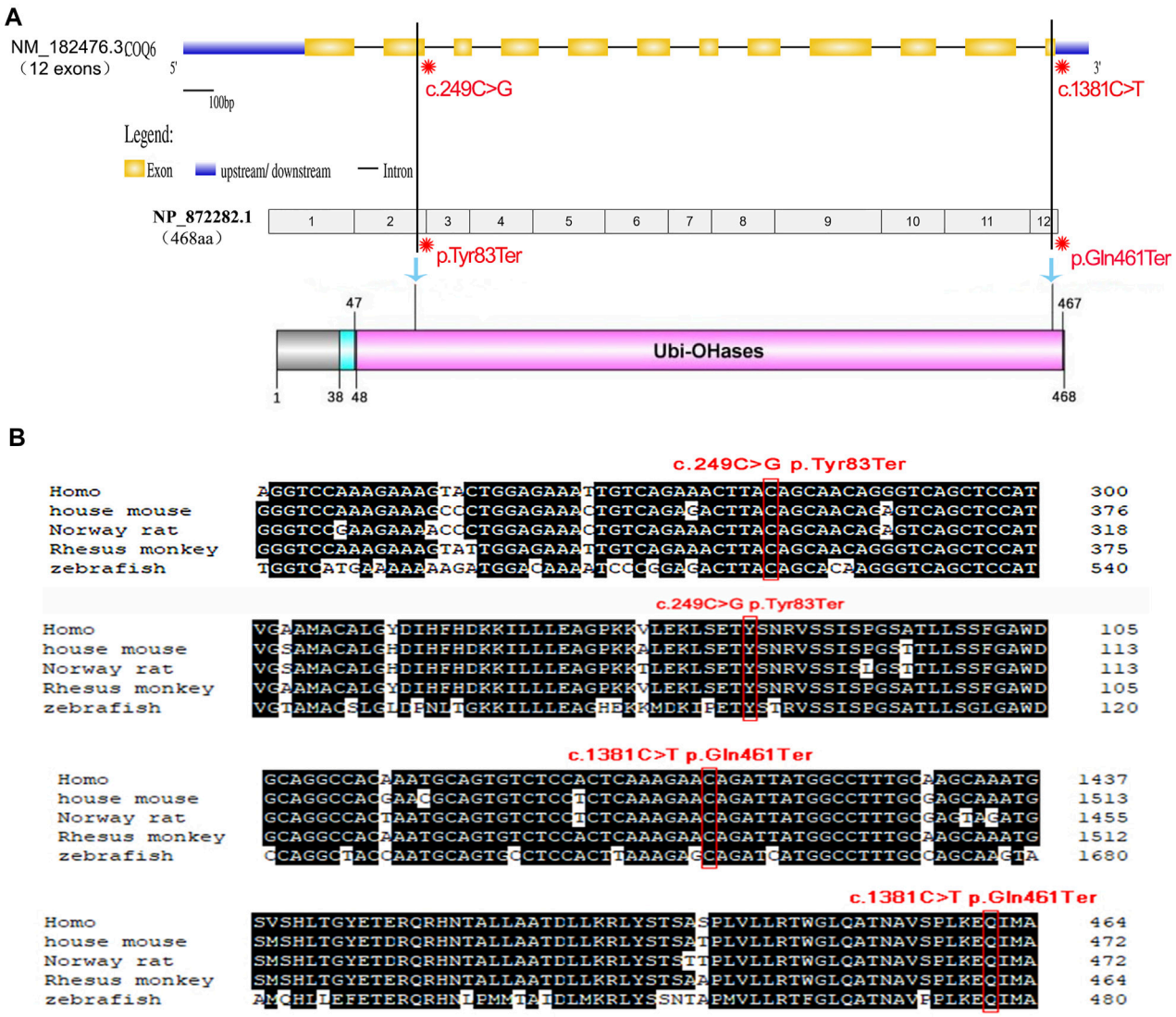

FIGURE 3 | Schematic of the gene structure and domain structure of *COQ6* protein and conservation analysis of the two nonsense mutations detected in the family. **(A)** The *COQ6* gene containing 12 exons (yellow boxes) was exhibited using the UDSD online database, and the location of the two variants is tagged in the *COQ6* exon region and its corresponding Ubi-OHases domain. **(B)** Comparative analysis of genome sequences or CDSs across species indicates that the two mutant sites are evolutionarily highly conserved.

synthesis (Acosta et al., 2019). These results suggest that the two novel *COQ6* mutants identified in our study are likely both loss-of-function variants; the p.Try81Ter causes NMD and p.Gln461Ter perturbs the active site and secondary structure of the COQ6 protein. In addition, *COQ6* was found to correlate closely with *COQ3*, *COQ4*, *COQ5*, *COQ7*, and *COQ9* in a PPI network (**Figure 4B**). Human PDSS2, *COQ4*, *COQ6*, and *COQ7* could form a protein complex in human mitochondria, and the knockdown of *COQ6* markedly resulted in reduced levels of *COQ3*; this, in turn, causes an obvious decrease of *COQ7*, which is crucial for maintaining the mitochondrial function (Yen et al., 2020). Furthermore, the decreased expression of the COQ6 protein was revealed to cause kidney damage by inducing mitochondrial dysfunction and apoptosis in podocytes (Song et al., 2018). Thus, we suspect that the candidate pathogenic variants (p.Tyr83Ter and p.Gln461Ter) may impede the interaction between COQ6 and other mitochondrial proteins in the CoQ complex, thus disrupting the pathway of CoQ10 biosynthesis and ultimately impairing renal function. This may be the reason for the more severe phenotype in the current cases.

However, the present study had some limitations. Due to premature mortality in infancy, we could not confirm our molecular finding through the detection of CoQ10 levels in skeletal muscle and the level of COQ6 protein in skin fibroblasts from patients. Although the pathogenicity of the two novel *COQ6* variants identified in our study is explained by several findings, including the clinical phenotype of the two

TABLE 2 | Genotypic and phenotypic characteristics of the detected *COQ6* variants in the published literature and the present study.

Origin	Age at onset (year)	Age at ESRD (year)	*COQ6* mutations	Zygosity	Renal involvement	Extra-renal involvement	Effect of CoQ10 and its analogue treatment	References
China	0.4	No	c.249C > G (p.Tyr83Ter) c.1381C > T (p.Gln461Ter)	Heterozygous	NS	Growth retardation, seizures, muscle hypotonia	ND	Current study
China	0.3	No	c.249C > G (p.Tyr83Ter) c.1381C > T (p.Gln461Ter)	Heterozygous	Proteinuria	Growth retardation, muscle hypotonia	ND	Current study
Turkey	0.2	NA	c.763G > A (p.Gln255Arg)	Homozygous	SRNS	SNHL, bilateral nephrolithiasis, growth retardation	Recovery of kidney function	Heeringa et al. (2011)
Turkey	0.3	0.4	c.763G > A (p.Gln255Arg)	Homozygous	SRNS	SNHL, facial dysmorphism	SNHL substantially improved	Heeringa et al. (2011)
Turkey	0.3	0.4	c.763G > A (p.Gln255Arg)	Homozygous	SRNS	Seizures	ND	Heeringa et al. (2011)
Lebanon	0.3	1.7	c.763G > A (p.Gln255Arg)	Homozygous	SRNS	SNHL	ND	Heeringa et al. (2011)
Lebanon	<1.0	3.0	c.763G > A (p.Gln255Arg)	Homozygous	SRNS	SNHL	ND	Heeringa et al. (2011)
Lebanon	1.2	1.4	c.763G > A (p.Gln255Arg)	Homozygous	SRNS	SNHL, ataxia	ND	Heeringa et al. (2011)
Lebanon	6.4	9.3	c.763G > A (p.Gln255Arg)	Homozygous	SRNS	SNHL	ND	Heeringa et al. (2011)
Turkey	2.5	3.4	c.1058C > A (p.Ala353Asp)	Homozygous	SRNS	SNHL, seizures, white matter abnormalities	ND	Heeringa et al. (2011)
Turkey	6.0	6.5	c.1058C > A (p.Ala353Asp)	Homozygous	SRNS	SNHL	ND	Heeringa et al. (2011)
Turkey	2.5	NA	c.1058C > A (p.Ala353Asp)	Homozygous	SRNS	SNHL	Remission of proteinuria	Heeringa et al. (2011)
Turkey	3.0	NA	c.1341G > A (p.Trp447Ter) c.1383delG (p.Gln461fsTer478)	Heterozygous	SRNS	SNHL	ND	Heeringa et al. (2011)
European	4.5	NA	c.1154A > C (p.Asp385Ala) c.1235A > G (p.Tyr412Cys)	Heterozygous	SRNS	NA	ND	Sadowski et al. (2015)
China	0.8	NA	c.1078C > T (p.R360W)	Homozygous	SRNS	SNHL, growth retardation, muscle hypotonia	Complete remission of NS; improved psychomotor development	Cao et al. (2017)
Korea	1.2	1.4	c.189_191delGAA (p.Lys64del); c.782C > T (p.Pro261Leu)	Heterozygous	SRNS	SNHL, bilateral optic nerve atrophy	NA	Park et al. (2017)
Korea	1.9	2.6	c.189_191delGAA (p.Lys64del); c.686A > C (p.Gln229Pro)	Heterozygous	SRNS	SNHL, extropia with nistagmus on both eyes	NA	Park et al. (2017)
Korea	2.0	3.6	c.189_191delGAA (p.Lys64del); c.782C > T (p.Pro261Leu)	Heterozygous	SRNS	SNHL, mild muscle weakness in the lower extremities	NA	Park et al. (2017)
Korea	2.6	4.6	c.189_191delGAA (p. Lys64del); c.782C > T (p.Pro261Leu)	Heterozygous	SRNS	SNHL	NA	Park et al. (2017)
Korea	3.8	6.1	c.189_191delGAA (p. Lys64del); c.782C > T (p.Pro261Leu)	Heterozygous	SRNS	SNHL, mild muscle weakness in the lower extremities	NA	Park et al. (2017)
Korea	3.9	4.0	c.189_191delGAA (p. Lys64del); c.782C > T (p.Pro261Leu)	Heterozygous	SRNS	SNHL	NA	Park et al. (2017)
Italy	0.6	1.7	c.782C > T (p.Pro261Leu)	Homozygous	SRNS	None	Delayed neurological disease	Gigante et al. (2017)
China	16	NA	c.41G > A (p.Try14Ter)	Homozygous	SRNS	None	ND	Song et al. (2018)
China	0.2	NA	c.1078C > T (p.R360W)	Homozygous	Congenital NS	None	ND	Li et al. (2018)
Poland	2.0	NA	c.1078C > T (p. Arg360Trp); c.804delC (p.Leu269TrpfsTer13)	Heterozygous	SRNS	None	Complete remission of NS	Stanczyk et al. (2018)

(Continued on following page)

TABLE 2 | (*Continued*) Genotypic and phenotypic characteristics of the detected *COQ6* variants in the published literature and the present study.

Origin	Age at onset (year)	Age at ESRD (year)	*COQ6* mutations	Zygosity	Renal involvement	Extra-renal involvement	Effect of CoQ10 and its analogue treatment	References
Japan	0.8	NA	c.782C > T (p.Pro261Leu)	Heterozygous	SRNS	None	Complete remission of proteinuria	Nakanishi et al. (2019)
Turkey	7.0	8.0	c.1058C > A (p.Ala353Asp)	Homozygous	SRNS	None	Kidney function improved with No complications related with the renal transplantation	Yuruk et al. (2020)
Turkey	10	NA	c.1058C > A (p.Ala353Asp)	Homozygous	None	SNHL	Delayed renal or neurological disease	Yuruk et al. (2020)
Turkey	NA	5.0	c.1058C > A (p.Ala353Asp)	Homozygous	SRNS	SNHL, optic atrophy	Visual acuity improved	Justine et al. (2020)
Turkey	4.0	NA	c.1058C > A (p.Ala353Asp)	Homozygous	SRNS	SNHL	Remission of proteinuria; unchanged hearing loss	Justine et al. (2020)

Note: ESRD, end-stage renal disease; NS, nephrotic syndrome; SNHL, sensorineural hearing loss; SRNS, steroid-resistant nephrotic syndrome; ND, not done; NA, not available.

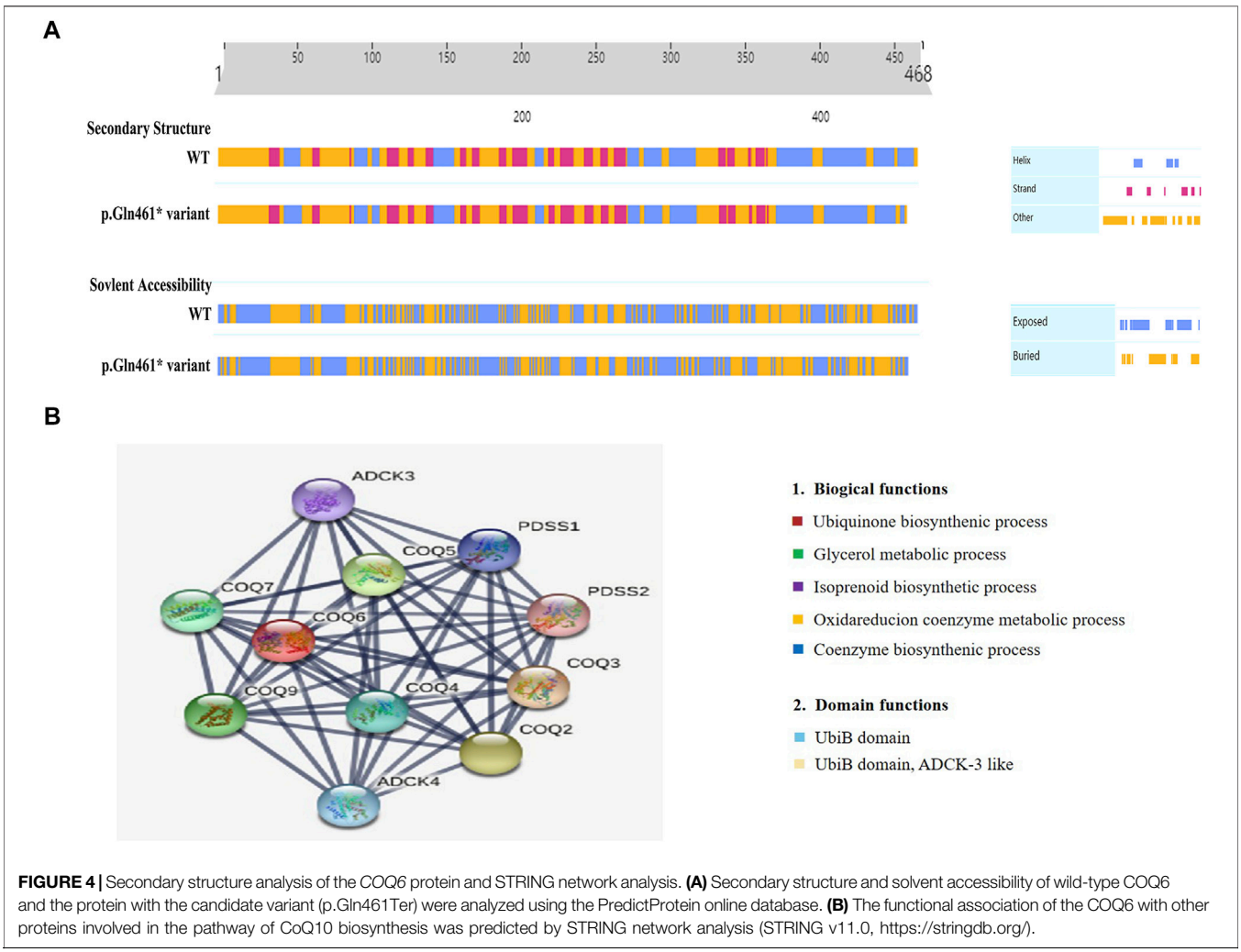

FIGURE 4 | Secondary structure analysis of the *COQ6* protein and STRING network analysis. **(A)** Secondary structure and solvent accessibility of wild-type COQ6 and the protein with the candidate variant (p.Gln461Ter) were analyzed using the PredictProtein online database. **(B)** The functional association of the COQ6 with other proteins involved in the pathway of CoQ10 biosynthesis was predicted by STRING network analysis (STRING v11.0, https://stringdb.org/).

probands overlapping with patients harboring *COQ6* mutations as previously reported, the segregation with the disease, and bioinformatics predictions, in-depth studies are still needed to further determine the impact of the two candidate mutations on *COQ6* gene expression and function.

In conclusion, our study provides the first report of a novel compound heterozygous pathogenic variant of the *COQ6* gene in a Chinese family with severe COQ10D6. Our cases widen the genotypic spectrum of COQ10D6 and highlight the heterogeneity and severity of clinical features associated with *COQ6* mutations. An early diagnosis of *COQ*6 pathogenic mutations in such cases with clinical presentations suggestive of COQ10D6 will facilitate disease diagnosis and therapeutic interventions as well as disease prevention in future generations.

MATERIALS AND METHODS

Ethics Statement

The study was performed in accordance with the Declaration of Helsinki and approved by the Ethics Committee of Taizhou Hospital of Zhejiang Province Affiliated to Wenzhou Medical University. Informed consent was obtained from the family before gene testing.

Subjects

We collected blood samples and pedigrees after obtaining informed consent from the family. The two affected siblings were diagnosed with infantile NS by pediatric nephrologists based on the age of presentation (4–12 months) and the diagnostic criteria of NS, including serum albumin ≤25 g/L, proteinuria (24 h urine greater than 50 mg/kg/day), and hyperlipidemia (elevated cholesterol and/or triglycerides) (Lombel et al., 2013); (Wang and Greenbaum 2019). The clinical and molecular biological characteristics of the affected individuals were analyzed retrospectively.

Genetic Testing

Genomic deoxyribonucleic acid was isolated from the patient's whole blood, and exome sequencing was conducted using an Illumina NovaSeq 6000 sequencing system with 150 bp paired-end reads at an average 100× sequencing depth to cover the maximum genomic variations. The DNA sequence was aligned to the UCSC hg19/GRCh37 reference sequence. Variant calls and annotation were performed with a pipeline based on the Burrows–Wheeler aligner, in-house software, the Genome Aggregation Database (gnomAD), ClinVar, and custom annotation scripts. Thereafter, Sanger sequencing analysis was performed for variant confirmation and segregation using target sequence-specific primers on an ABI 3730xl sequencer and analyzed using Sequencing Analysis Software v5.2 (Applied Biosystems) and SeqMan (DNASTAR) according to the manufacturer's instructions.

In Silico Analysis

For the evolutionary conservation analysis of *COQ6* candidate variants, the alignment of gene sequences and complete coding sequences from different species were conducted using DNAMAN, including human (NP_872282.1), rhesus monkey (XP_014999576.2), house mouse (NP_766170.2), Norway rat (NP_001011 983.1), and zebrafish (NP_001038869.1). Next, the pathogenicity of the variants was predicted by using MutationTaster, and the possible influence of the detected variants on the structure and function of the COQ6 protein was evaluated by PredictProtein. The diagram of the functional protein association network was depicted based on the STRING (https://string-db.org/) database, which was used to predict protein–protein interactions.

DATA AVAILABILITY STATEMENT

The datasets for this article are not publicly available due to concerns regarding participant/patient anonymity. Requests to access the datasets should be directed to the corresponding authors.

ETHICS STATEMENT

The studies involving human participants were reviewed and approved by The Ethics Committee of Taizhou Hospital of Zhejiang Province affiliated with Wenzhou Medical University. Written informed consent to participate in this study was provided by the participants' legal guardian/next of kin. Written informed consent was obtained from the individual(s), and minor(s)' legal guardian/next of kin, for the publication of any potentially identifiable images or data included in this article.

AUTHOR CONTRIBUTIONS

NW conceived of the study, analyzed the data and wrote the manuscript. YZ provided the clinical samples. YZ and LZ participated in the clinical data collection and clinical evaluations. XT conducted the bioinformatics analysis. FC interpreted the brain MRI and head CT of the patients. MQ, JD, and SC performed the genetics analysis. SC and JL conducted the biochemical analysis. BS and LW critically commented and revised the manuscript. All authors have read and approved the final version of the manuscript.

ACKNOWLEDGMENTS

We would like to thank the patients and their family members for participating in our study. We also thank Dian Diagnostics for their excellent technical assistance. Finally, we sincerely thank Children's Hospital of Fudan University and The Children's Hospital, Zhejiang University School of Medicine for providing patient imaging data.

REFERENCES

Acosta Lopez, M. J., Trevisson, E., Canton, M., Vazquez-Fonseca, L., Morbidoni, V., Baschiera, E., et al. (2019). Vanillic Acid Restores Coenzyme Q Biosynthesis and ATP Production in Human Cells LackingCOQ6. *Oxidative Med. Cell Longevity* 2019, 1–11. doi:10.1155/2019/3904905

Acosta, M. J., Vazquez Fonseca, L., Desbats, M. A., Cerqua, C., Zordan, R., Trevisson, E., et al. (2016). Coenzyme Q Biosynthesis in Health and Disease. *Biochim. Biophys. Acta (Bba) - Bioenerg.* 1857 (8), 1079–1085. doi:10.1016/j.bbabio.2016.03.036

Cao, Q., Li, G. M., Xu, H., Shen, Q., Sun, L., Fang, X. Y., et al. (2017). Coenzyme Q(10) Treatment for One Child with COQ6 Gene Mutation Induced Nephrotic Syndrome and Literature Review. *Zhonghua Er Ke Za Zhi* 55 (2), 135–138. doi:10.3760/cma.j.issn.0578-1310.2017.02.016

Cheong, H. I. (2020). Genetic Tests in Children with Steroid-Resistant Nephrotic Syndrome. *Kidney Res. Clin. Pract.* 39 (1), 7–16. doi:10.23876/j.krcp.20.001

Desbats, M. A., Lunardi, G., Doimo, M., Trevisson, E., and Salviati, L. (2015). Genetic Bases and Clinical Manifestations of Coenzyme Q10 (CoQ10) Deficiency. *J. Inherit. Metab. Dis.* 38 (1), 145–156. doi:10.1007/s10545-014-9749-9

Doimo, M., Trevisson, E., Airik, R., Bergdoll, M., Santos-Ocaña, C., Hildebrandt, F., et al. (2014). Effect of Vanillic Acid on COQ6 Mutants Identified in Patients with Coenzyme Q10 Deficiency. *Biochim. Biophys. Acta (Bba) - Mol. Basis Dis.* 1842 (1), 1–6. doi:10.1016/j.bbadis.2013.10.007

Gigante, M., Diella, S., Santangelo, L., Trevisson, E., Acosta, M. J., Amatruda, M., et al. (2017). Further Phenotypic Heterogeneity of CoQ10 Deficiency Associated with Steroid Resistant Nephrotic Syndrome and Novel COQ2 and COQ6 Variants. *Clin. Genet.* 92 (2), 224–226. doi:10.1111/cge.12960

Greenbaum, L. A., Benndorf, R., and Smoyer, W. E. (2012). Childhood Nephrotic Syndrome-Current and Future Therapies. *Nat. Rev. Nephrol.* 8 (8), 445–458. doi:10.1038/nrneph.2012.115

Hargreaves, I., Heaton, R. A., and Mantle, D. (2020). Disorders of Human Coenzyme Q10 Metabolism: An Overview. *Ijms* 21 (18), 6695. doi:10.3390/ijms21186695

Heeringa, S. F., Chernin, G., Chaki, M., Zhou, W., Sloan, A. J., Ji, Z., et al. (2011). COQ6 Mutations in Human Patients Produce Nephrotic Syndrome with Sensorineural Deafness. *J. Clin. Invest.* 121 (5), 2013–2024. doi:10.1172/JCI45693

Justine Perrin, R., Rousset-Rouvière, C., Garaix, F., Cano, A., Conrath, J., Boyer, O., et al. (2020). COQ6 Mutation in Patients with Nephrotic Syndrome, Sensorineural Deafness, and Optic Atrophy. *JIMD Rep.* 54 (1), 37–44. doi:10.1002/jmd2.12068

Li, G.-m., Cao, Q., Shen, Q., Sun, L., Zhai, Y.-h., Liu, H.-m., et al. (2018). Gene Mutation Analysis in 12 Chinese Children with Congenital Nephrotic Syndrome. *BMC Nephrol.* 19 (1), 382. doi:10.1186/s12882-018-1184-y

Lombel, R. M., Gipson, D. S., and Hodson, E. M. (2013). Treatment of Steroid-Sensitive Nephrotic Syndrome: New Guidelines from KDIGO. *Pediatr. Nephrol.* 28 (3), 415–426. doi:10.1007/s00467-012-2310-x

Lovric, S., Ashraf, S., Tan, W., and Hildebrandt, F. (2016). Genetic Testing in Steroid-Resistant Nephrotic Syndrome: When and How? *Nephrol. Dial. Transpl.* 31 (11), 1802–1813. doi:10.1093/ndt/gfv355

Nagano, C., Yamamura, T., Horinouchi, T., Aoto, Y., Ishiko, S., Sakakibara, N., et al. (2020). Comprehensive Genetic Diagnosis of Japanese Patients with Severe Proteinuria. *Sci. Rep.* 10 (1), 270. doi:10.1038/s41598-019-57149-5

Nakanishi, K., Okamoto, T., Nozu, K., Hara, S., Sato, Y., Hayashi, A., et al. (2019). Pair Analysis and Custom Array CGH Can Detect a Small Copy Number Variation in COQ6 Gene. *Clin. Exp. Nephrol.* 23 (5), 669–675. doi:10.1007/s10157-018-1682-z

Noone, D. G., Iijima, K., and Parekh, R. (2018). Idiopathic Nephrotic Syndrome in Children. *The Lancet* 392 (10141), 61–74. doi:10.1016/S0140-6736(18)30536-1

Park, E., Ahn, Y. H., Kang, H. G., Yoo, K. H., Won, N. H., Lee, K. B., et al. (2017). COQ6 Mutations in Children with Steroid-Resistant Focal Segmental Glomerulosclerosis and Sensorineural Hearing Loss. *Am. J. Kidney Dis.* 70 (1), 139–144. doi:10.1053/j.ajkd.2016.10.040

Park, E., Lee, C., Kim, N. K. D., Ahn, Y. H., Park, Y. S., Lee, J. H., et al. (2020). Genetic Study in Korean Pediatric Patients with Steroid-Resistant Nephrotic Syndrome or Focal Segmental Glomerulosclerosis. *Jcm* 9 (6), 2013. doi:10.3390/jcm9062013

Quinzii, C. M., Emmanuele, V., and Hirano, M. (2014). Clinical Presentations of Coenzyme Q10 Deficiency Syndrome. *Mol. Syndromol* 5 (3-4), 141–146. doi:10.1159/000360490

Sadowski, C. E., Lovric, S., Ashraf, S., Pabst, W. L., Gee, H. Y., Kohl, S., et al. (2015). A Single-Gene Cause in 29.5% of Cases of Steroid-Resistant Nephrotic Syndrome. *J. Am. Soc. Nephrol.* 26 (6), 1279–1289. doi:10.1681/ASN.2014050489

Song, C.-C., Hong, Q., Geng, X.-D., Wang, X., Wang, S.-Q., Cui, S.-Y., et al. (2018). New Mutation of Coenzyme Q10 Monooxygenase 6 Causing Podocyte Injury in a Focal Segmental Glomerulosclerosis Patient. *Chin. Med. J. (Engl).* 131 (22), 2666–2675. doi:10.4103/0366-6999.245158

Stańczyk, M., Bałasz-Chmielewska, I., Lipska-Ziętkiewicz, B., and Tkaczyk, M. (2018). CoQ10-related Sustained Remission of Proteinuria in a Child with COQ6 Glomerulopathy-A Case Report. *Pediatr. Nephrol.* 33 (12), 2383–2387. doi:10.1007/s00467-018-4083-3

Trautmann, A., Schnaidt, S., Lipska-Ziętkiewicz, B. S., Bodria, M., Ozaltin, F., Emma, F., et al. (2017). Long-Term Outcome of Steroid-Resistant Nephrotic Syndrome in Children. *Jasn* 28 (10), 3055–3065. doi:10.1681/ASN.2016101121

Wang, C.-s., and Greenbaum, L. A. (2019). Nephrotic Syndrome. *Pediatr. Clin. North America* 66 (1), 73–85. doi:10.1016/j.pcl.2018.08.006

Wang, F., Zhang, Y., Mao, J., Yu, Z., Yi, Z., Yu, L., et al. (2017). Spectrum of Mutations in Chinese Children with Steroid-Resistant Nephrotic Syndrome. *Pediatr. Nephrol.* 32 (7), 1181–1192. doi:10.1007/s00467-017-3590-y

Warejko, J. K., Tan, W., Daga, A., Schapiro, D., Lawson, J. A., Shril, S., et al. (2018). Whole Exome Sequencing of Patients with Steroid-Resistant Nephrotic Syndrome. *Cjasn* 13 (1), 53–62. doi:10.2215/CJN.04120417

Yen, H.-C., Yeh, W.-Y., Lee, S.-H., Feng, Y.-H., and Yang, S.-L. (2020). Characterization of Human Mitochondrial PDSS and COQ Proteins and Their Roles in Maintaining Coenzyme Q10 Levels and Each Other's Stability. *Biochim. Biophys. Acta (Bba) - Bioenerg.* 1861 (7), 148192. doi:10.1016/j.bbabio.2020.148192

Yuruk Yildirim, Z., Toksoy, G., Uyguner, O., Nayir, A., Yavuz, S., Altunoglu, U., et al. (2020). Primary Coenzyme Q10 Deficiency-6 (COQ10D6): Two Siblings with Variable Expressivity of the Renal Phenotype. *Eur. J. Med. Genet.* 63 (1), 103621. doi:10.1016/j.ejmg.2019.01.011

Conflict of Interest: Author MQ is employed by DIAN Diagnostics.

The remaining authors declare that the research was conducted in the absence of any commercial or financial relationships that could be construed as a potential conflict of interest.

frontiers in Pediatrics

CASE REPORT
published: 03 February 2022
doi: 10.3389/fped.2021.803732

Case Report: Reinterpretation and Reclassification of *ARSB*:p.Arg159Cys Variant Identified in an Emirati Patient With Hearing Loss Caused by a Pathogenic Variant in the *CDH23* Gene

Nahid Al Dhahouri[1], *Amanat Ali*[1], *Jozef Hertecant*[2] *and Fatma Al-Jasmi*[1,2*]

[1] *Department of Genetics and Genomics, College of Medicine and Health Sciences, United Arab Emirates University, Al-Ain, United Arab Emirates,* [2] *Department of Pediatrics, Tawam Hospital, Al-Ain, United Arab Emirates*

OPEN ACCESS

Edited by:
Huiwen Zhang,
Xinhua Hospital, China

Reviewed by:
Munis Dundar,
Erciyes University, Turkey
Mohiuddin Mohammed Taher,
Umm Al-Qura University, Saudi Arabia

***Correspondence:**
Fatma Al-Jasmi
aljasmif@uaeu.ac.ae

Specialty section:
This article was submitted to Genetics of Common and Rare Diseases, a section of the journal Frontiers in Pediatrics

Received: *28 October 2021*
Accepted: *16 December 2021*
Published: *03 February 2022*

Citation:
Al Dhahouri N, Ali A, Hertecant J and Al-Jasmi F (2022) Case Report: Reinterpretation and Reclassification of ARSB:p.Arg159Cys Variant Identified in an Emirati Patient With Hearing Loss Caused by a Pathogenic Variant in the CDH23 Gene. Front. Pediatr. 9:803732. doi: 10.3389/fped.2021.803732

Arylsulfatase B is an enzyme present in the lysosomes that involves in the breakdown of large sugar molecules known as glycosaminoglycans (GAGs). Arylsulfatase B chemically modifies two GAGs, namely, dermatan sulfate and chondroitin sulfate, by removing the sulfate group. Mutations in the gene encoding the arylsulfataseB enzyme causes lysosomal storage disorder, mucopolysaccharidosis type VI (MPS VI), or Maroteaux–Lamy syndrome. In this study, we report a case of congenital hearing loss with mild pigmentary changes in the retina, indicative of Usher syndrome, and a missense variant reported as likely pathogenic for MPS VI. Sequencing results identified a pathogenic missense variant p.Arg1746Gln in the *CDH23* gene. However, another missense variant *ARSB*:p.Arg159Cys was reported as likely pathogenic to the treating physician. Mutations in *ARSB* gene have been associated with MPS VI. Subsequently, ARSB enzyme activity was found low twice in dried blood spot (DBS), suggestive of MPS VI. The patient did not have the clinical features of MPS VI, but considering the wide clinical spectrum, progressive nature of MPS VI, and the fact that a treatment for MPS VI is available to prevent disease progression, further biochemical, enzymatic, and *in silico* studies were performed to confirm the pathogenicity of this variant. *In silico* tools predicted this variant to be pathogenic. However, the results of urine and serum GAGs and ARSB enzyme levels measured from patient's fibroblast were found normal. Based on clinical and biochemical findings, *ARSB*:p.Arg159Cys is likely benign and did not support the diagnosis of MPS VI. However, *CDH23*:p.Arg1746Gln, a pathogenic variant, supports the underlying cause of hearing loss. This study highlights the importance of a robust correlation between genetic results and clinical presentation, and biochemical and enzymatic studies, to achieve a differential diagnosis.

Keywords: arylsulfatase B, glycosaminoglycans, non-syndromic hearing loss, Cdh23, whole exome sequencing

INTRODUCTION

Mucopolysaccharidoses (MPSs) are lysosomal storage disorders (LSDs) caused by inherited deficiencies of lysosomal hydrolases responsible for the catabolism of mucopolysaccharide molecules known as glycosaminoglycans (GAGs) (1). To date, 13 enzyme deficiencies have been identified that lead to an accumulation of different species of GAGs including dermatan sulfate (DS), heparan sulfate (HS), keratan sulfate (KS), chondroitin sulfate (CS), and hyaluronic acid in blood, tissues, and urine (2). MPSs are autosomal recessive disorders, except for MPS type II also known as Hunter syndrome, which is an X-linked disorder (3). MPS VI have a variable clinical phenotype in terms of severity and progression of disease, with multisystemic involvement that can include skeletal deformities, coarse facial features, and organomegaly. Hearing loss is one of the most common clinical presentation in MPSs (4). Studies have reported confirmed cases of conductive hearing loss, sensorineural hearing, and mixed hearing loss in MPS VI (5). However, patients with MPSs usually do not present with congenital hearing loss. Therefore, an intensive clinical evaluation is crucial to establish a differential diagnosis. MPS VI, or Maroteaux–Lamy syndrome, is caused by a deficiency of N-acetylgalactosamine-4-sulfatase deficiency (arylsulfatase B), leading to an accumulation of DS (OMIM: 253200). In newborns, the incidence of MPS VI is 1 in 250,000–600,000. However, the prevalence was observed to be higher in consanguineous populations (6, 7). Primary treatment options for MPSs include hematopoietic stem cell transplantation (HSCT) and enzyme replacement therapy (ERT) (8). ERT in MPS VI has been shown to reduce GAG accumulation in clinical trials (9). However, the effects of ERT on the hearing loss is inconclusive (10). Differential diagnosis based solely on clinical observations are rarely conclusive, and therefore, additional biochemical and genetic confirmatory tests are often required. Liquid chromatography tandem mass spectrometry (LC-MS/MS) is an effective method for the measurement of metabolites such as disaccharides derived from glycosaminoglycans (11). The CDH23 is a long protein made up of 27 extracellular cadherin (EC) repeats and a non-canonical domain. Each EC repeat is composed of approximately 110 residues. Linker regions that connect different EC repeats are highly conserved and are important for the binding of Ca^{2+} ions (12).

In this study, we report a pathogenic variant *CDH23*:p.Arg1746Gln in a case of congenital hearing loss with mild pigmentary changes in the retina, indicative of Usher syndrome, and a missense variant reported as likely pathogenic for MPS VI identified through whole exome sequencing (WES). However, biochemical confirmatory results for MPS VI were found negative. This report highlights the importance to identify, classify, and characterize variants using computational, biochemical, and clinical approaches.

MATERIALS AND METHODS

Ethical Approval

The Ethical Approval was obtained from Abu Dhabi Health Research and Technology Committee, reference number (DOH/CVDC/2020/1185). The affected case was diagnosed with hearing loss at birth and referred to Tawam Hospital, Abu Dhabi, for further clinical evaluation. Different biological samples such as blood, urine, and fibroblasts were collected to conduct several assays as part of the clinical investigation. Patient was consented for WES, and after that, his blood was spotted on CentoCard (Centogene AG, Germany).

Biochemical Analysis

Arylsulfatase B Fluorimetry Assay

The enzymatic assay is a screening method for MPS VI based on the quantitative determination of ARSB (aryl-sulfatase B) activity in dried blood spots (DBS). The patient's blood was spotted on CentoCard, left to dry for 24 h, and was shipped to Centogene AG (Rostock, Germany). The protocol involves extraction of the ARSB from the DBS, incubation with a specific synthetic substrate for 20 h, and detection of the enzymatic product using fluorimetry. Quantification was performed on a fluorimeter using an external calibration line of the enzymatic product. Affected MPS VI patients show low activity of ARSB, while the healthy controls show high activity of the same enzyme (13).

Dimethylene Blue Assay

Total urine GAGs were measured using the dimethylene blue (DMB) assay, which involves binding of GAGs to the dye DMB followed by a spectrophotometric analysis of the GAG-DMB complex (14).

Mucopolysaccharidosis Quant S

The patient's serum sample was shipped to Mayo Clinic (FL, USA) for quantification of glycosaminoglycans (GAGs). The selected reaction monitoring (SRM) mode in liquid chromatography–electrospray ionization–tandem mass spectrometry (LC–ESI–MS/MS) was used for quantitative measurement of GAGs. The simultaneous quantification of 23 differently sulfated disaccharides from four GAG classes (8 chondroitin/dermatan sulfates, 1 hyaluronic acid, 12 heparan sulfates, and 2 keratan sulfates) was achieved using MS/MS technique. Apart from the internal disaccharides as mentioned previously, some saccharides derived from the non-reducing terminal were also observed. The chain length of GAGs was estimated based on the simultaneous quantification of both internal and non-reducing terminal saccharides (15).

Arylsulfatase B Enzymatic Assay

Enzymatic assay was performed on the fibroblast cell culture obtained from the index skin biopsy. Enzyme assay is the gold standard for diagnosis of patients with MPS VI. It can also determine the pathogenicity effect of the detected novel variants. Skin biopsy was shipped to South Australia Pathology Laboratory (Adelaide, Australia). In normal physiological conditions, the ARSB enzyme chemically modifies chondroitin-4-sulfate and dermatan sulfate by removing the sulfate group. The kinetic parameters, Michaelis–Menten constant (Km), and maximum velocity of human ARSB activity in cultured skin fibroblasts were measured with a different synthetic substrate similar to chondroitin 4-sulfate and dermatan sulfate. The natural

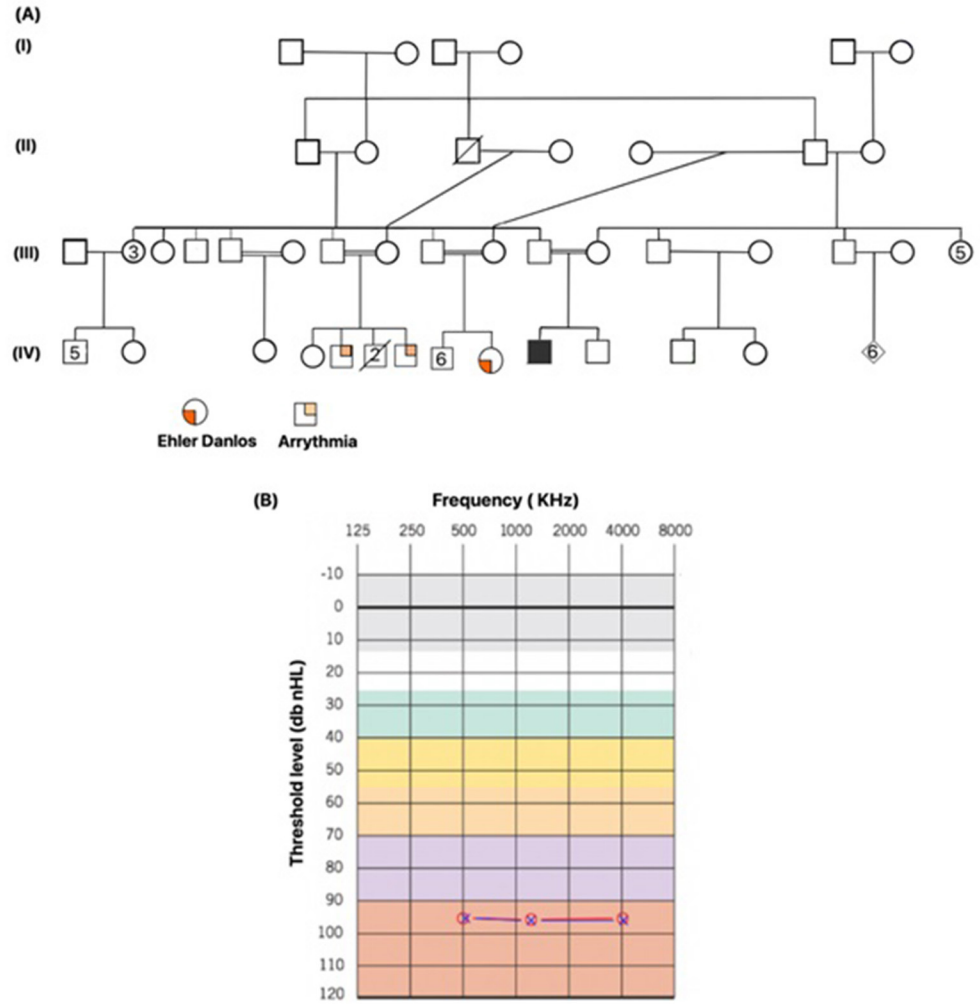

FIGURE 1 | The affected patient's family pedigree and the results of a confirmatory hearing loss test. **(A)** Family pedigree of the index patient, showing a highly inbred family. Family has a history of Ehler Danlos syndrome and history of cardiac arrythmia. The index patient is indicated with filled square. Male and female are shown in squares and circles, respectively. **(B)** Threshold test indicating the level of hearing loss recorded from the auditory brainstem response (ABR), classifying it to be severe. Background colors represent the severity of hearing loss. Normal hearing (gray and white), mild hearing loss (green), moderate hearing loss (yellow), moderately severe hearing loss (orange), severe hearing loss (purple), and profound hearing loss (red). Measurements were recorded in both ears at three frequencies. Red circle indicates the value recorded in left ear, blue cross in a red circle indicates the value recorded in right ear.

substrate's aglycon structures were desulfated up to 4,400 times faster than the substrates specific for arylsulfatase-B (N-acetylgalactosamine 4-sulfate). The enzyme activity of arylsulfatase B in skin fibroblast was measured using O-(beta-N-acetylgalactosamine 4-sulfate)-(1−−4)-O-D-(beta-glucuronic acid)-(1−−3)-O-D-N-acetyl[1-3H] galactosaminitol 4-sulfate. These substrates are used to identify Maroteaux–Lamy syndrome patients from normal controls or/and MPSs patients (16).

DNA Extraction and Whole Exome Sequencing

The patient's blood was spotted on CentoCard and left to dry for 24 h. DNA extraction was performed on QIAcube instrument with QIAamp DNA Blood Mini QIAcube Kit (Qiagen, Valencia, CA, USA) following the manufacturer's instructions. NanoQuant plate was used for the quality and quantity analysis of DNA samples. The diagnostic WES was carried out by Centogene AG (Rostock, Germany). Briefly, twist Human Core Exome Plus kit was used for the exome capture, and the captured libraries were target enriched and indexed. A Novaseq 6000 sequencer was used to sequence the target enriched libraries. For the WES data analysis, sequencing reads were initially converted into normal FastQ format and were processed via locally maintained bioinformatics pipeline. The short reads were aligned to the GRCh37 (hg19) build of the human reference genome. Aligned sequences were further converted to a binary BAM file format, followed by variant calling, which was performed on the secondary alignment files using GATK Haplotype Caller, free

TABLE 1 | Description of variants detected during whole exome analysis.

Gene	Variant coordinates	Amino acid change	Zygosity	Type	Clinvar ACMG Classification
CDH23	NM_022124.5:c.5237G>A	p.(Arg1746Gln)	Homozygous	Missense	Pathogenic
ARSB	NM_000046.3:c.475C<T	p.(Arg159Cys)	Homozygous	Missense	Variant of unknown significance

bayes, and sam tools. Locally maintained bioinformatics tools and Annovar were used for variants annotation. Alignments were conducted and visually confirmed by using Alamut v.2.4.5. The identified variants were further analyzed for genotype phenotype correlation according to the guidelines of the American College of Medical Genetics (ACMG).

In silico Analysis

To further examine the deleterious effect of the identified missense variants on CDH23, and ARSB, several *in silico* tools, namely, Sorting Intolerant from Tolerant (SIFT) (17), Polymorphism Phenotyping v2 (PolyPhen-2.0) (18), Fathmm (19), and Mutation Taster (20), were used. Multiple sequence alignment (MSA) was performed to determine the conservation of amino acids at the missense position (p. Arg159Cys) in ARSB and (p.Arg1746Gln) in CDH23, and Jensen–Shannon Divergence (JSD) scores were also calculated (21). Amino acid sequences of CDH23, and ARSB protein from *Homo sapiens* (human), *Mus musculus* (house mouse), *Rattus norvegicus* (Norway rat), *Callorhinchus milii* (elephant shark), *Bos taurus* (cattle), *Danio rerio* (zebrafish), *Felis catus* (domestic cat), *Pan troglodytes* (chimpanzee), and *Vulpes Vulpes* (red fox) were retrieved from National Center for Biotechnology Information (NCBI) RefSeq and aligned using Clustal Omega (22). JSD scores were calculated using aligned sequences in FASTA format. The protein sequence of the human CDH23 (accession number: Q9H251) and ARSB (accession number: P15484) were obtained from UniProt for homology modeling. Protein databank (PDB) IDs 1FSU and 5VVM were used as templates to produce the homology models of wild-type and mutant CDH23 and ARSB, respectively, using SWISS-MODEL. PyMOL was used for the evaluation and visualization of generated models (23).

RESULTS

Case Report Summary

A male proband was born after full-term pregnancy *via* spontaneous vaginal delivery (SVD) to consanguineous Emirati parents. During newborn screening, hearing loss measurements were performed using distortion product oto-acoustic emission with the interacoustic instrument at 30–40 db prior to the infant's discharge. The proband failed the test at 40 db and was suggestive of congenital hearing loss. A diagnostic auditory brainstem response (ABR) was performed to measure the degree of hearing loss, and threshold estimation was computed during normal sleep. ABR results revealed no reproducible wave V traced out at 90 dB nHL for click stimulus and tone burst (0.5, 1.0, and 2.0 kHz) in both ears, indicative of bilateral hearing loss. Cochlear microphonics was absent. Moreover, two additional audiology tests performed every 2 months showed no repeatable and reliable response even at 90dB nHL for clicks at 0.5, 1.0, 2.0, and 4 kHz tone burst in both ears, confirming a profound sensorineural hearing loss (**Figure 1B**). Patient underwent an ear tube surgery at 8 months of age followed by a cochlear implant at the age of 10 months. Mild pigmentary changes in the retina were observed during an eye examination, suggestive of Usher syndrome. To investigate the genetic causes of congenital hearing loss, gene panel for hearing loss at Prevention Genetics (Marshfield, WI, USA) was ordered, and results came negative. Additionally, the results of microarray were also found to be negative when compared to a normal male array. The patient is from a highly consanguineous family, and his parents are first cousins. The proband also had a family history of Ehlers–Danol syndrome (EDS) and sudden cardiac death for several family members (**Figure 1A**). Whole exome sequencing was ordered to determine the genetic reasoning of hearing loss. Sequencing results identified a missense variant *CDH23*:p.Arg1746Gln in a homozygous state associated with hearing loss. *In silico* tools predicted this as pathogenic. ClinVar ACMG classifies it as pathogenic. Furthermore, an incidental finding of likely pathogenic mutation *ARSB*:p.Arg159Cys based on Centogene ACMG criteria, suggestive of MPS VI diagnosis, was also reported to the treating physician. As per Centogene local database, this variant has been previously identified in one second affected patient in a homozygous state with partial phenotype overlap with no enzymatic analysis. ARSB enzyme activity (EA) measured twice in DBS revealed low levels of EA. Based on this, *ARSB*:p.Arg159Cys variant was reported as likely pathogenic. At that time, this variant was not reported in any public database. However, this variant has recently been classified as variant of unknown significance (VUS) in ClinVar. MPS VI is a disease that progresses slowly or quickly, but early intervention is critical for the patient's outcome. The proband had a history of inguinal hernia repair, recurrent ear infection, recurrent fever, and reactive airway disease. Patient's developmental milestones were normal, rolling over 40 days, sitting at 6/12 months, standing at 1.5 years. Gross motor and fine motor skills were also observed normal. Moreover, he received a speech therapy three times per week. Physical examination performed at 30 months of age showed head circumference of 47 cm (5th percentile), height of 92 cm (25th percentile), weight of 13 kg (25th percentile), no corneal clouding, no coarse fascial feature, no organomegaly, and no joint restriction. Furthermore, skeletal survey did not show any evidence of dysostosis multiplex; ultrasound of abdomen was observed normal with no hepatosplenomegaly. Echo of the heart was also normal. The patient did not have the clinical features of MPS VI, but considering the wide clinical spectrum, progressive nature of MPS VI, and the fact that a treatment

TABLE 2 | Results of mucopolysaccharides quant assay performed on patient's serum.

Mucopolysaccharides quant, S	Concentration (ng/ml)	Reference value
Dermatan sulfate	61.16	<300
Heparan sulfate	16.52	<55
Total keratan sulfate	1,078.87	<1,800

for MPS VI is available to prevent disease progression, further *in silico*, biochemical, and enzymatic studies were performed to confirm the pathogenicity of *ARSB*:p.Arg159Cys variant. *In silico* tools predicted this variant to be pathogenic. However, the results of urine and serum GAGs came normal. ARSB enzyme levels measured from patient's fibroblast were also found normal. These studies conclusively ruled out the diagnosis of MPS VI.

Molecular and Biochemical Studies

WES was performed to determine the genetic basis of hearing loss. Variants were prioritized on the basis of clinical phenotypes of the patient, family history, suspected disease pathways, and minor allele frequency ($\leq$0.05). Sequencing results identified a homozygous missense variant *CDH23*:p.Arg1746Gln. It has already been reported in ClinVar as pathogenic. This confirmed the diagnosis of hearing loss (**Table 1**). Additionally, a missense variant *ARSB*:p.Arg159Cys was found during WES analysis in a homozygous state. At the time of identification, this variant was not reported in any public database. Moreover, variant around this region in ARSB has been found associated with MPS VI (24). ARSB enzyme was estimated in DBS, and results showed low levels of ARSB enzyme 6.3 μmol/L/h (reference, >8.8 μmol/L/h), supporting the diagnosis of MPS VI. Since it is a screening assay and has high false-positive rate, further biochemical and enzymatic studies were performed. Urine GAGs assay was performed as part of the biochemical clinical investigation, and the result was normal at 18.8 mg/mmol creatinine (reference value, <24.0 mg/mmol creatinine). MPS serum assay was carried out, and results indicated the GAGs levels including dermatan sulfate, heparin sulfate, and total Keratan sulfate to be normal (**Table 2**). Furthermore, an enzymatic assay was performed on the patient's skin fibroblast to determine the deficiency in ARSB enzyme. However, ARSB enzyme levels were found to be normal at 12.0 pmol/min/mg protein (reference range, 11.8–39.4 pmol/min/mg/protein). This variant has recently been deposited in ClinVar database and classified as VUS based on ClinVar ACMG classification. However, our results conclusively indicated the likely benign nature of *ARSB*:p.Arg159Cys variant.

In silico Analysis

Several *in silico* variant predictions tools and molecular modeling were utilized to assess the variant pathogenicity effect on the overall protein structure, stability, and function. CDH23 and ARSB protein sequences of different mammals were retrieved from NCBI's reference sequence (RefSeq), and MSA was carried out using Clustal Omega (22). Arg1746 and Arg159 residues of CDH23 and ARSB are highly conserved as indicated by their JSD scores (**Figures 2G,H**). *In silico* tools consistently predicted these variants to be pathogenic. I-Mutant tool was used to compute the impact of *CDH23*:p.Arg1746Gln and *ARSB*:p.Arg159Cys variants on the overall stability of the protein. Both variants decreased the protein stability as indicated by their Gibbs free energy change value ($\Delta\Delta G$) (**Figures 2G,H**). Importantly, the results of *in silico* tools for the *ARSB*:p.Arg159Cys variant were found to be contradictory to its functional studies. Moreover, three-dimensional models of wild-type and variants of ARSB and CDH23 were generated using SWISS-MODEL to observe the effect of missense variants on the protein structure and function. Initially, the full amino acid sequence of human CDH23 was used for the identification of appropriate templates. However, no good quality template was found. In order to obtain a reasonable template, only EC17 and EC18 residues of human CDH23 were selected for template search. Human CDH23 (EC17 and EC18) produced 90% sequence identity with three-dimensional structure of mouse CDH23 (EC17 and EC18), indicating a good template for modeling. Arg1746Gln variant is located in EC17 of CDH23 (**Figure 2A**). The substitution of a charged residue arginine to glutamine is physiochemically significant (**Figures 2B,C**). Arg1746 forms a hydrogen bond with Glu1749. The substituted Gln1746 is likely to disrupt this interaction. It is also perceivable that this loss of charge mutation could likely affect salt bridges and hydrogen bonds that are essential in the CDH23 cis homodimer interface.

The 3D structure of human ARSB is available in PDB (PDB ID: 1FSU) and was used as a template for generating the 3D model of *ARSB*:p.Arg159Cys variant (**Figure 2D**). Arg159 is located in a loop region of ARSB (**Figures 2E,F**). This region is considered the probable recognition site for targeting to the lysosomes (25). The substitution of arginine to cystine is physiochemical significant. However, Arg159 is not the part of residues that line the active site pocket of ARSB, which is essential for enzyme activity. Aside from the loss of a charged residue at the surface of enzyme, no notable impact is expected.

DISCUSSION

This study presents a pathogenic variant p.Arg1746Gln in *CDH23* gene associated with congenital hearing loss with mild pigmentary changes in the retina, indicative of Usher syndrome, and an incidental finding of a missense variant (*ARSB*:p.Arg159Cys) reported as likely pathogenic for MPS VI in an Emirati patient.

A series of biochemical and enzymatic assays were performed to establish the pathogenicity of *ARSB*:p.Arg159Cys associated with MPS VI. The normal results of enzyme activity on fibroblast and normal level of GAGs indicate that this variant is likely benign. This study also highlights the limitations of *in silico* tools that consistently predicted this variant to be pathogenic. Therefore, a careful evaluation of clinical phenotypes and functional studies is imperative to confirm variant pathogenicity.

It is critical to establish a clear genotype–phenotype correlation early in the diagnostic process. Generally, a

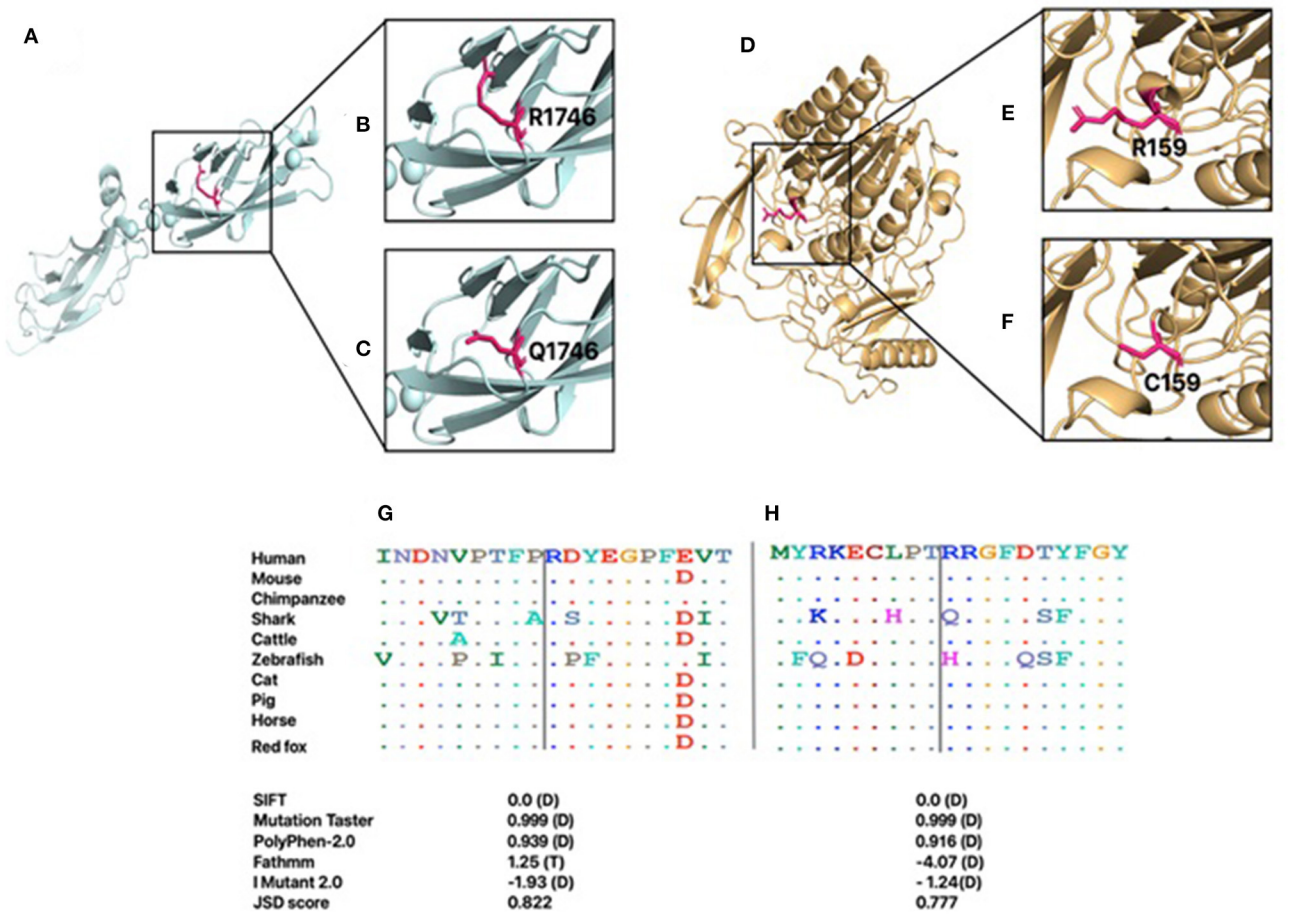

FIGURE 2 | The generated homology models for CDH23 and ARSB. The proteins are shown in cartoon representation, and the amino acid is demonstrated with a stick representation. The boxed region in A and D is enlarged in subsequent images. **(A)** Modeled structure of CDH23. **(B)** Wild-type R1746. **(C)** Mutant Q1746. **(D)** Modeled structure of ARSB. **(E)** Wild-type R159. **(F)** Mutant C159. Conservation of each amino acid is shown across species for both CDH23 **(G)** and ARSB **(H).** Predicted effects of the variants on protein structure and function based on SIFT, Fathmm, Mutation Taster, PolyPhen2.0, and I Mutant2.0 programs. D, damaging; T, tolerated.

combination of clinical and laboratory findings is needed to establish the diagnosis of MPSs. The patients of MPS VI often present with skeletal deformities, coarse facial features, conductive hearing loss, and corneal clouding. It is worth mentioning that the physical examination of index patient was inconsistent with the clinical signs and symptoms of MPS VI. Despite a clear physical examination, the patient's history of inguinal hernia repair, the detection of *ARSB*:p.Arg159Cys variant, and positive results of ARSB enzyme activity in DBS, this patient was suspected with MPS VI. It is also worth mentioning that the variant present close to this region in ARSB is reported to be associated with MPS VI (1, 26).

Interestingly, the gene panel performed in the first place failed to identify any variant associated with hearing loss. There are several limitations associated with the use of gene panel assays, such as variants are limited to pre-selected gene. Additionally, it requires regular updates, as new variants are being discovered (27). It is also important to mention that *CDH23*, a disease-causing gene linked with hearing loss was not included in the design of gene panel. This is why the gene panel failed to identify any mutation in genes linked to hearing loss. However, WES results identified a pathogenic variant *CDH23*:p.Arg1746Gln associated with hearing loss.

Finding likely pathogenic variants necessitates immediate action in patients' management plan, especially if a treatment is available. According to ACMG/AMP guidelines, pathogenic and likely pathogenic variants are reported with 99.1 and 90% confidence (28). However, physicians generally interpret both pathogenic and likely pathogenic variants to be disease associated. According to a recent study that evaluated 36,808 variants classified as likely pathogenic in ClinVar, only 2.16% were reclassified to other categories (29). Interestingly, only four variants were reclassified from likely pathogenic to likely benign (29). This suggests that likely pathogenic variants are rarely found to be benign. Therefore, exhaustive interpretation of genetic data should be performed, before reporting genetic results to the treating physicians.

Here, sequencing results initially reported a likely pathogenic variant *ARSB*:p.Arg159Cys. *ARSB* gene variants have often been associated to the lysosomal storage disorder MPS VI (30). Conductive hearing loss has been linked to MPS VI and other MPS subtypes (31). ARSB enzyme levels in the patient's DBS were measured twice, and the results supported the MPS VI diagnosis. It is worth highlighting that this assay is a screening assay and has high false-positive rate. Therefore, additional biochemical assays should be performed to confirm the diagnosis of MPS VI due to its experimental limitations. Measuring ARSB in DBS is performed using a fluorescence-based method that is being used for detecting LSD in newborn screening (NBS), where different β-methylumbelliferone sulfate (β-MU)-derived substrates similar to natural substrates are applied to quantify lysosomal enzyme deficiency in DBS samples (32). β-MU molecule is known to be highly fluorescent; its detection is often hindered when it is found in a DBS (13). Normally, known standards of β-MU are prepared in an aqueous matrix lacking blood components. Therefore, the enzyme activity (EA) calculated by interpolating sample fluorescence values in a blood-free calibration curve provides data that underestimate the real EA. This could potentially explain the reason why enzyme ARSB on DBS was found lower twice (32). Therefore, enzymatic screenings performed in DBS are not always conclusive, and it required further confirmatory biochemical assays. Additional biochemical and enzymatic studies were performed to establish the pathogenicity of *ARSB*:p.Arg159Cys; however, results were found normal (**Table 2**). These findings concluded that the enzyme is functional, and thus, the patient cannot be diagnosed with MPS VI.

As the number of genetics and genomics tests are increasing, interpreting sequence variants becomes more difficult. Recently, several sequence variants of VUS have been identified (31). Although ACMG guidelines provides a robust framework for laboratories to determine the pathogenicity of sequence variants in a systematic manner, the degree of uncertainty provided by these guidelines can produce contrary classification among different clinical laboratories (32). A study performed on variants reported in ClinVar observed a conflicting interpretation rate of 11.7% among four clinical laboratories (33). Moreover, variability in the *in silico* tools and classification of functionally relevant variants also pose a challenge on the interpretation of variants. In clinical settings, predictions from *in silico* algorithms are considered as one of the eight evidence criteria recommended for variant interpretation by ACMG guidelines (34). *In silico* tools often produce high rate of false-negative and false-positive results. In our study, multiple *in silico* tools consistently predicted *ARSB*:p.Arg159Cys variant as pathogenic, contradicting functional studies that found the variant to be likely benign. Therefore, the patient does not require immediate enzyme replacement therapy.

CONCLUSION

In this study, we report the utility of WES in identifying the genetic variants associated with clinical phenotypes. A robust genotype–phenotype correlation and functional studies are needed to establish the pathogenicity of detected variants during differential diagnosis. Our biochemicals and enzymatic studies indicate that *ARSB*:p.Arg159Cys variant is likely benign and should be reclassified from VUS to likely benign.

DATA AVAILABILITY STATEMENT

The original contributions presented in the study are included in the article/supplementary materials, further inquiries can be directed to the corresponding author.

ETHICS STATEMENT

The studies involving human participants were reviewed and approved by Abu Dhabi Health Research and Technology Committee, Department of Health, Abu Dhabi, United Arab Emirates. Written informed consent to participate in this study was provided by the participants' legal guardian/next of kin.

AUTHOR CONTRIBUTIONS

FA-J conceived and managed the funding of this study. NA, AA, and FA-J designed the study. Material preparation and molecular analysis were performed by NA, AA, and FA-J. Patient examination and clinical analysis were performed by FA-J, and JH. NA, and AA wrote the manuscript. All authors have read and agreed to the published version of the manuscript.

FUNDING

The research project was funded by the United Arab Emirates University grant (31M491) to FA-J. The funder has no role in study design, data collection, and decision to publish.

ACKNOWLEDGMENTS

We are grateful to the patient and family members for their participation in this study.

REFERENCES

1. Tomanin R, Karageorgos L, Zanetti A, Al-Sayed M, Bailey M, Miller N, et al. Mucopolysaccharidosis type VI (MPS VI) and molecular analysis: Review and classification of published variants in the ARSB gene. *Hum Mutat.* (2018) 39:1788–802. doi: 10.1002/humu.23613
2. Coutinho MF. Ucia Lacerda L, Alves S, Alaniz L. Glycosaminoglycan storage disorders: a review. *Biochem Res Int.* (2012) 2012:16. doi: 10.1155/2012/471325
3. Muenzer J. Overview of the mucopolysaccharidoses. *Rheumatology.* (2011) 50 (Suppl 5):v19–25. doi: 10.1093/rheumatology/ker394

4. Giugliani R, Harmatz P, Lin SP, Scarpa M. Assessing the impact of the five senses on quality of life in mucopolysaccharidoses. *Orphanet J Rare Dis.* (2020) 15:1–8. doi: 10.1186/s13023-020-01368-x
5. Silveira MRM da, Buriti AKL, Martins AM, Gil D, Azevedo MF de. Audiometric evaluation in individuals with mucopolysaccharidosis. *Clinics (São Paulo, Brazil).* (2018) 73:e523. doi: 10.6061/clinics/2018/e523
6. Khan SA, Peracha H, Ballhausen D, Wiesbauer A, Rohrbach M, Gautschi M, et al. Epidemiology of mucopolysaccharidoses. *Mol Genet Metab.* (2017) 121:227–40. doi: 10.1016/j.ymgme.2017.05.016
7. Al-Jasmi FA, Tawfig N, Berniah A, Ali BR, Taleb M, Hertecant JL, et al. Prevalence and novel mutations of lysosomal storage disorders in United Arab Emirates: LSD in UAE. *JIMD Rep.* (2013) 10:1–9. doi: 10.1007/8904_2012_182
8. Stapleton M, Hoshina H, Sawamoto K, Kubaski F, Mason RW, Mackenzie WG, et al. Critical review of current MPS guidelines and management. Mol Genet Metab. (2019) 126:238–45. (2019). doi: 10.1016/j.ymgme.2018.07.001
9. Concolino D, Deodato F, Parini R. Enzyme replacement therapy: efficacy and limitations. *Ital J Pediatr.* (2018) 44:120. doi: 10.1186/s13052-018-0562-1
10. Horovitz DDG, Leão EKEA, Ribeiro EM, Martins AM, Barth AL, Neri JICF, et al. Long-term impact of early initiation of enzyme replacement therapy in 34 MPS VI patients: a resurvey study. *Mol Genet Metab.* (2021) 133:94–9. doi: 10.1016/j.ymgme.2021.02.006
11. Auray-Blais C, Lavoie P, Tomatsu S, Valayannopoulos V, Mitchell JJ, Raiman J, et al. UPLC-MS/MS detection of disaccharides derived from glycosaminoglycans as biomarkers of mucopolysaccharidoses. *Anal Chim Acta.* (2016) 936:139–48. doi: 10.1016/j.aca.2016.06.054
12. Vanniya SP, Srisailapathy CRS, Kunka Mohanram R. The tip link protein Cadherin-23: from hearing loss to cancer. *Pharmacol Res.* (2018) 130:25–35. doi: 10.1016/j.phrs.2018.01.026
13. Civallero G, Michelin K, de Mari J, Viapiana M, Burin M, Coelho JC, et al. Twelve different enzyme assays on dried-blood filter paper samples for detection of patients with selected inherited lysosomal storage diseases. *Clin Chim Acta.* (2006) 372:98–102. doi: 10.1016/j.cca.2006.03.029
14. Stone JE, Akhtar N, Botchway S, Pennock CA. Interaction of 1,9-dimethylmethylene blue with glycosaminoglycans. *Ann Clin Biochem.* (1994) 31:147–52. doi: 10.1177/000456329403100206
15. Osago H, Shibata T, Hara N, Kuwata S, Kono M, Uchio Y, et al. Quantitative analysis of glycosaminoglycans, chondroitin/dermatan sulfate, hyaluronic acid, heparan sulfate, and keratan sulfate by liquid chromatography-electrospray ionization-tandem mass spectrometry. *Anal Biochem.* (2014) 467:62–74. doi: 10.1016/j.ab.2014.08.005
16. Hopwood JJ, Elliott H, Muller VJ, Saccone GTP. Diagnosis of Maroteaux-Lamy syndrome by the use of radiolabelled oligosaccharides as substrates for the determination of arylsulphatase B activity. Biochem J. (1986) 234:507–14. doi: 10.1042/bj2340507
17. Sim NL, Kumar P, Hu J, Henikoff S, Schneider G, Ng PC, et al. web server: predicting effects of amino acid substitutions on proteins. *Nucleic Acids Res.* (2012) 40:W452. doi: 10.1093/nar/gks539
18. Adzhubei I, Jordan DM, Sunyaev SR. Predicting functional effect of human missense mutations using PolyPhen-2. *Curr Protoc Hum Genet.* (2013) 76:7–20. doi: 10.1002/0471142905.hg0720s76
19. Shihab HA, Gough J, Cooper DN, Stenson PD, Barker GLA, Edwards KJ, et al. Predicting the functional, molecular, and phenotypic consequences of amino acid substitutions using hidden markov models. *Hum Mutat.* (2013) 34:57–65. doi: 10.1002/humu.22225
20. Schwarz JM, Cooper DN, Schuelke M, Seelow D. MutationTaster2: mutation prediction for the deep-sequencing age. *Nat meth.* (2014) 11:361–2.
21. Dalton JE, Benish WA, Krieger NI. An information-theoretic measure for balance assessment in comparative clinical studies. *Entropy.* (2020) 22:218. doi: 10.3390/e22020218
22. Sievers F, Higgins DG. Clustal Omega for making accurate alignments of many protein sequences. *Protein Sci.* (2018) 27:135–45. doi: 10.1002/pro.3290
23. Seeliger D, De Groot BL. Ligand docking and binding site analysis with PyMOL and Autodock/Vina. *J Comput Aided Mol Des.* (2010) 24:417–22. doi: 10.1007/s10822-010-9352-6
24. Mathew J, Jagadeesh SM, Bhat M, Udhaya Kumar S, Thiyagarajan S, Srinivasan S. Mutations in ARSB in MPS VI patients in India. *Mol Genet Metab Rep.* (2015) 4:53–61. doi: 10.1016/j.ymgmr.2015.06.002
25. Bond CS, Clements PR, Ashby SJ, Collyer CA, Harrop SJ, Hopwood JJ, et al. Structure of a human lysosomal sulfatase. *Structure.* (1997) 5:277–89. doi: 10.1016/S0969-2126(97)00185-8
26. Voskoboeva E, Isbrandt D, von Figura K, Krasnopolskaya X, Peters C. Four novel mutant alleles of the arylsulfatase B gene in two patients with intermediate form of mucopolysaccharidosis VI (Maroteaux-Lamy syndrome). *Hum Genet.* (1994) 93:259–64. doi: 10.1007/BF00212019
27. Biesecker LG, Green RC. Diagnostic clinical genome and exome sequencing. *N Engl J Med.* (2014) 370:2418–25. doi: 10.1056/NEJMra1312543
28. Richards S, Aziz N, Bale S, Bick D, Das S, Gastier-Foster J, et al. Standards and guidelines for the interpretation of sequence variants: a joint consensus recommendation of the American College of Medical Genetics and Genomics and the Association for Molecular Pathology. *Gen Med.* (2015) 17:405–24. doi: 10.1038/gim.2015.30
29. Harrison SM, Rehm HL. Is "likely pathogenic" really 90% likely? Reclassification data in ClinVar. *Genome Med.* (2019) 11:72–5. doi: 10.1186/s13073-019-0688-9
30. Malekpour N, Vakili R, Hamzehloie T. Mutational analysis of ARSB gene in mucopolysaccharidosis type VI: Identification of three novel mutations in Iranian patients. *Iran J Basic Med Sci.* (2018) 21:950–6. doi: 10.22038/IJBMS.2018.27742.6760
31. Wolfberg J, Chintalapati K, Tomatsu S, Nagao K. Hearing loss in mucopolysaccharidoses: current knowledge and future directions. *Diagnostics*. (2020) 10:554. doi: 10.3390/diagnostics10080554
32. Franco PG, Pérez MJ, Aranda C, Adamo A, Silvestroff L. Improving arylsulfatase activity determination in dried blood spots: Screening and diagnostic approaches for Maroteaux-Lamy syndrome (MPS VI). *Clin Chim Acta.* (2015) 446:86–92. doi: 10.1016/j.cca.2015.04.011
33. Vears DF, Sénécal K, Borry P. Reporting practices for variants of uncertain significance from next generation sequencing technologies. *Eur J Med Genet.* (2017) 60:553–8. doi: 10.1016/j.ejmg.2017.07.016
34. Harrison SM, Dolinsky JS, Knight Johnson AE, Pesaran T, Azzariti DR, Bale S, et al. Clinical laboratories collaborate to resolve differences in variant interpretations submitted to ClinVar. *Genet Med.* (2017) 19:1096–104. doi: 10.1038/gim.2017.14

Conflict of Interest: The authors declare that the research was conducted in the absence of any commercial or financial relationships that could be construed as a potential conflict of interest.

frontiers in Genetics

ORIGINAL RESEARCH
published: 08 February 2022
doi: 10.3389/fgene.2022.808919

Molecular and Phenotypic Expansion of Alström Syndrome in Chinese Patients

Qianwen Zhang[1†], Yu Ding[1†], Biyun Feng[1], Yijun Tang[1], Yao Chen[1], Yirou Wang[1], Guoying Chang[1], Shijian Liu[2], Jian Wang[3], Qian Li[4,5], Lijun Fu[6]* and Xiumin Wang[1,4]**

[1]Department of Endocrinology and Metabolism, Shanghai Children's Medical Center, School of Medicine, Shanghai Jiao Tong University, Shanghai, China, [2]Department of Clinical Epidemiology and Biostatistics, Shanghai Children's Medical Center, School of Medicine, Shanghai Jiao Tong University, Shanghai, China, [3]Department of Medical Genetics and Molecular Diagnostic Laboratory, Shanghai Children's Medical Center, School of Medicine, Shanghai Jiao Tong University, Shanghai, China, [4]Center for Brain Science, Shanghai Children's Medical Center, School of Medicine, Shanghai Jiao Tong University, Shanghai, China, [5]Department of Anatomy and Physiology, Ministry of Education-Shanghai Key Laboratory of Children's Environmental Health in Xinhua Hospital, Shanghai Jiao Tong University School of Medicine, Shanghai, China, [6]Department of Cardiology, Shanghai Children's Medical Center, School of Medicine, Shanghai Jiao Tong University, Shanghai, China

OPEN ACCESS

Edited by:
Huiwen Zhang,
Xinhua Hospital, China

Reviewed by:
Chunhua Zeng,
Guangzhou Women and Children's Medical Center, China
Feihong Luo,
Fudan University, China

***Correspondence:**
Qian Li
liqian@shsmu.edu.cn
Lijun Fu
fulinjun@scmc.com.cn
Xiumin Wang
wangxiumin1019@126.com

†These authors have contributed equally to this work

Specialty section:
This article was submitted to Genetics of Common and Rare Diseases, a section of the journal Frontiers in Genetics

Received: 04 November 2021
Accepted: 13 January 2022
Published: 08 February 2022

Citation:
Zhang Q, Ding Y, Feng B, Tang Y, Chen Y, Wang Y, Chang G, Liu S, Wang J, Li Q, Fu L and Wang X (2022) Molecular and Phenotypic Expansion of Alström Syndrome in Chinese Patients. Front. Genet. 13:808919. doi: 10.3389/fgene.2022.808919

Alström syndrome (ALMS) is a rare inherited metabolic disease and ciliopathy. Large cohorts of ALMS are lacking around the world. Detailed genetic and phenotypic data were obtained from all affected individuals. Olfactory function was evaluated by the Chinese Smell Identification Test and facial pattern was analyzed with Face2gene. Fifty ALMS patients were included in this study, aged from 0.3 to 21.7 years old. Sixty-one *ALMS1* variants in 50 patients from 47 different families were confirmed, including 59 truncating and two exon deletions. Twenty-four of those variants were novel. We also summarized all previously reported cases of Chinese ALMS patients (69 patients) and identified specific and common variants within the Chinese population. Besides, the Chinese Smell Identification Test scores in patients was lower than that in controls (11.97 Vs. 10.44, $p < .05$), indicating olfactory identification impairments in ALMS patients. The facial pattern in ALMS patients was also distinctive from that of the controls ($p < .05$). In conclusion, this is the largest cohort of Chinese ALMS patients. We have successfully identified both specific and common variants in our cohort. We found a new phenotype of olfactory impairments in ALMS patients through a case-control study.

Keywords: alström syndrome, ALMS1, next-generation sequencing, rare disease, variants

INTRODUCTION

Alström syndrome (ALMS; MIM #203800), a ciliopathy caused by mutations of the *ALMS1* gene, is inherited in an autosomal recessive pattern. The incidence of this disease is approximately 1/1,000,000 (Tahani et al., 2020). ALMS is a complex multisystem disease whose main symptoms include retinal dystrophy, hearing loss, early-onset obesity, cardiomyopathy, type 2 diabetes mellitus, and multiple organ fibrosis. Retinal dystrophy occurs in all ALMS patients and is a critical manifestation that can be detected from a few weeks to 6 months of age. Hearing loss usually presents with progressive bilateral sensorineural hearing loss, and obesity is usually observed within 6 months to 2 years of age alongside an increased appetite. There are two forms of cardiomyopathy: infantile- and later-onset cardiomyopathy, both of which vary in severity and prognosis. Infantile-onset cardiomyopathy is severe and usually transient; however, later-onset cardiomyopathy is progressive and has a poor prognosis (Tahani et al., 2020).

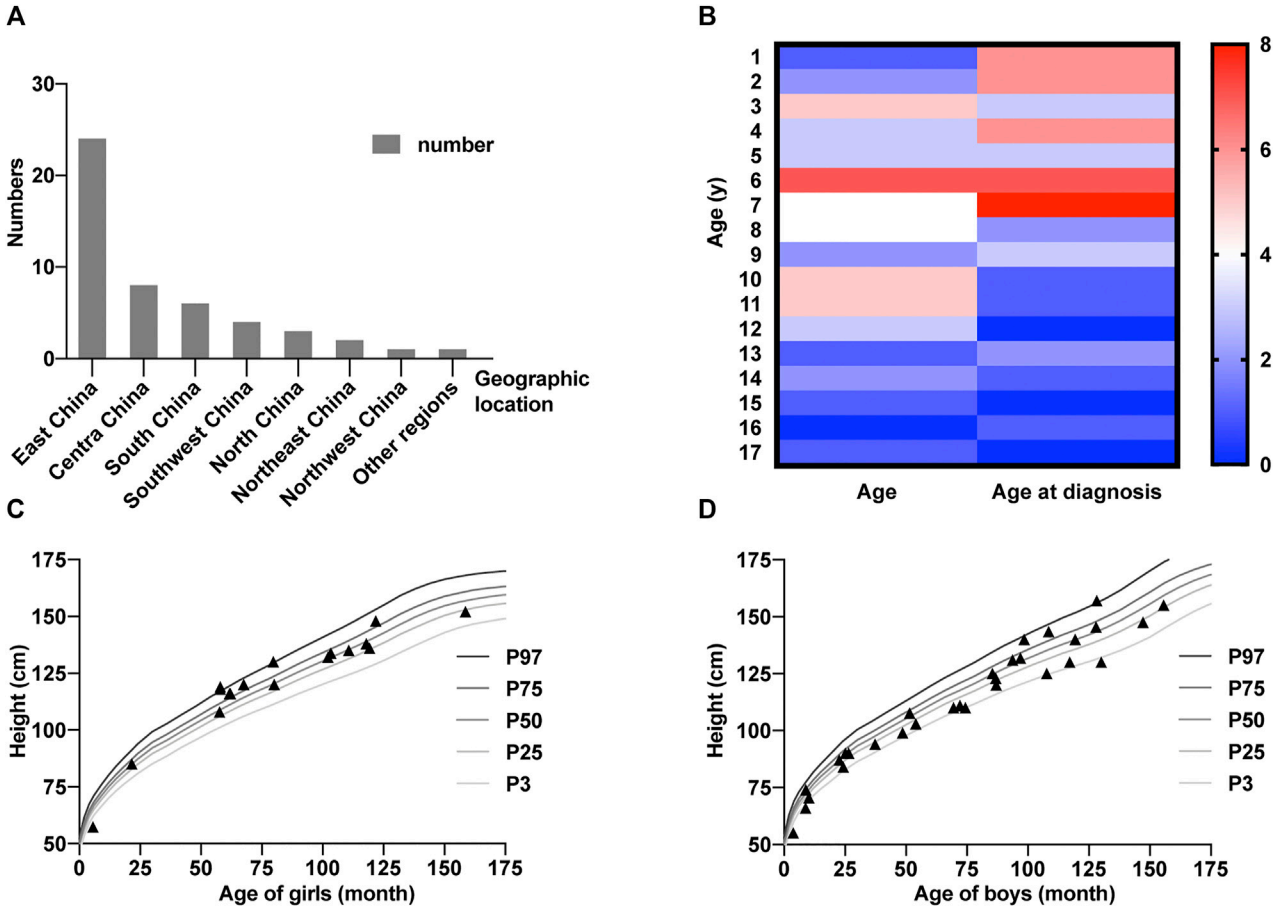

FIGURE 1 | Basic characters of the Chinese cohort. **(A)** Numbers of patients in different areas of China. **(B)** Heatmap representing age distribution of 50 ALMS patients. The columns represent the number of patients with ages at present and at diagnosis. The color bar shows the range of numbers. **(C,D)** Height of girls **(C)** and boys **(D)** included in this study. The standard child growth curves are extracted from Li et al. (2009).

The *ALMS1* gene is located in chromosome two at locus 2p13 and spans 23 exons. Most disease-causing variants of *ALMS1* are truncating mutations that result in loss-of-function proteins (Marshall et al., 2015). To date, 278 variants of *ALMS1* have been identified according to The Human Gene Mutation Database with the mutational hotspots being in exons 8, 10, and 16. There have been no disease-causing variants identified in exons 1, 2, 6, 7, 13, 22, and 23 thus far (Marshall et al., 2015). Such variants were mainly reported by studies of ALMS patient cohorts from Turkey, American, and Poland (Ozantürk et al., 2015; Zmyslowska et al., 2016; Brofferio et al., 2017). However, although there are a few case reports of ALMS patients in China (Rethanavelu et al., 2020), large-scale cohort studies of Chinese patients are still lacking, making it difficult to summarize the common features of ALMS in China.

The ALMS1 protein is located in the basal body of the primary cilia and plays an important role in ciliary function. Therefore, ALMS is a ciliopathy (Hearn et al., 2005). The defective ALMS1 protein is believed to affect primary cilia function in ALMS patients (Hearn et al., 2005; Heydet et al., 2013). Primary cilia are present in most mature mammalian cells. They are essential in many organs such as the eyes, inner ears, and hypothalamus, which may explain the phenotypes of retinal dystrophy, hearing loss, and obesity in ALMS patients. Additionally, primary cilia contribute to olfactory sensory neuron function. Olfactory dysfunction has been identified in other ciliopathies such as Bardet-Biedl syndrome (BBS) (Kulaga et al., 2004). However, it has not been reported in ALMS patients.

Here, we report the clinical and genetic spectrum of 50 ALMS patients in China, which is, to our knowledge, the largest ALMS cohort in East Asia. In total, we identified 61 variants in the *ALMS1* gene, including 50 truncating variants and two exon deletions, of which 24 are novel. Notably, we also identified the first variant c.1415_1416insTCCT in exon 7. Furthermore, genotype-phenotype correlations were analyzed, and the phenotypes of ALMS patients in China were compared to those found in three cohorts from Turkey, American, and Poland. We also summarized all of the variants identified in the Chinese ALMS patients ($n = 69$) from our study and previous reports. We identified distinct and common variants within the Chinese patients. To expand on new phenotypes and explore new diagnostic tools, we further designed a cases-control study to

TABLE 1 | Features of our Chinese cohort compared with other cohorts.

Features	Chinese cohort (N = 50)	Turkish cohort[g] (N = 33)	American's cohort (N = 38)	Polish cohort (N = 12)
Age (mean ± SD, y)	6.95 ± 4.42	**15.83 ± 9.19*****[a]**	**16.04 ± 10.46*****[a]**	**13.50 ± 6.08*****[a]**
Gender (M/F)	31/19	18/15[b]	18/20[b]	8/4[c]
Obesity[h], n/N (%)	33/49 (67)	12/33 (36)**[b]	24/38 (63)[b]	**12/12 (100)*[d]**
Overweight[h], n/N (%)	38/49 (78)	27/33 (82)[b]	33/38 (87)[b]	ND
Vision, n/N (%)	48/48 (100)	33/33 (100)[d]	37/37 (100)[d]	12/12 (100)[d]
SNHL, n/N (%)	19/45 (42)	**24/31 (77)**[b]	**29/32 (91)**[c]	7/10 (70)[c]
Cardiomyopathy, n/N (%)	18/49 (37)	ND	ND	4/12 (33)[c]
Infantile-onset Cardiomyopathy, n/N (%)	16/49 (33)	4/31 (13)[c]	13/38 (34)[b]	ND
Late-onset Cardiomyopathy, n/N (%)	4/49 (8)	4/31 (13)[c]	4/38 (11)[c]	ND
Diabetes mellitus, n/N (%)	4/47 (9)	**11/33 (33)*[c]**	**14/38 (37)**[c]	**5/12 (42)*[c]**
Renal symptom, n/N (%)[e]	3/15 (20)	11/24 (46)[c]	**21/37 (57)*[c]**	2/12 (17)[d]
Hepatic symptom, n/N (%)[f]	17/28 (61)	26/33 (79)[b]	ND	5/10 (50)[d]

F, female; M, male; SNHL, sensorineural hearing loss; ND, no data. Bold indicates that there are significant differences between the two groups (p < .05).

[a]p-value by the Kruskal–Wallis test.

[b]p-value by the Pearson Chi-square.

[c]p-value by the Pearson Chi-square with continuity correction.

*[d]p-value by the Fisher exact test, *p < .05, **p < .01, ***p < .001.*

[e]Renal symptom includes proteinuria, fat liver, and elevated liver enzymes.

[f]Hepatic symptom includes hepatic steatosis, fat liver, and elevated liver enzymes.

[g]33/44 patients from Turkish cohort were included for the including criteria of carrying at least one pathogenic/likely pathogenic variant of ALMS1.

[h]Obesity and overweight was defined as BMI ≥28 kg/m^2 or BMI ≥24 kg/m^2 for adults according to the WGOC, criteria. For children between 6 and 18 years old, overweight/obesity was defined according to Chinese reference values released by the National Health and Family Planning Commission of the People's Republic of China. For patients aged 5,6 years, obesity was defined as a BMI-for-age greater than two SD, above the WHO, growth reference median; and overweight is greater than one SD, above the WHO, Growth Reference median. Obesity in children less than 5 years was defined as a weight-for-height ≥ 2 SD, and overweight ≥3 SD, above the WHO, growth reference median.

assess the facial patterns and the olfactory function of ALMS patients, which may be used as auxiliary diagnostic methods for ALMS.

MATERIALS AND METHODS

Patients

A total of 50 patients, aged from 0.3 to 21.7 years old, were recruited through the Alström Syndrome Greater China Association, a patient-centered group for ALMS (https://www.alstrom.cn/) for genetic consulting in Shanghai Children's Medical Center. They were diagnosed with ALMS at different districts throughout China. Phenotypic and genetic data were obtained from all affected individuals, including general information, medical history, personal history, inspection reports, and laboratory reports. Diagnosis was then confirmed by professional physicians at Shanghai Children's Medical Center. Obesity was defined as BMI ≥28 kg/m^2 and overweight was defined as BMI ≥24 kg/m^2 for adults according to the criteria from Working Group on Obesity in China (WGOC) (Pan et al., 2021). For children between 6 and 18 years old, overweight/obesity was defined according to Chinese reference values released by the National Health and Family Planning Commission of the People's Republic of China (China, N.H.C. o.t.P.s.R.o., 2018; Liu, 2021). Obesity in children less than 5 years was defined as a weight-for-height ≥ 2 standard deviation (SD) and overweight ≥3 SD above the WHO Growth Reference median (https://www.who.int/news-room/fact-sheets/detail/obesity-and-overweight). And in children aged 5,6 years, obesity was defined as a BMI-for-age greater than two SD above the WHO Growth Reference median; and overweight is greater than one SD above the WHO Growth Reference median (https://www.who.int/news-room/fact-sheets/detail/obesity-and-overweight). Written informed consent was obtained from all the participants or their guardians before information was collected.

Genetic Sequencing

For patients 36 and 42–46, exome sequencing was performed at Shanghai Children's Medical Center as previously described (Hu et al., 2018; Li et al., 2019). Candidate variants were screened by a minor allele frequency <1% against the 1,000 Genomes Project, the NHLBI exome variant server or in 50 HapMap control exomes. Then retinal degeneration, obesity, and cardiomyopathy were selected as the filtering clinical symptoms to further analyze those variants. Next-generation sequencing (NGS) in other patients were performed through other commercial companies or hospitals. Variants detected were confirmed by Sanger sequencing in each proband and their parents except for patients 35, 42, 44, and 45. The potential pathogenicity of the variant was evaluated with PolyPhen-2 (http://genetics.bwh.harvard.edu/pph2/), SIFT (http://sift.jcvi.org/), and MutationTaster (http://www.mutationtaster.org/ChrPos.html). The allele frequencies of all identified variants were much lower than 0.1%. All variants were re-identified by the geneticists at Shanghai Children's Medical Center according to the guidelines recommended by the American College of Medical Genetics and Genomics (ACMG) (NM_015120.4).

Automated Image Analysis

Face2Gene (https://face2gene.com) was used as a tool to analyze phenotypic traits based on pattern recognition of frontal

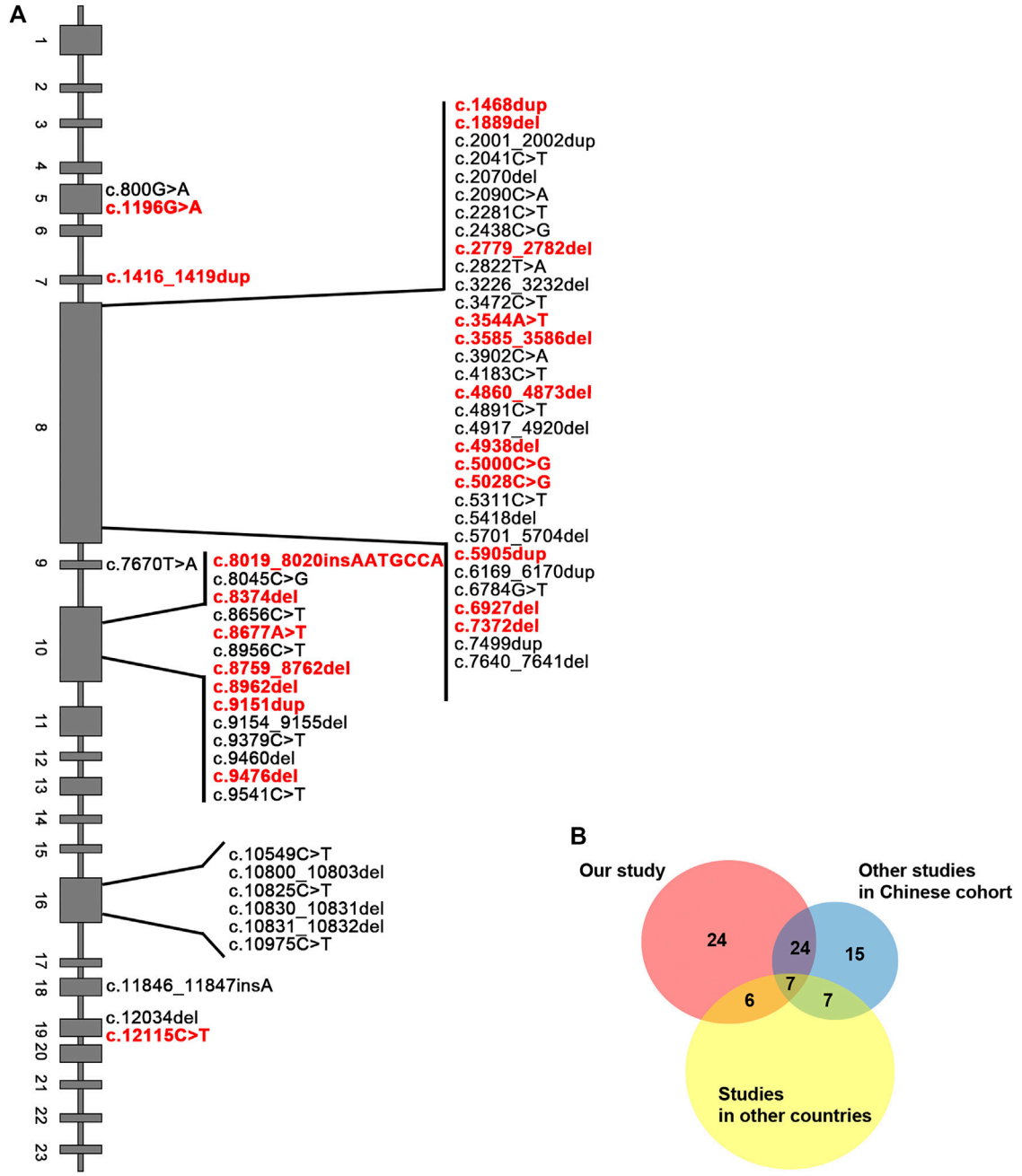

FIGURE 2 | Summary of *ALMS1* variants. **(A)** *ALMS1* variants identified in this study. Novel variants are shown in red. **(B)** Pie chart for the number of variants identified in our study and other cohorts.

photographs of the patients. Because Face2Gene's CLINIC application was not yet designed to differentiate ALMS patients, we used the Face2Gene RESEARCH application to analyze facial features (Knaus et al., 2018).

Olfactory Identification Assessment

ALMS patients and healthy children (controls) were included if the following criteria were met: 1) aged 6–18 years; 2) willing to participate in this study; 3) no difficulty in language communication. Cases and controls were excluded if they had a history of respiratory allergies, upper respiratory infections, rhinitis within the past 14 days, smoking or drinking. Controls with any chronic diseases were also excluded.

The smell identification test includes 16 different odorized items selected from the Chinese Smell Identification Test (CSIT), which has been used as a validated tool to assess olfactory function in the Chinese people (Feng et al., 2019; Wu et al., 2019). The test was conducted in a quiet room free of odors and

TABLE 2 | Novel variants in *ALMS1* identified in this study.

Exon	Nucleotide change	Amino acid change
5	c. 1196G > A	p. W399*
7	c. 1,416_1419dup	p. K474Sfs*2
8	c. 1468dup	p. T490Nfs*15
8	c. 1889del	p. G630Vfs*12
8	c. 2779_2782del	p. L927Sfs*6
8	c. 3544A > T	p. K1182*
8	c. 3585_3586del	p. K1198Tfs*12
8	c. 4860_4873del	p. L1621Hfs*15
8	c. 4938del	p. A1647Lfs*44
8	c. 5000C > G	p. S1667*
8	c. 5028C > G	p. Y1676*
8	c. 5905dup	p. S1969Ffs*19
8	c. 6927del	p. T2310Rfs*34
8	c. 7372del	p. T2458Qfs*20
10	c. 8019_8020insAATGCCA	p. D2674Efs*4
10	c. 8374del	p. G2792Vfs*22
10	c. 8677A > T	p. K2893*
10	c. 8759_8762del	p. P2920Lfs*19
10	c. 8962del	p. L2988Ffs*8
10	c. 9151dup	p. T3051Nfs12
10	c. 9476del	p. I3159Nfs*3
19	c. 12115C > T	p. Q4039*
	Exon 8 del	
	Exon 17-21del	

with proper ventilation. During the CSIT, felt-tip pens containing different odorants were placed 2 cm below the individuals' noses for 2 s after removing the cap. Participants were requested to distinguish the correct smell from four different odor options. Each correct choice was scored one point; otherwise, 0 point was recorded. Each individual only had one chance to complete the test to avoid smell fatigue. After the CSIT, a self-reported olfactory scale was obtained based on a 5-point scale.

Statistics Analysis

Qualitative data are expressed as frequency (%) and compared using Chi-squared test of Fisher test, quantitative data showed as mean ± SD and comparisons were performed by unpaired *t*-test or nonparametric tests where appropriate. SPSS 25.0 (Statistical Package for the Social Sciences Inc., Chicago, IL, United States) was used for statistical analyses. $p < .05$ was considered statistical significance with two-sides.

RESULTS

Clinical Manifestations

A total of 50 patients from 47 different families were included in this study (19 women and 31 men, **Supplementary Table S1**). Families 17, 21, and 47 each had two siblings. All probands from a non-consanguineous family are of Han nationality, except for patients 49 and 50, who are of Tibetan nationality. Among them, sixteen patients (patients 1–8, 10–13, 15, 19, 21–22) were previously reported by Rethanavelu et al. (Rethanavelu et al., 2020) and one patient (patient 9) was reported by Xu et al., (2016). Most patients are from East China, Central China, and South China (**Figure 1A**) and younger than 10 years of age (**Figure 1B**). Patient heights are almost close to normal ranges according to the Chinese Growth Reference (**Figures 1C,D**) (Li et al., 2009). Furthermore, the distribution of height among girls is higher than that among boys.

Detailed clinical manifestations of the patients are summarized in **Supplementary Table S1**. The average age at onset (vision impairment or cardiomyopathy) is 0.7 years, and the average age at diagnosis is 4.7 years. Visual impairment, including nystagmus, photophobia, and impaired vision, is the first symptom in 72% of the patients, and the remaining 28% of patients are referred to the hospital for infantile-onset cardiomyopathy. Overall, one-third of the patients (18/49, 37%) have a history of cardiomyopathy. Obesity and hepatic symptoms are observed in more than 50% of the patients. The prevalence of diabetes mellitus (DM), late-onset cardiomyopathy, and renal symptoms is lower than that of other symptoms (9%, 8%, and 20% respectively).

Phenotypic Comparison Between Our Chinese Cohort and Cohorts From Other Countries

To understand whether the major clinical manifestations of ALMS are consistent across patients worldwide, we compared phenotypes between our Chinese cohort and three cohorts from other countries: Turkey, America, and Poland (Ozantürk et al., 2015; Zmyslowska et al., 2016; Brofferio et al., 2017) (**Table 1**). The overall clinical features were similar between these cohorts. Vision loss, the typical symptom of ALMS, occurred in all patients from all four cohorts. There were also no significant differences in the incidence of overweight status, cardiomyopathy, and hepatic symptoms between these cohorts. However, we observed significant differences in the incidence of sensorineural hearing loss (SNHL), DM, and renal symptoms between the Chinese cohort and the other cohorts. This could be because of differences in patient ages with an average of 7.0 years in the Chinese cohort and an average of 15.1 years in the other cohorts (**Table 1**). Thus, the different clinical symptoms could occur or become more severe as age increases. In addition, many patients in the Chinese cohort lacked the necessary renal function and liver function evaluations, which could have resulted in the incidence of associated symptoms being underestimated. In general, we believe that the major clinical symptoms are common for ALMS patients in the world.

Spectrum of *ALMS1* Variants in Chinese Patients

Next, we sought to define the variant spectrum of *ALMS1* in the Chinese ALMS patients, aiming to identify the prevalent variants in patients globally, and the distinct variants in the Chinese patients. We totally identified 61 different variants of *ALMS1* (59 truncating variants and two exon-deletions) in total in the 50 patients using exome sequencing (**Figure 2A**). The allele frequencies of these variants were <0.1% against the 1,000 Genomes Project and the Exome Aggregation Consortium databases. Additionally, a variety of in silico studies were conducted to evaluate the pathogenicity of these variants.

TABLE 3 | Summary of *ALMS1* variants in 69 Chinese ALMS families (47families in this study and 22 families in previous reports).

Exon	Nucleotide change	Amino acid change	No. of alleles	Allele frequency (%)	References
Novel variants identified in this study					
5	c. 800G > A	p. W267*	1	0.72	This study
5	c. 1196G > A	p. W399*	1	0.72	This study
7	c. 1415_1416insTCCT	p. A472Afs*4	1	0.72	This study
8	c. 1467_1468insA	p. T490Nfs*15	1	0.72	This study
8	c. 1889delG	p. G630Vfs*12	1	0.72	This study
8	c. 2779_2782delCTTT	p. L927Sfs*6	1	0.72	This study
8	c. 2822T > A	p. L941*	2	1.45	This study
8	c. 3544A > T	p. K1182*	1	0.72	This study
8	c. 3585_3586delAA	p. K1198Tfs*12	1	0.72	This study
8	c. 4183C > T	p. Q1395*	1	0.72	This study
8	c.4860_4873delACTTGGAGAGAAGC	p. L1621Hfs*15	1	0.72	This study
8	c. 4938delA	p. A1647Lfs*44	1	0.72	This study
8	c. 5000C > G	p. S1667*	1	0.72	This study
8	c. 5028C > G	p. Y1676*	1	0.72	This study
8	c. 5905_5906insT	p. S1969Ffs*19	1	0.72	This study
8	c. 6927delC	p. T2310Rfs*34	1	0.72	This study
8	c. 7372delA	p. T2458Qfs*20	1	0.72	This study
10	c. 8019_8020insAATGCCA	p. D2674Efs*4	1	0.72	This study
10	c. 8045C > G	p. S2682*	1	0.72	This study
10	c. 8374delG	p. G2792Vfs*22	1	0.72	This study
10	c. 8656C > T	p. R2886*	1	0.72	This study
10	c. 8677A > T	p. K2893*	1	0.72	This study
10	c. 8759_8762delCTTC	p. P2920Lfs*19	1	0.72	This study
10	c. 8959delC	p. P2987Pfs*9	1	0.72	This study
10	c. 9152dupA	p. T3051Nfs*12	1	0.72	This study
10	c. 9379C > T	p. Q3127*	1	0.72	This study
10	c. 9460delG	p. V3154*	2	1.45	This study
10	c. 9476delT	p. I3159Nfs*3	1	0.72	This study
19	c. 12115C > T	p. Q4039*	2	1.45	This study
	Exon 8 del		1	0.72	This study
	Exon 17-21del		2	1.45	This study
Known variants identified in previous reports but not in this study					
5	c. 805C > T	p. R269*	1	0.72	Wang et al. (2015)
5	c. 1054C > T	p. R352*	1	0.72	Xu et al. (2016)
8	c. 2994_2995delAG	p. T996Tfs*9	1	0.72	Zhou et al. (2020)
8	c. 3181C > T	p. Q1061*	1	0.72	Wang et al. (2015)
8	c. 3727A > T	p. K1243*	1	0.72	Rethanavelu et al. (2020)
8	c. 5049dupA	p. P1684Tfs*2	1	0.72	Rethanavelu et al. (2020)
8	c. 5631dupA	p. G1878Rfs*7	1	0.72	Xu et al. (2016)
8	c. 6305C > A	p. S2102*	1	0.72	Xu et al. (2016)
8	c. 6436C > T	p. R2146*	1	0.72	Yang et al. (2017)
8	c. 6823C > T	p. R2275*	1	0.72	Rethanavelu et al. (2020)
8	c. 7402G > T	p. E2468*	1	0.72	Xu et al. (2016)
8	c. 7436C > G	p. S2479*	2	1.45	Liang et al. (2013)
10	c. 8041G > T	p. E2681*	1	0.72	Rethanavelu et al. (2020)
10	c. 8335C > T	p. Q2471*	2	1.45	Liu et al. (2009)
10	c. 8782C > T	p. R2928*	1	0.72	Xu et al. (2016)
10	c. 9441_9442insAATA	p. Q3147Qfs*2	1	0.72	Liang et al. (2013)
10	c. 9448insA	p. N3150Kfs*2	1	0.72	Liang et al. (2013)
10	c. 9535C > T	p. R3179*	1	0.72	Zhou et al. (2020)
16	c. 10883insG	p. R3611Efs7*	1	0.72	Liang et al. (2013)
16	c. 11015delA	p. N3672Ifs11*	1	0.72	Liang et al. (2013)
16	c. 11107C > T	p. R3703*	1	0.72	Liang et al. (2013)
16	c. 11110_11128del	p. R3704Lfs*11	3	2.17	Wang et al. (2015)
Common variants in this study and previous reports					
8	c. 1995_1996insCT	p. T666Lfs*7	1	0.72	This study and Rethanavelu et al. (2020)
8	c. 2041C > T	p. R681*	3	2.17	This study and Xu et al. (2016)
8	c. 2070delT	p. D691Ifs*4	2	1.45	This study and (Wang et al., 2015)
8	c. 2090C > A	p. S697*	11	7.97	

(Continued on following page)

TABLE 3 | (*Continued*) Summary of *ALMS1* variants in 69 Chinese ALMS families (47families in this study and 22 families in previous reports).

Exon	Nucleotide change	Amino acid change	No. of alleles	Allele frequency (%)	References
					This study and Liang et al. (2013), Wang et al. (2015), Xu et al. (2016)
8	c. 2281C > T	p. Q761*	1	0.72	This study and Rethanavelu et al. (2020)
8	c. 2438C > G	p. S813*	1	0.72	This study and Rethanavelu et al. (2020)
8	c. 3226_3232delAAAGTTT	p. K1076Qfs*10	1	0.72	This study and Rethanavelu et al. (2020)
8	c. 3466C > T	p. Q1156*	1	0.72	This study and Rethanavelu et al. (2020)
8	c. 3902C > A	p. S1301*	5	3.62	This study and (Yang et al., 2017)
8	c. 4891C > T	p. Q1631*	2	1.45	This study and Xu et al. (2016)
8	c. 4917_4920delTAAA	p. N1639Kfs*4	5	3.62	This study and Xu et al. (2016), Rethanavelu et al. (2020)
8	c. 5311C > T	p. Q1771*	1	0.72	This study and Rethanavelu et al. (2020)
8	c. 5418delC	p. Y1807Tfs*23	2	1.45	This study and Rethanavelu et al. (2020)
8	c. 5701_5704_delGAGA	p. E1901Rfs*18	2	1.45	This study and Xu et al. (2016)
8	c. 6169_6170dupAT	p. L2058Ffs*17	4	2.90	This study and Xu et al. (2016)
8	c. 6784G > T	p. E2262*	1	0.72	This study and Rethanavelu et al. (2020)
8	c. 7499dupT	p. L2501Tfs*25	1	0.72	This study and Rethanavelu et al. (2020)
8	c. 7640_7641delAG	p. E2547Vfs*9	1	0.72	This study and Rethanavelu et al. (2020)
9	c. 7670T > A	p. L2557*	1	0.72	This study and Rethanavelu et al. (2020)
10	c. 8653C > T	p. Q2885*	1	0.72	This study and Rethanavelu et al. (2020)
10	c. 9154_9155delCT	p. C3053Sfs*9	7	5.07	This study and Rethanavelu et al. (2020)
10	c. 9541C > T	p. R3181*	1	0.72	This study and Rethanavelu et al. (2020)
16	c. 10549C > T	p. Q3517*	3	2.17	This study and Rethanavelu et al. (2020)
16	c. 10800_10803delTGAA	p. E3601Cfs*60	1	0.72	This study and Rethanavelu et al. (2020)
16	c. 10825C > T	p. R3609*	9	6.52	This study and Rethanavelu et al. (2020)
16	c. 10830_10831delGA	p. R3611Afs*6	1	0.72	This study and Rethanavelu et al. (2020)
16	c. 10831_10832delAG	p. R3611Afs*6	5	3.62	This study and Xu et al. (2016)
16	c. 10975C > T	p. R3659*	1	0.72	This study and Rethanavelu et al. (2020)
18	c. 11846_11847insA	p. N3952Lfs*10	1	0.72	This study Rethanavelu et al. (2020)
19	c. 12034delC	p. L4012Wfs*19	1	0.72	This study and Rethanavelu et al. (2020)

TABLE 4 | Allele rate and distribution of *ALMS1* variants in different exons from 69 Chinese ALMS families.

Exon	Exon size (bp)	Number of alleles	Allele rate[a] (%)
5	473	4	0.8
7	94	1	1.1
8	6108	71	1.2
9	134	1	0.7
10	1865	28	1.5
16	1,163	26	2.2
18	204	1	0.5
19	242	3	1.2

[a]*Allele rate = Number of alleles/Exon size.*

According to the guidelines recommended by ACMG, all of the 59 truncating variants were classified as pathogenic. Among them, twenty-four were novel and are located in exons 5, 7, 8, 10, and 19 (**Table 2** and **Figure 2A**). Notably, we identified the first *ALMS1* variant in exon 7, i.e., c.1415_1416insTCCT. The remaining 37 variants have been reported previously in other cohorts (Minton et al., 2006; Flintoff and Josifova, 2007; Liang et al., 2013; Consugar et al., 2015; Marshall et al., 2015; Ozantürk et al., 2015; Wang et al., 2015; Rethanavelu et al., 2020). To better understand the commonality of those 37 variants, we summarized the variants reported by other Chinese cohorts and cohorts from other countries. We retrieved 24 Chinese ALMS patients from 22 families from the literature (Liu et al., 2009; Liang et al., 2013; Wang et al., 2015; Xu et al., 2016; Yang et al., 2017; Rethanavelu et al., 2020; Zhou et al., 2020). All variants of the *ALMS1* gene from 69 Chinese families are summarized in **Table 3** and the distribution of these variants in Chinese and other countries' cohorts are shown in **Figure 2B**. Twenty-four variants were only identified in our cohort and 23 variants were identified in both our cohort and the other Chinese cohorts. Of them, ranking variants included c.2090C > A (11/138, 7.97%), c.10825C > T (9/138, 6.52%), c.10831_10832del (5/138, 3.62%), c.4917_4920del (5/138, 3.62%), c.3902C > A (5/138, 3.62%), and c.6169_6170dup (4/138, 2.9%). Variant c.9154_9155del (7/138, 5.07%) was recurrent in our cohort but was not found in the other cohorts. Interestingly, c.2090C > A was a distinct variant in the Chinese patients and only identified in them. Based on our analysis, exons 8, 10, and 16 were mutational hotspots, harboring 51.45%, 20.29%, and 18.84% of variants, respectively. Exon 16 had a particularly high mutation rate considering its size (**Table 4**). Generally, we found that the spectrum of *ALMS1* variants in Chinese ALMS patients showed clusters in some exons (8, 10, and 16) and specific variants.

Genotype-Phenotype Correlations

Interestingly, the siblings from family 17 suffered from severe infantile-onset cardiomyopathy, which indicated the possibility

TABLE 5 | Genotype-Phenotype correlation for Infantile-onset cardiomyopathy ALMS patient.

Subjects	Patients with a history of infantile-onset cardiomyopathyN = 16	Patients without a history of infantile-onset cardiomyopathyN = 34	*p* Value
Age (mean ± SD, y)	5.84 ± 4.01	7.46 ± 4.39	.201[a]
Gender (male/female)	8/8	23/11	.230[b]
Carrying variants before exon 8, n (%)	15 (93.75)	23 (67.65)	.097[c]

[a]p-*value by the Mann-Whitney* U *test.*
[b]p-*value by the Pearson Chi-square.*
[c]p-*value by the Pearson Chi-square with continuity correction.* *p < .05.

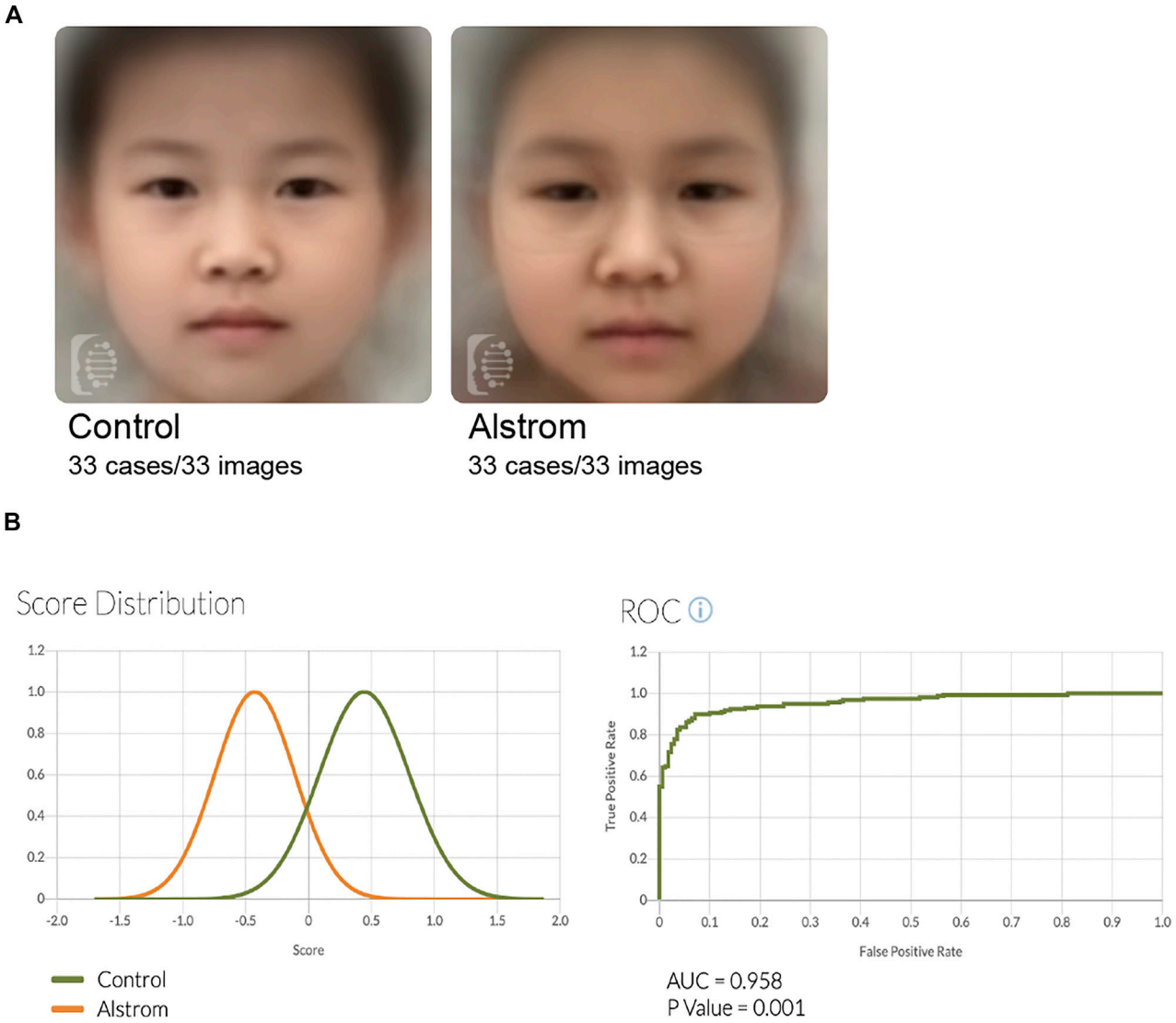

FIGURE 3 | Facial analysis of patients and controls. **(A)** Composite photos computed from age-matched images of ALMS patients and controls. **(B)** Score distribution and ROC curves of the comparison results of ALMS patients and controls.

of a genotype-phenotype correlation. Therefore, we tried to find genotype-phenotype correlations in the ALMS patients. We analyzed patients with a history of infantile-onset cardiomyopathy and compared them to patients without a history of cardiomyopathy. In total, 32% (16/50) of the patients suffered from infantile-onset cardiomyopathy in our

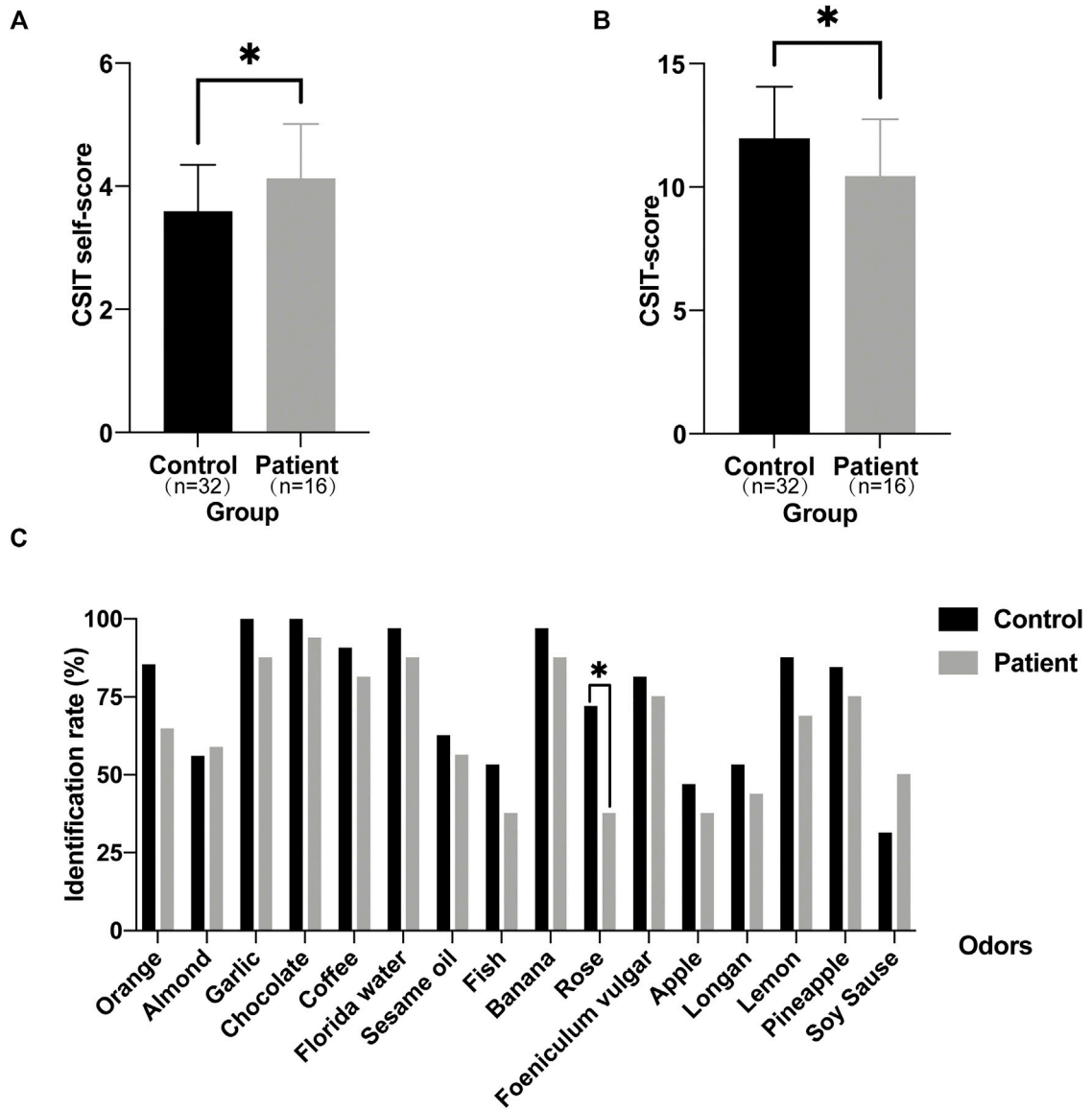

FIGURE 4 | Olfactory assessment in ALMS patients and controls. **(A)** The CSIT self-scores of ALMS patients and controls. **(B)** The tested CSIT scores of ALMS patients and controls. **(C)** The identification rate of each odor in ALMS patients and controls. *$p < .05$.

cohort. Of these patients, 93.75% (15/16) carried at least one truncated variant before exon 8 (including exon 8); only 67.65% (23/34) of the patients without cardiomyopathy had similar truncated variants (**Table 5**). However, no significant statistical difference was identified ($p = .097$), likely because of the limited number of patients. These results suggest that earlier translation termination may be correlated with infantile-onset cardiomyopathy and that the fragment encoded by exon 8 may be important for cardiac function.

Computer Facial Recognition Analysis

Next, we wondered if we could develop novel methods which might aid in the diagnosis of ALMS. Firstly, we tested whether ALMS patients had distinct facial features. We used the Face2Gene RESEARCH tools to assess patient facial patterns. Thirty-three facial photographs of ALMS patients were collected, along with those from 33 age- and sex-matched controls. The receiver operating characteristic (ROC) curves showed that the facial patterns in ALMS patients were indeed different from those in the controls, with an Area Under Curve (AUC) of 0.96 ($p < .001$) (**Figures 3A,B**). This suggests that the facial recognition analysis could be an auxiliary diagnostic method for ALMS.

Olfactory Assessment

Next, we tended to find other potential diagnosis method. *ALMS1* variants have been reported to result in defective cilia structures and trafficking of key signaling molecules in

TABLE 6 | Detailed information of Chinese Smell Identification Test in ALMS patients and controls.

Smell	Patients N = 16 (%)	Control N = 32 (%)	*p* Value
Orange	10 (64.71)	27 (85.29)	.089[c]
Almond	10 (58.82)	18 (55.88)	.679[c]
Garlic	14 (87.50)	32 (100.00)	.106[b]
Chocolate	15 (93.75)	32 (100.00)	0.333[b]
Coffee	13 (81.25)	29 (90.63)	.643[d]
Florida water	14 (87.50)	31 (96.88)	.527[d]
Sesame oil	9 (56.25)	20 (62.50)	.676[c]
Fish	6 (37.50)	17 (53.13)	.307[c]
Banana	14 (87.50)	31 (96.88)	.527[d]
Rose	6 (37.50)	23 (71.88)	**.022*[c]**
Foeniculum vulgar	12 (75.00)	26 (81.25)	.900[d]
Apple	6 (37.50)	15 (46.88)	.537[c]
Longan	7 (43.75)	17 (53.13)	.540[c]
Lemon	11 (68.75)	28 (87.50)	.239[d]
Pineapple	12 (75.00)	27 (84.38)	.695[d]
Soy Sauce	8 (50.00)	10 (31.25)	.206[c]

*Data are shown as the number of patients and controls that successfully identified the odors. The identification rates are calculated as the percentages and are placed inside the parentheses. Bold indicates that there are significant differences between the two groups (*p < *.05).*

[b]p *value by the Fisher exact test.*

[c]p *value by the Pearson Chi-square.*

[d]p *value by the Pearson Chi-square with continuity correction.* *p < *.05.*

the cilia (Hearn et al., 2005; Heydet et al., 2013). Therefore, ALMS patients have visual and auditory dysfunctions. Interestingly, olfactory sensory neurons detect volatile odorants using olfactory receptors and other signaling molecules located in the cilia. However, it is unknown if olfactory function is normal in ALMS patients. We used CSIT, a toolkit specifically designed to assess olfactory function in the Chinese population, to evaluate olfactory function in ALMS patients (Feng et al., 2019; Wu et al., 2019). Sixteen patients were recruited and were matched with 32 individual controls by age and sex. The average age of patients was 9.50 ± 2.28 years and of controls, 9.63 ± 2.12 years. Although the CSIT self-score was higher in patients than that in controls, the tested CSIT score in patients was 10.44 in patients and 11.97 in controls. The slightly lower but significant CSIT score in ALMS patients indicated that olfactory identification (OI) impairments occurred in ALMS patients (**Figures 4A,B**). Further analysis showed that, for most odors, the identification rate was slightly lower in patients than that in controls. Only the identification rate of rose odor in the patients was significantly lower in patients than that in the controls (**Table 6** and **Figure 4C**). We further compared the differences in age, sex, early-onset cardiomyopathy, and genotypes between ALMS patients who could identify the rose odor and those who could not (**Table 7**). Unfortunately, no differences between the two groups were found. It should be noted that the patients and controls included in this study were very young and may not have been able to describe the odors correctly, which could have resulted in the olfactory impairment in ALMS patients being underestimated. In conclusion, the olfactory assessment could be used as another auxiliary diagnosis method for ALMS.

DISCUSSION

In this study, we recruited 50 Chinese ALMS patients for genetic and phenotypic analyses. To the best of our knowledge, this is the largest cohort study of Chinese ALMS patients. The average age of this Chinese cohort is also the youngest in the world of all ALMS cohorts. Most of the patients in this study were diagnosed before 7 years old, possibly owing to the rapid development of NGS in China. Furthermore, the time from age at onset to age at diagnosis was approximately 4 years in our cohort compared to approximately 13 years in the Polish cohort (Zmyslowska et al., 2016).

Our study has revealed that exons 8, 10, and 16 are mutational hotspots, which is consistent with previous reports (Marshall et al., 2015). However, previous studies directly sequenced exons 8, 10, and 16, whereas we performed NGS without exon bias. The preference of *ALMS1* variants in those exons is partly due to the relatively larger sizes of these exons. Among these three exons, exon 16 has the highest mutation rate (**Table 4**). Further, ethnicity greatly contributed to the distribution of the *ALMS1* variants. According to our study, c.2090C > A (11/138, 7.97%) in exon eight is the most common variants in

TABLE 7 | Comparison analysis between ALMS patients who could identify the rose odor and those could not.

Subject	Group 1[c]N = 10	Group 2[d]N = 6	*p* Value
Gender (M/F)	7/3	3/3	.089[a]
Age (mean ± SD, y)	9.74 ± 1.95	9.54 ± 3.47	.792[b]
Obesity[h], n/N (%)	7/10 (70)	5/6 (83)	1.000[a]
Overweight[h], n/N (%)	9/10 (90)	6/6 (100)	1.000[a]
Vision, n/N (%)	10/10 (100)	6 (100)	1.000[a]
SNHL, n/N (%)	8/10 (80)	3/6 (50)	.299[a]
Infantile-onset Cardiomyopathy, n/N (%)	3/10 (30)	1/6 (17)	1.000[a]
Late-onset Cardiomyopathy, n/N (%)	2/10 (20)	0/6 (0)	.500[a]
Cardiomyopathy, n/N (%)	5/10 (50)	1/6 (17)	.307[a]
Diabetes mellitus, n/N (%)	1/10 (10)	0/6 (0)	1.000[a]

[a]p *value by the Fisher exact test.*

[b]p *value by the Mann-Whitney* U *test.*

[c]*Group 1 refers to patients who could identify the rose odor and.*

[d]*Group 2 refers to patients who could not identify the rose odor.*

China. The high carrier rate of this variant in East Asians (0.006%) may account for this pattern (Marshall et al., 2015). Other recurrent variants included: c.2041C > T (3/138, 2.17%), c.3902C > A (5/138, 3.62%), c.4917_4920del (5/138, 3.62%), and c.6169_6170dup (4/138, 2.90%) in exon 8; c. 9154_9155del (7/138, 5.07%) in exon 10, and c. 10549C > T (3/138, 2.17%), c. 10825C > T (9/138, 6.52%), and c. 10831_10832del (5/138, 3.62%) in exon 16. Of those 8 recurrent variants, c. 2041C > T, c. 2090C > A, c. 3902C > A, c. 6169_6170dup, c. 9154_9155del, and c. 10831_10832del are specific to Chinese patients, whereas c.10825C > T is common worldwide. Regarding recurrent variants in other countries, c.8177_8187del, c.8164C > T, and c.10945G > T are specific to patients of West Asian/Middle Eastern kindreds, whereas c.10775del (24/557) and c.11449C > T (15/557) are specific to Northern European and American populations (Marshall et al., 2015).

ALMS symptoms either develop or become more severe with age; thus, diagnosis is difficult during the early ages of patients. Consequently, exploring new diagnostic tools is necessary. In this study, we explored the possibility of two auxiliary diagnostic methods. The first is computer facial recognition, which has been successfully applied in diagnosis of some diseases, such as Noonan syndrome with characteristic facial features (Li et al., 2019). Facial patterns in ALMS patients are rarely mentioned, likely because of the low incidence of this disease. Since we had 50 patients, we performed facial analysis. We showed that there are significant differences in facial patterns between ALMS patients and age- and sex-matched controls. However, further studies are still required to identify the distinctive facial features of ALMS patients, which will greatly benefit the clinical diagnosis of ALMS, especially in juveniles. The second is olfactory assessment. We used the CSIT that was specifically developed for Chinese populations to evaluate the olfactory function in patients. We observed olfactory identification impairments in ALMS patients. However, we could not exclude the possibility that the patients were simply unfamiliar with the odors due to their limited exposures to them. In addition, we found that the ALMS patients particularly struggled to recognize the rose odor instead of other odors. This may suggest that ALMS1 is expressed in subsets of olfactory sensory neurons that detect distinct volatile odors. We will continue to follow-up with these patients and perform computer facial recognition and olfactory assessment annually, which may further validate our findings as the patients grow up.

In summary, we reported 50 Chinese ALMS patients with 61 pathogenic variants, including 24 novel variants. We identified recurrent variants of 138 variants in 69 Chinese ALMS families totally. Olfactory identification impairments can occur in ALMS patients, and these patients have some distinctive facial features. Early-onset cardiomyopathy is likely related to earlier transcription termination of the *ALMS1* gene. Our study expands on the *ALMS1* gene genetic and phenotypic spectrum and provides new insights into the understanding of ALMS.

DATA AVAILABILITY STATEMENT

The data that support the findings of this study are available from the corresponding authors upon reasonable request.

ETHICS STATEMENT

The studies involving human participants were reviewed and approved by The Research Ethics Committee of Shanghai Children's Medical Center School of Medicine, Shanghai Jiao Tong University. Written informed consent to participate in this study was provided by the participants' legal guardian/next of kin. Written informed consent was obtained from the individual(s), and minor(s)' legal guardian/next of kin, for the publication of any potentially identifiable images or data included in this article.

AUTHOR CONTRIBUTIONS

Conceptualization: XW and QL; Data curation: QZ; Funding acquisition: GC, XW, and LF; Methodology: QL and JW; Investigation: YT, BF, QZ, YD, YC, and YW; Supervision: QL, XW, LF, and SL; Writing—original draft: QZ; Writing—review and editing: XW, QL, LF, YD, and SL.

FUNDING

This work was supported by National Nature Science Foundation of China (81900722, 82170190, 32122038, and 31970933), Shanghai Clinical Medical Research Center for children's rare diseases (20MC1920400), Pudong New Area Science and Technology Development Fund (PKJ2018-Y46), the National Key Research and Development Program of China (2021ZD0203100), the Basic Research Project (21JC1404500) and Shanghai Brain-Intelligence Project (18JC1420302) from the Science and Technology Commission of Shanghai Municipality, Shuguang Program supported by Shanghai Education Development Foundation and Shanghai Municipal Education Commission (21SG16), Program for Young Scholars of Special Appointment at Shanghai Institutions of Higher Learning (QD2018017), and Fundamental Research Funds for the Central Universities (Shanghai Jiao Tong University, 17X100040037).

ACKNOWLEDGMENTS

We acknowledge the collaborations of the patients and their guardians.

SUPPLEMENTARY MATERIAL

The Supplementary Material for this article can be found online at: https://www.frontiersin.org/articles/10.3389/fgene.2022.808919/full#supplementary-material

REFERENCES

Brofferio, A., Sachdev, V., Hannoush, H., Marshall, J. D., Naggert, J. K., Sidenko, S., et al. (2017). Characteristics of Cardiomyopathy in Alström Syndrome: Prospective Single-center Data on 38 Patients. *Mol. Genet. Metab.* 121 (4), 336–343. doi:10.1016/j.ymgme.2017.05.017

China, N.H.C.o.t.P.s.R.o. (2018). *Screening for Overweight and Obesity Among School-Age Children and Adolescents*. Beijing: National Health Commission of the People's Republic of China, 25, 103–108.

Consugar, M. B., Navarro-Gomez, D., Place, E. M., Bujakowska, K. M., Sousa, M. E., Fonseca-Kelly, Z. D., et al. (2015). Panel-based Genetic Diagnostic Testing for Inherited Eye Diseases Is Highly Accurate and Reproducible, and More Sensitive for Variant Detection, Than Exome Sequencing. *Genet. Med.* 17 (4), 253–261. doi:10.1038/gim.2014.172

Feng, G., Zhuang, Y., Yao, F., Ye, Y., Wan, Q., and Zhou, W. (2019). Development of the Chinese Smell Identification Test. *Chem. Senses* 44 (3), 189–195. doi:10.1093/chemse/bjz006

Flintoff, K. J., and Josifova, D. (2007). Gene Symbol: ALMS1. *Hum. Genet.* 121 (2), 297.

Hearn, T., Spalluto, C., Phillips, V. J., Renforth, G. L., Copin, N., Hanley, N. A., et al. (2005). Subcellular Localization of ALMS1 Supports Involvement of Centrosome and Basal Body Dysfunction in the Pathogenesis of Obesity, Insulin Resistance, and Type 2 Diabetes. *Diabetes* 54 (5), 1581–1587. doi:10.2337/diabetes.54.5.1581

Heydet, D., Chen, L. X., Larter, C. Z., Inglis, C., Silverman, M. A., Farrell, G. C., et al. (2013). A Truncating Mutation of Alms1 Reduces the Number of Hypothalamic Neuronal Cilia in Obese Mice. *Devel Neurobio* 73 (1), 1–13. doi:10.1002/dneu.22031

Hu, X., Li, N., Xu, Y., Li, G., Yu, T., Yao, R.-e., et al. (2018). Proband-only Medical Exome Sequencing as a Cost-Effective First-Tier Genetic Diagnostic Test for Patients without Prior Molecular Tests and Clinical Diagnosis in a Developing Country: the China Experience. *Genet. Med.* 20 (9), 1045–1053. doi:10.1038/gim.2017.195

Knaus, A., Pantel, J. T., Pendziwiat, M., Hajjir, N., Zhao, M., Hsieh, T.-C., et al. (2018). Characterization of Glycosylphosphatidylinositol Biosynthesis Defects by Clinical Features, Flow Cytometry, and Automated Image Analysis. *Genome Med.* 10 (1), 3. doi:10.1186/s13073-017-0510-5

Kulaga, H. M., Leitch, C. C., Eichers, E. R., Badano, J. L., Lesemann, A., Hoskins, B. E., et al. (2004). Loss of BBS Proteins Causes Anosmia in Humans and Defects in Olfactory Cilia Structure and Function in the Mouse. *Nat. Genet.* 36 (9), 994–998. doi:10.1038/ng1418

Li, H., Ji, C. Y., Zong, X. N., and Zhang, Y. Q. (2009). Height and Weight Standardized Growth Charts for Chinese Children and Adolescents Aged 0 to 18 Years. *Zhonghua Er Ke Za Zhi* 47 (7), 487–492.

Li, X., Yao, R., Tan, X., Li, N., Ding, Y., Li, J., et al. (2019). Molecular and Phenotypic Spectrum of Noonan Syndrome in Chinese Patients. *Clin. Genet.* 96 (4), 290–299. doi:10.1111/cge.13588

Liang, X., Li, H., Li, H., Xu, F., Dong, F., and Sui, R. (2013). Novel ALMS1 Mutations in Chinese Patients with Alström Syndrome. *Mol. Vis.* 19, 1885–1891.

Liu, L., Dong, B., Chen, X., Li, J., and Li, Y. (2009). Identification of a Novel ALMS1 Mutation in a Chinese Family with Alström Syndrome. *Eye* 23 (5), 1210–1212. doi:10.1038/eye.2008.235

Liu, Z. (2021). Effectiveness of a Multifaceted Intervention for Prevention of Obesity in Primary School Children in China: A Cluster Randomized Clinical Trial. *JAMA Pediatr.* 176, e214375. doi:10.1001/jamapediatrics.2021.4375

Marshall, J. D., Muller, J., Collin, G. B., Milan, G., Kingsmore, S. F., Dinwiddie, D., et al. (2015). Alström Syndrome: Mutation Spectrum ofALMS1. *Hum. Mutat.* 36 (7), 660–668. doi:10.1002/humu.22796

Minton, J. A. L., Owen, K. R., Ricketts, C. J., Crabtree, N., Shaikh, G., Ehtisham, S., et al. (2006). Syndromic Obesity and Diabetes: Changes in Body Composition with Age and Mutation Analysis of ALMS1 in 12 United Kingdom Kindreds with Alstrom Syndrome. *J. Clin. Endocrinol. Metab.* 91 (8), 3110–3116. doi:10.1210/jc.2005-2633

Ozantürk, A., Marshall, J. D., Collin, G. B., Düzenli, S., Marshall, R. P., Candan, Ş., et al. (2015). The Phenotypic and Molecular Genetic Spectrum of Alström Syndrome in 44 Turkish Kindreds and a Literature Review of Alström Syndrome in Turkey. *J. Hum. Genet.* 60 (1), 1–9. doi:10.1038/jhg.2014.85

Pan, X.-F., Wang, L., and Pan, A. (2021). Epidemiology and Determinants of Obesity in China. *Lancet Diabetes Endocrinol.* 9 (6), 373–392. doi:10.1016/s2213-8587(21)00045-0

Rethanavelu, K., Fung, J. L. F., Chau, J. F. T., Pei, S. L. C., Chung, C. C. Y., Mak, C. C. Y., et al. (2020). Phenotypic and Mutational Spectrum of 21 Chinese Patients with Alström Syndrome. *Am. J. Med. Genet.* 182 (2), 279–288. doi:10.1002/ajmg.a.61412

Tahani, N., Maffei, P., Dollfus, H., Paisey, R., Valverde, D., Milan, G., et al. (2020). Consensus Clinical Management Guidelines for Alström Syndrome. *Orphanet J. Rare Dis.* 15 (1), 253. doi:10.1186/s13023-020-01468-8

Wang, H., Wang, X., Zou, X., Xu, S., Li, H., Soens, Z. T., et al. (2015). Comprehensive Molecular Diagnosis of a Large Chinese Leber Congenital Amaurosis Cohort. *Invest. Ophthalmol. Vis. Sci.* 56 (6), 3642–3655. doi:10.1167/iovs.14-15972

Wu, X., Geng, Z., Zhou, S., Bai, T., Wei, L., Ji, G.-J., et al. (2019). Brain Structural Correlates of Odor Identification in Mild Cognitive Impairment and Alzheimer's Disease Revealed by Magnetic Resonance Imaging and a Chinese Olfactory Identification Test. *Front. Neurosci.* 13, 842. doi:10.3389/fnins.2019.00842

Xu, Y., Guan, L., Xiao, X., Zhang, J., Li, S., Jiang, H., et al. (2016). ALMS1null Mutations: a Common Cause of Leber Congenital Amaurosis and Early-Onset Severe Cone-Rod Dystrophy. *Clin. Genet.* 89 (4), 442–447. doi:10.1111/cge.12617

Yang, L., Li, Z., Mei, M., Fan, X., Zhan, G., Wang, H., et al. (2017). Whole Genome Sequencing Identifies a Novel ALMS1 Gene Mutation in Two Chinese Siblings with Alström Syndrome. *BMC Med. Genet.* 18 (1), 75. doi:10.1186/s12881-017-0418-3

Zhou, C., Xiao, Y., Xie, H., Liu, S., and Wang, J. (2020). A Novel Variant in ALMS1 in a Patient with Alström Syndrome and Prenatal Diagnosis for the Fetus in the Family: A Case Report and Literature Review. *Mol. Med. Rep.* 22 (4), 3271–3276. doi:10.3892/mmr.2020.11398

Zmyslowska, A., Borowiec, M., Antosik, K., Ploski, R., Ciechanowska, M., Iwaniszewska, B., et al. (2016). Genetic Evaluation of Patients with Alström Syndrome in the Polish Population. *Clin. Genet.* 89 (4), 448–453. doi:10.1111/cge.12656

Conflict of Interest: The authors declare that the research was conducted in the absence of any commercial or financial relationships that could be construed as a potential conflict of interest.

frontiers in Pediatrics

ORIGINAL RESEARCH
published: 09 February 2022
doi: 10.3389/fped.2022.824399

Prenatal Diagnosis of Two Common Inborn Errors of Metabolism by Genetic and Mass Spectrometric Analysis of Amniotic Fluid

Congcong Shi[1†], *Sitao Li*[2†], *Yu Gao*[3], *Zhirong Deng*[2], *Hu Hao*[2] *and Xin Xiao*[2*]

[1] Inborn Errors of Metabolism Laboratory, The Sixth Affiliated Hospital, Sun Yat-sen University, Guangzhou, China, [2] Department of Pediatrics, The Sixth Affiliated Hospital, Sun Yat-sen University, Guangzhou, China, [3] Department of Obstetrical, The Sixth Affiliated Hospital, Sun Yat-sen University, Guangzhou, China

OPEN ACCESS

Edited by:
Huiwen Zhang,
Xinhua Hospital, China

Reviewed by:
Orna Staretz Chacham,
Ben-Gurion University of the Negev, Israel
Hidde Huidekoper,
Erasmus Medical Center, Netherlands

***Correspondence:**
Xin Xiao
xiaoxin2@mail.sysu.edu.cn

[†]These authors have contributed equally to this work and share first authorship

Specialty section:
This article was submitted to Genetics of Common and Rare Diseases, a section of the journal Frontiers in Pediatrics

Received: 29 November 2021
Accepted: 17 January 2022
Published: 09 February 2022

Citation:
Shi C, Li S, Gao Y, Deng Z, Hao H and Xiao X (2022) Prenatal Diagnosis of Two Common Inborn Errors of Metabolism by Genetic and Mass Spectrometric Analysis of Amniotic Fluid. Front. Pediatr. 10:824399. doi: 10.3389/fped.2022.824399

Methylmalonic acidaemia (MMA) and ornithine transcarbamylase deficiency (OTCD) are both intoxication-type inborn errors of metabolism (IEM). Presently, genetic testing is the primary method for prenatally diagnosing these diseases. However, some reports have demonstrated that mass spectrometry approaches can prenatally diagnose some forms of inborn errors of metabolism using amniotic fluid. Therefore, in this study, genetic and mass spectrometry approaches were used for prenatally diagnosing MMA and OTCD. We collected amniotic fluid samples from 19 foetuses referred, 15 cases were referred for MMA and 4 for OTCD. Of the 15 MMA cases, seven were affected, as determined by genetic testing and the metabolite levels; the characteristic metabolites propionylcarnitine (C3), C3/acetylcarnitine (C2) ratio, methylmalonic acid and methylcitrate levels were significantly higher than the reference range. Eight foetuses were unaffected, and the C3, C3/C2 ratio, methylmalonic acid and methylcitrate levels were within the reference range. The C3, C3/C2, methylmalonic acid, and methylcitrate levels in the amniotic fluid significantly differed between the affected and unaffected foetuses ($P = 0.0014$, $P = 0.0014$, $P = 0.0003$, $P = 0.0014$, respectively). Moreover, the homocysteine level increased in the amniotic fluid of affected foetuses with *MMACHC* gene mutations. Of the four OTCD cases, genetic testing confirmed that two foetuses were affected and two were unaffected. However, the characteristic metabolite levels were within the reference range for all foetuses, including citrulline, orotic acid, and uracil. The genetic testing results were confirmed to be correct through the abortion tissue of the foetus and the postnatal follow-up. Our results suggest that mass spectrometry approaches are convenient method for improving the prenatal diagnosis of MMA. The characteristic metabolites C3, C3/C2, methylmalonic acid, and methylcitrate levels in amniotic fluid were reliable biochemical markers for the prenatal diagnosis of MMA.

Keywords: methylmalonic acidaemia, ornithine transcarbamylase deficiency, gas chromatography mass spectrometry, tandem mass spectrometry, prenatal diagnosis

INTRODUCTION

Methylmalonic acidaemia (MMA) and ornithine transcarbamylase deficiency (OTCD) are both common intoxication-type inborn errors of metabolism (IEM) in China (1, 2). The estimated incidence of MMA is 1.5–3 cases per 100 000 people, and the OTCD incidence is between 1 case per 77 000 people and 1 per 14,000 people (3, 4). MMA is an autosomal recessive organic acidaemia associated with methylmalonyl-CoA mutase and cobalamin metabolic defects. There are five common clinical MMA subtypes, namely mut, cblA, cblB, cblC, and cblD. OTCD is an X-linked inherited metabolic disease caused by pathogenic variants of the OTC gene, and is the most common type of congenital urea cycle disorder (5). MMA and OTCD patients either die shortly after birth or present with acute deterioration, metabolic acidosis, or hyperammonaemia, and later in life, the presentations include intellectual disabilities or abnormal growth and development (1, 6, 7). Early diagnosis and treatment can prevent complications, and prenatal diagnosis is an important way for families with an IEM proband to prevent IEM recurrence.

Presently, tandem mass spectrometry (MS/MS) and gas chromatography-mass spectrometry (GC/MS) are important methods for screening and clinically diagnosing IEM (8, 9). Some reports have demonstrated that MS/MS and GC/MS can prenatally diagnose some forms of IEM using amniotic fluid, such as MMA, propionic acidaemia, isovaleric acidaemia, and β-ketothiolase deficiency (10–14). Therefore, together with gene sequencing, mass spectrometry provides a new method for prenatally diagnosing IEM.

Since the MS/MS and GC/MS methodologies are mature for diagnosing IEMs, this study describes our experiences with prenatally diagnosing IEM by measuring metabolites in the supernatant of amniotic fluid together with direct mutation analysis in MMA and OTC high-risk pregnancies.

MATERIALS AND METHODS

Probands

From January 2019 to June 2021, we recruited 15 unrelated families with MMA probands, 4 unrelated families with OTCD probands, and 73 pregnant women undergoing routine prenatal diagnoses with no history of IEM referrals. Five amniotic fluid samples from the referred MMA cases were collected by the Centre for Prenatal Diagnosis of Xinhua Hospital, Shanghai, China, all other samples were collected by our hospital (The Sixth Affiliated Hospital of Sun Yat-sen University, Guangzhou, China). The probands were diagnosed based on clinical symptoms, GC/MS and MS/MS biochemical results, and genetic testing. Written informed consent was obtained from all participants. The study protocols were approved by the Ethics Committee of the Sixth Affiliated Hospital of Sun Yat-Sen University (ethics committee batch number 2019ZSLYEC-105).

Amniocyte Samples

The pregnant women with MMA or OTCD probands underwent amniocentesis by an experienced obstetrician; 10 mL of amniotic fluid was obtained from each pregnant woman. The amniotic fluid was centrifuged at 3000 r/min. Then, the amniotic fluid cells were collected for DNA extraction, and the supernatant was collected for mass spectrometry detection in separate sterile test tubes and stored at −80°C until use. All samples were collected before beginning the analyses, and the tests for all samples were performed at the same time.

Metabolite Detection and Analysis

The characteristic metabolites detected by MS/MS in the peripheral blood of MMA patients were propionylcarnitine (C3), the C3/acetylcarnitine (C2) ratio (C3/C2), methylmalonic acid, and methylcitrate (15). We also assessed the level of homocysteine (Hcy), which is a specific metabolite of the MMA cblC subtype (16); cblC is caused by mutations of the metabolism of cobalamin associated C (*MMACHC*)gene. The characteristic metabolite detected by MS/MS in the peripheral blood of OTCD patients was citrulline, and the metabolites detected by GC/MS were orotic acid and uracil (3, 5).

The diagnostic criteria for characteristic metabolites of MMA and OTCD are consistent between amniotic fluid and peripheral blood. We used the 95th and 5th percentile mass spectrometry results from the 73 cases of normal (i.e. control) amniotic fluid to establish the upper and lower limits of the normal reference interval, the reference range of the different metabolites were displayed in the results section. All samples were sent to the Inborn Errors of Metabolism laboratory of the Sixth Affiliated Hospital of Sun Yat-sen University for MS/MS and GC/MS testing.

MS/MS Analysis

Several amino acid and carnitine, methylmalonic acid, methylcitrate, and total Hcy determination kits (Zhipu Biotechnology Corporation, Shandong, China) were used for the analysis. MS/MS (Xevo TQ-DIVD, Waters Corporation, Milford, MA, USA) was used to detect the metabolites in 3 μL of amniotic fluid.

GC/MS Analysis

GC/MS (Q1000, Japan Electronics Co., Ltd.) was used to evaluate orotic acid and uracil in 100 mL of amniotic fluid. The amniotic fluid samples were processed by adding internal standard, deproteinizing, vacuum drying, and trimethylsilyl derivatization (BSTFA/TMCS) before testing.

Mutation Analysis

The QIAamp DNA Blood Mini Kit (Qiagen Inc., Valencia, CA, USA) was used to extract DNA from the amniotic fluid exfoliated cells, and then, polymerase chain reaction amplification and Sanger sequencing were used to test the candidate variants. The reference gene sequences were obtained from National Centre for Biotechnology Information GenBank database. Short tandem repeat analyses were performed to exclude maternal blood contamination and perform linkage analysis.

Diagnostic Criteria

Foetuses were considered affected by MMA if the characteristic metabolites in the amniotic fluid were higher than the upper

TABLE 1 | Gene mutations and clinical diagnosis of 19 probands.

Family no.	Gender	Gene	Mutation 1 (paternal)	Mutation 2 (maternal)	Clinical diagnosis
F1	Female	*MMUT*	c.1741C > T (p.Arg581Ter)	c.385 + 5G > A (splicing)	mut-type MMA
F2	Male	*MMUT*	c.1630_1631del insTA (p.Gly544Ter)	c.753G > T (p.Lys251Asn)	mut-type MMA
F3	Male	*MMUT*	c.1106C > T (p.Arg369His)	c.1159T > G (p.Thr387Pro)	mut-type MMA
F4	Female	*MMUT*	c.424A > G (p.Thr142Ala)	c.323G > A (p.Arg108His)	mut-type MMA
F5	Male	*MMUT*	c.729_730insTT (p.Asp244LeufsTer39)	c.1850T > C (p. Leu617Arg)	mut-type MMA
F6	Male	*MMUT*	c.729_730insTT (p.Asp244LeufsTer39)	c.1663G > A (p.Ala555Thr)	mut-type MMA
F7	Male	*MMUT*	c.323G > A(p.Arg108His)	c.323G > A(p.Arg108His)	mut-type MMA
F8	Female	*MMUT*	c.1280G > A (p.Gly427Asp)	c.1031C > A (p.Ser344Cys)	mut-type MMA
F9	Male	*MMUT*	c.1106G > A (p.Arg369His)	c.1677-1G > A (splicing)	mut-type MMA
F10	Female	*MMAB*	c.289_290delGG (p.Gly97ValfsTer120)	c.566G > A (p.Cys189Tyr)	cblB-type MMA
F11	Female	*MMACHC*	c.482G > A (p.Arg161Gln)	c.80A > G (p.Gln27Arg)	cblC-type MMA
F12	Male	*MMACHC*	c.228_231delTGAC (p.Asp77GlnfsTer22)	c.609G > A (p.Trp203Ter)	cblC-type MMA
F13	Female	*MMACHC*	c.567dupT (p.Ile190TyrfsTer13)	c.609G > A (p.Trp203Ter)	cblC-type MMA
F14	Male	*MMACHC*	c.80A > G (p.Gln27Arg)	c.217C > T (p.Arg73Ter)	cblC-type MMA
F15	Male	*MMACHC*	c.609G > A (p.Trp203Ter)	c.658_660del (p.Lys220del)	cblC-type MMA
F16	Male	*OTC*	-	c.782T > C (p.Ile261Thr)*	OTCD
F17	Male	*OTC*	-	c.867 + 1G > C (splicing)*	OTCD
F18	Male	*OTC*	-	c.103insA (p.Val35SerfsX7)*	OTCD
F19	Male	*OTC*	-	c.512A > G (p.Gln171Arg)*	OTCD

*MMA, Methylmalonic Acidemia; OTCD, Ornithine transcarbamylase deficiency. *The Mutation is Hemizygous.*

limit of the reference range and the genetic test results of the amniotic fluid cells were consistent with the genetic test results of the proband.

Foetuses were considered affected by OTCD if the concentration of citrulline in the amniotic fluid was lower than the lower limit of the reference range and the concentrations of orotic acid and uracil were higher than the upper limit of the reference range. Further, the genetic test results of the amniotic fluid cells must be consistent with the genetic test results of the proband.

Statistical Analyses

SPSS version 21.0 (IBM Corp., Armonk, NY, USA) was used for the analyses. The reference range for each analyte was determined by a nonparametric approach, identified the 95th and 5th percentiles from the cumulative levels of the 73 normal foetuses as the upper and lower reference limits, respectively. Wilcoxon rank-sum tests with exact P-values were performed to compare the levels of the characteristic metabolites between affected and unaffected groups. $P < 0.05$ was considered statistically significant.

RESULTS

Patient Demographics

We included 19 pregnant women with MMA or OTCD probands aged between 27 and 36 years with gestational ages from 16–21 weeks. We also included 72 pregnant women undergoing routine prenatal diagnosis (i.e. healthy controls) aged between 25 and 38 years with gestational ages from 16–23 weeks.

Table 1 presents the gene mutation spectrum for cases in this study. There were 9 MMA probands with methylmalonyl-CoA mutase (i.e. *MMUT*) mutations, 5 with *MMACHC* mutations, and 1 with metabolism of cobalamin associated B (i.e. *MMAB*) mutations. The OTCD probands all had the ornithine transcarbamylase (*OTC*) gene mutations.

Reference Range

We established a reference range for each analyte using the 95th and 5th percentiles. The following values were considered normal: C3 = 0.16–1.53 μmol/L, C3/C2 = 0.08–0.57 μmol/L, methylmalonic acid 0.97–1.81 μmol/L, and methylcitrate 0.01–0.79 μmol/L. Further, the specific product of cblC also has Hcy 2.40–6.95 μmol/L, citrulline (Cit) > 3.30 μmol/L, orotic acid (Orotate) 0.00 mmol/mol creatinine, and uracil (Uracil) 0.00 mmol/mol creatinine.

MMA and OTCD Diagnoses

We found no maternal contamination in the amniotic fluid samples by short tandem repeat analysis. **Table 2** presents the amniotic fluid metabolite and DNA sequencing results of the 15 pregnancies from MMA families referred. The genetic and metabolite analyses had high consistency. Seven foetuses were affected by MMA, and eight were unaffected. The seven affected foetuses had the same compound heterogeneous mutations as their probands. The C3 (median: 8.47 μmol/L, range: 3.56–15.55), C3/C2 (median: 1.46, range: 0.76–2.20), methylmalonic acid (median: 35.85 μmol/L, range: 9.81–66.78), and methylcitrate (median: 6.48 μmol/L, range: 3.69–17.62) levels in amniotic fluid were higher than the reference ranges. The Hcy concentration in the amniotic fluid of two foetuses

TABLE 2 | The characteristic metabolite levels and DNA sequencing results in the amniotic fluid samples of 15 foetuses from MMA families referred.

Family no.	Gestational ages	C3 (μmol/L)	C3/C2	Methylmalonic acid (μmol/L)	Methylcitrate (μmol/L)	Hcy (μmol/L)	Gene	Mutation 1 (Paternal)	Mutation 2 (Maternal)	Foetus status
F1	17 weeks	**1.79**	0.25	1.58	0.17	**10.60**	*MMUT*	–	c.385 + 5G > A (splicing)	Unaffected
F2	19 weeks	**8.71**	**1.59**	**35.85**	**4.81**	4.31	*MMUT*	c.1630_1631delinsTA (p.Gly544Ter)	c.753G > T (p.Lys251Asn)	Affected
F3	17 weeks	**13.85**	**1.73**	**66.78**	**7.45**	5.77	*MMUT*	c.1106C > T (p.Arg369His)	c.1159T > G (p.Thr387Pro)	Affected
F4	16 weeks	**7.21**	**1.46**	**15.97**	**6.48**	4.68	*MMUT*	c.424A > G (p.Thr142Ala)	c.323G > A (p.Arg108His)	Affected
F5	17 weeks	**15.55**	**2.20**	**43.04**	**17.62**	6.07	*MMUT*	c.729_730insTT (p.Asp244LeufsTer39)	c.1850T > C (p. Leu617Arg)	Affected
F6	16 weeks	1.09	0.13	1.63	0.02	4.66	*MMUT*	–	–	Unaffected
F7	18 weeks	0.82	0.17	1.15	0.52	2.37	*MMUT*	–	–	Unaffected
F8	16 weeks	1.29	0.18	1.30	0.46	6.29	*MMUT*	–	c.1031C > A (p.Ser344Cys)	Unaffected
F9	18 weeks	**4.94**	**1.01**	**49.96**	**9.90**	6.44	*MMUT*	c.1106G > A (p.Arg369His)	c.1677-1G > A (splicing)	Affected
F10	20 weeks	0.48	0.07	1.24	0.26	4.27	*MMAB*	c.289_290delGG (p.Gly97ValfsTer120)	–	Unaffected
F11	17 weeks	**8.47**	**0.94**	**9.81**	**3.69**	**20.67**	*MMACHC*	c.482G > A (p.Arg161Gln)	c.80A > G (p.Gln27Arg)	Affected
F12	19 weeks	**3.56**	**0.76**	**15.91**	**4.73**	**18.50**	*MMACHC*	c.228_231delTGAC (p.Asp77GlnfsTer22)	c.609G > A (p.Trp203Ter)	Affected
F13	18 weeks	0.77	0.24	1.28	0.10	4.07	*MMACHC*	–	–	Unaffected
F14	18 weeks	0.79	0.14	1.53	0.10	3.84	*MMACHC*	c.80A > G (p.Gln27Arg)	–	Unaffected
F15	17 weeks	0.91	0.14	0.8	0.7	1.3	*MMACHC*	c.609G > A (p.Trp203Ter)	–	Unaffected

MMA, Methylmalonic Acidemia; C3, Propionylcarnitine; C2, Acetylcarnitine; Hcy, Homocysteine. Reference range: C3 (0.16–1.53) μmol/L, C3/C2 (0.08–0.57), Methylmalonic acid (0.97–1.81)μmol/L, Methylcitrate (0.01–0.79) μmol/L, Hcy (2.40–6.95) μmol/L. Elevated metabolites are shown in bold.

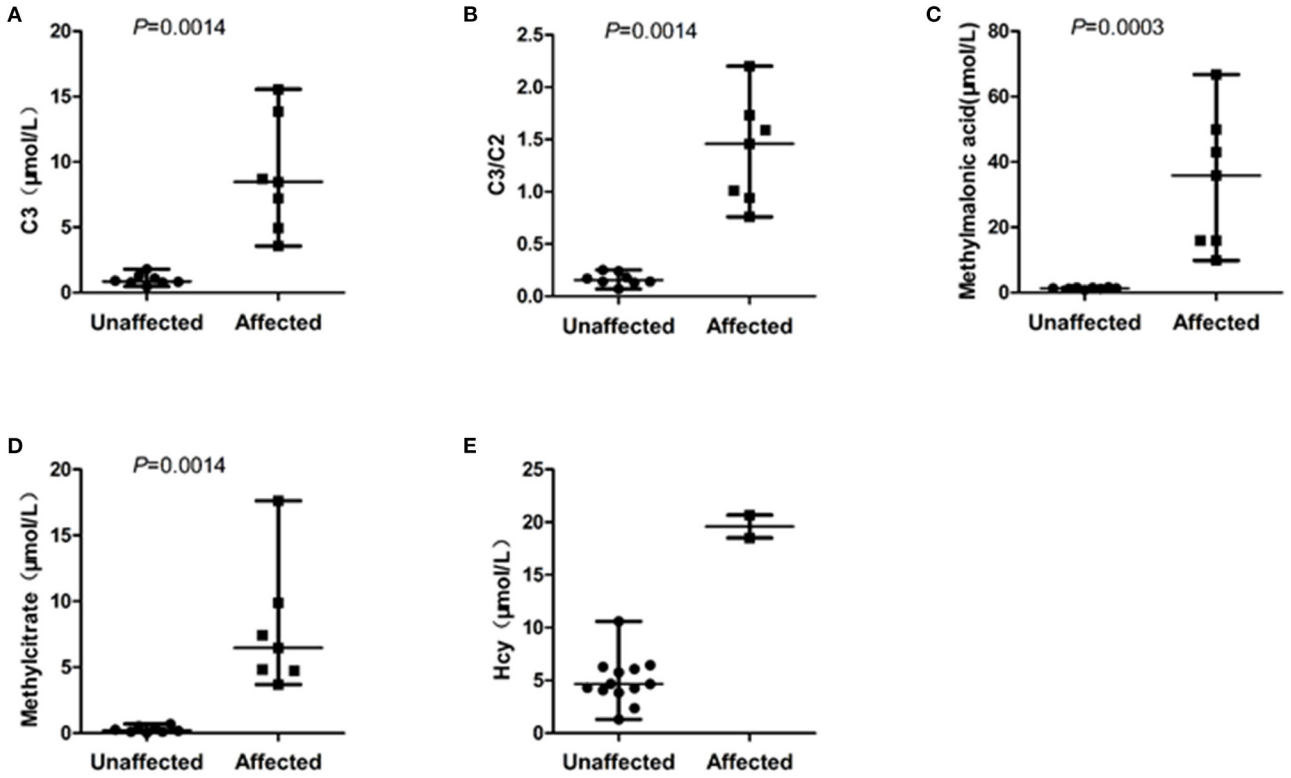

FIGURE 1 | Scatterplot showing the distribution of characteristic metabolite levels in unaffected and affected of 15 cases amniotic fluids referred for MMA. **(A)** The distribution of C3 levels in amniotic fluids between affected and unaffected samples. **(B)** The distribution of C3/C2 ratios in amniotic fluids between affected and unaffected samples. **(C)** The distribution of methylmalonic acid levels in amniotic fluids between affected and unaffected samples. **(D)** The distribution of methylcitrate in amniotic fluids between affected and unaffected samples. **(E)** The distribution of Hcy in amniotic fluids between two foetuses with compound heterogeneous *MMACHC* gene mutations and other amniotic fluid samples unaffected for the *MMACHC* gene. Horizontal lines, median values. *P* values were determined by the Wilcoxon rank sum test.

TABLE 3 | The characteristic metabolites levels and DNA sequencing results in the amniotic fluid samples of four foetuses from OTCD families referred.

Family no.	Gestational ages	Cit (μmol/L)	Orotate (mmol/mol creatinine)	Uracil (mmol/mol creatinine)	Gene	Mutation	Foetus status
F16	17weeks	15.27	0	0	*OTC*	–	Unaffected
F17	17weeks	8.99	0	0	*OTC*	c.867 + 1G > C (splicing)*	Affected
F18	18weeks	9.86	0	0	*OTC*	–	Unaffected
F19	16weeks	8.86	0	0	*OTC*	c.512A > G (p.Gln171Arg)*	Affected

*OTCD, Ornithine transcarbamylase deficiency; Cit, Citrulline; orotic acid, Orotate; Reference range: citrulline > 3.30 μmol/L, orotic acid (Orotate) = 0.00 mmol/mol creatinine, and Uracil = 0.00 mmol/mol creatinine. *The Mutation is Hemizygous.*

with compound heterogeneous *MMACHC* gene mutations was significantly higher than the concentration of the normal range and other affected amniotic fluid samples.

The eight unaffected foetuses carried one heterogeneous mutation ($n = 5$) or no mutation ($n = 3$), and the median levels of C3, C3/C2, methylmalonic acid, and methylcitrate in the amniotic fluid were 0.87 μmol/L(range: 0.48–1.79), 0.16 (range: 0.07–0.25), 4.17 μmol/L(range: 1.30–10.60), 1.29 μmol/L(range: 0.80–1.63), and 0.22 μmol/L(range: 0.02–0.70), respectively. The C3, C3/C2, methylmalonic acid, and methylcitrate levels in the 7 samples amniotic fluid were within normal ranges. The C3 and Hcy levels in F1 was slightly higher than the normal range, while the levels of the other three metabolites were in the normal range. The C3, C3/C2, methylmalonic acid, and methylcitrate levels did not overlap between the affected and unaffected foetuses (**Figure 1**).

Table 3 presents the amniotic fluid metabolite and DNA sequencing results of the 4 pregnancies from OTCD families

referred. Two foetuses were affected, and two were unaffected based on the *OTC* gene mutations analysis, but the citrulline (8.86–15.27 μmol/L, Reference range: Cit > 3.30 μmol/L), orotic acid, and uracil (0.00 mmol/mol creatinine, Reference range: 0.00 mmol/mol creatinine) levels were in the normal ranges for all samples. The amniotic fluid metabolite and genetic testing results were inconsistent. Thus, the prenatal diagnosis was based on the genetic test results. The abortion tissue of the foetus and the postnatal follow-up confirmed the genetic testing.

DISCUSSION

Currently, the standard method for prenatally diagnosing IEM is the detection of genetic mutations in amniotic fluid cells or chorionic tissues, but the disease-causing genes and mutation sites of the proband must be confirmed to complete the prenatal diagnosis. The genetic testing process is also complicated and slow, usually taking 10–25 days. Further, studies have shown that for autosomal recessive diseases, the foetus has only one causative variant as same as the proband, and the genetic testing results of the foetus cannot give a clear conclusion, but mass spectrometry can detect specific metabolite levels in the amniotic fluid, helping the prenatal diagnostic of foetus (13, 17). Importantly, the speed of mass spectrometry is advantageous; the samples in this study were tested by MS/MS and GC/MS within one day. Also, only a small amount of amniotic fluid is required for testing and provides results for multiple metabolites. Therefore, mass spectrometry is a powerful supplement to genetic testing. Current domestic and foreign research indicate that the prenatal diagnosis of genetic metabolic diseases, such as MMA, propionic acidaemia, isovaleric acidaemia, and β-ketothiolase deficiency, can be performed using mass spectrometry (10–14). This study highlights our experience in prenatally diagnosing MMA and OTCD with genetic testing and mass spectrometry.

Some studies have shown that MS/MS detection of C3, methylmalonic acid, and methylcitrate concentrations in amniotic fluid can be used for prenatally diagnosing MMA (10, 12). In this study, the C3, C3/C2, methylmalonic acid, and methylcitrate levels in amniotic fluid were tested by MS/MS in 15 samples from women referred with MMA. These results showed that four biochemical markers significantly differed between the unaffected and affected groups without overlap. Furthermore, all of the three biochemical markers (C3/C2, methylmalonic acid, and methylcitrate) were identical and consistent with the genetic analysis results. However, the C3 levels in F1 was slightly higher than the normal range; the likely reason might be associated with the selection of the reference range. One study suggested that clinical reference ranges may need to be adjusted in response to the degree of overlap between the normal population and the disorder range (18). However, due to the small number of affected samples, it is difficult to establish more reasonable ranges in this manner. Moreover, the normal samples selected in this study are only 73 cases, so the 95th and 5th percentiles were identified as the upper and lower reference limits, respectively. If the number of samples is large enough, the 99.5th and 0.5th percentiles as the upper and lower reference limits may be more reasonable. Nevertheless, our results are also consistent with other related studies, confirming that C3, C3/C2 ratio, methylmalonic acid, and methylcitrate detection in amniotic fluid by MS/MS is feasible for the prenatal diagnosis of MMA.

In this study, we evaluated three MMA subtypes (mut, cblB, and cblC). The cblC subtype, the most common subtype, is caused by biallelic pathogenic variants in the *MMACHC* gene, which encodes a protein involved in the processing and trafficking of intracellular cobalamin. This subtype is also associated with increased Hcy and methylmalonic acid plasma concentrations (17, 19). In our study, five women were referred with MMA type cblC. Three foetuses were unaffected, and two were affected. Except C3, C3/C2, methylmalonic acid, and methylcitrate, the Hcy level in the amniotic fluid of these affected foetuses was significantly higher than the normal reference range and the Hcy level in the other affected MMA subtypes, consistent with the genetic analysis results. This result suggests that the Hcy level in amniotic fluid is an indicator for the prenatal diagnosis of cblC subtype. However, the Hcy levels in F1 was higher than the normal range, the likely reason may be the same as the C3, further data are warranted to prove the reliability of Hcy in the prenatal diagnosis.

OTCD, also known as hyperammonaemia type II, is an X-linked recessive genetic disorder; therefore, almost all hemizygous males develop this disease. Approximately, 20% of female carriers present some neurocognitive disorders due to random X-inactivation. However, the symptoms are substantially milder than those experienced by male patients. Presently, genetic testing is the primary method for prenatal diagnosis of OTCD; although male foetuses can be diagnosed, due to the unpredictability of random X chromosome inactivation, it is impossible to determine whether foetal female carriers have the disease. Prenatal diagnosis of OTCD in female foetuses using mass spectrometry will therefore be difficult. In this study, four women were referred with OTCD, and all foetuses were confirmed to be male through genetic testing. The MS/MS and GC/MS results showed that the citrulline, orotic acid, and uracil levels in all amniotic fluid samples were within the reference range, suggesting that none of the foetuses had OTCD. However, the genetic testing indicated a c.512A > G hemizygous mutation and c.867 + 1G > C hemizygous mutation in the *OTC* gene in two samples, consistent with the proband, there was no mutation in the other two samples. The metabolite and genetic testing results were inconsistent, suggesting that metabolite analyses using amniotic fluid at 16–22 weeks of pregnancy is not suitable for prenatally diagnosing OTCD. This result has not been suggested in other studies, and more data are warranted to prove the conclusion.

In summary, mass spectrometric approaches are a convenient prenatal diagnostic method for pregnancies at risk for MMA. Characteristic metabolite (C3, C3/C2, methylmalonic acid, and methylcitrate) levels in the amniotic fluid were reliable biochemical markers for prenatally diagnosing MMA. A combined genetic

and biochemical approach would provide increased diagnostic accuracy.

ETHICS STATEMENT

The studies involving human participants were reviewed and approved by the Ethics Committee of the Sixth Affiliated Hospital of Sun Yat-sen University (Ethics Committee Batch no. 2019ZSLYEC-105). The patients/participants provided their written informed consent to participate in this study.

AUTHOR CONTRIBUTIONS

XX conceived and designed the study. CS wrote the manuscript draft. SL, ZD, HH, and XX enrolled the patients. YG performed amniocentesis. CS and SL performed the metabolite test, mutation test, and data analysis. All authors read and approved this manuscript.

FUNDING

This work was supported by Guangzhou Science and Technology Plan Project (No. 201604020154) and Guangdong Science and Technology Plan Project (No. 2020A1414010111).

ACKNOWLEDGMENTS

We acknowledge all patients and their family for participating in this study. Moreover, thanks to the team of Prof. Lianshu Han (Centre for Prenatal Diagnosis, Xinhua Hospital, School of Medicine, Shanghai Jiao Tong University, Shanghai, China) for their support for our research and helpful discussion.

REFERENCES

1. Peng MZ, Li XZ, Mei HF, Sheng HY, Yin X, Jiang MY, et al. Clinical and biochemical characteristics of patients with ornithine transcarbamylase deficiency. *Clin Biochem.* (2020) 84:63–72. doi: 10.1016/j.clinbiochem.2020.06.011
2. Yi ZJ, Yu S, Ying S, Lan XG, Yuan YK, Zhi JZ, et al. Methylmalonic and propionic acidemia among hospitalized pediatric patients: a nationwide report. *Orphanet J Rare Dis.* (2019) 14:292. doi: 10.1186/s13023-019-1268-1
3. Gu XF. *Clinical Genetic Metabolic Diseases*. Beijing: People's Medical Publishing House. (2015).
4. Caldovic L, Abdikarim I, Narain S, Tuchman M, Morizono H. Genotype-phenotype correlations in ornithine transcarbamylase deficiency: a mutation update. *J Genet Genomics.* (2015) 42:181–94. doi: 10.1016/j.jgg.2015.04.003
5. Gordon N. Ornithine transcarbamylase deficiency: a urea cycle defect. *Eur J Paediatr Neurol.* (2003) 7:115–21. doi: 10.1016/S1090-3798(03)00040-0
6. Forny P, Grunewald S. An expanding spectrum of complications in isolated methylmalonic aciduria. *J Mother Child.* (2020) 24:9–13. doi: 10.34763/jmotherandchild.20202402si.2014.000003
7. Haijes HA, Jans JJM, Tas SY, Verhoeven-Duif NM, van Hasselt PM. Pathophysiology of propionic and methylmalonic acidemias. *Part 1: Complications J Inherit Metab Dis.* (2019) 42:730–44. doi: 10.1002/jimd.12129
8. Pandor A, Eastham J, Beverley C, Chilcott J, Paisley S. Share Clinical effectiveness and cost-effectiveness of neonatal screening for inborn errors of metabolism using tandem mass spectrometry: a systematic review. *Health Technol Assess.* (2004) 8:1–121. doi: 10.3310/hta8120
9. Xu K, Wang L, Cai H, Zhang T, Zhang C, Matsumoto I. Screening for inborn errors of metabolism using gas chromatography-mass spectrometry. *J Chromatogr B Biomed Sci Appl.* (2001) 758:75–80. doi: 10.1016/S0378-4347(01)00042-1
10. Cavicchi C, Donati MA, Funghini S, Marca G, Malvagia S, Ciani F, et al. Genetic and biochemical approach to early prenatal diagnosis in a family with mut methylmalonic aciduria. *Clin Genet.* (2006) 69:72–6. doi: 10.1111/j.1399-0004.2005.00547.x
11. Dai M, Xiao B, Zhang H, Ye J, Qiu W, Zhu H, et al. Biochemical and genetic approaches to the prenatal diagnosis of propionic acidemia in 78 pregnancies. *Orphanet J Rare Dis.* (2020) 15:276. doi: 10.1186/s13023-020-01539-w
12. Ji X, Wang H, Ye J, Qiu W, Zhang H, Liang L, et al. Prenatal diagnosis of methylmalonic aciduria from amniotic fluid using genetic and biochemical approaches. *Prenat Diagn.* (2019) 39:993–7. doi: 10.1002/pd.5519
13. Xiao B, Qiu W, Ye J, Zhang H, Zhu H, Wang L, et al. Prenatal diagnosis of glutaric acidemia I based on amniotic fluid samples in 42 families using genetic and biochemical approaches. *Front Genet.* (2020) 11:496. doi: 10.3389/fgene.2020.00496
14. Xu F, Han LS, Ji WJ, Chen T, Zhan X, Ye J, et al. Mass spectrometry combined with gene analysis for prenatal diagnosis of β-ketothiolase deficiency. *J Development Med.* (2018) 6:25–9.
15. Keyfi F, Talebi S, Varasteh AR. Methylmalonic acidemia diagnosis by laboratory methods. *Rep Biochem Mol Biol.* (2016) 5:1–14.
16. Wang F, Han L, Yang Y, Gu X, Ye J, Qiu W, et al. Clinical, biochemical, and molecular analysis of combined methylmalonic acidemia and hyperhomocysteinemia (cblC type) in China. *J Inherit Metab Dis.* (2010) 33:S435–442. doi: 10.1007/s10545-010-9217-0
17. Chen T, Liang L, Zhang H, Ye J, Qiu W, Xiao B, et al. Value of amniotic fluid homocysteine assay in prenatal diagnosis of combined methylmalonic acidemia and homocystinuria, cobalamin C type. *Orphanet J Rare Dis.* (2021) 16:125. doi: 10.1186/s13023-021-01762-z
18. McHugh DM, Cameron CA, Abdenur JE, Abdulrahman M, Adair O, Al Nuaimi SA, et al. Clinical validation of cutoff target ranges in newborn screening of metabolic disorders by tandem mass spectrometry: a worldwide collaborative project. *Genet Med.* (2011) 13:230–254. doi: 10.1097/GIM.0b013e31820d5e67
19. Zhang Y, Yang YL, Hasegawa Y, Yamaguchi S, Shi CY, Song JQ, et al. Prenatal diagnosis of methylmalonic aciduria by analysis of organic acids and total homocysteine in amniotic fluid. *Chin Med J (Engl).* (2008) 121:216–9. doi: 10.1097/00029330-200802010-00006

Conflict of Interest: The authors declare that the research was conducted in the absence of any commercial or financial relationships that could be construed as a potential conflict of interest.

Publisher's Note: All claims expressed in this article are solely those of the authors and do not necessarily represent those of their affiliated organizations, or those of the publisher, the editors and the reviewers. Any product that may be evaluated in this article, or claim that may be made by its manufacturer, is not guaranteed or endorsed by the publisher.

frontiers in Genetics

ORIGINAL RESEARCH
published: 15 February 2022
doi: 10.3389/fgene.2022.805599

The Follow-Up of Chinese Patients in cblC Type Methylmalonic Acidemia Identified Through Expanded Newborn Screening

*Shiying Ling[1†], Shengnan Wu[2†], Ruixue Shuai[1], Yue Yu[1], Wenjuan Qiu[1], Haiyan Wei[2], Chiju Yang[3], Peng Xu[3], Hui Zou[4], Jizhen Feng[5], Tingting Niu[6], Haili Hu[7], Huiwen Zhang[1], Lili Liang[1], Deyun Lu[1], Zhuwen Gong[1], Xia Zhan[1], Wenjun Ji[1], Xuefan Gu[1] and Lianshu Han[1]**

[1]Department of Pediatric Endocrinology/Genetics, Shanghai Institute for Pediatric Research, Xinhua Hospital, School of Medicine, Shanghai Jiao Tong University, Shanghai, China, [2]Department of Endocrinology and Metabolism, Henan Key Laboratory of Children's Genetics and Metabolic Diseases, Children's Hospital Affiliated to Zhengzhou University, Henan Children's Hospital, Zhengzhou Children's Hospital, Zhengzhou, China, [3]Center of Neonatal Disease Screening, Jining Maternal and Child Health Care Hospital, Jining, China, [4]Center of Neonatal Disease Screening, Jinan Maternal and Child Health Care Hospital, Jinan, China, [5]Center of Neonatal Disease Screening, Shijiazhuang Maternal and Child Health Care Hospital, Shijiazhuang, China, [6]Center of Neonatal Disease Screening, Shandong Maternal and Child Health Care Hospital, Jinan, China, [7]Center of Neonatal Disease Screening, Hefei Maternal and Child Health Care Hospital, Hefei, China

Objective: The cblC type of combined methylmalonic acidemia and homocystinuria, an inherited disorder with variable phenotypes, is included in newborn screening (NBS) programs at multiple newborn screening centers in China. The present study aimed to investigate the long-term clinical benefits of screening individual.

Methods: A national, retrospective multi-center study of infants with confirmed cblC defect identified by NBS between 2004 and 2020 was conducted. We collected a large cohort of 538 patients and investigated their clinical data in detail, including disease onset, biochemical metabolites, and gene variation, and explored different factors on the prognosis.

Results: The long-term outcomes of all patients were evaluated, representing 44.6% for poor outcomes. In our comparison of patients with already occurring clinical signs before treatment to asymptomatic ones, the incidence of intellectual impairment, movement disorders, ocular complications, hydrocephalus, and death were significantly different ($p <$ 0.01). The presence of disease onset [Odd ratio (OR) 12.39, 95% CI 5.15–29.81; $p =$ 0.000], variants of c.609G>A (OR 2.55, 95% CI 1.49–4.35; $p = 0.001$), and c.567dupT (OR 2.28, 95% CI 1.03–5.05; $p = 0.042$) were independently associated with poor outcomes, especially for neurodevelopmental deterioration.

Conclusion: NBS, avoiding major disease-related events and allowing an earlier treatment initiation, appeared to have protective effects on the prognosis of infants with cblC defect.

Keywords: methylmalonic acidemia combined with homocysteinemia, long-term outcome, newborn screening, MMACHC gene, tandem mass spectrometry

OPEN ACCESS

Edited by:
Carmen Gherasim, University of Michigan, United States

Reviewed by:
Jennifer Sloan, National Human Genome Research Institute (NHGRI), United States
Harvey L. Levy, Boston Children's Hospital and Harvard Medical School, United States

****Correspondence:***
Lianshu Han
hanlianshu@xinhuamed.com.cn

[†]These authors have contributed equally to this work

Specialty section:
This article was submitted to Genetics of Common and Rare Diseases, a section of the journal Frontiers in Genetics

Received: *30 October 2021*
Accepted: *21 January 2022*
Published: *15 February 2022*

Citation:
Ling S, Wu S, Shuai R, Yu Y, Qiu W, Wei H, Yang C, Xu P, Zou H, Feng J, Niu T, Hu H, Zhang H, Liang L, Lu D, Gong Z, Zhan X, Ji W, Gu X and Han L (2022) The Follow-Up of Chinese Patients in cblC Type Methylmalonic Acidemia Identified Through Expanded Newborn Screening. Front. Genet. 13:805599. doi: 10.3389/fgene.2022.805599

1 INTRODUCTION

Methylmalonic acidemia combined with homocysteinemia (OMIM 277400) is a series of inherited autosomal recessive defects in cobalamin [vitamin B12 (VitB12)] metabolism resulting in impaired synthesis of adenosylcobalamin (AdoCbl) and methylcobalamin (MeCbl), which both are essential coenzymes for the conversion of methylmalonyl-CoA to succinyl-CoA (catalyzed by methylmalonyl-CoA mutase) and remethylation of homocysteine to methionine (catalyzed by methionine synthase) (Dionisi-Vici et al., 2006; Lerner-Ellis et al., 2009; Watkins and Rosenblatt, 2011). The cblC type of combined methylmalonic acidemia and homocystinuria is the most common defect in the intracellular cobalamin metabolism pathway (Nogueira et al., 2008), characterized by variable and non-specific symptoms, especially in childhood. The phenotype has a wide expression, with early-onset (before 1 year from birth) often associated with multisystem involvement, neurological deterioration, maculopathy, failure to thrive, cytopenias, renal and hepatic dysfunction (Rosenblatt et al., 1997; Carrillo-Carrasco et al., 2012; Fischer et al., 2014; He et al., 2020). Neurological damage is often with hydrocephalus, cerebral atrophy, white matter abnormalities, and basal ganglia lesions (Weisfeld-Adams et al., 2013; Fischer et al., 2014; Zhang et al., 2019). Developmental delay and intellectual deficits are also frequently impaired (Weisfeld-Adams et al., 2013).

The incidence of cblC defect ranges from 1:46,000 to 1:200,000 in European and American countries (Morel et al., 2006; Weisfeld-Adams et al., 2010) and varies hugely from 1:3,220 to 1:21,488 in China (Zhou et al., 2018; Wang et al., 2019). Previously, individuals with cblC defects were diagnosed symptomatically. However, since tandem mass spectrometry (MS/MS) has been increasingly used in newborn screening (NBS) programs in China, technically enabling identification of more than 30 inherited metabolic diseases (IMDs) by using a single method, it is recommended to identify those infants who are at risk for IMDs, including cblC defect. Most NBS pilot studies have demonstrated a positive effect on early identification of cblC defect by NBS and the neonatal start of treatment on the neurological outcome to a variable extent (Martínez-Morillo et al., 2016; Mütze et al., 2020). However, the impact on the long-term outcome of individuals with cblC defects in the era of newborn screening is yet to be comprehensively explored. This national multicenter retrospective study, therefore, aims at elucidating the long-term outcome of screened individuals and at investigating the impact of different factors on the disease outcome.

2 PATIENTS AND METHODS

2.1 Patients

From January 2004 to December 2020, a total of 560 patients with cblC defects identified by NBS were diagnosed and treated at multiple hospitals in China. Among them, 9 cases died and 22 cases were lost to follow-up. All patients were ascertained on DNA-based and MS/MS NBS and most receive personalized treatment as well as regular follow-up. To evaluate clinical outcomes, patients were divided into two groups, with the normal outcome group being healthy and the poor outcome group suffering from varying degrees of physical and mental damage. Among poor outcomes, five different types of clinical parameters were included—intellectual impairment, movement disorders, ocular complications, hydrocephalus, and death. "Intellectual impairment" was categorized based on the presence of developmental delay according to age, or neuropsychological test results, or in the absence of neuropsychological test results on educational level or professional employment. "Movement disorders" mainly manifested as involuntary tremor, gait instability, and disability to walk that developed throughout the disease course, objectified during follow-up examinations by pediatricians and physiotherapists shortly after the symptomatic phase. "Ocular complications" included the presence of strabismus, nystagmus, and a range of ocular findings from unremarkable and mild phenotypes to significant retinopathy. "Hydrocephalus" was detected at cranial MRI, which usually depicted ventriculomegaly, extensive cerebral parenchyma atrophy, and subdural effusion. And the most severe clinical outcome is failure to thrive. Parents or legal guardians of the participants signed an informed consent form, approving analysis of their clinical records, and publication of the anonymous data, in agreement with institutional and national legislation. This study was approved by the Ethics Committee of Xinhua Hospital (approval number XHEC-D-2021-140).

2.2 Newborn Screening and Confirmatory Testing

NBS samples of dried blood spots are taken between the ages of 72–120 h according to the recommended time frame (Mak et al., 2013). Blood levels of acylcarnitines, including propionylcarnitine (C3) and acetylcarnitine (C2) were detected by MS/MS (API 4000, American Bio-System Inc., Foster City, CA, United States,) using blood filter papers. The ratio of C3/C2 was calculated at the same time. Second blood spots were requested upon abnormal first-screening results (Niu et al., 2010). To further confirm the diagnosis, urinary organic acids, including methylmalonic acid (MMA) and methylcitric acid (MCA) were measured by gas chromatography-mass spectrometry (GC-MS) (Shimadzu Limited., Shimadzu, Kyoto, Japan, QP 2010) (Al Dhahouri et al., 2018; Al-Dirbashi et al., 2019). Moreover, plasma total homocysteine (tHcy) were assessed using fluorescence polarization immunoassay.

2.3 Molecular Genetic Analysis

Genomic DNA was extracted from peripheral blood using the DNA extraction kit (TIANGEN Biotech, Beijing, China) according to the manufacturer's instructions. All coding exons and flanking regions of *MMACHC* were amplified using polymerase chain reaction (PCR) with primers designed by Primer3 Input (v. 0.4.0, http://bioinfo.ut.ee/primer3-0.4.0/). After PCR, Nucleotide variations were identified using a reference sequence from Genbank (MMACHC: NM_015506). We used the ClinVar database, the HGMD database, and previous literature to identify whether the mutations had been

TABLE 1 | comparison of baseline demographic, clinical, and biochemical characteristics between patients with normal and poor outcomes.

Variable	Normal outcome	Poor outcome	*p* value
No.	298 (55.4%)	240 (44.6%)	
Age at diagnosis (months)	1 (0.8–1.5)	1.5 (1–2.2)	
Age during follow-up (years)	3.34 (0.63–4.52)	3.8 (0.48–5.25)	
Biochemical features at NBS			
C3	7.35 (4–22.47)	7.71 (4–31.5)	0.119
C3/C2	0.52 (0.2–9.19)	0.62 (0.21–3.27)	0.000
MMA	78.82 (5–3,253.72)	112.6 (5.3–2,348.8)	0.01
MCA	2.51 (0–397.13)	3.86 (0.17–209.1)	0.000
tHcy	102.99 (31–1,139)	131.2 (31–750)	0.02
Onset of symptoms, n (%)	63 (21.1%)	187 (77.9%)	0.000
Initial symptoms			
Milk refusal, n (%)	37 (12.4%)	114 (47.5%)	0.000
Vomiting, n (%)	29 (9.7%)	71 (29.6%)	0.000
Drowsiness, n (%)	38 (12.8%)	105 (43.8%)	0.000
Seizures, n (%)	13 (4.4%)	41 (17.1%)	0.000
Coma, n (%)	5 (1.7%)	17 (7.1%)	0.002
Dyskinesia, n (%)	8 (2.7%)	82 (34.2%)	0.000
Developmental delay, n (%)	12 (4%)	80 (33.3%)	0.000
Treatment			
With VB12 before onset	248 (83.2%)	89 (37.1%)	
With VB12 after onset	50 (16.8%)	151 (62.9%)	0.000
Biochemical features during follow-up			
C3	3 (0.06–10.83)	3.39 (0.16–13.96)	0.002
C3/C2	0.12 (0.01–0.36)	0.15 (0.02–0.39)	0.001
MMA	4.29 (0–45.19)	6.85 (0–49.57)	0.002
MCA	0.48 (0–4.99)	0.71 (0–4.95)	0.021
tHcy	30.15 (2–59)	35.35 (6.2–59.5)	0.000
Nucleotide variant			
c.609G>A	173 (58.1%)	178 (74.2%)	0.000
c.658_660delAAG	52 (17.4%)	41 (17.1%)	0.911
c.80A>G	55 (18.5%)	26 (10.8%)	0.014
c.567dupT	20 (6.7%)	30 (12.5%)	0.022
c.482G>A	77 (25.8%)	10 (4.2%)	0.000
Others	140 (47%)	134 (55.8%)	0.041

Reference range: C3 in the blood: 0.5–4 μmol/L; C3/C2 in the blood: 0–0.2 μmol/L; MMA in the urine: 0–4 mmol/mol creatinine; MCA in the urine: 0–0.8 mmol/mol creatinine; tHcy in the blood: 0–15 μmol/L.

reported. The pathogenicity of novel variants was evaluated based on the American College of Medical Genetics and Genomics (ACMG) standards and guidelines.

2.4 Treatment

The treatment of cblC defect varies with different vitamin B12 responsiveness and is adjusted depending on the condition of individual patients (Baumgartner et al., 2014). According to the guideline, the long-term therapy involved parenteral cobalamin, L-carnitine, and oral betaine (Forny et al., 2021). Then, the treatment is adjusted based on levels of biochemical metabolites. Generally, for most patients, intramuscular injections of hydroxocobalamin were the first choice at a dose of 1–20 mg each time, once every 1–20 days, L-carnitine at 50–100 mg/kg/day and oral betaine at 50–100 mg/kg/day.

All patients followed a normal diet. In patients with methionine deficiency, methionine was supplemented orally (Manoli et al., 2016; Huemer et al., 2017).

2.5 Statistical Analysis

All statistical analyses were performed using SPSS 24.0 (IBM, Chicago, IL). Continuous data are expressed either as medians and interquartile range or mean ± standard deviation (SD). Categorical variables are presented as percentages (%). The demographic, clinical, and biochemical characteristics were compared between patients with or without symptoms and patients with different prognoses using 2-sample t test, χ^2/Fisher exact test, or Wilcoxon rank-sum test as appropriate. Overall univariate odds ratios and by different categories of poor outcome were calculated using the logistic regression. Multivariate logistic regression analysis was performed using variables that were significantly associated with a poor outcome in univariate analysis to determine the independent risk factors. A value of $p < 0.05$ was considered to indicate statistical significance.

3 RESULTS

3.1 Study Population

Among all 538 (280 males, 253 females) patients, who were enrolled in our study, 298 (55.4%) were with normal physical and neurocognitive development, 240 (44.6%) had poor outcomes, in which 9 children died of frequent and severe

TABLE 2 | Comparison of baseline demographic, clinical, and biochemical characteristics between patients with or without symptoms before treatment.

	Asymptomatic before treatment	Symptomatic before treatment	*p* value
No.	337 (62.6%)	201 (37.4%)	
Age during follow-up (yeas)	3.59 (0.48–4.86)	3.52 (0.67–5.25)	
Age at diagnosis (months)	0.8 (1–1.73)	1.5 (1–2.2)	
Biochemical features at NBS			
C3	7.33 (4–26.13)	7.97 (4.01–31.5)	0.087
C3/C2	0.52 (0.2–9.19)	0.65 (0.22–3.34)	0.000
MMA	85.38 (5–3,253.72)	116.31 (5.3–1,693)	0.022
MCA	2.71 (0–397.13)	3.45 (0.17–209.1)	0.01
tHcy	100 (31–1,139)	134.2 (31–750)	0.001
Biochemical features after treatment			
C3	3.08 (0.26–10.96)	3.66 (0.06–13.96)	0.002
C3/C2	0.12 (0.01–0.37)	0.14 (0.03–0.39)	0.005
MMA	4.7 (0–49.57)	6.45 (0–44.61)	0.036
MCA	0.53 (0–4.99)	0.7 (0–4.95)	0.086
tHcy	30.5 (2–59.5)	35.4 (6.47–59)	0.001
Nucleotide variant			
c.609G>A	205 (60.8%)	146 (72.6%)	0.005
c.658_660delAAG	61 (18.1%)	32 (15.9%)	0.518
c.80A>G	60 (17.8%)	21 (10.4%)	0.021
c.567dupT	24 (7.1%)	26 (12.9%)	0.025
c.482G>A	80 (23.7%)	7 (3.5%)	0.000
others	166 (49.3%)	108 (53.7%)	0.315
Outcome			
Normal	248 (73.6%)	50 (24.9%)	
Poor	89 (26.4%)	151 (75.1%)	0.000
Intellectual impairment	88 (26.1%)	146 (72.6%)	0.000
Movement disorders	39 (11.6%)	65 (32.3%)	0.000
Ocular Complications	6 (1.8%)	25 (12.4%)	0.000
Hydrocephalus	2 (0.6%)	7 (3.5%)	0.016
Deceased	2 (0.6%)	7 (3.5%)	0.016

Reference range: C3 in the blood: 0.5–4 μmol/L; C3/C2 in the blood: 0–0.2 μmol/L; MMA in the urine: 0–4 mmol/mol creatinine; MCA in the urine: 0–0.8 mmol/mol creatinine; tHcy in the blood: 0–15 μmol/L.

relapses of metabolic decompensations or hydrocephalus. For nearly all patients, data were available from NBS to the last moment of follow-up. **Table 1** is a comparison of demographic variables between those with and without poor outcomes. The median age during the follow-up period in two groups was 3.34 years (range 0.63–4.52 years) and 3.8 years (range 0.48–5.25 years), respectively. The age at diagnosis was 1 month (range 0.8–1.5 months) in the normal outcome group, while 1.5 months (range 1–2.2 months) in the poor outcome group. Although all patients were identified by NBS, a total of 201 (37.4%) patients already developed symptoms before treatment, which included poor feeding, vomiting, drowsiness, seizures, developmental delay, and so on. The incidence of variable clinical features was compared between individuals with or without normal physical and neurocognitive development. As shown in **Table 1**, the incidence of different kinds of initial symptoms was significantly higher in the poor outcome group ($p < 0.05$), which indicates the onset of symptoms might have an adverse impact on the long-term outcome.

3.2 Biochemical Features

In the study, all the patients were screened by MS/MS presented with elevated C3 levels (>4 μmol/L), an increased C3/C2 ratio (>0.2 μmol/L) in dried blood spots. Subsequently, the increased MMA and MCA levels in urine as well as elevated total plasma homocysteine were exhibited in confirmatory testing. Importantly, the ratio of blood C3/C2, the level of urinary MMA, and MCA in the NBS sample were higher in the poor outcome group than in the normal group (all $p < 0.05$), except for the blood C3 ($p = 0.119$). Data about tHcy levels showed similar differences between the two groups ($p < 0.05$). As can be seen from **Table 1**, the biochemical markers after treatment showed the difference between individuals with different outcomes, which the blood C3, blood C3/C2 ratio, urinary MMA, urinary MCA, and tHcy were lower in the normal outcome group than those in poor outcome group (all $p < 0.05$). Additionally, all of the biochemical parameters reached the normal range after treatment, laboratory values of blood C3, blood C3/C2 ratio, urinary MMA, urinary MCA, and tHcy showed remarkably decrease tendency than those before treatment, with a significant statistical difference (all $p < 0.01$). As is evident from **Table 2**, the greatest differences in biochemical data including the blood C3/C2 ratio, urinary MMA, and MGA, tHcy, were observed between asymptomatic or symptomatic subjects as well. However, there were no statistically significant differences in blood C3 at NBS ($p = 0.087$). The urinary MCA at the last available visit between affected infants with or without symptomatic presentation also did not reveal statistically significant results ($p = 0.086$), which may be the reason for there being limited and insufficient data, partly caused by the patient referral process.

3.3 Gene Analysis

MMACHC mutations were found on both alleles in 510 of 534 patients (95.5%), whereas a single mutation on one allele was noted in 24 patients (4.5%). Among them, 74 different mutations were identified, including 16 nonsense mutations that account for 52.5% (552/1,052) of alleles; the remainder consisted of 18 missense mutations, 3 duplications, 27 deletions, 5 insertions, 5 splice-site mutations. Sequencing analysis identified *MMACHC* mutation in 97.8% (1,052 of 1,076) of all disease alleles. Among them, the common mutation was c.609G>A (p.W203X), c.658_660delAAG (p.K220del), c.482G>A (p.R161Q), c.80A>G (p.Q27R), c.567dupT (p.I190Yfs*13), which accounted for 41.3% (434 of 1,052), 9.2% (97 of 1,052), 9.0% (95 0f 1,052), 8.3% (87 of 1,052) and 4.9% (51 of 1,052), respectively. Between groups with good and poor outcomes or groups whether showed symptoms when therapy was initiated, the types of mutation sites strongly differed. In poor outcome group, the variant of c.609G>A (p.W203X) was more common (74.2% vs. 58.1%), as was c.567dupT (p.I190Yfs*13) (12.5% vs. 6.7%), while these patients appeared to have less incidence of c.482G>A (p.R161Q) (4.2% vs. 25.8%) and c.80A>G (p.Q27R) (10.8% vs. 18.5%) in *MMACHC*. In analogy, c.609G>A (p.W203X) and c.567dupT (p.I190Yfs*13) in *MMACHC* were increasingly observed in symptomatic patients, while c.482G>A (p.R161Q) and c.80A>G (p.Q27R) were more often in asymptomatic patients. Therefore receiving a disease-specific therapy, individuals with these variants in our cohort were more likely to have a better prognosis.

3.4 Follow-Up and Outcomes

We evaluated the current health condition of the patients up to December 2020. The prognosis is shown in detail in **Table 1**. However, of the 240 patients who showed poor prognosis, 234 (97.5%) developed progressive intellectual impairment, 104 (43.3%) manifested movement disorders, 31 (12.9%) exhibited ocular problems, 9 (3.8%) had hydrocephalus and 9 (3.8%) died from disease onset. By dividing them into two groups which depend on whether they suffered from early symptoms of disease before therapy, there is a significant difference between good or poor outcomes ($p < 0.01$). Unfortunately, patients detected by newborn screening but treated after disease onset were more likely to show poor outcomes. In comparison with individuals who remained asymptomatic before treatment, the proportion of intellectual impairment (72.6% vs. 26.1%), movement disorders (32.3% vs. 11.6%), ocular complications (12.4% vs. 1.8%), hydrocephalus (3.5% vs. 0.6%), and death (3.5% vs. 0.6%) were higher in symptomatic group. It is worth noting that among patients deceased, all developed severe symptoms, except two cases without specific symptoms at first who then progressively developed clinical manifestations later even if they received therapy. This might be due to poor treatment compliance.

3.5 Factors Affecting Variable Outcomes

Two hundred and forty patients with different types of poor outcomes were analyzed by both univariate and multivariate logistic regression. Factors including the onset of symptoms, nucleotide variants, biochemical markers at NBS, time from onset to treatment initiation were analyzed.

Univariate analysis showed onset of symptom [Odd ratio (OR) 13.16, 95% CI 8.71–19.89; $p = 0.000$], presence of c.609G>A (OR 2.07, 95% CI 1.43–3.00; $p = 0.000$), and c.567dupT in the *MMACHC* gene (OR 1.99, 95% CI 1.1–3.6; $p = 0.023$), baseline C3 (OR 1.06, 95% CI 1.01–1.12; $p = 0.031$) and C3/C2 (OR 1.5, 95% CI 1.04–2.17; $p = 0.031$) were associated with poor outcomes in the whole sample (**Table 3**). In multivariate logistic regression analysis, onset of symptom (OR 12.39, 95% CI 5.15–29.81; $p = 0.000$), the presence of c.609G>A (OR 2.55, 95% CI 1.49–4.35; $p = 0.001$), and c.567dupT in the *MMACHC* gene (OR 2.28, 95% CI 1.03–5.05; $p = 0.042$) remained independently associated with poor outcomes.

The results of the logistic regression analysis for the poor outcomes are listed in **Table 3**. In subjects with intellectual impairment, the multivariate logistic regression analysis showed that onset of symptoms (OR 12.31, 95% CI 5.11–29.66; $p = 0.000$), the mutation of c.609G>A (p.W203X) (OR 2.53, 95% CI 1.48–4.31; $p = 0.001$) and c.567dupT in the *MMACHC* gene (OR 2.57, 95% CI 1.17–5.66; $p = 0.019$) independently predicted the outcome of intellectual impairment (**Table 4**). While in patients who had ocular abnormalities, the mutation of c.567dupT in the *MMACHC* gene (OR 3.72, 95% CI 1.55–8.94; $p = 0.003$) was an independent predictor as well as the onset of symptoms (OR 5.84, 95% CI 1.13–30.12; $p = 0.035$) (**Table 5**). In the group with movement disorders, the independent predictor was the onset of disease (OR 13.47, 95% CI 5.6–32.33; $p = 0.000$) as well as the concentration of MMA (OR 1.00, 95% CI 1.00–1.00; $p = 0.027$), whereas the type of nucleotide variant was not significantly correlated with it (**Table 6**). Additionally, none of the factors were independently associated with the outcome of hydrocephalus (**Table 7**).

4 DISCUSSION

Previous NBS programs enormously improved the health outcomes of affected individuals, since early diagnosis is known to have a great benefit for effectively treating some inborn errors of metabolism (Mütze et al., 2020; Lüders et al., 2021). However, many European countries do not generally advocate widespread screening for the disease of propionate metabolism on the basis that long-term outcomes may not be significantly influenced by early detection (Leonard et al., 2003). In the United States, screening is advocated: it has been argued that even in the absence of clear clinical benefit, early diagnosis enables families to receive genetic counseling more promptly and avoids expensive and time-consuming radiologic and biochemical investigations in affected children. Although there are no national detailed expanded NBS standards in China due to regional differences in the application of MS/MS and lack of valid studies, some work has been done on epidemiology, technical aspects, and clinic validity of MS/MS screening in several provinces and cities in China (Zhang et al., 2021), indicated that NBS programs can prevent irreversible neurological damage

TABLE 3 | Univariate and multivariate analysis of predictors for poor outcome.

	Univariable analysis			Multivariable analysis		
	OR	**95% CI**	***p* value**	**OR**	**95% CI**	***p* value**
Onset of symptoms	13.16	8.71–19.89	0.000	12.39	5.15–29.81	0.000
Nucleotide variant						
c.609G>A	2.07	1.43–3.00	0.000	2.55	1.42–3.8	0.001
c.658_660delAAG	0.98	0.62–1.53	0.911			
c.80A>G	0.54	0.33–0.89	0.015			
c.567dupT	1.99	1.1–3.6	0.023	2.28	1.03–5.05	0.042
c.482G>A	0.13	0.06–0.25	0.000			
Others	1.43	1.01–2.01	0.041	1.95	1.23–3.09	0.005
Biochemical features at baseline						
C3	1.06	1.01–1.12	0.031	1.02	0.96–1.08	0.577
C3/C2	1.50	1.04–2.17	0.031	0.78	0.53–1.14	0.194
MMA	1.00	1.00–1.00	0.079			
MCA	1.01	1.00–1.01	0.323			
tHcy	1.00	1.00–1.00	0.057			
With VB12 after onset	8.42	5.63–12.57	0.000	0.82	0.35–2.00	0.66

TABLE 4 | Univariate and multivariate analysis of predictors for intellectual impairment.

	Univariable analysis			Multivariable analysis		
	OR	**95% CI**	***p* value**	**OR**	**95% CI**	***p* value**
Onset of symptoms	12.15	8.07–18.30	0.000	12.30	5.11–29.66	0.000
Nucleotide variant						
c.609G>A	2.01	1.39–2.91	0.000	2.31	1.41–3.77	0.001
c.658_660delAAG	0.93	0.59–1.46	0.739			
c.80A>G	0.53	0.32–0.88	0.014			
c.567dupT	2.09	1.15–3.78	0.015	2.49	1.17–5.29	0.018
c.482G>A	0.12	0.06–0.24	0.000			
Others	1.52	1.08–2.15	0.016	2.14	1.35–3.39	0.001
Biochemical features at baseline						
C3	1.07	1.02–1.13	0.012	1.03	0.97–1.10	0.287
C3/C2	1.55	1.07–2.25	0.021	0.86	0.61–1.21	0.387
MMA	1.00	1.00–1.00	0.079			
MCA	1.01	1.00–1.01	0.298			
tHcy	1.00	1.00–1.00	0.054			
With VB12 after onset	7.51	5.07–11.14	0.000	0.72	0.31–1.72	0.464

TABLE 5 | Univariate and multivariate analysis of predictors for ocular complication.

	Univariable analysis			Multivariable analysis		
	OR	**95% CI**	***p* value**	**OR**	**95% CI**	***p* value**
Onset of symptoms	11.98	3.6–39.92	0.000	5.84	1.13–30.12	0.035
Nucleotide variant						
c.609G>A	0.55	0.26–1.13	0.105			
c.658_660delAAG	1.73	0.75–3.99	0.201			
c.80A>G	0.59	0.18–1.99	0.394			
c.567dupT	4.65	2.01–10.76	0.000	3.72	1.55–8.94	0.003
c.482G>A	0	0	0.997			
Others	1.18	0.57–2.45	0.654			
Biochemical features at baseline						
C3	1.01	0.91–1.12	0.858			
C3/C2	0.79	0.34–1.81	0.570			
MMA	1.00	1.00–1.00	0.708			
MCA	1.01	1.00–1.02	0.189			
tHcy	1.00	1.00–1.00	0.363			
With VB12 after onset	7.84	3.16–19.46	0.000	2.12	0.60–7.42	0.242

TABLE 6 | Univariate and multivariate analysis of predictors for movement disorders.

	Univariable analysis			Multivariable analysis		
	OR	**95% CI**	***p* value**	**OR**	**95% CI**	***p* value**
Onset of symptoms	7.87	4.57–13.55	0.000	13.47	5.61–32.33	0.000
Nucleotide variant						
c.609G>A	1.57	0.98–2.52	0.063			
c.658_660delAAG	0.51	0.26–0.99	0.047			
c.80A>G	0.77	0.41–1.45	0.418			
c.567dupT	1.72	0.89–3.32	0.107			
c.482G>A	0.12	0.04–0.4	0.000			
Others	1.40	0.91–2.16	0.125			
Biochemical features at baseline						
C3	0.99	0.93–1.06	0.785			
C3/C2	1.29	0.92–1.80	0.140			
MMA	1.00	1.00–1.00	0.012	1.00	1.00–1.00	0.021
MCA	1.01	1.00–1.02	0.080			
tHcy	1.00	1.00–1.00	0.180			
With VB12 after onset	3.65	2.34–5.70	0.000	0.43	0.20–0.92	0.030

TABLE 7 | Univariate and multivariate analysis of predictors for hydrocephalus.

	Univariable analysis			Multivariable analysis		
	OR	**95% CI**	***p* value**	**OR**	**95% CI**	***p* value**
Onset of symptoms	9.49	1.18–76.39	0.035	5.98	0.37–97.21	0.209
Nucleotide variant						
c.609G>A	1.07	0.26–4.31	0.928	1.29	0.69–2.42	0.425
c.658_660delAAG	1.38	0.28–6.73	0.694			
c.80A>G	0.71	0.089–5.77	0.75			
c.567dupT	2.86	0.58–14.17	0.197			
c.482G>A	0.64	0.08–5.21	0.68			
Others	0.48	0.12–1.92	0.297			
Biochemical features at baseline						
C3	0.76	0.55–1.05	0.092			
C3/C2	0.37	0.05–2.90	0.344			
MMA	1.00	1.00–1.00	0.499			
MCA	1.00	0.97–1.03	0.935			
tHcy	1.00	0.99–1.01	0.985			
With VB12 after onset	6.04	1.24–29.38	0.026	1.73	0.21–14.41	0.611

and death by allowing treatment to be started, ideally, before the onset of symptoms. We conducted a national multicenter study including 538 patients identified by NBS with confirmed cblC defect to investigate their long-term outcome and to identify the major predictors of the disease outcome.

In the present study, we investigated the clinical and biochemical characteristics of patients with different outcomes to discuss the potential risk factor of poor outcomes. As expected, there were significant differences in clinical phenotypes, pathogenic variants, and biochemical features both at NBS and during follow-up. Meanwhile, infants with poor outcomes appeared to take therapeutic measures after disease onset, conversely, the normal group was more likely to take timely treatment once positive NBS results had been reported at birth, underlining the importance of optimal diagnostic process quality and early NBS results. Importantly, cblC defect is with a high frequency of severe and potentially fatal neonatal decompensations often already during the first days of life (Heringer et al., 2016), a delay in treatment might lead to irreversible damage, pointing out emphatically the importance of pre-symptomatic treatment (He et al., 2020). The mortality rate of patients identified by NBS tended to be lower (Dionisi-Vici et al., 2006). The nine deceased patients in our study, though detected by newborn screening, were all treated after disease onset. Among them, eight died because of recurrent metabolic decompensation and only one died of hydrocephalus, suggesting that onset of the disease is negatively correlated with prognosis.

To identify the effect of onset disease on the long-term outcomes of neonatally screened individuals with cblC defect, we analyzed the detailed information between asymptomatic individuals and symptomatic ones before treatment. In the majority of asymptomatic individuals, the long-term outcomes tended to be more favorable. Unfortunately, two of them appeared no clinical symptoms firstly before therapy but died of acute metabolic crisis due to poor treatment compliance. NBS, though not preventing clinical disease course in all screened

individuals, is associated with favorable long-term outcomes. With pre-symptomatic treatment, developmental milestones of the majority of patients detected by newborn screening were normal. These cases benefited from early diagnosis, the timely start of treatment, and the prevention of severe complications.

Regarding biochemical data at NBS, patients with poor prognosis had slightly elevated blood C3/C2 ratio, urinary MCA, but obviously increased plasma tHcy and urinary MMA, which are considered to be correlated with severe brain damage (Kruman et al., 2000; Huemer et al., 2017). However, the relevant metabolic indicators still need to be further explored. Besides, there is no significant difference in the value of blood C3 between groups, which is the opposite of the blood C3/C2 ratio, representing a significant difference. This serves to illustrate that the absolute value of C3 is not sensitive enough since it can be affected by body weight, breastfeeding, and so on. Moreover, compared to severely affected individuals who appeared symptoms before treatment, mildly affected patients who remained asymptomatic showed lower blood C3 and blood C3/C2 ratio concentrations. Interestingly, blood C3 of some patients with the milder disease might not reach the cutoff because of low plasma carnitine obscured elevations in C3 (Ahrens-Nicklas et al., 2015), which results in the possibility of missing mild disease with newborn screening and questioning the sensitivity of newborn screening in identifying these infants. As a consequence, some reports suggested that the C3/C2 ratio can be used as a marker for cblC defect due to the fact that this ratio was elevated on the first and second newborn screens whereas C3 was not above the cutoff (Ahrens-Nicklas et al., 2015). Besides C3/C2 ratio, low methionine could be an additional secondary analyte and was demonstrated to be associated with improved specificity and positive predictive value in one study (Weisfeld-Adams et al., 2010). Moreover, there exists a mild difference in the cut-off value nationwide and a high false-positive or false-negative rates of NBS results based on MS/MS, some experts suggested using next-generation sequencing (NGS) as a second-tier diagnostic test for abnormal NBS results (Luo et al., 2018).

It is noteworthy that genotype-phenotype correlations seem to have a huge impact on the onset of this disorder as well as the prognosis (Lerner-Ellis et al., 2009). For example, in comparison with individuals who remained asymptomatic, those who had already shown clinical manifestations before initiation of treatment were more likely to carry c.609G>A as well as c.567dupT in the *MMACHC* gene. Consistent with previous reports (Liu et al., 2010), both pathogenic variants showed early onset of disease, usually during the neonatal period. This could be related to the fact that c.609G>A variant is nonsense and results in a premature termination codon, which is predicted to cause a truncated or absent MMACHC protein. Similarly, c.567dupT in the *MMACHC* gene, a duplication and frameshift mutation, can also have an adverse effect on the function of this protein. Furthermore, patients carrying these homozygous or heterozygous variants are more likely to develop bad outcomes. On the contrary, individuals who remained asymptomatic before initiation of treatment appeared to carry c.482G>A or c.80A>G in the *MMACHC* gene, both missense pathogenic variants, which predicted excellent clinical outcomes. This result was nearly in line with previous reports (Lerner-Ellis et al., 2009; Huemer et al., 2014; Liu et al., 2020), which described that c.482G>A (p.R161Q) and c.80A>G (p.Q27R) variants were known to predict an attenuated or even benign phenotype with late onset. In a more recent study, Almannai et al. showed that patients with c.482G>A pathogenic variant have a milder disease as indicated by later-onset of symptoms (Almannai et al., 2017), thus when detected by NBS, they were still asymptomatic and once treatment was to be started, the irreversible damage caused by the onset of symptoms could be prevented.

Our findings suggested that symptomatic onset, independently from other predictors like pathogenic variant, metabolic analytes, and treatment, is a strong predictor of poor outcomes, such as intellectual impairment, movement disorders, ocular complications except for hydrocephalus. But the underlying mechanism remains obscure. Results from this current study also suggested that c.609G>A and c.567dupT variants were independent factors of poor prognosis, especially for intellectual impairment. In addition, the odds ratio of c.609G>A variant is a little higher than that of c.567dupT variant in poor outcome, but when intellectual impairment was analyzed, the odds ratio of c.567dupT variant was higher than that of c.609G>A variant. Considering a much higher carrier prevalence of c.609G>A in the *MMACHC* gene among the Chinese population, we proposed that c.609G>A mutant allele, the mutational hotspots, could be potential candidates for gene screening and should be listed in the pre-pregnancy carrier screening panel in China (Qiao et al., 2020). Furthermore, eye diseases are common in patients with the *MMACHC* gene c.271dupA homozygous mutation and are characterized by early maculopathy (Gizicki et al., 2014; Brooks et al., 2016). Ruxuan He et al. showed that the incidence of ocular problems in patients with the c.609G>A variant is much lower (He et al., 2020). And in our study, there is a strong link between c.567dupT variant and ocular abnormalities which is not reported before. This may be because we included the presence of strabismus and nystagmus, which are obvious phenotypes, as criteria of ocular complications. Due to the lack of formal assessment of ocular complications, this result remains to be investigated in the future. In addition, our study found that MMA seems to be a strong biochemical marker of movement disorder because MMA is associated with a high risk of basal ganglia stroke (Dionisi-Vici et al., 2006). This result substantiates the fact that movement disorder could be recovered after treatment once MMA decreases (Matos et al., 2013). However, in our study, we did not observe any risk factors that independently predict the outcome of hydrocephalus.

Although the incidence of cblC defect is low, the outcomes of affected patients are not favorable. The rate of death in our cohort (3.8%) is lower than that of a historical cohort diagnosed before initiation of NBS (26%) (Rosenblatt et al., 1997). In addition, compared to previous studies (Liu et al., 2018; He et al., 2020), the proportion of poor outcomes as well as mortality in our study is lower, demonstrating that NBS reduces mortality and allows a favorable outcome. For late-onset patients, there is no doubt that early detection by NBS and timely treatment improved long-term outcomes (Weisfeld-Adams et al., 2010). Several studies have demonstrated that early-onset patients, though identified by NBS, still have suboptimal outcomes with a high residual burden of

neurologic and ophthalmologic disease (Weisfeld-Adams et al., 2013; Ahrens-Nicklas et al., 2017). In our study, NBS data were typically reported at 2–3 days of life, which enable early diagnostic treatment, thus reducing the frequency of hospitalization and severity of symptoms. Overall, based on our large sample, NBS for cblC defect should be considered since survival and prevention of severe complications in early-onset patients can be improved by early treatment (Dionisi-Vici et al., 2006; Weisfeld-Adams et al., 2010; Huemer et al., 2015; Huemer et al., 2017).

In all screened individuals, there is still a minority at risk of mild to severe psychomotor impairment or complications. This might be the reason that some patients had already developed neonatal disease manifestations, therefore initiation of treatment with intramuscular hydroxocobalamin should even precede recalling screening.

5 CONCLUSION

The present study has discussed a large cohort of individuals with cblC defects. Our study emphasizes the factors affecting outcomes in individuals with cblC defects. Those with a better prognosis have milder diseases as indicated by less symptomatic manifestations, less prominent biochemical abnormalities on NBS, and easier control as made evident by the biochemical profile on the last follow-up. The onset of symptoms is an independent risk factor for poorer outcomes and independently carries a greater risk than pathogenic variants. Newborn screening facilitates early diagnosis, improves the quality of therapy, allows longer survival, and prevents the damage of symptoms, which is the most important prognostic factor. There is no doubt that NBS is a highly successful preventive care program, resulting in favorable clinical outcomes for screened individuals.

DATA AVAILABILITY STATEMENT

The original contributions presented in the study are included in the article/supplementary files, further inquiries can be directed to the corresponding author.

ETHICS STATEMENT

The studies involving human participants were reviewed and approved by Ethics Committee of Xinhua Hospital Affiliated to Shanghai Jiao Tong University School of Medicine (No.XHEC-D-2021-140). Written informed consent to participate in this study was provided by the participants' legal guardian/next of kin. Written informed consent was obtained from the individual(s), and minor(s)' legal guardian/next of kin, for the publication of any potentially identifiable images or data included in this article.

AUTHOR CONTRIBUTIONS

SL contributed to reorganizing and analyzing the clinical data of the patients and drafting the manuscript. SW, as the doctor of many of these patients, contributed to reorganizing and analyzing the clinical data of the patients and revised the manuscript. RS, YY contributed to collecting the clinical data of the patients. WQ, HW, CY, PX, HZo, JF, TN, HH, HZh, LL, DL, XG contributed to collecting and treating the patients and providing the clinical data. ZG contributed to the gene variation analysis. XZ contributed to the detection of blood acylcarnitines of the patients by tandem mass spectrometry. WJ contributed to the detection of urinary organic acids of the patients by gas chromatography-mass spectrometry. LH, as the doctor of most of the patients, contributed to designing the research, treating the patients, providing the clinical data, and revising the manuscript. All authors contributed to the article.

FUNDING

This work was supported by the National Key Research and Development Program of China (No. 2016YFC0901505).

ACKNOWLEDGMENTS

The authors thank all the patients and their families for their active participation in this study.

REFERENCES

Ahrens-Nicklas, R. C., Serdaroglu, E., Muraresku, C., and Ficicioglu, C. (2015). Cobalamin C Disease Missed by Newborn Screening in a Patient with Low Carnitine Level. *JIMD Rep.* 23, 71–75. doi:10.1007/8904_2015_429

Ahrens-Nicklas, R. C., Whitaker, A. M., Kaplan, P., Cuddapah, S., Burfield, J., Blair, J., et al. (2017). Efficacy of Early Treatment in Patients with Cobalamin C Disease Identified by Newborn Screening: a 16-year Experience. *Genet. Med.* 19, 926–935. doi:10.1038/gim.2016.214

Al Dhahouri, N., Langhans, C.-D., Al Hammadi, Z., Okun, J. G., Hoffmann, G. F., Al-Jasmi, F., et al. (2018). Quantification of Methylcitrate in Dried Urine Spots by Liquid Chromatography Tandem Mass Spectrometry for the Diagnosis of Propionic and Methylmalonic Acidemias. *Clinica Chim. Acta* 487, 41–45. doi:10.1016/j.cca.2018.09.017

Al-Dirbashi, O. Y., Alfadhel, M., Al-Thihli, K., Al Dhahouri, N., Langhans, C.-D., Al Hammadi, Z., et al. (2019). Assessment of Methylcitrate and Methylcitrate to Citrate Ratio in Dried Blood Spots as Biomarkers for Inborn Errors of Propionate Metabolism. *Sci. Rep.* 9, 12366. doi:10.1038/s41598-019-48885-9

Almannai, M., Marom, R., Divin, K., Scaglia, F., Sutton, V. R., Craigen, W. J., et al. (2017). Milder Clinical and Biochemical Phenotypes Associated with the c.482G>A (p.Arg161Gln) Pathogenic Variant in Cobalamin C Disease: Implications for Management and Screening. *Mol. Genet. Metab.* 122, 60–66. doi:10.1016/j.ymgme.2017.06.011

Baumgartner, M. R., Hörster, F., Dionisi-Vici, C., Haliloglu, G., Karall, D., Chapman, K. A., et al. (2014). Proposed Guidelines for the Diagnosis and Management of Methylmalonic and Propionic Acidemia. *Orphanet J. Rare Dis.* 9, 130. doi:10.1186/s13023-014-0130-8

Brooks, B. P., Thompson, A. H., Sloan, J. L., Manoli, I., Carrillo-Carrasco, N., Zein, W. M., et al. (2016). Ophthalmic Manifestations and Long-Term Visual

Outcomes in Patients with Cobalamin C Deficiency. *Ophthalmology* 123, 571–582. doi:10.1016/j.ophtha.2015.10.041

Carrillo-Carrasco, N., Chandler, R. J., and Venditti, C. P. (2012). Combined Methylmalonic Acidemia and Homocystinuria, cblC Type. I. Clinical Presentations, Diagnosis and Management. *J. Inherit. Metab. Dis.* 35, 91–102. doi:10.1007/s10545-011-9364-y

Dionisi-Vici, C., Deodato, F., Röschinger, W., Rhead, W., and Wilcken, B. (2006). 'Classical' Organic Acidurias, Propionic Aciduria, Methylmalonic Aciduria and Isovaleric Aciduria: Long-Term Outcome and Effects of Expanded Newborn Screening Using Tandem Mass Spectrometry. *J. Inherit. Metab. Dis.* 29, 383–389. doi:10.1007/s10545-006-0278-z

Fischer, S., Huemer, M., Baumgartner, M., Deodato, F., Ballhausen, D., Boneh, A., et al. (2014). Clinical Presentation and Outcome in a Series of 88 Patients with the cblC Defect. *J. Inherit. Metab. Dis.* 37, 831–840. doi:10.1007/s10545-014-9687-6

Forny, P., Hörster, F., Ballhausen, D., Chakrapani, A., Chapman, K. A., Dionisi-Vici, C., et al. (2021). Guidelines for the Diagnosis and Management of Methylmalonic Acidaemia and Propionic Acidaemia: First Revision. *J. Inherit. Metab. Dis.* 44, 566. doi:10.1002/jimd.12370

Gizicki, R., Robert, M.-C., Gómez-López, L., Orquin, J., Decarie, J.-C., Mitchell, G. A., et al. (2014). Long-term Visual Outcome of Methylmalonic Aciduria and Homocystinuria, Cobalamin C Type. *Ophthalmology* 121, 381–386. doi:10.1016/j.ophtha.2013.08.034

He, R., Mo, R., Shen, M., Kang, L., Song, J., Liu, Y., et al. (2020). Variable Phenotypes and Outcomes Associated with the MMACHC c.609G>A Homologous Mutation: Long Term Follow-Up in a Large Cohort of Cases. *Orphanet J. Rare Dis.* 15, 200. doi:10.1186/s13023-020-01485-7

Heringer, J., Valayannopoulos, V., Valayannopoulos, V., Lund, A. M., Wijburg, F. A., Freisinger, P., et al. (2016). Impact of Age at Onset and Newborn Screening on Outcome in Organic Acidurias. *J. Inherit. Metab. Dis.* 39, 341–353. doi:10.1007/s10545-015-9907-8

Huemer, M., Diodato, D., Schwahn, B., Schiff, M., Bandeira, A., Benoist, J.-F., et al. (2017). Guidelines for Diagnosis and Management of the Cobalamin-Related Remethylation Disorders cblC, cblD, cblE, cblF, cblG, cblJ and MTHFR Deficiency. *J. Inherit. Metab. Dis.* 40, 21–48. doi:10.1007/s10545-016-9991-4

Huemer, M., Kožich, V., Rinaldo, P., Baumgartner, M. R., Merinero, B., Pasquini, E., et al. (2015). Newborn Screening for Homocystinurias and Methylation Disorders: Systematic Review and Proposed Guidelines. *J. Inherit. Metab. Dis.* 38, 1007–1019. doi:10.1007/s10545-015-9830-z

Huemer, M., Scholl-Bürgi, S., Hadaya, K., Kern, I., Beer, R., Seppi, K., et al. (2014). Three New Cases of Late-Onset cblC Defect and Review of the Literature Illustrating when to Consider Inborn Errors of Metabolism beyond Infancy. *Orphanet J. Rare Dis.* 9, 161. doi:10.1186/s13023-014-0161-1

KrumanII, Culmsee, C., Chan, S. L., Kruman, Y., Guo, Z., Penix, L., et al. (2000). Homocysteine Elicits a DNA Damage Response in Neurons that Promotes Apoptosis and Hypersensitivity to Excitotoxicity. *J. Neurosci.* 20, 6920–6926. doi:10.1523/jneurosci.20-18-06920.2000

Leonard, J. V., Vijayaraghavan, S., and Walter, J. H. (2003). The Impact of Screening for Propionic and Methylmalonic Acidaemia. *Eur. J. Pediatr.* 162 (Suppl. 1), S21–S24. doi:10.1007/s00431-003-1345-1

Lerner-Ellis, J. P., Anastasio, N., Liu, J., Coelho, D., Suormala, T., Stucki, M., et al. (2009). Spectrum of Mutations inMMACHC, Allelic Expression, and Evidence for Genotypeâ€"phenotype Correlations. *Hum. Mutat.* 30, 1072–1081. doi:10.1002/humu.21001

Liu, J., Tang, X., Zhou, C., Xu, H., Yang, H., He, R., et al. (2020). Cobalamin C Deficiency Presenting with Diffuse Alveolar Hemorrhage and Pulmonary Microangiopathy. *Pediatr. Pulmonol* 55, 1481–1486. doi:10.1002/ppul.24781

Liu, M.-Y., Yang, Y.-L., Chang, Y.-C., Chiang, S.-H., Lin, S.-P., Han, L.-S., et al. (2010). Mutation Spectrum of MMACHC in Chinese Patients with Combined Methylmalonic Aciduria and Homocystinuria. *J. Hum. Genet.* 55, 621–626. doi:10.1038/jhg.2010.81

Liu, Y., Liu, Y. P., Zhang, Y., Song, J. Q., Zheng, H., Dong, H., et al. (2018). Heterogeneous Phenotypes, Genotypes, Treatment and Prevention of 1 003 Patients with Methylmalonic Acidemia in the mainland of China. *Zhonghua Er Ke Za Zhi* 56, 414–420. doi:10.3760/cma.j.issn.0578-1310.2018.06.003

Lüders, A., Blankenstein, O., Brockow, I., Ensenauer, R., Lindner, M., Schulze, A., et al. (2021). Neonatal Screening for Congenital Metabolic and Endocrine Disorders. *Dtsch Arztebl Int.* 118, 101–108. doi:10.3238/arztebl.m2021.0009

Luo, X., Wang, R., Fan, Y., Gu, X., and Yu, Y. (2018). Next-generation Sequencing as a Second-Tier Diagnostic Test for Newborn Screening. *J. Pediatr. Endocrinol. Metab.* 31, 927–931. doi:10.1515/jpem-2018-0088

Mak, C. M., Lee, H.-C. H., Chan, A. Y.-W., and Lam, C.-W. (2013). Inborn Errors of Metabolism and Expanded Newborn Screening: Review and Update. *Crit. Rev. Clin. Lab. Sci.* 50, 142–162. doi:10.3109/10408363.2013.847896

Manoli, I., Myles, J. G., Sloan, J. L., Carrillo-Carrasco, N., Morava, E., Strauss, K. A., et al. (2016). A Critical Reappraisal of Dietary Practices in Methylmalonic Acidemia Raises Concerns about the Safety of Medical Foods. Part 2: Cobalamin C Deficiency. *Genet. Med.* 18, 396–404. doi:10.1038/gim.2015.107

Martínez-Morillo, E., Prieto García, B., and Álvarez Menéndez, F. V. (2016). Challenges for Worldwide Harmonization of Newborn Screening Programs. *Clin. Chem.* 62, 689–698. doi:10.1373/clinchem.2015.240903

Matos, I. V., Castejón, E., Meavilla, S., O'Callaghan, M., Garcia-Villoria, J., López-Sala, A., et al. (2013). Clinical and Biochemical Outcome after Hydroxocobalamin Dose Escalation in a Series of Patients with Cobalamin C Deficiency. *Mol. Genet. Metab.* 109, 360–365. doi:10.1016/j.ymgme.2013.05.007

Morel, C. F., Lerner-Ellis, J. P., and Rosenblatt, D. S. (2006). Combined Methylmalonic Aciduria and Homocystinuria (cblC): Phenotype-Genotype Correlations and Ethnic-specific Observations. *Mol. Genet. Metab.* 88, 315–321. doi:10.1016/j.ymgme.2006.04.001

Mütze, U., Garbade, S. F., Gramer, G., Lindner, M., Freisinger, P., Grünert, S. C., et al. (2020). Long-term Outcomes of Individuals with Metabolic Diseases Identified through Newborn Screening. *Pediatrics* 146, e20200444. doi:10.1542/peds.2020-0444

Niu, D. M., Chien, Y. H., Chiang, C. C., Ho, H. C., Hwu, W. L., Kao, S. M., et al. (2010). Nationwide Survey of Extended Newborn Screening by Tandem Mass Spectrometry in Taiwan. *J. Inherit. Metab. Dis.* 33, S295–S305. doi:10.1007/s10545-010-9129-z

Nogueira, C., Aiello, C., Cerone, R., Martins, E., Caruso, U., Moroni, I., et al. (2008). Spectrum of MMACHC Mutations in Italian and Portuguese Patients with Combined Methylmalonic Aciduria and Homocystinuria, cblC Type. *Mol. Genet. Metab.* 93, 475–480. doi:10.1016/j.ymgme.2007.11.005

Qiao, L. Y., Ge, J., Li, W. J., Wang, J., Zhou, G. C., and Li, T. (2020). Screening for Carriers of Pathogenic Genes for Methylmalonic Acidemia and Wilson's Disease in Neonates in Qingdao. *Zhonghua Er Ke Za Zhi* 58, 596–599. doi:10.3760/cma.j.cn112140-20191208-00786

Rosenblatt, D. S., Aspler, A. L., Shevell, M. I., Pletcher, B. A., Fenton, W. A., and Seashore, M. R. (1997). Clinical Heterogeneity and Prognosis in Combined Methylmalonic Aciduria and Homocystinuria (cblC). *J. Inherit. Metab. Dis.* 20, 528–538. doi:10.1023/a:1005353530303

Wang, T., Ma, J., Zhang, Q., Gao, A., Wang, Q., Li, H., et al. (2019). Expanded Newborn Screening for Inborn Errors of Metabolism by Tandem Mass Spectrometry in Suzhou, China: Disease Spectrum, Prevalence, Genetic Characteristics in a Chinese Population. *Front. Genet.* 10, 1052. doi:10.3389/fgene.2019.01052

Watkins, D., and Rosenblatt, D. S. (2011). Inborn Errors of Cobalamin Absorption and Metabolism. *Am. J. Med. Genet.* 157, 33–44. doi:10.1002/ajmg.c.30288

Weisfeld-Adams, J. D., Bender, H. A., Miley-Åkerstedt, A., Frempong, T., Schrager, N. L., Patel, K., et al. (2013). Neurologic and Neurodevelopmental Phenotypes in Young Children with Early-Treated Combined Methylmalonic Acidemia and Homocystinuria, Cobalamin C Type. *Mol. Genet. Metab.* 110, 241–247. doi:10.1016/j.ymgme.2013.07.018

Weisfeld-Adams, J. D., Morrissey, M. A., Kirmse, B. M., Salveson, B. R., Wasserstein, M. P., McGuire, P. J., et al. (2010). Newborn Screening and Early Biochemical Follow-Up in Combined Methylmalonic Aciduria and Homocystinuria, cblC Type, and Utility of Methionine as a Secondary Screening Analyte. *Mol. Genet. Metab.* 99, 116–123. doi:10.1016/j.ymgme.2009.09.008

Zhang, K., Gao, M., Wang, G., Shi, Y., Li, X., Lv, Y., et al. (2019). Hydrocephalus in cblC Type Methylmalonic Acidemia. *Metab. Brain Dis.* 34, 451–458. doi:10.1007/s11011-018-0351-y

Zhang, R., Qiang, R., Song, C., Ma, X., Zhang, Y., Li, F., et al. (2021). Spectrum Analysis of Inborn Errors of Metabolism for Expanded Newborn Screening in a Northwestern Chinese Population. *Sci. Rep.* 11, 2699. doi:10.1038/s41598-021-81897-y

Zhou, W., Li, H., Wang, C., Wang, X., and Gu, M. (2018). Newborn Screening for Methylmalonic Acidemia in a Chinese Population: Molecular Genetic Confirmation and Genotype Phenotype Correlations. *Front. Genet.* 9, 726. doi:10.3389/fgene.2018.00726

Conflict of Interest: The authors declare that the research was conducted in the absence of any commercial or financial relationships that could be construed as a potential conflict of interest.

Publisher's Note: All claims expressed in this article are solely those of the authors and do not necessarily represent those of their affiliated organizations, or those of the publisher, the editors and the reviewers. Any product that may be evaluated in this article, or claim that may be made by its manufacturer, is not guaranteed or endorsed by the publisher.

frontiers in Genetics

ORIGINAL RESEARCH
published: 04 March 2022
doi: 10.3389/fgene.2021.816779

Clinical, Biochemical, Molecular, and Outcome Features of Mitochondrial 3-Hydroxy-3-Methylglutaryl-CoA Synthase Deficiency in 10 Chinese Patients

Shengnan Wu[1], Linghua Shen[1], Qiong Chen[1], Chunxiu Gong[2], Yanling Yang[3], Haiyan Wei[1], Bingyan Cao[2] and Yongxing Chen[1]**

[1]Department of Endocrinology and Metabolism, Henan Key Laboratory of Children's Genetics and Metabolic Diseases, Children's Hospital Affiliated to Zhengzhou University, Henan Children's Hospital, Zhengzhou Children's Hospital, Zhengzhou, China, [2]Department of Endocrinology, Genetics and Metabolism, Beijing Children's Hospital, Capital Medical University, National Center for Children's Health, Beijing, China, [3]Department of Pediatrics, Peking University First Hospital, Beijing, China

OPEN ACCESS

Edited by:
Huiwen Zhang,
Xinhua Hospital, China

Reviewed by:
Julnar A. R. Usta,
American University of Beirut, Lebanon
Laura Patterson Rosa,
University of Florida, United States

***Correspondence:**
Yongxing Chen
cyx75@126.com
Bingyan Cao
caoby1982@163.com

Specialty section:
This article was submitted to Genetics of Common and Rare Diseases, a section of the journal Frontiers in Genetics

Received: *17 November 2021*
Accepted: *31 December 2021*
Published: *04 March 2022*

Citation:
Wu S, Shen L, Chen Q, Gong C, Yang Y, Wei H, Cao B and Chen Y (2022) Clinical, Biochemical, Molecular, and Outcome Features of Mitochondrial 3-Hydroxy-3-Methylglutaryl-CoA Synthase Deficiency in 10 Chinese Patients. Front. Genet. 12:816779. doi: 10.3389/fgene.2021.816779

Background: Mitochondrial 3-hydroxy-3-methylglutaryl-CoA synthase deficiency (HMGCS2D) is a rare autosomal recessive metabolic disorder caused by mutations of the *HMGCS2* gene. To date, no more than 60 patients have been reported throughout the world.

Purpose: To analyze the clinical, biochemical, molecular, and outcome features of HMGCS2D in a case series of 10 new Chinese patients.

Methods: This retrospective study includes 10 Chinese patients diagnosed with HMGCS2D. We collected and analyzed clinical data for all patients. We also reviewed clinical data for 39 cases that had been reported previously.

Results: All of our patients had experienced their first metabolic crisis before 12 months old. The most common clinical manifestations were anorexia, dyspnea, and disturbance of consciousness (10/10), followed by vomiting (8/10), fever (7/10), cough (4/10), diarrhea, and seizures (3/10). Each patient (10/10) had a different degree of hepatomegaly and increased aminotransferase, severe metabolic acidosis, and hypofibrinogenemia. 9 patients presented with severe hypoglycemia and weak positives on qualitative tests of urinary ketone body. Patient 3 was the only one without hypoglycemia. Five patients had hypocalcemia, five patients had hyperammonemia, four patients had hyperuricemia, and three had hypertriglyceridemia. During the metabolic acidosis episode, we observed high dicarboxylic acid values in urine, and the elevated ratio of blood acetylcarnitine to free carnitine may have been an additional biochemical signature. However, all returned to normal during the interictal interval. Molecular analysis identified 15 variants in the *HMGCS2* gene, of which 10 were novel (c.220G>A/p.E74K, c.407A>G/p.D136G, c.422T>A/p.V141D, c.719A>C/p.D240A, c.821G>A/p.R274H, c.39dupA/p.L14Tfs*59, c.1394delA/p.N465Tfs*10, c.788delT/p.L263Cfs*36, c.717T>G/p.Y239*, and c.1017-2A>G). Combining these with previous cases, the known mutation c.1201G>T/p.E401* has

been found in 6/40 (15.0%) of mutated alleles in 21 Chinese patients from 20 families, while none have been found in other populations. We found that patients with biallelic truncation mutation appeared to show a more severe clinical condition through a literature review.

Conclusion: This study analyzed the phenotypic and genetic features of HMGCS2D in a Chinese case series. We also expanded the *HMGCS2* mutational spectrum with 10 novel variants. The c.1201G>T/p.E401* mutation was the most frequent, representing 15.0% of the mutated alleles in reported unrelated Chinese patients, and thus, it may be a hot spot mutation.

Keywords: 3-hydroxy-3-methylglutaryl-CoA synthase deficiency, hypoglycemia, ketogenesis, HMGCS2 gene, HMGCS2D

INTRODUCTION

Mitochondrial 3-hydroxy-3-methylglutaryl-CoA synthase deficiency (mitochondrial HMG-CoA synthase deficiency; HMGCS2D; OMIM#605911) is a rare autosomal recessive metabolic disorder caused by mutations in the *HMGCS2* gene (OMIM*600234). The *HMGCS2* gene encodes mitochondrial HMG-CoA synthase, which catalyzes the reactions of acetyl-CoA and acetoacetyl-CoA into HMG-CoA during ketone body synthesis. Ketone bodies are an important energy supply for the brain, heart and kidneys during long-term fasting and carbohydrate deprivation. Pathogenic mutations on the *HMGCS2* gene cause mitochondrial HMG-CoA synthase deficiency which disrupts the ketogenesis and blocks the energy supply to the brain during the fasting state. Patients present with intermittent vomiting, lethargy, respiratory distress, encephalopathy, and hepatomegaly, usually precipitated by an intercurrent infection or prolonged fasting (Aledo et al., 2006). Hypoketotic hypoglycemia, metabolic acidosis, increased transaminitis and dicarboxylic aciduria are common laboratory findings during the acute attack stage. Nevertheless, the clinical manifestations and biochemical abnormalities usually return to normal during the interictal period. In 1997, Thompson described the first case of mitochondrial HMGCS2D (Thompson et al., 1997). To date, no more than 60 patients carrying over 40 variants have been reported throughout the world among different ethnic groups. Among them, only 11 patients, from 10 families, are of Chinese descent.

In the present study, we report 10 new Chinese patients with HMGCS2D, and summarize their clinical, biochemical, molecular and outcome characteristics. We reviewed 39 patients with relatively complete clinical data reported for overall understanding of the molecular genetics features of Chinese patients, and to explore the correlation between genotype and clinical features and disease severity. This has not been reported in previous studies.

MATERIALS AND METHODS

Subjects and Clinical Evaluation

Ten unrelated patients (two boys and eight girls) from different Chinese families identified between 2015 and 2021 were included in this retrospective analysis. They had each been diagnosed with HMGCS2D based on clinical features (encephalopathy, and hepatomegaly, usually precipitated by an intercurrent infection or prolonged fasting), biochemical detection results (hypoketotic hypoglycemia, transaminitis, metabolic acidosis and dicarboxylic aciduria), as well as molecular analysis. We collected clinical data through the review of patients' medical records, including the age at onset, primary clinical symptoms, medical management, and biochemical and clinical outcomes following therapy.

Biochemical Analysis

We performed routine blood and urine examination to assess blood gas analysis, ammonia, glucose, liver function, renal function, blood lipids and plasma electrolytes. Then, we applied tandem mass spectrometry to test serum amino acids and acylcarnitines, and analyzed the results using ChemoView software. To analyze urine organic acids, we used gas chromatography-mass spectrometry and the Inborn Errors of Metabolism Screening System. We also performed abdominal ultrasonography and cranial MRI on most patients.

Molecular Analysis

We extracted genomic DNA from peripheral blood leucocytes using a QIAamp DNA Blood Midi kit (Qiagen, Hilden, Germany), and generated sequences using the Agilent Bioanalyzer. Then, we applied whole-exome sequencing for mutation screening. Additionally, we performed Sanger sequencing validation on all patients who we found to be harbouring gene mutations, as well as their parents. The pathogenicity of novel variants was evaluated according to the American College of Medical Genetics and Genomics (ACMG) standards and guidelines (Richards et al., 2015). For the novel mis-sense variants, multiple sequence alignment studies were performed to verify the amino acid conservation using the UCSC Genome Bioinformatics Database, and potential pathogenicity was analyzed using Mutation taster, PolyPhen-2, and Sorting Intolerant From Tolerant (SIFT). Swiss model (https://swissmodel.expasy.org/) was also used to predict the protein 3D structure and evaluate the impact of these novel missense variants on protein structure.

Treatment, Follow Up and Outcome Evaluation

When initial metabolic decompensation occurred, all patients were admitted to the hospital and received regular supportive treatment including intravenous glucose and sodium bicarbonate. We also administered liver-protecting and carnitine therapy. We gave mechanical ventilation and continuous renal replacement therapy to any patients who were critically ill because of persistent metabolic acidosis and multiple organ dysfunction. Once the HMGCS2D diagnosis was confirmed, all patients were instructed to avoid long periods of fasting, and put on a low-fat diet.

All patients were enrolled into a simple follow-up study. During the follow-up period, each patient had several telephone survey or outpatient visits. We performed physical growth and psychomotor evaluation, as well as routine laboratory tests such as urine organic acids, plasma amino acids and acylcarnitines and other biochemical investigations, every 6–12 months. Psychomotor evaluation was based on the intellectual test results according to Gesell Developmental Schedules at the last follow-up.

Case Review and Grouping

For overall understanding of Chinese patients' molecular genetics features, and to explore the correlation between genotype and clinical features and disease severity, we reviewed 39 previously reported patients with relatively complete clinical data, including the genetic analysis results. In our study, we divided the patients into 3 phenotypic groups according to their clinical severity: A deceased group, a severe group, and a mild group. The deceased group included patients who had died because of disease onset. The severe group included patients who met one of the following conditions: Recurrent attacks on multiple occasions; blood pH value lower than 7.0 in metabolic decompensation; had required mechanical ventilation or CRRT treatment in metabolic decompensation; had become cognitively disabled after disease onset. The mild group included patients with milder symptoms. According to their disease-causing variation type, we divided them into 3 genotypic groups: The A group included patients carrying 2 truncating mutations on the *HMGCS2* gene; the B group included patients carrying only 1 truncating mutation on the *HMGCS2* gene; and the C group included patients carrying no truncating mutations.

Statistical Analysis

We performed statistical analysis in SPSS 22.0. We analyzed the correlations between different phenotypic groups and genotypic groups with a Cochran-Mantel-Haenszel test. We considered any results with $p < 0.05$ as having a statistically significant difference.

RESULTS

Patients' Clinical Characteristics, Biochemical Detection

As summarized in **Table 1**, there were 8 females and 2 males in our study. All of their parents were non-consanguineous. Among the 10 cases, patient 1 had a deceased sister who had died of a sudden coma after respiratory infections at the age of 8 months, while patient 4 had an older brother who had died of Reye Syndrome at 1 year and 10 months. For patient 10, his mother had experienced spontaneous abortion in her first two pregnancies with no specific cause. None of the other patients had positive family history. Patients had experienced their first metabolic crises at ages ranging from 5 to 12 months. The most common clinical manifestations were anorexia, fever and cough, which then developed into vomiting, dyspnea and disturbance of consciousness. The time from onset to progression to dyspnea and disturbance of consciousness ranged from 2 to 7 days. During the course of disease, all patients had anorexia, dyspnea and disturbance of consciousness (10/10). The second most common symptom was vomiting (8/10), followed by fever (7/10), cough (4/10), diarrhea and seizures (3/10).

Routine biochemical laboratory results at onset are shown in **Table 1**. Each patient had a different degree of hepatomegaly, about 2–7 cm below the right costal margin. Laboratory examinations showed severe metabolic acidosis (10/10), increased aminotransferase from mild to severe (10/10), hypofibrinogenemia (10/10), slightly increased creatine kinase isoenzyme (8/10), increased creatine kinase (3/10), and normal lactate (10/10). Among all patients, 9 presented with severe hypoglycemia and weak positives in qualitative urinary ketone body tests, while we observed no hypoglycemia in Patient 3. Five patients (Patient 1, 2, 4, 5 and 9) had hyperammonemia. Five (Patient 1, 2, 4, 9 and 10) had hypocalcemia. Three (Patient 2, 4, and 8) had hypertriglyceridemia. Eight received cranial MRI examinations, and 3 cases (Patient 1, 2 and 3) showed widening of the sulcus and bilateral frontal and temporal subarachnoid space, two (Patient 3 and 10) showed abnormal signal in the basal ganglia, one (Patient 2) showed delayed myelination in white matter, while four (Patient 6, 7, 8 and 9) were normal. During acute metabolic decompensation, eight patients (all except for Patient 5 and 6) received mechanical ventilation for respiratory failure resulting from serious metabolic acidosis. Four (Patient 3, 4, 8, and 10) had to undergo continuous renal replacement therapy (CRRT) because of serious and/or obstinate metabolic acidosis.

We performed urine organic acid analysis during the acute episode of metabolic acidosis. While we detected a massive amount of dicarboxylic acid in all patients, ketone body excretion was only mildly elevated. Plasma amino acids and acylcarnitine analysis revealed that free carnitine levels were low with a mildly increased acetylcarnitine in Patients 1–3, 5 and 7. Patients 4 and 6 had decreased free carnitine but normal acetylcarnitine, while Patients 8–10 had normal free carnitine but elevated acetylcarnitine.

Molecular Genetic Analysis

We performed molecular analysis on all patients, and detected biallelic mutations in the *HMGCS2* gene in all of them. In our study, we identified fifteen molecular variants in the *HMGCS2* gene, ten of which were novel. Five were known mutations, including 2 missense mutations (c.160G > A/p.V54M, c.1502G > A/p.R501Q), 2 splicing mutations (c.559+1G > T, c.1187+1G >

TABLE 1 | Clinical information, biochemical assays, and outcome findings of 10 new patients with HMGCS2D.

		Patient 1	Patient 2	Patient 3	Patient 4	Patient 5	Patient 6	Patient 7	Patient 8	Patient 9	Patient 10
Gender		Female	Female	Female	Female	Female	Female	Female	Male	Female	Male
Age at onset		11.5m	5m	9m	12m	12m	6m	9m	8m	10m	12m
Anorexia		+	+	+	+	+	+	+	+	+	+
Vomiting		+	–	–	+	+	+	+	+	+	+
Diarrhea		–	–	–	–	+	–	–	+	+	–
Fever		+	–	+	+	+	+	+	–	+	–
Cough		–	+	+	+	–	-	–	+	–	–
Dyspnea		+	+	+	+	+	+	+	+	+	+
Consciousness disorder		+	+	+	+	+	+	+	+	+	+
Seizure		–	–	–	+	–	+	–	–	+	–
Blood glucose (mmol/L)		2.3	2.4	9.3	0.6	2.0	0.3	1.8	1.2	0.12	0.3
Blood gas analysis		PH 7.03 BE -25 AG 35	PH 7.07 BE -25.5 AG 29	PH 6.79 BE -31 AG 48	PH 6.81 BE -28.5 AG 67	PH 7.30 BE -17 AG 37	PH 7.12 BE -23.4 AG 39	PH 7.03 BE -26 AG 38	PH 7.01 BE -31 AG 30.8	PH 6.9 BE -30 AG 35.8	PH 7.046 BE -27.5 AG 39.3
Lactic acid (mmol/L)		0.8	0.5	0.4	0.6	0.4	0.69	0.7	0.8	0.5	1.9
Blood ammonia (umol/L)		123	131.5	NA	468	48	8	NA	NA	166.3	NA
Hepatomegaly		+	+	+	+	+	+	+	+	+	+
ALT (U/L)		206	94	82	3,216	1,333	57	44	99	91	91
AST (U/L)		247	135	113	6,608	1893	120	113	167	128	105
Hyperuricemia		–	–	NA	+	–	–	–	+	+	+
Hypocalcemia		+	-	–	+	–	–	–	+	+	+
Hypofibrinogenemia		+	+	+	+	+	+	NA	NA	+	+
Triglyceride (mmol/L)		NA	5.37	NA	8.34	–	NA	–	2.69	NA	NA
CK (U/L)		154	198	106	239	492	133	157	171	304	105
CKMB (U/L)		22	62.3	43	34.6	192	31	19	39	44	67
C0 (free carnitine)		Low	Low	Low	Low	Low	Low	Low	Normal	Normal	Normal
C2 (acetylcarnitine)		Elevated	Elevated	Elevated	Elevated	Elevated	Normal	Elevated	Elevated	Elevated	Elevated
Dicarboxylic aciduria		+	+	+	+	+	+	+	+	+	+
Ketonuria		Mild	Mild	Mild	Mild	Mild	Mild	Mild	Mild	Mild	Mild
Brain MRI		Widening of sulcus and bilateral frontal and temporal subarachnoid space	Abnormal myelination of white matter	Abnormal signal in bilateral basal ganglia; broaden bilateral frontal and temporal subarachnoid space	NA	NA	Normal	NA	Normal	Normal	Abnormal signal in bilateral basal ganglia
Mechanical ventilation		+	+	+	+	–	–	+	+	+	+
CRRT		–	–	+	+	–	–	–	+	–	+
At last follow-up	Age	5y1m	5y7m	3y2m	—	3y	4y10m	6y10m	2y2m	2y	1y7m
	Height (cm)	114.8	111.3	97.1	—	98.5	107.5	120.9	88.5	85.2	85.8
	Weight (kg)	22.6	18.2	14.7	—	15.2	17.7	19.5	12.6	11	13
	DQ score	93	92	90	—	94	ND	ND	91	96	93
Variation (Allele 1)		▲c.39dupA/p.L14Tfs*59 (Exon 1)	▲c.422A>T/ p.V141D (Exon 2)	▲c.821G>A/p.R274H (Exon 4)	▲c.1394delA/ p.N465Tfs*10 (Exon 8)	c.160G>A/ p.V54M (Exon 2)	c.1502G>A/ p.R501Q (Exon 9)	c.1201G>T/ p.E401* (Exon 7)	c.1201G>T/ p.E401* (Exon 7)	c.1201G>T/ p.E401* (Exon 7)	▲c.788delT/ p.L263Cfs*36 (Exon 4)
Variation (Allele 2)		▲c.220G>A/p.E74K (Exon 2)	c.559+1G>T (Intron 2)	c.1187+1G>C (Intron 6)	c.1201G>T/p.E401* (Exon 7)	▲c.220G>A/ p.E74K (Exon 2)	▲c.719A>C/ p.D240A (Exon 4)	c.559+1G>T (Intron 2)	▲c.1017-2A>G (Intron 5)	▲c.407A>G/ p.D136G (Exon 2)	▲c.717T>G/p.Y239* (Exon 4)

Abbreviations and reference range: ALT, alanine aminotransferase; AST, aspartate aminotransferase; CK, creatine kinase; CKMB, creatine kinase isoenzyme; CRRT, continuous renal replacement therapy; DQ, development quotient; NA, not available; ND, not detected; ▲ novel variation. Reference range: ALT: 0-40U/L; AST: 0-40U/L; CK: 20-200U/L; CKMB: 0-24U/L; Triglyceride: 0.38-2.25 mmol/L; Lactic acid: 0–2.2 mmol/L; Blood ammonia: 9–33umol/L.

C) and one nonsense mutation (c.1201G > T/p.E401*). The ten novel potentially pathogenic variants have not been previously reported in the literature or registered in the HGMD, ClinVarMiner, ExAC or gnomAD databases. This includes the 5 missense mutations (c.220G > A/p.E74K, c.407A > G/p.D136G, c.422T > A/p.V141D, c.719A > C/p.D240A, c.821G > A/p.R274H), 3 frame-shift mutations (c.39dupA/p.L14Tfs*59, c.1394delA/p.N465Tfs*10, c.788delT/p. L263Cfs*36), one nonsense mutation (c.717T > G/p.Y239*) and one splicing mutation (c.1017-2A > G). Multiple sequence alignment studies suggested all the amino acids were conserved. Multiple lines of computational evidence supported a deleterious effect on the gene about the novel mutations. Detailed results of the 15 variants and prediction of effects of some novel mutations are shown in **Table 2**. In addition, we have performed a computational evaluation of the impact of the novel missense variants on protein structural using Swiss-model software. The results show that the 3D structure of HMGCS2 protein may be affected by these 5 novel mis-sense variants. Detailed results were shown in **Supplementary Figure S1**.

Outcome Evaluation

Except for Patient 4 who died of multiple organ failure due to severe metabolic disorder at onset, all patients had complete recovery with symptomatic and supportive treatment. Each maintained well-being by avoiding long-term fasting and taking glucose supplements during illness. Hitherto, all 9 cases had followed up, made good progress, and reported no further episodes. The follow-up time varied from 7 months to 5 years and 3 months. As of October 2021, their ages ranged from 2 to 6 years and 9 months. During follow-up, we surveyed the routine laboratory tests including plasma amino acids and acylcarnitines, urine organic acids and other biochemical investigations. All results were within the normal range. We also summarized patients' physical growth and developmental quotients (DQ) at the latest follow up, and found normal outcomes in all patients. Both height and weight were between mean±1SD. For the four individuals older than 4 years (Patients 1, 2, 6, and 7), all performed well in school. Additionally, DQ tests revealed that all patients examined had age-appropriate intelligence. Detailed results are shown in **Table 1**.

Case Review and Exploration of the Correlation Between Genotype and Clinical Features and Disease Severity

A review of previous literature has revealed that from October 1997 to January 2021, 59 patients, carrying 54 variants of the *HMGCS2* gene, have been reported. Among them, only 11 individuals, from 10 families, were of Chinese descent. Including the 10 cases in our research, 27 mutations have been identified in the 21 Chinese patients from 20 families, including 15 (15/27, 55.6%) missense mutations, 5 (5/27, 18.5%) frame-shift mutations, 4 (4/27, 14.8%) nonsense mutations and 3 (3/27, 11.1%) splicing mutations. The frequency of the *HMGCS2* variants in the 20 unrelated Chinese patients is shown in **Table 3**. The recurrent *HMGCS2* mutations in the Chinese population were c.1201G > T/p.E401* (detected in 7 individuals from 6 unrelated families, mutated allele frequency 6/40, 15.0%), c.559+1G > T, c.1187+1G > C and c.1502G > A/p.R501Q (respectively detected in 3 mutated alleles, 3/40, 7.5%), c.220G > A/p.E74K (detected in 2 unrelated individuals, mutated allele frequency 2/40, 5.0%).

Including our 10 patients and the previously reported 39 patients with relatively complete clinical data, we analysed the clinical and molecular characteristics of 49 patients to explore the correlation between genotype and clinical features and disease severity. Detailed clinical data is presented in **Supplementary Table S1**, and the statistical analysis results are shown in **Table 4**. 16 patients carried biallelic truncating mutations (either nonsense, frame-shift or splicing mutation) (Group A). During acute metabolic decompensation, 4 of them (25%) died, and 7 (43.7%) had severe phenotypes. 13 patients carried monoallelic truncating mutations (Group B). Among them, one patient (7.7%) died, and 10 (76.9%) had severe phenotypes. For the 20 patients carrying biallelic non-truncating mutations (Group C), only one (5%) died, and 7 (35%) showed severe phenotypes, while 12 (60%) had mild symptoms. From another perspective, within the deceased group 66.7% (4/6) had 2 truncating mutations; within the severe group 70.9% (17/24) had at least 1 truncating mutation; and within the mild group 63.2% (12/19) had non truncating mutations. We analysed the correlation between phenotypic groups and genotypic groups with a Cochran-Mantel-Haenszel test. The results indicated that disease severity was correlated with how many truncating variations the patients carried ($p < 0.05$).

DISCUSSION

Mitochondrial HMGCS2D is a life-threatening, but treatable, inherited metabolic disorder caused by a defect in the critical enzyme that regulates ketone body formation (Aledo et al., 2006). Therefore, patients with HMGCS2D are prone to episodic metabolic decompensation triggered by fasting or stressful conditions that require fatty acid decomposition for the provision of energy. In the present study, we reported 10 new unrelated Chinese patients with HMGCS2D. All patients had suffered their first metabolic crisis before their first birthday. Prior to metabolic crisis, there had been prodromic infection of either the digestive tract or the respiratory tract in all cases. The most common clinical manifestations before admission were poor intake, fever, cough and vomiting, which progressed rapidly to life-threatening dyspnea and coma. One third of patients had seizures, although each had only one throughout the disease course. Nonetheless, this still suggests there may have been an insufficient energy supply to the brain which may have harmed the nervous system, or even caused sequelae. All of our patients presented with severe metabolic acidosis with significantly increased anion gap, hepatomegaly, increased aminotransferase, and abnormal coagulation function, but normal lactate. Although their primary clinical characteristics were similar to those previously reported, there were several points of concern.

TABLE 2 | Molecular analysis of *HMGCS2* gene identified in 10 new Chinese patients with HMGCS2D.

Case	Region	Nucleotide change	Amino-acid change	MutationTaster prediction	SIFT prediction (score)	Polyphen-2.0 prediction (score)	Conservation	Novel or reported	Assession number
Patient 1	Exon 1	c.39dupA	p.L14Tfs*59	—	—	—	Yes	Novel	SCV002032067
	Exon 2	c.220G>A	p.E74K	Disease causing	Damaging (0.008)	Probably damaging (0.999)	Yes	Novel	SCV002032068
Patient 2	Exon 2	c.422T>A	p.V141D	Disease causing	Damaging (0)	Probably damaging (1.00)	Yes	Novel	SCV002032069
	Intron 2	c.559+1G>T	—	Disease causing	—	—	Yes	Reported	rs587603096
Patient 3	Exon 4	c.821G>A	p.R274H	Disease causing	Tolerated (0.166)	Probably damaging (0.999)	Yes	Novel	SCV002032070
	Intron 6	c.1187+1G>C	—	Disease causing	—	—	Yes	Reported	rs764706394
Patient 4	Exon 8	c.1394delA	p.N465Tfs*10	—	—	—	Yes	Novel	SCV002032071
	Exon 7	c.1201G>T	p.E401*	Disease causing	—	—	Yes	Reported	rs1454719802
Patient 5	Exon 2	c.160G>A	p.V54M	Disease causing	Damaging (0)	Probably damaging (1.00)	Yes	Reported	rs28937320
	Exon 2	c.220G>A	p.E74K	Disease causing	Damaging (0.008)	Probably damaging (0.999)	Yes	Novel	SCV002032068
Patient 6	Exon 9	c.1502G>A	p.R501Q	Disease causing	Damaging (0)	Probably damaging (1.00)	Yes	Reported	rs372079931
	Exon 4	c.719A>C	p.D240A	Disease causing	Damaging (0)	Probably damaging (1.00)	Yes	Novel	SCV002032072
Patient 7	Exon 7	c.1201G>T	p.E401*	Disease causing	—	—	Yes	Reported	rs1454719802
	Intron 2	c.559+1G>T	—	Disease causing	—	—	Yes	Reported	rs587603096
Patient 8	Exon 7	c.1201G>T	p.E401*	Disease causing	—	—	Yes	Reported	rs1454719802
	Intron 5	c.1017-2A>G	—	Disease causing	—	—	Yes	Novel	SCV002032073
Patient 9	Exon 7	c.1201G>T	p.E401*	Disease causing	—	—	Yes	Reported	rs1454719802
	Exon 2	c.407A>G	p.D136G	Disease causing	Damaging (0)	Probably damaging (1.00)	Yes	Novel	SCV002032074
Patient 10	Exon 4	c.788delT	p.L263Cfs*36	—	—	—	Yes	Novel	SCV002032075
	Exon 4	c.717T>G	p.Y239*	Disease causing	—	—	Yes	Novel	SCV002032076

All of our patients, with the exception of Patient 3, had hypoglycemia. According to previously reported data, 3 patients had no hypoglycemia during metabolic decompensation (Lee et al., 2019; Conlon et al., 2020; Wang et al., 2020a). The specific mechanism for this is unknown, and it may be related to compensatory glycogen decomposition and gluconeogenesis. However, the evidence suggested that hypoketotic hypoglycemia was important, but not indispensable, to HMGCS2D diagnosis. Similar to the patients observed by other researchers (Fukao et al., 2014; Conboy et al., 2018), urinary ketones in all of our patients were weakly positive (i.e., not negative). This may have interfered with the initial HMGCS2D diagnosis. Moreover, the observed ketones may have been due to the moderate amounts of ketone bodies produced by leucine catabolism pathway. In addition, in our study, four patients developed hypocalcemia during acute decompensation. Previously, this had only been reported in two patients (Wolf et al., 2003; Kilic et al., 2020). The specific pathogenesis of hypocalcemia remains unclear. We speculate the activation of coagulation and the fibrinolytic system, cell membrane damage caused by severe acidosis and tissue energy deficiency, Vitamin D deficiency and insufficient calcium intake in the acute stage could each be factors. Three patients had transient hyperuricemia, similar to the recent Turkish cases (Kilic et al., 2020). Many organic acids can stimulate the transporter, increasing the reabsorption of uric acid, which may account for the hyperuricemia (George and Minter, 2021). Moreover, Patient 3 had a concomitant disease, congenital laryngeal web, which had been diagnosed when she was 10-months-old based on clinical symptoms including recurrent cough, asthma, laryngeal stridor and hoarseness, and the results of electronic bronchoscopy. Then she accepted interventional therapy, with exceptional results. To our knowledge, this is the first time this has been reported in patients with HMGCS2D.

Detection of metabolic markers are crucial to diagnosing most inherited metabolic diseases. However, as far as we know, there are no specific biochemical markers in HMGCS2D. All patients in this study showed elevated dicarboxylic acid in their urine during decompensation. It has been reported that this can provide an indication, but cannot differentiate HMGCS2D from other fatty acid metabolic disorders (Kilic et al., 2020; Wang et al., 2020b). It has been reported that increased urine 4-hydroxy-6-methyl-2-pyrone (4-HMP) can be a specific biochemical hallmark indicator which can distinguish HMGCS2D from fatty acid oxidation defects (Pitt et al., 2015; Wang et al., 2020a). Unfortunately, in our study, only 3 patients received urine 4-HMP tests. Among them, 2 had elevated urinary 4-HMP and the other patient's urinary 4-HMP was normal. These results indicated that using 4-HMP as a positive prediction needs further study through more patients. We also detected the blood acylcarnitine profile in all individuals. As previously reported in the literature, blood acetylcarnitine (C2) can be either normal or increased during decompensation (Aledo et al., 2006; Ramos et al., 2013; Liu et al., 2019). In our study, the blood C2 level in 8 of the patients increased, while the free carnitine (C0) level in 7 of the patients

TABLE 3 | The frequency of *HMGCS2* variations in 20 unrelated Chinese patients (total number of mutated alleles = 40).

Variation	Region	Nucleotide change	Amino-acid change	Variation type	Variation frequency	Variation	Region	Nucleotide change	Amino-acid change	Variation type	Variation frequency
1	Exon 7	c.1201G>T	p.E401*	Nonsense	6/40 (15.0%)	15	Exon 3	c.616C>T	p.R206C	Missense	1/40 (2.5%)
2	Intron 2	c.559+1G>T	—	Splicing	3/40 (7.5%)	16	Exon 3	c.648G>T	p.M216I	Missense	1/40 (2.5%)
3	Intron 6	c.1187+1G>C	—	Splicing	3/40 (7.5%)	17	Exon 4	c.717T>G	p.Y239*	Nonsense	1/40 (2.5%)
4	Exon 9	c.1502G>A	p.R501Q	Missense	3/40 (7.5%)	18	Exon 4	c.719A>C	p.D240A	Missense	1/40 (2.5%)
5	Exon 2	c.220G>A	p.E74K	Missense	2/40 (5.0%)	19	Exon 4	c.758T>C	p.V253A	Missense	1/40 (2.5%)
6	Exon 2	c.520T>C	p.F174L	Missense	2/40 (5.0%)	20	Exon 4	c.788delT	p.L263Cfs*36	Frame-shift	1/40 (2.5%)
7	Exon 8	c.1347_1351del	p.A450Pfs*7	Frame-shift	1/40 (2.5%)	21	Exon 4	c.821G>A	p.R274H	Missense	1/40 (2.5%)
8	Exon 1	c.39dupA	p.L14Tfs*59	Frame-shift	1/40 (2.5%)	22	Intron 5	c.1017-2A>G	—	Splicing	1/40 (2.5%)
9	Exon 1	c.100C>T	p.Q34*	Nonsense	1/40 (2.5%)	23	Exon 6	c.1175C>T	p.S392L	Missense	1/40 (2.5%)
10	Exon 2	c.160G>A	p.V54M	Missense	1/40 (2.5%)	24	Exon 7	c.1259T>C	p.F420S	Missense	1/40 (2.5%)
11	Exon 2	c.407A>G	p.D136G	Missense	1/40 (2.5%)	25	Exon 7	c.1279C>T	p.Q427*	Nonsense	1/40 (2.5%)
12	Exon 2	c.422T>A	p.V141D	Missense	1/40 (2.5%)	26	Exon 8	c.1394delA	p.N465Tfs*10	Frame-shift	1/40 (2.5%)
13	Exon 2	c.476G>T	p.G159V	Missense	1/40 (2.5%)	27	Exon 9	c.1465delA	p.T489Lfs*55	Frame-shift	1/40 (2.5%)
14	Exon 3	c.563G>A	p.R188H	Missense	1/40 (2.5%)	—	—	—	—	—	—

TABLE 4 | Analysis of the correlation between severity of disease and number of truncating variations patients carried.

Group	Deceased (*n*, %)	Severe (*n*, %)	Mild (*n*, %)
A group (*n* = 16)	4, 25%	7, 43.7%	5, 31.25%
B group (*n* = 13)	1, 7.7%	10, 76.9%	2, 15.4%
C group (*n* = 20)	1, 5%	7, 35%	12, 60%
p-value		0.0255	

decreased. This led to elevated C2/C0 ratios in all cases. These data suggest that for clinically suspected patients, the high ratio of C2 to C0 may have been more specific and informative than the solitary high C2 or low C0 levels. Consequently, we considered that simultaneous detection of blood acylcarnitine profile and urinary organic acids was essential for HMGCS2D diagnosis. An elevated C2/C0 ratio combined with plenty of dicarboxylic acids in urine during an episode of acute hypoglycemia and metabolic acidosis may be an additional biochemical signature of HMGCS2D. This observation needs further research to identify whether there is sufficient specificity for clinical utilization.

As mentioned above, the lack of specificity in clinical and biochemical characteristics, as well as any abnormalities, may turn normal during intermissions. This complicates HMGCS2D diagnosis. On the other hand, detecting enzyme activity is invasive and complex, and the results are unstable. Therefore, at present, molecular genetic analysis of the *HMGCS2* gene still consists of the recommended diagnostic method (Zschocke et al., 2002; Ramos et al., 2013). In recent years, more and more patients have been confirmed as carrying biallelic pathogenic variants on *HMGCS2* gene by genetic testing. The *HMGCS2* gene is located on chromosome 1p13-p12, with a length of 20.9 kb. It consists of 10 exons, encoding 508 amino acids. Since the first description of the disease in 1997 (Thompson et al., 1997), over 40 variants have been identified. Prior reports have shown that these mutations have an irregular distribution and involve all exons (Wang Q. et al., 2020). Most of them are sporadic, specific to families, and have ethnic and regional differences. The c.634A > G/p.G212R has been identified in 3 families, respectively from Poland (Conlon et al., 2020), Britain (Pitt et al., 2015) and Germany (Zschocke et al., 2002). This implies that it was a common HMGCS2D mutation in Europe. The large deletion on exon 1, denoted as c.1-?_104+?del, has only been identified in patients of Mediterranean descent (Pitt et al., 2015), while c.725-2A > C has only been reported in two families from Turkey (Kilic et al., 2020). No relevant research on phenotype-genotype correlations has been reported to date.

Our finding is unlike similar studies conducted on other populations. In our cohort, the recurrent variants were c.1201G > T/p.E401*, c.559+1G > T and c.220G > A/p.E74K. If combined with the 11 patients reported previously (Thompson et al., 1997; Ma and Yu, 2018; Liu et al., 2019; Wang et al., 2019; Wang et al., 2020a; Wang et al., 2020b; Yang et al., 2020), the most frequent mutation was c.1201G > T/p.E401*. This may result in a premature termination codon at amino acid residue 401 located in exon 7 of *HMGCS2*. This leads to a truncated protein, and causes the loss of gene function. We detected this mutation as compound heterozygous in 7 Chinese patients from 6 families, while no patient in any other population has been a carrier of c.1201G > T/p.E401* in prior studies. All of these observations suggested that c.1201G > T/p.E401* may be a hot-spot mutation in Chinese HMGCS2D patients. The second most common mutations were c.559+1G > T, c.1187+1G > C and c.1502G > A/p.R501Q, all accounting for 3/42 mutated alleles, repectively. All had been reported in previous Chinese HMGCS2D patients, but not in other populations. c.559+1G > T was reported to be the second described splicing mutation of the *HMGCS2* gene, and

minigene assay results revealed that it may influence protein structure and function (Wang et al., 2020b). c.1187+1G > C is the classical site splicing mutation, which may cause abnormal splicing resulting in loss of protein function. We detected the missense mutation c.1502G > A/p.R501Q in Patient 6 in the compound heterozygous state, and a previous study has reported a Chinese case in the homozygous state (Ma and Yu, 2018). Previous reports have also suggested that arginine at position 501 is critical to enzymatic function (Bagheri-Fam et al., 2020). Moreover, variation in amino acids in the same position, c.1502G > C/p.R501P, has also been found in two Thai patients (Rojnueangnit et al., 2020). All of these factors imply that it was a causative variant.

Furthermore, our study also identified 10 novel mutations of *HMGCS2*. The c.1017-2A > G was the fifth splicing mutation of *HMGCS2*. It occurred at a classical splicing site and may lead to abnormal formation of *HMGCS2* protein, demonstrating its pathogenicity. c.717T > G/p.Y239*, c.39dupA/p.L14Tfs*59, c.788delT/p.L263Cfs*36 and c.1394delA/p.N465Tfs*10 all led to a premature termination codon respectively in exons 4, 1, 4, and 8. This led to encoded truncated peptides, thereby resulting in an enzyme defect. The 5 missense mutations each occurred in highly conserved regions. They were predicted to be damaged by Mutation taster, SIFT, and Polyphen 2. The computational evaluation using Swiss-model software showed that they may affect the 3D structure of HMGCS2 protein. Among them, c.220G > A/p.E74K was detected in two unrelated patients. We speculated that it is a common mutation in Chinese patients.

In order to explore the correlation between genotype and clinical features and disease severity, which had remained unknown according to previous studies, we analysed the clinical and molecular characteristics of 49 patients. This included our 10 patients, as well as the previously reported 39 patients with relatively complete clinical data (as shown in **Supplementary Table S1**). In **Table 4**, Group A (patients carrying biallelic truncating mutations) had the highest mortality (25%), while Group C (patients carrying biallelic non-truncating mutations) had the highest percentage of mild cases (60%). Group B (carrying monoallelic truncating mutations) had the highest percentage of severe cases (76.9%). Statistical analysis showed a correlation between disease severity and how many truncating variations patients carried. This suggests that patients with biallelic truncation mutation are likely to have more severe phenotypes. However, there was no convincing evidence indicating that individuals with biallelic missense mutation would have milder or later presentation. On the other hand, due to the limited number of patients, the frequency of compound heterozygotes, and the lack of enzymatic studies, it is difficult to assess the precise relationship between genotype and phenotype. Furthermore, inter-allelic complementation complicated the predictions of potential genotype-phenotype correlations. Therefore, more cases are needed for further exploration.

With regard to the prognosis, most of our patients had full recovery after symptomatic and supportive treatment, and maintained normal growth and development, without further episodes during follow-up. According to the literature, only one case had neurological sequelae (Conboy et al., 2018). However, there still were 6 patients who died of hypoglycemic crisis and serious metabolic acidosis during acute metabolic decompensation (Liu et al., 2019; Kilic et al., 2020; Wang et al., 2020a; Yang et al., 2020). These results suggest that HMGCS2D is a fatal, but treatable, hereditary metabolic disease. If we can diagnose it before onset, and then prevent those trigger factors like long-term fasting, and administrate oral glucose when patients have poor food intake, we may be able to prevent metabolic crises. However, patients cannot be diagnosed before disease onset through the current newborn screening program. We believe that the combination of rapid and accurate next-generation sequencing technology and biochemical screening may improve newborn HMGCS2D screening efficiency in the future (Luo et al., 2020).

CONCLUSION

In summary, mitochondrial HMGCS2 deficiency is a rare ketone synthesis disorder. We have described clinical symptoms, biochemical features, clinical outcomes, and molecular analysis of 10 new Chinese patients. We have also expanded the *HMGCS2* mutational spectrum with 10 novel variants. The variation c.1201G > T/p.E401* is the most common, and may be a hot-spot mutation of the *HMGCS2* gene in Chinese patients. Through a literature review, we found that patients with biallelic truncation mutation appeared to show a more severe clinical condition.

DATA AVAILABILITY STATEMENT

The data that support the findings of this study are submitted to ClinVar through ClinVar Submission Portal and available from the corresponding author upon reasonable request. Accession link to HMGCS2 cDNA sequence NM_005518 https://www.ncbi.nlm.nih.gov/nuccore/NM_005518.4. ClinVar accession link of new variants of HMGCS2 gene identified in this study https://www.ncbi.nlm.nih.gov/clinvar/?term= SUB10769664.

ETHICS STATEMENT

The studies involving human participants were reviewed and approved by The Research and Ethics Committee of Zhengzhou Children's Hospital. Written informed consent to participate in this study was provided by the participants' or legal guardian/next of kin.

AUTHOR CONTRIBUTIONS

YC and BC contributed to conception and design of the study. SW performed the statistical analysis, and wrote the first draft of the manuscript. HW and YY collected the clinical data. CG made many suggestions for the revised manuscript. All authors critically reviewed, revised, and approved the final version of the manuscript.

ACKNOWLEDGMENTS

We would like to thank our patients and their families for their corporation, and all pediatricians who sent us patients' information.

SUPPLEMENTARY MATERIAL

The Supplementary Material for this article can be found online at: https://www.frontiersin.org/articles/10.3389/fgene.2021.816779/full#supplementary-material

REFERENCES

Aledo, R., Mir, C., Dalton, R. N., Turner, C., Pié, J., Hegardt, F. G., et al. (2006). Refining the Diagnosis of Mitochondrial HMG-CoA Synthase Deficiency. *J. Inherit. Metab. Dis.* 29 (1), 207–211. doi:10.1007/s10545-006-0214-2

Bagheri-Fam, S., Chen, H., Wilson, S., Ayers, K., Hughes, J., Sloan-Bena, F., et al. (2020). The Gene Encoding the Ketogenic Enzyme HMGCS2 Displays a Unique Expression during Gonad Development in Mice. *PLoS One* 15 (1), e0227411. doi:10.1371/journal.pone.0227411

Conboy, E., Vairo, F., Schultz, M., Agre, K., Ridsdale, R., Deyle, D., et al. (2017). Mitochondrial 3-Hydroxy-3-Methylglutaryl-CoA Synthase Deficiency: Unique Presenting Laboratory Values and a Review of Biochemical and Clinical Features. *JIMD Rep.* 40, 63–69. doi:10.1007/8904_2017_59

Conlon, T. A., Fitzsimons, P. E., Borovickova, I., Kirby, F., Murphy, S., Knerr, I., et al. (2020). Hypoglycemia Is Not a Defining Feature of Metabolic Crisis in Mitochondrial 3-Hydroxy-3-Methylglutaryl-CoA Synthase Deficiency: Further Evidence of Specific Biochemical Markers Which May Aid Diagnosis. *JIMD Rep.* 55 (1), 26–31. doi:10.1002/jmd2.12146

Fukao, T., Mitchell, G., Sass, J. O., Hori, T., Orii, K., and Aoyama, Y. (2014). Ketone Body Metabolism and its Defects. *J. Inherit. Metab. Dis.* 37 (4), 541–551. doi:10.1007/s10545-014-9704-9

George, C., and Minter, D. A. (2021). "Hyperuricemia," in *Treasure Island (FL): In StatPearls*. [Internet].

Kılıç, M., Dorum, S., Topak, A., Yazıcı, M. U., Ezgu, F. S., and Coskun, T. (2020). Expanding the Clinical Spectrum of Mitochondrial 3-Hydroxy-3-Methylglutaryl-CoA Synthase Deficiency with Turkish Cases Harboring Novel HMGCS2 Gene Mutations and Literature Review. *Am. J. Med. Genet.* 182 (7), 1608–1614. doi:10.1002/ajmg.a.61590

Lee, T., Takami, Y., Yamada, K., Kobayashi, H., Hasegawa, Y., Sasai, H., et al. (2019). A Japanese Case of Mitochondrial 3-Hydroxy-3-Methylglutaryl-CoA Synthase Deficiency Who Presented with Severe Metabolic Acidosis and Fatty Liver without Hypoglycemia. *JIMD Rep.* 48 (1), 19–25. doi:10.1002/jmd2.12051

Liu, H., Miao, J.-k., Yu, C.-w., Wan, K.-x., Zhang, J., Yuan, Z.-j., et al. (2019). Severe Clinical Manifestation of Mitochondrial 3-Hydroxy-3-Methylglutaryl-CoA Synthase Deficiency Associated with Two Novel Mutations: a Case Report. *BMC Pediatr.* 19 (1), 344. doi:10.1186/s12887-019-1747-5

Luo, X., Sun, Y., Xu, F., Guo, J., Li, L., Lin, Z., et al. (2020). A Pilot Study of Expanded Newborn Screening for 573 Genes Related to Severe Inherited Disorders in China: Results from 1,127 Newborns. *Ann. Transl. Med.* 8 (17), 1058. doi:10.21037/atm-20-1147

Ma, D., and Yu, D. (2018). Mitochondrial 3-Hydroxy-3-Methylglutaryl CoA Synthase Deficiency: a Case Report and Literature Review. *Zhongguo Dang Dai Er Ke Za Zhi* 20 (11), 930–933. doi:10.7499/j.issn.1008-8830.2018.11.010

Pitt, J. J., Peters, H., Boneh, A., Yaplito-Lee, J., Wieser, S., Hinderhofer, K., et al. (2015). Mitochondrial 3-Hydroxy-3-Methylglutaryl-CoA Synthase Deficiency: Urinary Organic Acid Profiles and Expanded Spectrum of Mutations. *J. Inherit. Metab. Dis.* 38 (3), 459–466. doi:10.1007/s10545-014-9801-9

Ramos, M., Menao, S., Arnedo, M., Puisac, B., Gil-Rodríguez, M. C., Teresa-Rodrigo, M. E., et al. (2013). New Case of Mitochondrial HMG-CoA Synthase Deficiency. Functional Analysis of Eight Mutations. *Eur. J. Med. Genet.* 56 (8), 411–415. doi:10.1016/j.ejmg.2013.05.008

Richards, S., Aziz, N., Bale, S., Bick, D., Das, S., Gastier-Foster, J., et al. (2015). Standards and Guidelines for the Interpretation of Sequence Variants: a Joint Consensus Recommendation of the American College of Medical Genetics and Genomics and the Association for Molecular Pathology. *Genet. Med.* 17 (5), 405–424. doi:10.1038/gim.2015.30

Rojnueangnit, K., Maneechai, P., Thaweekul, P., Piriyanon, P., Khositseth, S., Ittiwut, C., et al. (2020). Expanding Phenotypic and Mutational Spectra of Mitochondrial HMG-CoA Synthase Deficiency. *Eur. J. Med. Genet.* 63 (12), 104086. doi:10.1016/j.ejmg.2020.104086

Thompson, G. N., Hsu, B. Y. L., Pitt, J. J., Treacy, E., and Stanley, C. A. (1997). Fasting Hypoketotic Coma in a Child with Deficiency of Mitochondrial 3-Hydroxy-3-Methylglutaryl-CoA Synthase. *N. Engl. J. Med.* 337 (17), 1203–1207. doi:10.1056/NEJM199710233371704

Wang, H., Li, D., Song, C., Yang, Y., Qian, S., and Cheng, Y. (2020a). Case Report of Mitochondrial 3-Hydroxy-3-Methylglutaryl-CoA Synthase Deficiency. *Zhonghua Shi Yong Er Ke Lin Chuang Za Zhi* 35 (16), 1269–1271. doi:10.3760/cma.j.cn101070-20190621-00559

Wang, M., Gong, Y., Ma, X., Zhu, D., and Zhong, X. (2019). Clinical Features of a Chinese Infant with Mitochondrial 3-Hydroxy-3-Methylglutaryl CoA Synthase Deficiency and Review of the Literature. *Lin Chuang Er Ke Za Zhi* 37 (11), 858–861. doi:10.3969/j.issn.1000-3606.2019.11.015

Wang, Q., Yang, Y.-L., Liu, M., Chen, J.-J., Li, X.-q., Cao, B.-y., et al. (2020b). Clinical, Biochemical, Molecular and Therapeutic Characteristics of Four New Patients of Mitochondrial 3-Hydroxy-3-Methylglutaryl-CoA Synthase Deficiency. *Clinica Chim. Acta* 509, 83–90. doi:10.1016/j.cca.2020.04.004

Wolf, N. I., Rahman, S., Clayton, P. T., and Zschocke, J. (2003). Mitochondrial HMG-CoA Synthase Deficiency: Identification of Two Further Patients Carrying Two Novel Mutations. *Eur. J. Pediatr.* 162 (4), 279–280. doi:10.1007/s00431-002-1110-x

Yang, Q., Li, S., Xiong, H., Cai, Y., Shi, C., Xiao, X., et al. (2020). 3-Hydroxy-3-methylglutaryl-CoA Synthase Deficiency: a New Case and Literature Review. *Zhongguo Xiao Er Ji Jiu Yi Xue Za Zhi* 27, 10. doi:10.3760/cma.j.issn.1673-4912.2020.10.016

Zschocke, J., Penzien, J. M., Bielen, R., Casals, N., Aledo, R., Pié, J., et al. (2002). The Diagnosis of Mitochondrial HMG-CoA Synthase Deficiency. *J. Pediatr.* 140 (6), 778–780. doi:10.1067/mpd.2002.123854

Conflict of Interest: The authors declare that the research was conducted in the absence of any commercial or financial relationships that could be construed as a potential conflict of interest.

Publisher's Note: All claims expressed in this article are solely those of the authors and do not necessarily represent those of their affiliated organizations, or those of the publisher, the editors and the reviewers. Any product that may be evaluated in this article, or claim that may be made by its manufacturer, is not guaranteed or endorsed by the publisher.

frontiers in Pediatrics

CASE REPORT
published: 10 March 2022
doi: 10.3389/fped.2022.831284

Case Report: A Novel Compound Heterozygote Mutation of the *SCNN1B* Gene Identified in a Chinese Familial Pseudohypoaldosteronism Disease Type I With Persistent Hyperkalemia

Zongzhi Liu[1,2†], *Xiaojiao Wang*[3†], *Zilong Zhang*[4], *Zixin Yang*[3], *Junyun Wang*[5*] and *Yajuan Wang*[6*]

[1] Shenzhen Key Laboratory of Synthetic Genomics, Guangdong Provincial Key Laboratory of Synthetic Genomics, CAS Key Laboratory of Quantitative Engineering Biology, Shenzhen Institute of Synthetic Biology, Shenzhen Institutes of Advanced Technology, Chinese Academy of Sciences, Shenzhen, China, [2] Central Laboratory, National Cancer Center/National Clinical Research Center for Cancer/Cancer Hospital and Shenzhen Hospital, Chinese Academic of Medical Sciences and Peking Union Medical College, Shenzhen, China, [3] Department of Neonatal Center, Beijing Children's Hospital, Capital Medical University, National Center for Children's Health, Beijing, China, [4] Tianjin Novogene Bioinformatic Technology Co., Ltd., Tianjin, China, [5] CAS Key Laboratory of Genome Sciences and Information, China National Center for Bioinformation, Beijing Institute of Genomics, Chinese Academy of Sciences, Beijing, China, [6] Department of Neonatology, Children's Hospital, Capital Institute of Pediatrics, Beijing, China

OPEN ACCESS

Edited by:
Hui Xiong,
Peking University First Hospital, China

Reviewed by:
John William Foreman,
School of Medicine Duke University, United States
Roberto Chimenz,
University of Messina, Italy

***Correspondence:**
Yajuan Wang
cxswyj@vip.sina.com
Junyun Wang
jywang@big.ac.cn

[†] *These authors have contributed equally to this work*

Specialty section:
This article was submitted to Genetics of Common and Rare Diseases, a section of the journal Frontiers in Pediatrics

Received: *08 December 2021*
Accepted: *02 February 2022*
Published: *10 March 2022*

Citation:
Liu Z, Wang X, Zhang Z, Yang Z, Wang J and Wang Y (2022) Case Report: A Novel Compound Heterozygote Mutation of the SCNN1B Gene Identified in a Chinese Familial Pseudohypoaldosteronism Disease Type I With Persistent Hyperkalemia. Front. Pediatr. 10:831284. doi: 10.3389/fped.2022.831284

Background: Pseudohypoaldosteronism (PHA) diseases are difficult to diagnose because symptoms are often non-specific and an in-depth pathogenesis study is still lacking.

Case Presentation: We present the case of a 19-day-old neonate who presented with unexplained recurrent hyperkalaemia, hypovolemia and metabolic acidosis, whose parents did not have significant clinical disease characteristics. Whole-exome sequencing was performed to confirm the disease and genetic pattern of the neonate. Sanger sequencing was performed to identify the mutation sites. Secondary structure comparisons and 3D model construction were used to predict changes in protein structure. Two novel frameshift mutations in the *SCNN1B* gene were identified (c.1290delA and c.1348_1361del), which resulted in amino acid synthesis termination (p.Gln431ArgfsTer2 and p.Thr451AspfsTer6). Considering the clinical phenotype and genetic analysis, this case was finally identified as a PHA type I disease. Genetic analysis showed that the neonate suffered complex heterozygosity in the *SCNN1B* gene inherited from the parents, which is passed on in an autosomal recessive inheritance pattern. These two deleterious mutations resulted in an incomplete protein 3D structure.

Conclusions: Our results have confirmed the associations of mutations in the SCNN1B gene with recurrent hyperkalaemia, which can cause severe PHA type I disease, meanwhile suggested clinical attention should be paid when persistent recurrent hyperkalemia is accompanied by these types of mutations.

Keywords: pseudohypoaldosteronism type I, whole-exome sequencing, *SCNN1B*, frameshift mutations, genetic pattern, rare disease

INTRODUCTION

Pseudohypoaldosteronism (PHA) is a severe disease first described by Cheek and Perry (1), characterized by congenital resistance to the action of aldosterone on epithelial tissue, failure to thrive, hyperkalaemia, hypovolemia, and metabolic acidosis. PHAs can be divided into types I and II. PHA type I often harbors mutations in the *SCNN1A*, *SCNN1B*, and *SCNN1G* genes, which encode the epithelial sodium channel (ENaC) (2, 3). PHA type II is caused by mutations in the *WNK1* and *WNK4* genes, which encode lysine-deficient protein kinases. PHA type I results in excessive salt wasting despite very high plasma aldosterone and renin levels, whereas PHA type II leads to blood pressure disorder-related diseases (4–6). Molecular level research on PHA type I shows the *SCNN1A* (12p13), *SCNN1B* (16p12.2–p12.1), and *SCNN1G* (16p12) genes encoding the three homologous α, β, and γ subunits of ENaCs (7–10), which are membrane-bound ion channels that are selectively permeable to Na^+ ions. Changes in Na? concentration affect the movement of fluids and, consequently, fluid volume and blood pressure (11, 12). ENaC activity is modulated by the mineralocorticoid aldosterone, and the α, β, and γ subunits of ENaC are essential for transport to the membrane assembly of functional channels on the membrane; mutations in *SCNN1A*, *SBNN1B*, and *SCNN1G* lead to loss of ENaC activity (13–15).

Here, we report the case of a 19-day-old neonate presumptively diagnosed with PHA with two novel frameshift mutations in *SCNN1B* (c.1290delA and c.1348_1361del), which resulted in premature amino acid synthesis termination (p.Gln431ArgfsTer2 and p.Thr451AspfsTer6) by both two chromosomes. We also reviewed and analyzed the clinical features of the neonate to further clarify the correlation between the deletion region and the phenotype.

MATERIALS AND METHODS

Editorial Policies and Ethical Considerations

This study was agreed by the Research Ethical Review Committee, Beijing Children's Hospital Affiliated to Capital Medical University (approved protocol no.2017-k-81). Written informed consent was obtained from the individual(s), and minor(s)' legal guardian/next of kin, for the publication of any potentially identifiable images or data included in this article. All blood samples were obtained after written informed patient consent and were fully anonymized. The participants and legal guardian provided written informed consent to participate in this study.

Clinical Presentation

A 19-day-old neonate suffered an inexplicable electrolyte disturbance for 15 days and was admitted to the neonatal intensive care unit at the Beijing Children's Hospital with a history of poor feeding, hypothermia, lethargy, and bradycardia. She was born by cesarean section after a full-term pregnancy with a birth weight of 3,490 g (10–90th percentile) and lost 15% of her weight 5 days after birth. She was the first child of her parents, and the mother had no perinatal problems. Neither of the parents had a family history of significant illness or unexplained death.

On physical examination, her weight and height were 3.09 kg (<3rd percentile) and 50.2 cm (3rd-10th percentile), respectively, and her head circumference was 34.1 cm (10–50th percentile). Routine examination showed a blood pressure of 73/39 mmHg, pulse rate of 148/min, respiratory rate of 44/min, and temperature of 37.2°C. The neonate was pale and lethargic and exhibited hypotonic extremities and severe dehydration. Her external genitals developed normally, and other physical examination results were within the normal range.

The initial serum laboratory examinations results were as follows: hyponatraemia: sodium 111 mmol/L (normal range = 130–150 mmol/L), hyperkalaemia: potassium 9.0 mmol/L (normal range = 3.5–5.5 mmol/L), hypochloraemia: chloride 83.6 mmol/L (normal range = 98–108 mmol/L), urea nitrogen 4.2 mmol/L (normal range = 1.7–7.1 mmol/L), and creatinine 23 μmol/L (normal range = 30–104 μmol/L). Arterial blood gas analysis revealed metabolic acidosis: pH = 7.227 (normal range = 7.251–7.429) and base excess:−14 mmol/L (normal range = −6–2). Plasma adrenocorticotropic hormone < 5–11.9 pg/ml(normal range = 0–46 pg/ml), Plasma cortisol 1.27–9.28 umol/dl (normal range =5–25 μmol/dl), Plasma testosterone < 20 ng/dl (normal range = 0–106.9), Plasma 17-α-hydroxyprogesterone 5.18 nmol/L (normal range = 0.31–38.1). Further laboratory studies subsequently revealed markedly increased plasma renin 5.36 ng/mL/h (normal range = 0.00–0.79 ng/mL/h), serum aldosterone 22.78 ng/dL (normal range = 5.9–17.4 ng/dL), and angiotensin II 398.7 pg/mL (normal range = 40.6–90.0 pg/mL). B-ultrasound of adrenal gland showed that the structure of adrenal gland was normal. Symptoms of hyperkalaemia persisted during the treatment from day 1 to day 4 (**Figure 1**). Meanwhile, through differential diagnosis, we ruled out renal failure, hypovolemia: shock or dehydration, adrenocortical insufficiency: adrenal hemorrhage, adrenal hypoplasia, etc., congenital adrenal hyperplasia, potassium retention diuretics and other diseases. Based on these clinical tests, a presumptive diagnosis of PHA was made (**Table 1**), metabolic acidosis was corrected, and blood potassium was lowered using simultaneous high-salt milk feeding (1 g Nacl/day, 20–30 ml/feeding). Because the PHA disease was not confirmed, the type and genetic pattern was also unclear, accurate treatment could not be provided; therefore, whole-exome sequencing and Sanger sequencing were performed on the neonate and her parents who without typical PHA disease symptoms.

Genomic DNA Extraction

We obtained the peripheral blood of the neonate and her parents at Beijing Children's Hospital and extracted the DNA immediately using the QIAamp DNA Blood Mini Kit according to the manufacturer's instructions.

Whole-Exome Sequencing and Single Nucleotide Polymorphism Calling

Exome capture was performed using the Agilent SureSelect Human All Exon V6, according to the manufacturer's standard protocols. The Illumina Hiseq 2500 platform was used to

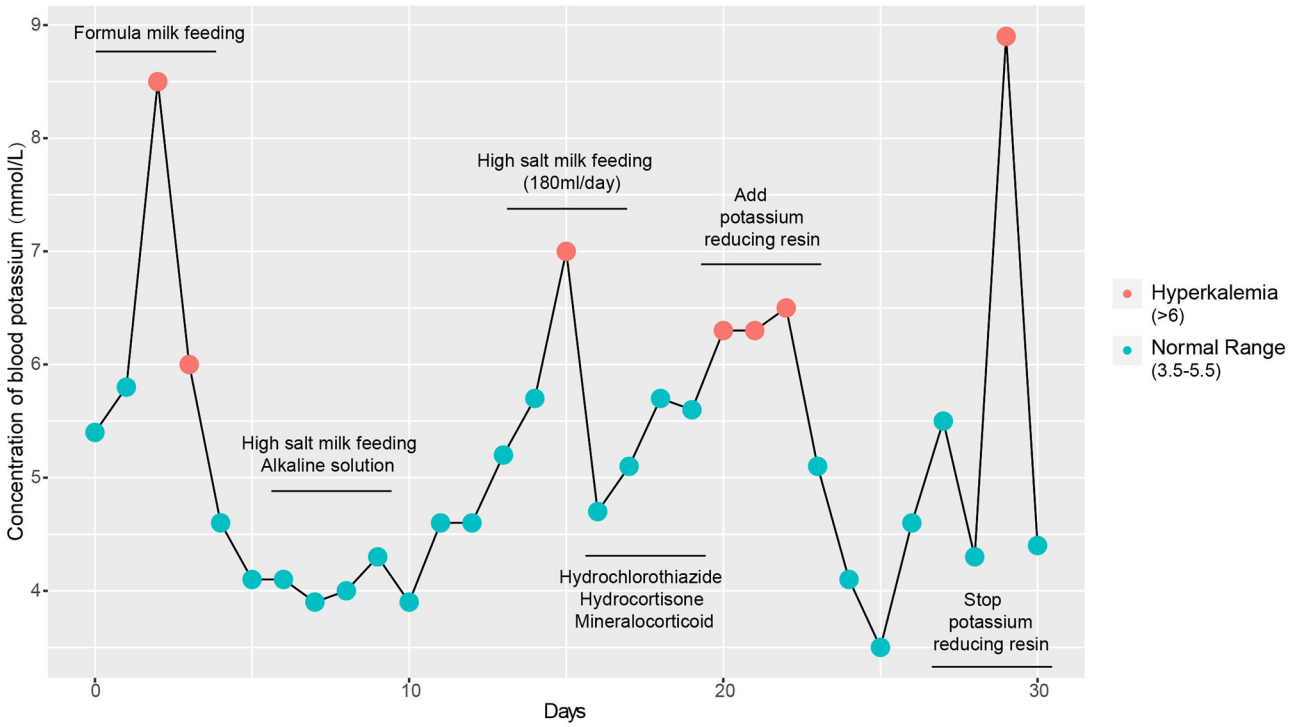

FIGURE 1 | Detection of blood potassium from admission to discharge. Repeated clinical symptoms of hyperkalaemia in the infant from day 1 to day 30.

TABLE 1 | Differential diagnosis of the neonate.

Pathogeny	Diagnosis	The neonate
Excessive potassium intake	Intravenous infusion a large amount of potassium liquid	No
Renal potassium depletion disorder	Renal failure	No
	Hypovolemia: shock or dehydration	No
	Adrenocortical insufficiency: adrenal hemorrhage, adrenal hypoplasia, etc.	No
	Congenital adrenal hyperplasia	No
	Potassium retention diuretics	No
	Pseudohypoaldosteronism	Highly suspicious

detect the DNA sequence, and paired-end sequencing was conducted with a read length of 150 bp (16). More than 10 GB of clean sequence data and more than 100 × read depth were obtained for each DNA sample. All individual sequence reads were aligned to the human reference genome (NCBI build GRH37/hg19) using the Burrows-Wheeler Aligner software (17). The genome analysis toolkit, SAMtools, and Picard tools were used for bioinformatic analysis, and SNPs and insertion-deletions (indels) were identified using the genome analysis toolkit (18, 19).

3D Modeling

Amino acid sequence alignment and the 3D structure of SCNN1B were constructed using Swiss-Model software (https://swissmodel.expasy.org/).

RESULTS

Mutation Analysis and Verification

In order to identify the PHA disease and the type of PHA, SNPs and indels in the *SCNN1A*, *SCNN1B*, *SCNN1G*, *WNK1*, and *WNK4* genes were investigated. As shown in **Table 2**, two novel frameshift mutations in *SCNN1B* (c.1290delA and c.1348_1361del) were revealed, both of which led to the production of the stop codon TGA. We further verified the two new mutations using Sanger sequencing (**Figure 2A**). Neither mutation had been described previously (http://www.ncbi.nlm.nih.gov/projects/SNP). Other candidate genes were also analyzed, but no significant pathogenic SNPs or indels were found (**Table 2**). Based on the molecular-level results, PHA type I was preliminarily identified.

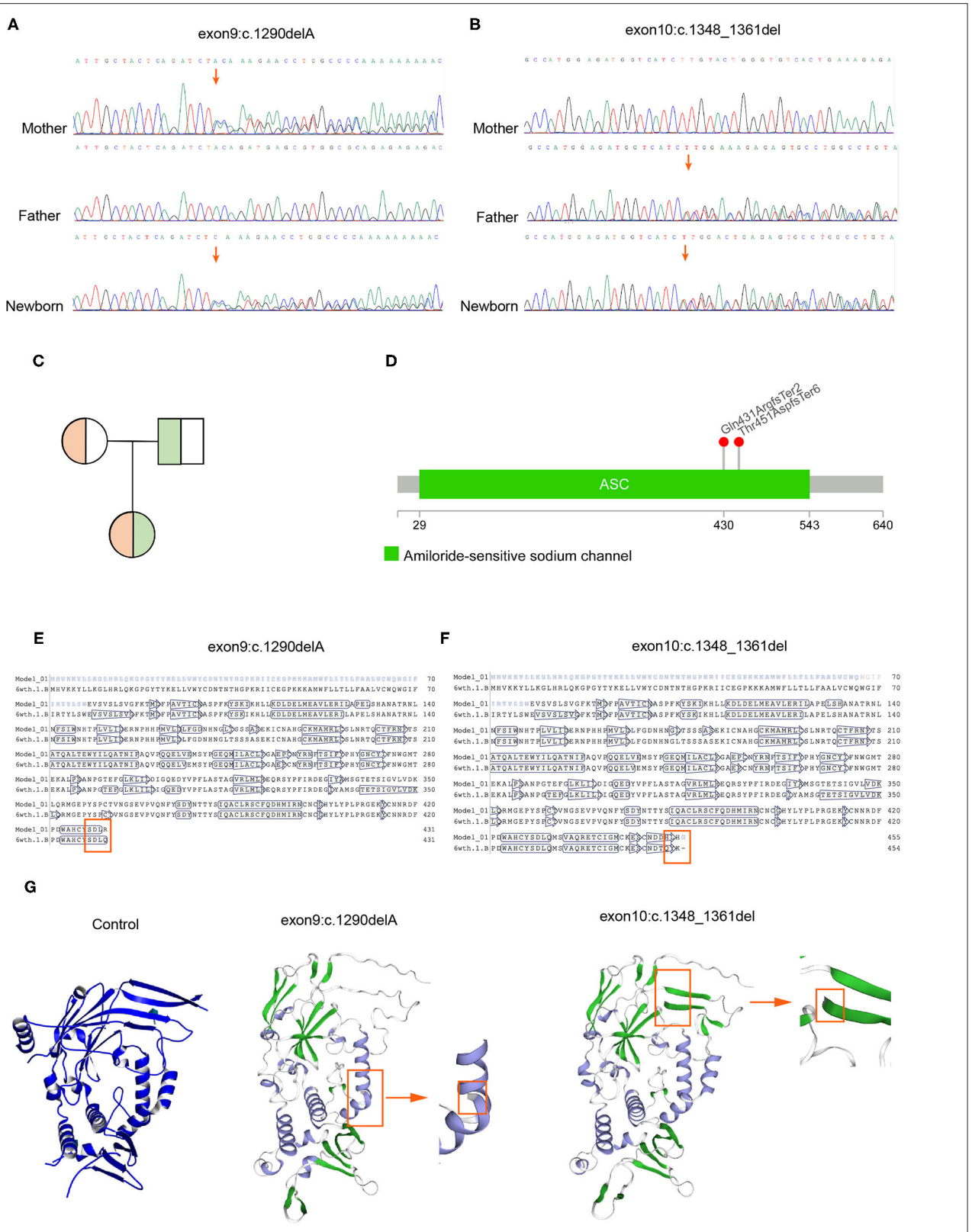

FIGURE 2 | Mutation verification and protein 3D structure prediction. **(A)** Sanger sequencing demonstrated that c.1290delA was inherited from the mother. **(B)** Sanger sequencing demonstrated that c.1348_1361del was inherited from the father. **(C)** Genetic pattern analysis of compound heterozygotes. **(D)** Location of the mutation sites in the *SCNN1B* gene. **(E,F)** Amino acid sequence alignment indicated that both mutations caused early termination of amino acid synthesis (6wth.1.b refers to the amino acid sequence after mutation; Model_01 refers to the non-mutated amino acid sequence). **(G)** The 3D model predicted an incomplete ENaC structure after mutation.

TABLE 2 | SNPs and indels analysis of SCNN1B and WNK1 in the neonate.

Gene name	Chromosome position	RS number	Ref Allele	SNP allele	Functional consequence	Allele frequency	Global MAF	Clinical significance
SCNN1B	16:23388504	-	TA	T	-	0.5	-	-
SCNN1B	16:23388650	-	TGACACCCAGTACAA	T	-	0.5	-	-
SCNN1B	16:23360199	rs238547	T	C	Synonymous codon	1	T:0.2115	Benign
WNK1	12:1017197	rs4766334	C	T	Synonymous codon	1	C:0.0130	Benign
WNK1	12:862989	rs3168640	T	C	Synonymous codon	1	T:0.0244	Benign
WNK1	12:987482	rs1012729	G	A	Synonymous codon	1	G:0.3205	Benign
WNK1	12:990912	rs956868	A	C	Missense	1	A:0.1472	Benign
WNK1	12:993930	rs7300444	C	T	Synonymous codon	1	T:0.3990	Benign
WNK1	12:994487	rs7955371	G	C	Synonymous codon	1	G:5008:0.0132	Benign
WNK1	12:862641	rs3088353	T	G	5'utr variant	0.5	G:5008:0.3399	Benign
WNK1	12:939302	rs10774466	A	G	Synonymous codon	1	A:5008:0.3065	Benign

Confirmation of Compound Heterozygosity and Genetic Pattern

Because the neonate's parents do not have typical PHA disease characteristics, next, we explored the genetic patterns of these mutations. As shown in **Figures 2A–C**, c.1290delA was carried by her mother, whereas c.1348_1461del was carried by her father, and the neonate inherited these two frameshift mutations concurrently. Her parents possessed heterozygous mutations with a normal phenotype, indicating a recessive inheritance pattern (**Figure 2C**). Thereafter, we confirmed that these two mutations were distributed in different chromosomes in the neonate, so the translation of the *SCNN1B* gene was terminated prematurely in both chromosomes. Whole-exome sequencing results showed that c.1290delA occurred at chr16:23388505, whereas c.1348_1461del occurred at chr16:23388651, and the distance between these two mutations was 146 bp (**Figure 2D**). We then counted the number of reads covered in this range, there was no single read containing both mutations, all the reads covered from chr16:23388505 to chr16:23388651 had only one mutation, either c.1290delA or c.1348_1461del, which indicates that the two mutations occurred in different chromosomes. Based on these findings, the neonate suffered a "double-stop" compound heterozygous mutation in the *SCNN1B* gene, which led to no functional B-subunit protein of ENaC and severe and persistent electrolyte abnormalities.

Amino Acid Sequence Alignment and 3D Prediction of Protein Structure

Further, we want to know whether these two mutations will cause changes in the three-dimensional structure of the protein. We found that the two mutations at the amino acid level were p.Gln431ArgfsTer2 and p.Thr451AspfsTer6. After amino acid sequence alignment, we found that these two frameshift mutations led to the early termination of amino acid synthesis (**Figures 2E,F**). We also found that both mutations led to an incomplete structure in the protein 3D prediction model (**Figure 2G**).

Follow Up and Outcome

After confirmation of recessive hereditary PHA type I using genetic analysis, the parents were asked to go back to the local hospital for treatment after a clear diagnosis, we recommend continuing oral potassium lowering resin (1–2g/kg/day) and high-salt milk feeding (1 g Nacl/day, 20–30 ml/feeding) as therapeutic approach. Serum electrolytes returned to the normal range after initial parenteral hydration, oral sodium supplementation, and kayexalate usage; all clinical indicators were within the normal range after returning to the local hospital, but the development level was slightly slower than that of normal infants. At 3 months of age, the following measurements were obtained: weight 3.8 kg (normal range = 4.4–8.71 kg), height 55 cm (normal range = 54.2–67.5 cm), and head circumference 37 cm (normal range = 37.4–42.2 cm). At the age of 4 months, the infant returned to Beijing Children's Hospital due to convulsions without obvious causes, respiratory infection symptoms, increased blood potassium level, decreased blood sodium level, and ventricular tachycardia. Subsequently, resuscitative efforts were unsuccessful and the infant died.

DISCUSSION

PHA is a mineralocorticoid resistance disease characterized by renal salt wasting, dehydration, and failure to thrive. PHA type

I typically presents in the neonatal period with severe salt-wasting crisis with hyponatraemia, hyperkalaemia, acidosis, and dehydration due to sodium loss through the kidneys, colon, sweat, and salivary glands (20, 21). Patients may also present with lethargy and failure to thrive. PHA type I is often recessively inherited, and genetic mutations cause manifold loss of function of ENaC protein subunits and sodium reabsorption disfunction (3, 22). There is no specific treatment for PHA type I, except for the potassium ion exchange resin.

We present a case of PHA type I identified using whole-exome sequencing, with two novel frameshift mutations in the *SCNN1B* gene, which resulted in severe hyperkalaemia, hyponatraemia, metabolic acidosis, moreover, the emergence of compound heterozygotes of this mutant type may lead to growth retardation and early neonatal mortality. These mutations were inherited from the parents, who did not exhibit typical PHA clinical symptoms. Although several cases of patients with PHA type I have previously been presented, and mutations such as c.1466 $+1\,G > A$, c.1288delC, and c.1266-1G > C have been reported (9, 23–26). This neonate carried novel compound heterozygote mutations in the *SCNN1B* gene, both of which resulted in an abnormal stop codon.

The ENaC plays a critical role in cellular functions, such as Na^+ and water balance, blood pressure stabilization, and response to aldosterone. As a result, mutations in ENaC genes generally produce clinical symptoms of failure to thrive, hypovolemia caused by sodium wasting, metabolic acidosis, and severe hyperkalaemia.c.1290delA and c.1348_1461del changed the reading frame, resulting in a completely different translation compared with the original (27, 28), and these two deletions lead to abnormal stop codons that were distributed in different chromosome. These two novel frameshift mutations led to p.Gln431ArgfsTer2 and p.Thr451AspfsTer6 (29). The advantage of our study is we established the mutations identified were inherited from both parents, who had novel frameshift mutations. The parents were not diagnosed with PHA because the mutation in the *SCNN1B* gene only occurred in one of the homologous chromosome. The other homologous chromosome had a *SCNN1B* gene with normal structure and function; therefore, the parents did not exhibit significant clinical symptoms. However, both of them carried different mutations in the *SCNN1B* gene, and their daughter inherited these mutations.

This case increased our understanding of phenotypes resulting from *SCNN1B* mutations. Our results highlight the need for increased attention to parents or children with such genotypes in clinical practice.

DATA AVAILABILITY STATEMENT

The original contributions presented in the study are included in the article/supplementary files, further inquiries can be directed to the corresponding authors.

ETHICS STATEMENT

The studies involving human participants were reviewed and approved by Research Ethical Review Committee, Beijing Children's Hospital Affiliated to Capital Medical University (Approved Protocol No. 2017-k-81). Written informed consent to participate in this study was provided by the participants' legal guardian/next of kin. Written informed consent was obtained from the individual(s), and minor(s)' legal guardian/next of kin, for the publication of any potentially identifiable images or data included in this article.

AUTHOR CONTRIBUTIONS

ZL analyzed the data. XW and ZY collected the samples and treated the patient. ZZ contributed reagents, materials, and analysis tools. JW and YW participated in writing and correction. All authors read and approved the final manuscript.

FUNDING

This work was supported by the National Natural Science Foundation of China (Grant Nos. 22005343 and 81702796), the Precision Medicine Research Program of the Chinese Academy of Sciences (Grant No. KJZD-EW-L14), the Sanming Project of Medicine in Shenzhen (Grant Nos. SZSM201812062 and SZSM201612097), and Shenzhen Key Medical Discipline Construction Fund (Grant No. SZXK075).

ACKNOWLEDGMENTS

We are sincerely grateful to advice given by Xiaoting Mu and professor Fan Liu, thanks the patients family for providing samples and offering us enough trust.

REFERENCES

1. Cheek DB, Perry JW. A salt wasting syndrome in infancy. *Arch Dis Child.* (1958) 33:252–6. doi: 10.1136/adc.33.169.252
2. Yin LP, Zhu H, Zhu RY, Huang L. A novel SCNN1G mutation in a PHA I infant patient correlates with nephropathy. *Biochem Biophys Res Commun.* (2019) 519:415–21. doi: 10.1016/j.bbrc.2019.07.026
3. Karacan Küçükali G, Çetinkaya S, Tunç G, Oguz MM, Çelik N, Akkaş KY, et al. Clinical management in systemic type pseudohypoaldosteronism due to SCNN1B variant and literature review. *J Clin Res Pediatr Endocrinol.* (2020) 13:446–51. doi: 10.4274/jcrpe.galenos.2020.2020.0107
4. Zennaro MC, Hubert EL, Fernandes-Rosa FL. Aldosterone resistance: structural and functional considerations and new perspectives. *Mol Cell Endocrinol.* (2012) 350:206–15. doi: 10.1016/j.mce.2011.04.023
5. Kawashima Sonoyama Y, Tajima T, Fujimoto M, Hasegawa A, Miyahara N, Nishimura R, et al. A novel frameshift mutation in NR3C2 leads to decreased expression of mineralocorticoid receptor: a family with renal pseudohypoaldosteronism type 1. *Endocr J.* (2017) 64:83–90. doi: 10.1507/endocrj.EJ16-0280
6. Bonny O, Rossier BC. Disturbances of Na/K balance: pseudohypoaldosteronism revisited. *J Am Soc Nephrol.* (2002) 13:2399–414. doi: 10.1097/01.ASN.0000028641.59030.B2

7. Strautnieks SS, Thompson RJ, Hanukoglu A, Dillon MJ, Hanukoglu I, Kuhnle U, et al. Localisation of pseudohypoaldosteronism genes to chromosome 16p12.2-13.11 and 12p13.1-pter by homozygosity mapping. *Hum Mol Genet*. (1996) 5:293–9. doi: 10.1093/hmg/5.2.293
8. Hanukoglu A, Edelheit O, Shriki Y, Gizewska M, Dascal N, Hanukoglu I. Renin-aldosterone response, urinary Na/K ratio and growth in pseudohypoaldosteronism patients with mutations in epithelial sodium channel (ENaC) subunit genes. *J Steroid Biochem Mol Biol.* (2008) 111:268–74. doi: 10.1016/j.jsbmb.2008.06.013
9. Dogan CS, Erdem D, Mesut P, Merve A, Iffet B, Afig B. A novel splice site mutation of the beta subunit gene of epithelial sodium channel (ENaC) in one Turkish patient with a systemic form of pseudohypoaldosteronism Type 1. *J Pediatr Endocrinol Metab*. (2012) 25:1035–9. doi: 10.1515/jpem-2012-0083
10. Boscardin E, Perrier R, Sergi C, Maillard M, Loffing J, Loffing-Cueni D, et al. Severe hyperkalemia is rescued by low-potassium diet in renal βENaC-deficient mice. *Pflugers Archiv*. (2017) 469:1387–99. doi: 10.1007/s00424-017-1990-2
11. Sorokin A, Staruschenko A. Inhibition of ENaC by endothelin-1. *Vitam Horm.* (2015) 98:155–87. doi: 10.1016/bs.vh.2015.01.001
12. Willam A, Aufy M, Tzotzos S, Evanzin H, Chytracek S, Geppert S, et al. Restoration of epithelial sodium channel function by synthetic peptides in pseudohypoaldosteronism type 1B mutants. *Front Pharmacol.* (2017) 8:85. doi: 10.3389/fphar.2017.00085
13. Chen L, Zhang X, Zhang W. Regulation of αENaC transcription. *Vitam Horm.* (2015) 98:101. doi: 10.1016/bs.vh.2014.12.004
14. Hanukoglu I, Hanukoglu A. Epithelial sodium channel (ENaC) family: phylogeny, structure–function, tissue distribution, and associated inherited diseases. *Gene.* (2016) 579:95. doi: 10.1016/j.gene.2015.12.061
15. W. SM. Renal intercalated cells and blood pressure regulation. *Kidney Res Clin Pract.* (2017) 36:305. doi: 10.23876/j.krcp.2017.36.4.305
16. Bentley DR, Balasubramanian S, Swerdlow HP, Smith GP, Milton J, Brown CG, et al. Accurate whole human genome sequencing using reversible terminator chemistry. *Nature.* (2008) 456:53–9. doi: 10.1038/nature07517
17. Li H, Durbin R. Fast and accurate short read alignment with Burrows–Wheeler transform. *Bioinformatics*. (2009) 25:1754–60. doi: 10.1093/bioinformatics/btp324
18. McKenna A, Hanna M, Banks E, Sivachenko A, Cibulskis K, Kernytsky A, et al. The genome analysis toolkit: a mapreduce framework for analyzing next-generation DNA sequencing data. *Genome Res*. (2010) 20:1297–303. doi: 10.1101/gr.107524.110
19. Wang K, Li M, Hakonarson H. ANNOVAR: functional annotation of genetic variants from high-throughput sequencing data. *Nucleic Acids Res.* (2010) 38:e164. doi: 10.1093/nar/gkq603
20. Delforge X, Kongolo G, Cauliez A, Braun K, Haraux E, Buisson P. Transient pseudohypoaldosteronism: a potentially severe condition affecting infants with urinary tract malformation. *J Pediatr Urol.* (2019) 15:265. doi: 10.1016/j.jpurol.2019.03.002
21. Kumar S, McDermott H, Kamupira S, Agwu JC. Rare case of pseudohypoaldosteronism in a neonate secondary to congenital hydrometrocolpos. *BMJ Case Rep.* (2020) 13:e234813. doi: 10.1136/bcr-2020-234813
22. Alzahrani AS, Alswailem M, Abbas BB, Qasem E, Alsagheir A, Al Shidhani A, et al. A unique genotype of pseudohypoaldosteronism type 1b in a highly consanguineous population. *J Endocr Soc.* (2021) 5:bvab095. doi: 10.1210/jendso/bvab095
23. Nobel YR, Lodish MB, Raygada M, Rivero JD, Faucz FR, Abraham SB, et al. Pseudohypoaldosteronism type 1 due to novel variants of SCNN1B gene. *Endocrinol Diabetes Metab Case Rep*. (2016) 2016:150104. doi: 10.1530/EDM-15-0104
24. Nam HK, Nam MH, Kim HR, Rhie YJ, Yoo KH, Lee KH. Clinical manifestation and molecular analysis of three Korean patients with the renal form of pseudohypoaldosteronism Type 1. *Ann Clin Lab Sci.* (2017) 47:83–7.
25. Nissen M, Dettmer P, Thränhardt R, Winter K, Niemeyer T, Tröbs R-B. Congenital jejunal membrane causing transient pseudohypoaldosteronism and hypoprothrombinemia in a 7-week-old infant. *Klin Padiatr*. (2017) 229:302–3. doi: 10.1055/s-0043-113570
26. Nur N, Lang C, Hodax JK, Quintos JB. Systemic pseudohypoaldosteronism Type I: a case report and review of the literature. *Case Rep Pediatr*. (2017) 2017:7939854. doi: 10.1155/2017/7939854
27. Brenner S, Barnett L, Katz ER, Crick FH. UGA: a third nonsense triplet in the genetic code. *Nature*. (1967) 213:449–50. doi: 10.1038/213449a0
28. Gagniuc P, Constantin Ionescutirgoviste. Gene promoters show chromosome-specificity and reveal chromosome territories in humans. *BMC Genomics.* (2013) 14:278. doi: 10.1186/1471-2164-14-278
29. Chang SS, Grunder S, Hanukoglu A, Rösler A, Mathew PM, Hanukoglu I, et al. Mutations in subunits of the epithelial sodium channel cause salt wasting with hyperkalaemic acidosis, pseudohypoaldosteronism type 1. *Nat Genet.* (1996) 12:248–53. doi: 10.1038/ng0396-248

Conflict of Interest: ZZ was employed by company Tianjin Novogene Bioinformatic Technology Co., Ltd., China.

The remaining authors declare that the research was conducted in the absence of any commercial or financial relationships that could be construed as a potential conflict of interest.

Publisher's Note: All claims expressed in this article are solely those of the authors and do not necessarily represent those of their affiliated organizations, or those of the publisher, the editors and the reviewers. Any product that may be evaluated in this article, or claim that may be made by its manufacturer, is not guaranteed or endorsed by the publisher.

frontiers in Genetics

CASE REPORT
published: 11 March 2022
doi: 10.3389/fgene.2022.845246

Case Report: Be Aware of "New" Features of Niemann–Pick Disease: Insights From Two Pediatric Cases

Fan Chen[1†], Shan Guo[2†], Xuesong Li[1], Shengxuan Liu[1], Li Wang[3], Victor Wei Zhang[3], Hui Xu[4], Zhihua Huang[1], Yanqin Ying[1] and Sainan Shu[1]**

[1]Department of Pediatrics, Tongji Hospital, Tongji Medical College, Huazhong University of Science and Technology, Wuhan, China, [2]Department of Gastroenterology, Wuhan Children's Hospital of Tongji Medical College, Huazhong University of Science and Technology, Wuhan, China, [3]AmCare Genomics Lab, Guangzhou, China, [4]Department of Pathology, School of Basic Medicine, Tongji Medical College, Huazhong University of Science and Technology, Wuhan, China

OPEN ACCESS

Edited by:
Huiwen Zhang,
Xinhua Hospital, China

Reviewed by:
Hasan Orhan Akman,
Columbia University Irving Medical Center, United States
Reena V. Kartha,
University of Minnesota Twin Cities, United States

***Correspondence:**
Yanqin Ying
yingtea0909@126.com
Sainan Shu
shusainan@163.com

†These authors have contributed equally to this work and share first authorship

Specialty section:
This article was submitted to Genetics of Common and Rare Diseases, a section of the journal Frontiers in Genetics

Received: 29 December 2021
Accepted: 15 February 2022
Published: 11 March 2022

Citation:
Chen F, Guo S, Li X, Liu S, Wang L, Zhang VW, Xu H, Huang Z, Ying Y and Shu S (2022) Case Report: Be Aware of "New" Features of Niemann–Pick Disease: Insights From Two Pediatric Cases. Front. Genet. 13:845246. doi: 10.3389/fgene.2022.845246

Niemann–Pick disease is a relatively common lysosomal storage disease. Cholestatic liver disease is a typical clinical phenotype of Niemann–Pick disease in infancy. The diagnosis is traditionally based on Niemann–Pick cells in bone marrow smears or liver biopsies. Treatment for cholestatic liver disease mainly includes ursodeoxycholic acid and liver protection drugs. Here, we reported two cases of Niemann–Pick disease type C, diagnosed by genetic analysis during early infancy. Besides cholestatic jaundice, the two patients also exhibited signs of immune system hyperactivity, such as elevated immunoglobulins or multiple autoantibodies, which might require the application of glucocorticoids. In addition, three novel missense variants of the NPC1 gene were identified. The findings suggest that immune activation should be considered as a "new" clinical phenotype of lysosomal storage diseases.

Keywords: niemann-pick disease, lysosomal storage diseases, NPC1, immune, child

INTRODUCTION

Lysosomal storage diseases (LSDs) comprise a group of more than 70 distinct genetic diseases. LSDs are characterized by the accumulation of undigested macromolecules in lysosomes of various body cells. Although these disorders are rare, they affect 1 in 5,000 live births, accounting for 14% of all inherited metabolic diseases. LSDs have similar clinical features despite different pathogenetic mechanisms (Rigante et al., 2017; Platt et al., 2018). Niemann–Pick disease is a relatively common autosomal recessive LSD. Clinical manifestations and pathogenic genes are mainly classified into types A, B, and C (Vanier, 2013). Niemann–Pick disease type C (NPC) is a progressive and fatal disorder caused by mutations in the NPC1 (OMIM 257220) or NPC2 (OMIM 607625) gene, which results in the intracellular accumulation of unesterified cholesterol. As cholesterol accumulates in cells, it affects the brain, liver, spleen, and lungs, leading to premature death. The estimated incidence of NPC is 1:100,000, with variable age of onset and clinical features (Vanier, 2010; Patterson et al., 2012; Geberhiwot et al., 2018). Perinatal manifestations of NPC often include splenomegaly, hepatomegaly, fetal ascites, or nonimmune fetal hydrops (Spiegel et al., 2009; Surmeli-Onay et al., 2013). Severe hepatic diseases, associated or not with pulmonary disease, are neonatal manifestations of NPC (Bjurulf et al., 2008; Griese et al., 2010). In comparison with the adult period, cholestatic liver disease is a typical clinical phenotype in infants. However, some affected infants may also present hypotonia and developmental delay with little hepatic and pulmonary involvement (Vanier et al., 1988). Later in childhood and adulthood, patients can present a

progressive neurodegenerative disorder characterized by developmental delay, clumsiness, cataplexy, supranuclear gaze palsy, ataxia, dystonia, and progressive dementia (Vanier, 2010).

Autoimmune diseases are systemic diseases that affect approximately 5% of the population in western countries. They are characterized by chronic, systemic excessive immune activation and inflammation (Davidson and Diamond, 2001; Xiao et al., 2021). Many studies have reported an association between autoimmune phenomena and LSDs (Rigante et al., 2017). Recently, autoantibodies in NPC have been reported in several studies (Dimitriou et al., 2019; Chu et al., 2021). Herein, we reported two clinical cases of NPC in the form of cholestatic jaundice combined with immune activation in early infancy diagnosed by genetic analysis.

CASE PRESENTATION

Clinical Features

Two independent patients were recruited into this study after the parents signed the informed consent. Both patients presented early-onset jaundice, abnormal liver function, and hepatosplenomegaly, suggestive of cholestatic liver disease. In addition, both patients showed signs of the immune system hyperactivity, such as elevated levels of immunoglobulins.

Patient 1

A female patient (Patient 1) was born at term after an uneventful pregnancy by cesarean delivery, with a birth weight of 3,400 g (50–75th centile). The patient was breastfed and was the first child of a nonconsanguineous Chinese couple. The patient's mother had once miscarried before because of a bad pregnancy outcome. The father is healthy without any known comorbidity. The patient had developed progressive jaundice since the third day after birth. At 1.8 months, the patient was initially admitted to a local hospital, and hepatosplenomegaly was identified. After more than 1 month of conservative medical treatment, the patient developed yellowing of the skin and sclera, which slowly improved, while hepatosplenomegaly progressively worsened. Therefore, the patient was referred to Tongji Hospital at the age of 3.1 months. Malnutrition was documented based on a low body weight (4,400 g, < third centile). Physical examination revealed slight yellowing of the skin, increased respiratory rate, and moist rales of the lungs. The patient's liver was 3.5 cm below the right costal margin, while the spleen was 6.0 cm below the left costal margin.

Laboratory tests showed an elevation in the serum levels of alanine aminotransferase (ALT), aspartate aminotransferase (AST), total bilirubin (TBIL), direct bilirubin (DBIL), indirect bilirubin (IBIL), γ-glutamyl transferase (γ-GT), total bile acid (TBA), globulin (GLB), and alpha-fetoprotein (AFP). Blood routine test results, prothrombin time (PT), activated partial thromboplastin time (APTT), and international normalized ratio (INR) were normal. Blood amino acid spectrum analysis performed by tandem mass spectrometry (MS-MS) and urinary gas chromatography-mass spectrometry (GC-MS) analysis was unremarkable. Infectious causes were also investigated. Serological markers of hepatotropic viruses, rubella virus, herpes simplex virus, Epstein–Barr virus, human immunodeficiency virus, syphilis, and toxoplasma were negative, but markers for cytomegalovirus and human parvovirus B19 were positive. Notably, immunological evaluation revealed an increased serum level of immunoglobulins tested, including IgA, IgG, and IgM. Antinuclear antibody was positive in the range of 1:3,200; moreover, anti-scl-70 antibody and IgM anticardiolipin antibody were also positive (**Table 1**).

Abdominal ultrasound revealed hepatosplenomegaly and uneven distribution of echogenic dots, and multiple hyperechoic and hypoechoic masses within the liver parenchyma. The maximum size of the masses was 20 × 12 mm. Subsequent liver magnetic resonance imaging (MRI) showed multiple abnormal signal foci of the liver, suggesting possible fatty infiltration within the liver mass. In addition, echocardiography indicated patent ductus arteriosus, while high-resolution chest computed tomography (CT) showed severe pulmonary infection. A liver biopsy under ultrasonic guidance was performed at the age of 3.3 months. Light microscopy examination of the collected liver tissue showed some vacuolated hepatocytes with positive periodic-acid-Schiff (PAS) staining. In contrast, immunohistochemistry examination indicated that a diagnosis of hepatoblastoma could not be completely excluded because of the limited size of the tissue sample. Electron microscopy revealed intrahepatic cholestasis, giant hepatocytes, and extramedullary hematopoiesis. The collected hepatocytes had a reduced rough endoplasmic reticulum, a fuzzy mitochondrial structure, and lipid deposits. Niemann–Pick cells were not found in the liver. The bone marrow biopsy found no abnormal cells.

The patient was treated with supportive medical treatment, including liver protection drugs, ursodeoxycholic acid (UDCA), supplementary fat-soluble vitamins, and antibiotics. After ruling out contraindications and obtaining informed parental consent, methylprednisolone was started at a low dose (1 mg/kg per day) since the patient had presented the activation of the immune system and severe pulmonary infection at the age of 3.7 months. Subsequently, the patient's clinical symptoms gradually improved. At 4 months, the patient was clinically stable and discharged. Biochemical parameters gradually improved and returned to the standard value (**Table 1**). At the age of 6.2 months, serum immune globulin also normalized. At the age of 9 months, the serum level of antinuclear antibodies was within a normal range. After the discontinuation of methylprednisolone at 12.4 months, there were no further abnormalities in these indicators. During the 29-month follow-up period, the patient never suffered from jaundice or pneumonia. There were no abnormalities in head MRIs or the Child Development Scale Assessment. The patient was last evaluated at 32 months. The patient's height was 91.5 cm (25–50th centile) and weight was 14.8 kg (50–75th centile). Her liver was 2.0 cm below the xiphoid process but not below the right costal margin, while the spleen was 5.0 cm below the left costal margin. The patient is still under clinical follow-up.

TABLE 1 | Results of blood examinations.

Serum biochemistry (References range)	Patient 1									Patient 2
	1.8 m	3.1 m	3.6 m	4.6 m[a]	6.2 m[b]	9.0 m[b]	12.4 m[b]	25.7 m[b]	32.0 m[b]	3.5 m
White blood cell count (3.50–9.50 × 10^9/L)	5.89	7.54	9.14	NA	5.28	NA	NA	6.25	7.32	7.65
Hemoglobin (115–150 g/L)	117	117	106	NA	120	NA	NA	129	123	75
Platelet count (125–350 × 10^9/L)	225	254	279	NA	161	NA	NA	237	283	94
Alanine aminotransferase (0–40 U/L)	134	79	58	53	40	25	27	17	17	34
Aspartate aminotransferase (0–40 U/L)	382	234	113	66	41	46	43	38	35	199
Albumin (38–54 g/L)	36.2	47.7	40.1	37.9	41.3	47.4	45.8	46.5	46.7	31.6
Globulin (20–30 g/L)	NA	35.5	35.1	19.8	18.1	17.7	21.6	18.8	23.2	17.2
Total bilirubin (3.4–17.1 μmol/L)	210.3	58.3	26.6	7.0	4.5	3.7	5.1	6.0	4.9	256.1
Direct bilirubin (0–5.0 μmol/L)	151.6	18.8	22.1	5.3	2.5	1.6	1.8	2.2	2.3	117.6
Indirect bilirubin (0–13.3 μmol/L)	58.7	39.5	4.5	1.7	2.0	2.1	3.3	3.8	2.6	138.5
Alkaline phosphatase (1–281 U/L)	409	209	245	253	200	268	283	288	240	939
γ-Glutamyl transferase (6–42 U/L)	420	504	677	251	105	37	24	12	16	64
Total bile acid (0–10 μmol/L)	130.4	132.1	68.1	14.6	10.8	4.5	4.7	4.5	5.0	142.8
Total cholesterol (<5.18 mmol/L)	NA	4.38	4.46	2.86	NA	3.66	3.81	3.47	3.34	3.20
Triglycerides (0.05–1.70 mmol/L)	NA	2.87	NA	NA	NA	NA	NA	NA	NA	1.09
Blood glucose (4.11–6.05 mmol/L)	NA	2.33	4.34	NA	NA	NA	NA	6.00	5.60	6.83
Lactate (0.50–2.20 mmol/L)	NA	2.01	1.28	NA	NA	NA	NA	NA	NA	3.70
Ammonia (11–51 μmol/L)	NA	75	80	NA	NA	NA	NA	NA	NA	39
Pyruvate (20–100 μmol/L)	NA	223.4	73.1	NA	NA	NA	NA	NA	NA	NA
Alpha-fetoprotein (≤7.0 ng/ml)	NA	50,792	NA	814.7	146.9	62.55	48.31	5.91	3.92	128,575
Immunoglobulin A (≤0.34 g/L)	NA	0.54	NA	0.39	0.40	0.25	0.26	0.30	0.45	1.45
Immunoglobulin G (2.0–6.9 g/L)	NA	15.8	NA	7.9	5.0	4.6	5.3	6.3	6.3	10.1
Immunoglobulin M (0.06–0.66 g/L)	NA	8.98	NA	1.42	0.87	1.20	1.12	1.59	2.19	2.84
Antinuclear antibody (negative)	NA	1: 3,200	NA	1: 1,000	1:320	negative	negative	negative	negative	NA
Anti-scl-70 antibody (0–1.0 IU/ml)	NA	4.3	NA	0.3	<0.2	<0.2	<0.2	<0.2	<0.2	NA
IgM anticardiolipin antibody (0–20.0 CU)	NA	164.6	NA	4.8	NA	NA	NA	NA	NA	NA

m, months.

[a]*The reference range for immunoglobulin A is 0.05–0.57 g/L, for immunoglobulin G is 2.0–6.9 g/L, and for immunoglobulin M is 0.17–1.00 g/L.*

[b]*The reference range for immunoglobulin A is 0.11–1.45 g/L, for immunoglobulin G is 3.3–12.3 g/L, and for immunoglobulin M is 0.33–1.75 g/L.*

NA, not available.

Patient 2

The second patient was also a female and was delivered at term after a protected pregnancy. She was born with a low birth weight of 1,960 g and was breastfed. The patient was the first child of nonconsanguineous and healthy parents of Chinese origin. The father's sister died of acute jaundice hepatitis at the age of 9 years. The patient had developed progressive jaundice since the first day after birth. At the age of 3.2 months, the patient began to develop epistaxis and cough. However, there was no improvement in her clinical symptoms after treatment with drugs for 1 week. At the age of 3.5 months, the patient was admitted to Wuhan Children's Hospital. On physical examination, severe yellowing of the skin and sclera was noticed. In addition, edema in both lower extremities and a few scattered needle-like bleeding spots were observed. The liver was 4.0 cm below the right costal margin, while the spleen was 4.0 cm below the left costal margin.

A biochemical exam revealed elevated AST, TBIL, DBIL, IBIL, alkaline phosphatase (ALP), TBA, and AFP levels. Blood routine test results showed hemoglobin level of 75 g/L (normal range: 115–150 g/L) and platelet count of 94 × 10^9/L (normal range: 125–350 × 10^9/L). The clotting tests revealed PT of 15.9 s (normal range: 10.2–13.4 s), APTT of 63.9 s (normal range: 25.7–39.0 s), and INR of 1.34 (normal range: 0.88–1.16). Tests for infectious causes, including hepatotropic viruses, Epstein–Barr virus, human immunodeficiency virus, and syphilis were all negative, while the test for cytomegalovirus was positive. Serum levels of the tested immunoglobulins were elevated (**Table 1**). At that time, autoantibodies were not tested because the doctor did not recognize the phenomenon of immune hyperactivity.

Abdominal ultrasound showed hepatomegaly 4.1 cm below the right costal margin, splenomegaly 4.7 cm below the left costal margin, and bilateral inguinal hernia. Echogenic dots were unevenly distributed. There were multiple hyperechoic masses within the liver parenchyma, and the size of the maximum mass was 6 × 6 mm. Furthermore, no bile duct dysplasia was observed. The chest radiography revealed pulmonary infection. The head CT showed no significant abnormality.

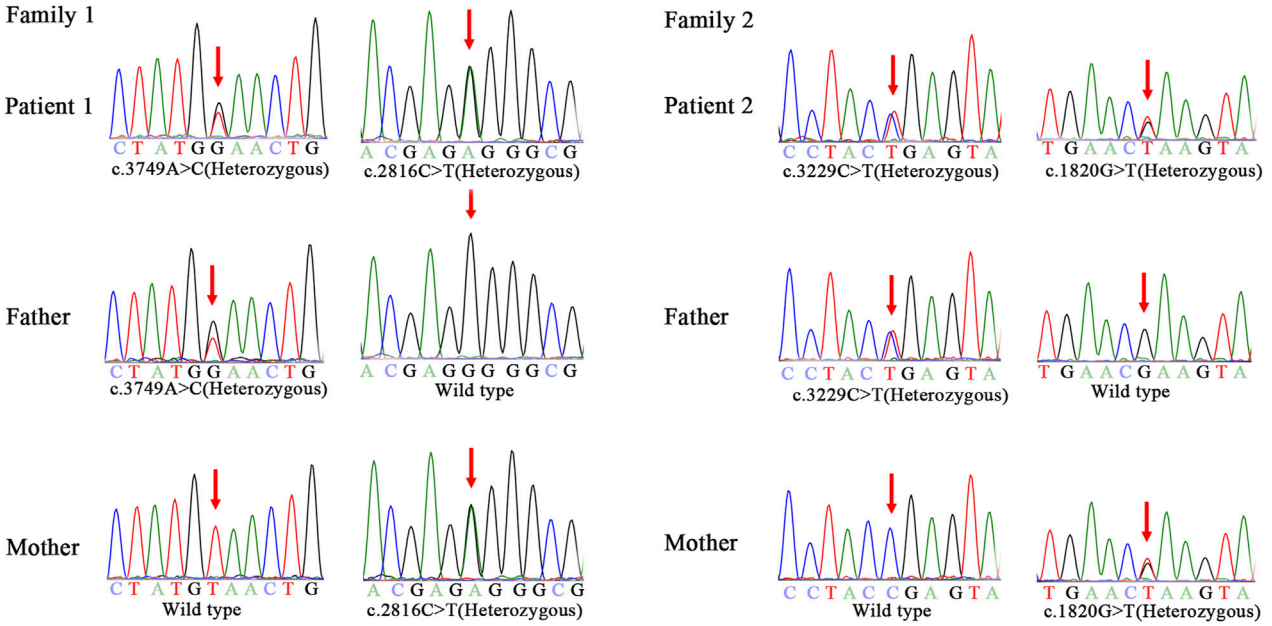

FIGURE 1 | Genotyping results on NPC1 by Sanger Sequencing analysis in the two families.

Patient 2 received antibiotics, liver protection drugs, UDCA, and supplementary fat-soluble vitamins. However, jaundice was progressive, and there was no improvement in epistaxis, cough, or edema. After 3 days of medication, her parents gave up and refused further examination and treatment. The patient was referred to Tongji Hospital at the age of 3.9 months. Physical examination showed that her previous symptoms were worsening, and she developed anuria and lethargy. Regretfully, this patient was taken home by her parents after just a genetic test, and the parents refused any other examination and treatment, including bone marrow smears or liver biopsies. A short time later, the patient died at home.

Genetic Analysis

Genomic DNA of the patients and their parents was extracted from peripheral blood samples. Library preparation, custom-designed Medical Exome capture (MES, AmCare Genomic Lab), next-generation sequencing (PE 150Illumina, Inc), data alignment (Human GRCh37/hg19 assembly), and family genetic analyses were performed by in-house pipelines, with details described in previous studies (Wang et al., 2019; Li et al., 2020). Genetic diagnosis was confirmed for these two patients suspected of having NPC, and three novel missense variants (c.2816C > T, c.3749A > C, c.1820G > T) of the NPC1 gene were identified. Patient 1 carries compound heterozygous missense

TABLE 2 | Summary of NPC1 variants reported in this study.

Patient	cDNA	Protein	Chromosome position	Domain	Inheritance	gnomAD	Polyphen-2_HDIV Polyphen-2_HVAR	SIFT	PROVEAN	GERP++	Revel	ACMG
1	c.2816C > T	p.Pro939Leu	18:21,119,414	CTD	maternal	-	Possibly damaging Benign	D	D	Conserved	D	VUS (PM2, PP3)
	c.3749A > C	p.Tyr1250Ser	18:21,113,324	C-terminal	paternal	-	Probably damaging	D	D	Conserved	D	VUS (PM2, PP3)
2	c.3229C > T	p.Arg1077*	18:21,116,653	CTD	paternal	$3.98*10^{-6}$	-	-	-	Conserved	-	LP (PVS1, PM2)
	c.1820G > T	p.Arg607Leu	18:21,125,051	MLD	maternal	-	Probably damaging	D	D	Conserved	D	VUS (PM2, PM3, PP3)

NM_000,271.5 for cDNA, and NP_000,262.2 for protein sequence. CTD, C-terminal domain; MLD, Middle luminal Domain; D, Damaging; VUS, variant of uncertain significance; LP, Likely pathogenic

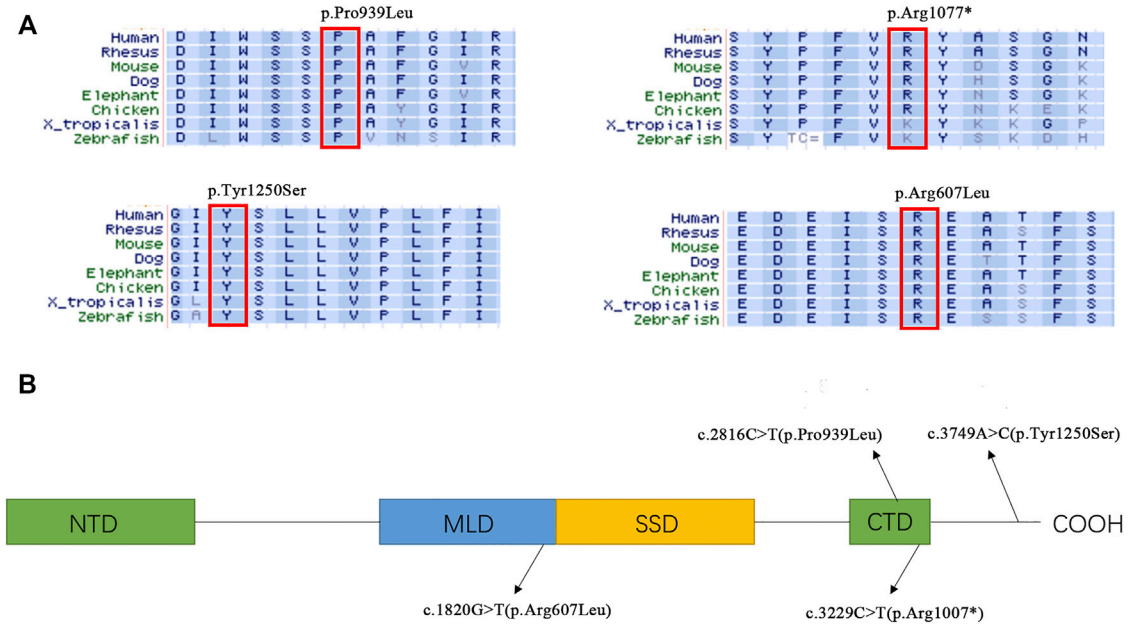

FIGURE 2 | (A) Alignment of amino acid sequences in different organism. **(B)** Distribution of the variants in different NPC1 domains NTD, N-terminal domains. MLD, Middle Lumenal Domain; SSD, Sterol sensing domain; CTD, C-terminal Domain.

variant of c.2816C > T (p.Pro939Leu) inherited from the mother and c.3749A > C (p.Tyr1250Ser) inherited from the father. In the case of patient 2, the maternal missense variant is c.1820G > T (p.Arg607Leu), and the paternal variant c.3229C > T (p.Arg1077*) is a nonsense variant (**Figure 1**). Based on the guidelines of the American College of Medical Genetics and Genomics (ACMG) for SNV interpretation (Richards et al., 2015), these three missense variants were classified as "uncertain significance" and the nonsense variant as "likely pathogenic" (**Table 2**). The alignment of amino acid sequences in different organisms highly indicates the conservation of these mutations (**Figure 2A**). The three missense variants of these two patients have not been reported in any of the previously published cases. They were predicted to be deleterious by multiple bioinformatics tools. The nonsense variant c.3229C > T (p.Arg1077*) can lead to stop-gain at exon 21 and is predicted to cause nonsense-mediated mRNA decay (NMD) (**Figure 2B**). This variant has been previously reported in two individual NPC1 cases (Liu et al., 2017).

DISCUSSION

Considering the wide range in age of onset and clinical presentations of NPC, it is a prolonged and complicated process to establish the diagnosis. Many physicians lack knowledge about the disease, so it is often missed or misdiagnosed. The presence of Niemann–Pick cells (foam cells) in bone marrow smears, spleen, or liver biopsies is one of the histological features of Niemann–Pick disease; however, these cells have not always been found (Rodrigues et al., 2006). In addition, Filipin staining in cultured skin fibroblasts is considered a key diagnostic test for NPC (Spiegel et al., 2009; Patterson et al., 2012; Mengel et al., 2013). At present, the combination of cell biology (cholestane-3β, 5α, 6β-triol, lyso-sphingomyelin isoforms, and bile acid metabolites) laboratory testing and genetic analyses is considered the first-line laboratory testing when the NPC is clinically suspected (Vanier et al., 2016; Patterson et al., 2017; Geberhiwot et al., 2018).

In this study, the two patients presented cholestatic liver disease, a typical clinical phenotype in infantile-onset Niemann–Pick disease. After excluding viral hepatitis, biliary atresia, and autoimmune hepatitis, inherited metabolic liver disease was highly suspected. However, traditional diagnostic methods failed to provide helpful information. Although liver and bone marrow biopsies of patient 1 were obtained, no significant changes were found. At that time, liver tumors could not be ruled out because of multiple liver masses and extremely high AFP levels. Therefore, next-generation DNA sequencing technologies were performed. The genetic analysis confirmed the diagnosis of NPC.

The NPC1 gene encodes NPC intracellular cholesterol transporter 1 (or Niemann–Pick C1 protein), a transmembrane protein located in the lysosome membrane. This protein interacts with NPC2 for the export of cholesterol from lysosome. Dysfunction of NPC proteins leads to the abnormal accumulation of cholesterol in lysosomes of different human tissue cells and causes Niemann–Pick syndrome with variable severity. Many studies have revealed the structure of NPC1 protein as well as the critical role of its conservative domains. The sterol-sensing domain (SSD) is the transmembrane structure of NPC1 and is the major domain for the exporting of cholesterol. The N-terminal domain (NTD) is a potential sterol-binding site for

cholesterol transferred by NPC2. The middle luminal domain (MLD) is also involved in the binding process. C-terminal domain (CTD) interacts with NTD to keep it in the proper orientation for receiving cholesterol during the export process (Cologna and Rosenhouse-Dantsker, 2019; Elghobashi-Meinhardt, 2020). Three novel variants reported in this study are located in highly conserved regions related to CTD and MLD, indicating their potential roles in maintaining the NPC1 protein function. Although the p.Pro939Leu carried by Patient 1 has not previously been reported, there are several other known pathogenic variants nearby (p.Ser940Leu, p.Asp948Asn, p.Val950Met), which indicates the importance of this region (Park et al., 2003; Skorpen et al., 2012; Abela et al., 2014; Reunert et al., 2016; Pipalia et al., 2017). The variant p.Tyr1250Ser is located downstream of CTD. There are also quite a few variants reported in this C-terminal region, such as p.Val1212Leu, p.Leu1213Phe, and p.Ser1249Gly (Yamamoto et al., 1999; Garver et al., 2010; Xiong et al., 2012), indicating that there may be a specific function of the C-terminal region. However, a further functional study is necessary to better understand the mechanism by which these variants affect the NPC1 function and/or structure.

Lysosome, a subcellular organelle responsible for digestion and recycling of different macromolecules, is necessary for many cellular processes (Ballabio and Bonifacino, 2020). Therefore, it is not surprising that LSDs can display different impairments in immune responses, such as inflammation, disrupted autophagy, and autoimmunity (Rigante et al., 2017). Nevertheless, it is uncertain whether an altered immune response directly contributes to pathogenesis in LSDs. LSDs can largely be divided into two categories, where some diseases are predisposed to immunosuppression, while others are prone to immune system hyperactivity (Castaneda et al., 2008). Gaucher disease (GD), the most common LSD, is associated with immunoglobulin abnormalities (Nguyen et al., 2020). Shoenfeld *et al.* analyzed the sera of 43 patients with GD to study the presence of autoantibodies against 14 autoantigens. The immunization of naive mice with a pool of purified anti-DNA antibodies from GD patients did not result in the induction of any experimental manifestation of systemic lupus erythematosus, suggesting that these autoantibodies were nonpathogenic (Shoenfeld et al., 1995). Also, a high incidence of autoantibodies or autoimmune disorders has been reported in patients with Fabry disease (Faggiano et al., 2006; Martinez et al., 2007; Katsumata et al., 2011). The phenomenon of neuroimmune responses in Niemann–Pick disease has been widely reported, concerning mainly inappropriate microglia activation (Ledesma et al., 2011; Pressey et al., 2012; Platt et al., 2016). Sideris *et al.* showed that Niemann–Pick disease type B could coexist with autoimmune pulmonary alveolar proteinosis in an 8-year-old girl (Sideris and Josephson, 2016). Recent studies have reported the rare association of Niemann–Pick disease type B and systemic lupus erythematosus in adult cases (Murgia et al., 2015; Baya et al., 2020). Furthermore, NPC has also been linked to inflammatory bowel disease (Jolliffe and Sarkany, 1983; Steven and Driver, 2005; Schwerd et al., 2017; Dike et al., 2019).

The clinical cases presented in this study are unique since the patients did not have any typical neurological symptoms at diagnosis but showed immune system hyperactivity in early infancy. In both patients, elevated immunoglobulins were noticed. In addition, there were multiple autoantibodies in the first patient. We excluded other possible factors that may cause immune activation. Before the immunoglobulin blood test, none of the patients were treated with any medications (*e.g.*, gamma globulin) that may have affected the immune system. The first patient's mother was examined. There were no abnormalities in her immune function or symptoms of rheumatism, which ruled out the possibility of maternal antibody transmission through the placenta. However, we do not know whether the child may develop a secondary autoimmune disease, such as systemic lupus erythematosus, in the future.

NPC has no disease-specific treatment to modify the onset of neurologic progression or prolong lifespan. The disease usually progresses to premature death. Therefore, before the onset of neurological symptoms, treatment is essentially palliative and aims at alleviating specific symptoms (Geberhiwot et al., 2018; Matencio et al., 2020). The two infants included in this study mainly presented with cholestatic liver disease, which was treated with symptomatic support. In addition, given the presence of severe pneumonia and activation of immunity in the first patient, methylprednisolone, a common immunosuppressant drug, was used, and produced a good response. It indicates that methylprednisolone effectively treated the patient's immune system irregularities. However, we do not know yet whether this treatment would be suitable for other similar cases. Indeed, the limitation of our study is that it is difficult to draw any wider conclusions regarding these findings.

In conclusion, this study reported two unique cases that presented the typical clinical features of infantile NPC and immune system hyperactivity. Genetic analysis of these patients further confirmed the diagnosis of NPC, and three novel NPC1 variants were identified by exome sequencing. Our findings suggest that recognizing immune activation in LSDs is essential, and expand both the clinical phenotype and genetic mutation spectrum of NPC1.

DATA AVAILABILITY STATEMENT

The datasets for this article are not publicly available due to concerns regarding participant/patient anonymity. Requests to access the datasets should be directed to the corresponding authors.

ETHICS STATEMENT

The studies involving human participants were reviewed and approved by Medical Ethics Committee of Tongji Hospital, Tongji Medical College, Huazhong University of Science and Technology. Written informed consent to participate in this study was provided by the participants' legal guardian/next of kin.

AUTHOR CONTRIBUTIONS

FC organized the database and drafted the manuscript. SG performed data collection. SL, XL, HX, and ZH checked the data. LW and VZ carried out the genetic analyses. YY and SS followed up the patients. SS conceptualized and designed the study, and critically reviewed the manuscript. All authors contributed to manuscript revision, and read and approved the submitted version.

ACKNOWLEDGMENTS

We thank all the research subjects for their support and cooperation.

REFERENCES

Abela, L., Plecko, B., Palla, A., Burda, P., Nuoffer, J.-M., Ballhausen, D., et al. (2014). Early Co-occurrence of a Neurologic-Psychiatric Disease Pattern in Niemann-Pick Type C Disease: a Retrospective Swiss Cohort Study. *Orphanet J. Rare Dis.* 9, 176. doi:10.1186/s13023-014-0176-7

Ballabio, A., and Bonifacino, J. S. (2020). Lysosomes as Dynamic Regulators of Cell and Organismal Homeostasis. *Nat. Rev. Mol. Cel Biol* 21, 101–118. doi:10.1038/s41580-019-0185-4

Baya, W., Fredj, F. B., Hassine, I. B., Anoun, J., Mzabi, A., Karmani, M., et al. (2020). Systemic Lupus Erythematosus, Antiphospholipid Syndrome and Hashimoto Thyroiditis Occurring in a Patient with Niemann-Pick Disease: a Second Case. *Pan Afr. Med. J.* 36, 367. doi:10.11604/pamj.2020.36.367.25116

Bjurulf, B., Spetalen, S., Erichsen, A., Vanier, M. T., Strøm, E. H., and Strømme, P. (2008). Niemann-Pick Disease Type C2 Presenting as Fatal Pulmonary Alveolar Lipoproteinosis: Morphological Findings in Lung and Nervous Tissue. *Med. Sci. Monit.* 14, CCS71–5.

Castaneda, J. A., Lim, M. J., Cooper, J. D., and Pearce, D. A. (2008). Immune System Irregularities in Lysosomal Storage Disorders. *Acta Neuropathol.* 115, 159–174. doi:10.1007/s00401-007-0296-4

Chu, T.-T., Tu, X., Yang, K., Wu, J., Repa, J. J., and Yan, N. (2021). Tonic Prime-Boost of STING Signalling Mediates Niemann-Pick Disease Type C. *Nature* 596, 570–575. doi:10.1038/s41586-021-03762-2

Cologna, S. M., and Rosenhouse-Dantsker, A. (2019). Insights into the Molecular Mechanisms of Cholesterol Binding to the NPC1 and NPC2 Proteins. *Adv. Exp. Med. Biol.* 1135, 139–160. doi:10.1007/978-3-030-14265-0_8

Davidson, A., and Diamond, B. (2001). Autoimmune Diseases. *N. Engl. J. Med.* 345, 340–350. doi:10.1056/nejm200108023450506

Dike, C. R., Bernat, J., Bishop, W., and Degeeter, C. (2019). Niemann-Pick Disease Type C Presenting as Very Early Onset Inflammatory Bowel Disease. *BMJ Case Rep.* 12, e229780. doi:10.1136/bcr-2019-229780

Dimitriou, E., Paschali, E., Kanariou, M., and Michelakakis, H. (2019). Prevalence of Antibodies to Ganglioside and Hep 2 in Gaucher, Niemann - Pick Type C and Sanfilippo Diseases. *Mol. Genet. Metab. Rep.* 20, 100477. doi:10.1016/j.ymgmr.2019.100477

Elghobashi-Meinhardt, N. (2020). Cholesterol Transport in Wild-type NPC1 and P691S: Molecular Dynamics Simulations Reveal Changes in Dynamical Behavior. *Ijms* 21, 2962. doi:10.3390/ijms21082962

Faggiano, A., Pisani, A., Milone, F., Gaccione, M., Filippella, M., Santoro, A., et al. (2006). Endocrine Dysfunction in Patients with Fabry Disease. *J. Clin. Endocrinol. Metab.* 91, 4319–4325. doi:10.1210/jc.2006-0858

Garver, W. S., Jelinek, D., Meaney, F. J., Flynn, J., Pettit, K. M., Shepherd, G., et al. (2010). The National Niemann-Pick Type C1 Disease Database: Correlation of Lipid Profiles, Mutations, and Biochemical Phenotypes. *J. Lipid Res.* 51, 406–415. doi:10.1194/jlr.P000331

Geberhiwot, T., Moro, A., Moro, A., Dardis, A., Ramaswami, U., Sirrs, S., et al. (2018). Consensus Clinical Management Guidelines for Niemann-Pick Disease Type C. *Orphanet J. Rare Dis.* 13, 50. doi:10.1186/s13023-018-0785-7

Griese, M., Brasch, F., Aldana, V., Cabrera, M., Goelnitz, U., Ikonen, E., et al. (2010). Respiratory Disease in Niemann-Pick Type C2 Is Caused by Pulmonary Alveolar Proteinosis. *Clin. Genet.* 77, 119–130. doi:10.1111/j.1399-0004.2009.01325.x

Jolliffe, D. S., and Sarkany, I. (1983). Niemann-Pick Type III and Crohn's Disease. *J. R. Soc. Med.* 76, 307–308. doi:10.1177/014107688307600414

Katsumata, N., Ishiguro, A., and Watanabe, H. (2011). Fabry Disease Superimposed on Overt Autoimmune Hypothyroidism. *Clin. Pediatr. Endocrinol.* 20, 95–98. doi:10.1297/cpe.20.95

Ledesma, M. D., Prinetti, A., Sonnino, S., and Schuchman, E. H. (2011). Brain Pathology in Niemann Pick Disease Type A: Insights from the Acid Sphingomyelinase Knockout Mice. *J. Neurochem.* 116, 779–788. doi:10.1111/j.1471-4159.2010.07034.x

Li, Y.-T., Chen, J.-S., Jian, W., He, Y.-D., Li, N., Xie, Y.-N., et al. (2020). L1CAM Mutations in Three Fetuses Diagnosed by Medical Exome Sequencing. *Taiwanese J. Obstet. Gynecol.* 59, 451–455. doi:10.1016/j.tjog.2020.03.022

Liu, R., Zou, Y., Hong, J., Cao, M., Cui, B., Zhang, H., et al. (2017). Rare Loss-Of-Function Variants in NPC1 Predispose to Human Obesity. *Diabetes* 66, 935–947. doi:10.2337/db16-0877

Martinez, P., Aggio, M., and Rozenfeld, P. (2007). High Incidence of Autoantibodies in Fabry Disease Patients. *J. Inherit. Metab. Dis.* 30, 365–369. doi:10.1007/s10545-007-0513-2

Matencio, A., Navarro-Orcajada, S., González-Ramón, A., García-Carmona, F., and López-Nicolás, J. M. (2020). Recent Advances in the Treatment of Niemann Pick Disease Type C: A Mini-Review. *Int. J. Pharmaceutics* 584, 119440. doi:10.1016/j.ijpharm.2020.119440

Mengel, E., Klünemann, H.-H., Lourenço, C. M., Hendriksz, C. J., Sedel, F., Walterfang, M., et al. (2013). Niemann-Pick Disease Type C Symptomatology: an Expert-Based Clinical Description. *Orphanet J. Rare Dis.* 8, 166. doi:10.1186/1750-1172-8-166

Murgia, G., Firinu, D., Meleddu, R., Lorrai, M. M., Manconi, P. E., and Del Giacco, S. R. (2015). Systemic Lupus Erythematosus Occurring in a Patient with Niemann-Pick Type B Disease. *Lupus* 24, 1332–1334. doi:10.1177/0961203315585818

Nguyen, Y., Stirnemann, J., Lautredoux, F., Cador, B., Bengherbia, M., Yousfi, K., et al. (2020). Immunoglobulin Abnormalities in Gaucher Disease: an Analysis of 278 Patients Included in the French Gaucher Disease Registry. *Ijms* 21, 1247. doi:10.3390/ijms21041247

Park, W. D., O'brien, J. F., Lundquist, P. A., Kraft, D. L., Vockley, C. W., Karnes, P. S., et al. (2003). Identification of 58 Novel Mutations in Niemann-Pick Disease Type C: Correlation with Biochemical Phenotype and Importance ofPTC1-like Domains inNPC1. *Hum. Mutat.* 22, 313–325. doi:10.1002/humu.10255

Patterson, M. C., Clayton, P., Gissen, P., Anheim, M., Bauer, P., Bonnot, O., et al. (2017). Recommendations for the Detection and Diagnosis of Niemann-Pick Disease Type C. *Neurol. Clin. Pract.* 7, 499–511. doi:10.1212/cpj.0000000000000399

Patterson, M. C., Hendriksz, C. J., Walterfang, M., Sedel, F., Vanier, M. T., and Wijburg, F. (2012). Recommendations for the Diagnosis and Management of Niemann-Pick Disease Type C: an Update. *Mol. Genet. Metab.* 106, 330–344. doi:10.1016/j.ymgme.2012.03.012

Pipalia, N. H., Subramanian, K., Mao, S., Ralph, H., Hutt, D. M., Scott, S. M., et al. (2017). Histone Deacetylase Inhibitors Correct the Cholesterol Storage Defect in Most Niemann-Pick C1 Mutant Cells. *J. Lipid Res.* 58, 695–708. doi:10.1194/jlr.M072140

Platt, F. M., d'Azzo, A., Davidson, B. L., Neufeld, E. F., and Tifft, C. J. (2018). Lysosomal Storage Diseases. *Nat. Rev. Dis. Primers* 4, 27. doi:10.1038/s41572-018-0025-4

Platt, N., Speak, A. O., Colaco, A., Gray, J., Smith, D. A., Williams, I. M., et al. (2016). Immune Dysfunction in Niemann-Pick Disease Type C. *J. Neurochem.* 136 (136 Suppl. l), 74–80. doi:10.1111/jnc.13138

Pressey, S. N. R., Smith, D. A., Wong, A. M. S., Platt, F. M., and Cooper, J. D. (2012). Early Glial Activation, Synaptic Changes and Axonal Pathology in the Thalamocortical System of Niemann-Pick Type C1 Mice. *Neurobiol. Dis.* 45, 1086–1100. doi:10.1016/j.nbd.2011.12.027

Reunert, J., Fobker, M., Kannenberg, F., Du Chesne, I., Plate, M., Wellhausen, J., et al. (2016). Rapid Diagnosis of 83 Patients with Niemann Pick Type C Disease and Related Cholesterol Transport Disorders by Cholestantriol Screening. *EBioMedicine* 4, 170–175. doi:10.1016/j.ebiom.2015.12.018

Richards, S., Aziz, N., Bale, S., Bick, D., Das, S., Gastier-Foster, J., et al. (2015). Standards and Guidelines for the Interpretation of Sequence Variants: a Joint Consensus Recommendation of the American College of Medical Genetics and Genomics and the Association for Molecular Pathology. *Genet. Med.* 17, 405–424. doi:10.1038/gim.2015.30

Rigante, D., Cipolla, C., Basile, U., Gulli, F., and Savastano, M. C. (2017). Overview of Immune Abnormalities in Lysosomal Storage Disorders. *Immunol. Lett.* 188, 79–85. doi:10.1016/j.imlet.2017.07.004

Rodrigues, A. F., Gray, R. G., Preece, M. A., Brown, R., Hill, F. G., Baumann, U., et al. (2006). The Usefulness of Bone Marrow Aspiration in the Diagnosis of Niemann-Pick Disease Type C in Infantile Liver Disease. *Arch. Dis. Child.* 91, 841–844. doi:10.1136/adc.2005.088013

Schwerd, T., Pandey, S., Yang, H.-T., Bagola, K., Jameson, E., Jung, J., et al. (2017). Impaired Antibacterial Autophagy Links Granulomatous Intestinal Inflammation in Niemann-Pick Disease Type C1 and XIAP Deficiency with NOD2 Variants in Crohn's Disease. *Gut* 66, 1060–1073. doi:10.1136/gutjnl-2015-310382

Shoenfeld, Y., Beresovski, A., Zharhary, D., Tomer, Y., Swissa, M., Sela, E., et al. (1995). Natural Autoantibodies in Sera of Patients with Gaucher's Disease. *J. Clin. Immunol.* 15, 363–372. doi:10.1007/bf01541326

Sideris, G. A., and Josephson, M. (2016). Pulmonary Alveolar Proteinosis and Niemann Pick Disease Type B: An Unexpected Combination. *Respir. Med. Case Rep.* 19, 37–39. doi:10.1016/j.rmcr.2016.06.009

Skorpen, J., Helland, I. B., and Tennøe, B. (2012). Use of Miglustat in a Child with Late-Infantile-Onset Niemann-Pick Disease Type C and Frequent Seizures: a Case Report. *J. Med. Case Rep.* 6, 383. doi:10.1186/1752-1947-6-383

Spiegel, R., Raas-Rothschild, A., Reish, O., Regev, M., Meiner, V., Bargal, R., et al. (2009). The Clinical Spectrum of Fetal Niemann-Pick Type C. *Am. J. Med. Genet.* 149A, 446–450. doi:10.1002/ajmg.a.32642

Steven, L., and Driver, C. (2005). Niemann-pick Disease Type C and Crohn's Disease. *Scott Med. J.* 50, 80–81. doi:10.1177/003693300505000213

Surmeli-Onay, O., Yakarisik, S., Korkmaz, A., Akcoren, Z., Yuce, A., Runz, H., et al. (2013). Prenatal-onset Niemann-Pick Type C Disease with Nonimmune Hydrops Fetalis. *Pediatr. Neonatal.* 54, 344–347. doi:10.1016/j.pedneo.2013.01.015

Vanier, M. T., Gissen, P., Bauer, P., Coll, M. J., Burlina, A., Hendriksz, C. J., et al. (2016). Diagnostic Tests for Niemann-Pick Disease Type C (NP-C): A Critical Review. *Mol. Genet. Metab.* 118, 244–254. doi:10.1016/j.ymgme.2016.06.004

Vanier, M. T. (2010). Niemann-Pick Disease Type C. *Orphanet J. Rare Dis.* 5, 16. doi:10.1186/1750-1172-5-16

Vanier, M. T. (2013). Niemann-Pick Diseases. *Handb Clin. Neurol.* 113, 1717–1721. doi:10.1016/b978-0-444-59565-2.00041-1

Vanier, M. T., Wenger, D. A., Comly, M. E., Rousson, R., Brady, R. O., and Pentchev, P. G. (1988). Niemann-Pick Disease Group C: Clinical Variability and Diagnosis Based on Defective Cholesterol Esterification: A Collaborative Study on 70 Patients. *Clin. Genet.* 33, 331–348. doi:10.1111/j.1399-0004.1988.tb03460.x

Wang, Z., Lin, J., Qiao, K., Cai, S., Zhang, V. W., Zhao, C., et al. (2019). Novel Mutations in HINT1 Gene Cause the Autosomal Recessive Axonal Neuropathy with Neuromyotonia. *Eur. J. Med. Genet.* 62, 190–194. doi:10.1016/j.ejmg.2018.07.009

Xiao, Z. X., Miller, J. S., and Zheng, S. G. (2021). An Updated advance of Autoantibodies in Autoimmune Diseases. *Autoimmun. Rev.* 20, 102743. doi:10.1016/j.autrev.2020.102743

Xiong, H., Higaki, K., Wei, C.-j., Bao, X.-H., Zhang, Y.-H., Fu, N., et al. (2012). Genotype/phenotype of 6 Chinese Cases with Niemann-Pick Disease Type C. *Gene* 498, 332–335. doi:10.1016/j.gene.2012.01.026

Yamamoto, T., Nanba, E., Ninomiya, H., Higaki, K., Taniguchi, M., Zhang, H., et al. (1999). NPC1 Gene Mutations in Japanese Patients with Niemann-Pick Disease Type C. *Hum. Genet.* 105, 10–16. doi:10.1007/s004399900059

Conflict of Interest: Authors LW and VWZ are employed by AmCare Genomics Lab.

The remaining authors declare that the research was conducted in the absence of any commercial or financial relationships that could be construed as a potential conflict of interest.

Publisher's Note: All claims expressed in this article are solely those of the authors and do not necessarily represent those of their affiliated organizations, or those of the publisher, the editors and the reviewers. Any product that may be evaluated in this article, or claim that may be made by its manufacturer, is not guaranteed or endorsed by the publisher.

frontiers in Genetics

ORIGINAL RESEARCH
published: 14 March 2022
doi: 10.3389/fgene.2022.823687

Newborn Screening for Mitochondrial Carnitine-Acylcarnitine Cycle Disorders in Zhejiang Province, China

Duo Zhou[1], Yi Cheng[1], Xiaoshan Yin[2], Haixia Miao[1], Zhenzhen Hu[1], Jianbin Yang[1], Yu Zhang[3], Benqing Wu[4] and Xinwen Huang[1]**

[1]Department of Genetics and Metabolism, Children's Hospital, Zhejiang University School of Medicine, National Clinical Research Center for Child Health, National Regional Medical Center for Children, Hangzhou, China, [2]School of Health in Social Science, The University of Edinburg, Edinburg, United Kingdom, [3]Zhejiang Bosheng Biotechnology Co, Ltd, Hangzhou, China, [4]Children's Medical Center, University of Chinese Academy of Science - Shenzhen Hospital, Shenzhen, China

Background: Disorders of mitochondrial carnitine–acylcarnitine cycle is a heterogeneous group of hereditary diseases of mitochondrial β-oxidation of fatty acids tested in NBS program in Zhejiang province, China. Large-scale studies reporting disorders of mitochondrial carnitine–acylcarnitine cycle among Chinese population in NBS are limited. The aim of this study was to explain the incidence and biochemical, clinical, and genetic characteristics of disorders of mitochondrial carnitine–acylcarnitine cycle in NBS.

Methods: From January 2009 to June 2021, 4,070,375 newborns were screened by tandem mass spectrometry. Newborns with elevated C0 levels and/or C0/(C16 + C18) ratios were identified as having CPT1D, whereas those with decreased C0 levels and/or C0/(C16 + C18) ratios and/or elevated C12-C18:1 level were identified as having CPT2D or CACTD. Suspected positive patients were further subjected to genetic analysis. All confirmed patients received biochemical and nutritional treatment, as well as follow-up sessions.

Results: Overall, 20 patients (12 with CPT1D, 4 with CPT2D, and 4 with CACTD) with disorders of mitochondrial carnitine–acylcarnitine cycle were diagnosed by NBS. The overall incidence of these disorders was one in 203,518 newborns. In toal, 11 patients with CPT1D exhibited increased C0 levels and C0/(C16 + C18) ratios. In all patients of CPT2D, all long chain acyl-carnitines levels were elevated except for case 14 having normal C12 levels. In all patients with CACTD, all long chain acyl-carnitines levels were elevated except for case 17 having normal C12, C18, and C18:1 levels. Most patients with CPT1D were asymptomatic. Overall, two of 4 patients with CPT2D did not present any clinical symptom, but other two patients died. In 4 cases with CACTD, the disease was onset after birth, and

OPEN ACCESS

Edited by:
Yang Sun,
Stanford University, United States

Reviewed by:
Ke Ning,
Stanford University, United States
Rui Lu,
Stanford University, United States

***Correspondence:**
Benqing Wu
wubenqing783@126.com
Xinwen Huang
6305022@zju.edu.cn

Specialty section:
This article was submitted to Genetics of Common and Rare Diseases, a section of the journal Frontiers in Genetics

Received: 28 November 2021
Accepted: 20 January 2022
Published: 14 March 2022

Citation:
Zhou D, Cheng Y, Yin X, Miao H, Hu Z, Yang J, Zhang Y, Wu B and Huang X (2022) Newborn Screening for Mitochondrial Carnitine-Acylcarnitine Cycle Disorders in Zhejiang Province, China. Front. Genet. 13:823687. doi: 10.3389/fgene.2022.823687

Abbreviations: CPT1, carnitine palmitoyltransferase 1; CPT2, carnitine palmitoyltransferase 2; CACT, carnitine-acylcarnitine translocase; CPT1D, carnitine palmitoyltransferase 1 deficiency; CPT2D, carnitine palmitoyltransferase 2 deficiency; CACTD, carnitine-acylcarnitine translocase deficiency; NBS, newborn screening; C0, free carnitine; C2, Acetylcarnitine; C3, Propionylcarnitine; C4, Butyrylcarnitine; C12, Lauroylcarnitine; C14, Myristoylcarnitine; C16, Palmitoylcarnitine; C16:1, Palmitoylcarnitine; C18, Octadecanoylcarnitine; C18:1, Oleylcarnitine; MS/MS, tandem mass spectrometry; DBS, dried blood spot; NGS, next-generation sequencing; PCR, Polymerase chain reaction-restriction.

75% patients died. In total, 14 distinct mutations were identified in CPT1A gene, of which 11 were novel and c.1910C > A (p.S637T), c.740C > T (p.P247L), and c.1328T > C (p.L443P) were the most common mutations. Overall, 3 novel mutations were identified in CPT2 gene, and the most frequent mutation was c.1711C > A (p.P571T). The most common variant in SLC25A20 gene was c.199-10T > G.

Conclusion: Disorders of mitochondrial carnitine–acylcarnitine cycle can be detected by NBS, and the combined incidence of these disorders in newborns was rare in Zhejiang province, China. Most patients presented typical acylcarnitine profiles. Most patients with CPT1D presented normal growth and development, whereas those with CPT2D/CACTD exhibited a high mortality rate. Several novel CPT1A and CPT2 variants were identified, which expanded the variant spectrum.

Keywords: mitochondrial carnitine-acylcarnitine cycle disorders, carnitine palmitoyl transferase 2 deficiency, carnitine palmitoyltransferase 2 deficiency, carnitine-acylcarnitine translocase deficiency, newborn screening

INTRODUCTION

Carnitine cycle is essential for transporting long-chain fatty acids into the mitochondrial matrix for β-oxidation (Watkins et al., 2007). Mitochondrial carnitine–acylcarnitine cycle is an important component of carnitine cycle, which consists of carnitine palmitoyl-transferases 1 (CPT1), carnitine palmitoyl-transferases 2 (CPT2), and the transporter protein carnitine-acylcarnitine translocase (CACT), which can uptake fatty acyl-CoAs across the mitochondrial membrane (Lodhi and Semenkovich, 2014). First, CPT1 located on the outer mitochondrial membrane converts the long-chain acyl-CoAs to their acylcarnitine equivalents. Further, acyl-carnitines are transported into the mitochondrial matrix by CACT. In the end, acyl-carnitine is converted back to the acyl-CoA species and carnitine by CPT2 associated with the inner mitochondrial membrane (McGarry and Brown, 1997). CPT1 deficiency (CPT1D), CPT2 deficiency (CPT2D), and CACT deficiency (CACTD) are rare autosomal inherited recessive disorders, and the causative genes are CPT1A, CPT2, and SLC25A20, respectively (Wieser et al., 2003; Collins et al., 2010; Indiveri et al., 2011). Differences in the age of onset and clinical manifestations were observed in these disorders (Houten and Wanders, 2010). Late onset forms may present muscular symptoms such as myalgia, myoglobinuria, and muscle weakness during adolescence or adulthood. The condition can be triggered by fasting, illnesses, or high energy demand resulting in hypoketotic hypoglycaemia, hepatomegaly, cardiomyopathy, liver dysfunction, seizures, and sudden death at an early age. Disorders of mitochondrial carnitine–acylcarnitine cycle present different mortality and morbidity rates. In particular, CACTD was characterised with high mortality (Baruteau et al., 2014; Houten et al., 2016). Early detection and medical interventions can prevent individuals from metabolic decompensation and improve prognosis (Maguolo et al., 2020).

Infants with these diseases presented characteristic acylcarnitine profile are detectable by using tandem mass spectrometry (MS/MS), which has been widely implemented in NBS. With the application of MS/MS, the diagnosis of these disorders through newborn screening has become easier (Wilcken et al., 2003). The combined incidence of disorders of mitochondrial carnitine–acylcarnitine cycle was thought to be rare, which is estimated to be 1:186,833 in mainland China, 1: 250,000 to 1:666,6671 in Australia, Germany, and <1:189,136 in the United States (Lindner et al., 2010; Deng et al., 2020). Disorders of mitochondrial carnitine–acylcarnitine cycle have great phenotypic variability and molecular heterogeneity. Herein, we present our over 12-years experience of NBS for the diagnosis and treatment of disorders of mitochondrial carnitine–acylcarnitine cycle in Zhejiang Province, China. The aim of this study was to determine the incidence and biochemical, clinical, and genetic characteristics of these disorders by NBS. With this study, the awareness about these rare disorders can be improved, and further implications of treatment can be considered.

MATERIALS AND METHODS

Study Population

From January 2009 to June 2021, 4,070,375 newborns were screened by MS/MS at Children's Hospital, Zhejiang University School of Medicine. Among 4,070,375 participants who were recruited in this study, 3,784,837 were normal-term infants, 276,482 were premature infants, and 9,056 were post-term infants. The ratio of male to female was 1.1:1. The Ethical Committee of Children's Hospital, Zhejiang University School of Medicine approved this research. The information sheet with consent information containing the explanation on the aim of this study was sent to participants and their parents and was signed by participants' parents.

NBS for Disorders of Mitochondrial Carnitine–Acylcarnitine Cycle

Dried blood spot (DBS) samples were randomly collected between 3 and 7 days after birth and delivered through cold-chain transportation to the NBS centre of Children's Hospital,

Zhejiang University School of Medicine within 3 days. Acylcarnitine profiles were assessed at our centre using NeoBase™ MS/MS reagent kits (PekinElmer, United States) according to the manufacturers' protocol. Newborns with elevated C0 levels and/or C0/(C16 + C18) ratios were identified to have CPT1D. Newborns with decreased C0 levels and/or C0/(C16 + C18) ratios and/or elevated C12-C18:1 level were identified to have CPT2D or CACTD. Newborns were subjected to further confirmatory tests if the initial screening value exceeded the diagnostic cut-off. Newborns were subjected to a repeated test if the initial screening value was equal to or exceeding the screening cut-off. If the second screening results were still positive, confirmatory detection tests were performed, including biochemical laboratory tests and genetic analysis.

Genetic Testing

Genomic DNA was extracted from patients. Genetic testing was performed by Genetic Diagnostic Laboratory at Children's Hospital, Zhejiang University School of Medicine (Hangzhou, Zhejiang, China). The target next-generation sequencing (NGS) was used on the probands with a target sequencing panel covering 306 known genes associated with inherited metabolic disorders. All potentially pathogenic mutations identified by NGS were further confirmed via Sanger sequencing. PolyPhen-2, PROVEAN, and Mutation Taster were used to predict the pathogenicity of the missense variants. The Structure stability analysis of novel missense variants were performed by Chimera version 1.15. The protein PDB number was entered in the Chimera software, and the three-level structure of protein was obtained. We selected the amino acid sequence and optimised the structure to find out whether the mutant amino acid triggers the atoms clash and contact. The three-dimensional structure of the protein was constructed after mutation, and the effect of mutation on protein stability was analysed.

Diagnosis and Follow-Up

Diagnosis was assessed by metabolic disease specialists based on the patients' free carnitine and acylcarnitine levels, genetic variations, as well as additional clinical symptoms. All confirmed patients were followed up in our hospital. Dietary guidance including more frequent feeding, avoiding fasting, limiting fat intake, and appropriate supplementation of L-carnitine were applied for the confirmed patients. The follow-up time was once every 3–6 months if the confirmed patients presented stable performances. Patients were regarded as lost to follow-up if the follow-up time exceeded over 3 months and the patient still did not return to the clinical centre. The monitoring items included physical and biochemical examinations; levels of free carnitine and acylcarnitine, blood glucose, lactic acid, and blood ammonia; and blood routine test.

RESULTS

Incidences Determined From NBS

In this study, 4,070,375 newborns were screened and 20 patients (12 with CPT1D, 4 with CPT2D, and 4 with CACTD) were identified, with a total incidence of one in 203,518 live births. The incidence of CPT1D, CPT2D, and CACTD was 1:339,197, 1:1,017,593, 1:1,017,593, respectively. Among all the disorders of mitochondrial carnitine–acylcarnitine cycle, CPT1D was the most prevalent. There were two pairs of monozygotic twins among patients with CPT1D.

Initial Screening Results of Acylcarnitine Levels

Overall, 11 patients (91.7%) with CPT1D had increased C0 levels and C0/(C16 + C18) ratios. C0 levels and C0/(C16 + C18) ratios of case 12 were normal in initial screening accompanied with lower C12-C18:1 level. In these patients, the average C0 level was 125.1 ± 61.68 μmol/L (range: 14.84–240.28 μmol/L) and C0/(C16 + C18) was 206.3 ± 278.5 (range: 25.59–1,007.27).

Overall, two of 4 patients with CPT2D had low C0 levels, and those of other two patients were normal. All long chain acyl-carnitines levels were elevated except in case 14 with normal C12 levels. The C14, C16, C16:1, C18, and C18:1 levels were 1.59 ± 0.25, 19.36 ± 2.33, 1.69 ± 0.18, 4.28 ± 0.74, and 6.67 ± 0.89 μmol/L, respectively. The ratios of long-chain acyl-carnitines to C0 were decreased and those to C2 and C3 were increased in all cases (C16 + C18:1)/C2, C14/C3, C16/C3, C16:1/C3, C18/C3, C18:1/C3, (C16 + C18:1)/C3, and C0/(C16 + C18) were, 3.6 ± 2.7, 8.2 ± 2.55, 89.36 ± 53.08, 8.39 ± 5.25, 23.89 ± 14.61, 33.41 ± 21.43, 122.8 ± 73.72, and 0.51 ± 0.29, respectively.

In total, three patients with CACTD had decreased C0 levels. ALL C0/(C16+C18) ratios were decreased. All long-chain acyl-carnitines levels were elevated except in case 17 with normal C12, C18, and C18:1 levels. The C14, C16, and C16:1 levels were 1.33 ± 0.54, 18.97 ± 8.5, and 1.5 ± 0.7 μmol/L, respectively. All the ratios of long-chain acyl-carnitines to C2 and C3 were increased except in case 17 with normal C18/C3 level. The (C16 + C18:1)/C2, C14/C3, C16/C3, C16:1/C3, C18/C3, C18:1/C3, (C16 + C18:1)/C3, and C0/(C16 + C18) were 2.84 ± 1.71, 1.43 ± 0.45, 20,52 ± 7.99, 1.63 ± 0.51, 3.57 ± 1.72, 6.42 ± 4.09, 26.9 ± 11.33, and 0.38 ± 0.13, respectively.

C14/C3, C16/C3, C16:1/C3, C18/C3, C18:1/C3, and (C16 + C18:1)/C3 ratios were higher in patients with CPT2D when compared with those with CACTD. The differences were statistically significant (p = 0.038, 0.042, 0.042, 0.032, 0.048, and 0.042, respectively) (**Table 1**).

Initial Clinical Manifestations

The follow-up period of these patients lasted from 7 days to 4 years. Among 12 patients with CPT1D, 10 patients were asymptomatic. Case 2 presented clinical symptoms after birth, including hyperammonaemia and metabolic acidosis and passed away at 18 days-point. Follow-up data of case 1 were not available.

Patients 13 to 16 were identified as having CPT2D. Patient 13 died suddenly at 8 months at home with no available data. Patient 14 presented with poor feeding, poor response, and hypoglycaemia. Her condition deteriorated rapidly, and she died at 10 days after birth. No clinical symptoms were found in patients 15 and 16; however, patient 15 had incomplete right

TABLE 1 | Initial screening results of acylcarnitine levels in Mitochondrial Carnitine-Acylcarnitine Cycle Disorders.

Acylcarnitine index	**C0**	**C2**	**C3**	**C12**	**C14**	**C16**	**C16: 1**	**C18**	**C18: 1**	**C0/(C16 + C18)**	—	—	—	—	—	—	—
CPT1D	—	—	—	—	—	—	—	—	—	—	—	—	—	—	—	—	—
1	119.08	11.01	0.89	0.03	0.03	0.29	0.02	0.16	0.16	237.33	—	—	—	—	—	—	—
2	110.8	13.1	1.28	0.03	0.01	0.07	0.01	0.04	0.03	1,007.27	—	—	—	—	—	—	—
3	156	37.83	2.01	0.05	0.08	0.86	0.06	0.27	0.3	138.01	—	—	—	—	—	—	—
4	66.9	23.3	1.19	0.06	0.09	0.32	0.04	0.18	0.64	133.8	—	—	—	—	—	—	—
5	117.45	35.71	1.86	0.08	0.11	0.37	0.05	0.17	0.55	217.5	—	—	—	—	—	—	—
6	165.49	36.16	2.3	0.14	0.15	0.76	0.09	0.19	0.2	174.2	—	—	—	—	—	—	—
7	240.28	33.83	3.21	0.08	0.08	0.59	0.05	0.17	0.25	316.16	—	—	—	—	—	—	—
8	131.13	15.47	2.41	0.01	0.02	0.11	0.01	0.1	0.05	624.43	—	—	—	—	—	—	—
9	199.04	28.7	2.42	0.06	0.09	0.79	0.05	0.23	0.25	195.14	—	—	—	—	—	—	—
10	172.35	23.03	0.83	0.02	0.03	0.2	0.01	0.12	0.06	538.59	—	—	—	—	—	—	—
11	72.46	31.68	3.66	0.05	0.09	0.37	0.04	0.15	0.56	139.35	—	—	—	—	—	—	—
12	14.84	4.67	0.46	0.01	0.03	0.4	0.02	0.18	0.27	25.59	—	—	—	—	—	—	—
Acylcarnitine index	C0	C2	C3	C12	C14	C16	C16: 1	C18	C18: 1	C0/(C16 + C18)	(C16 + C18: 1)/C2	C14/ C3	C16/ C3	C16: 1/C3	C18/ C3	C18: 1/C3	(C16 + C18: 1)/C3
CPT2D																	
13	25.34	23.83	0.19	0.72	1.85	17.87	1.63	5.92	7.78	0.91	1.08	9.74	94.05	8.58	31.16	40.95	135
14	5.86	11.47	1.68	0.23	1.24	22.31	1.54	4.24	5.9	0.22	2.46	0.74	13.28	0.92	2.52	3.51	16.79
15	12.41	3.27	0.13	0.59	1.61	17.15	1.63	4.54	7.02	0.57	7.39	12.38	131.92	12.54	34.92	54.00	185.92
16	9.25	7.33	0.17	0.47	1.69	20.09	1.96	4.58	5.98	0.37	3.56	9.94	118.18	11.53	26.94	35.18	153.35
CACTD																	
17	5.56	11.11	0.95	0.18	0.73	8.8	0.9	1.07	2.01	0.56	0.97	0.77	9.26	0.95	1.13	2.12	11.38
18	7.24	7.96	0.63	0.89	1.08	15.23	1	3.07	7.43	0.4	2.85	1.71	24.17	1.59	4.87	11.79	35.97
19	6.86	6	0.88	0.4	1.52	24.36	1.9	4.12	6.15	0.24	5.09	1.73	27.68	2.16	4.68	6.99	34.67
20	10.29	12.83	1.31	0.65	1.99	27.49	2.39	4.73	6.27	0.32	2.63	1.52	20.98	1.82	3.61	4.79	25.77

Cutoff value: C0 10.28–54.24 μmol/L; C2 3–50 μmol/L; C3 0.43–3.8 μmol/L C12 0.03–0.28 μmol/L; C12:1 0.01–0.23 μmol/L; C14 0.07–0.40 μmol/L; C14:1 0.03–0.26 μmol/L; C16 0.49–6.00 μmol/L; C16:1 0.02–0.49 μmol/L; C18 0.24–1.90 μmol/L; C18:1 0.38–2.92 μmol/L; C0/(C16 + C18) 2.76–35.1 (C16 + C18:1)/C2 0.11–0.54; C14/C3; C16/C3 0.35–4.92; C16:1/C3 0.01–0.34; C18/C3 0.6–1.69 (C16 + C18:1)/C3 0.71–7.21.

bundle branch block in ECG, and patient 16 presented transient increase in alanine aminotransferase (ALT; 102 U/L) level.

Patients 17 to 20 were identified to have CACTD. All the patients had disease onset after birth. They presented feeding dysfunction, poor response, hypoglycaemia [1.9–3.2 mmol/L (normal range 3.6–6.1 mmol/L)], acidosis [1.8–17 mmol/L (normal range 0.5–1.6 mmol/L)], and hyperammonaemia [52–226 μmol/L (normal range 9–30 μmol/L)]. After diet management, L-carnitine supplementation, and acidosis correction, the clinical presentations and biochemical results of case 17 became normal, and the data were good after 15-months follow-up. case 18 developed hepatic impairment, hepatomegaly, and cardiac hypertrophy; further, the parents stopped the treatment, and the infant died at the age of 2 months. The condition of cases 19 and 20 deteriorated rapidly, and they died at 7 days after birth (**Table 2**).

Genetic Findings

A total of 14 distinct mutations were identified in CPT1A gene; 85.72% (12/14) were missense, 7.14% (1/14) were deletion, and 7.14% (1/14) were spicing variants. Overall, 11 of these CPT1A variants were novel, and the other three were previously reported. The most frequent mutation was c.1910C > A (p.S637T), with an allelic frequency of 16.67% (4/24). The relatively frequent mutations were c.740C > T (p.P247L) and c.1328T > C (p.L443P), and each of mutation was identified three times, with an allelic frequency of 12.5% (3/24). c.2125G > A (p.G709R) and c.1295C > T (p.P432L) were each identified twice. The remaining six mutations were identified only once.

A total of six distinct mutations were identified in CPT2 gene. Among which, 83.33% (4/6) were missense, and 16.67% (2/6) were frameshift variants. Overall, three of these CPT2 variants were novel. The most frequent mutation was c.1711C > A (p.P571T), with an allelic frequency of 37.5% (3/8). Each of the remaining five mutations were identified only once.

There were 4 distinct mutations in the SLC25A20 gene. All the mutations were previously reported. The most common variant was c.199-10T > G, which accounted for 62.6% (5/8). Each of the remaining three mutations was identified only once.

For all these novel missense variants, all were predicted to be potentially pathogenic byPolyphen-2, PROVEAN, and the MutationTaster predictor (**Table 3**). Structure stability analysis was performed using Chimera version 1.15. Atoms clash and contacts decreased structure stability. c.740C > T (p.P247L), c.1328T > C (p.L443P), c.1817G > A (p.R606H), c.1910C > A (p.S637T), c.2246G > A, (p.A749H). c.205G > A (p.V69M),

TABLE 2 | Clinical presentation, biochemical, and genetic investigation of confirmed patients with CPT1D, CPT2D, CACTD.

Patient no	Gender	Age[a]	Genotype		Onset	Clinical presentation
			Allele 1	Allele 2		
CPT1D						
1	Female	3M	c.740C > T	c.1328T > C	ND	ND
2	Female	18D	c.1817G > A	c.1817G > A	After birth	died at 18D hyperammonemia, metabolic acidosis
3	Female	4Y3M	c.979C > T	c.1336G > A	None	asymptomatic
4	Female	5M	c.1910C > A	c.1910C > A	None	asymptomatic
5	Female	5M	c.1910C > A	c.1910C > A	None	asymptomatic
6	Male	3Y9M	c.281+1G > A	c.956G > T	None	asymptomatic
7	Male	3Y	c.2246G > A	c.1131G > C	None	asymptomatic
8	Male	3Y2M	c.577delC	c.740C > T	None	asymptomatic
9	Male	2Y4M	c.205G > A	c.740C > T	None	asymptomatic
10	Female	2Y4M	c.1328T > C	c.1328T > C	None	asymptomatic
11	Male	2Y8M	c.2125G > A	c.1295C > T	None	asymptomatic
12	Male	2Y8M	c.2125G > A	c.1295C > T	None	asymptomatic
CPT2D						
13	Female	8M	c.988dupT	c.1711C > A	8M	died at 8M
14	Female	10D	c.1711C > A	c.520G > A	2D	died at 10D metabolic acidosis, hypoglycemia
15	Male	2Y3M	c.895-896insGGGCAGAGCTC	c.1711C > A	None	asymptomatic incomplete right bundle branch block
16	Male	6M	c.1054T > C	c.1301T > C	None	asymptomatic impaired liver function
CACTD						
17	Male	1Y3M	c.1A > G	c.199-10T > G	After birth	acidosis, hypoglycemia, hyperammonemia, survive
18	Female	3M	c.270delC	c.804delG	After birth	died at 2M metabolic acidosis, impaired liver function, hepatomegaly, cardiac hypertrophy, hyperammonemia
19	Male	7D	c.199-10T > G	c.199-10T > G	After birth	died at 7D acidosis, hypoglycemia, hyperammonemia
20	Female	7D	c.199-10T > G	c.199-10T > G	After birth	died at 7D acidosis, hypoglycemia, hyperammonemia

[a]*Y: years; M: months; D: days; Age[a]: age at last follow-up; ND: no data;* CPT1A *gene for CPTID;* CPT2 *gene for CPTIID;* SLC25A20 *gene for CACTD.*

c.2125G > A (p.G709R), and (p.P432L). c.1054T > C (p.F352L) might cause 5, 5, 3, 1, 3, 7, 37, and one atom clash and contacts, respectively. No atom clash and contacts were caused by c.1295C > T (p.P432L), c.979C > T (p.H327T), and c.1131G > C (p.G377A). Atoms clash and contact are shown in yellow lines in **Figure 1**.

DISCUSSION

In this study, 20 patients with disorders of mitochondrial carnitine–acylcarnitine cycle were identified (12 with CPT1D, 4 with CPT2D, and 4 with CACTD) in approximately 4 million newborns in Zhejiang province, China between 2009 and 2021. The data revealed the largest series of cases with disorders of mitochondrial carnitine–acylcarnitine cycle detected by NBS in the Chinese Population. The incidence of newborns with disorders of mitochondrial carnitine–acylcarnitine cycle was 1: 203,518 (CPT1D: 1:339,197; CPT2D: 1:1,017,593; and CACTD: 1: 1,017,593) in Zhejiang province. CPT1D was the most common disorder of mitochondrial carnitine–acylcarnitine cycle. The incidence of these disorders in Taiwan was 1:263,523 (CPT1D: 1:790,567 and CPT2D/CACTD: 1:395,283) according to NBS data in 2013 (Chien et al., 2013). Data from the largest nationwide cross-sectional study illustrated that the total incidence in mainland China was 1:236,655 (CPT1D: 1: 546,128, CPT2D: 1:1,014,237, and CACTD: 1:709.996) (Deng et al., 2020). Incidence of these disorders in Australia, Germany, and the United States was 1:250,000 to 1:666,667 (Lindner et al., 2010). Disorders of mitochondrial carnitine–acylcarnitine cycle seem to be rare diseases in general population. The incidence of these disorders, especially that of CPT1D, in Zhejiang province seems to be higher than that reported in previous studies. This difference may be due to the awareness of these disorders, ethnic backgrounds, different cut-off values, recall criteria, and development of diagnostic methods. Previous reports revealed that these disorders may present normal acyl-carnitine levels at birth, resulting in false-negative cases (Dowsett et al., 2017). Case 12 with CPT1D was overlooked at the initial screening. Hence, the actual incidence may be higher than the reported data. A looser cut-off value can decrease false-negative cases but increase the false-positive cases. To handle these issues, a previous report revealed that they have developed second-tier molecular tests for these diseases (Lin et al., 2020).

NBS plays an important role in the early detection of deficiency in enzymes of mitochondrial carnitine–acylcarnitine

TABLE 3 | Variants detected in confirmed patients with CPT1D, CPT2D, CACTD.

No	Nucleotide	Protein	Location	Effect	Frequency(%)	Prediction of pathogenicity			
						PolyPhen-2	PROVEAN	Mutation taster	References
CPT1A									
1	**c.740C > T**	**p.P247L**	Exon3	Missense	12.5	D (1)	D (–8.135)	D (0.999)	Novel
2	**c.1328T > C**	**p.L443P**	Exon11	Missense	12.5	D (1)	D (–5.826)	D (0.999)	Novel
3	**c.1817G > A**	**p.R606H**	Exon15	Missense	8.33	D (1)	D (–4.557)	D (0.999)	Novel
4	**c.979C > T**	**p.H327T**	Exon10	Missense	4.16	D (0.995)	D (–8.678)	D (0.999)	Novel
5	c.1336G > A	p.G446S	Exon11	Missense	4.16	D (0.995)	D (–5.351)	D (0.999)	Zhang et al. (2021)
6	**c.1910C > A**	**p.S637T**	Exon16	Missense	16.67	D (1)	N (–0.945)	P (0.998)	Novel
7	c.281+1G > A	—	Exon4	Splicing	8.33	N/A	N/A	N/A	Yu et al. (2021)
8	c.956G > T	p.G319V	Exon9	Missense	8.33	B (0.005)	D (–8.203)	D (1)	Yu et al. (2021)
9	**c.2246G > A**	**p.R749H**	Exon19	Missense	8.33	D (1)	N (–0.771)	D (0.999)	Novel
10	**c.1131G > C**	**p.E377D**	Exon10	Missense	8.33	D (0.906)	D (–7.425)	D (0.999)	Novel
11	**c.577delC**	**p.M194***	Exon6	Deletion	8.33	N/A	N/A	N/A	Novel
12	**c.205G > A**	**p.V69M**	Exon7	Missense	8.33	D (1)	N (–1.494)	D (0.996)	Novel
13	**c.2125G > A**	**p.G709R**	Exon17	Missense	16.67	D (0.985)	D (–6.766)	D (0.999)	Novel
14	**c.1295C > T**	**p.P432L**	Exon11	Missense	16.67	D (1)	D (–7.054)	D (0.999)	Novel
CPT2									
15	**c.988dupT**	**p.I332Hfs*2**	Exon4	Frameshift	12.5	N/A	N/A	N/A	Novel
16	c.1711C > A	p.P571T	Exon5	Missense	37.5	D (0.985)	D (-6.169)	D (0.999)	Qian J, et al. (2020)
17	c.520G > A	p.G174L	Exon4	Missense	12.5	P (0.997)	N (-0.989)	D (0.999)	T Takahashi et al. (2015)
18	**c.895-896insGGGCAGAGCTC**	**p.R303Gfs*6**	Exon4	Frameshift	12.5	N/A	N/A	N/A	Novel
19	**c.1054T > C**	**p.F352L**	Exon4	Missense	12.5	B (0.118)	D (-5.229)	D (0.999)	Novel
20	c.1301T > C	p.F434S	Exon4	Missense	12.5	B (0.118)	D (-5.851)	D (0.999)	Nathalie et al. (2021)
SLC25A20									
21	c.1A > G	p.M1V	Exon1	start codon	12.5	B (0.028)	N (-1.132)	D (0.999)	Yan et al. (2017)
22	c.199-10T > G	—	Intron2	Intron	62.5	N/A	N/A	N/A	Chen M et al. (2020)
23	c.270delC	p.F91Lfs*37	Exon3	Frameshift	12.5	N/A	N/A	N/A	BB Gürbüz et al. (2021)
24	c.804delG	p.F269Sfs*3	Exon8	Frameshift	12.5	N/A	N/A	N/A	T Fukushima et al. (2013)

Reference sequence for CPT1A, CPT2, SLC25A20 *are NM_001876.3, NM_000098.2, NM_000098.3 respectively. The previously unreported novel variants of this study are in boldface type. N/A: not available. PolyPhen-2: http://genetics.bwh.harvard.edu/pph2/, HVAR score ranges from 0 (neutral, N) to 1 (damaging, D), B: benign. PROVEAN: http://provean.jcvi.org/index.php, score ranges from ≤ –2.5 (deleterious, D) to > –2.5 (neutral, N). Mutation Taster: http://www.mutationtaster.org/, a score close to one indicates a high "security" of the prediction (P: polymorphism, D: disease causing).*
Novel mutations are in boldface type.

cycle (Wilcken et al., 2003). Most patients with CPT1D presented increased C0 levels and C0/(C16 + C18) ratios and/or decreased long-chain acyl-carnitines levels. For instance, patient 12 with normal C0 levels and C0/(C16 + C18) ratios was overlooked at the initial screening and exhibited slight reduction of C12 to C18:1 level. Milder forms of CPT1D may present normal C0 levels and C0/(C16 + C18) ratios or slight changes can easily be missed by NBS (de Sain-van der Velden et al., 2013; Dowsett et al., 2017). Combining a lower C18:1 level with higher C0/(C16 + C18) ratios in plasma and high sensitivity and specificity for CPT1D could be found in a previous study (Heiner-Fokkema et al., 2017). The reduction in C18:1 level might be an important inducer of CPT1D, which is consistent with a previous study which reported nine patients with a low C18:1 level. The number of patients with low C18:1 level was more than that with low C12 to C16:1 level. Increased C12–C18:1 level (particularly C16 and C18:1) and/or decreased C0, C2 levels were the major characteristics in CACTD and CPT2D. Some patients had normal concentrations of C12, C14, C16, C18, and C18:1. Elevation of (C16 + C18:1)/C2 ratios could reduce the false negative rate and improve the sensitivity (Sigauke et al., 2003; Edmondson et al., 2017; Tajima et al., 2017; Tang et al., 2019). However, this ratio sometimes may be normal (de Sain-van der Velden et al., 2013; Edmondson et al., 2017). The ratio of several long-chain acyl-carnitines to C3 like C14/C3, C16/C3, C18/C3, and (C16 + C18:1)/C3 can be used as better indices for CPT2D screening (Edmondson et al., 2017). In this study, it was observed that C14/C3, C16/C3, C16:1/C3, C18:1/C3, and (C16 + C18:1)/C3 ratios were increased in all patients with CACTD and CPT2D, which were significantly higher in CPT2D; this might be considered to distinguish between these two similar diseases. The results might be caused by very low concentrations of C3 levels in patients with CPT2D.

Patients with CPT1AD presented normal growth and development following a strict diet management and follow-up (Gan et al., 2021). CPT1D can be triggered by fasting or illnesses

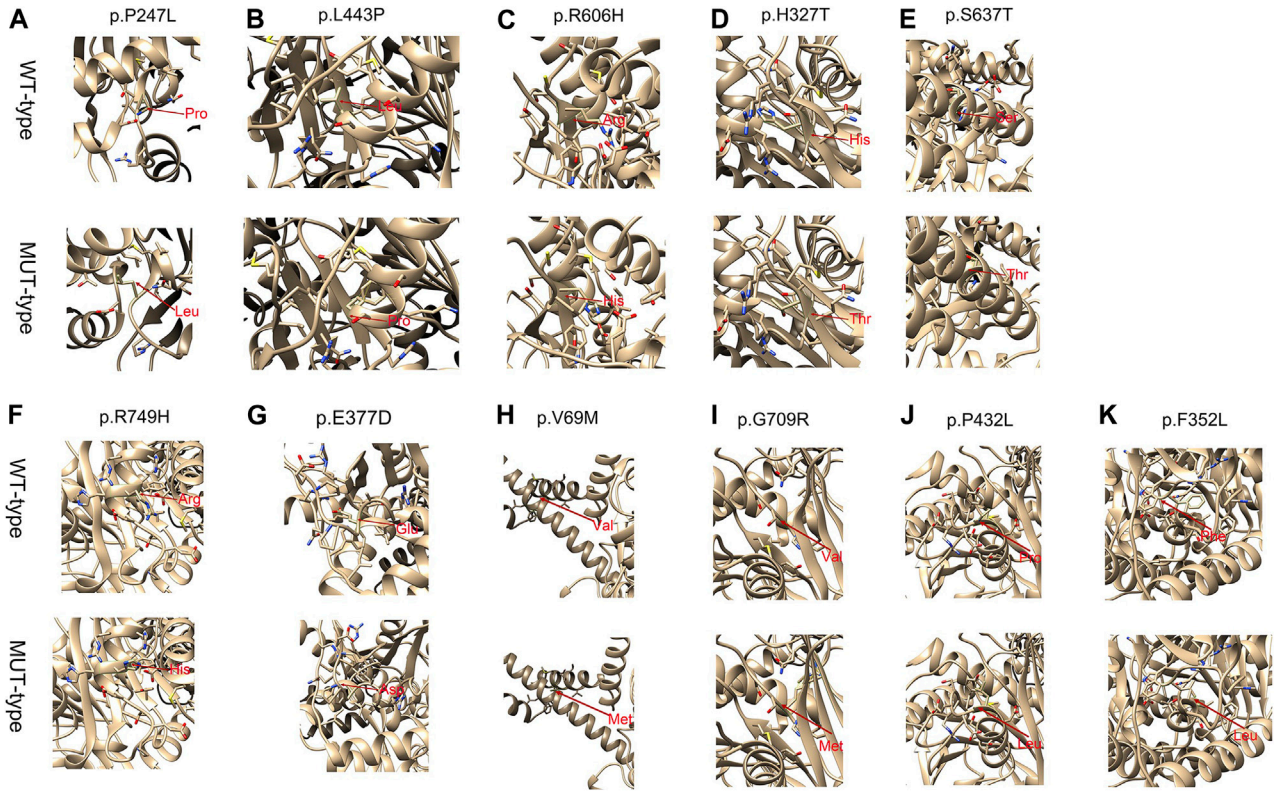

FIGURE 1 | Structure stability analysis of the p.P247L, p.L443P, p.R606H, p.H327T, p.S637T, p.R749H, p.E377A, p.V69M, p.G709R, p.P432L mutations on the partial tertiary structure of CPT1Aprotein (Uniprot: AF-P50416-F1). Structure stability analysis of the p.F352L mutation on the partial tertiary structure of CPT2 protein (Uniprot: AF-P23786-F1). A: The wildtype amino-acid residue at 247 site, 443 site, 606 site, 327 site, 637 site, 749 site, 377 site, 69 site, 709 site, 432 site and 352 site (CPT2 protein) colored green has no contact with the amino-acid residue nearby. **(A)** base on this model, after amino-acid was substituted by the Leucine amino acid residue at this site, five atoms clash and contacts were found in this region. **(B)** After amino-acid was substituted by the Proline amino acid residue at this site, five atoms clash and contacts were found in this region. **(C)** After amino-acid was substituted by the Histidine amino acid residue at this site, three atoms clash and contacts were found in this region. **(D)** After amino-acid was substituted by the Threonine amino acid residue at this site, no atom clash and contacts were found in this region. **(E)** After amino-acid was substituted by the Threonine amino acid residue at this site, one atoms clash and contacts were found in this region. **(F)** After amino-acid was substituted by the Histidine amino acid residue at this site, three atom clash and contacts were found in this region. **(G)** After amino-acid was substituted by the Aspartic acid residue at this site, 0 atoms clash and contacts were found in this region. H After amino-acid was substituted by the Methionine amino acid residue at this site, seven atoms clash and contacts were found in this region. **(I)** After amino-acid was substituted by the Argnine amino acid residue at this site, 37 atoms clash and contacts were found in this region. **(J)** After amino-acid was substituted by the Leucine amino acid residue at this site, 0 atoms clash and contacts were found in this region **(K)** After amino-acid was substituted by the Leucine amino acid residue at this site, one atoms clash and contacts were found in this region. Amino acid change marked with red arrows. Atoms clash and contacts are shown in yellow lines. The Structure stability analysis of novel mutations were performed by Chimera version 1.15.

and presented with hypoketotic hypoglycaemic episodes and hepatomegaly in the early period of life; few cases may die in neonatal period (Baruteau et al., 2014; Fohner et al., 2017). Several cases with mild cardiomegaly, heartbeat disorders, or distal renal tubular acidosis have been reported (Olpin et al., 2001; Yu et al., 2021). Most patients with CPT1D had no clinic symptoms and only one case presented with hyperammonaemia and metabolic acidosis and died in the early neonatal period. Additionally, data suggested that early diagnosis and proper treatment resulted in good prognosis in patients with CPT1D. It remains to be observed whether patients with CPT1D will present further clinical symptoms. Overall, three different phenotypes of CPT2D have myopathic, lethal neonatal, and severe infantile forms. The most common form of CPT2D is the myopathic form, and the symptoms in 70% cases of this form were presented during 0–12 years of ages. The most common clinical symptoms were myalgia, myoglobinuria, and muscle weakness trigged by exercise and infection (Joshi et al., 2014; Joshi and Zierz, 2020). The severe infantile forms always presented hypoketotic hypoglycaemia, hepatomegaly, metabolic acidosis, cardiac manifestations, weakness, seizures, and sudden death (Sigauke et al., 2003). The lethal neonatal form is fatal, which causes death during the neonatal period (Isackson et al., 2008; Du et al., 2017). Overall, 4 CPT2D cases were detected in this study. One lethal neonatal form (patient 14) presented metabolic acidosis and hypoketotic hypoglycaemia and died soon in the neonatal period. One severe infantile form (patient 13) presented sudden death at 8 months at home without any available data. The two remaining cases (patients 15 and 16) were asymptomatic along with incomplete right and transient elevation of ALT, respectively. Critically ill patients with CACTD presented a severe phenotype in the neonatal time, including rapidly progressive condition and

a high fatality rate (Chen et al., 2020). Late onset form has been less common (Morris et al., 1998). In this study, the 4 cases with CACTD presented feeding dysfunction, poor response, hypoglycaemia, metabolic acidosis, hepatic impairment, hepatomegaly, and cardiac hypertrophy. In addition, two patients died in the early neonatal period, and 1 case died at 2 months after birth. Patient 17 survived. Although CACT deficiency diagnosed via NBS had a surely high mortality rate, early detection and treatment may save lives.

In general, more than 30 CPT1A pathogenic mutations have been reported (Tsuburaya et al., 2010; Gan et al., 2021). c.1436C > T (p.P479L) was the common mutation in northern Canada, Greenland, Colombia, and the native Alaskan population (Park et al., 2006). Moreover, c.2129G > A (p.G710E) was mainly detected in the US Alaskan and Hutterite populations, and a homozygous mutation might lead to severe clinical manifestations (Prasad et al., 2001; Prip-Buus et al., 2001). Hotspot mutations with CPT1D in the Chinese population have not yet been reported. c.1910C > A (p.S637T), c.740C > T (p.P247L), and c.1328T > C (p.L443P) presented highest occurring mutations in this study and might be the potential hotpot variants in Zhejiang province of South China.

Seventy pathogenic variants in CPT2 gene were reported and phenotype–genotype association was observed in CPT2D (Joshi et al., 2014). c.680C > T (p.P227L), c.1923_1935del, and c.983A > G (p.D328G) were thought to be correlated with lethal neonatal and severe infantile forms and generally not detected in patients with myopathic forms (Isackson et al., 2006; Isackson et al., 2008). Furthermore, the c.338C > T (p.S113L) mutation was detected in almost 70% patients with myopathic forms (Joshi et al., 2014; Fontaine et al., 2018). The c.338C > T (p.S113L) compound heterozygotic patients were easily triggered by low temperature compared with c.338C > T (p.S113L) homozygotic patients. Patients with truncating mutations were significantly easily triggered by fasting compared with those with missense mutations on both two alleges. The c.338C > T (p.S113L) mutation of CPT2 is a common variant in the Caucasian population, whereas c.1148T > A (p.F383Y) mutation is common in Japanese population (Yasuno et al., 2008). According to dataset, the most frequent mutation was c.1711C > A (p.P571T), which was previously reported in the northern China and might be the potential hotspot of CPT2D in Chinese population (Qian et al., 2017).

More than 40 SLC25A20 pathogenic mutations have been identified (Yan et al., 2017). Phenotype–genotype association in CACTD have been reported previously. The c.241G > A (G81R) mutation was associated with severe phenotype, whereas the c.955insC mutation was associated with a milder form in the Netherlands (IJlst et al., 2001). c.199-10T > G mutation was the most common in East Asia, which accounted for 83% of the variant alleles in Chinese population (Tang et al., 2019; Chen et al., 2020). The homozygous c.199-10T > G mutation was correlated with lethal neonatal form in Asian cases; two cases with homozygous c.199-10T > G mutation in our study were died early. c.199-10T > G mutation may cause premature protein truncation and translocate enzyme without activity which may explain the severe genotype of c.199-10T > G mutation (Hsu et al., 2001). A compound heterozygous case with c.199-10T > G and c.1A > G (p.M1V) mutation died at 6 days after birth (Yan et al., 2017), whereas a case in our study with the same mutation survived. Early timely treatment is crucial for CACTD and may reverse the metabolic decompensation. This good prognosis of our case might have benefitted from early detection and early management after NBS.

This study identified 11 novel CPT1A variants and 3 novel CPT2 variants. Deletion (c.577delC (p.M194*)) and frameshift variants (c.988dupT (p.I332Hfs*2) and c.895-896insGGGCAGAGCTC (p.R303Gfs*6)) would result in truncated proteins which would potentially affect protein function. All novel missense variants were predicted as possibly pathogenic by bioinformatics analysis. We further predicted structure stability analysis of novel missense mutations. In addition to c.1295C > T (p.P432L), c.979C > T (p.H327T), and c.1131G > C (p.G377A), all missense variants might cause atom clash and contacts and decreased structure stability of protein resulting in a loss-of-function effect. Nevertheless, the pathogenicity of all these novel variants needs to be confirmed by further functional investigations.

CONCLUSION

In conclusion, disorders of mitochondrial carnitine–acylcarnitine cycle, with a rare combined incidence among newborns, were detected through NBS in Zhejiang, China. Most of the patients presented different typical acylcarnitine profiles. To be more specific, most patients with CPT1D presented normal growth and development, whereas those with CPT2D/CACTD had a high mortality rate. Overall, 11 novel CPT1A variants and 3 novel CPT2 variants were identified, which further expanded the mutational spectrum. All novel missense variants were predicted as possibly pathogenic by bioinformatics analysis. This study may help in enhancing overall awareness of disorders of mitochondrial carnitine–acylcarnitine cycle through clarifying the signification of early diagnosis and proper treatment on the prevention and recovery of patients.

DATA AVAILABILITY STATEMENT

The data presented in the study are deposited in the Figshare. The accession numbers were 10.6084/m9.figshare.18392345 and 10.6084/m9.figshare.18392426.

AUTHOR CONTRIBUTIONS

DZ performed the data analysis, drafted the initial manuscript, reviewed and revised the manuscript; YC assisted with data collection; XY revised the manuscript; ZH, JY, a followed the patients and collected the clinical data; HM, YZ performed the genetic tests, variats analysis; XH, BW designed and supervised

the study. All authors approved the final manuscript for submission and publication. These authors contributed equally to this work.

FUNDING

This work was supported by the National Key Research and Development Program of China (grant number: 2018YFC1002204), the National Natural Science Foundation of China (82073560); Basic Public Welfare Research Program of Zhejiang province (LGC19B050013).

ACKNOWLEDGMENTS

Thank you for all participation of patients and their family members.

REFERENCES

Baruteau, J., Sachs, P., Broué, P., Brivet, M., Abdoul, H., Vianey-Saban, C., et al. (2014). Clinical and Biological Features at Diagnosis in Mitochondrial Fatty Acid Beta-Oxidation Defects: a French Pediatric Study from 187 Patients. Complementary Data. *J. Inherit. Metab. Dis.* 37 (1), 137–139. doi:10.1007/s10545-013-9628-9

Chen, M., Cai, Y., Li, S., Xiong, H., Liu, M., Ma, F., et al. (2020). Late-Onset Carnitine-Acylcarnitine Translocase Deficiency with SLC25A20 c.199-10T>G Variation: Case Report and Pathologic Analysis of Liver Biopsy. *Front. Pediatr.* 8, 585646. doi:10.3389/fped.2020.585646

Chien, Y.-H., Lee, N.-C., Chao, M.-C., Chen, L.-C., Chen, L.-H., Chien, C.-C., et al. (2013). Fatty Acid Oxidation Disorders in a Chinese Population in Taiwan. *JIMD Rep.* 11, 165–172. doi:10.1007/8904_2013_236

Collins, S. A., Sinclair, G., McIntosh, S., Bamforth, F., Thompson, R., Sobol, I., et al. (2010). Carnitine Palmitoyltransferase 1A (CPT1A) P479L Prevalence in Live Newborns in Yukon, Northwest Territories, and Nunavut. *Mol. Genet. Metab.* 101, 200–204. doi:10.1016/j.ymgme.2010.07.013

de Sain-van der Velden, M. G. M., Diekman, E. F., Jans, J. J., van der Ham, M., Prinsen, B. H. C. M. T., Visser, G., et al. (2013). Differences between Acylcarnitine Profiles in Plasma and Bloodspots. *Mol. Genet. Metab.* 110, 116–121. doi:10.1016/j.ymgme.2013.04.008

Deng, K., Zhu, J., Yu, E., Xiang, L., Yuan, X., Yao, Y., et al. (2020). Incidence of Inborn Errors of Metabolism Detected by Tandem Mass Spectrometry in China: A Census of over Seven Million Newborns between 2016 and 2017. *J. Med. Screen.* 28, 223–229. doi:10.1177/0969141320973690

Dowsett, L., Lulis, L., Ficicioglu, C., and Cuddapah, S. (2017). Utility of Genetic Testing for Confirmation of Abnormal Newborn Screening in Disorders of Long-Chain Fatty Acids: A Missed Case of Carnitine Palmitoyltransferase 1A (CPT1A) Deficiency. *Ijns* 3 (2), 10. doi:10.3390/ijns3020010

Du, S.-H., Zhang, F., Yu, Y.-G., Chen, C.-X., Wang, H.-J., and Li, D.-R. (2017). Sudden Infant Death from Neonate Carnitine Palmitoyl Transferase II Deficiency. *Forensic Sci. Int.* 278, e41–e44. doi:10.1016/j.forsciint.2017.06.020

Edmondson, A. C., Salant, J., Ierardi-Curto, L. A., and Ficicioglu, C. (2016). Missed Newborn Screening Case of Carnitine Palmitoyltransferase-II Deficiency. *JIMD Rep.* 33, 93–97. doi:10.1007/8904_2016_528

Fohner, A. E., Garrison, N. A., Austin, M. A., and Burke, W. (2017). Carnitine Palmitoyltransferase 1A P479L and Infant Death: Policy Implications of Emerging Data. *Genet. Med.* 19 (8), 851–857. doi:10.1038/gim.2016.202

Fontaine, M., Kim, I., Dessein, A.-F., Mention-Mulliez, K., Dobbelaere, D., Douillard, C., et al. (2018). Fluxomic Assay-Assisted Diagnosis Orientation in a Cohort of 11 Patients with Myopathic Form of CPT2 Deficiency. *Mol. Genet. Metab.* 123 (4), 441–448. doi:10.1016/j.ymgme.2018.02.005

Gan, Y., Yu, F., and Fang, H. (2021). Novel Mutation in Carnitine Palmitoyltransferase 1A Detected through Newborn Screening for a Presymptomatic Case in China: a Case Report. *Ital. J. Pediatr.* 47 (1), 154. doi:10.1186/s13052-021-01094-5

Heiner-Fokkema, M. R., Vaz, F. M., Maatman, R., Kluijtmans, L. A. J., van Spronsen, F. J., and Reijngoud, D.-J. (2016). Reliable Diagnosis of Carnitine Palmitoyltransferase Type IA Deficiency by Analysis of Plasma Acylcarnitine Profiles. *Acylcarnitine Profiles* 32, 33–39. doi:10.1007/8904_2016_564

Houten, S. M., Violante, S., Ventura, F. V., and Wanders, R. J. A. (2016). The Biochemistry and Physiology of Mitochondrial Fatty Acid β-Oxidation and its Genetic Disorders. *Annu. Rev. Physiol.* 78, 23–44. doi:10.1146/annurev-physiol-021115-105045

Houten, S. M., and Wanders, R. J. A. (2010). A General Introduction to the Biochemistry of Mitochondrial Fatty Acid β-oxidation. *J. Inherit. Metab. Dis.* 33 (5), 469–477. doi:10.1007/s10545-010-9061-2

Hsu, B. Y. L., Iacobazzi, V., Wang, Z., Harvie, H., Chalmers, R. A., Saudubray, J.-M., et al. (2001). Aberrant mRNA Splicing Associated with Coding Region Mutations in Children with Carnitine-Acylcarnitine Translocase Deficiency. *Mol. Genet. Metab.* 74, 248–255. doi:10.1006/mgme.2001.3235

IJlst, L., van Roermund, C. W. T., Iacobazzi, V., Oostheim, W., Ruiter, J. P. N., Williams, J. C., et al. (2001). Functional Analysis of Mutant Human Carnitine Acylcarnitine Translocases in Yeast. *Biochem. Biophysical Res. Commun.* 280 (3), 700–706. doi:10.1006/bbrc.2000.4178

Indiveri, C., Iacobazzi, V., Tonazzi, A., Giangregorio, N., Infantino, V., Convertini, P., et al. (2011). The Mitochondrial Carnitine/acylcarnitine Carrier: Function, Structure and Physiopathology. *Mol. aspects Med.* 32, 223–233. doi:10.1016/j.mam.2011.10.008

Isackson, P. J., Bennett, M. J., Lichter-Konecki, U., Willis, M., Nyhan, W. L., Sutton, V. R., et al. (2008). CPT2 Gene Mutations Resulting in Lethal Neonatal or Severe Infantile Carnitine Palmitoyltransferase II Deficiency. *Mol. Genet. Metab.* 94 (4), 422–427. doi:10.1016/j.ymgme.2008.05.002

Isackson, P. J., Bennett, M. J., and Vladutiu, G. D. (2006). Identification of 16 New Disease-Causing Mutations in the CPT2 Gene Resulting in Carnitine Palmitoyltransferase II Deficiency. *Mol. Genet. Metab.* 89 (4), 323–331. doi:10.1016/j.ymgme.2006.08.004

Joshi, P. R., Deschauer, M., and Zierz, S. (2014). Carnitine Palmitoyltransferase II (CPT II) Deficiency: Genotype-Phenotype Analysis of 50 Patients. *J. Neurol. Sci.* 338, 107–111. doi:10.1016/j.jns.2013.12.026

Joshi, P. R., and Zierz, S. (2020). Muscle Carnitine Palmitoyltransferase II (CPT II) Deficiency: A Conceptual Approach. *Molecules* 25 (8), 1784. doi:10.3390/molecules25081784

Lin, Y., Liu, Y., Zhu, L., Le, K., Shen, Y., Yang, C., et al. (2020). Combining Newborn Metabolic and Genetic Screening for Neonatal Intrahepatic Cholestasis Caused by Citrin Deficiency. *Jrnl Inher Metab. Disea* 43 (3), 467–477. doi:10.1002/jimd.12206

Lindner, M., Hoffmann, G. F., and Matern, D. (2010). Newborn Screening for Disorders of Fatty-Acid Oxidation: Experience and Recommendations from an Expert Meeting. *J. Inherit. Metab. Dis.* 33 (5), 521–526. doi:10.1007/s10545-010-9076-8

Lodhi, I. J., and Semenkovich, C. F. (2014). Peroxisomes: a Nexus for Lipid Metabolism and Cellular Signaling. *Cel Metab.* 19 (3), 380–392. doi:10.1016/j.cmet.2014.01.002

Maguolo, A., Rodella, G., Dianin, A., Nurti, R., Monge, I., Rigotti, E., et al. (2020). Diagnosis, Genetic Characterization and Clinical Follow up of Mitochondrial Fatty Acid Oxidation Disorders in the new era of Expanded Newborn Screening: A Single centre Experience. *Mol. Genet. Metab. Rep.* 24, 100632. doi:10.1016/j.ymgmr.2020.100632

McGarry, J. D., and Brown, N. F. (1997). The Mitochondrial Carnitine Palmitoyltransferase System - from Concept to Molecular Analysis. *Eur. J. Biochem.* 244 (1), 1–14. doi:10.1111/j.1432-1033.1997.00001.x

Morris, A. A. M., Olpin, S. E., Brivet, M., Turnbull, D. M., Jones, R. A. K., and Leonard, J. V. (1998). A Patient with Carnitine-Acylcarnitine Translocase Deficiency with a Mild Phenotype. *J. Pediatr.* 132, 514–516. doi:10.1016/s0022-3476(98)70030-7

Olpin, S. E., Allen, J., Bonham, J. R., Clark, S., Clayton, P. T., Calvin, J., et al. (2001). Features of Carnitine Palmitoyltransferase Type I Deficiency. *J. Inherit. Metab. Dis.* 24 (1), 35–42. doi:10.1023/a:1005694320063

Park, J. Y., Narayan, S. B., and Bennett, M. J. (2006). Molecular Assay for Detection of the Common Carnitine Palmitoyltransferase 1A 1436(C>T) Mutation. *Clin. Chem. Lab. Med.* 44 (9), 1090–1091. doi:10.1515/CCLM.2006.196

Prasad, C., Johnson, J. P., Bonnefont, J. P., Dilling, L. A., Innes, A. M., Haworth, J. C., et al. (2001). Hepatic Carnitine Palmitoyl Transferase 1 (CPT1 A) Deficiency in North American Hutterites (Canadian and American): Evidence for a Founder Effect and Results of a Pilot Study on a DNA-Based Newborn Screening Program. *Mol. Genet. Metab.* 73 (1), 55–63. doi:10.1006/mgme.2001.3149

Prip-Buus, C., Thuillier, L., Abadi, N., Prasad, C., Dilling, L., Klasing, J., et al. (2001). Molecular and Enzymatic Characterization of a Unique Carnitine Palmitoyltransferase 1A Mutation in the Hutterite Community. *Mol. Genet. Metab.* 73 (1), 46–54. doi:10.1006/mgme.2001.3176

Qian, J., Wang, X., Liu, J., Zhong, J., Le, Y., Melchior Tellier, L. C. A., et al. (2017). Applying Targeted Next Generation Sequencing to Dried Blood Spot Specimens from Suspicious Cases Identified by Tandem Mass Spectrometry-Based Newborn Screening. *J. Pediatr. Endocrinol. Metab.* 30 (9), 979–988. doi:10.1515/jpem-2017-0003

Sigauke, E., Rakheja, D., Kitson, K., and Bennett, M. J. (2003). Carnitine Palmitoyltransferase II Deficiency: A Clinical, Biochemical, and Molecular Review. *Lab. Invest.* 83 (11), 1543–1554. doi:10.1097/01.lab.0000098428.51765.83

Tajima, G., Hara, K., Tsumura, M., Kagawa, R., Okada, S., Sakura, N., et al. (2017). Newborn Screening for Carnitine Palmitoyltransferase II Deficiency Using (C16 + C18:1)/C2: Evaluation of Additional Indices for Adequate Sensitivity and Lower False-Positivity. *Mol. Genet. Metab.* 122 (3), 67–75. doi:10.1016/j.ymgme.2017.07.011

Tang, C., Liu, S., Wu, M., Lin, S., Lin, Y., Su, L., et al. (2019). Clinical and Molecular Characteristics of Carnitine-Acylcarnitine Translocase Deficiency: Experience with Six Patients in Guangdong China. *Clinica Chim. Acta* 495, 476–480. doi:10.1016/j.cca.2019.05.018

Tsuburaya, R., Sakamoto, O., Arai, N., Kobayashi, H., Hasegawa, Y., Yamaguchi, S., et al. (2010). Molecular Analysis of a Presymptomatic Case of Carnitine Palmitoyl Transferase I (CPT I) Deficiency Detected by Tandem Mass Spectrometry Newborn Screening in Japan. *Brain Develop.* 32 (5), 409–411. doi:10.1016/j.braindev.2009.03.004

Watkins, P. A., Maiguel, D., Jia, Z., and Pevsner, J. (2007). Evidence for 26 Distinct Acyl-Coenzyme A Synthetase Genes in the Human Genome. *J. lipid Res.* 48 (12), 2736–2750. doi:10.1194/jlr.M700378-JLR200

Wieser, T., Deschauer, M., Olek, K., Hermann, T., and Zierz, S. (2003). Carnitine Palmitoyltransferase II Deficiency: Molecular and Biochemical Analysis of 32 Patients. *Neurology* 60 (8), 1351–1353. doi:10.1212/01.wnl.0000055901.58642.48

Wilcken, B., Wiley, V., Hammond, J., and Carpenter, K. (2003). Screening Newborns for Inborn Errors of Metabolism by Tandem Mass Spectrometry. *N. Engl. J. Med.* 348 (23), 2304–2312. doi:10.1056/NEJMoa025225

Yan, H.-M., Hu, H., Ahmed, A., Feng, B.-B., Liu, J., Jia, Z.-J., et al. (2017). Carnitine-acylcarnitine Translocase Deficiency with c.199-10 T>G and Novel c.1A>G Mutation. *Medicine* 96 (45), e8549. doi:10.1097/md.0000000000008549

Yasuno, T., Kaneoka, H., Tokuyasu, T., Aoki, J., Yoshida, S., Takayanagi, M., et al. (2008). Mutations of Carnitine Palmitoyltransferase II (CPT II) in Japanese Patients with CPT II Deficiency. *Int. J. Genet. Mol. Personalized Med.* 73 (5), 496–501. doi:10.1111/j.1399-0004.2008.00986.x

Yu, Y., Shen, L. H., Qiu, W. J., Zhang, H. W., Ye, J., Liang, L. L., et al. (2021). Clinical Features and Gene Mutations of 6 Patients with Carnitine Palmitoyltransferase 1A Deficiency. *Zhonghua Yi Xue Za Zhi* 101 (14), 1041–1044. doi:10.3760/cma.j.cn112137-20200724-02206

Conflict of Interest: Author YZ is employed by Zhejiang Bosheng Biotechnology Co, Ltd, Hangzhou, China.

The remaining authors declare that the research was conducted in the absence of any commercial or financial relationships that could be construed as a potential conflict of interest.

Publisher's Note: All claims expressed in this article are solely those of the authors and do not necessarily represent those of their affiliated organizations, or those of the publisher, the editors and the reviewers. Any product that may be evaluated in this article, or claim that may be made by its manufacturer, is not guaranteed or endorsed by the publisher.

frontiers in Genetics

ORIGINAL RESEARCH
published: 16 March 2022
doi: 10.3389/fgene.2022.825793

Novel *SEPN1* Mutations in Exon 1 Are Common in Rigid Spine With Muscular Dystrophy Type 1 in Chinese Patients

*Yanbin Fan[1], Zhifei Xu[2], Xing Li[1], Feng Gao[3], Enyu Guo[4], Xingzhi Chang[1], Cuijie Wei[1], Cheng Zhang[5], Qing Yu[5], Chengli Que[5], Jiangxi Xiao[6], Chuanzhu Yan[7], Zhaoxia Wang[8], Yun Yuan[8] and Hui Xiong[1]**

[1]Department of Pediatrics, Peking University First Hospital, Beijing, China, [2]Department of General Pediatrics, Beijing Children's Hospital, Capital Medical University, Beijing, China, [3]Department of Neurology, Children's Hospital, Zhejiang University School of Medicine, Hangzhou, China, [4]Department of Pediatrics, Jining No. 1 People's Hospital, Jining, China, [5]Department of Respiratory and Critical Care Medicine, Peking University First Hospital, Beijing, China, [6]Department of Radiology, Peking University First Hospital, Beijing, China, [7]Department of Neurology, Qilu Hospital, Shandong University, Qingdao, China, [8]Department of Neurology, Peking University First Hospital, Beijing, China

Congenital muscular dystrophy with early rigid spine, also known as the rigid spine with muscular dystrophy type 1 (RSMD1), is caused by *SEPN1* mutation. We investigated the clinical manifestations, pathological features, and genetic characteristics of 8 Chinese RSMD1 patients in order to improve diagnosis and management of the disease. Eight patients presented with delayed motor development, muscle weakness, hypotonia, and a myopathic face with high palatine arches. All patients could walk independently, though with poor running and jumping, and most had a rigid spine, lordosis, or scoliosis. The symptoms of respiratory involvement were present early, and upper respiratory tract infections and pneumonia often occurred. Five patients had severe pneumonia, pulmonary hypertension, and respiratory failure. Lung function tests showed variable restrictive ventilation dysfunction. Polysomnography suggested hypoxia and hypoventilation. The serum creatine kinase (CK) level was normal or mildly increased. Muscle biopsy indicated chronic myopathic changes and minicores. Muscle magnetic resonance imaging (MRI) showed diffuse fatty infiltration of the gluteus maximus and thigh muscle. *SEPN1* gene analysis revealed 16 compound heterozygous variants, 81.3% of which are unreported, including 7 exon 1 variants. Our study expands the spectrum of clinical and genetic findings in RSMD1 to improve diagnosis, management, and standards of care. *SEPN1* mutations in exon 1 are common and easily missed, and exon 1 should be carefully analyzed when RSMD1 is suspected, which will provide valuable genetic counseling for the family and useful information for future natural history studies and clinical trials.

Keywords: congenital muscular dystrophy with spinal rigidity, rigid spine with muscular dystrophy type 1, respiratory insufficiency, *SEPN1* gene, selenoprotein N

OPEN ACCESS

Edited by:
Matthew E. R. Butchbach, Nemours Children's Health Delaware, United States

Reviewed by:
Ester Zito, Mario Negri Pharmacological Research Institute (IRCCS), Italy
Santasree Banerjee, Beijing Genomics Institute (BGI), China

****Correspondence:***
Hui Xiong
xh_bjbj@163.com

Specialty section:
This article was submitted to Genetics of Common and Rare Diseases, a section of the journal Frontiers in Genetics

Received: *30 November 2021*
Accepted: *14 February 2022*
Published: *16 March 2022*

Citation:
Fan Y, Xu Z, Li X, Gao F, Guo E, Chang X, Wei C, Zhang C, Yu Q, Que C, Xiao J, Yan C, Wang Z, Yuan Y and Xiong H (2022) Novel SEPN1 Mutations in Exon 1 Are Common in Rigid Spine With Muscular Dystrophy Type 1 in Chinese Patients. Front. Genet. 13:825793. doi: 10.3389/fgene.2022.825793

INTRODUCTION

Congenital muscular dystrophy with early rigid spine, also known as the rigid spine with muscular dystrophy type 1 (RSMD1), is caused by *SEPN1/SELENON* (MIM 606210) mutation. RSMD1 is characterized by slowly progressive muscle weakness, early-onset spinal rigidity, scoliosis, and progressive and potentially life-threatening respiratory insufficiency induced by diaphragm weakness (Koul et al., 2014).

In addition to RSMD1, *SEPN1* gene mutations also cause congenital fiber-type disproportion, a severe form of classic multiminicore myopathy, and desmin-related myopathy with Mallory body-like inclusions (Cagliani et al., 2011). Due to the clinical and genetic overlap between these four autosomal recessive conditions, there is an emerging idea that they are all manifestations of the same disease, namely, *SEPN1*-related myopathy (*SEPN1*-RM) (Scoto et al., 2011). However, there is no clear correlation between genotype and pathologic or genetic findings.

The *SEPN1* gene, located on chromosome 1p36.13, contains 13 exons and encodes selenoprotein N, encompassing transmembrane domain, EF-hand domain (Ca^{2+}-interacting region), thioredoxin domain, and SCUG motif (Chernorudskiy et al., 2020; Zhu et al., 2021). The underlying mechanisms of *SEPN1*-RM are unclear as the function of the selenoprotein N is incompletely understood. Selenoprotein N, an endoplasmic reticulum (ER) glycoprotein and an enzyme containing a selenium atom, has an established role in redox-based calcium hemostasis and protects muscle cells from oxidative damage and ER stress (Arbogast et al., 2009; Arbogast and Ferreiro, 2010; Pozzer et al., 2019; Varone et al., 2019). Mutations in *SEPN1* lead to the absence or malfunction of selenoprotein N, and one study has suggested that some compounds effectively rescued the *SEPN1*-devoid cell phenotype *ex vivo* (Arbogast et al., 2009). However, the lack of natural history data, the complications of disease progression or prognosis determinants, and unclear phenotype–genotype correlations hinder the clinical trial implementation.

In this study, we investigated the clinical manifestations, pathological features, and genetic characteristics of 8 Chinese RSMD1 patients in order to improve the diagnosis and management of this disease.

MATERIALS AND METHODS

Clinical Studies

We studied eight patients with a clinical diagnosis of *SEPN1*-RM, performed a retrospective review of medical records, and carried out a prospective cohort study. Clinical and laboratory data, including motor development, family history, serum creatine kinase (CK) levels, pulmonary function test and polysomnography data, electrocardiography (ECG), ultrasound cardiography, and electromyography (EMG) findings, and muscle magnetic resonance imaging (MRI) were collected and analyzed based on the medical records provided by the attending physicians.

Pathological Studies

Skeletal muscle biopsies were performed on probands for pathological diagnosis. Muscle biopsies from the biceps brachii or quadriceps muscle were embedded, frozen in isopentane, and cooled in liquid nitrogen. Frozen sections (6 μm) were cut and processed for routine historical and immunohistochemical staining. A Nikon Eclipse TE2000-S microscope was used to obtain images.

Genetic Analysis

Genomic DNA was extracted from peripheral blood leukocytes using standard protocols. The genomic DNA was first prepared as a DNA library, amplified, and then analyzed by next-generation sequencing (NGS) using a myopathy panel or whole-exon sequencing. After sequencing, the sequencing reads were mapped to the GRC37/hg19 human reference genome using Burrows–Wheeler Aligner software (version 0.59). Then the single-nucleotide variants (SNVs) and small insertions or deletions (InDels) were detected using the GATK UnifiedGenotyper (broadinstitute.org/). Finally, we filtered and selected the variants according to the minor allele frequency (MAF) with a cutoff value of <0.05 in multiple databases (such as 1000 Genome Project, dbSNP, HGMD, HapMap, and in-house Chinese local database). Variants' pathogenicity was evaluated using the variant-classification guidelines of the American College of Medical Genetics and Genomics (ACMG) (Richards et al., 2015) and determined based on the population frequency, phylogenetic conservation analysis, *in silico* prediction programs, and reporting in locus-specific databases. The candidate variants detected using NGS were verified in the probands and family members using Sanger sequencing. Exon 1 of *SEPN1* and its flanking intronic regions were amplified by polymerase chain reaction (PCR) and directly sequenced using Sanger sequencing. The primers of exon 1 are as follows: F- 5′-CTT GGCGTTCCGGTGTAG-3′, R- 5′-ACTCGTCCATGCCCA TGTC-3′; F- 5′-GATCAGCCCCTCTTGGCGTTC-3′, R: CTCTGGATAGAGACCCCTCCAGTC-3′. The reference sequence NM_020451 of *SEPN1* was used.

RESULTS

In total, eight patients were clinically diagnosed with RSMD1, and *SEPN1* gene mutations were confirmed. The clinical features of these patients are summarized in **Tables 1**, **2**.

Clinical Characteristics

Onset of Signs

The age of onset ranged from birth to 1 year old. Five patients (5/8, 62.5%) had a congenital presentation with hypotonia (5/5) and feeding difficulties (3/5). All seven patients presented with delayed motor milestones or gross motor difficulties, subdivided into the following categories: 5/8 (62.5%) poor or delayed head control (after 4 months of age), 4/8 (50.0%) delayed ability to sit unsupported (after 10 months of age), 4/8 (50.0%) delayed walking (after 18 months of age), and 8/8 (100%) difficulty in running or jumping, frequent falls, or easy fatigability.

Muscle Weakness and Functional Abilities

Four patients (4/8, 50.0%) presented with facial weakness, high palatine arches, and a nasal, high-pitched voice. All patients had

TABLE 1 | Clinical features of 8 RSMD1 patients.

Patient	Sex/age	Age of onset	Onset of symptoms	Maximum motor milestone	Contractures	Spinal deformities	CK level (U/L)	ECG	UCG	EMG	Muscle biopsy
1	F/9 y 3 m	Birth	Delayed motor milestones and weakness	Walking and running	Long finger flexor	Rigid spine and mild scoliosis	281	Normal (9 y)	Normal (9 y)	Myogenic	No significant pathological changes (1 y 2 m)
2	M/18 y	Birth	Delayed motor milestones and weakness	Walking	No	Rigid spine and scoliosis	<195	Sinus tachycardia (12 y)	Right ventricular enlargement, interventricular septal hypertrophy, pulmonary hypertension and mild tricuspid regurgitation (12 y); normal (18 y)	Myogenic	Myopathic, minicore (12 y)
3	F/11 y 9 m	<6 m	Delayed motor milestones	Walking	No	Rigid spine, scoliosis, and lordosis	<195	n/a	Mild enlargement of the right heart and mild pulmonary hypertension (6 y 8 m); normal (11 y)	No significant changes	n/a
4	F/12 y 4 m	Birth	Delayed motor milestones and weakness	Walking	No	Rigid spine and scoliosis	<195	Sinus tachycardia (8 y)	Normal (12 y)	No significant changes	n/a
5	F/8 y deceased	Birth	Delayed motor milestones and weakness	Walking and running	No	Rigid spine	<195	Sinus tachycardia (5 y)	Normal (8 y)	No significant changes	Myopathic, minicore (3 y)
6	M/13 y 8 m	1 y	Frequent falls and difficulty running	Walking and running	Elbow, Achilles tendon	Rigid spine, and mild scoliosis	664	n/a	Normal (13 y)	Myogenic	Myopathic, minicore (3 y)
7	F/13 y 5 m	<1 y	Delayed motor milestones and difficulty jumping	Walking	No	Scoliosis	<195	Sinus tachycardia (12 y)	Enlargement of right heart, decreased diastolic function of left ventricle, mild pulmonary hypertension, and mild tricuspid regurgitation (12 y)	Myogenic	n/a
8	F/7 y	<1 y	Delayed motor milestones	Walking, running	No	No	<195	Normal (7 y)	Normal (7 y)	n/a	n/a

F, female; M, male; y, year; m, month; CK, creatine kinase; ECG, electrocardiogram; UCG, ultrasound cardiography; EMG, electromyography; n/a, not available. The upper limit of the normal CK level is 195 U/L.

muscle weakness, especially axial weakness, in the neck flexors, abdominal muscles, and predominantly mild proximal limb muscles, with relatively well-preserved neck extensors. Deep-tendon reflexes were invariably diminished or absent. All patients remained fully ambulant and were able to walk independently indoors and outdoors when last followed up.

TABLE 2 | Respiratory function of 8 *RSMD1* patients.

Patient	Lung function tests		Polysomnography						Severe pneumonia/Age	Respiratory insufficiency/Age	NIV/age
	Age	FVC (% predicted)	Age	Mean nocturnal SpO2 (%)	Minimum nocturnal SpO2 (%)	NH	AHI (/h)	OSAHS			
1	6 y 4 m	75.5	6 y 4 m	96	76	Yes	11.2	No	No	No	No
2	12 y	50.0	12 y	93	60	Yes	n/a	No	No	Yes/12 y	Yes/12 y
			12 y (NIV)	95 (NIV)	80 (NIV)						
3	8 y 7 m	32.2	6 y 3 m	77	23	Yes	41.5	Yes	Yes/5 y	Yes/5 y	Yes/6 y
			9 y (NIV)	97 (NIV)	93 (NIV)						
4	10 y 11 m	31.3	7 y 2 m	91	43	Yes	23.7	Yes	Yes/7 y	Yes/7 y	Yes/7 y
			10 y (NIV)	94 (NIV)	44 (NIV)						
5	6 y 3 m	33.7	6 y 3 m	88	64	Yes	15	No	Yes/5 y	Yes/5 y	Yes/5 y
6	12 y 11 m	42.8	12 y 11 m	82	60	Yes	47.3	Yes	No	No	Yes/13 y
			13 y (NIV)	96 (NIV)	93 (NIV)						
7	12 y 7 m	36.6	12 y	90	80	Yes	n/a	No	No	Yes/12 y	Yes/12 y
			12 y (NIV)	98 (NIV)	93 (NIV)						
8	7 y	n/a	n/a	n/a	n/a	No	n/a	No	No	No	No

y, year; m, month; FVC, forced vital capacity; NH, nocturnal hypoventilation; AHI, apnea–hypopnea index; h, hour; OSAHS, obstructive sleep apnea–hypopnea syndrome; NIV, noninvasive ventilation; n/a, not available.

Spine and Joint Deformity

Six patients (except patients 7 and 8) were first referred for rigid spines between 4 and 12 years old (mean age 6.8 years). In 6 patients, presentation with scoliosis was between 4 and 12 years of age (mean age 8.8 years); patient 3 presented lordosis at 6 years of age. Patient 6 showed contractures involving the elbow and Achilles tendon at 12 years old. After birth, the right ring finger, left pinky finger, and ring finger of patient 1 could not be straightened, and the contracture of the long finger flexor was more pronounced at the age of 1 year old.

Respiratory and Cardiac Involvement

The symptoms of respiratory involvement were present in all patients. They often had upper respiratory tract infections, five (5/8, 62.5%) were susceptible to pneumonia, and three (3/8, 37.5%) had severe pneumonia between the ages of 5 and 7 years.

The respiratory function data of 8 patients are summarized in **Table 2**. Forced vital capacity (FVC) data were available, and all had predicted FVC values (FVC%) below 80%. Pulmonary function tests suggested mild (in patient 1), moderate (in patients 2 and 6), and severe (patients 3, 4, 5, and 7) restrictive ventilation dysfunction. Polysomnography indicated variable hypoxia and nocturnal hypoventilation in all patients (see **Table 2**), and three (3/8) showed low oxygen saturation, apnea, and a high apnea–hypopnea index (AHI), suggestive of obstructive sleep apnea–hypopnea syndrome (OSAHS). Five patients had varying degrees of respiratory insufficiency from 5 to 12 years old (mean age 8.2 years; median 7), requiring nocturnal noninvasive ventilation (NIV) at a mean age of 9.2 years (median 9.5). After NIV treatment, all patients slept well at night, the symptoms of hypoxia and hypoventilation improved, and oxygen saturation at night improved significantly compared with before. Patient 6 declined regular respiratory follow-up and nocturnal NIV, and died at 8 years old. Patients 1 and 8 did not receive NIV in the first decade.

All patients underwent cardiac assessment. Three (3/8) had sinus tachycardia without abnormal electrocardiogram. Although right ventricular enlargement and mild pulmonary hypertension secondary to respiratory insufficiency were observed in the echocardiogram of three patients (3/8, 37.5%), their cardiac function improved after the active non-invasive respiratory support. A normal echocardiogram was obtained for the remaining 5 patients.

Survival

Patient 6 declined regular nocturnal NIV and died from respiratory failure at the age of 8 years because of severe pneumonia.

Auxiliary Tests

Serum CK levels were normal or mildly increased in all patients (see **Table 1**). EMG revealed myogenic changes in 4/8 patients, and no significant changes were found in 3/8 patients.

Muscle MRI

Muscle MRI of probands 1, 3, 4, and 6 showed diffuse fatty infiltration of the gluteus maximus and thigh muscle (**Figure 1**).

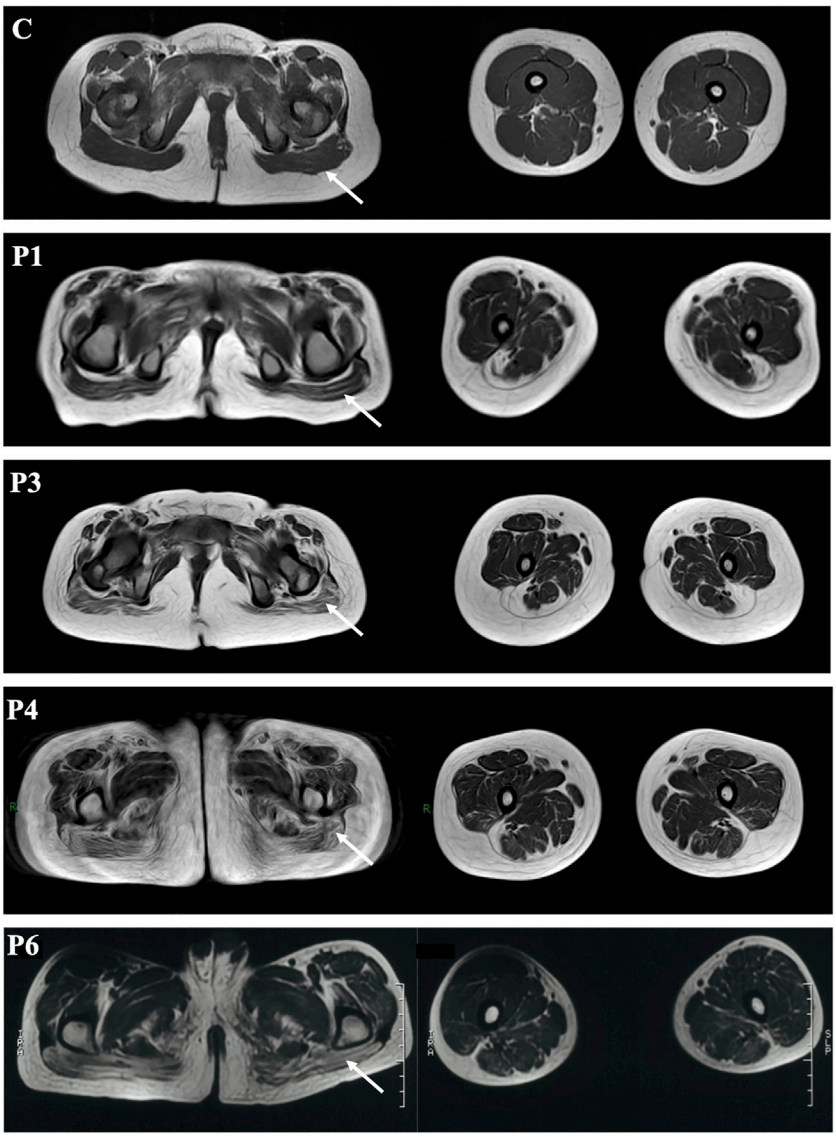

FIGURE 1 | Muscle MRI of RSMD1 patients. Arrows showed the gluteus maximus and thigh. C: control.

All the four patients exhibited fatty infiltration and atrophy of the gluteus maximus, and the adductor magnus was severely affected in patients 4 and 6. The semimembranosus was severely atrophic and absent in patient 1. Several muscles were preserved and mildly affected, including the gracilis, semitendinosus, rectus femoris and tibialis anterior, and tibialis posterior muscles in the lower leg (patients 1 and 6).

Muscle Pathology

Muscle biopsy was performed in patients 1, 2, 5, and 6. Most (patients 2, 5, and 6) indicated chronic myopathic changes with fiber size variation, mild atrophic and regenerative fibers, internalized nuclei, and a mild increase in endomysial connective tissue (see **Figure 2**). NADH staining showed that minicores present small areas of reduced oxidative enzyme reactivity. No significant changes in patient 1 were observed, and the lesions were minimal.

Genetic Analysis

Genomic sequencing revealed 16 compound heterozygous variants (13 unreported, 81.3%) of the *SEPN1* gene (**Figure 3**; **Table 3**), and all tested parents of probands were healthy heterozygous carriers. We observed a cluster of variants in exons 1 (7/16, 43.8%), 10 (2/16, 12.5%), and 11 (3/16, 18.8%) (**Figure 3A**). Exon 1, which included the high GC sequence, harbored the largest number of mutations and was the most frequent variable sequence in our cohort. The types of *SEPN1* mutations mainly included missense (6/16, 37.5%), deletion (5/16, 31.3%), insertion (2/16, 12.5%), duplication (2/16, 12.5%), and insertion–duplication (1/16, 6.2%) (**Figure 3B**).

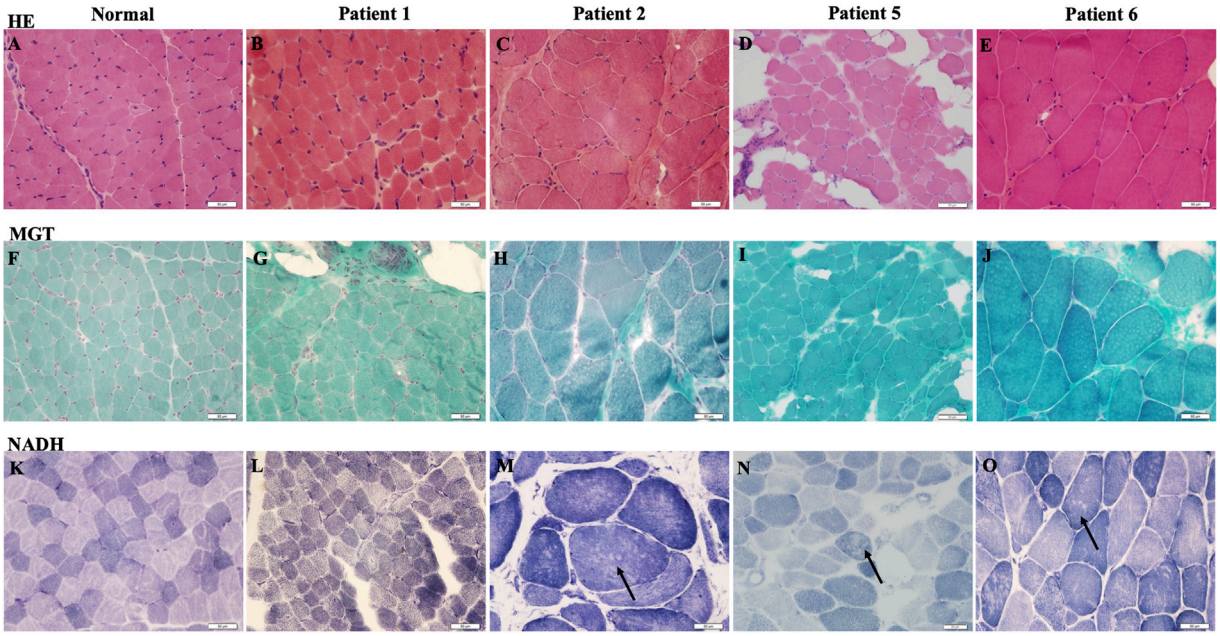

FIGURE 2 | Muscle biopsy of RSMD1 patients: **(A–E)** hematoxylin and eosin (H&E) staining, **(F–J)** modified Gomori Trichrome (MGT) staining, and **(K–O)** β-nicotinamide–adenine dinucleotide (NADH) staining. Arrows showed minicore changes.

The mutations mainly affected the transmembrane domain and thioredoxin (Trx) domain (encompassing the SCUG motif) of selenoprotein N. Ten mutations (62.5%) result in nonsense variants and are predicted to produce truncated proteins. Most missense mutations (5/6, 83.3%) mainly affect the Trx domain, including the SCUG motif (encoding the selenoprotein N putative catalytic site), a variant (c.1384T>A), and causing a loss of selenocysteine (Sec).

DISCUSSION

In this study, we clinically and genetically analyzed a cohort of 8 Chinese RSMD1 patients in detail to improve our understanding of the disease, extend the disease phenotypic spectrum, and facilitate diagnosis and management of the disease. In agreement with previous studies (Scoto et al., 2011), we characterized the clinical phenotype of RSMD1 patients with delayed motor milestones, slowly progressive muscle weakness, spinal rigidity, and progressive and potentially life-threatening respiratory insufficiency.

Although all our patients had a congenital onset, they fully remained ambulant with poor running and jumping, and none needed a wheelchair for an outdoor activity. This suggests that clinical severity is independent of the age at its onset. Axial weakness was generally present with an early onset but often neglected. Since the patients showed preserved limb strength and ambulation, they rarely complained of axial weakness. The muscular disease was suspected when scoliosis and respiratory insufficiency were detected at the end of the first decade.

Joint contractures were not significant in our patients, with only two cases of long finger flexors, elbow, and Achilles tendon. As reported, the contractures most commonly affected the Achilles tendons and elbow, and less frequently the long finger flexors (Scoto et al., 2011). However, in contrast to contractures, spinal rigidity was a presenting feature and a significantly progressive factor in our cohort. *SEPN1*-RM predominantly manifests as cervico-dorsal spinal rigidity that differs from the rigid spine in myopathies caused by mutations in *LMNA* (Quijano-Roy et al., 2008), *EMD* (Kubo et al., 1998), *COL6* (Bönnemann, 2011), or *RYR1* (Bharucha-Goebel et al., 2013). Our patients presented a rigid spine at a mean age of 6.8 years and developed scoliosis at a mean age of 8.8 years, earlier than the reported age of 10 years (Scoto et al., 2011).

Pulmonary function tests showed abnormal FVC values, and PSG suggested variable hypoxia and nocturnal hypoventilation in our patients. In our patients, respiratory insufficiency was found at a mean age of 8.2 years, requiring nocturnal NIV at a mean age of 9.2 years, which was earlier than the reported age of 13 years (Villar-Quiles et al., 2020). Due to obvious diaphragmatic weakness in patients with RSMD1, sleep-related respiratory disorders are likely to occur, which will eventually lead to respiratory insufficiency (Cagliani et al., 2011). In our cohort, pulmonary hypertension secondary to respiratory insufficiency improved with nocturnal NIV, and there was no clear progressive deterioration of the respiratory function with good oxygen saturation at night. FVC values are reported to be essentially stable after the 2nd decade of life following the introduction of NIV (Scoto et al., 2011). In our cohort, one patient who refused NIV died of respiratory failure. The respiratory function declines systematically from the end of the third decade, and early NIV

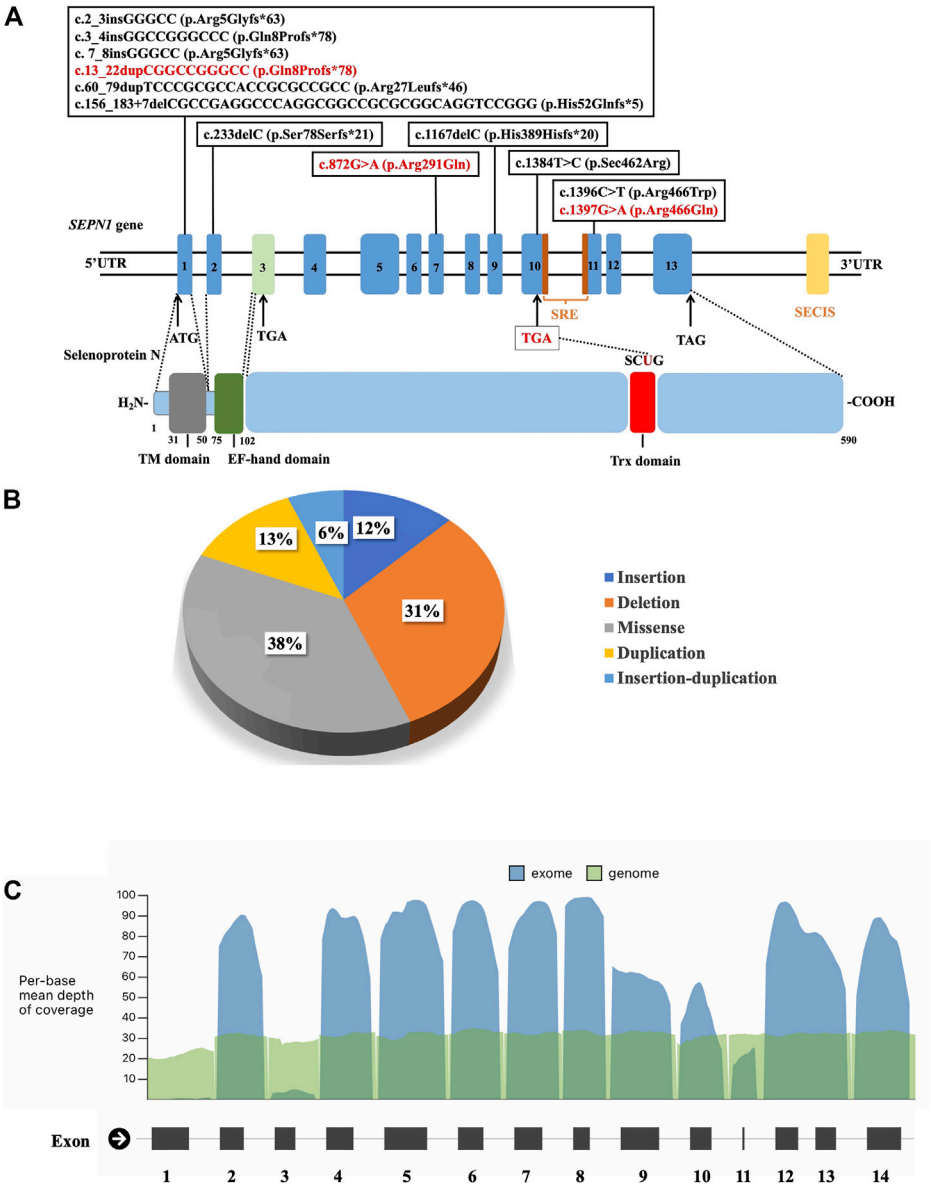

FIGURE 3 | (A) Schematic localization of the variants identified in the *SEPN1* gene. ATG: initiation codon. EF-hand domain: Ca^{2+}-interacting region. SECIS: selenocysteine insertion sequence. SRE: selenocysteine redefinition element. TAG, TGA: termination codon. TM domain: transmembrane domain. Trx domain: thioredoxin domain, encompassing SCUG motif. UTR: untranslated region. **(B)** The types of *SEPN1* variants. **(C)** Mean depth of coverage in *SEPN*1 exons and genome by next-generation sequencing (https://gnomad.broadinstitute.org).

may initially stabilize the respiratory muscle strength (Caggiano et al., 2017). Respiratory involvement might be aggravated by spinal deformities, especially scoliosis. Indeed, one study reported that one-third of patients had a spinal fusion at a mean age of 13.9 years, with good tolerance and no deterioration of motor or respiratory function after surgery (Scoto et al., 2011). Therefore, it is important to improve the prognosis by managing scoliosis and respiratory insufficiency.

Muscle MRI in our patients revealed the involvement of the gluteus maximus and adductor magnus, and the lower leg was mildly affected. The semimembranosus is reportedly the most abnormal muscle in all *SEPN1*-RM patients (Flanigan et al., 2000). However, it was present in patient 1 but not in some RSMD1 patients (Mercuri et al., 2010). A distinct radiological pattern in *SEPN1*-RM with predominant axial and cervical muscle involvement, severe wasting of sternocleidomastoid muscles, and dramatic atrophy of semimembranosus, with relative preservation of the rectus femoris, long adductor, and gracilis, has been reported (Hankiewicz et al., 2015). This information might be useful for diagnosis even in very young patients or those with mild disease. We found no clear correlation between histopathological findings and clinical

TABLE 3 | Genetic analysis of 8 RSMD1 patients.

Patient	Exon	Nucleotide change	Predicted amino acid change	Protein domain affected	Inheritance	Novel/ reported
1	1	c.7_8insGGGCC	p.(Arg5Glyfs*63)	Transmembrane domain	Maternal	Novel
	9	c.1167delC	p.(His389Hisfs*20)	Non-cytoplasmic domain	Paternal	Novel
2	2	c.233delC	p.(Ser78Serfs*21)	Ca^{2+}-interacting region (EF-hand domain)	Paternal	Novel
	10	c.1384T>C	p.(Sec462Arg)	SCUG motif (Selenocysteine)	Maternal	Novel
3	1	c.2_3insGGGCC	p.(Arg5Glyfs*63)	Transmembrane domain	Maternal	Novel
	1	c.3_4insdupGGCCGGGCCC	p.(Gln8Profs*78)	Transmembrane domain	Paternal	Novel
4	2	c.233delC	p.(Ser78Serfs*21)	Ca^{2+}-interacting region (EF-hand domain)	Paternal	Novel
	11	c.1397G>A	p.Arg466Gln	Thioredoxin domain	Maternal	Reported
5	1	c.60_79dupTCCCGCGCCACCGCGCCGCC	p.(Arg27Leufs*46)	Transmembrane domain	Maternal	Novel
	10	c.1384T>C	p.(Sec462Arg)	SCUG motif (Selenocysteine)	Paternal	Novel
6	1	c.13_22dupCGGCCGGGCC	p.Gln8Profs*78	Transmembrane domain	Maternal	Reported
	7	c.872G>A	p.Arg291Gln	Non-cytoplasmic domain	Paternal	Reported
7	1	c.156_183+7delCGCCGAGGCCCAGGCGGCCGCGCGGCAGGTCCGGG	p.(His52Glnfs*5)	Transmembrane domain	Maternal	Novel
	11	c.1396C>T	p.(Arg466Trp)	Thioredoxin domain	Paternal	Novel
8	1	c.156_183+7delCGCCGAGGCCCAGGCGGCCGCGCGGCAGGTCCGGG	p.(His52Glnfs*5)	Transmembrane domain	Maternal	Novel
	11	c.1396C>T	p.(Arg466Trp)	Thioredoxin domain	Paternal	Novel

features. Muscle biopsy indicated chronic myopathic changes and minicores, as previously described (Scoto et al., 2011; Villar-Quiles et al., 2020), and the age and site of biopsy correlated with the histopathological variability. Muscle biopsy is recommended at the school age to promote diagnosis.

In our study, exon 1 harbored the highest number of mutations. Mutations in *SEPN1* are distributed along with the whole gene, except for exon 3. GC-rich exon 1 has been reported as a major hotspot, although it is poorly or not covered by NGS panels (see **Figure 3C**). Hence, mutations in exon 1 of *SEPN1* are easily missed by NGS, and NGS data should be re-analyzed, or the detection of exon 1 using Sanger sequencing should be performed. Moreover, the first *SEPN1* copy number variation (c.(872+1_873-1)(1602+1_1603-1) del), a large out-of-frame deletion affecting exons 7 to 12, was identified (Villar-Quiles et al., 2020). Mutations in the *SEPN1* 3′ UTR selenocysteine insertion sequence (SECIS), an untranslated cis element necessary for selenocysteine integration, were also found (Villar-Quiles et al., 2020). All these findings highlight the need to search for *SEPN1* copy number variations and mutations in SECIS, particularly when only one *SEPN1* pathogenic variant has been detected.

Most *SEPN1* mutations in our cohort were null mutations producing truncated proteins prone to nonsense-mediated decay (NMD). As reported, all mutations located around or in the sequence encoding the potential catalytic site (SCUG motif) were missense. The codon UGA encoding selenocysteine is located in exon 10 (c. 1384_1386); UGA is usually a termination codon, which causes coding termination, but selenoprotein N is unique. The SECIS located in the 3′UTR of the mRNA and the selenocysteine redefinition element (SRE) downstream of the UGA jointly mediate the selenocysteine insertion into the selenoprotein N polypeptide chain (Moghadaszadeh et al., 2013). Mutations in the codon UGA encoding selenocysteine, SECIS, and SRE can reduce the insertion efficiency of selenocysteine, reduce the level of mRNA, and ultimately affect the synthesis and expression of selenoprotein N (Maiti et al., 2009). We also detected mutations in the EF-hand domain-encoding sequence. We did not observe a clear genotype–phenotype correlation. Biallelic null mutations may be associated with higher disease severity, which is the only genotype–phenotype correlation that has been proposed (Villar-Quiles et al., 2020).

Selenoprotein N, an endoplasmic reticulum glycoprotein, is a member of an enzyme family containing one selenium atom that binds covalently to form selenocysteine in the catalytic region (Castets et al., 2012). Selenoprotein N participates in redox reactions (Moghadaszadeh et al.,

2013) and calcium homeostasis (Lescure et al., 2009), protects cells from the oxidative stress (Arbogast and Ferreiro, 2010), and plays a role in early embryonic development, cell proliferation, and regeneration (Castets et al., 2009). Excessive oxidative damage induces dysfunction and degradation of muscle fibers, which is considered a primary pathophysiological mechanism of *SEPN1*-RM (Varone et al., 2019). Selenoprotein N is required for calcium transients between the ER–mitochondria, thereby controlling mitochondrial bioenergetics. The mutation of *SEPN1* leads to impaired ER–mitochondria contacts and decreased ATP levels in muscle cells (Filipe et al., 2021). The antioxidant N-acetylcysteine has been identified as an effective protective agent against oxidative stress-induced cell death (Arbogast and Ferreiro, 2010) and should be considered in future clinical trials. Multidisciplinary management should be provided to patients, including physical rehabilitation and nursing, cardiovascular and respiratory management, nutritional support, orthopedic surgery, and psychological care. We recommend yearly follow-up, including respiratory and cardiac evaluations and spine surveillance. Regular pulmonary function tests and PSG are recommended for all patients, and NIV should be used as soon as nocturnal hypoventilation or respiratory failure is detected.

In summary, our study expands the spectrum of clinical and genetic findings in RSMD1 and provides valuable genetic counseling for the families. The findings will contribute to improving diagnosis, management, and standards of care, and provide useful information on future natural history studies and clinical trials.

DATA AVAILABILITY STATEMENT

All datasets generated for this study are included in the article/supplementary material.

ETHICS STATEMENT

The studies involving human participants were reviewed and approved by the Ethics Committee of Peking University First Hospital. Written informed consent to participate in this study was provided by the participants' legal guardian/next of kin.

AUTHOR CONTRIBUTIONS

YF conducted the patient follow-up and wrote the first draft of the manuscript. XL and CW helped collect the clinical and laboratory data, and followed up on patients. FG, EG, CY, ZW, and YY provided patients' data as multi-center participants. ZX, CZ, QY, and CQ helped analyze the respiratory data of all the patients. XC analyzed muscle biopsies of the patients. JX analyzed muscle MRI. HX conceived the study, participated in its design and coordination, and helped to draft the manuscript. All the authors participated in drafting and critically revising the article, and approved the final manuscript.

FUNDING

This study was supported by grants from the Natural Science Foundation of Beijing Municipality (No. 7212116), the National Natural Science Foundation of China (No. 82171393), the National Key Research and Development Program of China (No. 2016YFC0901505), and Beijing Key Laboratory of Molecular Diagnosis and Study on Pediatric Genetic Diseases (No. BZ0317).

ACKNOWLEDGMENTS

The authors appreciated all the grant supports that enabled this research. The authors thank all the health providers, patients, and their families who have participated in this study.

REFERENCES

Arbogast, S., Beuvin, M., Fraysse, B., Zhou, H., Muntoni, F., and Ferreiro, A. (2009). Oxidative Stress inSEPN1-Related Myopathy: From Pathophysiology to Treatment. *Ann. Neurol.* 65, 677–686. doi:10.1002/ana.21644

Arbogast, S., and Ferreiro, A. (2010). Selenoproteins and protection against Oxidative Stress: Selenoprotein N as a Novel Player at the Crossroads of Redox Signaling and Calcium Homeostasis. *Antioxid. Redox Signaling* 12, 893–904. doi:10.1089/ars.2009.2890

Bharucha-Goebel, D. X., Santi, M., Medne, L., Zukosky, K., Dastgir, J., Shieh, P. B., et al. (2013). Severe Congenital RYR1-Associated Myopathy: the Expanding Clinicopathologic and Genetic Spectrum. *Neurology* 80, 1584–1589. doi:10.1212/WNL.0b013e3182900380

Bönnemann, C. G. (2011). The Collagen VI-related Myopathies. *Handb Clin. Neurol.* 101, 81–96. doi:10.1016/B978-0-08-045031-5.00005-0

Caggiano, S., Khirani, S., Dabaj, I., Cavassa, E., Amaddeo, A., Arroyo, J. O., et al. (2017). Diaphragmatic Dysfunction in SEPN1-Related Myopathy. *Neuromuscul. Disord.* 27, 747–755. doi:10.1016/j.nmd.2017.04.010

Cagliani, R., Fruguglietti, M. E., Berardinelli, A., D'Angelo, M. G., Prelle, A., Riva, S., et al. (2011). New Molecular Findings in Congenital Myopathies Due to Selenoprotein N Gene Mutations. *J. Neurol. Sci.* 300, 107–113. doi:10.1016/j.jns.2010.09.011

Castets, P., Lescure, A., Guicheney, P., and Allamand, V. (2012). Selenoprotein N in Skeletal Muscle: from Diseases to Function. *J. Mol. Med.* 90, 1095–1107. doi:10.1007/s00109-012-0896-x

Castets, P., Maugenre, S., Gartioux, C., Rederstorff, M., Krol, A., Lescure, A., et al. (2009). Selenoprotein N Is Dynamically Expressed during Mouse Development and Detected Early in Muscle Precursors. *BMC Dev. Biol.* 9, 46. doi:10.1186/1471-213X-9-46

Chernorudskiy, A., Varone, E., Colombo, S. F., Fumagalli, S., Cagnotto, A., Cattaneo, A., et al. (2020). Selenoprotein N Is an Endoplasmic Reticulum Calcium Sensor that Links Luminal Calcium Levels to a Redox Activity. *Proc. Natl. Acad. Sci. USA* 117 (35), 21288–21298. doi:10.1073/pnas.2003847117

Filipe, A., Chernorudskiy, A., Arbogast, S., Varone, E., Villar-Quiles, R.-N., Pozzer, D., et al. (2021). Defective Endoplasmic Reticulum-Mitochondria Contacts and Bioenergetics in SEPN1-Related Myopathy. *Cell Death Differ* 28, 123–138. doi:10.1038/s41418-020-0587-z

Flanigan, K. M., Kerr, L., Bromberg, M. B., Leonard, C., Tsuruda, J., Zhang, P., et al. (2000). Congenital Muscular Dystrophy with Rigid Spine Syndrome: a Clinical, Pathological, Radiological, and Genetic Study. *Ann. Neurol.* 47, 152–161. doi:10.1002/1531-8249(200002)47:2<152::aid-ana4>3.0.co;2-u

Hankiewicz, K., Carlier, R. Y., Lazaro, L., Linzoain, J., Barnerias, C., Gómez-Andrés, D., et al. (2015). Whole-body Muscle Magnetic Resonance Imaging inSEPN1-Related Myopathy Shows a Homogeneous and Recognizable Pattern. *Muscle Nerve* 52, 728–735. doi:10.1002/mus.24634

Koul, R., Al-Yarubi, S., Al-Kindy, H., Al-Futaisi, A., Al-Thihli, K., Chacko, P. A., et al. (2014). Rigid Spinal Muscular Dystrophy and Rigid Spine Syndrome. *J. Child. Neurol.* 29, 1436–1440. doi:10.1177/0883073813479173

Kubo, S., Tsukahara, T., Takemitsu, M., Yoon, K. B., Utsumi, H., Nonaka, I., et al. (1998). Presence of Emerinopathy in Cases of Rigid Spine Syndrome. *Neuromuscul. Disord.* 8, 502–507. doi:10.1016/s0960-8966(98)00069-8

Lescure, A., Rederstorff, M., Krol, A., Guicheney, P., and Allamand, V. (2009). Selenoprotein Function and Muscle Disease. *Biochim. Biophys. Acta (Bba) - Gen. Subjects* 1790, 1569–1574. doi:10.1016/j.bbagen.2009.03.002

Maiti, B., Arbogast, S., Allamand, V. r., Moyle, M. W., Anderson, C. B., Richard, P., et al. (2009). A Mutation in theSEPN1selenocysteine Redefinition Element (SRE) Reduces Selenocysteine Incorporation and Leads toSEPN1-Related Myopathy. *Hum. Mutat.* 30, 411–416. doi:10.1002/humu.20879

Mercuri, E., Clements, E., Offiah, A., Pichiecchio, A., Vasco, G., Bianco, F., et al. (2010). Muscle Magnetic Resonance Imaging Involvement in Muscular Dystrophies with Rigidity of the Spine. *Ann. Neurol.* 67, 201–208. doi:10.1002/ana.21846

Moghadaszadeh, B., Rider, B. E., Lawlor, M. W., Childers, M. K., Grange, R. W., Gupta, K., et al. (2013). Selenoprotein N Deficiency in Mice Is Associated with Abnormal Lung Development. *FASEB j.* 27, 1585–1599. doi:10.1096/fj.12-212688

Pozzer, D., Varone, E., Chernorudskiy, A., Schiarea, S., Missiroli, S., Giorgi, C., et al. (2019). A Maladaptive ER Stress Response Triggers Dysfunction in Highly Active Muscles of Mice with SELENON Loss. *Redox Biol.* 20, 354–366. doi:10.1016/j.redox.2018.10.017

Quijano-Roy, S., Mbieleu, B., Bönnemann, C. G., Jeannet, P.-Y., Colomer, J., Clarke, N. F., et al. (2008). De novoLMNAmutations Cause a New Form of Congenital Muscular Dystrophy. *Ann. Neurol.* 64, 177–186. doi:10.1002/ana.21417

Richards, S., Aziz, N., Bale, S., Bick, D., Das, S., Gastier-Foster, J., et al. (2015). Standards and Guidelines for the Interpretation of Sequence Variants: a Joint Consensus Recommendation of the American College of Medical Genetics and Genomics and the Association for Molecular Pathology. *Genet. Med.* 17, 405–424. doi:10.1038/gim.2015.30

Scoto, M., Cirak, S., Mein, R., Feng, L., Manzur, A. Y., Robb, S., et al. (2011). SEPN1-related Myopathies: Clinical Course in a Large Cohort of Patients. *Neurology* 76, 2073–2078. doi:10.1212/WNL.0b013e31821f467c

Varone, E., Pozzer, D., Di Modica, S., Chernorudskiy, A., Nogara, L., Baraldo, M., et al. (2019). SELENON (SEPN1) Protects Skeletal Muscle from Saturated Fatty Acid-Induced ER Stress and Insulin Resistance. *Redox Biol.* 24, 101176. doi:10.1016/j.redox.2019.101176

Villar-Quiles, R. N., von der Hagen, M., Métay, C., Gonzalez, V., Donkervoort, S., Bertini, E., et al. (2020). The Clinical, Histologic, and Genotypic Spectrum of SEPN1-Related Myopathy. *Neurology* 95, e1512–e1527. doi:10.1212/WNL.0000000000010327

Zhu, S. Y., Liu, L. L., Huang, Y. Q., Li, X. W., Talukder, M., Dai, X. Y., et al. (2021). In Silico analysis of Selenoprotein N (Gallus gallus): Absence of EF-Hand Motif and the Role of CUGS-helix Domain in Antioxidant protection. *Metallomics* 13, mfab004. doi:10.1093/mtomcs/mfab004

Conflict of Interest: The authors declare that the research was conducted in the absence of any commercial or financial relationships that could be construed as a potential conflict of interest.

Publisher's Note: All claims expressed in this article are solely those of the authors and do not necessarily represent those of their affiliated organizations, or those of the publisher, the editors, and the reviewers. Any product that may be evaluated in this article, or claim that may be made by its manufacturer, is not guaranteed or endorsed by the publisher.

frontiers in Genetics

ORIGINAL RESEARCH
published: 18 March 2022
doi: 10.3389/fgene.2022.867413

The Presence of Vacuolated Kupffer Cells Raises a Clinical Suspicion of Niemann-Pick Disease Type C in Neonatal Cholestasis

*Neng-Li Wang[1†], Lian Chen[2†], Yi Lu[1], Xin-Bao Xie[1], Jing Lin[3], Kuerbanjiang Abuduxikuer[1] and Jian-She Wang[1]**

[1]Center for Pediatric Liver Diseases, Children's Hospital of Fudan University, Shanghai, China, [2]Department of Pathology, Children's Hospital of Fudan University, Shanghai, China, [3]Department of Pediatrics, Icahn School of Medicine at Mount Sinai, New York, NY, United States

OPEN ACCESS

Edited by:
Yuan-Zong Song,
First Affiliated Hospital of Jinan University, China

Reviewed by:
Hanaa El-Karaksy,
Cairo University, Egypt
Andrés D. Klein,
Universidad del Desarrollo, Chile
Jan Lukas,
University Hospital Rostock, Germany

***Correspondence:**
Jian-She Wang
jshwang@shmu.edu.cn

†These authors have contributed equally to this work and share first authorship

Specialty section:
This article was submitted to Genetics of Common and Rare Diseases, a section of the journal Frontiers in Genetics

Received: 01 February 2022
Accepted: 22 February 2022
Published: 18 March 2022

Citation:
Wang N-L, Chen L, Lu Y, Xie X-B, Lin J, Abuduxikuer K and Wang J-S (2022) The Presence of Vacuolated Kupffer Cells Raises a Clinical Suspicion of Niemann-Pick Disease Type C in Neonatal Cholestasis. Front. Genet. 13:867413. doi: 10.3389/fgene.2022.867413

Early diagnosis of Niemann-Pick disease type C (NP-C) in neonatal cholestasis is still challenging because splenomegaly is non-specific and oxysterol profiling studies also have a relatively low specificity. This study explores a method for identifying infants with a high clinical suspicion of NP-C in neonatal cholestasis. We reviewed the clinical findings of 9 neonatal cholestatic infants with NP-C genetically diagnosed between January 2015 and December 2020. Seven underwent liver biopsy at ages ranging from 35 to 112 d. Foam cells were only detected in 2 (28.6%, 2/7) liver tissues obtained beyond 3 months of age. However, vacuolated Kupffer cells were detected in all 7 liver tissues. Their significance was explored by using 168 neonatal cholestatic infants, who underwent genetic tests and liver biopsy between January 2018 and December 2020. Of them, 26 detected vacuolated Kupffer cells. Six (23.1%, 6/26) were diagnosed as NP-C, comparing to none of the 142 neonatal cholestatic infants without vacuolated Kupffer cells ($\chi^2 = 33.983$, $p < 0.001$). The ratio of positive diagnosis of NP-C was 31.6% (6/19) in neonatal cholestatic infants with both vacuolated Kupffer cells and splenomegaly. Therefore, we conclude that the presence of vacuolated Kupffer cells can raise a high clinical suspicion of NP-C in neonatal cholestatic infants, especially in those with splenomegaly.

Keywords: neonatal cholestasis, infant, Niemann-Pick disease type C, Kupffer cell, diagnosis

INTRODUCTION

Niemann-Pick disease type C (NP-C) is a rare progressive and life limiting lysosomal storage disorder. It results from compound heterozygous or homozygous pathogenic variants in either of the two genes: *NPC1* or *NPC2* (Carstea et al., 1993; Vanier et al., 1996). Nearly 95% of cases are caused by NPC1 deficiency, with approximately 5% caused by NPC2 deficiency (Jahnova et al., 2014). It is classified as visceral-neurodegenerative form (early-infantile), neurodegenerative form (late-infantile and juvenile), and psychiatric-neurodegenerative form (adult) (Patterson, 2000; Geberhiwot et al., 2018). Primary manifestations are age dependent. In early infancy, clinical manifestations are predominantly visceral, with cholestasis and hepatosplenomegaly (Patterson, 2000). Cholestasis in the majority spontaneously resolves after 3–4 months of age, while splenomegaly persists and neurological symptoms develop with age (Evans et al., 2017; Geberhiwot et al., 2018). The early diagnosis is the key for reduction of organ damage since a medical treatment is available now (Pineda et al., 2018).

Newborn screening for NP-C still has not been developed. Splenomegaly in neonatal cholestatic infants raises a clinical suspicion of NP-C (Geberhiwot et al., 2018). Two plasma oxysterols, 7-ketocholesterol (7 KC) and cholestane-3β,5α,6β-triol (C-triol), are biomarkers for aiding diagnosis (Mazzacuva et al., 2016; Maekawa et al., 2020). Genetic tests can lead to a definite diagnosis. However, early diagnosing of NP-C is still challenging because splenomegaly is non-specific (Mazzacuva et al., 2016; Maekawa et al., 2020) and oxysterol profiling studies also have a relatively low specificity for NP-C in neonatal cholestasis (Polo et al., 2016; Degtyareva et al., 2019). Genetic tests are usually ordered if an inherited disorder is suspected. Therefore, an alternative is necessary for early identification of infants with a clinical suspicion of NP-C in neonatal cholestasis.

This study summarized the clinical findings of 9 NP-C infants presenting as neonatal cholestasis, and unexpectedly found that vacuolated Kupffer cells were detected in all liver tissues obtained in the early disease course. We also explored the significance of vacuolated Kupffer cells on early detection of infants with a high suspicion of NP-C in neonatal cholestasis.

METHODS

Patients and Definitions

This study enrolled neonatal cholestatic infants (onset <3 months of age) diagnosed as NP-C who were referred to the Children's Hospital of Fudan University between January 2015 and December 2020. The diagnosis of NP-C is established if *NPC1* or *NPC2* biallelic pathogenic/likely pathogenic variants are identified. Cholestasis is defined as follows (Togawa et al., 2016): serum direct bilirubin (DB) > 20.0% of total bilirubin (TB) if TB > 85.5 μmol/L; or DB > 17.1 μmol/L if TB < 85.5 μmol/L. Hepatomegaly and splenomegaly were diagnosed by ultrasonography.

To explore the significance of vacuolated Kupffer cells, this study also enrolled 168 consecutive infants with neonatal cholestasis, who underwent both genetic tests and liver biopsy, between January 2018 and December 2020. Following a work-up for neonatal cholestasis as described previously (Liu et al., 2010), surgical, infectious, parenteral nutrition, endocrinological, and drug-induced causes were excluded.

The study was approved by the ethics committees of the Children's Hospital, Fudan University and conducted in full compliance with medical ethics standards. Informed consent had been obtained from the parents/guardians during the admission. Clinical data were collected from their medical records.

Genetic Testing

Genetic testing was performed in the Translational Center of Children's Hospital of Fudan University. Genomic DNA was extracted from peripheral blood. *NPC1* variants (NM_000271) and *NPC2* variants (NM_006432) were screened by NGS, including panel, medical exome, and whole exome sequencing. The procedures of sequencing, data analyses, and variation classification were described previously (Wang et al., 2016; Qiu et al., 2017; Zhang et al., 2020). Variant pathogenicity was assessed according to the American College of Medical Genetics and Genomics (ACMG) standards and guidelines (Richards et al., 2015).

TABLE 1 | Molecular findings in *NPC1* (NM_000271) of 9 patients with neonatal cholestasis.

	Variant 1	Variant 2	Origin
P1	c.1757 + 3_1757+6delGAGT	**c.3254_3255delAT**	M/F
P2	**c.10delC**	c.1211G > A (p.R404Q)	ND
P3	**c.1024T > C (p.W342R)**	**c.2970_2971insTCCT**	M/F
P4	**c.3254A > C (p.Y1085S)**	**c.3254A > C (p.Y1085S)**	F/M
P5	c.1138C > T (p.L380F)	c.1211G > A (p.R404Q)	F/M
P6	c.352_353delAG	c.2000C > T (p.S667L)	ND
P7	**c.2207_2208dupTC**	c.2972_2973delAG	M/F
P8	c.1421C > T (p.P474L)	c.2728G > A (p.G910S)	ND
P9	c.1301C > T (p.P434L)	c.3425T > C (p.M1142T)	ND

P, patient; ND, not done; F, father; M, mother.
Novel pathogenic or likely pathogenic variants are shown in bold font.

Histologic Studies

Liver tissues were obtained by needle biopsy or intraoperative wedge biopsy. Liver tissues sections were stained by hematoxylin and eosin (HE), periodic acid-schiff (PAS), anti-CD68 (GENE, Shanghai, China), etc.

Smears of bone marrow aspirations were Wright's stained.

Statistical Analysis

Statistical analysis was performed using SPSS Inc. version 17.0 software (University of Chicago, Chicago, IL). Difference among ratios was tested by Chi-square test using Fisher's exact value. Comparison of two medians was done by nonparametric Mann-Whitney test. $p < 0.05$ was considered significant.

RESULTS

Molecular Findings

A total of 9 neonatal cholestatic infants, including 4 boys and 5 girls, were finally diagnosed as NP-C for harboring biallelic pathogenic or likely pathogenic variants in *NPC1* (**Table 1**). No infant was found to harbor biallelic pathogenic variants in *NPC2*. Sixteen distinct *NPC1* variants were identified, including 10 known disease-causing variants and 6 novel variants (4 frameshift indels and 2 missense variants) absented from the Genome Aggregation Database (GnomAD). The 2 novel missense variants, c.1024T > C (p.W342R) and c.3254A > C (p.Y1085S), were predicted to be disease causing and damaging by MutationTaster, Polyphen-2, and SIFT. Both were rated as likely pathogenic variants, while the 4 novel frameshift indels as pathogenic variants according to the ACMG standards and guidelines.

Clinical Findings

The 9 NP-C infants came from 9 distinct nonconsanguineous families. Jaundice and hepatosplenomegaly were identified in

TABLE 2 | Clinical findings of the 9 NPC patients presenting as neonatal cholestasis.

	P1	P2	P3	P4	P5	P6	P7	P8	P9
First symptoms	J	J	J	J	J	J	J	J	J
Age at first symptoms (d)	4	2	1	7	2	28	5	3	4
Other symptoms and signs									
Acholic stools	+	+	+	-	+	+	+	-	-
Hepatomegaly	+	+	+	+	+	+	+	+	+
Splenomegaly	+	+	+	+	+	+	+	+	+
Liver function tests (LFTs)									
Age at tests (d)	35	33	44	62	89	53	79	97	60
TB (μmol/L)	164	168	211	141	125	287	56	158	104
DB (μmol/L)	136	102	119	108	104	229	46	117	58
ALT (U/L)	55	59	41	110	152	117	63	72	58
AST (U/L)	206	199	309	338	371	250	174	283	177
GGT (U/L)	144	254	54	147	222	126	49	259	167
TBA (μmol/L)	69	96	96	84	66	114	59	158	106
Alb (g/L)	34.6	35.0	38.4	41.8	32.2	40.2	36.3	39.7	43.3
Glu (mmol/L)	4.0	ND	6.0	4.2	2.9	2.5	4.1	2.0	1.9

P, patient; J, jaundice; ND, not done; TB, total bilirubin; DB, direct bilirubin; ALT, alanine aminotransferase; AST, aspartate aminotransferase; GGT, γ-glutamyl transpeptidase; TBA, total bile acid; Alb, albumin; Glu, glucose.
-, negative; +, positive.

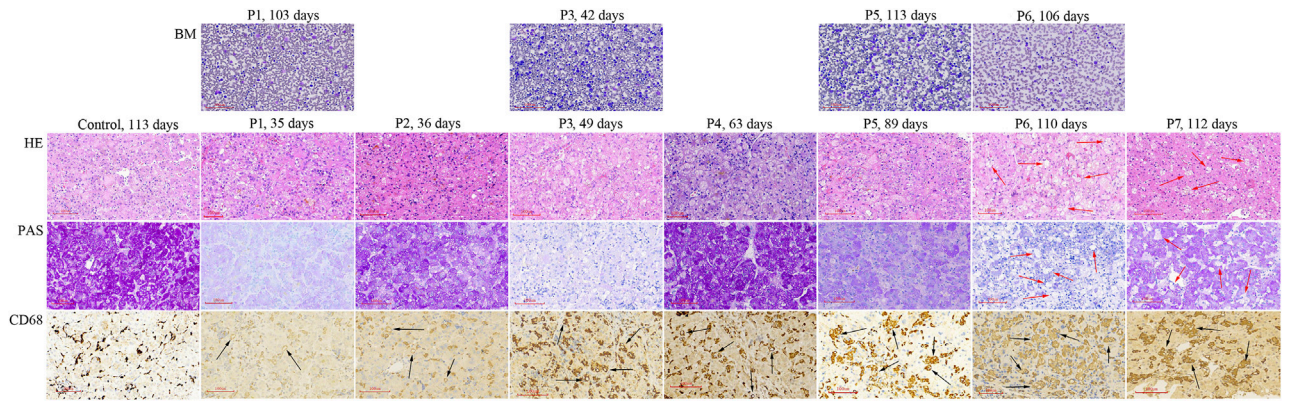

FIGURE 1 | Histologic studies of bone marrow aspirations and liver tissues obtained from NP-C patients presenting as neonatal cholestasis. Vacuolated Kupffer cells (black arrow) are observed in CD68 staining sections from liver tissues of all 7 NP-C infants (P1 ~ P7), but not in control (a neonatal cholestatic infant with unknown cause). Foam cells (red arrow) are observed in HE and PAS sections of P6 and P7 when vacuolated Kupffer cells with enlarged sizes become obvious. BM, bone marrow aspiration; LS, liver specimens; P, patient.

all 9 patients (**Table 2**). Six exhibited acholic stools. Seven, but not patient (P) 3 and P7, were classified into cholestasis with high serum γ-glutamyl transpeptidase (GGT >100U/L). Aspartate aminotransferase (AST) was elevated in all 9 patients, and the ratios of AST to alanine aminotransferase (ALT) ranged from 2.1 to 7.5. Hypoglycemia (blood glucose levels<3.0 mmol/L) was present in 4 patients (P5, P6, P8, and P9) after fasting for 3 h.

P1 ~ P7 underwent liver biopsy. Foam cells were only detected in HE staining sections of P6 and P7, but vacuolated Kupffer cells were detected in CD68 staining sections from all 7 liver tissues (**Figure 1**) Vacuolated Kupffer cells were scattered in P1 and P2, whose liver tissues were obtained at the age of 35 and 36 d, respectively. More vacuolated Kupffer cells were identified in P3 and P4 at the age of 49 and 63 d, respectively. Most Kupffer cells detected lipid vacuoles in P5 at 89 d of age, and a few had enlarged sizes. Vacuolated Kupffer cells with enlarged sizes became obvious in P6 and P7 at the age of 110 and 112 d, respectively.

Bone marrow aspiration was performed in P1, P3, P5, and P6 at ages ranging from 42 to 113 d, but no foam cell was observed (**Figure 1**).

Significance of Vacuolated Kupffer Cells

Of the 168 enrolled neonatal cholestatic infants, 26 detected vacuolated Kupffer cells, including 19 with splenomegaly (**Table 3**). Six of the 26 infants (P1 ~ P5, and P7) were diagnosed as NP-C, comparing to none of the 142 infants without vacuolated Kupffer cells (6/26 vs. 0/142, $\chi^2 = 33.983$, $p < 0.001$). The ratio of positive diagnosis of NP-C was 23.1% (6/26) in neonatal cholestatic infants with vacuolated Kupffer

TABLE 3 | Basic information of the 168 neonatal cholestatic infants with unexplained causes.

	With vacuolated Kupffer cells (*n* = 26)	Without vacuolated Kupffer cells (*n* = 142)
Gender (male/female)	14/12	92/50
Hepatomegaly	26 (100%)	142 (100%)
Splenomegaly	19 (73.1%)	47 (33.1%) *
Age at liver biopsy (d)	68 [46, 90]	73 [59, 100]
NP-C (*NPC1*)	6 (23.1%)	0 (0.0%) *
NP-C (*NPC2*)	0	0

NP-C, Niemann-Pick disease type C.
Interquartile range in square brackets.

cells, and it could increase to 31.6% (6/19) in neonatal cholestatic infants with both vacuolated Kupffer cells and splenomegaly.

DISCUSSION

The diagnosis of NP-C is often delayed in neonatal cholestasis. The measurement of biochemical markers, such as plasm oxysterols, is recommended for early detection of NP-C (Vanier et al., 2016; Geberhiwot et al., 2018), while liver biopsy is now rarely needed (Geberhiwot et al., 2018; Patterson, 2000). Disappointingly, oxysterol screening has a relatively low specificity on distinguishing NP-C from other causes in neonatal cholestasis (Polo et al., 2016; Degtyareva et al., 2019). The NP-C infants with neonatal cholestasis usually still have liver biopsy done for etiologic studies because clinical manifestations are non-specific in the early disease course (Yerushalmi et al., 2002; Evans et al., 2017). Liver foam cells, a typical light microscopic feature of NP-C, can raise a high clinical suspicion of NP-C, but are detectable in only 37–50% NP-C children (Kelly et al., 1993; Rodrigues et al., 2006). In this study, liver foam cells were detected in 2 (28.6%) NP-C infants beyond 3 months of age.

Differentiated from liver foam cells, vacuolated Kupffer cells were detected in all 7 NP-C infants who underwent liver biopsy at age ranging from 35 to 112 d. Abundant vacuolated Kupffer cells were detected at age 89 d and a few had enlarged sizes. When vacuolated Kupffer cells with enlarged sizes became obvious, liver foam cells were observed. A previous study also found that liver foam cells were negative in the early disease course and developed with age (Yerushalmi et al., 2002). These indicate that vacuolated Kupffer cells can evolve into liver foam cells. NP-C was finally diagnosed in 23.1% of neonatal cholestatic infants with vacuolated Kupffer cells, but none of those without vacuolated Kupffer cells. Hence, the presence of vacuolated Kupffer cells raises a clinical suspicion of NP-C in neonatal cholestatic infants, especially in those with splenomegaly, while their absence excludes a possibility of NP-C.

Demonstration of foam cells in bone marrow adds to clinical suspicion of NP-C (Kelly et al., 1993; Geberhiwot et al., 2018), but it can be negative in early infancy (Rodrigues et al., 2006). It is believed that foam cells may become apparent in bone marrow as the disease evolves. In the current study, foam cells were not identified in all 4 bone marrow samples obtained within 4 months of age. Therefore, the diagnosis of NP-C may be missed if early bone marrow aspiration is only relied on. It challenges the importance of bone marrow aspiration for the diagnosis of NP-C in younger infants with neonatal cholestasis.

NP-C infants usually present as neonatal cholestasis with high GGT (Woś et al., 2016; Yamada et al., 2019), but in some instances as neonatal cholestasis with low GGT (Evans et al., 2017). In the current study, we found 2 NP-C infants presented as neonatal cholestasis with low GGT (<100U/L). Furthermore, 4 NP-C infants were found to have fasting hypoglycemia. The reasons of hypoglycemia are still unclear. It may be associated with mitochondrial dysfunction which has been demonstrated in fibroblasts derived from NP-C patients (Woś et al., 2016). Therefore, blood glucose should be routinely monitored in NP-C infants presenting as neonatal cholestasis.

CONCLUSION

This study reports the molecular and clinical findings of 9 neonatal cholestatic infants diagnosed as NP-C. Vacuolated Kupffer cells are detected in all 7 NP-C infants who underwent liver biopsy in early disease course. The presence of vacuolated Kupffer cells raises a clinical suspicion of NP-C in neonatal cholestatic infants, especially in those with splenomegaly.

DATA AVAILABILITY STATEMENT

The datasets for this article are not publicly available due to concerns regarding participant/patient anonymity. Requests to access the datasets should be directed to the corresponding author.

ETHICS STATEMENT

The studies involving human participants were reviewed and approved by ethics committees of the Children's Hospital, Fudan University. Written informed consent to participate in

this study was provided by the participants' legal guardian/next of kin. Written informed consent was obtained from the individual(s), and minor(s)' legal guardian/next of kin, for the publication of any potentially identifiable images or data included in this article.

AUTHOR CONTRIBUTIONS

N-LW, LC, JL, and J-SW: Study design. N-LW, YL, KA, and X-BX: Data acquisition and interpretation. N-LW: Draft manuscript. All authors reviewed and approved the manuscript.

REFERENCES

Carstea, E. D., Polymeropoulos, M. H., Parker, C. C., Detera-Wadleigh, S. D., O'Neill, R. R., Patterson, M. C., et al. (1993). Linkage of Niemann-Pick Disease Type C to Human Chromosome 18. *Proc. Natl. Acad. Sci.* 90, 2002–2004. doi:10.1073/pnas.90.5.2002

Degtyareva, A. V., Proshlyakova, T. Y., Gautier, M. S., Degtyarev, D. N., Kamenets, E. A., Baydakova, G. V., et al. (2019). Oxysterol/chitotriosidase Based Selective Screening for Niemann-Pick Type C in Infantile Cholestasis Syndrome Patients. *BMC Med. Genet.* 20, 123. doi:10.1186/s12881-019-0857-0

Evans, W. R. H., Nicoli, E.-R., Wang, R. Y., Movsesyan, N., and Platt, F. M. (2017). Case Report: Ursodeoxycholic Acid Treatment in Niemann-Pick Disease Type C; Clinical Experience in Four Cases. *Wellcome Open Res.* 2, 75. doi:10.12688/wellcomeopenres.11854.1

Geberhiwot, T., Moro, A., Moro, A., Dardis, A., Ramaswami, U., Sirrs, S., et al. (2018). Consensus Clinical Management Guidelines for Niemann-Pick Disease Type C. *Orphanet J. Rare Dis.* 13, 50. doi:10.1186/s13023-018-0785-7

Jahnova, H., Dvorakova, L., Vlaskova, H., Hulkova, H., Poupetova, H., Hrebicek, M., et al. (2014). Observational, Retrospective Study of a Large Cohort of Patients with Niemann-Pick Disease Type C in the Czech Republic: a Surprisingly Stable Diagnostic Rate Spanning Almost 40 Years. *Orphanet J. Rare Dis.* 9, 140. doi:10.1186/s13023-014-0140-6

Kelly, D. A., Portmann, B., Mowat, A. P., Sherlock, S., and Lake, B. D. (1993). Niemann-Pick Disease Type C: Diagnosis and Outcome in Children, with Particular Reference to Liver Disease. *J. Pediatr.* 123, 242–247. doi:10.1016/s0022-3476(05)81695-6

Liu, L. Y., Wang, Z. L., Wang, X. H., Zhu, Q. R., and Wang, J. S. (2010). ABCB11 Gene Mutations in Chinese Children with Progressive Intrahepatic Cholestasis and Low Gamma Glutamyltransferase. *Liver Int.* 30, 809–815. doi:10.1111/j.1478-3231.2009.02112.x

Maekawa, M., Iwahori, A., and Mano, N. (2020). Biomarker Analysis of Niemann-Pick Disease Type C Using Chromatography and Mass Spectrometry. *J. Pharm. Biomed. Anal.* 191, 113622. doi:10.1016/j.jpba.2020.113622

Mazzacuva, F., Mills, P., Mills, K., Camuzeaux, S., Gissen, P., Nicoli, E.-R., et al. (2016). Identification of Novel Bile Acids as Biomarkers for the Early Diagnosis of Niemann-Pick C Disease. *FEBS Lett.* 590, 1651–1662. doi:10.1002/1873-3468.12196

Patterson, M. (2000). "Niemann-Pick Disease Type C," in *GeneReviews® [Internet]*. Editors MP Adam, HH Ardinger, RA Pagon, and S. E. Wallace (Seattle (WA): University of Washington, Seattle), 1993–2021. [Updated 2020 Dec 10].

Pineda, M., Walterfang, M., and Patterson, M. C. (2018). Miglustat in Niemann-Pick Disease Type C Patients: a Review. *Orphanet J. Rare Dis.* 13, 140. doi:10.1186/s13023-018-0844-0

Polo, G., Burlina, A., Furlan, F., Kolamunnage, T., Cananzi, M., Giordano, L., et al. (2016). High Level of Oxysterols in Neonatal Cholestasis: a Pitfall in Analysis of Biochemical Markers for Niemann-Pick Type C Disease. *Clin. Chem. Lab. Med.* 54, 1221–1229. doi:10.1515/cclm-2015-0669

Qiu, Y.-L., Gong, J.-Y., Feng, J.-Y., Wang, R.-X., Han, J., Liu, T., et al. (2017). Defects in Myosin VB Are Associated with a Spectrum of Previously Undiagnosed Low γ-glutamyltransferase Cholestasis. *Hepatology* 65, 1655–1669. doi:10.1002/hep.29020

Richards, S., Aziz, N., Bale, S., Bick, D., Das, S., Gastier-Foster, J., et al. (2015). Standards and Guidelines for the Interpretation of Sequence Variants: a Joint Consensus Recommendation of the American College of Medical Genetics and Genomics and the Association for Molecular Pathology. *Genet. Med.* 17, 405–424. doi:10.1038/gim.2015.30

Rodrigues, A. F., Gray, R. G., Preece, M. A., Brown, R., Hill, F. G., Baumann, U., et al. (2006). The Usefulness of Bone Marrow Aspiration in the Diagnosis of Niemann-Pick Disease Type C in Infantile Liver Disease. *Arch. Dis. Child.* 91, 841–844. doi:10.1136/adc.2005.088013

Togawa, T., Sugiura, T., Ito, K., Endo, T., Aoyama, K., Ohashi, K., et al. (2016). Molecular Genetic Dissection and Neonatal/infantile Intrahepatic Cholestasis Using Targeted Next-Generation Sequencing. *J. Pediatr.* 171, 171–177. doi:10.1016/j.jpeds.2016.01.006

Vanier, M. T., Duthel, S., Rodriguez-Lafrasse, C., Pentchev, P., and Carstea, E. D. (1996). Genetic Heterogeneity in Niemann-Pick C Disease: a Study Using Somatic Cell Hybridization and Linkage Analysis. *Am. J. Hum. Genet.* 58, 118–125.

Vanier, M. T., Gissen, P., Bauer, P., Coll, M. J., Burlina, A., Hendriksz, C. J., et al. (2016). Diagnostic Tests for Niemann-Pick Disease Type C (NP-C): a Critical Review. *Mol. Genet. Metab.* 118, 244–254. doi:10.1016/j.ymgme.2016.06.004

Wang, N.-L., Lu, Y.-L., Zhang, P., Zhang, M.-H., Gong, J.-Y., Lu, Y., et al. (2016). A Specially Designed Multi-Gene Panel Facilitates Genetic Diagnosis in Children with Intrahepatic Cholestasis: Simultaneous Test of Known Large Insertions/Deletions. *PLoS One* 11, e0164058. doi:10.1371/journal.pone.0164058

Woś, M., Szczepanowska, J., Pikuła, S., Tylki-Szymańska, A., Zabłocki, K., and Bandorowicz-Pikuła, J. (2016). Mitochondrial Dysfunction in Fibroblasts Derived from Patients with Niemann-Pick Type C Disease. *Arch. Biochem. Biophys.* 593, 50–59. doi:10.1016/j.abb.2016.02.012

Yamada, N., Inui, A., Sanada, Y., Ihara, Y., Urahashi, T., Fukuda, A., et al. (2019). Pediatric Liver Transplantation for Neonatal-Onset Niemann-Pick Disease Type C: Japanese Multicenter Experience. *Pediatr. Transpl.* 23, e13462. doi:10.1111/petr.13462

Yerushalmi, B., Sokol, R. J., Narkewicz, M. R., Smith, D., Ashmead, J. W., and Wenger, D. A. (2002). Niemann-pick Disease Type C in Neonatal Cholestasis at a North American Center. *J. Pediatr. Gastroenterol. Nutr.* 35, 44–50. doi:10.1097/00005176-200207000-00011

Zhang, J., Liu, L. L., Gong, J. Y., Hao, C. Z., Qiu, Y. L., Lu, Y., et al. (2020). *TJP2* Hepatobiliary Disorders: Novel Variants and Clinical Diversity. *Hum. Mutat.* 41, 502–511. doi:10.1002/humu.23947

Conflict of Interest: The authors declare that the research was conducted in the absence of any commercial or financial relationships that could be construed as a potential conflict of interest.

Publisher's Note: All claims expressed in this article are solely those of the authors and do not necessarily represent those of their affiliated organizations, or those of the publisher, the editors, and the reviewers. Any product that may be evaluated in this article, or claim that may be made by its manufacturer, is not guaranteed or endorsed by the publisher.

frontiers in Genetics

BRIEF RESEARCH REPORT
published: 24 March 2022
doi: 10.3389/fgene.2022.833495

TMEM199-Congenital Disorder of Glycosylation With Novel Phenotype and Genotype in a Chinese Boy

Yuan Fang[1†], Kuerbanjiang Abuduxikuer[2†], Yi-Zhen Wang[1], Shao-Mei Li[1], Lian Chen[3] and Jian-She Wang[2]**

[1]Department of Pathology, Anhui Provincial Children's Hospital, Hefei, China, [2]Department of Hepatology, Children's Hospital of Fudan University, Shanghai, China, [3]Department of Pathology, Children's Hospital of Fudan University, Shanghai, China

Background: TMEM199-congenital disorder of glycosylation (TMEM199-CDG) is a rare autosomal recessive inherited disease characterized by chronically elevated serum transaminase, decreased serum ceruloplasmin, steatosis and/or fibrosis, *TMEM199* mutation, reduced level of TMEM199 protein, and abnormal protein glycosylation.

Methods: The information of a Chinese patient with TMEM199-CDG in the Children's Hospital of Fudan University was reviewed. The patient's clinical, pathological, and molecular features were obtained by clinical data study, liver biopsy, immunohistochemistry, and molecular genetic analysis.

Results: A 4-year-old Chinese boy presented with hypertransaminasemia, hypercholesterolemia, elevated alkaline phosphatase, decreased serum ceruloplasmin and serum copper level, and coagulopathy since birth. To the best of our knowledge, novel findings included strabismus, cirrhosis by liver biopsy, reduced expression of TMEM199 by immunohistochemistry, and a frameshift variant of c.128delA/p.Lys43Argfs*25 in the *TMEM199* gene.

Conclusion: This case added to the phenotypic and genotypic spectrum of TMEM199-CDG.

Keywords: congenital disorders of glycosylation, TMEM199-CDG, inherited metabolic disease, liver disease, mutation

OPEN ACCESS

Edited by:
Hui Xiong,
Peking University First Hospital, China

Reviewed by:
Dario Ronchi,
University of Milan, Italy
Amir Hossein Saeidian,
Thomas Jefferson University, United States

****Correspondence:***
Lian Chen
doctchenlian@163.com
Jian-She Wang
jshwang@shmu.edu.cn

[†]The authors have contributed equally to this work and share first authorship

Specialty section:
This article was submitted to Genetics of Common and Rare Diseases, a section of the journal Frontiers in Genetics

Received: *11 December 2021*
Accepted: *14 February 2022*
Published: *24 March 2022*

Citation:
Fang Y, Abuduxikuer K, Wang Y-Z, Li S-M, Chen L and Wang J-S (2022) TMEM199-Congenital Disorder of Glycosylation With Novel Phenotype and Genotype in a Chinese Boy. Front. Genet. 13:833495. doi: 10.3389/fgene.2022.833495

INTRODUCTION

Congenital disorder of glycosylation (CDG) is an emerging group of metabolic diseases with autosomal recessive inheritance. One or more glycosylation enzyme defects lead to the abnormal glycosylation of protein or lipid in CDG, resulting in corresponding clinical symptoms (Yarema and Bertozzi, 2001; Jaeken, 2013). Common manifestations include dysmorphic features; diarrhea or malnutrition; abnormalities in the liver, coagulation, gland, and immune and nervous system; psychomotor disability; language retardation; ataxia; eye abnormalities; spinal or joint impairment; and cardiac disorders. Given the diversity of clinical performance, definitive diagnosis of CDG is difficult. With the development of whole-exome sequencing (WES), more than 140 CDG types have been identified. As a new subtype discovered in recent years, TMEM199-CDG (OMIM: 616829) is characterized by isolated or predominant liver involvement, which is different from most CDGs associated with multiple organ dysfunction (Marques-da-Silva et al., 2017). To date, only seven cases

of TMEM199-CDG have been reported worldwide (Jansen et al., 2016; Vajro et al., 2018). The patients presented with cryptogenic elevated alanine aminotransferase, aspartate aminotransferase, alkaline phosphatase, creatine kinase, total cholesterol, low-density lipoprotein cholesterol, and decreased serum ceruloplasmin. Liver biopsies revealed steatosis and/or fibrosis, and an ultrastructure of dilation and vesiculation of the Golgi and/or endoplasmic reticulum (ER). Several mutation sites of *TMEM199* were found by sequencing. Western blot confirmed reduced or undetectable levels of TMEM199 protein. Glycosylation analysis results were consistent with the type II CDG pattern.

Herein, we reported a Chinese boy with TMEM199-CDG, presenting with abnormal liver function, strabismus, and mild psychomotor delay. The liver biopsy showed steatosis, severe fibrosis as cirrhosis at stage 4, and reduced expression of TMEM199 by immunohistochemistry. WES revealed two compound heterozygous variants, c.20C > A mutation and c.128delA deletion in *TMEM199* exon 1, of which the latter had not been previously reported. Treatments with bicyclic alcohol, zinc sulfate, and penicillamine yielded no effect, while no significant progression in the course of the disease was observed after 1-year follow-up. To the best of our knowledge, he is the first Chinese patient described with TMEM199-CDG who carried a novel phenotype and genotype, which might expand the understanding of this rare disease.

MATERIALS AND METHODS

Patient

The information of a Chinese pediatric patient with TMEM199-CDG in the Children's Hospital of Fudan University was reviewed. Clinical, pathological, and molecular features of the patient were assessed by clinical manifestations, laboratory investigations, liver biopsy, immunohistochemistry, and molecular genetic analysis. This study conformed to the provisions of the institutional ethics committee and the Declaration of Helsinki (as revised in 2013). The patient's parents shared all procedures including treatment and signed the written informed consent. The written informed consent was obtained for publication of any potentially identifiable images or data included in this article.

Liver Biopsy

The specimen was obtained from core-needle biopsy, fixed in 10% buffered formalin, dehydrated in graded concentrations of ethyl alcohol, and embedded in paraffin. Then it underwent routine staining for hematoxylin and eosin (HE), and histochemical special staining for periodic acid–Schiff (PAS) with and without diastase, Masson, reticulin, copper, and iron.

Immunohistochemistry

Additional 4-μm sections were deparaffinized, rehydrated, and pretreated with 3% H_2O_2 to eliminate endogenous peroxidase activity. Moreover, they were treated with EDTA (pH 9) or citrate buffer (pH 6) for heat-mediated antigen retrieval before commencing with the immunohistochemical staining protocol. The primary antibodies used included CK7 (clone MX053, ready-to-use solution), CK19 (clone MX054, ready-to-use solution), CD68 (clone MX075, ready-to-use solution), CD163 (clone MX081, ready-to-use solution), CD3 (clone MX036, ready-to-use solution), and CD8 (clone C8/144B, ready-to-use solution), which were purchased from http://www.maxim.com.cn (Fuzhou, China). In addition to the series of conventional antibodies, a rabbit polyclonal antibody against TMEM199 (purchased from http://www.abcam.cn, product code: ab121907) with a 1:50 dilution was utilized. The sections were incubated overnight at 4°C, followed by incubating with a general secondary antibody for 1 h at room temperature. Finally, the sections were developed with DAB and counterstained with hematoxylin. A normal liver sample (donated by a surgical patient) was prepared as the positive control, while omitting the first antibody as the negative control.

Molecular Genetic Analysis

Genetic testing was performed by Running Gene Inc (http://www.mono-mz.com/auth, Beijing, China). EDTA-anticoagulated whole blood specimens were collected from the patient and his parents. DNA was isolated from peripheral blood using the DNA Isolation Kit (Blood DNA Kit V2, CW2553). Concentrations were determined on a Qubit fluorometer (Invitrogen, Q33216) using the Qubit dsDNA HS Assay Kit (Invitrogen, Q32851). Agarose gel (1%) electrophoresis was performed for the quality control. A total of 1 μg isolated DNA was sheared using the following parameters: duty cycle 10%, intensity 5, cycles per burst 200, and time six cycles per 60 s. This step was performed using a Bioruptor UCD-200 (Diagenode). All samples were sheared very consistently, and the size distribution peak was around 200 bp. In total, 3 μl of the sheared DNA was electrophoresed in a 2% agarose gel to confirm the presence of fragments of the desired size range. The multiplex ligation-dependent probe amplification assay (MLPA) was performed using the *ATP7B* MLPA kit (SALSA MLPA Probemix P098-D1, MRC-Holland, the Netherlands) (Chen et al., 2019). However, MLPA analysis excluded copy number variations in *ATP7B*. Then IDT-WES was performed to dig for potential genetic abnormalities. DNA libraries were prepared using the KAPA Library Preparation Kit (Kapa Biosystems, KR0453) following the manufacturer's instructions. The procedure comprised three standard steps: end-repair of fragmented DNA, A-tailing, adapter ligation, and amplification. Purifications between steps were carried out using Agencourt AMPure XP beads. The libraries were estimated using the Qubit dsDNA HS Assay kit (Invitrogen, Q32851). Hybridization of pooled libraries to the capture probes and removal of non-hybridized library molecules were carried out according to the SeqCap hybrid Mix system. DNA libraries were sequenced using the Illumina novaseq platform (Illumina, SanDiego, United States) as paired-end 200-bp reads. For data analysis, adapters and low-quality sequences were removed to obtain clean and basic data. Genome Analysis Toolkit (GATK) (https://gatk.broadinstitute.org) was used for variation calling to summarize single-nucleotide variants (SNVs) and indels. ANNOVAR software and Enliven® Variants Annotation

Interpretation System were employed for annotation and interpretation. Data were aligned against the Human Gene Mutation Database (HGMD) Professional (http://www.hgmd.cf.ac.uk), 1,000 Genome Database (www.1000genomes.org), Genome Aggregation Database (gnomAD) (https://gnomad.broadinstitute.org), dbSNP152 (https://www.ncbi.nlm.nih.gov/snp), and Exome Aggregation Consortium (ExAC) (http://exac.broadinstitute.org). The variants were filtered out only with a population frequency of <5% in 1,000 genomes and <2% in gnomAD. Damage prediction of the genetic variants was conducted by Combined Annotation-Dependent Depletion (CADD) (https://cadd.gs.washington.edu) for scoring and mutation significance cutoff (MSC) (https://lab.rockefeller.edu/casanova/MSC) for further comparison. The MSC server was applied to CADD, PolyPhen 2 (http://genetics.bwh.harvard.edu/pph2) and SIFT (https://sift.bii.a-star.edu.sg/www/SIFT_indels2.html), with a confidence interval of 99% and database source of HGMD and ClinVar (https://www.ncbi.nlm.nih.gov/clinvar). Genomics England PanelApp (https://panelapp.genomicsengland.co.uk), a crowdsourcing tool, was utilized for analysis based on variant–disease and gene–disease associations. Human Phenotype Ontology (HPO) (https://hpo.jax.org), Online Mendelian Inheritance in Man (OMIM) (https://www.omim.org), and HGMD database were used to match the phenotype descriptions with variant and gene prioritization results. According to the American College of Medical Genetics and Genomics (ACMG) guidelines, genetic variants were classified as pathogenic, likely pathogenic, variants of uncertain significance (VUS), likely benign, and benign. Thereafter, two pathogenic variants of *TMEM199* were identified with the transcript of NM_152464.1, which was validated by using Sanger sequencing. The pathogenicity of amino acid changes caused by gene mutations was predicted using MutationTaster (http://www.mutationtaster.org). We conducted protein modeling using the SWISS-model (https://www.swissmodel.expasy.org) with a UniProtKB code Q8N511, and the mutated structures were analyzed and visualized using PyMol (http://www.pymol.org).

RESULTS

Clinical History

The patient was born to healthy non-consanguineous parents as the second child of the family, whose older sister was healthy. At the age of 1 month, the patient was hospitalized for jaundice. During a routine blood test, remarkably elevated aspartate aminotransferase (253.0 IU/L, reference range 0–40 IU/L), γ-glutamyl transferase (540.0 IU/L, reference range 7–50 IU/L) and total bilirubin (303.8 μmol/L, reference range 5.1–17.1 μmol/L), and decreased globulin (9.6 g/L, reference range 20–30 g/L) and ceruloplasmin (0.04 g/L, reference range 0.22–0.58 g/L) were noticed. The patient was discharged after jaundice was treated. However, the hypertransaminasemia, hypercholesterolemia, elevated alkaline phosphatase, decreased serum ceruloplasmin and serum copper level, and coagulopathy persisted during the approximate 4-year follow-up.

Then the 4-year-old boy with abnormal liver function since birth was admitted to our in-patient department. Physical examination showed that his height was 108 cm (87th percentile by the WHO standard) and weight was 19 kg (88th percentile). Ocular strabismus was present, while the Kayser–Fleischer ring was absent. The liver was located 3 cm below the right costal and 4 cm below the xiphoid process, with a soft texture. The examination of the skin, abdomen, and nervous system showed no abnormalities. Abdominal ultrasonography indicated that the echogenicity of the liver was inhomogeneous, showing mild fatty liver manifestation. Cranial magnetic resonance imaging revealed that the anterior part of the right ventricle was slightly plentiful, and part of the sinus mucosa was thickened. The patient was assessed as having a mild intellectual disability by the development screening test (DST). The measured intellectual age was below his actual 51 months, showing 36 months in exercise, 27 months in social adaptation, and 36 months in intelligence. The majority of liver enzymes were elevated, including alanine aminotransferase (58.80 IU/L, reference range 0–40 IU/L), aspartate aminotransferase (123.20 IU/L, reference range 0–40 IU/L), alkaline phosphatase (1296.00 IU/L, reference range 42–383 IU/L), and creatine kinase isoenzyme (30.8 IU/L, reference range 0–30 IU/L). The lipid profile revealed increased total cholesterol (7.92 mmol/L, reference range 3.1–5.2 mmol/L), high-density lipoprotein cholesterol (1.61 mmol/L, reference range 0.91–2.05 mmol/L), and low-density lipoprotein cholesterol (5.72 mmol/L, reference range 1.30–3.90 mmol/L). Serum ceruloplasmin (0.04 g/L, reference range 0.22–0.58 g/L) and serum copper (2.80umol/L, reference range 10.99–21.98 μmol/L) levels were decreased. Transferrin (2.7 g/L, reference range 2.5–4.3 g/L) and ferritin (48.02 ng/ml, reference range 30–400 ng/ml) levels were normal. With the exception of prolonged activated partial thromboplastin time (46.6 s, reference range 28.0–44.5 s), increased D-dimer (0.57 mg/L, reference range 0–0.3 mg/L) and decreased fibrinogen (1.43 g/L, reference range 2–4 g/L), other coagulation indicators were normal. **Table 1** summarizes the predominant laboratory investigations of the patient in different phases. Subsequently, the patient was treated with bicyclic alcohol, zinc sulfate, and penicillamine for 1 year. To date, there has been no significant improvement or disease progression during the surveillance period. The follow-up showed elevated serum transaminases, alkaline phosphatase, and lipid profiles, and persistent low ceruloplasmin.

Liver Biopsy

Liver biopsy showed that the architecture of liver lobules was disordered, and pseudo-lobule was formed (**Figure 1A**). High power exhibited ground-glass-like hepatic cells, with a lightly stained cytoplasm and clear cell membrane, and vesicular steatosis, which were more evident in the portal area, rather than the regions around the central vein (**Figure 1B**). Infiltration of few lymphocytes in the portal area was also observed (**Figure 1C**). PAS staining identified small vacuoles in partial hepatocytes (**Figure 1D**), while PAS with diastase, copper, and iron staining were negative. The hyperplastic fibrous tissue in the

TABLE 1 | Predominant changes in laboratory investigations of the Chinese patient.

Age (m, month)		1 m	1.6 m	1.8 m	2.5 m	5.6 m	8.7 m	49.3 m	50.9 m	56.1 m	57.1 m	59.6 m	63.3 m
Serum biochemistry (reference range)	Albumin (35–55 g/L)	45.0	45.0	54.0	44.0	48.0	47.0	50.0	48.2	49.1	46.2	50.3	48.6
	Globulin (20–30 g/L)	9.6	15.0	18.0	14.0	14.0	16.0	NA	NA	14.6	18.3	12.8	14.1
	Alanine aminotransferase (0–40 IU/L)	63.0	88.0	69.0	80.0	99.0	129.0	156.5	58.8	297.7	169.4	77.7	128.6
	Aspartate aminotransferase (0–40 IU/L)	253.0	247.0	186.0	207.0	257.0	746.0	150.0	123.2	196.3	108.3	62.9	114.0
	Total bilirubin (5.1–17.1 μmol/L)	303.8	147.3	108.0	117.5	19.2	10.3	7.3	4.3	4.6	3.5	2.0	5.0
	Direct bilirubin (0–6 μmol/L)	14.3	14.9	19.7	14.5	8.5	6.2	0.9	NA	1.7	2.1	1.0	1.5
	γ-glutamyl transferase (7–50 IU/L)	540.0	557.0	459.0	497.0	201.0	343.0	22.6	25.7	25.0	19.0	18.0	17.0
	Total bile acid (0–10 μmol/L)	24.9	30.0	43.0	54.0	124.0	200.0	NA	2.8	3.1	12.6	7.7	8.7
	Alkaline phosphatase (42–383 IU/L)	410.0	757.0	974.0	700.0	769.0	789.0	1030.2	1296.0	1035.0	692.0	918.0	946.0
	Blood glucose (3.9–5.8 mmol/L)	NA	3.3	3.4	3.8	2.9	2.8	4.6	4.9	4.87	NA	NA	4.67
	Lactic acid (0–2 mmol/L)	NA	1.41	NA	NA	NA	NA	NA	NA	NA	NA	NA	NA
	Ammonia (10–47 μmol/L)	NA	24.8	NA	NA	NA	NA	NA	55.0	NA	NA	NA	NA
	Total cholesterol (3.1–5.2 mmol/L)	NA	7.74	9.30	7.00	6.73	8.73	NA	7.92	6.09	NA	NA	6.52
	LDL cholesterol (1.30–3.90 mmol/L)	NA	4.89	NA	NA	4.36	7.17	NA	5.72	4.66	NA	NA	4.93
	HDL cholesterol (0.91–2.05 mmol/L)	NA	3.03	NA	NA	2.46	1.17	NA	1.61	1.01	NA	NA	1.19
	Triglyceride (0.56–1.70 mmol/L)	NA	1.04	0.75	0.50	0.87	2.05	NA	0.90	0.82	NA	NA	0.66
	Procalcitonin (<0.05 ng/ml)	0.22	0.20	NA	NA	NA	0.54	NA	NA	NA	NA	NA	NA
	Ceruloplasmin (0.22–0.58 g/L)	0.04	0.03	0.04	NA	0.05	0.12	0.06	0.04	0.07	NA	NA	0.07
	Serum Copper (10.99–21.98 μmol/L)	NA	NA	NA	NA	4.0	8.6	2.8	2.8	NA	NA	NA	NA
Blood coagulation profiles (reference range)	Activated partial thromboplastin time (28.0–44.5 s)	53.8	39.2	NA	NA	NA	NA	NA	46.6	NA	NA	NA	34.5
	D-dimer (0–0.3 mg/L)	NA	NA	NA	NA	NA	NA	NA	0.57	NA	NA	NA	NA
	Fibrinogen (2–4 g/L)	1.76	1.67	NA	NA	NA	NA	NA	1.43	NA	NA	NA	1.64
	Thrombin time (14–21 s)	21.5	18.9	NA	NA	NA	NA	NA	17.0	NA	NA	NA	15.3
	International normalized ratio (0.8–1.2)	1.03	0.96	NA	NA	NA	NA	NA	1.09	NA	NA	NA	1.08
	Prothrombin time (12.0–14.8 s)	11.6	11.1	NA	NA	NA	NA	NA	14.4	NA	NA	NA	13.1
	Prothrombin time activity (80–100%)	85.4	83.1	NA	NA	NA	NA	NA	83.0	NA	NA	NA	88.0

portal area separated liver lobules, formatting bridging-like fibrosis and pseudo-lobules, which was highlighted by Masson staining (**Figure 1E**). The preserved reticular scaffold structure was displayed by reticulin staining. It presented cirrhosis with stage 4 assessment according to the Scheurer histopathologic scoring system (Scheuer, 1991).

Immunohistochemistry

Immunohistochemical staining of CK7 and CK19 showed mild hyperplasia of bile ducts along the margins of pseudo-lobules (**Figure 1F**). Slightly proliferated Kupffer cells in hepatic sinusoids were indicated by CD68 and CD163 staining, and lymphocytes infiltrating in the portal area were detected by CD3 and CD8 staining. It was worth noting that the expression of TMEM199 was reduced in this index patient sample (**Figure 1G**), compared with the normal liver sample (donated by a surgical patient), which displayed a cytoplasmic positive pattern in hepatic and bile duct cells (**Figure 1H**).

Molecular Genetic Analysis

With a suspected diagnosis of Wilson disease according to the clinical manifestation, a multi-gene panel was screened. However, the absence of *ATP7B* mutation and normal DNA copy number variant (CNV) ruled out Wilson disease. Thereafter, two compound heterozygous variations, c.20C > A and c.128delA, were found in *TMEM199* gene exon 1 (**Figure 2A**) by WES. The c.20C > A was inherited from the healthy father, leading to a change of alanine to glutamate at amino acid position 7 (p.Ala7Glu), which was reported in the HGMD (Jansen et al., 2016). The c.128delA as a deletion mutation was inherited from the healthy mother, which caused a frameshift with an early termination (p.Lys43Argfs*25), which was not reported in the HGMD. The amino acid residue of the splice-

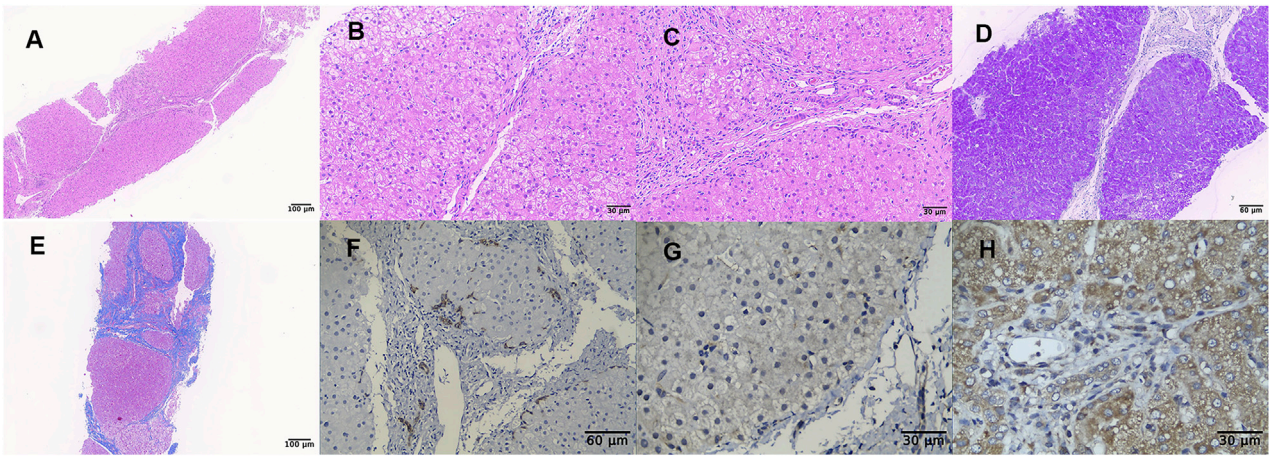

FIGURE 1 | Liver biopsy (all originally magnified principal images). Hematoxylin and eosin staining showed the discorded architecture of liver lobules and the formation of pseudo-lobules **(A×100)**, ground-glass-like hepatic cells with lightly stained cytoplasm and obvious vesicular steatosis in portal area **(B×400)**, and lymphocytic infiltration in the portal area **(C×400)**. PAS staining identified small vacuoles in partial hepatocytes **(D×200)**. Formation of bridging-like fibrosis and pseudo-lobule was highlighted by Masson staining **(E×100)**. Mild hyperplasia of bile ducts along the margins of pseudo-lobule was showed by immunohistochemical staining of CK7 **(F×200)**, while weaker staining in the index patient **(G×400)** than in normal control **(H×400)** was observed by TMEM199 immunohistochemical detection.

site mutation (p.Ala7Glu) was conserved across various species, while the frameshift mutation (p.Lys43Argfs*25) was not conserved (**Figure 2B**). The CADD score of c.20C > A and c.128delA was 14.560 and 11.410 respectively, both predicted as a high impact by MSC. Both mutations of c.20C > A (functional test PS3 + absent from controls PM2 + homozygous variants and distribution in trans PM3_Strong + phenotype match PP4) and c.128delA (frameshift variant with LOF PVS1 + absent from controls PM2 + phenotype match PP4) were evaluated to be pathogenic according to the guideline of the ACMG. The nomenclature of variants was based on the recommendations of the Human Genome Variation Society (HGVS, http://www.hgvs.org/varnomen). Wild-type and mutated TMEM199 were modeled by PyMol (http://www.pymol.org) which showed no effect of Ala7Glu residue change on the polar contact with them around amino acid Arg53 (**Figure 2C**). Spatial conformation of the frameshift mutation (p.Lys43Argfs*25) predicted by protein modeling showed that the amino acid at position 43 moved backward 25 positions and then terminated, resulting in protein truncation, which contained a loss of the Vam12 domain (**Figure 2D**). **Figure 2E** illustrates the TMEM199 protein domains, location of amino acid changes of the reported variants so far.

DISCUSSION

CDGs are clinically and genetically heterogenous disorders sharing a primary defect of glycosylation. Mandato et al. (2006) detected aberrant glycosylation of transferrin (Tf) by electrospray ionization mass spectrometry (ESI-MS) in four children with cryptogenic chronic hypertransaminasemia and/or liver steatosis and fibrosis, leading to the discovery of a new type of CDG-X with unknown disease-causing genetic alterations. With the development of WES, researchers found two cases of CDG-X and one unrelated case with *TMEM199* heterozygous mutations (Vajro et al., 2018). In addition, Jansen et al. (2016) confirmed that the abnormal glycosylation of serum protein was caused by Golgi homeostasis defects, and mutations at different sites in the *TMEM199* gene were found in four patients. Two heterozygous mutations in *TMEM199* were detected in our patient with the abnormal liver function since birth. Based on the mutations of the *TMEM199* gene, all the eight patients were diagnosed with TMEM199-CDG. The main features of the eight patients are listed in **Table 2**.

The eight patients with TMEM199-CDG included seven Europeans (originating from Greece and Italy) and one Chinese. There were six male and two female patients, with an age range of 2–41 years, four of whom were two pairs of siblings. Seven patients had the disease onset since early childhood. Intellectual disability or mild language retardation was found in three patients, among whom one also presented with hypotonia, while one Chinese patient also presented with strabismus. All patients reported to date presented high fluctuating levels of alanine aminotransferase (23–437 IU/L, reference range 0–40 IU/L), aspartate aminotransferase (31–746 IU/L, reference range 0–40 IU/L), and alkaline phosphatase (132–3990 IU/L, reference range 42–383IU/L). Total cholesterol (5.3–9.3 mmol/L, reference range 3.1–5.2 mmol/L) and low-density lipoprotein cholesterol (1.16–7.17 mmol/L, reference range 1.30–3.90 mmol/L) were elevated in seven patients, while high-density lipoprotein cholesterol (1.01–3.03 mmol/L, reference range 0.91–2.05 mmol/L) was normal or slightly increased in four patients. Low levels of serum ceruloplasmin (0.03–0.24 g/L, reference range 0.22–0.58 g/L) and serum copper (2.80–8.60 umol/L, reference range 10.99–21.98 μmol/L) were found. The coagulation function was normal, close to borderline or slightly weakened in six patients. These findings indicate that TMEM199-CDG mainly affects the liver, and nervous and muscular systems may be involved as well.

Liver biopsies were performed in six patients, four of whom showed various degrees of steatosis and periportal fibrosis, and two only showed steatosis. Among them, one patient underwent the

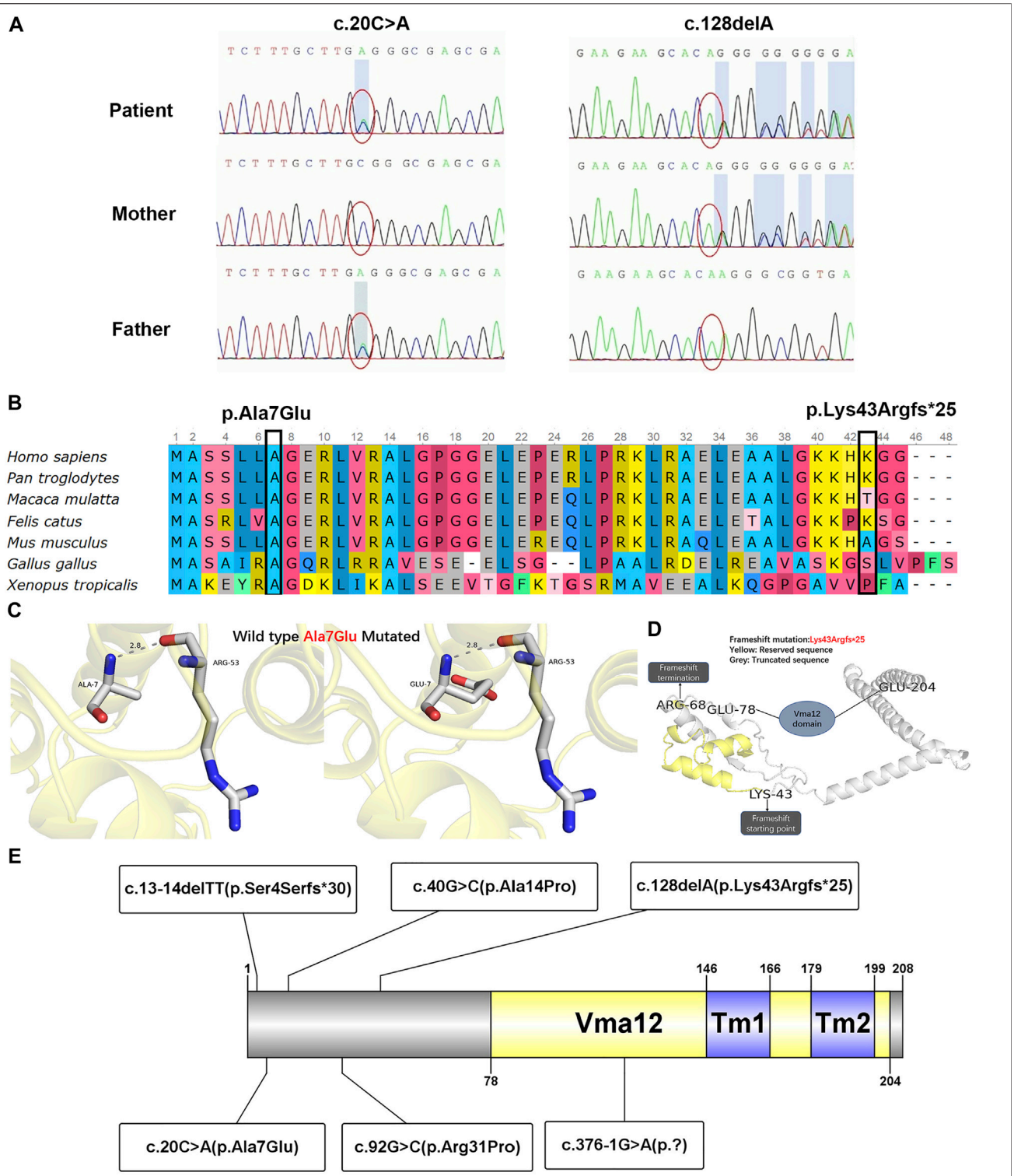

FIGURE 2 | Genetic testing results, conservation of amino acid residues, protein modulation, and distribution of reported variants with the TMEM199 protein. **(A)** Sanger sequencing confirmation of c.20C > A and c.128delA mutation of *TMEM199* in the index case and his parents. **(B)** Conservation status of amino acid residues of the two variants across various species. **(C)** Wild and mutated types of the p.Ala7Glu variant compared by PyMol. **(D)** Spatial conformation of the frameshift mutation (p.Lys43Argfs*25) showed by protein modeling. **(E)** Illustration of TMEM199 protein domains, location of amino acid changes of the reported variants so far.

TABLE 2 | Main findings of the eight patients with TMEM199-CDG.

Patient	Patient 1	Patient 2	Patient 3	Patient 4	Patient 5	Patient 6	Patient 7	Patient 8
	Siblings				Siblings			
Reference	Jansen et al. (2016)	Jansen et al. (2016)	Jansen et al. (2016)	Jansen et al. (2016)	Vajro et al. (2018)	Vajro et al. (2018)	Vajro et al. (2018)	Current report
Gender	Male	Male	Male	Female	Female	Male	Male	Male
Age (years)	26	18	41	23	27	24	2	4
Country of origin	Greece	Greece	ND	Greece	Italy	Italy	Italy	China
Developmental delay	None	None	ND	Psychomotor disability	None	None	Mild delay of speech	Mild delay of psychomotor
Other manifestation	None	None	None	Hypotonia	None	None	None	Strabismus
Alanine aminotransferase (0–40 IU/L)	54	210	46–190	36–172	23–329	50–221	104–437	58.8–297.7
Aspartate aminotransferase (0–40 IU/L)	73	246	40–153	31–119	53–349	98–299	156–656	62.9–746.0
Alkaline phosphatase (42–383 IU/L)	745	1,162	365–718	132–1,528	1,140–1995	903–3990	713–1,235	410.0–1296.0
Total cholesterol (3.1–5.2 mmol/L)	6.5	8.7	5.3–8.7	6.0–6.6	7.8–8.8	5.7–6.2	3.6–4.1	6.09–9.30
LDL cholesterol (1.30–3.90 mmol/L)	4.86	7.16	4.70–5.84	4.16–4.42	6.20–6.62	4.55–4.58	2.48–2.53	4.36–7.17
HDL cholesterol (0.91–2.05 mmol/L)	ND	ND	ND	ND	1.27–1.40	1.16–1.19	1.27–1.40	1.01–3.03
Ceruloplasmin (0.22–0.58 g/L)	0.11	0.16	0.09	0.17–0.24	0.06–0.08	0.04–0.06	0.08–0.084	0.03–0.12
Serum copper (10.99–21.98 μmol/L)	ND	ND	ND	ND	<6.25	<6.25	<6.25	2.8–8.6
Coagulation parameters	Slightly decreased ATIII, FXI, FXIII, and protein S	Slightly decreased ATIII, FXI, FXIII, and protein S	ND	ND	Normal/borderline	Normal/borderline	Low ATIII activity	Prolonged APTT, increased D-dimer and decreased fibrinogen
Liver histology	Steatosis	Steatosis	Steatosis and minimal fibrosis	ND	Mild periportal fibrosis; focal steatosis	Mild periportal fibrosis; focal steatosis	ND	Steatosis and cirrhosis
Hepatic ultrastructure	ND	ND	Dilation and vesiculation of the Golgi and/or ER	ND	ND	ND	ND	ND
Immunohistochemistry of TMEM199	ND	ND	ND	ND	ND	ND	ND	Weak positive
Western blot of TMEM199	Reduced	Reduced	Reduced	ND	Undetectable	Undetectable	ND	ND
Zygosity	Homozygous	Homozygous	Compound heterozygous	Homozygous	Compound heterozygous	Compound heterozygous	Compound heterozygous	Compound heterozygous
Mutation sites	c.20C > A	c.20C > A	c.40G > C/c.376-1G > A	c.92G > C	c.13-14delTT/c.92G > C	c.13-14delTT/ c.92G > C	c.13-14delTT/ c.92G > C	c.20C > A/c.128delA
Amino acid change	p.Ala7Glu	p.Ala7Glu	p.Ala14Pro/ND	p.Arg31Pro	p.Ser4Serfs*30/ p.Arg31Pro	p.Ser4Serfs*30/ p.Arg31Pro	p.Ser4Serfs*30/ p.Arg31Pro	p.Ala7Glu/ p.Lys43Argfs*25
Glycosylation studies	Abnormal N- and O-glycosylation	Abnormal N- and O-glycosylation	Abnormal N-glycosylation	Abnormal N- and O-glycosylation	Type II CDG pattern	Type II CDG pattern	Type 2 CDG pattern	ND
Treatment	ND	ND	ND			None	None	

(Continued on following page)

TABLE 2 | (*Continued*) Main findings of the eight patients with TMEM199-CDG.

Patient	Patient 1	Siblings Patient 2	Patient 3	Patient 4	Patient 5	Siblings Patient 6	Patient 7	Patient 8
				Carbamazepine × 2 years at age 6 for attention deficit	Vitamin D × 1 year at age 4; penicillamine for 6 months at age 5 with no effects			Bicyclic alcohol, zinc sulfate and penicillamine for 1 year at age 4 with no effects

ND, not described.

assessment of the ultrastructural characteristics of hepatocytes using a transmission electron microscope. Diffuse and severe vacuolization were observed to most likely derive from the rough ER, smooth ER, and/or Golgi apparatus (Jansen et al., 2016). Unlike the mild or minimal fibrosis manifested in European patients, the liver biopsy of the Chinese patient presented cirrhosis with bridging-like fibrosis and pseudo-lobule formation, which was assessed as stage 4 according to the Scheurer histopathologic scoring system (Scheuer, 1991). The presentation of cirrhosis in early childhood indicates that the severity of liver impairment caused by TMEM199-CDG may require more attention and early intervention.

WES demonstrated heterozygous *TMEM199* mutations in five patients and homozygous *TMEM199* mutations in three patients, including c.13-14delTT (p.Ser4Serfs*30), c.20C > A (p.Ala7Glu), c.40G > C (p.Ala14Pro), c.92G > C (p.Arg31Pro), c.128delA (p.Lys43Argfs*25), and c.376-1G > A (p.?) (**Figure 2E**). *TMEM199* (NM_152464.1, ENST00000292114) is located on chromosome 17 (chr17:26,684,604–26,690,705), containing six exons encoding a protein of 208 amino acids. The encoded TMEM199 (previously known as C17orf32), a transmembrane protein, is mainly located in the endoplasmic reticulum–Golgi apparatus intermediate compartment (ERGIC) and is involved in Golgi homeostasis. Moreover, as a human homolog of yeast Vma12p, TMEM199 participates in the formation of V-ATPase, which is the proton pump in the process of vesicle acidification via the secretory pathway (Miles et al., 2017). The homeostasis of Golgi apparatus cannot be maintained in TMEM199 deficiency due to the pH imbalance, leading to the abnormal glycosylation of serum proteins, which is closely related to the clinical manifestations of liver dysfunction in patients with TMEM199-CDG. In previously reported patients, glycosylation and functional studies showed aberrant N- and O-glycosylation as a type II CDG pattern, and deficient incorporation of galactose and sialic acid as seen in other Golgi homeostasis defects, which was confirmed by metabolic labeling and restored by lentiviral transduction with wild-type TMEM199 (Jansen et al., 2016; Vajro et al., 2018). Hence, the hepatic phenotype with abnormal glycosylation is considered to be resulted from TMEM199 deficiency. Glycosylation defects and the abnormal protein function of the Chinese patient need to be determined in future studies. Additionally, the expression level of TMEM199 in the Chinese patient's liver specimen detected by immunohistochemical staining was lower than normal control, which was consistent with the reduced or unmeasurable level of TMEM199 protein in skin fibroblasts detected using the Western blot in the European patients (Jansen et al., 2016; Vajro et al., 2018). The TMEM199 antibody (ab121907) is designed with a recombinant fragment corresponding to human TMEM199 amino acids at positions 7–143. Therefore, the unique c.128delA (p.Lys43Argfs*25) in *TMEM199* exon 1 in our patient caused a frameshift with an early termination, which was mainly responsible for the weak immunohistochemical signal.

Treatment and prognosis were reported in five patients, two of whom did not receive any medication. Despite the 2 years of carbamazepine usage for attention deficit starting at age 6, no other drugs were given to a Greek patient (Jansen et al., 2016). Vitamin D usage for 1 year starting at age 4 and penicillamine usage for 6 months starting at age 5 were reported in an Italian patient (Vajro et al., 2018), while the Chinese patient in the

present study was given bicyclic alcohol, zinc sulfate, and penicillamine for 1 year initiating at age 4. However, it seemed that medical treatments had no definite effect on improving the liver function of these patients. Nevertheless, the previous patients were reported to have no deterioration over several decades, and the Chinese patient presented no significant disease progression during 1-year follow-up. Therefore, there was a view that TMEM199-CDG had a more favorable course to avoid worries of the patients and their parents and unnecessary repeated blood sampling (Vajro et al., 2018). As far as our case is concerned, the early emergence of cirrhosis makes the outcome of the disease not too optimistic; more cohort observations are needed to verify our findings.

CONCLUSION

This report expands the phenotypic and genotypic spectra of TMEM199-CDG by presenting the first Chinese patient carrying strabismus, severe fibrosis, reduced expression of TMEM199, and a novel truncating mutation. Like the previously reported patients, this Chinese boy was monitored, without significant disease progression. But the appearance of cirrhosis in early childhood needs to be paid attention to, and more cases will help better understand the unclear course of this rare condition.

DATA AVAILABILITY STATEMENT

The data presented in this study is included in the article/Supplementary Material. The DNA datasets are not readily available due to privacy restrictions, further inquiries should be directed to the corresponding authors.

ETHICS STATEMENT

The studies involving human participants were reviewed and approved by the Children's Hospital of Fudan University. Written informed consent to participate in this study was provided by the participants' legal guardian/next of kin. Written informed consent was obtained from the individual(s), and minor(s)' legal guardian/next of kin, for the publication of any potentially identifiable images or data included in this article.

AUTHOR CONTRIBUTIONS

YF and KA drafted and revised the work, Y-ZW and S-ML analyzed and interpreted the data for the work, and LC and J-SW designed the work and approved the final version to be published.

ACKNOWLEDGMENTS

We acknowledge Running Gene Inc., for performing next-generation sequencing and Sanger sequencing and providing details of the genetic testing. We thank the patient and his parents for their participation in this study.

REFERENCES

Chen, Y.-C., Yu, H., Wang, R.-M., Xie, J.-J., Ni, W., and Zhang, Y. (2019). Contribution of Intragenic Deletions to Mutation Spectrum in Chinese Patients with Wilson's Disease and Possible Mechanism Underlying ATP7B Gross Deletions. *Parkinsonism Relat. Disord.* 62, 128–133. doi:10.1016/j.parkreldis.2019.01.001

Jaeken, J. (2013). Congenital Disorders of Glycosylation. *Handb Clin. Neurol.* 113, 1737–1743. doi:10.1016/B978-0-444-59565-2.00044-7

Jansen, J. C., Timal, S., van Scherpenzeel, M., Michelakakis, H., Vicogne, D., Ashikov, A., et al. (2016). TMEM199 Deficiency Is a Disorder of Golgi Homeostasis Characterized by Elevated Aminotransferases, Alkaline Phosphatase, and Cholesterol and Abnormal Glycosylation. *Am. J. Hum. Genet.* 98 (2), 322–330. doi:10.1016/j.ajhg.2015.12.011

Mandato, C., Brive, L., Miura, Y., Davis, J. A., Di Cosmo, N., Lucariello, S., et al. (2006). Cryptogenic Liver Disease in Four Children: a Novel Congenital Disorder of Glycosylation. *Pediatr. Res.* 59 (2), 293–298. doi:10.1203/01.pdr.0000196378.30165.26

Marques-da-Silva, D., Dos Reis Ferreira, V., Monticelli, M., Janeiro, P., Videira, P. A., Witters, P., et al. (2017). Liver Involvement in Congenital Disorders of Glycosylation (CDG). A Systematic Review of the Literature. *J. Inherit. Metab. Dis.* 40 (2), 195–207. doi:10.1007/s10545-016-0012-4

Miles, A. L., Burr, S. P., Grice, G. L., and Nathan, J. A. (2017). The Vacuolar-ATPase Complex and Assembly Factors, TMEM199 and CCDC115, Control HIF1alpha Prolyl Hydroxylation by Regulating Cellular Iron Levels. *Elife* 6. doi:10.7554/eLife.22693

Scheuer, P. J. (1991). Classification of Chronic Viral Hepatitis: a Need for Reassessment. *J. Hepatol.* 13 (3), 372–374. doi:10.1016/0168-8278(91)90084-o

Vajro, P., Zielinska, K., Ng, B. G., Maccarana, M., Bengtson, P., Poeta, M., et al. (2018). Three Unreported Cases of TMEM199-CDG, a Rare Genetic Liver Disease with Abnormal Glycosylation. *Orphanet J. Rare Dis.* 13 (1), 4. doi:10.1186/s13023-017-0757-3

Yarema, K. J., and Bertozzi, C. R. (2001). Characterizing Glycosylation Pathways. *Genome Biol.* 2 (5), REVIEWS0004. doi:10.1186/gb-2001-2-5-reviews0004

Conflict of Interest: The authors declare that the research was conducted in the absence of any commercial or financial relationships that could be construed as a potential conflict of interest.

Publisher's Note: All claims expressed in this article are solely those of the authors and do not necessarily represent those of their affiliated organizations, or those of the publisher, the editors, and the reviewers. Any product that may be evaluated in this article, or claim that may be made by its manufacturer, is not guaranteed or endorsed by the publisher.

frontiers in Pediatrics

ORIGINAL RESEARCH
published: 28 March 2022
doi: 10.3389/fped.2022.814461

Establishment of Cutoff Values for Newborn Screening of Six Lysosomal Storage Disorders by Tandem Mass Spectrometry

Ruotong Li†, Liping Tian†, Qing Gao, Yuanfang Guo, Gaijie Li, Yulin Li, Meng Sun, Yan Yan, Qing Li, Wenying Nie and Hui Zou**

Neonatal Disease Screening Center, Jinan Maternity and Child Care Hospital Affiliated With Shandong First Medical University, Jinan, China

OPEN ACCESS

Edited by:
Yuan-Zong Song, First Affiliated Hospital of Jinan University, China

Reviewed by:
Joseph J. Orsini, New York State Department of Health, United States
Michael H. Gelb, University of Washington, United States

***Correspondence:**
Hui Zou
zouhui819@163.com
Wenying Nie
goodddd@163.com

†*These authors have contributed equally to this work*

Specialty section:
This article was submitted to Genetics of Common and Rare Diseases, a section of the journal Frontiers in Pediatrics

Received: *13 November 2021*
Accepted: *11 February 2022*
Published: *28 March 2022*

Citation:
Li R, Tian L, Gao Q, Guo Y, Li G, Li Y, Sun M, Yan Y, Li Q, Nie W and Zou H (2022) Establishment of Cutoff Values for Newborn Screening of Six Lysosomal Storage Disorders by Tandem Mass Spectrometry. Front. Pediatr. 10:814461. doi: 10.3389/fped.2022.814461

Objective: Lysosomal storage disorders (LSDs) are becoming increasingly important in newborn screening, and tandem mass spectrometry (MS/MS) is widely used in newborn screening for LSDs through measurement of enzymatic activities in dried blood spots (DBSs). Overall, the determination of the cutoff value is important in such screening, and different laboratories have different methods of determining this value; most do not use a fixed cutoff value but rather calculate the corresponding batch cutoff value based on each batch of experimental data. In this study, we used MS/MS to screen for LSDs and sought to find an appropriate method to establish the cutoff value for LSD screening.

Methods: A total of 38,945 samples from newborn blood tablets collected from various maternity hospitals in six cities in Shandong province, including Jinan, Dezhou, Heze, Linyi, Weifang, and Zibo, were tested using a *Waters Xevo TQD* tandem mass spectrometer; the experimental data were analyzed with *MassLynx V4.1.* The laboratory used 30% of the median GLA enzyme activity and 20% of the median ABG, ASM, GALC, IDUA, and GAA enzyme activities in every test as the cutoff values for that batch of experiments.

Results: There were 254 suspicious positives in the initial screening test, including one case of Gaucher disease, one of Niemann-Pick disease, 47 of Krabbe disease, four of MPS-I, 21 of Fabry disease, and 180 of Pompe disease. After genetic screening, 11 children were diagnosed, including three with Pompe disease, three with Fabry disease, and five with Krabbe disease. In addition, the enzyme activity cutoff value of this experiment showed seasonal variation, which was initially believed to be related to the ambient temperature, such as the effect of ambient temperature on the human body or the temperature when the blood tablets dried naturally.

Conclusion: Overall, MS/MS can be used in LSD screening, and using different cutoff values in each batch of experiments is feasible. The ambient temperature might be a reason why the enzyme activity cutoff value has seasonal variation. More samples are needed to develop a method of determining cutoff values in laboratories.

Keywords: lysosomal storage disorders, newborn screening, cut-off value, tandem (hybrid) mass spectrometry, diagnose

INTRODUCTION

Lysosomal storage disorders (LSDs) are a group of rare genetic metabolic diseases, and it is found that early treatment can lead to the optimal clinical effect (1). Some research finds that there is approximately one LSD case among ∼7,700 newborns (2). Therefore, newborn screening for LSDs is increasingly important.

Lysosomes are organelles with monolayer membrane cystic structures containing a variety of hydrolytic enzyme substances that decompose many substances. Approximately 60 enzymes are involved in lysosomal catabolism (1). LSDs occur when some of these enzymes or other lysosomal proteins cannot perform their functions. Moreover, LSDs are believed to occur due to genetic variation (3). Indeed, mutation can lead to deficiency in certain lysosomal enzymes, which causes the corresponding substrates in the cells to be stored without being degraded, causing cell metabolism disorders and organ dysfunction (4). Nevertheless, some nonenzymatic lysosomal and nonlysosomal proteins related to lysosomal activity are considered to only represent a small component, and such accumulation might begin early in embryonic development (5). Currently, LSDs comprise more than 50 genetic metabolic disorders. Most of these disorders are inherited in an autosomal recessive manner with a small portion being X-chromosome linked (1). Lysosomal diseases can be classified in many ways, the most common of which is based on the nature of the accumulated substrate. For example, the corresponding enzymes in MPS-I, Fabry, Gaucher, Krabbe, Niemann-Pick, and Pompe diseases are IDUA, GLA, ABG, GALC, ASM, and GAA, respectively. However, some research in Chinese populations shows that the most common LSD in China is MPS-II (6).

The first disease screened for in neonates using dried blood tablets was phenylketonuria (PKU); the detection method reveals whether a neonate lacks phenylalanine hydroxylase by assessing the amount of the enzyme present (7). Previous studies find that the enzymatic activities of several lysosomal enzymes are retained in dried blood spots (DBSs) used for neonatal disease screening (8). Therefore, DBS testing can be used in the screening of LSDs. Tandem mass spectrometry (MS/MS) is currently the most common screening method for DBSs, and it can quantitatively assess lysosomal enzyme activity.

The gold standard for any test is the positive predictive value (PPV), which is the ratio of true positives to test positives (10). However, the determination of this value is difficult for LSD screening experiments because it is difficult to determine whether newborns who screen as positive truly have the disorder. First, some gene mutations lead to late-onset LSDs, such as late-onset Pompe disease, which would delay the determination of true positives (9). Second, LSDs are considered rare diseases, and the incidence of some is one in tens of or even hundreds of thousands (the incidence of MPS-VII could be <1 in 300,000) (11). Thus, a laboratory needs sufficiently large experimental data to prove the PPV. Based on the above, the false negative and positive rates are significant for NBS screening laboratories; determination of the cutoff value is also important. According to some research, most laboratories do not use a fixed enzyme activity cutoff value, but generally use the multiple or percentage of the median or mean of the enzyme activity of a test batch with unique cutoff values for each batch (7). According to the research of [Burlina et al. (12)], using 30% of the median GLA enzyme activity and 20% of the median of the other enzyme activities in each test as cutoff values would result in recalls that neither miss positive cases nor recall too many healthy children. For the first time, we used this method to determine cutoff values, such that the cutoff value could be flexibly adjusted according to the test situation to prevent excessive false positive or negative detection. Furthermore, a stable cutoff value would render data analysis relatively straightforward and allow screening results to be more comparable between studies. In this study, we sought to determine a fixed cutoff value.

This study summarizes 38,945 LSD screening data points, including MPS-I, Fabry, Gaucher, Krabbe, Niemann-Pick, and Pompe disease data obtained by MS/MS, from the Newborn Disease Screening Laboratory in Jinan City. We also verified the test method and the method used to establish the cutoff value.

METHODS

The main technique used for this project was MS/MS, which can determine the activity of six lysosomal enzymes in newborns, allowing for the risk of six LSDs to be assessed.

Instrumentation

A tandem mass spectrometer (*Waters Xevo TOD)* and incubation shaker (*Thermo MB100-4A*) were utilized in this study.

Reagents

A screening kit for six LSDs (NeoLSD MS/MS Kit, PerkinElmer) was used in this study.

Procedure

The samples used in this experiment were DBSs of newborns (age between 27 h and 7 days), which were sent to the Jinan Newborn Disease Screening Center from various maternity hospitals in six cities in Shandong province, including Jinan, Dezhou, Heze, Linyi, Weifang, and Zibo; informed consent was obtained from the parents. The collected dried blood tablets were stored under low-temperature drying conditions. Every week, the experimenter randomly selected ∼700 continuous samples from the screening samples for that week, which was convenient for associating newborn information with LSD data for LSD detection. Moreover, we conducted a reexamination of the original blood film of the positive samples in the previous batch of experiments as well as a call-up test for suspected positive cases.

The dried blood tablets were hole-punched into 96-well plates with one hole-punched sample per dried blood tablet. Each 96-well plate included two blank wells (BL), two sets of DBS quality controls (C1, C2, C3), and 88 samples. After adding 30 μl of reaction mixture containing buffer, six substrates, and six internal standards, the plates were covered with an aluminum

foil microplate sealing membrane and incubated on a shaker (400 rpm) for more than 18 h at 37°C. After incubation, the microplates were cooled to room temperature, and 100 μl of quencher (a mixture of methanol and NeoLSD extract with a volume ratio of 50:50) was added to stop the reaction; the samples were repeatedly pipetted up and down 10 times with pipette tips to ensure that the blood spot solution was completely mixed with the quencher. Then, all the liquid in the microplates was transferred to deep 96-well plates, and 400 μl of NeoLSD extract (ethyl acetate) and 200 μl of ultrapure water were added to each well with repeated blowing 20 times using a pipette tip. The aluminum foil microplates were sealed and centrifuged for 5 min at 2,500 rpm, after which 50 μl of the supernatant was pipetted into a U-shaped microplate. This step was conducted carefully to avoid collecting any of the lower water layers. The liquid in the microplate was blown dry using nitrogen. After the reagent was completely volatilized, 100 μl of flow solvent was added, the sealing film was attached, and the mixture was shaken at low speed for 10 min prior to analysis.

The analysts checked whether the quality control and total ion chromatogram (TIC) were normal and uploaded them to the Anaconda system to analyze the resulting data. For cutoff value establishment, the laboratory initially established the value based on the research of Burlina et al. (12), in which the cutoff value of GLA enzyme activity was 30% of the median activity in each test, and 20% of the median of IDUA, ABG, ASM, GALC, and GAA enzyme activities in each test was used as the cutoff values for these enzymes. If the first screening result was positive, the analysts performed a reexamination of the original DBS. Then, if the results of both tests were positive, the center recalled the newborns for a second blood sampling and DBS test. Finally, if the results of reexamination were positive, the child underwent DNA tests based on the doctors' judgment.

RESULTS

Summary of Screening Experimental Results

There were a total of 38,945 newborns who were screened for six LSDs by MS/MS using DBSs. If the results of the first newborn screening were positive, the original DBS was used for a second test. The newborns with two positives in screening were recalled to collect a new DBS for analysis. If the results of the review were positive, doctors combined the children's physical signs and genetic test results as confirmation of the diagnosis. **Table 1** shows the summary of the positives in the initial screening, positives in the original DBS reviews, positives in the second DBS reviews and confirmed number of cases. For all DBSs in LSD screening, there were 402 positives in the initial test, and 254 samples were still positive based on the original DBS review. Among them, GAA had the highest positive rate. For the children who were still positive in the original DBS reviews, the NBS center recalled them and collected a second DBS for testing. Finally, the children were subjected to genetic screening, and three children were diagnosed with Pompe disease, three were diagnosed with Fabry disease, and five were diagnosed with Krabbe disease (**Table 2**). Additionally, the genetic results revealed five Pompe disease carriers, two Fabry disease carriers, and three Krabbe disease carriers.

TABLE 1 | The rate of screening positive, review positive, and confirmed disorders in LSD newborn screening (due to lack of reagents, not all the initial screening positives on July 22 and July 27, 2020, were followed up).

Enzyme/LSD	ABG	ASM	GALC	IDUA	GLA	GAA	Total
Positives in initial screening	12	1	71	5	34	279	402
Positives in second original DBS review	1	1	47	4	21	180	254
Suspected cases	0	0	5	0	3	3	11

The type of gene sequence variation in nine suspected cases was "uncertain significance" but with a persistent decrease in enzyme activity as well as signs.

TABLE 2 | Genetic site information and enzyme activity in the screening experiment in confirmed cases.

Number	Disease	Enzyme	Genetic results	Screening result
1	Fabry	GLA	c.1019G > C	0.3 (2.54)
2	Fabry	GLA	c.1286–7del	2.12 (2.74)
3	Fabry	GLA	c.454T > C	0.48 (2.56)
4	Pompe	GAA	c.859-2A > T c.2065G > A	0.42 (1,73)
5	Pompe	GAA	c.752C > T c.761C > T	0.61 (1.92)
6	Pompe	GAA	c.752–761delins c.1757C > T	0.4 (1.72)
7	Krabbe	GALC	c.1901T > C c.2041G > A	0.33 (0.93)
8	Krabbe	GALC	c.1901T > C c.1901T > C	0.52 (0.92)
9	Krabbe	GALC	c.1901T > C c.1901T > C	0.45 (0.87)
10	Krabbe	GALC	c.1204G > A c.1535G > T	0.21 (0.7)
11	Krabbe	GALC	c.1901T > C c.1671–14G > A	0.35 (0.61)

In the "screening result" column, the parentheses are cutoff values for the batch of experiments.

Cutoff Value

ABG, ASM, GALC, IDUA, and GAA are lysosomal enzymes with reduced activity in Gaucher disease, Nimann-Pick disease, Krabbe disease, MPS-I, and Pompe disease, respectively. Thus, we decided to use 30% of the median enzyme activity of GLA in each experiment as the cutoff value for Fabry disease; the cutoff values for the other five diseases were 20% of the median enzyme activity. To determine the fixed cutoff value, the cutoff values for all experiments from August 2019 to June 2021 were

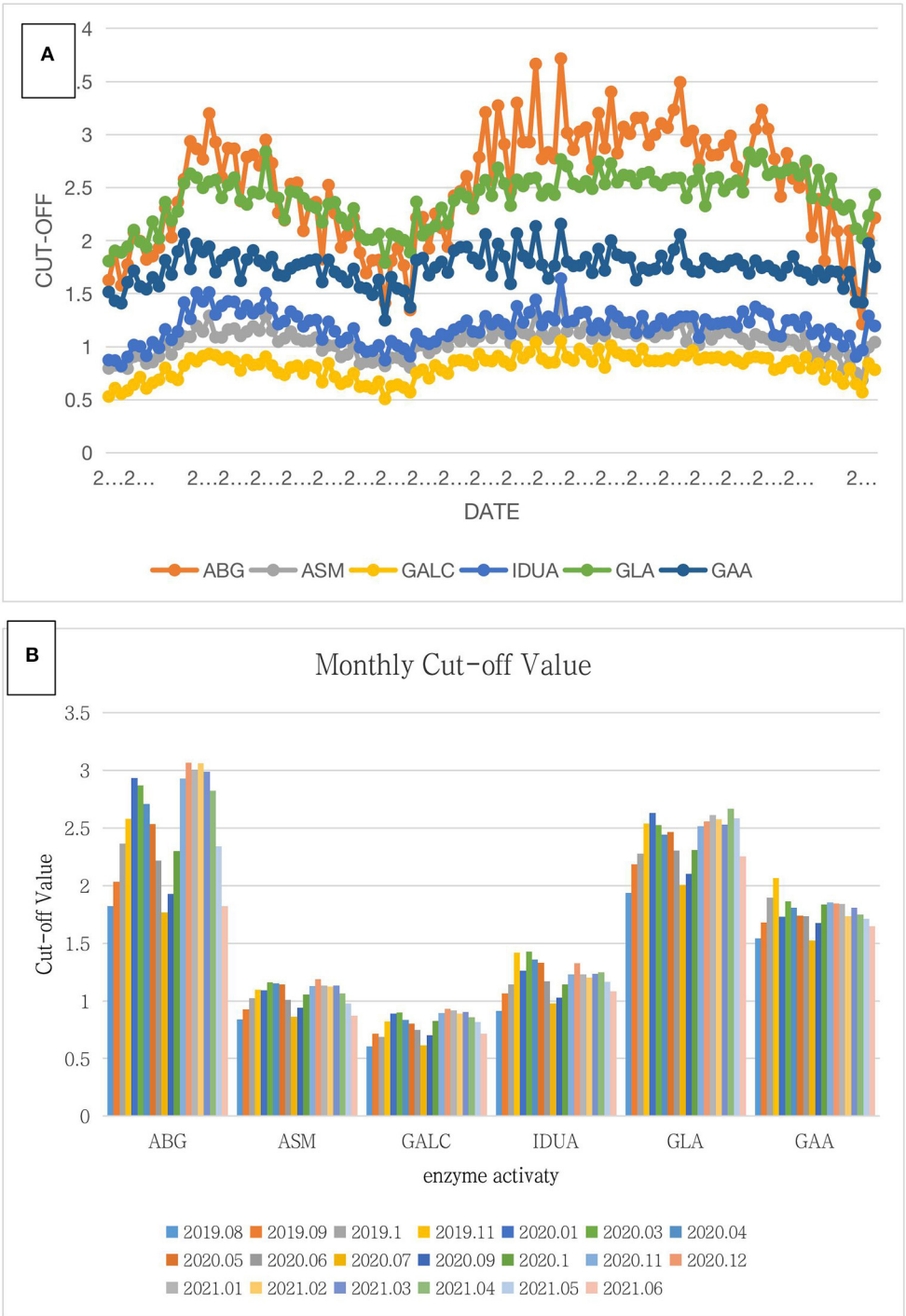

FIGURE 1 | Summary of the cutoff value for 38,945 screening samples. **(A)** In this chart, the abscissa is the date of the experiment, and the ordinate is the cutoff value of six lysosomal enzymes. The orange, gray, yellow, blue, green, and navy blue lines represent ABG, ASM, GALC, IDUA, GLA, and GAA, respectively. The overall trend of the six lysosomal enzymes was first an increase and then a decrease followed by another increase, finally showing a downward trend. Among them, the increasing trends of ABG and GLA were obvious though the changes in ASM, IDUA, GAA, and GALC were not significant. **(B)** In this chart, the abscissa is six lysosomal enzymes, and the ordinate is the average monthly cutoff value. Differently colored bars represent different months. For all six lysosomal enzymes, the average cutoff values were the lowest in July and highest in November, December, January, or February.

summarized (**Figure 1**). Activities of ABG and GLA lysosomal enzymes changed significantly over time, peaked in November 2019 and December 2020, and decreased to a minimum in July 2020. In contrast, the other four lysosomal enzymes did not show a significant seasonal change (**Figure 1A**). **Figure 1B** compares the monthly average cutoff values after statistical analysis of the data during the experiment. All six lysosomal enzymes showed the lowest activity in July, whereas the highest activity appeared in November, December, January, or February.

DISCUSSION

It is necessary to promote newborn screening for LSDs. In Europe, the United States, Taiwan, and many other countries, this screening has been ongoing for a long time (12). MS/MS, a high-throughput screening method, can detect enzyme activity by measuring the number of related products of the reaction (13). Moreover, the application of MS/MS to disease screening is common in neonatal disease-screening laboratories; it was first used to screen for PKU. In this study, MS/MS was mainly used to analyze the activity of IDUA, ABG, ASM, GALC, GLA, and GAA, which are reduced in MPS-I, Gaucher disease, Nimann-Pick disease, Krabbe disease, Fabry disease, and Pompe disease, respectively. Among these 38,945 samples, three children were diagnosed with Pompe disease, three with Fabry disease, and five with Krabbe disease through genetic screening. The total incidence of LSDs was nearly 1/3,000 though some research shows that the rate of these diseases is 1/6,000–7,000 (2). This discrepancy might be due to the inclusion of carriers in screen-positive specimens, and the enzyme activity of carriers would also be reduced. More samples are needed to verify the disease incidence in Shandong. The positive rate in Pompe disease was highest among the six diseases in the screening experiment, but the number of diagnosed children was not the largest either due to the effect on screening results of reduced enzyme activity in carriers or because current cutoff value establishment methods are not suitable for Pompe disease; more samples are needed to clarify this. On the other hand, there were no confirmed cases of Gaucher disease, Niemann-Pick disease, or MPS-I among any of the test samples. The incidence of Gaucher disease has strong regional and ethnic differences; it is relatively common in Eastern Europe (14), and the incidence is ∼1/500,000 to 1,000,000 (15). Similarly, Niemann-Pick disease has the lowest incidence in China, and it is mainly found in the Middle East, Western Europe, North America, and other countries, which may be why no confirmed cases of these two diseases were found in this study. Although some research shows that MPS is common in China, there were no confirmed cases in this study. This result might be because MPS with a relatively high incidence in China would be type II or type IVA (16), but the main MPS type analyzed in this study was MPS-I. Therefore, research on MPS-II and MPS-IV marker screening tests is needed.

We sought to determine a fixed cutoff value of the LSD screening experiment for this laboratory. However, lysosomal enzyme activity cutoff values differed according to the month. In fact, lysosomal enzyme activity cutoff values were lowest in July and August and highest in December and January. This situation made it difficult to establish a fixed cutoff value. We attempted to explore the reasons for this, and we initially thought changes in temperature to be a factor. The main principle of this experiment was to detect the activity of lysosomal enzymes in DBSs, and enzyme activity appears to be affected by temperature (17). This effect might be divided into the effect of low or high temperatures, but the main difference between these two conditions is that high temperatures would completely inactivate enzymes and low temperatures would not (18). This research was conducted in Shandong, China, and July and August are the 2 months with the highest average temperature in this region. Moreover, all six lysosomal enzymes showed low activity, which might be affected by high temperature. Conversely, low temperature would not inactivate an enzyme but cause a dormant state with activity being restored when the temperature returns to a suitable one (19). The results of this experiment are in accordance with this idea. All six lysosomal enzyme activities were highest in December and January, when the temperature was lowest in the 1-year test. This result might be because a relatively low ambient temperature would provide low-temperature storage conditions for lysosomal enzymes, which would better retain the enzyme activity. This is in accordance with the change in enzyme activity. Therefore, the change in the cutoff value might be related to the change in temperature. This experiment was carried out in a laboratory environment with constant temperature and humidity, and the blood tablets were transported to the laboratory through a cold chain. Nonetheless, the effect of different outdoor temperatures on enzyme activity in the human body and blood tablets at room temperature drying after collection might also cause changes in enzyme activity. In summary, using a fixed cutoff value leads to an increase in false positives in winter and false negatives in summer. However, more samples are required to further verify the effectiveness of the cutoff value establishment method. Although the incidence of lysosomal storage disease is 1 in 7,000 to 8,000, the incidence of each single disease is relatively low; for example, the incidence of Pompe disease is ∼1 in 40,000 (20).

Overall, MS/MS is feasible for screening LSDs. In this research, the highest initial screening positive rate was for Pompe disease (GAA), and there were eight children with suspected related gene mutation among the 38,945 newborns in the newborn screening test of LSDs but only three confirmed cases with two causative sites were detected. Moreover, we found that the lysosomal enzyme activity cutoff value exhibited seasonal variation, and we suggest that the main reason for this is the effect of seasonal temperature on enzyme activity. Therefore, it is optimal to change the cutoff value for each test batch. According to the current experimental data, the cutoff value establishment method was feasible, but the high rate of positivity in Pompe disease screening might reflect that this cutoff value establishment method is not suitable for screening for Pompe disease in this laboratory. More samples

are needed. Overall, 11 children with suspected mutations were successfully screened in this study. However, due to the low disease incidence, more samples are needed for further verification. Furthermore, as LSDs with high incidence in China are different from those in other countries, new markers need to be further studied to improve screening of LSDs in the Chinese population.

DATA AVAILABILITY STATEMENT

The original contributions presented in the study are included in the article/supplementary materials, further inquiries can be directed to the corresponding authors.

AUTHOR CONTRIBUTIONS

RL and LT designed the study and wrote the manuscript. RL, QG, YG, GL, YY, and QL prepared the materials used in the experiment and collated the data. RL, YL, and MS analyzed the data. HZ and WN were responsible for the supervision and leadership of the experiment and the review of the first draft of the manuscript. All authors contributed to the article and approved the submitted version.

FUNDING

This work was supported by the Shandong Provincial Natural Science Foundation (2021.01-2023.12).

REFERENCES

1. Schielen PCJI, Evelien KA, Gelb MH. Newborn screening for lysosomal storage diseases: a concise review of the literature on screening methods, therapeutic possibilities and regional programs. *Int J Neonatal Screen.* (2017) 3:6. doi: 10.3390/ijns3020006
2. Skrinjar P, Schwarz M, Lexmüller S, Mechtler TP, Zeyda M, Greber-Platzer S, et al. Rapid and modular assembly of click substrates to assay enzyme activity in the newborn screening of lysosomal storage disorders. *ACS Cent Sci.* (2018) 4:1688–96. doi: 10.1021/acscentsci.8b00668
3. Fuller M. Laboratory diagnosis of lysosomal diseases: newborn screening to treatment. *Clin Biochem Rev.* (2020) 41:53–66. doi: 10.33176/AACB-19-00037
4. Klein AD, Futerman AH. Lysosomal storage disorders: old diseases, present and future challenges. *Pediatr Endocrinol Rev.* (2013) 11(Suppl 1):59–63.
5. Filocamo M, Morrone A. Lysosomal storage disorders: molecular basis and laboratory testing. *Human Genomics.* (2011) 5:156–169(14). doi: 10.1186/1479-7364-5-3-156
6. Gong C, Li X. 黏多糖贮积症Ⅱ型的诊断及治疗进展.医学研究杂志(2021) 50:1–5. doi: 10.11969/j.issn.1673-548X.2021.06.001
7. Gelb MH, Lukacs Z, Ranieri E, Schielen PCJI. Newborn screening for lysosomal storage disorders: methodologies for measurement of enzymatic activities in dried blood spots. *Int J Neonatal Screen.* (2019) 5:1. doi: 10.3390/ijns5010001
8. Wilcken B, Wiley V. Fifty Years of Newborn Screening. *J Paediatr Child Health.* (2015) 51:103–7. doi: 10.1111/jpc.12817
9. Elliott S, Buroker N, Cournoyer JJ, Potier AM, Trometer JD, Elbin C, et al. Pilot study of newborn screening for six lysosomal storage diseases using Tandem Mass Spectrometry. *Mol Genet Metab.* (2016) 118:304–9. doi: 10.1016/j.ymgme.2016.05.015
10. Gelb M. Newborn screening for lysosomal storage diseases: methodologies, screen positive rates, normalization of datasets, second-tier tests, and post-analysis tools [J]. *Int J Neonatal Screen.* (2018) 4:23. doi: 10.3390/ijns4030023
11. Montaño AM, Lock-Hock N, Steiner RD, Graham BH, Szlago M, Greenstein R, et al. Clinical course of sly syndrome (mucopolysaccharidosis type VII). *J Med Genet.* (2016) 53:403–18. doi: 10.1136/jmedgenet-2015-103322
12. Burlina AB, Polo G, Salviati L, Duro G, Zizzo C, Dardis A, et al. Newborn screening for lysosomal storage disorders by tandem mass spectrometry in North East Italy. *J Inherit Metab Dis.* (2018) 41:209–19. doi: 10.1007/s10545-017-0098-3
13. Nakamura K, Hattori K, Endo F. Newborn screening for lysosomal storage disorders[J]. *Am J Med Genet C Semin Med Genet.* (2012) 157:63–71. doi: 10.1002/ajmg.c.30291
14. Beutler E, Gelbart T. Glucocerebrosidase (Gaucher disease). *Hum Mutat.* (1996) 8:207–13. doi: 10.1002/(SICI)1098-1004(1996)8:3<207::AID-HUMU2>3.0.CO;2-6
15. Zhou X, Yao R. 戈谢病1例报告. 温州医科大学学报. (2015) 6:76–7. doi: 10.3969/j.Issa.2095-9400.2015.06.019
16. 张惠文, 王瑜, 叶军, 等. 黏多糖贮积症47例的常见酶学分型[J]. 中华儿科杂志. (2009) 47:276–280. doi: 10.3760/cma.j.issn.0578-1310.2009.04.010
17. Tortorelli S, Turgeon CT, Gavrilov DK, et al. Simultaneous testing for 6 lysosomal storage disorders and x-adrenoleukodystrophy in dried blood spots by tandem mass spectrometry. *Clin Chem.* (2016) 62:1248–54. doi: 10.1373/clinchem.2016.256255
18. More N, Daniel RM, Petach HH. The effect of low temperatures on enzyme activity. *Biochem J.* (1995) 305:17–20. doi: 10.1042/bj3050017
19. Peterson ME, Daniel RM, Danson MJ, Eisenthal R. The dependence of enzyme activity on temperature: determination and validation of parameters. *Biochem J.* (2007) 402:331–7. doi: 10.1042/BJ20061143
20. *Effect of Temperature on Enzyme Activity StudyMode.com.* (2013). Available online at: https://www.studymode.com/essays/Effect-Of-Temperature-On-Enzyme-Activity-1344373.html (accessed 1, 2013).

Conflict of Interest: The authors declare that the research was conducted in the absence of any commercial or financial relationships that could be construed as a potential conflict of interest.

Publisher's Note: All claims expressed in this article are solely those of the authors and do not necessarily represent those of their affiliated organizations, or those of the publisher, the editors and the reviewers. Any product that may be evaluated in this article, or claim that may be made by its manufacturer, is not guaranteed or endorsed by the publisher.

frontiers | Frontiers in Genetics

CASE REPORT
published: 14 April 2022
doi: 10.3389/fgene.2022.856552

Acute Lymphoblastic Leukemia in Combined Methylmalonic Acidemia and Homocysteinemia (cblC Type): A Case Report and Literature Review

*Jun Zhu[1†], Shuisen Wan[1†], Xueqi Zhao[1†], Binlu Zhu[2], Yuan Lv[3] and Hongkun Jiang[1]**

[1]Department of Pediatrics, The First Hospital of China Medical University, Shenyang, China, [2]Department of Pediatrics, West China Second University Hospital, Chengdu, China, [3]Department of Gynecology and Obstetrics, Shengjing Hospital of China Medical University, Shenyang, China

OPEN ACCESS

Edited by:
Huiwen Zhang,
Xinhua Hospital, China

Reviewed by:
Wanjin Chen,
First Affiliated Hospital of Fujian Medical University, China
Maged Mostafa Mahmoud,
King Abdulaziz University, Saudi Arabia

***Correspondence:**
Hongkun Jiang
jianghongkun007@163.com

†These authors have contributed equally to this work and share first authorship

Specialty section:
This article was submitted to Genetics of Common and Rare Diseases, a section of the journal Frontiers in Genetics

Received: *17 January 2022*
Accepted: *21 March 2022*
Published: *14 April 2022*

Citation:
Zhu J, Wan S, Zhao X, Zhu B, Lv Y and Jiang H (2022) Acute Lymphoblastic Leukemia in Combined Methylmalonic Acidemia and Homocysteinemia (cblC Type): A Case Report and Literature Review. Front. Genet. 13:856552. doi: 10.3389/fgene.2022.856552

Background: Methylmalonic acidemia (MMA) can display many clinical manifestations, among which acute lymphoblastic leukemia (ALL) has not been reported, and congenital heart disease (CHD) is also rare.

Case presentation: We report an MMA case with ALL and CHD in a 5.5-year-old girl. With developmental delay and local brain atrophy in MRI, she was diagnosed with cerebral palsy at 9 months old. Rehabilitation was performed since then. This time she was admitted to hospital because of weakness and widespread bleeding spots. ALL-L2 (pre-B-cell) was confirmed by bone marrow morphology and immunophenotyping. Echocardiography showed patent foramen ovale. The girl was treated with VDLD and CAML chemotherapy, during which she developed seizures, edema and renal insufficiency. Decrease of muscle strength was also found in physical examination. Screening for inherited metabolic disorders showed significantly elevated levels of methylmalonate-2, acetylcarnitine (C2), propionylcarnitine (C3), C3/C2 and homocysteine. Gene analysis revealed a compound heterozygous mutaion in *MMACHC* (NM_015,560): c.80A > G (p.Gln27Arg) and c.609G > A (p.Trp203*). CblC type MMA was diagnosed. Intramuscular injection of cyanocobalamin and intravenous L-carnitine treatment were applied. The edema vanished gradually, and chemotherapy of small dosage of vindesine was given intermittently when condition permitted. 2 months later, muscle strength of both lower limbs were significantly improved to nearly grade 5. The levels of methylmalonic acid and homocysteine were improved.

Conclusion: Metabolic disease screening and gene analysis are very necessary for diseases with complex clinical symptoms. ALL can be a rare manifestation for MMA.

Synopsis: We report a case of methylmalonic acidemia with acute lymphoblastic leukemia and congenital heart disease, which uncovered the importance of genetic testing and metabolic diseases screening in patients with multiple systemic organ involvement.

Keywords: methylmalonic acidemia, acute lymphoblastic leukemia, congenital heart diseases, homocysteinemia, genetic analysis

INTRODUCTION

Methylmalonic acidemia (MMA) is an autosomal recessive disorder of methylmalonate and cobalamin (cbl; vitamin B12) metabolism first reported in 1967. Two main forms and different subtypes of the disease were identified based on enzymic and metabolic abnormalities: methylmalonyl-CoA mutase (MCM) defects, caused by mutation in *MUT* gene, including MUT^0 and MUT^- type; and synthesis and dysfunction of adenosylcobalamin (AdoCbl) and methylcobalamin (MeCbl), associated with mutation in *MMAA*, *MMAB*, *MMCHC*, *MMADHC*, *LMBRD1*, *HCFC1*, and *ABCD4* gene, including cblA, cblB, cblC, cblD, cblF, cblX, and cblJ type (Zhou et al., 2018). According to clinical and biochemical characteristics, MMA can also be classified into two phenotypes: isolated MMA, including *cblA*, *cblB*, *cblH*, and *MUT* deficiencies; and combined MMA, where the levels of both methylmalonic acid and homocysteine elevate, such as *cblC*, *cblD*, and *cblF* deficiencies (Watkins and Rosenblatt, 2013).

Abnormal accumulation of toxic metabolites can cause multisystem damages, including kidney, heart, eye, skin and nervous system, as well as gastrointestinal system and immune system. Symptoms may occur before 1 year of age or in early infancy (early-onset MMA), and may also appear between the ages of 4 and 14, even in adulthood (late-onset MMA). Clinical presentations are relatively non-specific, such as lethargy, seizures, developmental delay, hypotonia, movement disorders, feeding difficulties and vomiting (Zhou et al., 2018). Hematological disorders have been reported in some cases, such as megaloblastic anemia, neutropenia or pancytopenia. Cardiovascular changes have also been observed in few cases, such as cardiomyopathy and arrhythmias.

In this study, we reported a combined MMA (cblC type) case in a 5.5-year-old girl, with rare complications -- acute lymphoblastic leukemia (ALL) and patent foramen ovale (PFO). To our knowledge, no such complication has ever been described.

CASE PRESENTATION

The patient was a 5.5-year-old girl, whose primary symptom was developmental retardation—unable to crawl at 9 months. With no history of intrauterine infection or postnatal asphyxia, the girl was diagnosed with cerebral palsy by local hospital based on brain MRI changes. After receiving aggressive rehabilitation, she was barely able to walk without help until nearly 3 years old.

In January 2021, the girl was brought into hospital again because of weakness and widespread bleeding spots for 1 week. Pale lips and face, petechiae in skins and edema in eyelids were observed in physical examination. Blood routine examination showed severe anemia (hemoglobin of 53 g/L), moderate thrombocytopenia (platelets of 22×10^9/L), with normal white blood cell count (6.53×10^9/L). Liver function, kidney function and myocardial enzyme tests were all normal. Proteinuria (+) was detected, and 24-hour urine protein was 0.38 g. Echocardiography showed patent foramina ovale of 3.4 mm. In order to find out the reason of hematological abnormalities, bone marrow puncture was performed. Morphology and immunophenotyping confirmed the diagnosis of ALL-L2 (pre-B-cell). Ph-like ALL gene analysis showed positive mutated *IKZF1* gene, lower expression of *CRLF2* gene and positive mutated *WTI* gene. No abnormal karyotype was found in chromosome analysis. VDLD regimen (vindesine, daunorubicin, L-asparaginase and prednisone) was used as induction chemotherapy. Complete remission (CR) was achieved 15 days later, with the mutated *IKZF1* gene turning negative.

Treatment for leukemia continued for 2 months, when the girl developed vomiting, abdominal pain, distension and muscle tension during the early intensive CAML chemotherapy (cyclophosphamide, cytarabine, mercaptopurine and pegaspargase). Severe acute pancreatitis was diagnosed based on elevated serum amylase, lipase and characteristic abdominal CT changes. At same time, she showed recurrent attack of generalized seizures. Ambulatory electroencephalogram revealed lateralized periodic epileptic discharges in the left brain, and partial discharges from the left back side. Brain magnetic resonance imaging (MRI) showed encephalomalacia and gliosis in the left frontal and parietal lobe and basal ganglia, with regional brain atrophy, and abnormal signals in the left lateral ventricle and semicovale region (**Figure 1**). She also showed edema, hypertension, increased urinary protein (+++, 2.035 g/24 h) and hematuria (blood test +++, RBCs 25.52/HP). Chemotherapy was halted to deal with pancreatitis, seizures and renal injury. After her condition improved, the girl was discharged with prescriptions of oral levetiracetam, nifedipine, prednisone and furosemide.

1 month later, she showed gradually aggravated edema, hypertension, renal dysfunction, oliguria (about 200ml/24 h) and three episodes of seizures. Physical examination results at this admission were: BP 133/102 mmHg, severe edema in both eyelids and lower limbs, pale lips and face, and decrease of muscle strength (grade 3 in upper limbs, grade 2 in lower limbs), with normal muscle tone. Massive proteinuria (++++, 2.255 g/24 h) and hematuria (blood test +++, RBCs 38.42/HPF) was detected. Peripheral blood test results were: WBC of 8.26×10^9/L ($4\text{-}10\times10^9$/L), Neutrophil of 6.24×10^9/L ($1.8\text{-}6.3\times10^9$/L), hemoglobin of 85 g/L (110–140 g/L), platelets of 65×10^9/L ($100\text{-}300\times10^9$/L), albumin of 28.9 g/L (40–55 g/L), lactic dehydrogenase (LDH) of 2963U/L (120–250U/L), urea of 14.36 mmol/L (2.85–7.14 mmol/L) and creatinine of 88 μmol/L (59–104 μmol/L). Calculated creatinine clearance (Ccr) was 36 ml/min. Based on these results, the girl was diagnosed with CKD(G3b).

Considering the early-onset of symptoms and multisystem involvement, screening for metabolic diseases was performed. Results are: methylmalonic acid-2 of 8.68 umol/L (0.2-3.6 umol/L), serum homocysteine of >50 umol/L (4.44-13.56 umol/L), free carnitine of 177.194 umol/L (10-60 umol/L), acetylcarnitine (C2) of 58.959 umol/L (6-30 umol/L), propionylcarnitine (C3) of 17.561 umol/L (0.5-4 umol/L), and C3/C2 of 0.298 (0.04-0.25). MMA was suspected, whole exome sequencing (WES) was performed, and detected mutations was verified by Sanger

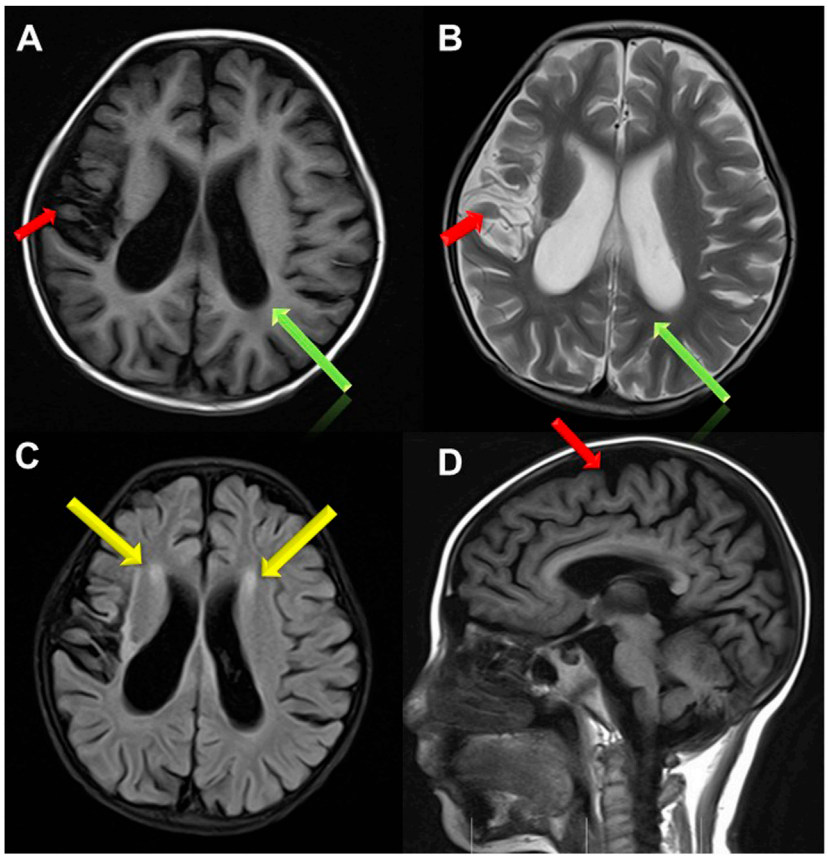

FIGURE 1 | Brain MRI images. **(A,B,D)** Brain atrophy was found in Transverse T1 and T2 weighted image and Sagittal T1 weighted image(the red arrow); Sulci fissure widened and deepened in Transverse T1 and T2 weighted image (the green arrow); **(C)** High signal in white matter near to bilateral periventricular in FLAIR sequence (the yellow arrow).

sequencing. The proband had a compound heterozygous mutation in MMACHC gene, c.80A > G (p.Gln27Arg) in exon 1 inherited from her mother, and c.609G > A (p.Trp203*) in exon 4 [reference sequence: NM_015560) from father (**Figure 2**). c.609G > A(p.Trp203*]is a nonsense mutation, which is expected to change the 203rd amino acid of encoded protein from Trp to stop codon, causing the encoded protein to be truncated and lose its normal function. As was reported in several literatures, this mutation is a hot mutation in Chinese patients with methylmalonic acidemia and homocysteinemia. In the gnomAD database, the frequency of this variation in East Asian population is 0.0005562. c. 80A > G (p.gln27arg) is a missense mutation, which is expected to change the 27th amino acid of the encoded protein from Gln to ARG. The frequency of this mutation in gnomAD database is 0.0001669 in East Asian population. Considering the ACMG score, both variants are pathogenic.

The final diagnosis was determined as combined methylmalonic acidemia and homocysteinemia (cblC type), secondary nephrotic syndrome (nephritis type), secondary hypertension (level 2), and chronic kidney disease (C3b). Vitamin B12 (cyanocobalamin; 1mg, twice-weekly) and L-carnitine (1000 mg, IV, qd) were given, together with oral antiepileptic drug, antihypotensive agents, diuretics and prednisone. When condition permitted, a low dose of vindesine (1.5 mg, IV) was administered intermittently for chemotherapy. About 1 week later, the edema vanished gradually. After 2 months of treatment of vitamin B12 and L-carnitine, the muscle strength of both lower limbs were significantly improved to nearly grade 5. In the following 3 months, the girl was treated with Chimeric Antigen Receptor T-Cell Immunotherapy (CAR-T) twice. After reinfusion of her own T cells, there was no abnormality in bone penetration, MRD and fusion gene. Then she received sequential treatment of CD19 and CD22, and 3 times of VDL chemotherapy. Now the girl receives intramuscular injection of cyanocobalamine twice a week, oral administration of L-carnitine and folic acid tablets. The levels of methylmalonic acid and homocysteine were improved.

DISCUSSION

Methylmalonic acid is the metabolite of methylmalonyl-CoA in the catabolism of branched chain amino acids (isoleucine, methionine, threonine and valine), odd-chain fatty acids, gut-derived propionate and cholesterol. In order to enter the

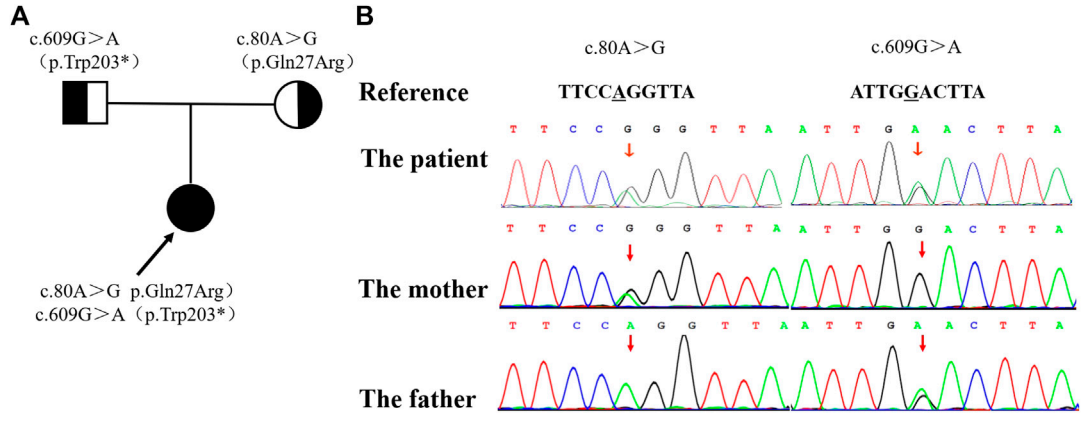

FIGURE 2 | The family pedigree showing the mutations detected in *MMACHC*. **(A)** The pedigree of the family with MMA. The arrow indicates the proband; her parents have no signs of MMA. **(B)** The mutations detected in the family. The proband has both mutations, while the c. 80A >G mutation was only detected in her mother and the c. 609G > A mutation was only detected in her father.

tricarboxylic acid cycle, methylmalonyl-CoA is reversibly isomerised to succinyl-CoA, which process is catalyzed by mitochondrial enzyme methylmalonyl-CoA mutase and requires adenosylcobalamin (AdoCbl) as an essential cofactor (Froese et al., 2015; Hu et al., 2018). Children with cblC type MMA have defects in *MMACHC* gene, whose coding proteins is related with the synthesis of Adocbl and methylcobalamin (MeCbl) (Bassila et al., 2017). MeCbl is the coenzyme of methyltetrahydrofolate-homocysteine methyltransferase, also known as methionine synthase (MS), located in the cytoplasm, catalyzing the methylation of homocysteine to methionine. Low levels of AdoCbl and MeCbl in cblC type patients cause abnormal accumulation of metabolites such as methylmalonate, methylcitrate and 3-hydroxybutyric acid, decreased serum methionine, and reduced activity of succinic dehydrogenase. As a result, mitochondrial energy metabolism was affected, and multiple symptoms appear (Bassila et al., 2017).

In China, most of *MMACHC* mutations are located in exons 3 and 4, and C. 609G > A (P.w203x) is the most common. In this case, clinical manifestations include cerebral palsy, developmental delay, epilepsy, hypertension, proteinuria, chronic renal insufficiency; laboratory findings showed elevated methylmalonic acid-2, acetyl carnitine, propionyl carnitine in blood and urine; genetic testing revealed a compound heterozygous mutation in *MMACHC* gene [c. 80A > G (P.q27r, from her mother) and c. 609G > A (P.w203x, from her father)], which has been reported in MMA cases before (Hu et al., 2018; Wang et al., 2019). Clinical features, laboratory findings and genetic testing all support the diagnosis of cblC-type MMA.

The diagnosis of MMA mainly depends on examination of blood acylcarnitine profile and urinary organic acids, characterized by remarkably increased blood C3, C3/C2 ratio and relatively high concentrations of methylmalonic acid and methyl citrate in urine (Keyfi et al., 2016). Genetic analysis is helpful for the classification of MMA (Chandler and Venditti, 2005). According to responses to vitamin B12, MMA can be divided into two sub-type: Vitamin B12 responsive and vitamin B12 unresponsive. B12 responsive ones are mostly caused by deficiency of coenzyme synthesis (Froese et al., 2009), while unresponsive ones are mostly caused by deficiency of mutase (Pela et al., 2006). Once MMA was suspected or diagnosed, initial treatments must be performed without delay. Basic principle of treatment is to reduce the production of methylmalonic acid and its bypass metabolites, and to accelerate their clearance. For acute management, treatments are stabilizing the patient, restricting protein intake, providing enough calories, and administering drugs including L-carnitine, vitamin B12 (preferably hydroxo-Cbl), biotin, sodium phenylbutyrate and arginine. For long-term management, vitamin B12 responsive MMA patients should be treated with vitamin B12 (1mg, IM, once or twice a week), followed by other oral drugs including vitamin B6, betaine, folic acid, L-carnitine, and sometimes methionine. If concentration of C3 and urinary methylmalonic acid are at appropriate levels, highly restricted diet may not necessarily be taken (Ribas et al., 2010). For vitamin B12 unresponsive cases, specialized amino acid formulations (containing minimal to no isoleucine, methionine, threonine, and proline, etc.) should be used, and nutritional intervention, such as strict restriction on the intake of natural protein and supplements, should be applied. L-carnitine is effective for both types of MMA because of its ability of promoting the excretion of both methylmalonic acid and C3 (Ribas et al., 2010). After diagnosis, the case was treated with intramuscular injection of vitamin B12 (1mg, twice a week), supplemented by L-carnitine (1g/day). The clinical course should be classified as early-onset: developmental delays in gross movement, brain atrophy in cerebral MR images, and seizures. The results of metabolic screening and genetic analysis confirmed the diagnosis. Symptoms improved significantly after vitamin B12 administration, so we speculate this case to be an early-onset and vitamin B12 responsive one.

B-acute lymphoblastic leukemia (B-ALL) is the most prevalent childhood hematological malignancy, whose development is a complex process of multiple gene mutations, involving fusion mutations in early-stage and collaborative genes mutations in

TABLE 1 | Multi-case analysis of MMA with cardiovascular and hematological disease.

NO.	References	Year	MMA type	Population origin	Total number	Hematological system performance	Cardiovascular system performance	Treatment	Outcome
1	Chao Wang	2021	NM	China	75	Anemia 23 (30.7%) Pancytopenia 3 (4.0%), Granulocytopenia 15 (20%), Thrombopenia 6 (8%), Haemolytic uremic 2 (2.7%)	Cardiomyopathy 1 (1.3%) PAH 1 (1.3%) ASD 6 (8%) VSD 1 (1.3%) PDA 5 (6.7%)	NM	NM
2	Ruxuan He	2020	NM	China	68	Anemia 27 (39.7%)	Cardiomyopathy 2 (2.9%)	CBL, CAR, BET	Lagerly Return
3	Lulu Kang	2020	NM	China	224	Anemia 66 (29.5%), Pancytopenia10 (4.5%)	Cardiomyopathy6 (2.7%), PAH 2 (0.9%)	CBL, CAR, PR	Lagerly return
4	Ruxuan He	2020	cblC	China	132	Anemia 37 (28%)	NM	CBL, CAR, BET	Lagerly return
5	Chao Wang	2019	cblC	China	28	Anemia 6 (21.4%), Granulocytopenia 3 (10.7%)	Atrial septal defect 3 (10.7%)	NM	NM
6	Yi Liu	2018	NM	China	1003	Anemia and haemolytic uremic260 (26.6%)	PAH17 (1.7%)	CBL, CAR, BET, PR	Lagerly return
7	Sabine Fischer	2014	cblC	Italy	86	Anemia 45 (53.3%), macrocytosis8 (7.9%), haemolytic uremic 4 (4.5%)	NM	BET, CAR, F	Lagerly return
				Portugal Spain		Macrocytosis 18 (20.9%) Haemolytic uremic 8 (9.3%)			
8	Fei Wang	2010	cblC	China	43	Anemia 36 (83.7%)	NM	NM	NM
9	Celia Nogueira	2008	cblC	Italy, Portugal	41	Anemia, thrombopenia and granulocytopenia 21 (51%)	NM	NM	NM

Abbreviation: PAH, pulmonary arterial hypertension; ASD, atrial septal defect; VSD, ventricular septal defect; PDA, patent ductus arteriosus; NM, not mentioned; CBL, hydroxocobalamin; CAR, carnitine; PR, protein restriction. BET, betaine. F, folic acid.

late-stage. In particular, gene mutations associated with B cell development play an increasingly important role in the pathogenesis of B-ALL (Pui et al., 2015).

We conducted a literature review about congenital hematological disease and cardiac disease in MMA. We searched for keywords "Hematological", "Cardiovascular", "heart", "blood" and "child" in all fields in PubMed and Webofscience, and screening out original articles focusing on cardiovascular disease and hematological disease in MMA. This section was summarized in **Tables 1**, **2**.

In summary, (Nogueira et al., 2008; Wang et al., 2010; Fischer et al., 2014; Liu et al., 2018; Wang et al., 2019; He et al., 2020a; He et al., 2020b; Kang et al., 2020; Wang et al., 2021), anemia is the most common blood system damage of MMA(**Table 1**), the incidence of which is 21.4–83.3%. Other hematological complications include granulocytopenia, thrombocytopenia, pancytopenia and hemolytic uremia.

The protein encoded by *MMACHC* is mainly involved in the biological synthesis of Adocbl and Mecbl (Bassila et al., 2017), and then affects the levels of methylmalonyl-coa mutase (MUT) and MMA, and also affects the activity of methionine synthase (MTR). MTR C. 2756 mutation has been reported to be positively correlated with the occurrence of ALL in Asian population in former studies (Yu et al., 2010), but its mechanism is still unclear.

Among the 14 methionine-dependent tumor lines tested by Watkins (Watkins, 1998), reduced methionine synthase function and reduced MeCbl and AdoCbl synthesis was observed only in MeWo LC1 melanoma cell lines. It was later proved that the decreased expression of MMACHC in MeWo LC1 was caused by methylation of CpG island at the end of the corresponding gene 5. Recent studies have shown that in some cblC patients, specific mutations in *PRDX1*, a contiguous gene of *MMACHC*, lead to secondary epigenetic mutations that affect methylation of the MMACHC promoter and expression of MMACHC (Guéant et al., 20172018). Both MeWo LC1 human melanoma cell line and cblC patient-derived cells have reduced AdoCbl and MeCbl synthesis, decreased intracellular cobalamin concentration, and impaired activity of these two cobalamine-dependent enzymes (Loewy et al., 2009). These similarities open up the possibilities to clarify whether there is a common mechanism of methionine dependence in cblC patient-derived cells and MeWo LC1 cell lines (Loewy et al., 2009).

The child suffered from methylmalonic acidemia, which leads to decreased expression of *MMACHC* gene, decreased intracellular cobalamin concentration, decreased activities of Adobe Cbl and MeCbl, two cobalamine-dependent enzymes, and increased levels of methionine and homocysteine, resulting in changes in blood microenvironment. Many syndromes can have complications of leukemia, of which the possible reason may be microenvironment changes caused by chromosomal, genetic and metabolic abnormalities. Simultaneous MMA and leukemia may be associated with abnormal amino acid levels and changes in blood microenvironment, or may be related to the genetic variation of MMACHC and MTR C. 2756 and the subsequent decrease of MTR activity. Further studies are needed to determine whether these changes lead to acute lymphoblastic leukemia. While, perhaps the presence of both ALL and cblC methylmalonic acidemia in this case may also be a coincidence.

In MMA cases combined with heart disease (**Table 1**), (Andersson et al., 1999; Heinemann et al., 2001; Tomaske

TABLE 2 | Case reports of MMA complicated with cardiovascular diseases.

NO.	References	Year	Sex	At diagnosis age	MMA-type	MMACHC mutation	Types of heart disease	Mean Hey (umol/L)	Mean urine MMA (mmol/mol cr)	Treatment	Outcome
1	Ling-yi Wen	2020	female	12 years	NM	c.80A > G/ c.609G > A	PAH and dilated right ventricle	155.8	↑	CBL, F, CYS	Largely return
2	Ya-Nan Zhang	2019	female	7 months	NM	NM	Dilated left ventricle	NM	NM	CBL, CYS	Largely return
3	Ya-Nan Zhang	2019	male	6 years	NM	NM	PAH and dilated right ventricle	NM	NM	CBL	died
4	Ya-Nan Zhang	2019	female	6 years	NM	NM	PAH and dilated right ventricle	NM	NM	CBL, CYS	died
5	Luciano De Simone	2018	male	2 years	cblC	c.271-272dupA/ c.347 T > C	PAH and dilated right ventricle	74	↑	CBL, F, CYS, CAR	Largely return
6	Jun KIDO	2017	female	39 years	NM	NM	PAH and dilated right ventricle	NM	NM	NM	Recovery (4Y)
7	Jinrong Liu	2017	female	21 months	cblC	c.80A >G/ c.331C > T	PAH and dilated right ventricle	>50	↑	CBL. CYS, F	Recovery (3Y)
8	Carlos E. Prada	2011	female	22 years	cblB	NM	Hypertrophic cardiomyopathy	NM	NM	NM	died
9	Carlos E. Prada	2011	male	2 years	Mut-0	NM	Dilated cardiomyopathy	NM	NM	CAR	died
10	Carlos E. Prada	2011	female	4 years	Mut-0	NM	Dilated cardiomyopathy	NM	NM	NM	died
11	Laurie E. Profitlich	2009	male	2 months	cblC	271dupA/ 271dupA	Mitral valve prolapse and Mild mitral regurgitation	95	266	CBL, PR, CYS, F	Largely return
12	Laurie E. Profitlich	2009	male	Prenatal	cblC	271dupA/ 271dupA	Focal left ventricular	107	196	CBL, PR, CYS, F	Largely return
13	Laurie E. Profitlich	2009	male	Birth	cblC	271dupA/ 271dupA	Normal structure	32	35	CBL, PR, CYS, F	Largely return
14	Laurie E. Profitlich	2009	female	Birth	cblC	271dupA/ 271dupA	Normal structure	30	34	CBL, PR, CAR, F	Largely return
15	Laurie E. Profitlich	2009	male	Birth	cblC	568insT/ 568insT	Secundum atrial septal defect	63	29	CBL, PR, CAR, F	Largely return
16	Laurie E. Profitlich	2009	female	2 months	cblC	G609A/G609A	Normal structure	35	24	CBL, PR, CYS, CAR, F	Largely return
17	Laurie E. Profitlich	2009	male	Birth	cblC	547-8delGT/ 285dupA	Secundum atrial septal defect	64	31	CBL, PR, CYS, CAR, F	Largely return
18	Laurie E. Profitlich	2009	male	Birth	cblC	G608A/G608A	Normal structure	42	20	CBL, PR, CAR, F	Largely return
19	Laurie E. Profitlich	2009	female	3 years	cblC	C666A/C666A	Normal structure	99	57	CBL, PR, CYS, ASA	Largely return
20	Laurie E. Profitlich	2009	male	3 months	cblC	C481T/C481T	Muscular ventricular septal defect	69	74	CBL, PR, CYS, ASA	Largely return
21	Isabelle De Bie	2009	female	27 years	cblC	NM	VSD and dilated cardiomyopathy	236	↑	CBL, PR, CAR, F, CYS	Largely return
22	M. Tomaske	2009	female	2 weeks	cblC	NM	VSD	282	1914	CBL, CAR, F, CYS	Largely return
23	Markus K. Heinemann	2001	female	19 days	NM	NM	VSD	NM	↑	CBL and Surgery	Largely return
24	Hans C. Andersson	1999	NM	5 year	cblC	NM	Pulmonic stenosis	↑	↑	CBL	Largely return
25	Hans C. Andersson	1999	NM	2 years	cblC	NM	VSD	↑	↑	CBL	Largely return

Abbreviation: PAH, pulmonary arterial hypertension; ASD, atrial septal defect; VSD, ventricular septal defect; PDA, patent ductus arteriosus; NM, not mentioned CBL, hydroxocobalamin; CAR, carnitine; PR, protein restriction. ↑, larger than the reference value. CBL, hydroxocobalamin; PR, protein restriction; CYS, cystadane; ASA, aspirin; CAR, carnitine; F, folic acid.

et al., 2001; De Bie et al., 2009; Profitlich et al., 2009), cardiomyopathy(1.2–2.9%) and pulmonary hypertension (0.9–1.7%) were more common (Andersson et al., 1999; Heinemann et al., 2001; Tomaske et al., 2001; De Bie et al., 2009; Profitlich et al., 2009; Prada et al., 2011; Kido et al., 2017; Liu et al., 2017; De Simone et al., 2018; Wen et al., 2020; Zhang et al., 2020). While mitral valve prolapse, mild mitral regurgitation, focal left ventricular uncompacting, atrial septal defect, ventricular

septal defect, patent ductus arteriosus and pulmonary artery stenosis were also reported (**Table 2**).

A study suggested that MTR polymorphisms (rs1770449 and rs1050993) may be associated with the risk of CHDs and modified the relation between maternal folate intake and CHDs (Deng et al., 2019). Three independent case-control studies in a total of 2,340 patients with CHD and 2,270 controls suggested that two regulatory variants of MTR, 2186T.G and +905G.A were associated with increased risk of CHD (Zhao et al., 2014). Patent foramen ovale, a secondary atrial septal defect, was detected in this case by echocardiography. We speculate that the main cause of this patent foramen ovale was MMA combined with homocysteine. The structural defects of heart in cblC MMA patients may be related to the increase of metabolites such as methionine, s-adenosine methionine and s-adenosine homocysteine, or the lack of methionine synthase.

This case was unable to crawl at 9 months old, and was diagnosed with cerebral palsy based on brain atrophy in brain MRI. Gestational age and birth weight were normal, and no history of postnatal asphyxia, hypoxia, hyperbilirubin encephalopathy, and intrauterine infections were found. Seizures occurred during chemotherapy, and the results of EEG suggested epilepsy. Therefore, when a patient showed cerebral palsy and epilepsy with no common causes, screening for metabolic diseases should be performed to exclude metabolic diseases.

CONCLUSION

1. Metabolic screening and genetic analysis are necessary for cases with multiple system involvement.
2. Cerebral palsy may have multiple causes, and genetic metabolic diseases should be taken into consideration apart from common causes such as preterm birth, low weight, history of postnatal asphyxia, and hypoxia, neonatal hyperbilirubin encephalopathy and intrauterine infection.
3. MMA and homocysteinemia should be considered in the differential diagnosis of congenital cardiac defects. Routine and regular cardiovascular assessments should be performed in patients with MMA to identify cases with cardiac structural defect and cases with risks of thromboembolism and stroke.
4. The lack of specific clinical manifestations causes difficulties in MMA diagnosis. Physicians, especially pediatricians in high-prevalence areas, should raise awareness for the diseases, screen high-risk patients timely and perform blood carnitines and urine organic acids analysis, so as to make early diagnosis and treatments, and improve prognosis of the disease.

DATA AVAILABILITY STATEMENT

The datasets for this article are not publicly available due to concerns regarding participant/patient anonymity. Requests to access the datasets should be directed to the corresponding author.

ETHICS STATEMENT

The studies involving human participants were reviewed and approved by the First Hospital of China Medical University. Written informed consent to participate in this study was provided by the participants' legal guardian/next of kin.

AUTHOR CONTRIBUTIONS

JZ, SW, and XZ were responsible for the acquisition of clinical information and drafted the manuscript. BZ analysed the patient data and edited manuscript. YL assisted in developing figures and images for the manuscript. HJ was responsible for acquisition of the clinical information and reviewed the manuscript. All authors approved the manuscript for submission.

FUNDING

This work was supported by the National Natural Science Foundation of China (Grant No. 81300130) and Liaoning Province Livelihood Science and Technology project (Grant No. 10300008). The role of funders was to sponsor the multiplex ligation-dependent probe amplification analysis for this case.

ACKNOWLEDGMENTS

We wish to thank the patients and their families for participating in this study, without whom none of this would be possible.

REFERENCES

Andersson, H. C., Marble, M., and Shapira, E. (1999). Long-term Outcome in Treated Combined Methylmalonic Acidemia and Homocystinemia. *Genet. Med.* 1 (4), 146–150. doi:10.1097/00125817-199905000-00006

Bassila, C., Ghemrawi, R., Flayac, J., Froese, D. S., Baumgartner, M. R., Guéant, J.-L., et al. (2017). Methionine Synthase and Methionine Synthase Reductase Interact with MMACHC and with MMADHC. *Biochim. Biophys. Acta (Bba) - Mol. Basis Dis.* 1863 (1), 103–112. doi:10.1016/j.bbadis.2016.10.016

Chandler, R. J., and Venditti, C. P. (2005). Genetic and Genomic Systems to Study Methylmalonic Acidemia. *Mol. Genet. Metab.* 86 (1–2), 34–43. doi:10.1016/j.ymgme.2005.07.020

De Bie, I., Nizard, S. D. P., and Mitchell, G. A. (2009). Fetal Dilated Cardiomyopathy: an Unsuspected Presentation of Methylmalonic Aciduria and Hyperhomocystinuria, cblC Type. *Prenat. Diagn.* 29 (3), 266–270. doi:10.1002/pd.2218

De Simone, L., Capirchio, L., Roperto, R. M., Romagnani, P., Sacchini, M., Donati, M. A., et al. (2018). Favorable Course of Previously Undiagnosed Methylmalonic Aciduria with Homocystinuria (cblC Type) Presenting with Pulmonary Hypertension and aHUS in a Young Child: a Case Report. *Ital. J. Pediatr.* 44 (1), 90. doi:10.1186/s13052-018-0530-9

Deng, C., Deng, Y., Xie, L., Yu, L., Liu, L., Liu, H., et al. (2019). Genetic Polymorphisms in MTR Are Associated with Non-syndromic Congenital Heart Disease from a Family-Based Case-Control Study in the Chinese Population. *Sci. Rep.* 9 (1), 5065. doi:10.1038/s41598-019-41641-z

Fischer, S., Huemer, M., Baumgartner, M., Deodato, F., Ballhausen, D., Boneh, A., et al. (2014). Clinical Presentation and Outcome in a Series of 88 Patients with the cblC Defect. *J. Inherit. Metab. Dis.* 37 (5), 831–840. doi:10.1007/s10545-014-9687-6

Froese, D. S., Kopec, J., Fitzpatrick, F., Schuller, M., McCorvie, T. J., Chalk, R., et al. (2015). Structural Insights into the MMACHC-MMADHC Protein Complex Involved in Vitamin B12 Trafficking. *J. Bio. Chemis.* 290 (49), 29167–29177. doi:10.1074/jbc.M115.683268

Froese, D. S., Zhang, J., Healy, S., and Gravel, R. A. (2009). Mechanism of Vitamin B12-Responsiveness in cblC Methylmalonic Aciduria with Homocystinuria. *Mol. Genet. Metab.* 98 (4), 338–343. doi:10.1016/j.ymgme.2009.07.014

Guéant, J.-L., Chéry, C., Oussalah, A., Nadaf, J., Coelho, D., Josse, T., et al. (20172018). Publisher Correction: A PRDX1 Mutant Allele Causes a MMACHC Secondary Epimutation in cblC Patients. *Nat. Commun.* 9, 9. doi:10.1038/s41467-018-03054-w

He, R., Mo, R., Shen, M., Kang, L., Song, J., Liu, Y., et al. (2020). Variable Phenotypes and Outcomes Associated with the MMACHC c.609G>A Homologous Mutation: Long Term Follow-Up in a Large Cohort of Cases. *Orphanet J. Rare Dis.* 15 (1), 200. doi:10.1186/s13023-020-01485-7

He, R., Zhang, H., Kang, L., Li, H., Shen, M., Zhang, Y., et al. (2020). Analysis of 70 Patients with Hydrocephalus Due to Cobalamin C Deficiency. *Neurology* 95 (23), e3129–e3137. doi:10.1212/WNL.0000000000010912

Heinemann, M. K., Tomaske, M., Trefz, F. K., Bosk, A., Baden, W., and Ziemer, G. (2001). Ventricular Septal Defect Closure in a Neonate with Combined Methylmalonic Aciduria/homocystinuria. *Ann. Thorac. Surg.* 72 (4), 1391–1392. doi:10.1016/s0003-4975(00)02605-9

Hu, S., Mei, S., Liu, N., and Kong, X. (2018). Molecular Genetic Characterization of cblC Defects in 126 Pedigrees and Prenatal Genetic Diagnosis of Pedigrees with Combined Methylmalonic Aciduria and Homocystinuria. *BMC Med. Genet.* 19 (1), 154. doi:10.1186/s12881-018-0666-x

Kang, L. L., Liu, Y. P., Shen, M., Chen, Z. H., Song, J. Q., He, R. X., et al. (2020). The Phenotypes and Genotypes in 314 Patients with Isolated Methylmalonic Acidemia. *Zhonghua Er Ke Za Zhi* 58 (6), 468–475. doi:10.3760/cma.j.cn112140-20200401-00339

Kido, J., Mitsubuchi, H., Sakanashi, M., Matsubara, J., Matsumoto, S., Sakamoto, R., et al. (2017). Pulmonary Artery Hypertension in Methylmalonic Acidemia. *Hemodialysis Int.* 21 (2), E25–E29. doi:10.1111/hdi.12506

Keyfi, F., Talebi, S., and Varasteh, A. R. (2016). Methylmalonic Acidemia Diagnosis by Laboratory Methods. *Rep. Biochem. Mol. Biol.* 5 (1), 1–14.

Liu, J., Peng, Y., Zhou, N., Liu, X., Meng, Q., Xu, H., et al. (2017). Combined Methylmalonic Acidemia and Homocysteinemia Presenting Predominantly with Late-Onset Diffuse Lung Disease: a Case Series of Four Patients. *Orphanet J. Rare Dis.* 12 (1), 58. doi:10.1186/s13023-017-0610-8

Liu, Y., Liu, Y. P., Zhang, Y., Song, J. Q., Zheng, H., Dong, H., et al. (2018). Heterogeneous Phenotypes, Genotypes, Treatment and Prevention of 1 003 Patients with Methylmalonic Acidemia in the mainland of China. *Zhonghua Er Ke Za Zhi* 56 (6), 414–420. doi:10.3760/cma.j.issn.0578-1310.2018.06.003

Loewy, A. D., Niles, K. M., Anastasio, N., Watkins, D., Lavoie, J., Lerner-Ellis, J. P., et al. (2009). Epigenetic Modification of the Gene for the Vitamin B12 Chaperone MMACHC Can Result in Increased Tumorigenicity and Methionine Dependence. *Mol. Genet. Metab.* 96 (4), 261–267. doi:10.1016/j.ymgme.2008.12.011

Nogueira, C., Aiello, C., Cerone, R., Martins, E., Caruso, U., Moroni, I., et al. (2008). Spectrum of MMACHC Mutations in Italian and Portuguese Patients with Combined Methylmalonic Aciduria and Homocystinuria, cblC Type. *Mol. Genet. Metab.* 93 (4), 475–480. doi:10.1016/j.ymgme.2007.11.005

Pela, I., Gasperini, S., Pasquini, E., and Donati, M. A. (2006). Hyperkalemia After Acute Metabolic Decompensation in Two Children with Vitamin B-12-Unresponsive Methylmalonic Acidemia and Normal Renal Function. *Clinical. Nephrology.* 66 (1), 63–66. doi:10.5414/cnp66063

Prada, C. E., Al Jasmi, F., Kirk, E. P., Hopp, M., Jones, O., Leslie, N. D., et al. (2011). Cardiac Disease in Methylmalonic Acidemia. *J. Pediatr.* 159 (5), 862–864. doi:10.1016/j.jpeds.2011.06.005

Profitlich, L. E., Kirmse, B., Wasserstein, M. P., Diaz, G. A., and Srivastava, S. (2009). High Prevalence of Structural Heart Disease in Children with cblC-type Methylmalonic Aciduria and Homocystinuria. *Mol. Genet. Metab.* 98 (4), 344–348. doi:10.1016/j.ymgme.2009.07.017

Pui, C.-H., Yang, J. J., Hunger, S. P., Pieters, R., Schrappe, M., Biondi, A., et al. (2015). Childhood Acute Lymphoblastic Leukemia: Progress through Collaboration. *Jco* 33 (27), 2938–2948. doi:10.1200/JCO.2014.59.1636

Ribas, C. S., Manfredini, V., de Marco, M. G., Vieira, R. B., Wayhs, C. Y., Vanzin, C. S., et al. (2010). Prevention by L-Carnitine of DNA Damage Induced by Propionic and L-Methylmalonic Acids in Human Peripheral Leukocytes *In Vitro*. *Mutat. Res.* 702 (1), 123–128. doi:10.1016/j.mrgentox.2010.07.008

Tomaske, M., Bosk, A., Heinemann, M. K., Sieverding, L., Baumgartner, E. R., Fowler, B., et al. (2001). CASE REPORT: CblC/D Defect Combined with Haemodynamically Highly Relevant VSD. *J. Inherit. Metab. Dis.* 24 (4), 511–512. doi:10.1023/a:1010541932476

Wang, C., Li, D., Cai, F., Zhang, X., Xu, X., Liu, X., et al. (2019). Mutation Spectrum of MMACHC in Chinese Pediatric Patients with Cobalamin C Disease: A Case Series and Literature Review. *Eur. J. Med. Genet.* 62 (10), 103713. doi:10.1016/j.ejmg.2019.103713

Wang, C., Liu, Y., Zhang, X., Wang, H., Cui, Y., Zhi, X., et al. (2021). Phenotypic and Genotypic Analysis of Children with Methylmalonic Academia: A Single-center Study in China and a Recent Literature Review. *Clinica Chim. Acta* 522, 14–22. doi:10.1016/j.cca.2021.08.008

Wang, F., Han, L., Yang, Y., Gu, X., Ye, J., Qiu, W., et al. (2010). Clinical, Biochemical, and Molecular Analysis of Combined Methylmalonic Acidemia and Hyperhomocysteinemia (cblC Type) in China. *J. Inherit. Metab. Dis.* 33 (Suppl. 3), 435–442. doi:10.1007/s10545-010-9217-0

Watkins, D. (1998). Cobalamin Metabolism in Methionine-dependent Human Tumour and Leukemia Cell Lines. *Clin. Invest. Med.* 21 (3), 151–158.

Watkins, D., and Rosenblatt, D. S. (2013). Lessons in Biology from Patients with Inborn Errors of Vitamin B12 Metabolism. *Biochimie* 95 (5), 1019–1022. doi:10.1016/j.biochi.2013.01.013

Wen, L.-y., Guo, Y.-k., and Shi, X.-q. (2020). Pulmonary Hypertension in Late-Onset Methylmalonic Aciduria and Homocystinemia: a Case Report. *BMC Pediatr.* 20 (1), 243. doi:10.1186/s12887-020-02130-9

Yu, K., Zhang, J., Zhang, J., Dou, C., Gu, S., Xie, Y., et al. (2010). Methionine Synthase A2756G Polymorphism and Cancer Risk: a Meta-Analysis. *Eur. J. Hum. Genet.* 18 (3), 370–378. doi:10.1038/ejhg.2009.131

Zhang, Y.-N., Pi, Y.-L., Yan, X., Li, Y.-Q., Qi, Z.-J., and Zhang, H.-F. (2020). Methylmalonic Acidemia Complicated by Homocystinuria Diseases: a Report of Three Cases. *Adv. Ther.* 37 (1), 630–636. doi:10.1007/s12325-019-01149-4

Zhao, J.-Y., Qiao, B., Duan, W.-Y., Gong, X.-H., Peng, Q.-Q., Jiang, S.-S., et al. (2014). Genetic Variants Reducing MTR Gene Expression Increase the Risk of Congenital Heart Disease in Han Chinese Populations. *Eur. Heart J.* 35 (11), 733–742. doi:10.1093/eurheartj/eht221

Zhou, X., Cui, Y., and Han, J. (2018). Methylmalonic Acidemia: Current Status and Research Priorities. *Irdr* 7 (2), 73–78. doi:10.5582/irdr.2018.01026

Conflict of Interest: The authors declare that the research was conducted in the absence of any commercial or financial relationships that could be construed as a potential conflict of interest.

Publisher's Note: All claims expressed in this article are solely those of the authors and do not necessarily represent those of their affiliated organizations, or those of the publisher, the editors and the reviewers. Any product that may be evaluated in this article, or claim that may be made by its manufacturer, is not guaranteed or endorsed by the publisher.

frontiers | Frontiers in Pediatrics

CASE REPORT
published: 15 April 2022
doi: 10.3389/fped.2022.860990

Case Report: Cystinosis in a Chinese Child With a Novel CTNS Pathogenic Variant

Yu-Jia Guan[1,2,3], *Yan-Nan Guo*[3,4]*, *Wen-Tao Peng*[1,2,3] and *Li-Li Liu*[1,2,3]

[1] Department of Nursing, West China Second University Hospital, Sichuan University, Chengdu, China, [2] West China School of Nursing, Sichuan University, Chengdu, China, [3] Key Laboratory of Birth Defects and Related Diseases of Women and Children (Sichuan University), Ministry of Education, Chengdu, China, [4] Department of Pediatrics, West China Second University Hospital, Sichuan University, Chengdu, China

Objective: To report a rare case of cystinosis with a novel CTNS pathogenic variant in the Chinese population.

Methods: Retrospective analysis of the clinical manifestations, laboratory results, and gene detection data of a child with cystinosis.

Results: A Chinese Zang ethnic girl could not stand or walk until 3 years old, with additional symptoms including a loss of appetite. Since then, the girl gradually exhibited "X" leg, double wrist joints, a bilateral ankle deformity, and rickets. At the age of 9 years, the girl was hospitalized. Laboratory testing showed that her blood phosphorus, blood calcium and blood potassium levels were significantly decreased. At the same time, the girl's urine glucose and urine protein were positive, although her fasting blood glucose, glycosylated hemoglobin, and 75 g glucose tolerance were not significantly abnormal. Further, blood gas analysis showed metabolic acidosis. These symptoms corresponded to Fanconi syndrome. Gene analysis showed that there was a homozygous pathogenic variant c.140 $\leq$ 5G > A (p.?) in the CTNS gene, which was a small variation in the intron region. To our knowledge, this is the first report of the rare variant.

Conclusion: Attention should be paid to the differential diagnosis of cystinosis by gene analysis in children whose clinical manifestations include exercise dysplasia, renal damage, or multiple organ damage (including bone, thyroid, etc) and who cannot be firmly diagnosed for the time being.

Keywords: cystinosis, CTNS gene mutation, Fanconi syndrome, renal tubular acidosis, genetics

OPEN ACCESS

Edited by:
Hui Xiong,
Peking University First Hospital, China

Reviewed by:
Roberto Chimenz,
University of Messina, Italy
Patryk Lipiński,
Children's Memorial Health Institute (IPCZD), Poland

***Correspondence:**
Yan-Nan Guo
theresa_guo@tom.com

Specialty section:
This article was submitted to Genetics of Common and Rare Diseases, a section of the journal Frontiers in Pediatrics

Received: *24 January 2022*
Accepted: *21 March 2022*
Published: *15 April 2022*

Citation:
Guan Y-J, Guo Y-N, Peng W-T and Liu L-L (2022) Case Report: Cystinosis in a Chinese Child With a Novel CTNS Pathogenic Variant. Front. Pediatr. 10:860990. doi: 10.3389/fped.2022.860990

INTRODUCTION

Cystinosis is an extremely rare autosomal recessive metabolic disease which is caused by the lack of L-cystine transporters on the lysosomal membrane resulted from the pathogenic variant of CTNS. This defect in lysosomal membrane transport leads to cystine accumulation, which eventually causes multiple organ dysfunction, including the eyes, kidneys, nerves, heart, and endocrine gland, amongst others. Until now, the majority of reported Cystinosis cases have occurred in Europe and the United States. The incidence of cystinosis in the general population is within the range

of 1:260,000–1:115,000 (1, 2), which varies greatly in different regions. It should be noted that the relevant data in China are still incomplete.

In recent years, some progress has been made in the study of the disease in developed countries. However, relatively few reviews or case reports from China have been published (3–6). Furthermore, cases of cystinosis in children are particularly rare, which may be related to the low incidence of the disease and also the understanding of the disease. Timely findings, accurate diagnosis, and extensive reporting will be helpful to increase awareness of this disease. Meanwhile, early diagnosis and early treatment have an important impact on the prognosis of the disease, and can help to reduce or delay the occurrence of complications and prolong the patient's life. In this paper, the clinical manifestations, laboratory results, and gene detection data of a child with cystinosis diagnosed in West China Second Hospital of Sichuan University were reported (see below). The clinical characteristics, diagnosis and treatment strategies were discussed.

CASE PRESENTATION

The patient was a 9-year-old girl who was the second child of non-consanguineous parents from the Zang ethnic minority group, Sichuan Province, China. Her mother was not exposed to or used alcohol, tobacco, or drugs during her pregnancy. She was carried full-term and had a normal vaginal delivery, although her birth weight and body length could not be provided by her family. She was breastfed after birth with supplementary foods added when appropriate. At the age of 1, the child began to crawl and sit by herself, which was not something her family paid particular attention to. However, by the age of 3, she could not stand or walk. Her mobility issues were accompanied by a poor diet, which mainly consisted of formula milk. The child's upper limb movement and cognitive and intellectual development were not significantly abnormal compared to children of the same age. Vitamin D and lysine were prescribed for her initial treatment in the outpatient department of a local hospital. At the age of 4 years, she could walk independently and appeared "X" leg. This patient was diagnosed with Fanconi syndrome, which based on renal tubular acidosis, vitamin D deficiency, growth retardation, normocytic anemia and the decreased serum phosphorus and calcium level during her first hospitalization, and diagnosed with bronchitis and hypocalcemia. Then she was treated with sodium dihydrogen phosphate, disodium hydrogen phosphate, sodium citrate + potassium citrate, vitamin D, and calcium.

After her symptoms were alleviated, it was suggested that she continue to take the above drugs after discharge and be followed up with the outpatient service. However, the child neither went to the clinic for follow-up on time, nor took medicine strictly according to the doctor's advice. Her family members admitted that they forgot occasionally and thought it was not such a serious problem. Their poor compliance may be related to distance from hospitals, lack of time, and family cultural background, concept and other reasons.

About 4 years later, at 8 years and 9 months old, the girl experienced fatigue and her hands were bent and claw-like. These symptoms were accompanied by pain, and at this time her family members independently decided to discontinue her medication. One month later, she presented with a paroxysmal dull ache in her hypogastrium, dizziness and headaches, and occasionally felt nauseous when eating greasy foods, soreness when exercised. She had occasional soft coughs, without polydipsia, urorrhagia, and so on.

At the age of 9, she was hospitalized in West China Second University Hospital of Sichuan University. The anthropometric evaluation showed that her stature (bodyweight 18 Kg, height 108 cm) was lower than the 3rd percentile of height and weight for individuals of the same age and sex, and also that her subcutaneous fat was thin. A Pectus carinatum brace was fitted. Upon testing, it was found that her blood phosphorus (1.07 mmol/L), blood calcium (1.72 mmol/L), and blood potassium (3.4 mmol/L) levels were significantly decreased. And it was found that her hemoglobin level (88 g/L) was decreased, while both of the level of Mean Corpuscular Volume (MCV) and the level of mean corpuscular hemoglobin (MCH) were within the normal range. This indicated that the patient can be diagnosed with normocytic anemia.

Meanwhile, laboratory tests showed a decreased Vitamin D (both 25-OH-D and 1.25-OH-D) level (9.6 ng/ml), an increased alkaline phosphatase level (575 U/L), significantly increased blood urea nitrogen level (6.98 mmol/L) and creatine level (163 μmol/L). Urine sugar (3 +) and urine protein (2 +) were positive. Her levels of free carnitine (6.1 umol/L), citrulline (44.86 umol/L), glucose (75 g) tolerance, glycosylated hemoglobin, fasting blood glucose, and thyroid function were normal. Blood gas analysis showed metabolic acidosis and anion gap. Renal ultrasound image (**Figure 1**) showed slightly enhanced parenchymal echo in both kidneys.

The child's clinical symptoms included abnormal motor development for 6 years, with bone deformity, "X" legs, chicken chest, double wrist joints, bilateral ankle joint deformity, and other changes in her left bone and distal radius, ulna distal osteoporosis, including the decreased bone mineral density detected by bone densitometry of child via Quantitative Ultrasound Bone Densitometry (QUS), and left radius and distal ulna rickets. The child had rickets and hypophosphatemia in the past. A diagnosis of Fanconi syndrome was the preliminary clinical consideration. In addition, according to Schwartz formula, the Epidermal Growth Factor Receptor (eGFR) of the patient was 20.17 mL/(min 1.73 m^2), indicating that the child was in chronic kidney diseases (stage IV) and did not meet the criteria for dialysis, so dialysis treatment was not performed for the time being. At the same time, we informed the patient's family that the patient was about to enter chronic kidney diseases (stage V), and preparations before dialysis should be made, including indwelling central venous catheterization for hemodialysis and peritoneal dialysis.

The patient suffered from renal tubular acidosis, hypokalemia, hypocalcemia and hypophosphatemia since childhood. The examination after admission showed that urine sugar (3 +) and urine protein (2 +) were positive, while glucose (75 g) tolerance,

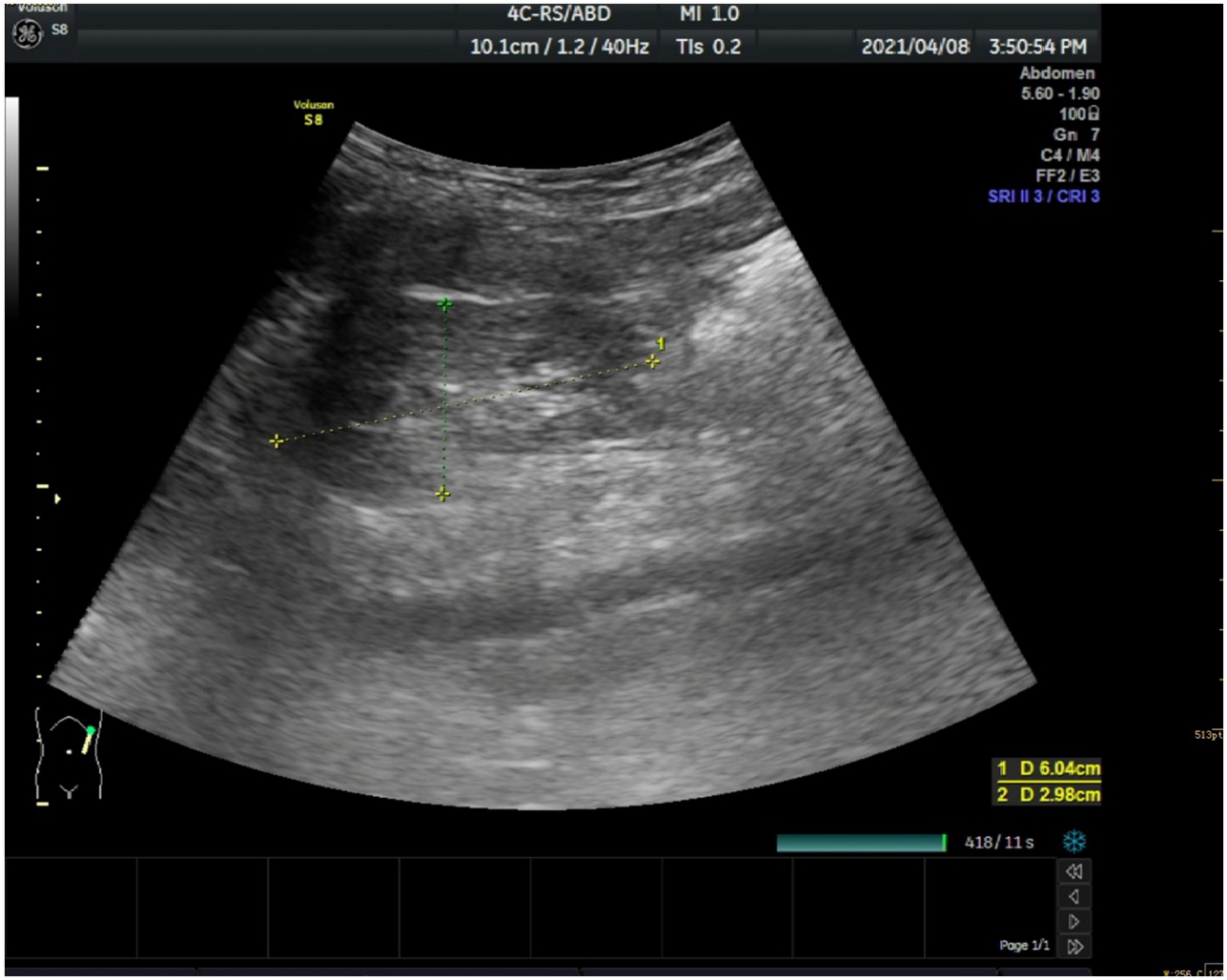

FIGURE 1 | Renal ultrasound image.

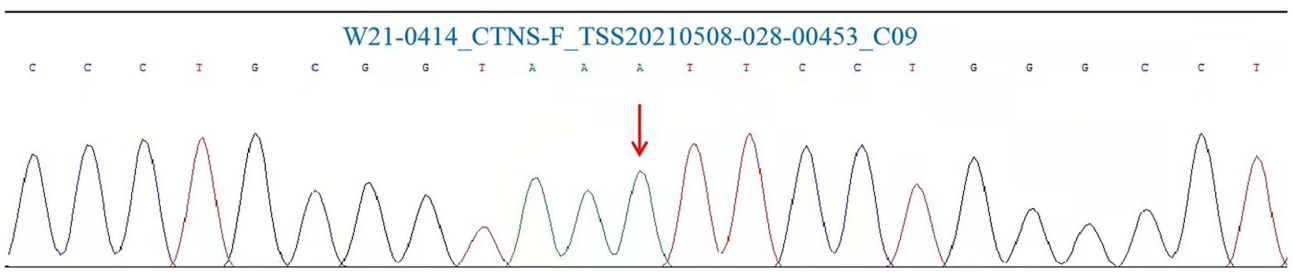

FIGURE 2 | CTNS mutation Sanger analysis results for the patient involved in this study. Polymerase chain reaction (PCR) and Sanger was performed in our test.

glycosylated hemoglobin and fasting blood glucose were normal. In addition, α1-microglobulin, β2-microglobulin and other proteins in urine that reflect the reabsorption function of renal tubules were increased. Therefore, the patient was considered to have renal tubular injury, which can lead to electrolyte disturbance, renal diabetes, and partial tubular proteinuria.

Meanwhile, considering the renal tubular injury, the decrease of serum calcium/phosphorus concentration/level and the increase of parathyroxine levels (945.8 pg/ml), the secondary hyperparathyropathy could be diagnosed. Furthermore, the girl had abdominal pain for more than 3 months prior to hospitalization. A CT scan showed slightly blurred mesenteric

fat space, multiple enlarged lymph nodes in the abdominal cavity were identified, thus mesenteric lymphadenitis was considered.

During hospitalization, the girl appeared tetany repeatedly, manifested as flexion and rigidity of the limbs as well as chicken claw-like hands accompanied by pain, and the lowest blood calcium level was 1.68 mmol/L. Calcium carbonate was then supplemented intravenously and oral calcium zinc gluconate and ossified triol were added. As citrate would combine with free calcium ions, which could further decrease blood calcium levels, the administration of citrate was stopped.

The girl underwent ophthalmologic examination in West China Fourth Hospital of Sichuan University. The conjunctiva, cornea, iris, lens, retina, intraocular pressure, and diopter were normal, no binocular corneal crystalline was found, and there was no visual field defect.

On the premise of informed consent, the whole exome sequencing (WES) of this girl was conducted. We decided to perform WES analysis because the initial onset age of the patient was early, accompanied by multiple organ system damage, and the treatment effect of oral sodium and potassium citrate mixture for renal tubular acidosis was not good. Meanwhile, the renal function of this patient showed progressive decline. The progression of renal tubular dysfunction, followed by glomerular involvement and renal decompensation, led us to strongly suspect that the patient had a mono-genetic inherited related renal tubule dysfunction.

Gene analysis showed that there was a homozygous pathogenic variant c.140 $\leq$ 5G > A (p.?) in the patient's CTNS gene (**Figure 2**). This was a small variation in the intron region, found for the first time. Notably, such a variant has not been reported in the literature and is rare in the population. Combined with the results of genetic examination, the diagnosis of cystinosis was made.

Although the child was in a serious condition, her parents asked for her to be discharged after 6 days of hospitalization. Research shows that hypophosphatemia and hypocalcemia in Fanconi syndrome and proximal renal tubular acidosis can be exacerbated by vitamin D deficiency, and the resulting tetany and obvious bone pain. And the above clinical symptoms can be effectively alleviated by the treatment with sodium hydrogen phosphate and sodium phosphate disodium buffer solution and active vitamin D.

After discharge, the parents were guided to supervise the girl to use drugs according to doctor's prescriptions (to take orally sodium dihydrogen phosphate, disodium hydrogen phosphate, lysine inositol vitamin B12, lysine calcium hydrogen phosphate tablets, calcitriol soft capsules, ferrous succinate tablets and vitamin C, and to recheck regularly).

The girl was asked to limit the intake of high protein foods, and return to the hospital if there was any discomfort. Twenty-eight days after the discharge, her family received the gene report results and were advised to carry out the related gene detection. Unfortunately, her family refused to carry out genetic testing. We used network follow-up to remind her family members to take her to the local hospital for urine review to monitor kidney function, but the patient did not follow up strictly according to the doctor's advice.

DISCUSSION

Up to date, most of the reported cases of cystinosis have occurred in Europe and the United States, with much less cases of cystinosis reported in Asia. Specifically, one case in Japan (7), 6 cases in Thailand (4 families involved) (8), 2 cases in India (9), and 21 cases in China have been reported (**Table 1**) (3, 5, 6, 10–13). The Chinese cases included 10 Mainland families (including 13 patients with CTNS homozygous mistranslation variant N323K, c.681 G > A(p.E227E), c.477C > G (p.S159R), c.274C > T (p.Q92X), c.680A > T (p.E227V) and CTNS pathogenic variant of (IVS6+1, del G and IVS8-1, and del GT), or with a deletion of c.18_21del GACT, (p.T7FfsX7)), and 5 Taiwanese families (including 8 patients with CTNS homozygous mistranslation variant N323K, 753G > A(W138X), exon 11 (IVS11+2T > C), 1178A-G (K280R) or mutation 57-kb deletion cystinosis).

At present, the known types of gene pathogenic variant include insertion, deletion, repetition, translocation, point variant, splice site variant, promoter variant, and genome rearrangement of CTNS gene sites. Here we report a new homozygous variant of the CTNS gene. The pathogenic variant site was lntron4 position on chr17:3550821 chromosome, and the protein level of reference transcript was NM 004937.3: c.140+5G > A (p.?). The variation is a small variation in the intron region, which has not been reported in the literature as this variant is rare in the population. The variation cannot be found in the ESP6500siv2 ALL, 1000g2015aug ALL, EXAC, gnomAD, and dbSNP147 databases. Unfortunately, the family members of the child refused to undergo genetic testing, and as such, we could not determine whether other members of the family had similar variations.

Also, among the cases reported in China, only Yong-jia Yang's report clarified ethnic groups of cystinosis patients, in which a Chinese Han family was affected.

Compared with adults, there are very few reports on cystinosis in children in China. However, in recent years, scholars are increasingly paying attention to cystinosis in children. Based on the duration of presented symptoms and the severity of renal involvement, Cystinosis can be divided into infant type (also known as kidney type), juvenile type (also known as intermediate type), and ophthalmopathy type, of which infant type is the most common and most serious, typically characterized by kidney involvement as the first symptom (14). In our report, the patient belongs to infant type, manifested as involvement of multiple organs such as kidney, bone, and thyroid. The girl began to develop symptoms at the age of 3 and was first diagnosed with Fanconi syndrome at the age of 4. At the age of 9, she was hospitalized due to the aggravation of the symptoms. At this time, following gene detection, she was diagnosed with cystinosis and chronic kidney disease. It took 5 years from the initial visit to the final diagnosis for this case. This may be related to the low medical cooperation of the patient's family members, characterized by irregular medical treatment, poor medication compliance, etc. There are also other factors, including the rarity of the cases, economic conditions, limit of diagnosis, and treatment technologies as well as the concept of medical behavior of the patient and her family members. In recent

TABLE 1 | Clinical and molecular characteristics of Chinese patients with cystinosis.

Study	Case	Nationality	Age of onset	Age of diagnosis	Mutation site	Cystinosis subtypes	Extra renal symptoms	Renal impailment	Treatment
Du et al. (3)	1	–	1 year	13 years	c. 969C > G, p. 323N > K	Nephropathic	Growth retardation, rickets, hypothyroidism	Tubular dysfunction, including glycosuria, urine protein, Amino acid urine, high phosphate urine	Taken neutral phosphorus mixture, citric acid mixture, sodium bicarbonate tablets, calcitriol, levothyroxine sodium. Limit the intake of high protein foods
	2	–	1 year	6 years	c. 969C > G, p. 323N > K	Nephropathic	Growth retardation, rickets	Tubular dysfunction, including glycosuria, urine protein, Amino acid urine, high phosphate urine	Taken neutral phosphorus mixture, citric acid mixture, sodium bicarbonate tablets, and calcitriol limit the intake of high protein food
Li et al. (10)	1	–	1 year	12 years	Homozygous c.969C > G, (p.N323K)	Nephropathic	Binocular corneal crystalline, growth retardation, rickets, hypothyroidism, metabolic acidosis	Glycosuria, urine protein, abdominal ultrasound showed renal damage	Citrate mixtures, phosphate supplements, oral calcium agents and calcitriol, GH treatment, Thyroid stimulating hormone, sodium levothyroxine tablets, calcium carbonate, sodium bicarbonate, gonadotropin releasing hormone. When this patient became 14 years old (40 kg), he was able to access cysteamine with international help. However, the patient suffered from severe pain in the legs and massive acne on both sides of the nose within 1 month of cysteamine treatment, which led to the halt of the treatment
	2	–	6 months	5 years	Homozygous c.969C > G, (p.N323K)	Nephropathic	Binocular corneal crystalline, growth retardation, rickets, hypothyroidism	Glycosuria, urine protein	Patient 2 was the brother of patient 1, and his symptoms were similar to patient 1 and he received comparable treatment as mentioned earlier
	3	–	1 year	4 years	c.18_21del GACT, (p.T7FfsX7); c.477C > G (p.S159R)	Nephropathic	Binocular corneal crystalline, growth retardation, rickets	Normal	Treated with alternative therapies to maintain the electrolyte levels, but none of them received either cysteamine or GH treatment

(Continued)

TABLE 1 | Continued

Study	Case	Nationality	Age of onset	Age of diagnosis	Mutation site	Cystinosis subtypes	Extra renal symptoms	Renal impailment	Treatment
	4	–	1 year	6 years	Homozygous c.18_21del GACT, (p.T7FfsX7)	Nephropathic	Binocular corneal crystalline, growth retardation, rickets	Could not acquire	Treated with alternative therapies to maintain the electrolyte levels, but none of them received either cysteamine or GH treatment
	5	–	3 years	5 years	c.274C > T (p.Q92X)a; c.680A > T (p.E227V)	Intermediate	Binocular corneal crystalline, growth retardation, rickets	Chronic renal insufficiency (stage III)	Treated with alternative therapies to maintain the electrolyte levels, but none of them received either cysteamine or GH treatment
	6	–	9 months	5 years	c.18_21del GACT, (p.T7FfsX7); c.600_700del GT, (p.S234LfsX61)	Nephropathic	Binocular corneal crystalline, growth retardation, RicketsH6:H9	Kidney failure (ESRD) and waiting for a kidney transplant	Treated with alternative therapies to maintain the electrolyte levels, but none of them received either cysteamine or GH treatment
Ling et al. (6)		–	–	4 years	c.681 G>A (p.E227E)	–	Binocular corneal crystalline, growth retardation, rickets, metabolic acidosis	Polyuria, glycosuria, urine protein	It is only mentioned that this patient did not comply with cysteamine treatment
Jiang et al. (11)		–	1 year	4 years	–	Ocular non-nephropathic cystinosis	Binocular corneal crystalline, growth retardation, rickets	Glycosuri, urine protein, Amino acid urine	Correct acidosis, supplement potassium, sodium and calcium, and topical eye drops of cysteine hydrochloride can effectively remove corneal crystallization
Yang et al. (5)	1	Han	7 months	7 years and 6 months	CTNS (IVS6+1, del G and IVS8-1, and del GT)	–	Binocular corneal crystalline, growth retardation, rickets, metabolic acidosis (severe), moderate anemia, secondary carnitine lack	Polydipsia and polyuria, Systemic amino acid uria, Fanconi syndrome	Lactose-free diet, supplemented with carnitine, VitB1, and VitB12
	2	Han	7 months	3 years and 4 months	CTNS (IVS6+1, del G and IVS8-1, and del GT).	–	Growth retardation, rickets, metabolic acidosis, hypokalemia, iron deficiency anemia, secondary carnitine deficiency	Glycosuria, urine protein, polydipsia and polyuria, renal Fanconi syndrome	Could not acquire
Chuang et al. (12)	1	–	–	5 years	–	–	Binocular corneal crystalline	Kidney failure (ESRD) and received allografts	Began cysteamine treatment until transplantation at ages 13.4, and delivered a girl without complication during gestation, and her renal function also remained good

(Continued)

TABLE 1 | Continued

Study	Case	Nationality	Age of onset	Age of diagnosis	Mutation site	Cystinosis subtypes	Extra renal symptoms	Renal impailment	Treatment
	2	–	–	9 years	–	–	Binocular corneal crystalline	Kidney failure (ESRD) and received allografts	Began cysteamine treatment until transplantation at ages 19.8 and 26.4 years. Obstructive nephropathy with progressive graft failure at age 26.4 years and was treated for vulvar condyloma and carcinoma *in situ* of cervix
Thoene et al. (13)	1	–	8 years and 1 months	–	1308C > G (N323K)	Nephropathic	Binocular corneal crystalline	Proteinuria, At age 12 her creatinine clearance had fallen to 67 mL/min/1.73 m^2 and her proteinuria had increased to 3.2 g/day	–
	2	–	5 years and 8 months	–	1308C > G (N323K)	Nephropathic	Binocular corneal crystalline	Proteinuria, At age 12 9/12 her daily protein excretion is 2.7 g and creatinine clearance 18 mL/min/1.73 m^2	–
	3	Unknown	7 years	13 years	753G > A (W138X), exon 11 (IVS11+2T > C)	Intermediate	Binocular corneal crystalline	Kidney failure (ESRD)	Renal transplant at age 15
	4		5 years	11 years	753G > A (W138X), exon 11 (IVS11+2T > C)	Intermediate	Binocular corneal crystalline	Kidney failure (ESRD)	Renal transplant at age 14
	5		16 years	18 years	753G > A (W138X), exon 11 (IVS11+2T > C)	Intermediate	Binocular corneal crystalline, moderate hypertension, minimal photophobia, thyroid gland is slightly enlarged	Proteinuria, creatinine clearance has declined to 42 mL/min/1.73 m^2	–
	6		12 years	25 years	57-kb deletion, 1178A-G (K280R)	Intermediate	Binocular corneal crystalline	ERSD	Hemodialysis and renal transplant at age 30 at age 43, the serum creatinine was 1.4 mg/dL
Ma et al. (4)	1	–	2 years	–	c.696C > G(p.323 N > K)	Nephropathic	Binocular corneal crystalline, growth retardation, rickets	Tubular dysfunction	It is only mentioned that supportive treatment and specific treatment can be used

years, with the development of economy and the progress of diagnosis and treatment technologies, gene detection technology has gradually become popularized in China, which has greatly enriched the means of diagnosis and treatment and improved the level of treatment.

At present, on the premise of combining clinical manifestations and laboratory results, there are three methods to assist in the diagnosis of suspected cystinosis patients: (1) Using mass spectrometer liquid chromatography to detect the level of cystine in blood leukocytes. This method has high sensitivity and specificity, and can monitor the therapeutic effect. However, as the requirements for instruments and testers are high, it cannot be easily conducted in a clinic. (2) Most patients can be diagnosed by gene detection, although the price is relatively high. (3) Using a slit lamp to detect characteristic corneal cystine crystallization is simple and economical; however, the scope of application is narrow: it is only suitable for patients with eye symptoms and cannot monitor the therapeutic effect.

Therefore, the corresponding medical testing methods can be selected based on the local medical conditions and the clinical manifestation type of the patient in question. At present, some cases of cystinosis in China have been analyzed by gene analysis, with the number of such cases increasing in recent years (3, 5, 6, 10–13). Gene diagnosis is beneficial to the diagnosis and analysis of cystinosis, and it is also an area for development in the future (15).

Some studies have pointed out that, the cases diagnosed may only be part of the actual cases because of the difficulty of diagnosis, such that some patients may not be able to be diagnosed (16). If patients with cystinosis cannot be diagnosed in time, they will not be treated in time, meanwhile the genetic information and clinical data of this population will be missing. From this case, it can be seen that the treatment compliance of the child and her families is not high. Thus, medical and nursing staff need to work to improve the treatment compliance of children and their families.

Health outcomes can be improved through health education and the improvement of drug research and treatment methods, such as developing sustained-release capsules to reduce the frequency of drug taking (17), and informing children and their families of the serious consequences of drug withdrawal through real cases examples.

At present, mercaptamine bitartrate, a drug that can specifically reduce cystine in lysosomes, is the preferred treatment for nephropathic cystinosis. The drug was transported to lysozyme by lysosomal membrane PQLC2 vector by forming cysteamine cysteine binding molecule with cystine in lysozyme. Early medication can effectively improve the growth and development, delay the occurrence of end-stage renal disease, but cannot prevent the progress of the disease. A new cysteamine preparation with delayed release simplifies the administration schedule, but still cannot cure cystinosis disease. Mercaptamine bitartrate is widely used in developed countries, but has not yet been introduced into China, which limits our research on this disease.

In the future, therapeutic research may be carried out based on CTNS-carrying stem cell transplantation, which has been successfully carried out in mouse model. Hematopoietic stem cell transplantation and gene editing technology are possible choices to cure the diseases (18).

As our understanding has developed, cystinosis has gradually become a treatable rare disease. Going forward, it is very important to improve the awareness by timely reporting of the disease and to adopt the behavior of actively seeking medical treatment. Early detection and early treatment can reduce and delay the occurrence of complications and improve the prognosis of patients with cystinosis.

DATA AVAILABILITY STATEMENT

The datasets for this article are not publicly available due to concerns regarding participant/patient anonymity. Requests to access the datasets should be directed to the corresponding author.

ETHICS STATEMENT

Written informed consent was obtained from the individual(s), and minor(s)' legal guardian/next of kin, for the publication of any potentially identifiable images or data included in this article.

AUTHOR CONTRIBUTIONS

All authors listed have made a substantial, direct, and intellectual contribution to the work and approved it for publication.

FUNDING

This article was supported by the fund of Science and Technology Bureau of Sichuan Province (Grant No. 2019YFS0240).

ACKNOWLEDGMENTS

We thank Dr. Wen Deng, from The University of Hong Kong, for editing the English text of a draft of this article.

REFERENCES

1. Hutchesson AC, Bundey S, Preece MA, Hall SK, Green A. A comparison of disease and gene frequencies of inborn errors of metabolism among different ethnic groups in the West Midlands,UK. *J Med Genet.* (1998) 35: 366–70.
2. Elmonem MA, Veys KR, Soliman NA, Van Dyck M, Van Den Heuvel LP, Levtchenko E. Cystinosis:a review. *Orphanet J Rare Dis.* (2016) 11:47. doi: 10.1186/s13023-016-0426-y
3. Du J, Pang R, Jiang Y, Wang O, Li M, Xing XP, et al. Clinical manifestations and CTNS gene mutation in two patients with cystinosis. *Chin J Osteoporosis Bone Miner Res.* (2017) 10:469–73. doi: 10. 3969/j.issn.1674-2591.2017.05.007

4. Ma YY, Shen YJ, Zhou L, Liu YP, Li DX, Ding Y, et al. CTNS gene mutation leads to cysteine nephropathy combined with corneal crystal in young child. *J Clin Pediatr.* (2016) 34:783–6. doi: 10.3969/j.issn.1000-3606.2016.10.017
5. Yang YJ, Hu Y, Zhao R, He XY, Zhao L, Tu M, et al. First report of CTNS mutations in a Chinese family with infantile cystinosis. *Sci World J.* (2015) 2015:309410. doi: 10.1155/2015/309410
6. Ling C, Liu XR, Chen Z, Jiang YP, Fan JF, Meng Q, et al. Corneal cystine crystals in cystinosis. *Arch Dis Childh.* (2017) 102:185. doi: 10.1136/archdischild-2016-312456
7. Okami T, Nakajima M, Higashino H, Aoki T. Ocular manifestations in a case of infantile cystinosis. *Nippon Ganka Gakkai Zasshi.* (1992) 96:1341.
8. Yeetong P, Tongkobpetch S, Kingwatanakul P, Deekajorndech T, Bernardini IM, Suphapeetiporn K, et al. Two novel CTNS mutations in cystinosis patients in Thailand. *Gene.* (2012) 499:323–5. doi: 10.1016/j.gene.2012.03.047
9. Tang S, Danda S, Zoleikhaeian M, Simon M, Huang T. An Indian boy with nephropathic cystinosis: a case report and molecular analysis of CTNS mutation. *Genet Test Mol Biomark.* (2009) 13:435–8. doi: 10.1089/gtmb.2008.0156
10. Li XQ, Wu D, Liang XJ, Li WJ, Liu M, Cao BY, et al. The diagnosis of cystinosis in patients reveals new CTNS gene mutations in the Chinese population. *J Pediatr Endocrinol Metab.* (2019) 32:375–82. doi: 10.1515/jpem-2018-0263
11. Jiang JJ, Bai DY, Yu G, Wu Q. Fanconi syndrome with corneal lesions secondary to cystine disease: a case report. *Natl Med J China.* (2014) 94:3357–8. doi: 10.3760/cma.j.issn.0376-2491.2014.42.019
12. Chuang YW, Wen MC, Wu MJ, Shu KH, Cheng CH, Yu TM, et al. Follow-up and treatment of renal transplantation with nephropathic cystinosis in central Taiwan. *Transplant Proc.* (2012) 44:80–2. doi: 10.1016/j.transproceed.2011.12.071
13. Thoene J, Lemons R, Anikster Y, Mullet J, Paelicke K, Lucero C, et al. Mutations of CTNS causing intermediate cystinosis. *Mol Genet Metab.* (1999) 67:283–93.
14. Harrison F, Yeagy BA, Rocca CJ, Kohn DB, Salomon DR, Cherqui S. Hematopoietic stem cell gene therapy for the multisystemic lysosomal storage disorder cystinosis. *Mol Ther.* (2013) 21:433–44. doi: 10.1038/mt.2012.214
15. Jiang XY, Rong LP. Progres of diagnosis and treatment for Gitelman syndrome and cystinosis. *Chin J Appl Clin Pediatr.* (2018) 33:1296–300. doi: 10.3760/cma.j.issn.2095-428X.2018.17.005
16. Gahl WA, Thoene JG, Schneider JA. Cystinosis. *N Engl J Med.* (2002) 347:111–21. doi: 10.1056/NEJMra020552
17. Dohil R, Fidler M, Gangoiti JA, Kaskel F, Schneider JA, Barshop BA. Twice-daily cysteamine bitartrate therapy for children with cystinosis. *J Pediatr.* (2010) 156:71–5. doi: 10.1016/j.jpeds.2009.07.016
18. Cherqui S. Hematopoietic stem cell gene therapy for cystinosis: updated results from a phase I/II clinical trial. *Mol Genet Metab.* (2021) 132:S25. doi: 10.1016/j.ymgme.2020

Conflict of Interest: The authors declare that the research was conducted in the absence of any commercial or financial relationships that could be construed as a potential conflict of interest.

Publisher's Note: All claims expressed in this article are solely those of the authors and do not necessarily represent those of their affiliated organizations, or those of the publisher, the editors and the reviewers. Any product that may be evaluated in this article, or claim that may be made by its manufacturer, is not guaranteed or endorsed by the publisher.

frontiers | Frontiers in Pediatrics

CASE REPORT
published: 28 April 2022
doi: 10.3389/fped.2022.825515

PC Splice-Site Variant c.1825+5G>A Caused Intron Retention in a Patient With Pyruvate Carboxylase Deficiency: A Case Report

*DongYing Tao[1], HuiQin Zhang[1], Jingmin Yang[2], HuanHong Niu[1], JingJing Zhang[1], Minghua Zeng[3] and ShengQuan Cheng[1]**

[1] Department of Pediatrics, XiJing Hospital, Fourth Military Medical University, Xi'an, China, [2] State Key Laboratory of Genetic Engineering, School of Life Sciences, Fudan University, Shanghai, China, [3] Medical Experiment and Training Center, Hanzhong Vocational and Technical College, Hanzhong, China

OPEN ACCESS

Edited by:
Hui Xiong,
Peking University First Hospital, China

Reviewed by:
Dario Balestra,
University of Ferrara, Italy
YoTsen Liu,
Taipei Veterans General Hospital, Taiwan
Athar Ansari,
Wayne State University, United States

***Correspondence:**
ShengQuan Cheng
chengsq999999@163.com

Specialty section:
This article was submitted to Genetics of Common and Rare Diseases, a section of the journal Frontiers in Pediatrics

Received: *30 November 2021*
Accepted: *28 March 2022*
Published: *28 April 2022*

Citation:
Tao D, Zhang H, Yang J, Niu H, Zhang J, Zeng M and Cheng S (2022) PC Splice-Site Variant c.1825+5G>A Caused Intron Retention in a Patient With Pyruvate Carboxylase Deficiency: A Case Report. Front. Pediatr. 10:825515. doi: 10.3389/fped.2022.825515

Background: Pyruvate carboxylase deficiency (PCD; MIM#266150) is a rare autosomal recessive disorder characterized by a wide range of clinical features, including delayed neurodevelopment, elevated pyruvate levels, lactic acidosis, elevated ketone levels, and hyperammonemia. The pyruvate carboxylase (PC) gene was identified to be the disease-causing gene for PCD. A novel homozygous splice variant in the PC gene was identified in a Chinese boy, but the pathogenicity is still unclear. The objective of the present study was to determine the effect of this splice-site variant by reverse transcription analysis.

Methods: We reported the clinical course of a 20-month-old Chinese pediatric patient who was diagnosed with PCD using whole-exome sequencing (WES). The effects of the variant on mRNA splicing were analyzed through the transcript analysis *in vivo*.

Results: The results of metabolic blood and urine screening suggested PCD by employing tandem mass spectrometry. WES revealed a novel homozygous splice-site variant (c.1825+5G>A) in the PC gene. *in vivo* transcript analysis indicated that the splice-site variant caused the retention of 192 bp of the intron.

Conclusion: Thus, c.1825+5G>A was established as a pathogenic variant, thereby enriching the mutational spectrum of the PC gene and providing a basis for the genetic diagnosis of PCD.

Keywords: pyruvate carboxylase deficiency, c.1825+5G>A, PC gene, splice-site variant, pathogenic variant

INTRODUCTION

Pyruvate carboxylase deficiency (PCD; MIM# 266150) is a rare autosomal recessive inherited disorder with an estimated prevalence of 1:250,000. It results from the insufficient activity of pyruvate carboxylase (PC), a mitochondrial matrix enzyme, which converts pyruvate to oxaloacetatic acid, thereby facilitating gluconeogenesis and energy production (1, 2). Low activity of PC causes the accumulation of pyruvate, which is subsequently converted into lactate in the

plasma by the enzyme lactate dehydrogenase. This eventually elevates plasma lactic acid levels. The decreased production of oxaloacetate decreases gluconeogenesis, thereby promoting hypoglycemia and preventing the liver from oxidizing pyruvate- and fatty acid-derived acetyl-CoA (2). This increases the acetyl-CoA pool, resulting in hepatic ketone body synthesis or ketoacidosis (2). It also affects the tricarboxylic acid (TCA) cycle and impairs the synthesis of aspartic acid, which consequently affects the urea cycle and the related biosynthetic pathways, thereby causing hyperammonemia. Another relevant role of PC activity involves astrocytes where the TCA cycle provides α-ketoglutarate as a precursor for the production of the neurotransmitter, glutamate (1–3).

Pyruvate carboxylase deficiency is associated with variants in the PC gene and is typically characterized by delayed development, recurrent seizures, elevated pyruvate levels, and lactic acidosis (3). PCD manifests in three main clinical forms: types A, B, and C. The infantile-onset form (type-A) manifests several months after birth; it is characterized by hypotonia, failure to thrive, delayed development, and lactic acidemia, followed by infection, diarrhea, and other symptoms, which eventually result in mortality during infancy or early childhood (4, 5). The neonatal-onset form (type-B) is usually characterized by severe lactic acidosis, hyperammonemia, and mortality within the first 3 months of life (6–8). The late-onset form (type C) presents with normal or mildly delayed neurological development and episodic metabolic acidosis (9, 10). To date, only 33 cases of PCD have been reported, and none of them are from the Chinese population. Here, we report the presence of a novel *PC* splice-site variant (c.1825+5G>A) in a 20-month-old Chinese boy and validate that the association of the variant is associated with abnormal *PC* mRNA processing, leading to intron retention.

MATERIALS AND METHODS

Patient

The proband was a 20-month-old boy who was transferred to XiJing Hospital after presenting with delayed neurodevelopment and recurrent lactic acidosis. The patient was the first child of healthy consanguineous Chinese parents, with no significant family history. The child was born at full-term with normal weight, length, and head circumference. At the age of 3 months, the patient presented with bilateral eyelid clonus seizures, lasting from 30 s to 1 min, and was completely controlled by the oral administration of levetiracetam. At the age of 9 months, the patient presented with severe lactic acidosis with failure to thrive, tachypnea, and lethargy after 2 days of upper respiratory symptoms. Laboratory investigations during the acute episode revealed a plasma pH of 6.96 and the plasma levels of lactate, ammonia, and glucose, and alanine and citrulline levels to be 7.95 mmol/L, 93.77 μmol/L (limit: < 40 mmol/L), 6.1 mmol/L, 715 μmol/L (normal range: 90–450 μmol/L), and 69.18 μ mol/L (normal range:5.5–45 μmol/L), respectively. The levels of lactate and ketones were also elevated in urine. MRI of the patient's brain revealed abnormal signal shadows in the white matter near the triangle of the bilateral lateral ventricles. Abdominal ultrasound indicated the absence of hepatomegaly. After intravenous administration of bicarbonate and hemodialysis, the patient's serum pH returned to normal. The patient subsequently presented with five additional episodes of lactate acidosis, which were treated with intensive fluid therapy; however, the patient's plasma lactic acid and ammonia levels remained elevated at 3.7–12 mmol/L and 36.25–93.77 μmol/L, respectively. The patient was slightly hypotonic, and his developmental milestones corresponded to those observed at 12 months of age. He could walk with support and pronounce approximately two words. Following diagnosis, the patient was administered biotin, aspartate, carnitine, thiamine, and citrate. At the age of 34 months, following one week of respiratory symptoms, the child developed severe metabolic acidosis. Despite treatment with dialysis, the patient's condition continued to deteriorate, with lactic acid levels increasing from 7.7 to 23.4 mmol/L, eventually followed by death.

Whole-Exome Sequencing for Mutation Screening

To identify the gene responsible for the patient's clinical presentation, peripheral blood was collected from the patient and sent to Running Gene, Inc. (Beijing, China) for whole-exome sequencing (WES). Briefly, DNA was isolated and fragmented to build a DNA library by using the KAPA Library Preparation Kit (Illumina, Inc., San Diego, USA). Then, the library was sequenced using an Illumina HiSeq4000 platform (Illumina, San Diego, USA) using a 150-bp paired-end read according to the standard manual. The sequencing data was filtered and aligned with the human reference genome (GRCh37/hg19) by using the BWA Aligner (https://bio-bwa.sourceforge.net/), and variants were annotated by ANNOVAR (annovar.openbioinformatics.org/en/latest/). The exclusion of variants with minor allele frequency (MAF) >1% according to the gnomAD database (https://gnomad.broadinstitute.org/) and/or the 1000 Genomes Project database (https://www.genome.gov/27528684/1000-genomes-project), as well as *in silico* pathogenicity predictions for missense variants (SIFT: http://sift.jcvi.org, PolyPhen2: http://genetics.bwh.harvard.edu/pph2, MutationTaster: http://www.mutationtaster.org, FATHMM: http://fathmm.biocompute.org.uk, and CADD: http://cadd.gs.washington.edu) and splice-site variants (Varseak: https://varseak.bio/, splice AI: https://spliceailookup.broadinstitute.org/, dbscSNV_ADA and dbscSNV_RF: https://sites.google.com/site/jpopgen/dbNSFP). Variants were classified as: pathogenic, likely pathogenic, benign, likely benign and VUS, according to American College of Medical Genetics (ACMG) guidelines. A candidate causal gene mutation was identified and confirmed using Sanger sequencing.

Transcript Analysis *in vivo*

Total RNA was extracted from the peripheral blood of the proband, his parents, and a healthy volunteer. Peripheral blood was collected in the PAXgene Blood RNA tube (BD Biosciences). RNA was isolated from the PAXgene Blood RNA kit (BD Biosciences) and then reverse-transcribed into cDNA

FIGURE 1 | Partial sequence chromatograms of pyruvate carboxylase (PC). The red arrows represent the mutation site. Index: homozygous splice-site variant c.1825+5G>A; father and mother: heterozygous splice-site variant c.1825+5G>A.

by using PrimeScript RT Master Mix (Takara). The target sequence was amplified from cDNA by PCR. The primer of the amplification is forward GCCCAAAAGCTGTTGCACTAC and reverse AAGTCATCCCAGACATGGAATC. PCR products were separated on 1.5% agarose and sequenced with an ABI 3130 genetic analyzer (Applied Biosystems). Generated next-generation sequencing (NGS) library using the PCR product was sequenced by Illumina HiSeq4000 platform. PCR products were separated on 1.5% agarose and sequenced with an ABI 3730XL DNA analyzer (Applied Biosystems).

RESULTS

Genetic Findings

Exome sequence analysis revealed that the patient was homozygous for a specific variant (c.1825+5G>A) in the PC gene (NM_022172), and Sanger sequencing confirmed that both parents were heterozygous carriers of the variant (**Figure 1**). The variant was not found in either the Genome Aggregation Database (gnomAD) or 1000 Genomes database. According to the American College of Medical Genetics and Genomics (ACMG) guidelines (11), the pathogenicity of c.1825+5G>A was unclear. However, *in silico* prediction of the variant's effects, using four different algorithms (Varseek, splice AI, dbscSNV_ADA, and dbscSNV_RF), consistently predicted that the variant would affect splicing (**Table 1**).

PC MRNA Expression *in vivo*

Agarose gel electrophoresis of RT-PCR-amplified genes showed that the band corresponding to that of the proband (mut) was larger than that of the control (wt) (**Figure 2A**). This indicates that the complementary DNA (cDNA) of the proband may have abnormal splicing. The cDNA amplification products of the proband, his parents, and healthy control were subjected to NGS. The results indicated that the proband cDNA retained a part of intron 13 (homozygous), and both the parents retained a part of intron 13 (heterozygous) (**Figure 2B**). Sanger sequencing indicated that the variant c.1825+5G>A caused aberrant splicing compared with that observed in the healthy control, resulting in the retention of the 192 bp intron 13 in the proband sample. Since the abnormal bands of his parents were too weak to be analyzed using the Sanger sequence, their sequencing results were similar to that of the control (**Figures 2C,D**). Eventually, the variant c.1825+5G>A was rated as pathogenic, based on the ACMG guidelines.

DISCUSSION

Pyruvate carboxylase deficiency is a rare neurometabolic disorder. Among the 34 cases reported to date, 10, including the proband of the present study, studies were born to consanguineous parents. The patient's symptoms first presented in the third month of his life and included

TABLE 1 | Summary of clinical findings of the proband.

	Proband			
Age of onset	3 months			
Clinical findings	Lactic acidosis	Developmental delay	Seziures	Recurrent metabolic neoacidosis
Laboratory	pH 6.96	Lactate 7.95	Ammonia 93.77 μmol/L	
	Plasma glucose 6.1	Alanine levels 715 μmol/L	Cit levels 69.18 μmol/L	
	Urinary organic acids:	elevated lactate and ketones		
MRI	Both abnormal signal shadows of the white matter near the triangle of bilateral lateral ventricles			
Genetic	PC:NM_022172 c.1825+5G>A			
in silico prediction	Varseek prediction level	4 [level range (1, 5)]		
	Splice AI	0.53 (range [0,1])		
	dbscSNV_ADA	0.9998 (range [0,1])		
	dbscSNV_RF	0.9499 (range [0,1])		
Time of diagnosis	At the age of 20-month-old			
Prognosis	At the age of 34 months, the child died of severe metabolic acidosis			

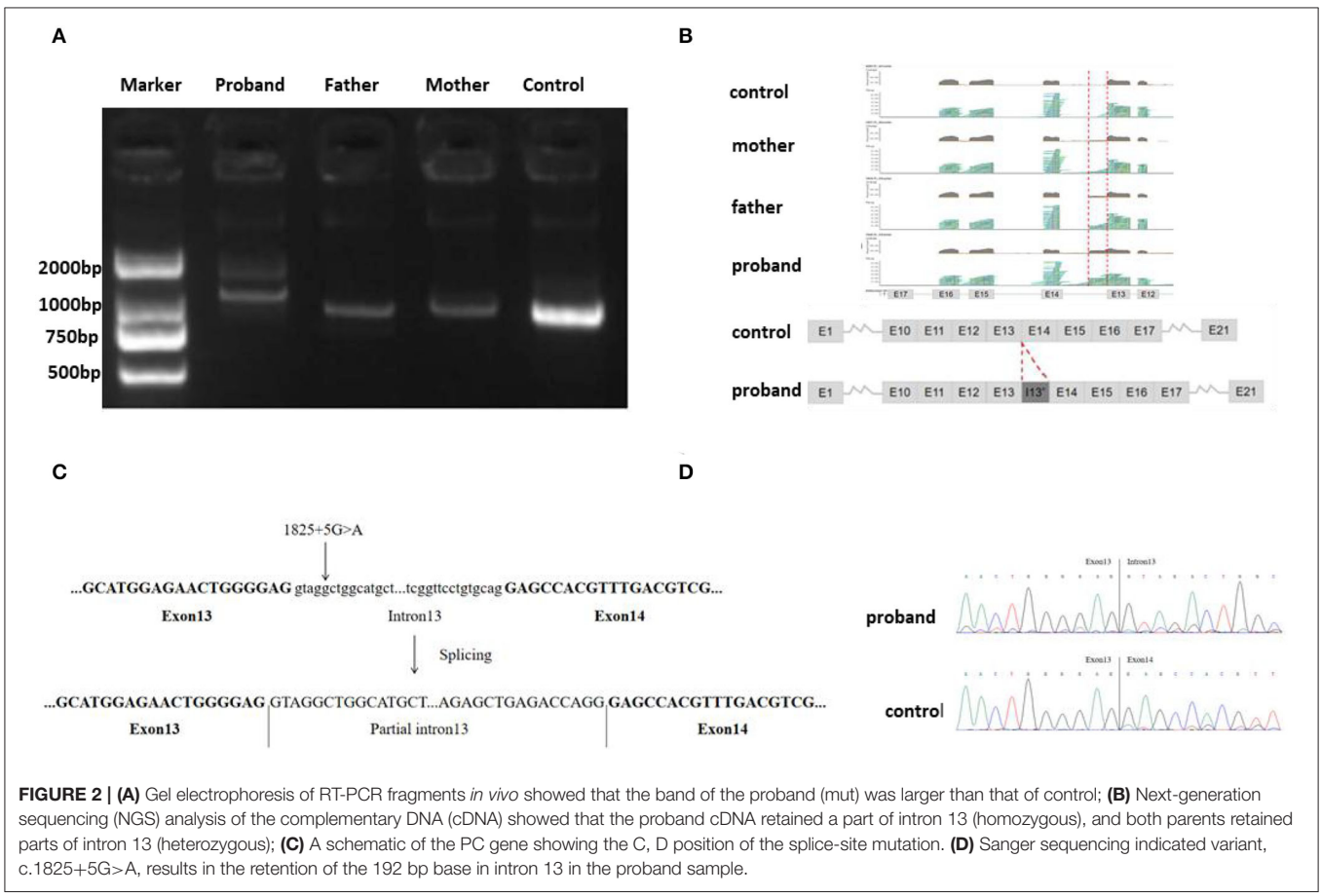

FIGURE 2 | (A) Gel electrophoresis of RT-PCR fragments *in vivo* showed that the band of the proband (mut) was larger than that of control; **(B)** Next-generation sequencing (NGS) analysis of the complementary DNA (cDNA) showed that the proband cDNA retained a part of intron 13 (homozygous), and both parents retained parts of intron 13 (heterozygous); **(C)** A schematic of the PC gene showing the C, D position of the splice-site mutation. **(D)** Sanger sequencing indicated variant, c.1825+5G>A, results in the retention of the 192 bp base in intron 13 in the proband sample.

delayed development, recurrent seizures, elevated pyruvate levels, lactic acidosis, hyperammonemia, and elevated ketone levels, which were consistent with the typical characteristics of type-A PCD (4). Among the eight patients that have been reported with type A PCD, two patients developed epilepsy, experiencing infantile spasms and tonic seizures.

The symptoms were controlled by using a combination of multiple epilepsy drugs. However, the patient in the current study experienced a mild seizure, with the only form of attack of clonic seizure, which was well controlled with levetiracetam. Lactic acidemia and hyperammonemia seemed to respond to treatment with aspartate, biotin, carnitine, and thiamine. However, for the remaining conditions, anaplerotic therapy did not seem to affect disease progression. Despite medical interventions, episodes of severe acidosis with lethargy still occurred in the proband, following a respiratory tract infection. Eventually, the proband died during early childhood similar to the outcomes of other patients with type A PCD.

Here, we reported the identification, via WES analysis, of a novel *PC* splice-site variant. This variant was homozygous in the 20-month-old study patient and was inherited from close relative parents, who carried the heterozygous mutation at the same site. Notably, the variant was not found in the Genome Aggregation Database (gnomAD). *in silico* prediction of the variant's effects, using four different algorithms (Varseak, splice AI, dbscSNV_ADA, and dbscSNV_RF), consistently indicated that the variant affected PC mRNA splicing. Thus, the splice-site variant could explain the proband phenotype. To determine the effect of this PC splice-site variant, total RNA isolated from venous blood was transcribed into cDNA *in vivo*. Sanger sequencing analysis of the cDNA revealed that the splice-site variant could cause the retention of 192 bp of intron 13. The pathogenicity of the splice-site variant was classified as like-pathogenic (PS3+PM2+PP4), according to the ACMG guidelines (11). After comprehensive consideration of the clinical manifestations, genetic analysis, and cDNA sequencing results, the c.1825+5G>A variant was identified as the cause of the patient's PCD.

The PC gene maps to 11q13.2 and includes 20 coding exons as well as four non-coding codons (12). Biallelic variants in the PC gene are associated with PCD. According to the Human Genome Mutation Database and other studies, approximately 44 causative variants (**Supplementary Table 1**), including nonsense, missense, splicing, insertion/deletion, and frameshift mutations, have been identified in 33 PCD-affected individuals. Genotype/phenotype correlations in both the fatal PCD forms (types A and B) are unclear. Theoretically, the presence of at least one truncating mutation in the PC gene should generate more severe clinical phenotypes. The current proband carried biallelic mutations and presented as type A PCD. However, one case that was similar to our patient was homozygous for splice-site variant c.321+1G>T and was diagnosed with type-B PCD (13), while another case with biallelic missense mutation 506G>A also presented with type-B PCD (14). Thus, the correlation between genotypes and clinical phenotypes certainly requires further investigation.

For the differential diagnosis of PCD, practitioners should focus on identifying other hereditary metabolic diseases that cause hyperlactatemia and abnormal neurodevelopment, such as carbohydrate metabolic diseases, including type-I glycogen accumulation syndrome (GSD1) (15), pyruvate dehydrogenase complex deficiency (PDHCD) (16), hereditary fructose intolerance (17), and the fructose-1,6-bisphosphatase deficiency (1,6-FBD) (18). These disorders can be distinguished based on the fact that hypoglycemia and hepatomegaly are common in type I glycogen accumulation syndrome and fructose-1,6-bisphosphatase deficiency but not in PCD, where these effects are only seen in individuals with the type B form. In addition, while PDHD and PCD have identical clinical manifestations, blood ketone bodies are not detectable in PDHCD.

To the best of our knowledge, this is the first case to be reported among the Chinese population (4–9, 13, 14, 16, 19–21). The patient had 6-times higher metabolic acidosis, accompanied by increased levels of lactic acid, blood ammonia, and pyruvate. Due to insufficient knowledge, it was not accurately clearly diagnosed in the early stages. Further, patients manifesting similar clinical characteristics need to be evaluated for PCD, and *PC* tests can be further confirmed.

In summary, we report the identification of a novel splice-site variant (c.1825+5G>A) in the PC gene of a Chinese boy with type-A PCD. In addition, we confirmed the variant's pathogenicity, which involves an alteration in mRNA splicing. This report enriches the mutational spectrum of the PC gene and provides a basis for the genetic diagnosis of PCD.

DATA AVAILABILITY STATEMENT

The original contributions presented in the study are included in the article/**Supplementary Material**, further inquiries can be directed to the corresponding author.

ETHICS STATEMENT

The studies involving human participants were reviewed and approved by the Medical Ethics Commilte of the first Afiliated Hospitat of the Air Force Medical University. The patients/participants provided their written informed consent to participate in this study. Written informed consent was obtained from the individual(s), and minor(s)' legal guardian/next of kin, for the publication of any potentially identifiable images or data included in this article.

AUTHOR CONTRIBUTIONS

DT, HN, and JZ was responsible for drafting the manuscript. DT did acquisition, analysis, and interpretation of data. HZ and JY designed and carried out the experiments. HN and JZ provided guidance and management for the patient. MZ made important comment for revision and polished the final version of the manuscript. SC was responsible for the revision of the manuscript for important intellectual content. All authors contributed to the article and approved the submitted version.

SUPPLEMENTARY MATERIAL

The Supplementary Material for this article can be found online at: https://www.frontiersin.org/articles/10.3389/fped.2022.825515/full#supplementary-material

REFERENCES

1. Wang D, *De Vivo* D. Pyruvate Carboxylase Deficiency. *GeneReviews*. Seattle, Washington, DC: University of Washington (2009).
2. Valle M. Pyruvate Carboxylase, Structure and Function. *Macromol Proteinm Complexes*. (2017) 83:291–322. doi: 10.1007/978-3-319-46503-6_11
3. Utter MF, Keech DB. Formation of oxaloacetate from pyruvate and carbon dioxide. *J Biol Chem*. (1960) 235:Pc17–8. doi: 10.1016/S0021-9258(18)69442-6
4. Coci EG, Gapsys V, Shur N, Shin-Podskarbi Y, de Groot BL, Miller K, et al. Pyruvate carboxylase deficiency type A and type C: Characterization of five novel pathogenic variants in PC and analysis of the genotype-phenotype correlation. *Hum Mutat*. (2019) 40:816–27. doi: 10.1002/humu.23742
5. Mangla P, Gambhir PS, Sudhanshu S, Srivastava P, Rai A, Bhatia V, et al. Pyruvate Carboxylase Deficiency Mimicking Diabetic Ketoacidosis. *Indian J Pediatr*. (2017) 84:959–60. doi: 10.1007/s12098-017-2430-1
6. Ostergaard E, Duno M, Møller LB, Kalkanoglu-Sivri HS, Dursun A, Aliefendioglu D, et al. Novel Mutations in the PC Gene in Patients with Type B Pyruvate Carboxylase Deficiency. *JIMD Rep*. (2013) 9:1–5. doi: 10.1007/8904_2012_173
7. Demir Köse M, Colak R, Yangin Ergon E, Kulali F, Yildiz M, Alkan S, et al. Challenges in the management of an ignored cause of hyperammonemic encephalopathy: pyruvate carboxylase deficiency. *J Pediatr Endocrinol Metabol*. (2020) 33:569–74. doi: 10.1515/jpem-2019-0307
8. Habarou F, Brassier A, Rio M, Chrétien D, Monnot S, Barbier V, et al. Pyruvate carboxylase deficiency: An underestimated cause of lactic acidosis. *Mol Genet Metab Rep*. (2014) 2:25–31. doi: 10.1016/j.ymgmr.2014.11.001
9. Almomen M, Sinclair G, Stockler-Ipsiroglu SG, Horvath GA. Pyruvate Carboxylase Deficiency Type C: A Rare Cause of Acute Transient Flaccid Paralysis with Ketoacidosis. *Neuropediatrics*. (2018) 49:369–72. doi: 10.1055/s-0038-1667171
10. Schiff M, Levrat V, Acquaviva C, Vianey-Saban C, Rolland MO, Guffon N. A case of pyruvate carboxylase deficiency with atypical clinical and neuroradiological presentation. *Mol Genet Metab*. (2006) 87:175–7. doi: 10.1016/j.ymgme.2005.10.007
11. Richards S, Aziz N, Bale S, Bick D, Das S, Gastier-Foster J, et al. Standards and guidelines for the interpretation of sequence variants: a joint consensus recommendation of the American College of Medical Genetics and Genomics and the Association for Molecular Pathology. *Genet Med*. (2015) 17:405–24. doi: 10.1038/gim.2015.30
12. Walker ME, Baker E, Wallace JC, Sutherland GR. Assignment of the human pyruvate carboxylase gene (PC) to 11q134 by flfluorescence in situ hybridization. *Cytogenet Cell Genet*. (1995) 69:187–9. doi: 10.1159/000133958
13. Wang D, Yang H, Kevin C, Lu JS, Shih LY, Briones P, et al. The Molecular Basis of Pyruvate Carboxylase Deficiency:Mosaicism correlates with prolonged survival. *Mol Genet Metab*. (2008) 95:31–8. doi: 10.1016/j.ymgme.2008.06.006
14. Breen C, White FJ, Scott CA, Heptinstall L, Walter JH, Jones SA, et al. Unsuccessful treatment of severe pyruvate carboxylase deficiency with triheptanoin. *Eur J Pediatr*. (2014) 173:361–6. doi: 10.1007/s00431-013-2166-5
15. Khoury J, Zohar Y, Shehadeh N, Saadi T. Glycogenic hepatopathy. *Hepatobiliary Pancreat Dis Int*. (2018) 17:113–8. doi: 10.1016/j.hbpd.2018.02.006
16. Hidalgo J, Campoverde L, Ortiz JF, Ruxmohan S, Eissa-Garcés A. A Unique Case of Pyruvate Carboxylase Deficiency. *Cureus*. (2021) 13:e15042. doi: 10.7759/cureus.15042
17. Kim MS, Moon JS, Kim MJ, Seong MW, Park SS, Ko JS. Hereditary Fructose Intolerance Diagnosed in Adulthood. *Gut Liver*. (2021) 15:142–5. doi: 10.5009/gnl20189
18. Adam MP, Ardinger HH, Pagon RA, Wallace SE, Bean LJH, Mirzaa G. Fructose-1,6-Bisphosphatase Deficiency. 2019 Dec 5. *GeneReviews®*. Seattle, WA: University of Washington, Seattle (1993–2021).
19. Monnot S, Serre V, Chadefaux-Vekemans B, Aupetit J, Romano S, De Lonlay P, et al. Structural insights on pathogenic effects of novel mutations causing pyruvatecarboxylase deficiency. *Hum Mutat*. (2009) 30:734–40. doi: 10.1002/humu.20908
20. Carbone MA, Applegarth DA, Robinson BH. Intron retention and frameshift mutations result in severe pyruvate carboxylasedeficiency in two male siblings. *Hum Mutat*. (2002) 20:48–56. doi: 10.1002/humu.10093
21. Ortez C, Jou C, Cortès-Saladelafont E, Moreno J, Pérez A, Ormazábal A, et al. A Infantile parkinsonism and GABAergic hypotransmission in a patient with pyruvate carboxylase deficiency. *Gene*. (2013) 532:302–6. doi: 10.1016/j.gene.2013.08.036

Conflict of Interest: The authors declare that the research was conducted in the absence of any commercial or financial relationships that could be construed as a potential conflict of interest.

Publisher's Note: All claims expressed in this article are solely those of the authors and do not necessarily represent those of their affiliated organizations, or those of the publisher, the editors and the reviewers. Any product that may be evaluated in this article, or claim that may be made by its manufacturer, is not guaranteed or endorsed by the publisher.

frontiers | Frontiers in Pediatrics

CASE REPORT
published: 18 May 2022
doi: 10.3389/fped.2022.812408

NDUFAF6-Related Leigh Syndrome Caused by Rare Pathogenic Variants: A Case Report and the Focused Review of Literature

Jaewon Kim[1], *Jaewoong Lee*[2] *and Dae-Hyun Jang*[1]*

[1] *Department of Rehabilitation Medicine, Incheon St. Mary's Hospital, College of Medicine, The Catholic University of Korea, Seoul, South Korea,* [2] *Department of Laboratory Medicine, Incheon St. Mary's Hospital, College of Medicine, The Catholic University of Korea, Seoul, South Korea*

Leigh syndrome is a neurodegenerative disorder that presents with fluctuation and stepwise deterioration, such as neurodevelopmental delay and regression, dysarthria, dysphagia, hypotonia, dystonia, tremor, spasticity, epilepsy, and respiratory problems. The syndrome characteristically presents symmetric necrotizing lesions in the basal ganglia, brainstem, cerebellum, thalamus, and spinal cord on cranial magnetic resonance imaging. To date, more than 85 genes are known to be associated with Leigh syndrome. Here, we present a rare case of a child who developed Leigh syndrome due to pathogenic variants of *NDUFAF6*, which encodes an assembly factor of complex I, a respiratory chain subunit. A targeted next-generation sequencing analysis related to mitochondrial disease revealed a missense variant (NM_152416.4:c.371T > C; p.Ile124Thr) and a frameshift variant (NM_152416.4:c.233_242del; p.Leu78Glnfs*10) inherited biparentally. The proband underwent physical therapy and nutrient cocktail therapy, but his physical impairment gradually worsened.

Keywords: Leigh syndrome, mitochondrial disease, *NDUFAF6*, complex I deficiency, neurodegenerative disorder

OPEN ACCESS

Edited by:
Huiwen Zhang,
Xinhua Hospital, China

Reviewed by:
Juan Dario Ortigoza-Escobar,
Hospital Sant Joan de Déu Barcelona, Spain
Xiaoping Luo,
Huazhong University of Science and Technology, China

***Correspondence:**
Dae-Hyun Jang
dhjangmd@naver.com

Specialty section:
This article was submitted to Genetics of Common and Rare Diseases, a section of the journal Frontiers in Pediatrics

Received: *10 November 2021*
Accepted: *31 March 2022*
Published: *18 May 2022*

Citation:
Kim J, Lee J and Jang D-H (2022) NDUFAF6-Related Leigh Syndrome Caused by Rare Pathogenic Variants: A Case Report and the Focused Review of Literature. Front. Pediatr. 10:812408. doi: 10.3389/fped.2022.812408

INTRODUCTION

Mitochondrial disease is a common inherited metabolic disorder that is clinically and genetically heterogeneous and occurs in approximately 10–25 cases per 100,000 individuals, many of which are childhood-onset usually by the age of 3 years (1). Mitochondria are present in all cells except erythrocytes and, given that mitochondria are responsible for oxidative phosphorylation and ATP synthesis, mitochondrial disease exhibits diverse phenotypes depending on the affected organs. Mitochondrial dysfunction leads to multiple system disorder, manifesting a progressive course with high morbidity and mortality (2). Mitochondrial disease is a genetic disorder resulting from pathogenic variants of mitochondrial DNA (mtDNA) and nuclear DNA (nDNA) associated with mitochondrial function. The mtDNA consists of 37 genes and encodes 13 proteins, and over 1,000 nuclear genes encode proteins related to mitochondrial function (3).

The most common mitochondrial disease that occurs during childhood is Leigh syndrome, with a prevalence of approximately 2.5 cases per 100,000 individuals (4). Most cases of Leigh

syndrome occur in childhood and rarely in adolescence or early adulthood. Leigh syndrome is a neurodegenerative disorder, with characteristic symmetric, necrotizing lesions in the basal ganglia, brainstem, cerebellum, thalamus, and spinal cord on cranial magnetic resonance imaging (MRI). The phenotypes of Leigh syndrome include neurological symptoms showing fluctuation and stepwise deterioration, such as neurodevelopmental delay and regression, dysarthria, dysphagia, hypotonia, dystonia, tremor, spasticity, epilepsy, and respiratory problems. Other non-neurologic symptoms include cardiac abnormalities, hepatorenal anomalies, anemia, and gastrointestinal symptoms such as constipation and vomiting (5). More than 85 genes are related to Leigh syndrome including mtDNA and nDNA, and genes related to complex I (NADH: ubiquinone oxidoreductase) deficiency are the most common causes. Approximately 75–80% of cases of Leigh syndrome are caused by pathogenic nDNA variants and more than half of the nDNA genes are related to complex I. *NDUFAF6* (NADH: ubiquinone oxidoreductase complex assembly factor 6) is one of them, and *NDUFAF6* is one of the major genes that cause reduced complex I activity by mitochondrial respiratory chain complex defect. Biallelic missense variants of *NDUFAF6* are known to cause Leigh syndrome.

Here, we present a rare case of a child who developed Leigh syndrome due to pathogenic variants of *NDUFAF6* on chromosome 8, which encodes an assembly factor of complex I, a respiratory chain subunit. A targeted next-generation sequencing study (NGS) enabled rapid genetic confirmation and avoided invasive diagnostic procedures such as skeletal muscle biopsy and skin fibroblast cell culture.

CASE PRESENTATION

A 56-month-old boy was referred to a rehabilitation clinic due to left hand clumsiness and frequent falling. The symptoms gradually began around the age of 3 years and slowly progressed. The patient had been born after an uncomplicated 40-week gestation with a birth weight of 3.07 kg. There were no perinatal problems and no specific family history of interest. There was no psychomotor developmental abnormalities prior to the onset of symptoms. The patient was brought to the primary clinic at 55 months due to language developmental delay, with simplified sentences and inaccurate pronunciation. In the evaluation, the patient's overall comprehension and language expression level was measured around 56–60 months, and his consonant accuracy was evaluated at approximately 87% in the pronunciation intelligibility assessment. The patient also presented with weakened tongue movement, simplification of middle consonants, and simplification of liquid consonants. In the psychoeducational profile–revised (PEP-R) evaluation, the overall developmental level was 64–65 months, and the other domains were above the normal ranges, except for fine motor function, which was below the average of 52–54 months. During the examination, the patient presented poor bimanual manipulation, with left hand clumsiness and slight weakness of the right ankle dorsiflexion; the patient was referred to a tertiary medical center.

Clinical Assessment

During the physical examination, the patient presented with dystonic and ataxic movements on the left side and clumsy movements of both hands. Weakness in ankle dorsiflexion involving both sides and spastic hypertonia in the left upper and lower extremities were observed. The strength of both ankle dorsiflexors was 3/5, and the strength of the other muscles was 5/5. The patient had difficulty jumping on both feet and stair-climbing and descending. Poor balance with one-leg standing with eyes open was also observed. The patient could independently walk but had tip-toeing and limping gait patterns. In the functional assessment, the balance evaluation using the Berg balance scale (BBS) revealed a poor standing balance of 36/56. The total score on the gross motor function measure-88 (GMFM-88) was 81.82%. The Beery–Buktenica developmental test of visual motor integration (6th edition) revealed a normal range of visual motor function of 99 (47%) with impaired motor coordination ability of 73 (4%).

Neuroimaging and Laboratory Tests

Due to a suspected brain pathology, an MRI of the head was performed, revealing abnormal signals in the bilateral putamen, with slight volume reduction and partial necrosis. The MRI revealed high signal intensity on T2- and diffusion-weighted images, an apparent diffusion coefficient (ADC), and fluid-attenuated inversion recovery (FLAIR) images with low signal intensity on T1-weighted images in the bilateral putamen (**Figure 1**). MR angiography showed normal cerebral vessels. To differentiate diseases that could show lesions of symmetric basal ganglia, we also performed MR spectroscopy, detecting normal N-acetylaspartate, choline, and creatine levels, and increased lipid and lactate levels (**Figure 2**). The high lactate peak would indicate acute mitochondrial dysfunction and with clinical features, we determined that there was a possibility of mitochondrial encephalopathy, especially Leigh syndrome. The laboratory test revealed a lactic acid level of 2.45 mmol/L (range, 0.50–2.20 mmol/L) and a creatine phosphokinase level of 287 U/L (range, 0–250 U/L). In the urine organic acid test, a slight increase was observed in tiglylglycine levels to 0.4 mmol/mol creatine (range, 0–0.2 mmol/mol creatine). The other laboratory test results, including serum aspartate aminotransferase, alanine aminotransferase, amino acid analysis, and acylcarnitine were all within normal ranges.

Cytogenetic and Molecular Analyses

We performed a mitochondrial DNA sequencing test and targeted NGS analysis of a multi-gene panel related to the mitochondrial disease. Informed consent from the patient's guardian was collected. Libraries were prepared with the Illumina^{TM} Truseq DNA kit, and sequencing was performed using the Illumina^{TM} Nextseq platform. The

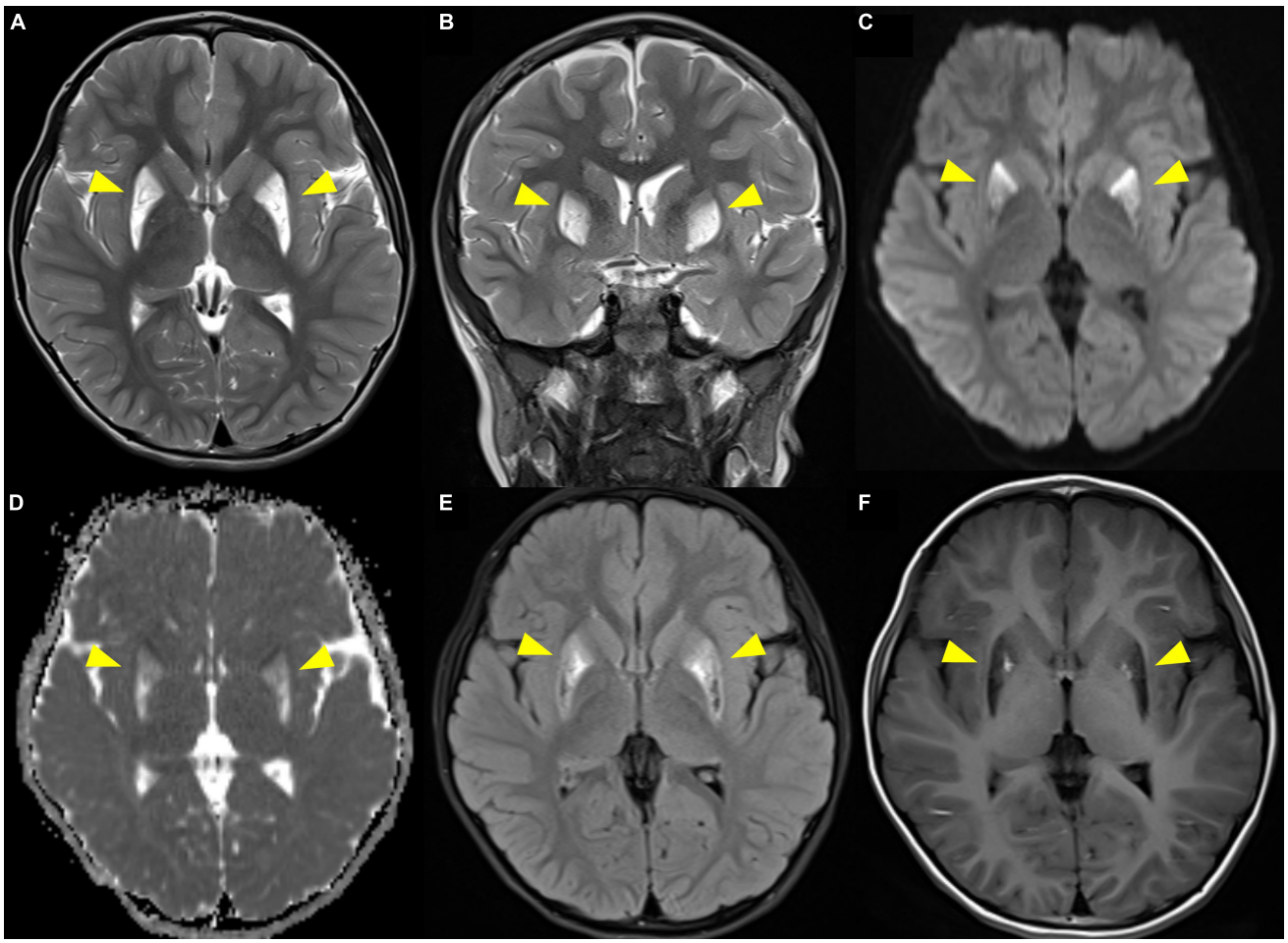

FIGURE 1 | Brain MRI showing high signal intensity on T2-weighted imaging (**A**. axial, **B**. coronal) and diffusion-weighted imaging **(C)**, apparent diffusion coefficient **(D)**, and fluid-attenuated inversion recovery **(E)** images with low signal intensity on T1-weighted imaging **(F)** in the bilateral putamen. Arrowheads indicate the lesions.

whole mtDNA test revealed a normal mtDNA sequence. The NGS test revealed two heterozygous variants of *NDUFAF6* in the different exons, identifying a missense variant (NM_152416.4:c.371T > C; p.Ile124Thr) and a frameshift variant (NM_152416.4:c.233_242del; p.Leu78GInfs*10), which were validated by Sanger sequencing. No other significant variants were found. The missense variant c.371T > C has been previously reported to cause Leigh syndrome, while the c.233_242del variant has not been reported (6–8). The missense variant c.371T > C was classified as a likely pathogenic variant and the frameshift variant (c.233_242del) was classified as a pathogenic variant by American College of Medical Genetics and Genomics (ACMG) Classification Standards and Guidelines for Genetic Variations. *In silico* prediction for the missense variant, SIFT predicted as deleterious (score: 0.05), PolyPhen-2 as benign (score 0.255), and MutationTaster as disease causing (probability: 0.99). For the frameshift variant, MutationTaster predicted as disease causing (probability: 1). To identify these compound heterozygous variants, we performed targeted gene sequencing of the parents, which revealed that the c.371T > C variant was inherited from the mother while the c.233_242del variant was inherited from the father (**Figure 3**). Finally, the proband was diagnosed with Leigh syndrome caused by biallelic pathogenic variants of *NDUFAF6*, inherited biparentally.

Clinical Progressions

After the diagnosis, the patient continued physiotherapy and occupational therapy while undergoing nutrient cocktail therapy. He was prescribed 10 mg of biotin, 500 mg of thiamine, 100 mg of Coenzyme Q10, and 100 mg of L-carnitine per day. However, worsening and improvement of spastic dystonia and balance impairment were repeated and his gait instability gradually worsened.

Five months after the first visit and at the age of 61 months, the patient's BBS dropped from 36/56 to 11/56, and his GMFM-88 score worsened from 81.82 to 58.33%. He required support from two hands for walking and for transitioning from sitting to standing. He was unable to maintain an upright

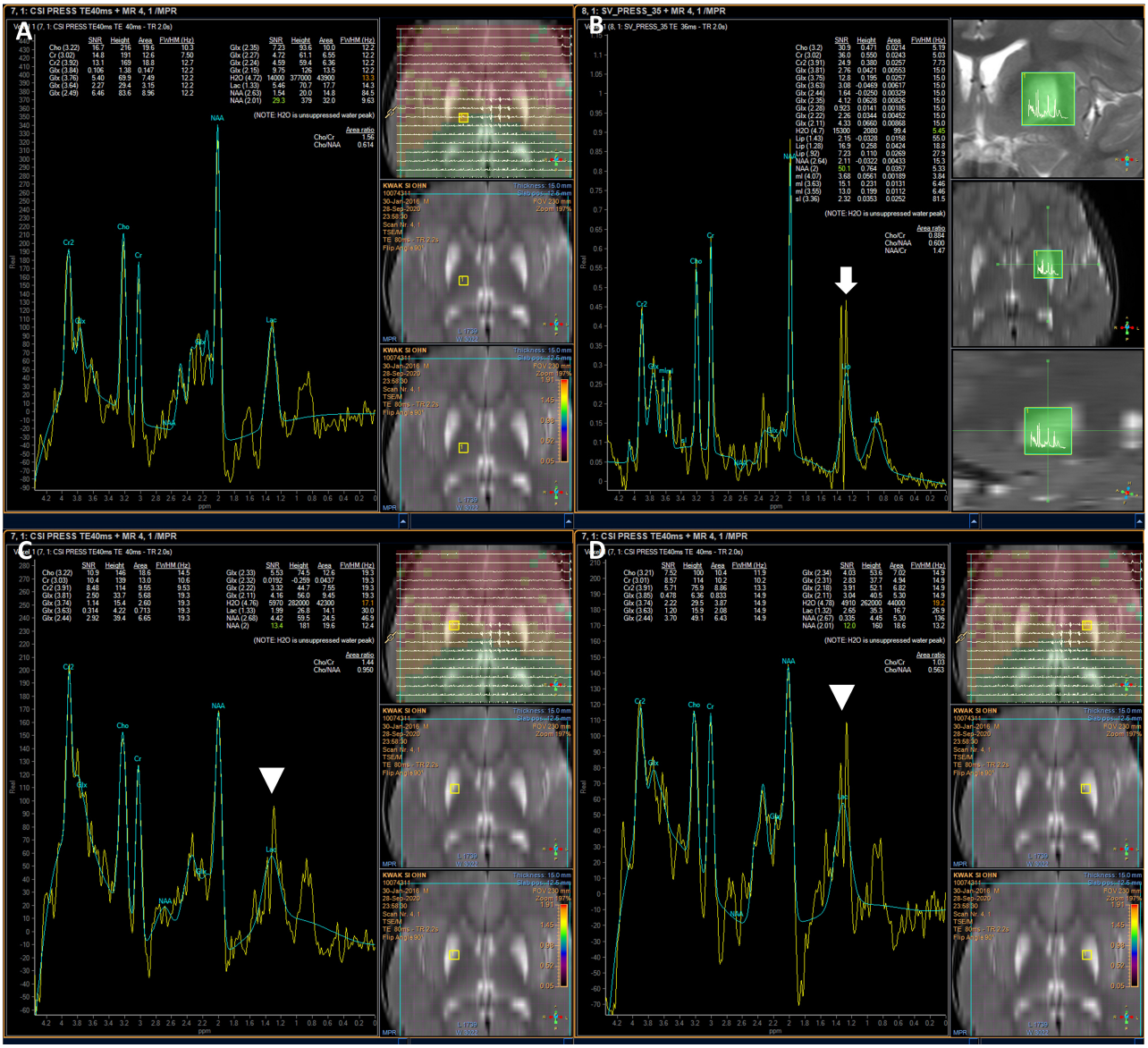

FIGURE 2 | Brain MR spectroscopy showing increased lipid and lactate in the lesions. Normal patterns outside lesions **(A)**, elevated lipids (white arrow) **(B)**, and elevated lactate in both putamen (arrowhead) **(C,D)**.

sitting or standing position and showed poor sitting balance. A symmetric tonic neck reflex appeared, and a hand-foot crawling pattern was observed.

DISCUSSION

We have reported a proband with biallelic pathogenic variants, c.371T > C and c.233_242del in *NDUFAF6*, who showed the typical phenotype of Leigh syndrome. The proband presented Leigh syndrome-appropriate clinical features, brain MRI and MR spectroscopy findings, and genetic confirmation. However, the serum biomarkers showing oxidative phosphorylation impairment such as lactate, pyruvate, creatine kinase, amino acid, acylcarnitine, and organic acid revealed no disease-specific findings. The patient underwent rehabilitation therapy and nutrient cocktail therapy, but his physical impairment rapidly worsened.

NDUFAF6 is an assembly factor of NADH-ubiquinone oxidoreductase (complex 1) and plays an important role in complex 1 maturation and activity. NDUFAF6 is a 38 kDa protein, consists of 333 amino acids, and is involved in the assembly of complex I in early stages, playing a role in regulating and stabilizing the complex I subunit MT-ND1. Defects in NDUFAF6 isoform 1 can disrupt complex I assembly by causing

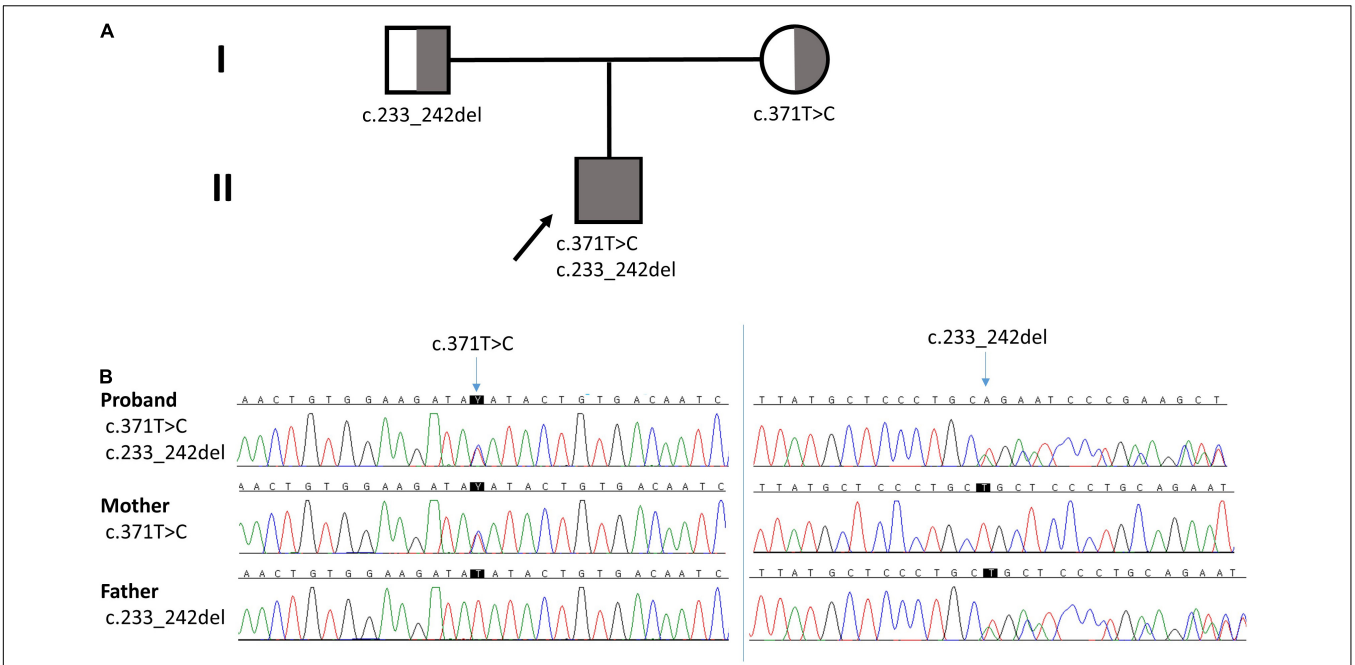

FIGURE 3 | (A) Pedigree of the family. Arrow indicates the proband. **(B)** Chromatographs of *NDUFAF6*. The proband had a missense variant (c.371T > C) from the mother and a frameshift variant (c.233_242del) from the father.

TABLE 1 | Variants and clinical features of patients with *NDUFAF6*-related Leigh syndrome.

	This case	Johnstone et al. (7)	Baide-Mairena et al. (8)	Bianciardi et al. (12) Catania et al. (18)	Fang et al. (19)	Pagliarini et al. (20)	Martikainen et al. (21)
Number of proband	1	1	3	4	1	2	2
Variants	c.371T > C c. 233_242del	c.371 T > C c.420 + 2_420 + 3insTA	c.371 T > C c.554_558del	c.532G > C c.420 + 784C > T	c.337C > T c.265G > A	c.296A > G*	c.226T > C*
Age of onset	3 years	4 years	17 months, 30 months, 30 months	21 months, 12 months, 3.5 years, 5 years	4 years	7 months, 10 months	1 year
Clinical features	Dysarthria, poor bimanual manipulation, dystonic and ataxic movement, poor balance, neurologic regression	Tiptoeing, increasingly severe focal hand dystonia which eventually became generalized dystonia, dysarthria, ataxic gait	Gait loss, speech difficulties, neurological deterioration, generalized dystonia, dysphagia, dysarthria	Ataxic gait, fine tremor, drooling, dysarthria, dysmetria, tremor, hypertonia, dystonic movement, fine motor difficulty, cognition preservation	Movement disorder, abnormal gait, exercise intolerance, weakness, difficulty swallowing, increased muscle tension	Focal right-hand seizures, decreased movement and strength, ataxia, and evolving rigidity	Generalized dystonia, stepwise deterioration
Lesions with abnormal signals on MRI	Bilateral putamen	Bilateral putamen	Bilateral caudate and putamen	Bilateral caudate and putamen	Bilateral basal ganglia, and gradually expand to centrum semiovale	Consistent with LS	Bilateral caudate, putamen, parietal cerebral white matter, dorsal pons
Serum lactate (mmol/L) (range, 0.50–2.20)	2.45 mmol/L	Normal	Normal	Slightly increased, normal	Normal	High	N/A

**Homozygous; Variants for which clinical features were not described [Khoda et al. (6)—four patients: c.226T > C, c.805C > G; c.206A > T, c.371T > C; c.371T > C, 805C > G; 820A > G*, Lee et al. (22)—two patients: c.265G > A, c.233_231del; c.874-2A > C, c.820A > G].*

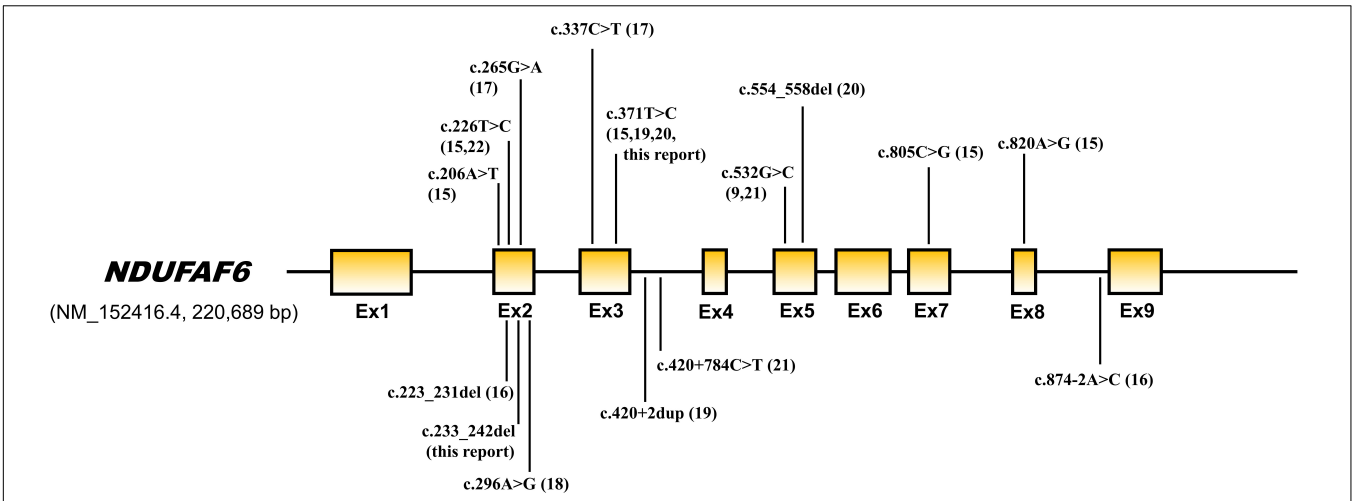

FIGURE 4 | Genetic structure of *NDUFAF6*. Pathogenic variants previously reported are indicated by arrows.

rapid proteolysis of the newly formed ND1 subunit, adversely affecting mitochondrial function (9, 10). Biallelic pathogenic variants cause Leigh syndrome, and 16 variants have been reported in 20 patients to date (**Table 1** and **Figure 4**). Among them, the most variants have been reported in exon 2, and 2 variants have also been reported in exons 3 and 5. All children with *NDUFAF6*-related Leigh syndrome show necrotic lesions in the symmetric basal ganglia, dystonia, and neurological regression. Characteristically, *NDUFAF6*-related Leigh syndrome tends to show normal or slight higher serum lactate, and our proband also showed lactate close to the normal range, revealing little diagnostic value for Leigh syndrome.

In a cohort study of 166 patients with Leigh syndrome, 8 had pathogenic variants of *NDUFAF6*. As a result of the analysis, mtDNA variants were associated with high mortality, and patients with *NDUFAF6* variants had better outcomes than those with other nDNA gene variants showing lower mortality and longer motor function preservation (11). However, not all patients with *NDUFAF6*-related Leigh syndrome show mild phenotypes, and the genotype does not appear to predict the prognosis sufficiently, given that there are patients with early disease onset with severe symptoms who have the same variants (12). Our proband showed normal psychomotor development with uneventful medical history until the age of 3, and symptoms developed gradually. At 55 months, he showed mild motor impairment, but from then on, he showed rapid deterioration. Since there is no report on long term functional prognosis in the *NDUFAF6*-related Leigh syndrome, additional reports will be helpful for prognosis prediction.

Mitochondrial disease is difficult to diagnose due to the diverse clinical features. Previously, tissue biopsy was often performed for diagnosis by histochemical and biochemical analysis. With the recent development of NGS technology, there have been numerous cases that relied on genetic tests. In addition, cases previously diagnosed with probable or uncertain mitochondrial disease have more frequently been genetically confirmed. As a result, overall diagnostic success has risen from less than 20% to more than 60% (1). In particular, given that 75–80% of cases of childhood-onset mitochondrial disease occur due to the pathogenic variant of nDNA, the NGS test increases the diagnosis success (13). In a study conducted in 2015, patients who were ultimately diagnosed with mitochondrial disease had met an average of 8.19 physicians before being confirmed, and 70% of the patients had undergone invasive muscle biopsy. Rapid diagnosis without invasive tests has been made possible with the advances in genetic diagnostic technology, including whole exome sequencing and whole genome sequencing (14).

Treatment for Leigh syndrome has no clear evidence, but cocktails of nutritional dietary supplements, such as antioxidants, vitamins, coenzyme Q10, and nitric acid precursors have been widely used (15). Given that Leigh syndrome is genetically heterogeneous, early intervention with tailored therapy according to the genotype rather than treatment according to the phenomenon will be an important treatment direction in the future. In terms of rehabilitation, exercise prescription including aerobic exercise training is often performed for patients with mitochondrial disease with gait disturbance, imbalance, frequent falling, fatigue, and exercise intolerance. In general, excessive physical activity is not recommended, and physiotherapy is contraindicated for patients with cardiac involvement. Physiotherapy is also not recommended for those with acute illness, severe fatigue, and a generally deconditioned status because of the expected excessive energy demand in addition to the body's energy demands (16). However, there was a report that oxygen utilization, exercise tolerance, and quality of life were better for the group who continued exercise training than for the group who did not (17). Therefore, rehabilitation therapy should be determined individually. Our patient underwent rehabilitation therapy because his general condition was not poor and did not correspond to discontinuation; however, his physical function gradually deteriorated.

CONCLUSION

We report a rare genetic disorder: *NDUFAF6*-related Leigh syndrome resulting from biallelic pathogenic variants, c.371T > C and c.233_242del in *NDUFAF6*. The proband showed typical Leigh syndrome features, and his physical impairment gradually worsened despite several therapies. This case report is distinguished from those previously reported in that we describe in detail the clinical features, including the developmental evaluation and clinical progressions.

DATA AVAILABILITY STATEMENT

The original contributions presented in the study are included in the article/supplementary material, further inquiries can be directed to the corresponding author.

ETHICS STATEMENT

The studies involving human participants were reviewed and approved by the Institutional Review Board for Clinical Research at Incheon St. Mary's Hospital. Written informed consent to participate in this study was provided by the participants' legal guardian/next of kin.

AUTHOR CONTRIBUTIONS

JK: acquisition of data, analysis and interpretation of data, and writing. JL: analysis and interpretation of data. D-HJ: study concept and design, acquisition of data, analysis and interpretation of data, study supervision, and critical revision of manuscript for intellectual content. All authors contributed to the article and approved the submitted version.

REFERENCES

1. Gorman GS, Chinnery PF, DiMauro S, Hirano M, Koga Y, McFarland R, et al. Mitochondrial diseases. *Nat Rev Dis Primers.* (2016) 2:16080. doi: 10.1038/nrdp.2016.80
2. McFarland R, Taylor RW, Turnbull DM. A neurological perspective on mitochondrial disease. *Lancet Neurol.* (2010) 9:829–40.
3. Calvo SE, Mootha VK. The mitochondrial proteome and human disease. *Annu Rev Genomics Hum Genet.* (2010) 11:25–44.
4. Lake NJ, Compton AG, Rahman S, Thorburn DR. Leigh syndrome: one disorder, more than 75 monogenic causes. *Ann Neurol.* (2016) 79:190–203. doi: 10.1002/ana.24551
5. Gerards M, Sallevelt SC, Smeets HJ. Leigh syndrome: resolving the clinical and genetic heterogeneity paves the way for treatment options. *Mol Genet Metab.* (2016) 117:300–12. doi: 10.1016/j.ymgme.2015.12.004
6. Kohda M, Tokuzawa Y, Kishita Y, Nyuzuki H, Moriyama Y, Mizuno Y, et al. A comprehensive genomic analysis reveals the genetic landscape of mitochondrial respiratory chain complex deficiencies. *PLoS Genet.* (2016) 12:e1005679. doi: 10.1371/journal.pgen.1005679
7. Johnstone T, Wang J, Ross D, Balanda N, Huang Y, Godfrey R, et al. Biallelic variants in two complex I genes cause abnormal splicing defects in probands with mild leigh syndrome. *Mol Genet Metab.* (2020) 131:98–106. doi: 10.1016/j.ymgme.2020.09.008
8. Baide-Mairena H, Gaudó P, Marti-Sánchez L, Emperador S, Sánchez-Montanez A, Alonso-Luengo O, et al. Mutations in the mitochondrial complex I assembly factor NDUFAF6 cause isolated bilateral striatal necrosis and progressive dystonia in childhood. *Mol Genet Metab.* (2019) 126:250–8.
9. Andrews B, Carroll J, Ding S, Fearnley IM, Walker JE. Assembly factors for the membrane arm of human complex I. *Proc Natl Acad Sci USA.* (2013) 110:18934–9. doi: 10.1073/pnas.1319247110
10. Lemire BD. Evolution, structure and membrane association of NDUFAF6, an assembly factor for NADH: ubiquinone oxidoreductase (Complex I). *Mitochondrion.* (2017) 35:13–22. doi: 10.1016/j.mito.2017.04.005
11. Ogawa E, Fushimi T, Ogawa-Tominaga M, Shimura M, Tajika M, Ichimoto K, et al. Mortality of Japanese patients with Leigh syndrome: Effects of age at onset and genetic diagnosis. *J Inherit Metab Dis.* (2020) 43:819–26. doi: 10.1002/jimd.12218
12. Bianciardi L, Imperatore V, Fernandez-Vizarra E, Lopomo A, Falabella M, Furini S, et al. Exome sequencing coupled with mRNA analysis identifies NDUFAF6 as a leigh gene. *Mol Genet Metab.* (2016) 119:214–22. doi: 10.1016/j.ymgme.2016.09.001
13. Thorburn DR. Mitochondrial disorders: prevalence, myths and advances. *J Inherit Metab Dis.* (2004) 27:349–62.
14. Grier J, Hirano M, Karaa A, Shepard E, Thompson JLP. Diagnostic odyssey of patients with mitochondrial disease: results of a survey. *Neurol Genet.* (2018) 4:e230. doi: 10.1212/NXG.0000000000000230
15. Pfeffer G, Majamaa K, Turnbull DM, Thorburn D, Chinnery PF. Treatment for mitochondrial disorders. *Cochrane Database Syst Rev.* (2012) 2012:CD004426. doi: 10.1002/14651858.CD004426.pub3
16. Newcastle University. *Physiotherapy Guidance for People with Mitochondrial Disease*. (2021). Available online at: https://www.newcastle-mitochondria.com/clinical-professional-home-page/clinical-publications/clinical-guidelines/ (Accessed August 19, 2021)
17. Taivassalo T, Gardner JL, Taylor RW, Schaefer AM, Newman J, Barron MJ, et al. Endurance training and detraining in mitochondrial myopathies due to single large-scale mtDNA deletions. *Brain.* (2006) 129:3391–401. doi: 10.1093/brain/awl282
18. Catania A, Ardissone A, Verrigni D, Legati A, Reyes A, Lamantea E, et al. Compound heterozygous missense and deep intronic variants in NDUFAF6 unraveled by exome sequencing and mRNA analysis. *J Hum Genet.* (2018) 63:563–8. doi: 10.1038/s10038-018-0423-1
19. Fang F, Liu Z, Fang H, Wu J, Shen D, Sun S, et al. The clinical and genetic characteristics in children with mitochondrial disease in China. *Sci China Life Sci.* (2017) 60:746–57. doi: 10.1007/s11427-017-9080-y
20. Pagliarini DJ, Calvo SE, Chang B, Sheth SA, Vafai SB, Ong SE, et al. A mitochondrial protein compendium elucidates complex I disease biology. *Cell.* (2008) 134:112–23. doi: 10.1016/j.cell.2008.06.016
21. Martikainen MH, Ng YS, Gorman GS, Alston CL, Blakely EL, Schaefer AM, et al. Clinical, genetic, and radiological features of extrapyramidal movement disorders in mitochondrial disease. *JAMA Neurol.* (2016) 73:668–74. doi: 10.1001/jamaneurol.2016.0355
22. Lee JS, Yoo T, Lee M, Lee Y, Jeon E, Kim SY, et al. Genetic heterogeneity in leigh syndrome: highlighting treatable and novel genetic causes. *Clin Genet.* (2020) 97:586–94. doi: 10.1111/cge.13713

Conflict of Interest: The authors declare that the research was conducted in the absence of any commercial or financial relationships that could be construed as a potential conflict of interest.

frontiers | Frontiers in Genetics

TYPE Original Research
PUBLISHED 29 August 2022
DOI 10.3389/fgene.2022.765637

OPEN ACCESS

EDITED BY
Hui Xiong,
First Hospital, Peking University, China

REVIEWED BY
Hao Hu,
Guangzhou Medical University, China
Caroline Evans,
The University of Sheffield,
United Kingdom

*CORRESPONDENCE
Hu Hao,
haohu@mail.sysu.edu.cn

†These authors have contributed equally to this work and share first authorship

SPECIALTY SECTION
This article was submitted to Genetics of Common and Rare Diseases, a section of the journal Frontiers in Genetics

RECEIVED 27 August 2021
ACCEPTED 01 July 2022
PUBLISHED 29 August 2022

CITATION
Li S, Shi C, Cai Y, Gu X, Xiong H, Liu X, Zhang Y, Xiao X, Ma F and Hao H (2022), Serum differential proteomic profiling of patients with isolated methylmalonic acidemia by iTRAQ.
Front. Genet. 13:765637.
doi: 10.3389/fgene.2022.765637

Serum differential proteomic profiling of patients with isolated methylmalonic acidemia by iTRAQ

Sitao Li[1†], Congcong Shi[2†], Yao Cai[1†], Xia Gu[1], Hui Xiong[1], Xiaoyu Liu[3], Yinchun Zhang[1], Xin Xiao[1], Fei Ma[2] and Hu Hao[1*]

[1]Department of Pediatrics, The Sixth Affiliated Hospital, Sun Yat sen University, Guangzhou, China, [2]Inborn Errors of Metabolism Laboratory, The Sixth Affiliated Hospital, Sun Yat sen University, Guangzhou, China, [3]Department of Child Care, The Maternity and Child Health Care Hospital of Tianhe District, Guangzhou, China

Isolated methylmalonic acidemia (MMA) is an inherited organic acid metabolic disorder in an autosomal recessive manner, caused by mutations in the methylmalonyl coenzyme A mutase gene, and the isolated MMA patients often suffer from multi-organ damage. The present study aimed to profile the differential proteome of serum between isolated MAA patients and healthy control. The *in vivo* proteome of isolated MAA patients and healthy subjects was detected by an isobaric tag for relative and absolute quantitation (iTRAQ). A total of 94 differentially expressed proteins (DEPs) were identified between MMA patients and healthy control, including 58 upregulated and 36 downregulated DEPs in MMA patients. Among them, the most significantly upregulated proteins were CRP and immunoglobulins, and the top five most significantly downregulated proteins were all different types of immunoglobulins in MMA patients. GO analysis showed that these DEPs were mainly enriched in immune-related function and membrane protein-related function. KEGG revealed that these DEPs were mainly enriched in lysosome and cholesterol metabolism pathways. Also, these DEPs were predicted to contribute to lipid metabolic diseases. We addressed the proteomes of isolated MMA patients and identified DEPs. Our study expands our current understanding of MMA, and the DEPs could be valuable for designing alternative therapies to alleviate MMA symptoms.

KEYWORDS

methylmalonic acidemia, iTRAQ, differential proteome, cholesterol metabolism, immunoglobulins, methylmalonyl coenzyme A mutase

Introduction

Methylmalonic acidemia (MMA) is an inherited organic acid metabolic disorder in an autosomal recessive manner. According to the biochemical manifestation, MMA can be classified into two common types: isolated MMA and MMA combined with homocysteinemia (Manoli and Venditti, 2005). Isolated MMA is mostly caused by mutations in the methylmalonyl coenzyme A mutase (MCM) gene (*MUT*) (Han et al., 2017), and a few cases have been shown to be the result of other gene mutations, such as *MMAA*, *MCEE*, and others (He et al., 2020). MMA usually resulted in various clinical symptoms, including severe metabolic acidosis, thrombocytopenia, hyperammonemia, ketosis and ketonuria, developmental delay, neutropenia, and hyperglycinemia (Manoli and Venditti, 2005). Clinical diagnosis of MMA relies upon specialized metabolic testing. Definitive diagnosis of MMA relies on the analysis of organic acids in plasma and/or urine by gas-liquid chromatography and mass spectrometry; the concentration of methylmalonic acid is greatly increased in the plasma, urine, and cerebrospinal fluid of affected individuals (Manoli et al., 1993). Based on complex and comprehensive clinical diagnosis, the abnormal production of metabolites in MMA patients has been relatively clear, but proteomic changes in MMA patients are rarely reported.

Isolated MMA patients with mutations in the *MUT* gene are usually severely ill with poor prognosis, high early mortality, and high lifelong morbidity (Jiang et al., 2020; Liang et al., 2021). The age of death in children with isolated MMA was 2 years, ranging from 5 days to 15 years, and 40% of individuals died and the overall mortality rate was 36%, with all deaths occurring during or after the acute metabolic crisis (Dionisi-Vici et al., 2006). The primary treatment for patients with isolated MMA is dietary restriction of propyl amino acid and carnitine supplementation. Despite treatment, the metabolite profile of the patients with isolated MMA remains abnormal, and the prognosis is still poor. Although several hypotheses have been proposed, the pathologic mechanism of abnormal protein expression in progressive isolated MMA systemic injury remains to be elucidated.

Recently, the characterization of MMA with homocystinuria and cobalamin deficiency type C (cblC) proteome in fibroblasts found that the downregulated proteins were mainly enriched in cellular detoxification (Hannibal et al., 2011). Also, the proteome in circulating lymphocytes in cblC patients has been demonstrated (Caterino et al., 2015). However, the proteomic characteristics of isolated MMA patients are still unclear. The present study investigated the proteome of serum isolated from three isolated MMA patients with *MUT* treated with a multi-drug combination. These three patients still have abnormal levels of metabolites although receiving treatment. This study of the proteome in isolated MMA patients was performed using the isobaric tag for relative and absolute quantitation (iTRAQ) analysis. Proteome identification helped bridge the gap between the role of *MUT* gene products and the clinical manifestations of MMA defects in humans.

Materials and methods

Ethics statement

This project was approved by the Ethical Committee of The Sixth Affiliated Hospital of Sun Yat-sen University and adhered to the World Medical Association's Declaration of Helsinki (WMADH 2008). In this study, MMA analysis was performed with written informed consent from guardians of each pediatric patient, following the approval of The Sixth Affiliated Hospital of Sun Yat-sen University.

Patient selection

The serum for three MMA patients and three healthy subjects from The Sixth Affiliated Hospital of Sun Yat-sen University was collected. Genotypes of MMA donors are listed in Table 1; the virulence gene of three MMA patients is *mut* gene. Clinical diagnosis of MMA patients relies upon specialized metabolic testing, which is performed by the Genetic Metabolic Disease Detection Laboratory of the Sixth Affiliated Hospital of Sun Yat-sen University. Table 2 listed the detailed clinical features of MMA patients determined by gas–liquid chromatography and mass spectrometry and also listed the detail of laboratory biochemical parameters. Serum from normal control and patients with confirmed MMA were subjected to iTRAQ assay for investigating the differentially expressed proteins (DEPs). Moreover, to verify the clinical characteristics of candidate DEPs, we subsequently collected the clinical biochemical data from 14 MMA patients and 15 non-MMA and uninfected patients. These 29 samples were in addition to those analyzed in the iTRAQ experiment. The information of these 29 samples is shown in Supplementary Table S1. All frozen tissue samples in liquid nitrogen were stored at −80°C.

Protein extraction and isobaric tag for relative and absolute quantitation labeling

Frozen serum samples were extracted by using RIPA lysis buffer (Elabscience, China) and subsequently homogenized by sonication (Scientz) on ice. The homogenate was cleared using centrifugation at 12,000 rpm for 15 min at 4°C. The major proteins of albumin and IgG were removed using ProteoExtract™ Albumin Removal Kit (Cat. No.:122640, MERCK). After that, the protein concentrations of supernatants were determined by Pierce BCA Protein Assay

TABLE 1 List of MMA donors with their genotypes and clinical features used in this study.

Sample ID	Age	Virulence gene	Genetic mutation	Medication before blood collection
001	16 months	Sequence alterations in *MUT*	c.636G>A homozygous	Tacrolimus, sesepin, lapindine, and zorcarnitine
002	10 months	Sequence alterations in *MUT*	c.323G>A, c.914 T>C compound heterozygote	Arginine, vitamin B_{12}, levocarnitine, and glutathione
003	1.5 months	Sequence alterations in *MUT*	c.755dupA, c.1159 A>C	Arginine, vitamin B_{12}, and levocarnitine
004	3 years	Healthy control	-	-
005	6 years	Healthy control	-	-
006	4 years	Healthy control	-	-

TABLE 2 Clinical information of MMA patients prior to sampling.

Biochemical	Sample 001	Sample 002	Sample 003
Body weight (kg)	8.5 kg	8 kg	3.44 kg
Height (cm)	80 cm	72 cm	54 cm
Malnutrition	Moderately nourished	Moderately nourished	Malnutrition: moderate
pH	7.353	7.47	7.38
PCO_2 (mmHg)	25.9	16.9	24
PO_2 (mmHg)	112.7	121.2	69
HCO_3 (mmol/L)	12.8	8.38	14.2
Lac (mmol/L)	3.1	2.9	6.6
Gap (mmol/L)	17.4	21.9	19.4
Ammonia (μmol/L)	176–84.5	149–66.9	170–67.6
CRP (mg/L)	0.91	<0.50	<0.50
White blood cell	5.97 × 10E9/L	6.58*10E9/L	7.75 × 10E9/L
Red blood cell	3.13 × 10E12/L	4.39*10E12/L	3.07 × 10E12/L
NEUTR	0.259	0.211	0.196
NLR	0.58	0.61	0.690
HGB (g/L)	89	99	87
PLT	228 × 10E9/L	253*10E9/L	758 × 10E9/L
Urine MMA (μmol/L)	964.8	1077.4	1278
C3 (μmol/L)	24.65	55.22	16.78
C0 (μmol/L)	32.56	76.13	22
C2 (μmol/L)	27.23	48.26	14.66
C3/C0 (0.01–0.25)	0.76	0.73	0.76
C3/C2 (0.01–0.25)	0.91	1.14	1.14
C3/C16 (0.15–2.0)	25.41	26.05	31.1
Glycine (μmol/L)	281.20	221.55	354.6
Valine (μmol/L)	20.97	88.53	116.65

Kit. Subsequently, 20 μg of each sample was taken and tested by SDS-PAGE. The qualified protein sample entered the iTRAQ labeling stage. Total protein (150 μg) from each sample solution was mixed with 200 μl of 8 mol/L urea in Nanosep Centrifugal Devices (PALL, United Kingdom) and centrifuged at 14,000 g at 20°C for 20 min. All following centrifugation steps were performed applying the same conditions allowing maximal concentration. Samples were incubated in 20 μl of 50 mmol/L iodoacetamide for 30 min in the dark to block reduced cysteine residues followed by centrifugation, and the liquid at the bottom was discarded. The Tris–HCl (pH 8.0) was added to every tube, centrifuged at 12,000 rpm for 10 min, and the solution was discarded at the bottom. Then, 200 μl of 100 mmol/L triethylammonium bicarbonate (TEAB) buffer was added to tubes and centrifuged twice. The solution was subjected to proteolytic digestion (1:50) overnight at 37°C. The digests of

peptides were collected by centrifugation following iTRAQ labeling.

Each iTRAQ-label reagent (AB Sciex, United States) was dissolved in 70 μl of isopropanol. The digested-peptide samples were dissolved in 30 μl TEAB buffer (200 mM). Next, the iTRAQ-label reagent was added to the respective peptide mixture for 2 h. The labeling reaction was quenched by the addition of 100 μl of MilliQ water, and six labeled samples were then pooled into one sample according to the manufacturer's instructions. After pooling, the samples were evaporated by vacuum concentration to remove excess water, TEAB, and isopropanol.

One-dimensional high-pH reversed-phase chromatography separation

The freeze-dried samples were dissolved in 100 μl of mobile phase A (10 nM ammonium formate, 5% acetonitrile, pH 10.0). Peptide separation was performed on a Thermo UltiMate 3000 UHPLC, and the chromatographic column was purchased from Agilent (ZORBAX Extended-C18, 2.1). The detection wavelength was UV 215 nm, and the flow rate was 0.3 ml/min. Mobile phase B (10 nM ammonium formate, 90% acetonitrile, and pH 10.0) separation gradient was linear from 5 to 38% in 80 min. One tube was collected every 1 min within the gradient range, and a total of 16 tubes of elution solution were collected, centrifuged, and dried for LC-MS analysis.

Liquid chromatography tandem mass spectrometry analysis and data reorganization

The LC-MS/MS analysis was conducted by Wininnovate Bio (China). Briefly, the lyophilized peptide fractions were re-suspended in 0.1% formic acid and then loaded into a nanoViper C18 (3 μm, 100Å) trap column, and online chromatography separation was performed on the Easy nLC 1200 system (ThermoFisher, United States). The trapping and desalting procedure was carried out with a volume of 20 μl 100% solvent A (0.1% formic acid). Then, an elution gradient of 5–38% solvent B (80% acetonitrile, 0.1% formic acid) at a flow rate of 300 nl/min (0–50 min, 5–38% B; 60–60 min, 38–100% B) in 60 min was used on an analytical column (50 μm × 15 cm C18-3 μm 100 Å). The data-dependent acquisition (DDA) mass spectrum techniques were used to acquire tandem mass spectrometry (MS) data on a ThermoFisher Q Exactive mass spectrometer (ThermoFisher, United States) fitted with a Nano Flex ion source. Data were acquired using an ion spray voltage of 1.9 kV, and an interface heater temperature of 275°C. The MS was operated with FULL-MS scans. For DDA, survey scans were acquired in 250 ms and up to 20 product ion scans (50 ms) were collected. Normalized collision energy (NCE) was set to 30 eV. Only spectra with a charge state of 2–4 were selected for fragmentation by higher-energy collision energy. Dynamic exclusion was set for 25 s. The proteomic raw data have been deposited on PRIDE Archive (https://www.ebi.ac.uk/pride/archive) with the project accession: PXD034075.

Data reorganization

The MS/MS data were analyzed for protein identification and quantification using the Proteome discoverer (v2.1.0.81). The local false discovery rate was 1.0% after searching against the Human protein database with a maximum of two missed cleavages and one missed termini cleavage. The following settings were selected: oxidation (M), acetylation (Protein N-term), deamidation (NQ), Pyro-glu from E, Pyro-glu from Q for variable modifications as well as carbamidomethylation (C), iTRAQ8plex (N-term), and iTRAQ8plex (K) for fixed modifications. Precursor and fragment mass tolerance were set to 10 ppm and 0.05 Da, respectively. A full list of proteins identified and relatively quantified by iTRAQ is shown in Supplementary Table S4. A full list of peptide groups identified and relatively quantified by iTRAQ is shown in Supplementary Table S5.

Statistical analysis of isobaric tags for relative and absolute quantitation data

DEPs were screened by t-test of the "*limma*" R package, and proteins with p-value < 0.05 and fold change (FC) ≥ 1.2 were considered DEPs.

Functional annotation

For functional annotation, the proteomic data were normalized, and then the protein expression of each sample was analyzed for differences to screen the DEPs using a t-test provided by the "*limma*" R package. The screening criterion of DEPs was that fold change (FC) ≥ 1.2 and the p-value < 0.05, between the two groups. Next, cluster analysis, principal component analysis (PCA), and partial least squares discrimination analysis (PLS-DA) were performed on DEPs, and they were referred to the Gene Ontology (GO) and Kyoto Encyclopedia of Genes and Genomes (KEGG) database, among which the "*ggplot2*" R package was used for volcano plots, heatmap, and PCA. The "*ropls*" R package was used for PLS-DA. For gene set enrichment analysis (GSEA), the whole genome was ranked from the largest to smallest based on the logFC of DEPs and matched to the KEGG pathway database, to draw a GSEA plot. A protein–protein interaction (PPI) network was constructed by Cytoscape version 3.6.1 using DEPs.

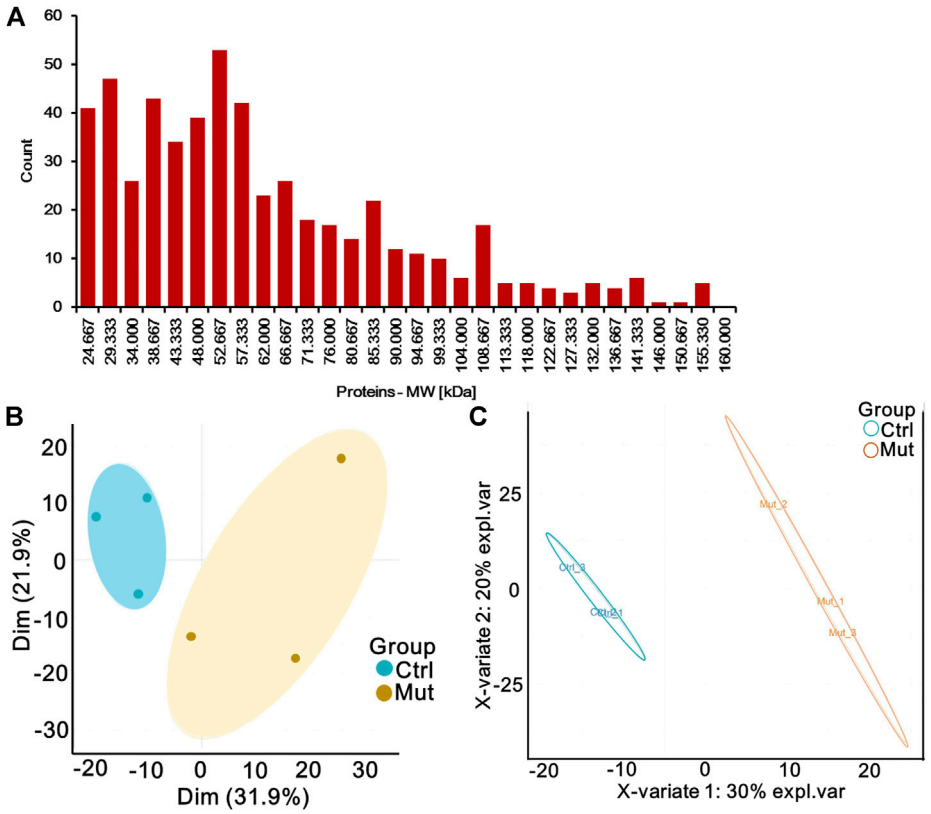

FIGURE 1
Quantitative proteomic profiling of serum of patients with MMA by iTRAQ labeling. **(A)** Histogram of the distribution of the average molecular weight of protein. **(B)** Principal component analysis (PCA) diagram of six samples. Oval indicates the 95% confidence intervals. **(C)** Partial least-squares discriminant analysis (PLS-DA) diagram of six samples based on all proteins. Oval indicates the 95% confidence intervals.

Results

Quantitative proteomic profiling of serum of patients with isolated methylmalonic acidemia by isobaric tags for relative and absolute quantitation labeling

Serum of patients with isolated MMA and healthy donators was subjected to proteomic analysis to elucidate proteomic changes. A total of 10306 peptides were identified, of which 9722 were uniquely mapped to known sequences of our iTRAQ proteomic results. Moreover, we identified 770 proteins whose average molecular weight was between 24 and 80 kDa (Figure 1A). PCA and PLS-DA analysis showed an obvious separation in the control group and mut group with the 95% confidence intervals, implicating that proteins were significantly separated (Figures 1B,C). Therefore, these data were used for further analysis.

Differential proteomics analysis

To search for MMA-induced specific proteins, proteome differential analysis was performed. As shown in the volcano plot, MMA induction upregulated the expression of 58 proteins and downregulated the expression of 36 proteins (Figure 2A). MMA and control groups were analyzed by the heatmap overview showing a good separation between the two groups, as well as confirmed by the PLSDA (Figures 2B,C). All the details of DEPs are listed in Supplementary Table S2, compared with the control group, the most significantly upregulated proteins were C-reactive protein (CRP), immunoglobulin, collagen alpha-2 (XI) chain (COL11A2), GTP-binding protein SAR1a (SAR1A), and dipeptidyl peptidase 1 (CTSC), and the top five most significantly downregulated proteins were all immunoglobulins, followed by apolipoprotein (APO), tubulin beta chain (TUBB), and cholesteryl ester transfer protein (CETP).

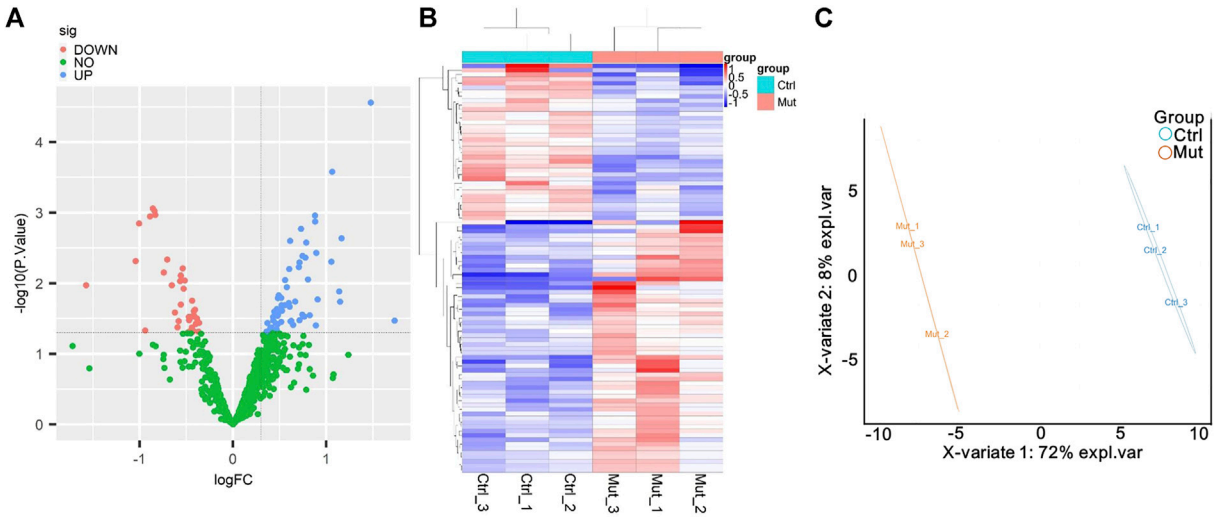

FIGURE 2
Analysis of the differentially expressed proteins (DEPs) between the MMA patients and healthy control. **(A)** Volcano plot of DEPs. The blue dot represents DEPs upregulated, and the red dot represents DEPs downregulated in the MMA patients compared with the healthy control. **(B)** Cluster heatmaps of significant DEPs. MUT represents the serum that was obtained from the MMA patients, and Ctrl represents the serum obtained from the healthy control. Each column represents a sample, and the row shaded in red represents upregulated, while shaded in blue represents downregulated when MMA patients vs. healthy control. **(C)** PL-SDA diagram of six samples based on DEPs. Oval indicates the 95% confidence intervals.

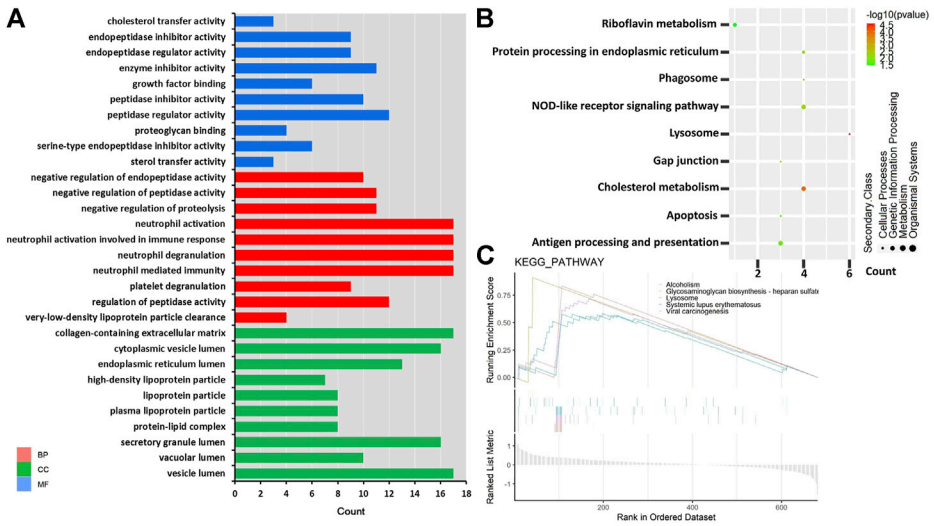

FIGURE 3
GO and KEGG pathway enrichment based on DEPs. **(A)** Top 30 GO terms in three domains. Red shows DEPs enriched in the biological process (BP); blue shows DEPs enriched in the molecular function (MF); and green shows DEPs enriched in the cellular component (CC). The left is the name of the GO term, while the right column represents the counts of DEPs. **(B)** KEGG enrichment items. The left is the name of the KEGG pathway, the right represents enrichment, and the size of the solid circle indicates the number of genes. **(C)** GSEA of identified DEPs. The abscissa is the list of whole genes sorted by logFC; the upper half of the ordinate is divided into enrichment scores, the lower half is divided into log2FC, and the pathway type is represented by the color label.

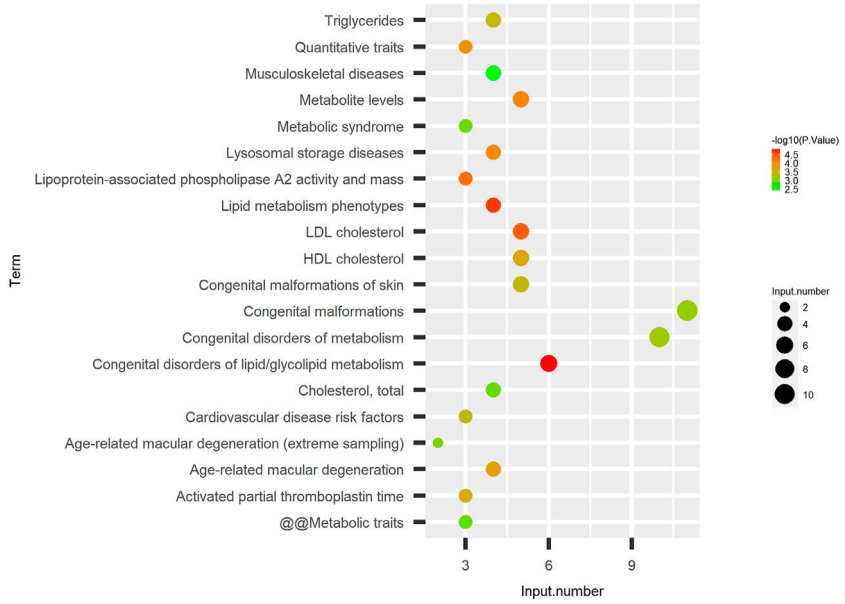

FIGURE 4
DEPs associated with lipid metabolic diseases. Disease enrichment analysis of identified DEPs. The left is the name of the disease, the right represents enrichment, and the size of the solid circle indicates the number of genes; the color of the solid circle indicates the−log10 (*p*-value) of enrichment.

Functional analysis of differentially expressed proteins

To further explore the potential functions of DEPs, GO, and KEGG predictions were performed. GO functional analysis showed that DEPs were mainly related to immune function (such as neutrophil-mediated immunity, neutrophil activation, neutrophil degranulation, neutrophil activation involved in immune response) and membrane protein function (such as vesicle lumen, cytoplasmic vesicle lumen, collagen-containing extracellular matrix) (Figure 3A). The KEGG pathway analysis showed that six DEPs were significantly enriched in the lysosome, including CTSC, tartrate-resistant acid phosphatase type 5 (ACP5), lysosomal protective protein (CTSA), cathepsin B (CTSB), prosaposin (PSAP), and tripeptidyl-peptidase 1 (TPP1), these six DEPs were downregulated in MMA patients (Figure 3B, Supplementary Figure S1). Also, four DEPs were significantly enriched in cholesterol metabolism, including APOE, APOC2, APOB, CETP, and these four DEPs were downregulated in MMA patients (Figure 3B, Supplementary Figure S2). We also found that the classical immune pathway of the NOD-like receptor pathway was also significantly enriched by these DEPs. Moreover, we used GSEA to further explore the potential function of DEPs, consistent with the KEGG results, the lysosome pathway was also observed in the GSEA-plot with the top five significant enrichment pathways, as well as an autoimmune disease pathway of systemic lupus erythematosus (Figure 3C). These results suggested that the disease progression of MMA may be involved not only in immune disorders but also related to abnormal lysosomal function and cholesterol metabolism.

Differentially expressed proteins associated with lipid metabolic diseases

Furthermore, we predicted the relationship between DEPs and human disease. As shown in Figure 4, the diseases most significantly associated with these DEPs were as follows: congenital disorders of lipid/glycolipid metabolism, lipid metabolism phenotypes, LDL cholesterol, lipoprotein-associated phospholipase A2 activity and mass, and HDL cholesterol. In addition, other diseases related to lipid metabolism were also predicted, such as triglycerides and cholesterol total. These results imply that DEPs are widely involved in lipid-abnormal metabolic diseases.

Protein–protein interaction network analysis

Subsequently, we interrogated the interaction relationship of these DEPs. The UNIPROT_ACCESSION of DEPs was input in Cytoscape, the data were retrieved from the HPIDB database to

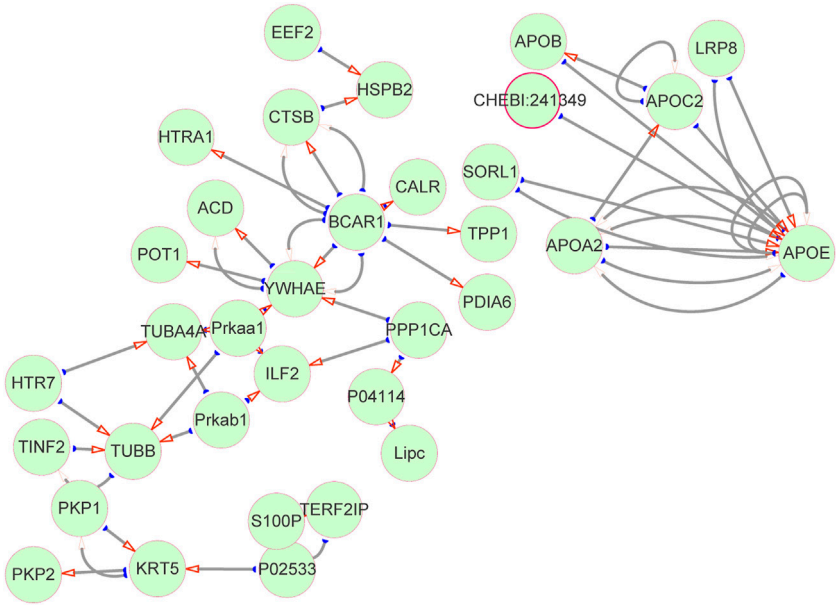

FIGURE 5
Protein–protein interaction network. DEPs interaction network diagram. The green circles represent proteins, and the red arrows point to target proteins (target proteins of DEPs), and the corresponding ones are source proteins (DEPs).

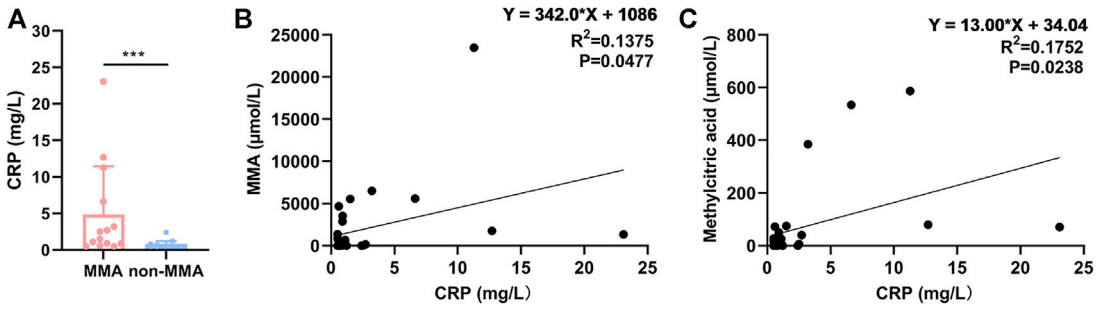

FIGURE 6
CRP was positively correlated with MMA. **(A)** Levels of CRP in serum of 14 MMA patients and 15 non-MMA (uninfected) patients. **(B)** Correlation analysis of serum CRP and MMA. **(C)** Correlation analysis of serum CRP and methylcitric acid.

plot the protein interaction network, and the results as shown in Figure 5. APOE is not only a target of itself but also a target protein of other APO family members. TPP1, which is significantly downregulated in MMA patients, is mainly a target protein of BCAR1, while the downregulated protein of TUBB interacts with multiple DEPs at the same time. Interestingly, both APO and TPP1 have been reported to be involved in lipid metabolism (Ghosh et al., 2017). It follows that there is a tight interaction relationship between the DEPs, which may co-act together on MMA progression, and this contribution may be related to lipid metabolism.

C-reactive protein was positively correlated with methylmalonic acidemia

To explore the reliability of the proteomic data, we expanded the sample size. We compared the levels of CRP in the serum of 14 MMA patients and 15 non-MMA (uninfected) patients, these values were in a range (MMA: 0.5–23.09; non-MMA: 0.5–2.41) consistent with the finding in serum levels of CRP (MMA: < 0.5, 0.91; no-MMA: < 0.5, 0.52) in serum of Table 2 and Supplementary Table S3. The results showed that CRP levels were significantly up-regulated in MMA patients compared with

those of non-MMA patients (Figure 6A). Further analysis showed that serum CRP levels were significantly positively correlated with MMA levels and methylcitric acid levels in MMA patients (Figures 6B,C). In fact, we have also analyzed the correlation between CRP content and patient age, gender, C3, C0, and other indicators, but no correlation was found. Together, these results support our proteomic data and suggest a positive correlation between CRP and MMA. The CRP validation is consistent with clinical metadata shown for the patients and thus gives confidence to the iTRAQ dataset as a whole.

Discussion

Isolated MMA is an inborn error of metabolism caused by the impaired isomerization of L-MCM to succinyl-CoA mutase. Normally, methylmalonic acid is the product of odd-chain fatty acids, some branched-chain amino acids, and cholesterol *via* the catabolic pathway of the propionyl coenzyme A to Krebs cycle (Richard et al., 2006). *MUT* gene mutations prevent the proper breakdown of these molecules, leading to the accumulation of a large number of compounds in the tissue that eventually form the pathologic characteristics of MMA. Considering Since the fact that the clinical diagnosis of MMA relies on metabolite detection, at present, the alteration of the metabolome caused by mutations in the *MUT* gene has been greatly recognized. In this study, we characterized the protein expression profiles of three isolated MMA patients and three healthy controls by iTRAQ technology in an attempt to connect the relationship between *MUT* mutations and abnormal protein expression at the global level in MMA patients.

In our study, a total of 94 DEPs were identified between MMA patients and healthy control, including 58 up-regulated and 36 down-regulated DEPs in MMA patients. Among them, compared with the control group, the most significantly up-regulated proteins were CRP and immunoglobulins, and the top five most significantly down-regulated proteins were all different types of immunoglobulins. Immunoglobulins appear repeatedly in the differential protein expression profiles of MMA patients and healthy control, which emphasizes that the immune environment may be strongly altered in MMA patients. This is consistent with the clinical outcome of MMA patients. Wong et al. (1992) reported that the population of B-lymphocytes was aggressively diminished and the ratio of CD4/CD8 was reversed in MMA infants which were regarded as having severe immunodeficiency. Altun et al. (2021) also proved that immunoglobulins and various immune cell types (including memory B cells, recent thymic emigrants, and Naïve helper T cells) exhibit marked defects. Importantly, intravenous administration of immunoglobulin has a dramatic rescue effect on the adverse clinical manifestations of MMA (Aikoh et al., 1997). Abnormal metabolism of MMA is located in mitochondria and leads to the failure of the citric acid cycle and affects the mitochondria function (Forny et al., 2021). It is reported that mitochondrial function determines individual B-cell fates, as well as their immunoglobulins (Jang et al., 2015). Therefore, immunoglobulins may be a potential idea to reverse-interrogate the consequences of *MUT* mutations in MMA patients.

In addition, CRP is massively elevated in the plasma of patients with MMA, and we speculate that there may be a point of association. It is generally agreed that CRP is highly conserved and is part of innate immune function, and occurs locally in inflamed or damaged tissues. As part of inflammation, elevated CRP is associated with cardiovascular disease, which is well-established by the Centers for Disease Control and the American Heart (Black et al., 2004). Wang et al. (2020) demonstrated that cardiovascular disease was strongly associated with mitochondria-derived MMA. Thus, the inflammatory response may be responsible for the accumulation of CRP protein in MMA serum. However, Del Giudice and Gangestad, (2018) proposed a new theory that CRP may exist in the absence of inflammation and have a net anti-inflammatory effect. In this case, elevated CRP indicates that the body is investing in protecting, preserving, and/or repairing somatic tissue. Depending on the state of the organism, maintenance may translate into responses including inflammation or tolerance. We conjecture that the currently recognized function of CRP may be only the tip of the iceberg and that the increase of CRP in MMA patients may be either a mechanism of clearance of damaged mitochondria or an unknown one. Collectively, CRP is one of the ways to understand the pathological mechanism of MMA.

Moreover, we found significant enrichment of DEPs in cholesterol metabolism pathways and lipid-related diseases. Similar results were found in zebrafish, where cobalamin C (cblC) deficiency caused by mutations in MMA resulted in deregulated expression of genes involved in cholesterol metabolism as demonstrated by Sloan et al. (2020). This can be explained by the physiological function of MCM enzymes. The MCM enzyme is encoded by the *MUT* gene and is also required for the degradation of a variety of amino acids, odd-chain fatty acids, and cholesterol (Keyfi et al., 2016). Thus, MMA patients with *MUT* mutations have abnormal cholesterol metabolic pathways. In addition, Manoli and Venditti (2005) reviewed that the major secondary complications of MMA include mental retardation, metabolic stroke, progressive impairment of renal function, pancreatitis, acrodermatitis-enteropathica-like lesions, and functional immune impairment. Interestingly, the occurrence of these diseases is associated with cholesterol or lipid abnormalities. For example, studies have shown that abnormal mutations in cholesterol biosynthetic genes are a possible cause of intellectual disability (Besnard et al., 2019). Mental retardation is also accompanied by a significant accumulation of lipids (Elmahgoub et al., 2009). The total cholesterol levels and incidence of severe acute pancreatitis

present a U-shaped relationship (Hong et al., 2020). Therefore, the disease predicted by DEPs may be similar to the complications of MMA, with the common denominator of abnormal cholesterol or lipid metabolism. Summarily, cholesterol metabolism may be one of the important bridges between communicating MUT gene mutations and MMA disease.

The CRP validation is consistent with clinical metadata shown for the patients and thus gives confidence to the iTRAQ dataset as a whole. However, the clinical validation of only one DEP also limits the generalizability of the results of this study to a certain extent. Therefore, in the further continuation, we will continue to explore the expression patterns and functions of four DEPs, including two upregulated DEPs (CTSC and SAR1A) and two downregulated DEPs (lactotransferrin and CETP) in MMA patients compared with healthy control. As mentioned in the results, DEPs associated with lipid metabolic diseases, which prompted us to examine the relationship between lipid-related DEPs and MMA progression. Therefore, CTSC (Rufinatscha et al., 2017), SAR1A (Sane et al., 2019), lactotransferrin (Kovacic et al., 2014), and CETP (Trinder et al., 2021) were selected for future validation due to their significant *p*-value and their correlation with lipid metabolism. We expect to provide more theoretical bases and evidence for clinical determination.

In conclusion, the present study characterized the protein expression profile of isolated MMA patients with *MUT* mutation and identified DEPs compared with healthy controls. These DEPs were mainly enriched in GO entries associated with an immune function such as neutrophil-mediated immunity, neutrophil activation, neutrophil degranulation, neutrophil activation involved in immune response, and membrane protein function. KEGG revealed that these DEPs were mainly enriched in lysosome and cholesterol metabolism pathways. Moreover, these DEPs contributed to lipid metabolic diseases. The DEPs and their pathways may be useful targets for new therapies to alleviate disease symptoms, importantly, candidate DEPs, such as CRP and immunoglobulins, and are associated with specific pathways were can be measured by routine tests (already available) and thus implemented in a clinical setting.

Data availability statement

The data presented in this study are deposited in the repository, accession number: PXD034075 (PRIDE Archive, https://www.ebi.ac.uk/pride/archive). The other data found in the article/Supplementary Material.

Ethics statement

The studies involving human participants were reviewed and approved by the Ethics Committee of the Sixth Affilia ted Hospital of Sun Yat sen University (Ethics Committee Batch no. 2019ZSLYEC-105). Written informed consent to participate in this study was provided by the p articipant's legal guardian/ next of kin.

Author contributions

Conceptualization and Funding acquisition, HH, and XL; Data curation, SL, XG, and CS; bioinformatics analyses, SL, CS, HX, and YZ; prepared the samples, YC, XL, XG, and HX; extracted serum protein, CS, YZ, and FM; Writing-original draft, SL, YC, and CS, Writing-review & editing, HH, XX, and FM. All authors read and approved the final manuscript, contributed to the article, and approved the submitted version.

Funding

This study was supported by the Guangzhou Science and Technology Project (202102080683).

Conflict of interest

The authors declare that the research was conducted in the absence of any commercial or financial relationships that could be construed as a potential conflict of interest.

Publisher's note

Supplementary material

The Supplementary Material for this article can be found online at: https://www.frontiersin.org/articles/10.3389/fgene.2022.765637/full#supplementary-material

References

Aikoh, H., Sasaki, M., Sugai, K., Yoshida, H., and Sakuragawa, N. (1997). Effective immunoglobulin therapy for brief tonic seizures in methylmalonic acidemia. *Brain Dev.* 19 (7), 502–505. doi:10.1016/S0387-7604(97)00059-4

Altun, I., Kiykim, A., Zubarioglu, T., Burtecene, N., Hopurcuoglu, D., Topcu, B., et al. (2021). Altered immune response in organic acidemia. *Pediatr. Int.* 64, e15082. doi:10.1111/ped.15082

Besnard, T., Sloboda, N., Goldenberg, A., Kury, S., Cogne, B., Breheret, F., et al. (2019). Biallelic pathogenic variants in the lanosterol synthase gene LSS involved in the cholesterol biosynthesis cause alopecia with intellectual disability, a rare recessive neuroectodermal syndrome. *Genet. Med.* 21 (9), 2025–2035. doi:10.1038/s41436-019-0445-x

Black, S., Kushner, I., and Samols, D. (2004). C-Reactive protein. *J. Biol. Chem.* 279 (47), 48487–48490. doi:10.1074/jbc.R400025200

Caterino, M., Pastore, A., Strozziero, M. G., Di Giovamberardino, G., Imperlini, E., Scolamiero, E., et al. (2015). The proteome of cblC defect: *in vivo* elucidation of altered cellular pathways in humans. *J. Inherit. Metab. Dis.* 38 (5), 969–979. doi:10.1007/s10545-014-9806-4

Del Giudice, M., and Gangestad, S. W. (2018). Rethinking IL-6 and CRP: why they are more than inflammatory biomarkers, and why it matters. *Brain Behav. Immun.* 70, 61–75. doi:10.1016/j.bbi.2018.02.013

Dionisi-Vici, C., Deodato, F., Roschinger, W., Rhead, W., and Wilcken, B. (2006). Classical' organic acidurias, propionic aciduria, methylmalonic aciduria and isovaleric aciduria: long-term outcome and effects of expanded newborn screening using tandem mass spectrometry. *J. Inherit. Metab. Dis.* 29 (2-3), 383–389. doi:10.1007/s10545-006-0278-z

Elmahgoub, S. M., Lambers, S., Stegen, S., Van Laethem, C., Cambier, D., Calders, P., et al. (2009). The influence of combined exercise training on indices of obesity, physical fitness and lipid profile in overweight and obese adolescents with mental retardation. *Eur. J. Pediatr.* 168 (11), 1327–1333. doi:10.1007/s00431-009-0930-3

Forny, P., Horster, F., Ballhausen, D., Chakrapani, A., Chapman, K. A., Dionisi-Vici, C., et al. (2021). Guidelines for the diagnosis and management of methylmalonic acidaemia and propionic acidaemia: first revision. *J. Inherit. Metab. Dis.* 44 (3), 566–592. doi:10.1002/jimd.12370

Ghosh, A., Rangasamy, S. B., Modi, K. K., and Pahan, K. (2017). Gemfibrozil, food and drug administration-approved lipid-lowering drug, increases longevity in mouse model of late infantile neuronal ceroid lipofuscinosis. *J. Neurochem.* 141 (3), 423–435. doi:10.1111/jnc.13987

Han, L. S., Huang, Z., Han, F., Wang, Y., Gong, Z. W., Gu, X. F., et al. (2017). Eight novel MUT loss-of-function missense mutations in Chinese patients with isolated methylmalonic academia. *World J. Pediatr.* 13 (4), 381–386. doi:10.1007/s12519-016-0085-z

Hannibal, L., DiBello, P. M., Yu, M., Miller, A., Wang, S., Willard, B., et al. (2011). The MMACHC proteome: hallmarks of functional cobalamin deficiency in humans. *Mol. Genet. Metab.* 103 (3), 226–239. doi:10.1016/j.ymgme.2011.03.008

He, R., Zhang, H., Kang, L., Li, H., Shen, M., Zhang, Y., et al. (2020). Analysis of 70 patients with hydrocephalus due to cobalamin C deficiency. *Neurology* 95 (23), e3129–e3137. doi:10.1212/WNL.0000000000010912

Hong, W., Zimmer, V., Basharat, Z., Zippi, M., Stock, S., Geng, W., et al. (2020). Association of total cholesterol with severe acute pancreatitis: a U-shaped relationship. *Clin. Nutr.* 39 (1), 250–257. doi:10.1016/j.clnu.2019.01.022

Jang, K. J., Mano, H., Aoki, K., Hayashi, T., Muto, A., Nambu, Y., et al. (2015). Mitochondrial function provides instructive signals for activation-induced B-cell fates. *Nat. Commun.* 6, 6750. doi:10.1038/ncomms7750

Jiang, Y. Z., Shi, Y., Shi, Y., Gan, L. X., Kong, Y. Y., Sun, L. Y., et al. (2020). Factors influencing in-hospital death for pediatric patients with isolated methylmalonic acidemia: a nationwide inpatient database analysis. *Orphanet J. Rare Dis.* 15 (1), 154. doi:10.1186/s13023-020-01446-0

Keyfi, F., Sankian, M., Moghaddassian, M., Rolfs, A., and Varasteh, A. R. (2016). Molecular, biochemical, and structural analysis of a novel mutation in patients with methylmalonyl-CoA mutase deficiency. *Gene* 576 (1 Pt 2), 208–213. doi:10.1016/j.gene.2015.10.002

Kovacic, B., Hoelbl-Kovacic, A., Fischhuber, K. M., Leitner, N. R., Gotthardt, D., Casanova, E., et al. (2014). Lactotransferrin-Cre reporter mice trace neutrophils, monocytes/macrophages and distinct subtypes of dendritic cells. *Haematologica* 99 (6), 1006–1015. doi:10.3324/haematol.2013.097154

Liang, L., Shuai, R., Yu, Y., Qiu, W., Shen, L., Wu, S., et al. (2021). A rare mutation c.1663G > A (p.A555T) in the MMUT gene associated with mild clinical and biochemical phenotypes of methylmalonic acidemia in 30 Chinese patients. *Orphanet J. Rare Dis.* 16 (1), 22. doi:10.1186/s13023-020-01632-0

Manoli, I., Sloan, J. L., and Venditti, C. P. (1993). *Isolated methylmalonic acidemia*. Seattle, Seattle (WA): University of Washington.

Manoli, I., and Venditti, C. P. (2005). *Methylmalonic acidemia*. GeneReviews™. Seattle: University of Washington. Available at: https://www.research gate.net/publication/221964133.

Richard, E., Monteoliva, L., Juarez, S., Perez, B., Desviat, L. R., Ugarte, M., et al. (2006). Quantitative analysis of mitochondrial protein expression in methylmalonic acidemia by two-dimensional difference gel electrophoresis. *J. Proteome Res.* 5 (7), 1602–1610. doi:10.1021/pr050481r

Rufinatscha, K., Radlinger, B., Dobner, J., Folie, S., Bon, C., Profanter, E., et al. (2017). Dipeptidyl peptidase-4 impairs insulin signaling and promotes lipid accumulation in hepatocytes. *Biochem. Biophys. Res. Commun.* 485 (2), 366–371. doi:10.1016/j.bbrc.2017.02.071

Sane, A., Ahmarani, L., Delvin, E., Auclair, N., Spahis, S., Levy, E., et al. (2019). SAR1B GTPase is necessary to protect intestinal cells from disorders of lipid homeostasis, oxidative stress, and inflammation. *J. Lipid Res.* 60 (10), 1755–1764. doi:10.1194/jlr.RA119000119

Sloan, J. L., Achilly, N. P., Arnold, M. L., Catlett, J. L., Blake, T., Bishop, K., et al. (2020). The vitamin B12 processing enzyme, mmachc, is essential for zebrafish survival, growth and retinal morphology. *Hum. Mol. Genet.* 29 (13), 2109–2123. doi:10.1093/hmg/ddaa044

Trinder, M., Wang, Y., Madsen, C. M., Ponomarev, T., Bohunek, L., Daisely, B. A., et al. (2021). Inhibition of Cholesteryl ester transfer protein preserves high-density Lipoprotein cholesterol and improves survival in sepsis. *Circulation* 143 (9), 921–934. doi:10.1161/CIRCULATIONAHA.120.048568

Wang, S., Liu, Y., Liu, J., Tian, W., Zhang, X., Cai, H., et al. (2020). Mitochondria-derived methylmalonic acid, a surrogate biomarker of mitochondrial dysfunction and oxidative stress, predicts all-cause and cardiovascular mortality in the general population. *Redox Biol.* 37, 101741. doi:10.1016/j.redox.2020.101741

Wong, S. N., Low, L. C., Lau, Y. L., Nicholls, J., and Chan, M. Y. (1992). Immunodeficiency in methylmalonic acidaemia. *J. Paediatr. Child. Health* 28 (2), 180–183. doi:10.1111/j.1440-1754.1992.tb02638.x

Advantages of publishing in Frontiers

OPEN ACCESS
Articles are free to read for greatest visibility and readership

FAST PUBLICATION
Around 90 days from submission to decision

HIGH QUALITY PEER-REVIEW
Rigorous, collaborative, and constructive peer-review

TRANSPARENT PEER-REVIEW
Editors and reviewers acknowledged by name on published articles

Frontiers
Avenue du Tribunal-Fédéral 34
1005 Lausanne | Switzerland

Visit us: www.frontiersin.org
Contact us: frontiersin.org/about/contact

REPRODUCIBILITY OF RESEARCH
Support open data and methods to enhance research reproducibility

DIGITAL PUBLISHING
Articles designed for optimal readership across devices

FOLLOW US
@frontiersin

IMPACT METRICS
Advanced article metrics track visibility across digital media

EXTENSIVE PROMOTION
Marketing and promotion of impactful research

LOOP RESEARCH NETWORK
Our network increases your article's readership